# Vessel wave wakes –
# new perspectives on their generation,
# propagation and shoreline impacts

## Gregory Cox

B.E. (Nav. Arch., Hons.) UNSW

Submitted in fulfilment of the requirements for the degree of
Doctor of Philosophy

Australian Maritime College
University of Tasmania

May 2020

# Declarations

## Declaration of Originality

This thesis does not contain material which has been accepted for a degree or diploma by the University or any other institution, except by way of background information and duly acknowledged in the thesis, and to the best of my knowledge and belief no material previously published or written by another person except where due acknowledgement is made in the text of the thesis, nor does the thesis contain any material that infringes copyright.

## Authority of Access

This thesis may be made available for loan and limited copying and communication in accordance with the *Copyright Act 1968*.

## Copyright

I warrant that I have obtained, where necessary, permission from the copyright owners to use any third-party copyright material reproduced in the thesis or to use any of my own published work in which the copyright is held by another party.

Gregory Lester Cox
May 2020

## Statement of Contribution

The paper "The Effects of Boat Waves on Sheltered Waterways – Thirty Years of Continuous Study," presented at *Australasian Coast and Ports 2019 Conference*, was co-authored with Gregor Macfarlane who contributed 10% to manuscript preparation and paper submission.

## Co-Author Agreement

We the undersigned agree with the above stated *proportion of work undertaken* in the above published peer-reviewed manuscript contributing to this thesis:

Signed on the 27th of November, 2019:

Assoc. Prof. Gregor Macfarlane
*Primary Supervisor*
National Centre for Maritime Engineering & Hydrodynamics,
Australian Maritime College,
University of Tasmania

Dr. Vikram Garaniya
*Acting Director*
National Centre for Maritime Engineering & Hydrodynamics,
Australian Maritime College,
University of Tasmania

Our fellow man,
Break him up, where him stand,
Slap away him open hand,
Steal him gold and take him land.
Then give him Jesus.
Jesus, save him soul, . . ..

Freedom.

*Cried, shouted, then sung.*
*All Rise*
Wynton Marsalis, 2002

# Abstract

The increasing prevalence of high-speed recreational and commercial craft utilising sheltered waterways has brought with it the commensurate degradation of the natural environment and public amenity. This is not new. Wave wake case studies for recreational craft in Australia were conducted as far back as the 1960s, but the growth in high-speed commuter ferry use since the 1980s to reduce urban transport pressures provided the impetus and requisite funding for more extensive research to be conducted.

Initially, the premise of this study was to formulate a systematic methodology for the quantification of environmental impacts. After several decades of describing and reporting the problems, there is a distinct and growing disjuncture between the science and its practical application in vessel management and regulation. Vessel wave wakes are complex and not easy to qualify, let alone quantify. Shallow water wakes are known to be quite different to those in deep water, yet both are described using the same techniques. Very little of the science transmits well to the general public and it is open to misinterpretation and manipulation.

Rather than continue towards a management and regulation methodology using science that has at times proved to be inadequate, if not questionable, the fundamental principles of wave wakes have been reviewed from the beginning to provide a more secure foundation for future application. A new method of ranking the erosive potential of wave wakes is proposed, subject to further validation.

Apart from the general introduction and conclusions, this document is arranged in a somewhat different manner to a traditional thesis. The principle tenets of wave wake science are reviewed and renewed, supported by subject-specific appendices.

**Section 2: *Literature Review***. A novel form of literature review is presented. Rather than a standard review of the available literature, which often can read as abstract summaries, nine selected technical reports and journal papers are appraised in detail, highlighting perpetual misinformation, problems of interpretation, and the limitations of the science.

**Section 3: *Waves.*** Waves are discussed from very basic concepts through to their propagation and interaction, but more in the context of how they are to be interpreted in a wave wake context rather than the principles of their existence.

**Section 4: *Deep Water.*** A comprehensive and updated review of the generation and propagation of wave wakes in deep water is presented. Its apparently simple relationships in fact give rise to complex interactions that lead to consistent misinterpretation of wave wake phenomena.

**Section 5: *Shallow Water***. In the past, a shallow-water wake was analysed in the same way as a deep-water wake. The composition of the shallow water wake is analysed, showing that the leading wave has the attributes of a wave packet and not a single wave. Moreover, the existence of solitary waves that come to dominate the leading shallow water wave at high depth super-critical Froude numbers and the results of novel experiments are discussed.

**Section 6: *Wave Energy and Power***. The two composite parameters of wave energy and power are commonly used as indicators of erosion potential. The distribution of energy in a shoaling wake is discussed and the results of past erosion experiments analysed. Wave power is shown to

have an intrinsic relationship with the wave wake itself, but wave energy and the form in which it is delivered are still believed the be two of the principal determinants of erosion potential.

**Section 7:** *Wave Height Decay*. This contentious subject is shown to be complex. It is proposed that a definitive wave height decay equation probably doesn't exist, and a new method of determining wave height decay based on group celerity is proposed.

**Section 8:** *Severity of Erosion*. A novel method is derived that determines a wave's propensity to entrain sediment, based on the summation of excess bottom shear stress above the threshold value, from threshold of sediment entrainment through to breaking. Promising correlation with field trials is demonstrated but based on a limited dataset.

A total of eleven comprehensive appendices contain the results of investigations and experiments and are written in a stand-alone manner:

> *Appendix A*: Review of nine existing wave wake studies.
> *Appendix B*: Deep water wave height decay.
> *Appendix C*: Shallow water wave height decay.
> *Appendix D*: Shallow water wavefront propagation.
> *Appendix E*: First wave in very shallow water.
> *Appendix F*: Extremely shallow water.
> *Appendix G*: Very shallow water – depth transition.
> *Appendix H*: Wave propagation from shallow to deep water.
> *Appendix J*: Correlation between bed shear stress and turbidity.
> *Appendix K*: Gordon River turbidity correlation.
> *Appendix L*: Wind waves.
> *Appendix M*: Error analysis and uncertainty.

# Acknowledgements

My thanks go to my supervisors, Assoc. Prof. Gregor Macfarlane and Dr. Jonathan Duffy, not only for their continuing support over the past many years but for leaving me alone to get on with it.

To my partner, Asst. Prof. Jeremy Leong, for his constant presence before, during and after this period, though he would probably describe the process as like trying to herd cats. Inherent recalcitrance is one trait that does not temper readily with age – which at least I acknowledge!

To my sons, Nathanael, Olin and Tristan, who did not abandon me when times were dark though had every right and reason to do so.

I acknowledge the influence of Greg Britton, who to me represents the consummate professional engineer. You can only ever look on and hope to learn.

It may come as a surprise to some that I acknowledge the early influence of Emeritus Professor Lawrence Doctors, who taught me hydrodynamics at an undergraduate level. I do not purport to be knowledgeable in the theory at all, but I doubt I would have come as far as I have without exposure to his fundamental approach. Wave wake did not form part of that education and our opinions on the subject diverge greatly, but I am not so stubborn as to deny history.

But this has been partly for me – to fulfil past dreams. A lot of time has been spent with *teach yourself practical wave mechanics*, often because much of what is available comes only in two forms: for those who qualify for the Fields Medal in mathematics or the trivialised, wave-of-the-hand generalisations that pass for engineering. I could never qualify for the first and I am too pedantic to accept the second. I want to know why.

I am pleased that, having graduated more than thirty years ago, I was still able to discover things for myself that are not explained clearly, or at all, in the literature. That comes from being able to imagine the problem and work through it qualitatively. There are many who excel at the mathematics but have no imagination, and there are plenty whose imagination extends no further than an EXCEL graph and a fitted trend line. As Albert Einstein said: "*imagination is more important than knowledge . . ,*" of which the modern-day equivalent is "*put away the computer and open your #@&%$ eyes*!" And dream.

And to Captain Cat, the retired blind sea-captain, asleep in his bunk in the seashelled, ship-in-bottled, shipshape best cabin of Schooner House.

"No, *I'll* take the mulatto, by God, who's captain here?
Parlez-vous jig jig, Madam?"

# Author's Statement

I did not come cold to this study. My work in the field as a consultant began twenty-five years ago, and even my undergraduate thesis from thirty-four years ago touched on transverse wave theory in a small way. Almost all that privilege was in the commercial sector, where the interest was not purely academic, and there were multiple commercial, regulatory and focus group forces pulling in different directions and not always with the purest of motives. Having to front members of angry community and boating interest groups at public information sessions, some of whom had already consumed more beers than what was really necessary, and giving them a presentation they really didn't want to hear, certainly sharpens the focus.

There were three important lessons learnt from this long involvement. The first was that everyone is looking for answers and there probably aren't as many simple ones as we would like. The idea that a simple or even complicated formula could take in a few basic parameters and reveal a definitive answer is just fanciful. It is often hard enough to determine the approximate weight of vessels being trialled let alone intimate and obscure design parameters. Vessels do produce orderly packets of waves, but those wave packets have characteristics specific to the vessel parameters and they propagate over and through each other in such a manner as to obscure their true form. Whether a shoreline responds to the aggregate or to the components has never been answered. It may be possible to dissect the aggregate into components analytically, but such a customised approach almost defeats the purpose of formulating a simplified approach to wave wake assessment.

The second lesson was that standards and standardised procedures for measurement and evaluation are important, and certainly more so than measuring wave parameters to three decimal places. As with all fluid mechanics, ship hydrodynamics is a study of scaling. Failure to recognise that can bias the outcome. Some parameters scale relative to the vessel, some to its speed, some to the water depth, and others to the wave parameters. There is inter-relation between these, but not always and not everywhere. A common technique for wave wake measurement is to measure the wake at a specific absolute lateral separation (example – fixed probe positions used by Osborne *et al.*, 2007, but with vessels ranging from *11.5 m* to *27 m* overall length and wave wake comparisons manually adjusted to a standard *300 m* lateral separation), yet this favours shorter vessels and allows their wake to decay in height to a greater relative extent. It is argued that a fixed distance rather than a distance relative to vessel length reflects a true operating condition, as would be found in a waterway of fixed width, though it could also be argued that there is potential for the misrepresentation or abuse of this method.

Similarly, many researchers focus endlessly on technology in data acquisition and forget the basics. The study of Ozeren *et al.* (2016) (refer review in Appendix A) is a prime example. Considerable technology was used to log the vessel track during wave wake field trials, yet it didn't occur to anyone to put out buoys to mark the course, or to measure the water depth at the sailing line. Consequently, the logged sailing lines varied in lateral separation by around *100%* (refer Ozeren *et al.*, 2016, Fig. 3). Measuring wave parameters to three decimal places is less important than maintaining repeatable conditions for their generation. My experience is that the two most difficult aspects of field trials to control are maintaining a straight course and a constant speed (ambient condition variations aside). Simple instructions to the helmsman about the need to maintain a straight course and constant speed (any speed!) are overwhelmed by their urge to

tweak the wheel, accelerate and decelerate abruptly, and nudge the throttle continually to maintain speed to the hundredth-of-a-knot accuracy of the speed log. Generally speaking, full-scale trials are rarely perfect and often waver between a necessary evil and a waste of time.

Lastly, and probably the most disconcerting lesson learnt, was the prevalence of politics over science.[1] Experience has demonstrated that concern for the environment is often a front for self-interest, as competing entities wrestle to preserve their subjective interpretation of *amenity*. Waterfront residents believe that with the purchase of their property comes stewardship (ownership) of, or special entitlement to, the waterway and the view beyond. Wave wake and shoreline erosion complaints are often a subterfuge for factors such as noise from passing vessels, which is a transient intrusion that leaves no residual for use as the basis of a formal complaint. Similarly, accelerated erosion from waves can highlight poor shoreside land management practices, but farming is viewed as being of national interest whereas water skiing is not. The softest targets are those that bring in the least direct revenue. Science and equitable access take second place to the proclivities of those with the loudest voices and deepest pockets. As was once explained to me as a junior engineer imbued with a naïve enthusiasm – *in this world, the person with the most rights is the person with the biggest gun*.

Few people want to acknowledge that politics and vested self-interest guide the conduct of environmental assessments, and science is often little more than window dressing. It is rare to find such comments in the published literature, though we have done so in the past (Cox, 2000; Macfarlane and Cox, 2003 and 2005). No amount of science could ever provide a definitive solution to wave wake problems. As an example, we are now able to define erosion thresholds with reasonable certainty. That has certainly been the case on the Gordon River, where thresholds have been used as the basis for sustainable tourist vessel operations (Bradbury *et al*., 1995). In that case, the threshold vessel service conditions are very low. Other boating activities with energetic wakes would initiate erosion; even the wakes of high-speed small craft. The question then becomes – *how much erosion above the threshold is tolerable?* That tolerance level would determine the type and extent of boating activity which, taken at a threshold level, may prohibit boating altogether. There most likely is no answer to that question; science cannot determine it and politics doesn't want to address it. Nominating a number and *putting a peg in the sand* extinguishes future opportunity for fluidity of conviction.

The premise of this study was the development of an assessment methodology that would allow a designer, operator or regulator to make an informed judgement about the effects of a specific vessel in a specific waterway. It would have required simplification in places to suit the limited knowledge of the user audience and almost certainly would have relied on the AMC's *Wave Wake Database* for the generation of vessel-specific wave parameters.[2] As the study progressed, it became clear that the past thirty years of work may have skipped over fundamental questions, the primary two being *what are we actually measuring,* and *does it correlate with the actual environmental impact*? An excellent example of that is analysed in Section 1.5.4. Small craft studies, the results of which have close correlation to deep water wave conditions, require few shallow water wave wake techniques. The desire to quantify larger vessels in shallow waterways requires a more intimate understanding of shallow water wave wakes than what is available.

---

[1] Politics both in terms of the involvement of government as well as self-interest.
[2] The AMC's Wave Wake Database (WWDB) is a collection of decades of wave wake model and full-scale experimental results that allows for the prediction of a vessel's principal wave wake heights and periods.

Waves are dynamic and transmute as they propagate, yet the language of waves gives them a static feel. I, too, am guilty of that at times, because the static explanation is convenient. We must learn to appreciate that waves are not individual entities that propagate largely unchanged or change only in height as they decay. Whatever we see is only valid at one point in space and time. The premise of this study changed over time as a consequence, with greater focus on better explanation of the principles of wave wake evaluation. It seemed pointless to press towards a conclusion on the top of thin (or flawed) foundations.

As most of my past work in this field has been for a public audience, the language used had to be of a simplified nature. There is more to be understood practically from descriptive prose than from pages of equations. Kelvin (1887) is the best example of that; it is *the* foundation paper on vessel wave wakes, and at the outset Kelvin stated his preference for words over mathematics for his educated but unedified audience. Conversely, the sections here on erosion prediction, as well as many of the appendices, are rich with reasoning and are not easily read. There is also a strong reliance on footnotes throughout, as would more be the case with the humanities than with science. The footnotes are used for additional referencing of sources considered incidental (there to substantiate a point and not as background reading), as well as additional comments that may otherwise clutter the prose. Too often technical papers make comments, in forms no better than throwaway lines, without proper background qualification. I make no apologies for the descriptive footnotes – it is how I want my work to be explained.

Much of the work is based on experimental results, but I have tried to avoid the tendency to use $R^2$ (goodness of fit or coefficient of determination) as an indication of causation. It isn't. In the cases where it is used, values greater than *0.9* are assumed to give good correlation, and values above *0.95* are assumed to show excellent correlation. Only in a few cases are values between *0.8* and *0.9* quoted; Figure J6 being the (hypocritical) exception. Anything below *0.8* is considered no better than shotgun scatter, where greater than *20%* variability is caused by unknown variables. It is quite common to see values of *0.6* to *0.8* reported in engineering studies, which at best could be regarded as *directional guidance* and nothing more. A dart board would give similar results at a cheaper price.

I also make no apologies for the length of the thesis. Unlike many of my fellow students who are undertaking studies that are quite narrow in focus, this topic is very broad and demands more than a cursory review of its myriad of component subjects. As it is, a considerable amount of necessary work has been culled from the final document. My intention has never been to complete an adequate amount of work to be awarded a doctorate, but rather complete a reference for which others in the academic and commercial fields may find useful applications. The guiding principle of my engineering career has always been the necessity for practical purpose rather than collecting badges – more so now in the late afternoon of my career.

After my three years of intense study following from twenty-two years of past work in the field, this is my philosophy – at least for now.


Greg Cox
November 2019

# Notes for the Reader

*Layout*

This thesis comprises a main body and many appendices. The main body is the over-arching story and the appendices are more detailed, subject-specific documents which can be consulted as required for more in-depth discussion. Those wanting only a descriptive understanding should find sufficient detail within the main body, without need to refer to the appendices.

There is sometimes repetition of discussion and diagrams between the main body and appendices. Each appendix is intended to be as complete and stand-alone as possible, sharing only common nomenclature and references with the main body.

There is also repetition of discussion within sections. Wave wake is not a linear progression of ideas: it is a network of intertwined conditions such as water depth, speed, vessel types, and locations requiring constant statement of the concepts that pertain to them.

Footnote numbering is continuous throughout the document.

*Diagrams and graphs*

Much of the work in this field is empirical, requiring an increased number of figures than would a more theoretical approach. Diagrams and figures are displayed in a manner that presents information as a detailed depiction at a suitable scale rather than a facile schematic at such a small scale that anything other than general relationships cannot be determined easily. Axes are fully labelled, and grids are provided so that the reader can manually extract the data to some extent, if desired.

Figure captions are deliberately expressive so that the reader can be referred to a figure and receive a summary of its salient features without returning to the main text. Captions are generally expressed in the present, not past, tense.

**Figure** indicates a figure within its relevant section of this document; in bold font for easy identification when moving from text to figure and back again (as per commercial engineering practice). Photographs are shown as figures for easier identification. The abbreviated terms *Fig.* and *Eqn.* refer to figures and equations in external references.

Note that most graphs have been prepared using Microsoft EXCEL, which does not support superscripts or subscripts in chart legend nomenclature.

*Equations*

Microsoft Equation Editor was used to present equations. It uses a specific font that cannot be varied. When equation parameters are referred to in the text, the standard font is used unless the Equation Editor font is required for clarity. Equations are generally left inline unless they are numbered for later reference.

Numbers within [square brackets] signify reference to an equation within the document.

$\sim$ signifies *about* or *in the order of*.
$\approx$ signifies *approximately equal to*.

## Terminology

When referring to waves, the term *celerity* and symbol $c$ are used to give some differentiation from *speed* and symbol $V$, which are reserved for vessel speed (and is always assumed to be a scalar quantity). Literature on waves often do not differentiate as they may assume waves already exist, and they may not have to describe a moving source as well (the exception being stream flows).

Wave period is always taken between concurrently periodic zero crossings (*zero up* to *zero up* or *zero down* to *zero down*). The term *maximum wave* always refers to the highest wave in the most energetic packet.

When referring to vessels, *length* is always taken as a vessel's static waterline length.

## Referencing

The APA referencing style is used throughout. References comply where possible with the University of Tasmania APA referencing style guide and the National Library of Australia (NLA) APA referencing style, noting that there are different interpretations of the APA standard worldwide.

Access dates are provided for all online references, including those considered permanent.

**Table i -** *Details of vessels used in this study.*

| Vessel | Type | L (m) | Δ | $L/\sqrt[3]{\nabla}$ | Notes |
|--------|------|-------|---|----------------------|-------|
| AMC 00-01 | Monohedron monohull | 1.042 | 10.55 kg | 4.75 | Model typical of small-to-medium recreational craft |
| AMC 17-05 | Catamaran | 3.57 | 62.4 kg | 9.00 | "Low-wash" catamaran model (passenger ferry) |
| Rivershuttle (AMC 99-17) | Slender monohedron monohull | 36.54 | 32.0 t (s.w.) | 11.60 | Scaled from 1:20 scale model (passenger ferry) |
| Supershuttle (AMC 97-30) | Monohedron monohull | 49.0 | 182.0 t (s.w.) | 8.72 | Scaled from 1:30 scale model (passenger ferry) |
| QG Cowan | Monohedron monohull | 6.75 | 2.48 t | 5.03 | From full-scale trials – government patrol boat |
| Large Ski Boat | Monohedron monohull | 5.30 | 1.44 t | 4.73 | From full-scale trials – recreational ski boat |

## Nomenclature

***Parameters***

| | |
|---|---|
| $a$ | Wave amplitude (m or mm, as shown); |
| | A generic power equation exponent ($y = x^a$) |
| $A_{nett}$ | Nett area under the normalised bed shear stress curve from threshold of sediment entrainment to breaking |
| $A_{total}$ | Total area under the normalised bed shear stress curve from threshold of sediment entrainment to breaking |
| $B$ | Vessel breadth, usually taken at the waterline (m) |
| $c$ | Wave celerity (m/s) |
| $c_g$ | Wave group celerity (m/s) |
| $c_L$ | Lateral celerity of a wave (perpendicular to the sailing line) (m/s) |
| $c_p$ | Wave phase celerity (m/s) |
| $d$ | Water depth (alternative form of $h$) (m) |
| $d_o$ | Orbital diameter of wave motion (m) |
| $D$ | Sediment diameter (usually mm) |
| $E$ | Wave energy (Joules per metre of crest length) |
| $E_o$ | Deep water wave energy (Joules per metre of crest length) |
| $E_T$ | Total wave energy of a packet of waves (Joules per metre of crest length) |
| $f$ | Frequency (Hz) |
| $F$ | Fetch (m or km, as shown) |
| $Fr_F$ | Fetch Froude number, ($= v/\sqrt{gF}$, where $v$ is a generic wind speed) |
| $Fr_h$ | Depth Froude number, ($= V/\sqrt{gh}$) |
| $Fr_L$ | Length Froude number, ($= V/\sqrt{gL}$) |
| $Fr_\nabla, Fr_V$ | Volumetric Froude number, ($= V/\sqrt{g\nabla}$) |
| $g$ | Acceleration due to gravity (m/s²) |
| $h$ | Water depth (m or mm, as shown) |
| $h_b$ | Water depth at the point of wave breaking (m or mm, as shown) |
| $h_t$ | Water depth at the sediment entrainment threshold (m or mm, as shown) |
| $h_0$ | Water depth in a super-critical flow (m or mm, as shown) |
| $h_1$ | Water depth in a sub-critical flow (m or mm, as shown) |
| $H$ | Wave height (m or mm, as shown) |
| $H_b$ | Wave height at breaking (m or mm, as shown) |
| $H_o$ | Deep water wave height (m or mm, as shown) |
| $H_m, H_{max}$ | Height of the highest wave in a group (m or mm, as shown) |
| $H_{rel}$ | Relative wave height (in decay calculation) |
| $k$ | Wavenumber, ($= 2\pi/\lambda$) (rad/m) |
| $k_o$ | Fundamental or characteristic wavenumber of a wave packet, ($= 2\pi/\lambda_o$) (rad/m) |
| $k_s$ | Shoaling factor, ($= H/H_o$) |

| $L, L_{WL}$ | Vessel waterline length (m) |
| --- | --- |
| $m$ | Beach slope (ratio expressed as a decimal); |
| | Modulus of the Jacobi elliptic function (for cnoidal waves) |
| $M_{crit}$ | Critical Mach number |
| $n$ | Wave height decay exponent; |
| | A generic power equation exponent ($y = x^n$) |
| $P$ | Wave power (Watts per metre of crest length) |
| $R_1$ | Wave reflection coefficient |
| $S$ | Normalised bed shear stress at a given depth |
| $S_t$ | Normalised threshold bed shear stress at a given depth |
| $S'$ | Quotient of the normalised shear stress and normalised threshold shear stress at a given depth, defined as $S/S_t$ |
| $S'_b$ | $S'$ measured at the point of wave breaking |
| $S'_{0.5}$ | $S'$ measured at a water depth of *0.5 m* |
| $t$ | Time (s) |
| $T$ | Wave period (s); |
| | Vessel draft, in the context of $L/T$ or $B/T$ ratio (m) |
| $T_m, T_{max}$ | Period of the maximum (highest) wave in a group (s) |
| $T_1$ | Wave transmission coefficient |
| $u$ | Relative wave height (ratio of wave height at $y$ to wave height at the sailing line) |
| $u_m$ | Near-bottom celerity beneath a wave, (m/s) |
| $U_R$ | Deep water Ursell number, ($= H\lambda^2/h^3$) |
| $U_S$ | Shallow water Ursell number, ($= gHT^2/h^2$) |
| $U_{10}$ | Windspeed measured at a reference height of *10 m* (m/s) |
| $V$ | Vessel speed (m/s) |
| $x$ | Spatial location relative to a reference point (m) |
| $y$ | Lateral separation perpendicular to the sailing line (m) |

### ***Greek Letters***

| $\alpha$ | Angle of wave crest propagation relative to the sailing line (degrees) |
| --- | --- |
| $\beta$ | Bore strength [$= (h_1 - h_0)/h_0$] |
| $\gamma$ | Vessel-dependent constant of wave height decay |
| $\zeta$ | Water surface elevation (analytical term) (m) |
| $\lambda$ | Wavelength (m) |
| $\lambda_o$ | Deep water wavelength (m); |
| | Fundamental or characteristic packet wavelength ($= 2\pi/k_o$) (m) |
| $\lambda_T$ | Transverse wavelength (m) |
| $\xi_o$ | Iribarren number ($= \tan m/\sqrt{H_o/\lambda_o}$) |
| $\rho$ | Density (generic form) (kg/m³, or as shown) |
| $\rho_s$ | Sediment density (kg/m³, or as shown) |
| $\psi$ | Wave function (generic) |

| | |
|---|---|
| $\psi^m$ | Kelvin angle (degrees) |
| $\Delta$ | Vessel displacement (kg or tonnes, as shown); |
| | Width of a solitary wave (m); |
| | Flow criticality parameter ($= Fr_h - 1$) |
| $\nabla$ | Vessel displaced volume (m³); |
| | Volume per unit crest width of a solitary wave (m³/m) |
| $\nabla_t$ | Temporal volume per unit crest width of a solitary wave (m²s/m) |

### *Subscripts*

| | |
|---|---|
| $1, 2, 3 \ldots$ | In general, indicate *first*, *second*, etc. (usually referring to individual waves) |
| $b$ | At the point of wave breaking |
| $crit$ | Critical (usually referring to a depth-critical condition) |
| $h$ | At depth $h$ |
| $m$ | Corresponding to the highest wave (≡*max*) |
| $max$ | Maximum value |
| $o$ | Deep water (used in coastal engineering); |
| | Packet fundamental or characteristic condition ($k_o$ and $\lambda_o$) |
| $rel$ | Relative to or relative value |
| $t$ | Threshold (at the threshold of sediment entrainment); |
| | Time (in reference to temporal volume $\nabla_t$) |
| $T$ | Total; |
| | Transverse (in reference to the transverse wavelength $\lambda_T$) |
| $WL$ | Waterline |

### *Abbreviations*

| | |
|---|---|
| AMC | Australian Maritime College |
| BBM | Benjamin Bona Mahoney (solitary wave form, refer Dingemans, 1997) |
| Bq | Boussinesq (solitary wave form, refer Dingemans, 1997) |
| CEM | Coastal Engineering Manual (United States, 2006) |
| iBq | Improved Boussinesq (solitary wave form, refer Dingemans, 1997) |
| KdV | Korteweg de Vries (cnoidal and solitary wave forms, refer Dingemans, 1997) |
| LOA | Length overall |
| SR | Slenderness ratio ($= L/\nabla^{1/3}$) |
| SPM | Shore Protection Manual (Coastal Engineering Research Center (CERC)(US), 1984) |
| WSE | Water surface elevation (general term) (m or mm, as shown) |

**Notes**:
1. Where possible, the ITTC standard nomenclature is applied.[3]
2. Some externally referenced equations have their own nomenclature, which is noted at the point of application.

---

[3] https://ittc.info/media/4004/structured-list2014.pdf (last accessed 5th September, 2019)

# Definitions

This study assumes the reader has had prior exposure to wave wake and vessel terminology. Only basic diagrams explaining wave features and vessel terms are included. Additional introductory material prepared by the author can be found in Macfarlane and Cox (2003, 2005).

### Wave Parameters (Figure i)

A *zero crossing* is the point where the water surface elevation returns to the still water level after the passing of a wave, defined in terms of upcrossings and downcrossings.

*Wave height* is measured between a consecutive crest and trough. No distinction is made between crest-to-trough or trough-to-crest.

The *maximum wave* is defined as the highest wave in a wave wake record, measured between a consecutive crest and trough, or trough and crest. No distinction is made between waves beginning with a zero upcrossing or zero downcrossing.

*Wave period* is measured between zero crossing points (consecutive upcrossings or downcrossings) spanning the complementary wave height measurement. Period is not measured from crest-to-crest or trough-to-trough because of potential discrepancy when consecutive crests or troughs are not of the same elevation. Wavelength therefore becomes the spatial equivalent of wave period.
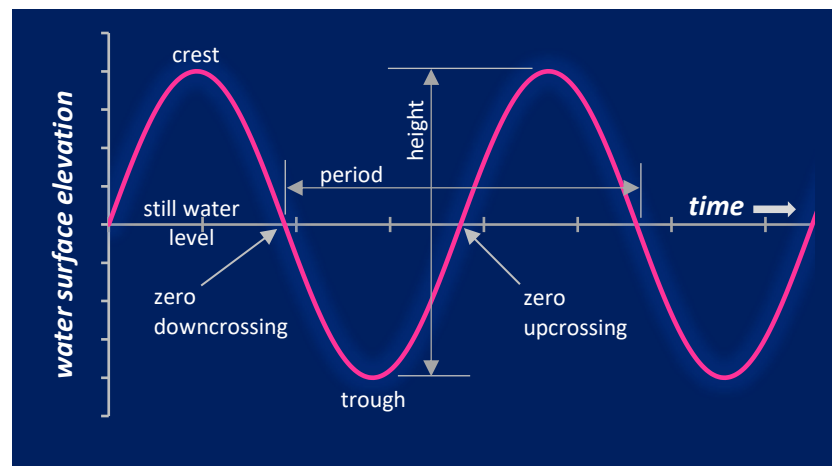


**Figure i** – *Wave parameters.*

### Wave Packet Parameters (Figure ii)

When numbering waves (*wave number*, not to be confused with wavenumber $k$), those waves beginning with zero upcrossings are given whole numbers and those beginning with zero downcrossings are given half numbers. Those waves with half numbers are therefore comprised of the trough of the preceding whole wave and the crest of the following whole wave. Often, the start of *wave 1* may be indeterminate or based on a nominal elevation that is a percentage of the height of the first crest.

A *wave packet* defines a group of related waves as they propagate or, more correctly, a group of waves defined by the same wave function.

A *packet envelope* describes the boundary of the packet of waves that circumscribes the crests and troughs. It is sometimes referred to as a packet soliton or envelope soliton, as its upper and lower boundaries have the properties of a soliton (a form of solitary wave).

The packet fundamental or characteristic wavelength ($\lambda_o$) and wavenumber ($k_o = 2\pi/\lambda_o$, not *wave number*) are defined by the wave parameters at the packet envelope maximum.
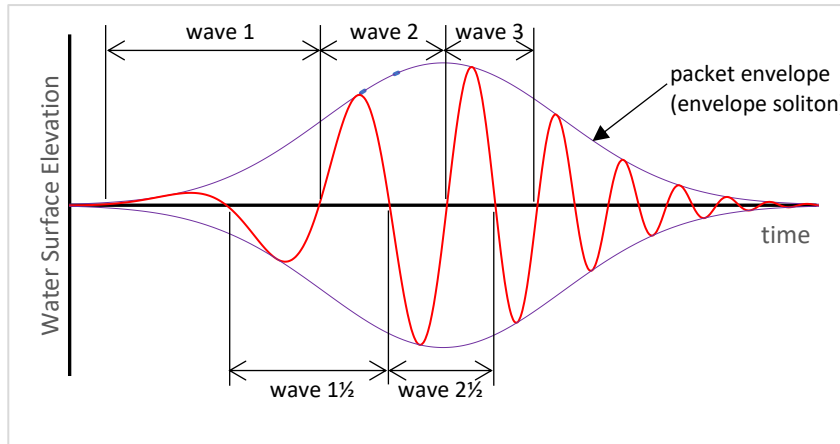


**Figure ii** – *Wave packet parameters.*

*Vessel Parameters*

*Length* ($L$) is always assumed to be the static waterline length, not the overall length or the dynamic waterline length.

The term *hull speed* (Figure iii) is a colloquial term that defines the speed where a hull has a wave at the bow and the stern and hence the transverse wavelength equals the static waterline length. Although it is a notional condition, it is used to signify the point where resistance increases substantially relative to speed. It also signifies the upper limit of the *displacement speed* range. The condition $\lambda_T = L$ would occur at $Fr_L = 0.399$ (or $V_{knots} = 1.34\sqrt{L_{feet}}$ in the imperial, colloquial form), though in reality the bow wave forms at a point aft of the forward end of $L$.
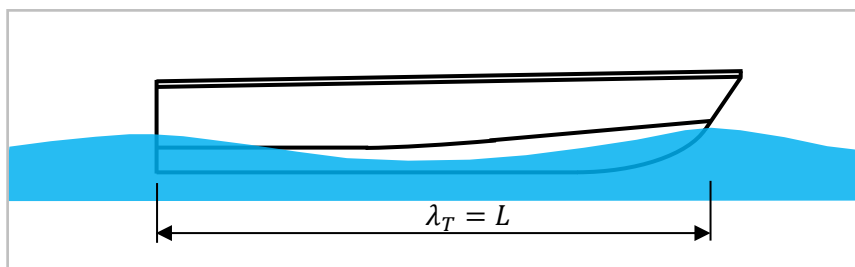


**Figure iii** – *Schematic definition of "hull speed."*

# Contents

# Figures and Tables

## Figures

xxvii

## Tables

# Preface

---

**i        Statement of the Problem**

The growth in recreational boating and the establishment of high-speed passenger vessel transport in sheltered waterways (rivers, harbours and bays) have put pressure on the natural and built-up environment. Sheltered waterways are dynamic environments that respond to ambient conditions and transmute accordingly. Forced changes in terms of new fluvial processes (damming of the Gordon River, and sand and gravel extraction on the Brisbane River, for instance), the construction of seawalls and revetments, the removal of riparian vegetation, and other anthropogenic factors have increased the propensity for shoreline erosion. The introduction of the high-speed vessels and a new wave paradigm has added increased pressure to already stressed waterways.

One complication is how we view these waterways. In the past, waterways were free to change dynamically, reaching a dynamic stability that would reset with cyclical flooding. Man's definition of stability is not dynamic; it is static. Shorelines are armoured and waterways are mapped with close precision, and any change to that static interpretation is considered to be degradation.

Vessel wave wakes have introduced waves with forms different to those occurring naturally, especially waves with longer wave periods. Also, vessels can generate very energetic waves in shallow water, giving them a form different to naturally-occurring waves that are effectively *deep* at the time of their generation.

It was not the intention of this study to quantify the mechanism of vessel wave wake generation based on vessel parameters. There are existing statistical and experimental methods available for that. The premise of this study was to:

    a.   not only determine those wave wake parameters that were primary causes of environmental concern, but to understand in detail how and why they were important;

    b.   understand how wave wakes were comprised of those parameters and under what conditions they were generated, with particular reference to waves generated in shallow water;

    c.   determine the relationships between the parameters of vessel-generated waves and shoreline erosion;

    d.   formulate a novel methodology for quantifying the propensity of wake waves to initiate erosion as well as rank the severity of erosion above threshold levels, understanding that there are many shoreline types and possible erosion mechanisms.

**ii       Research Questions to be Addressed**

The fundamental questions to be answered are:

    a.   What are we measuring and how does it correlate with the environmental impacts observed?

    b.   Does a portion of a wake represent the potential effects of the whole wake, and why?

    c.   What is the actual composition of wave wakes generated in shallow water and how do they relate to those generated in deep water?

    d.   How do shorelines react to different wave parameters?

e. What are reasonable threshold erosion limits and how are waves with parameters that exceed the threshold to be ranked according to their erosive potential?

In addressing these research questions, it is necessary to appreciate that there is a non-scientific aspect to this subject – one centred on the need to balance the public amenity of competing and at times disparate community, operator and regulatory interests.

## iii    Thesis Structure

The thesis is divided into a main body of nine sections. They are complemented by twelve detailed appendices on definitive topics. The main body of the thesis is a self-contained story, with the appendices providing interested readers with more comprehensive insights.

The introduction is divided into two themes - the classes of vessels and where they impact on the natural and built environment, and examples of the interpretation of the problem by the community, regulators, researchers and vessel designers.

The literature review of Section 2 takes a novel approach. It is too easy to repeat what has been published and perpetuate misinformation. Instead, nine existing (recent) wave wake investigations are reviewed in close detail to determine their strengths and weaknesses, as well as illuminate those areas where the discussion needs to be reset.

Sections 3 to 7 discuss how we view wave wakes and how we interpret them. Distinction is made between what is considered deep and shallow for the vessel and for the waves it generates. The difficult subjects of how the wave wake transforms as it propagates in terms of decay, energy and power are addressed.

Section 8 establishes a novel method of describing the potential of waves to cause erosion and how different waves may be ranked accordingly. Correlation with existing field trials is provided.

Lastly, the conclusions summarise where we have come from and where future work needs to focus in order to provide useful science for the community.

These are new perspectives on wave wakes and their generation, propagation and shoreline impacts.

## iv    Novel Concepts

Four investigations are considered novel and two are considered to be more developed than those available in the existing literature.

**Novel**
*Severity of Erosion* – a method is proposed that integrates the excess bottom shear stress (shear stress in excess of the threshold) beneath a shoaling wave that defines a wave's propensity to entrain sediment. This is useful in understanding the fundamental wave parameters that initiate and accelerate erosion. The method correlates with available field data. A method to rank the propensity of different waves is proposed, though further investigation of how that ranking correlates with recorded erosion is required.

*Shallow Water Wave Wakes* – It has previously been thought that the leading wave in shallow water was a single wave. It has been shown that the leading wave is a packet of waves that coalesce into what appears as a single wave, but with wave parameters that vary with

propagation. Several novel experiments demonstrated this. There is also a plausible relationship between deep and shallow water wave wakes.

*Solitary Waves* – It has been demonstrated that the leading wave of a depth super-critical shallow water wake has an underlying solitary wave component that becomes dominant as the water depth decreases. Moreover, it was previously believed that vessels only generated solitary waves under certain conditions and within a limited speed range around the depth-critical speed. A series of novel experiments were conducted that demonstrated the existence of solitary wave components across a wide speed range. Under the right conditions, these solitary components can energise themselves by trapping energy circulating through the shallow water wake. Once sufficiently energised, they can decouple from the depth super-critical wake and propagate independently. It is believed this is part of a probable mechanism that led to shoreline inundation, swamped small craft and caused several recorded deaths by what have been described as "*large breaking waves*" from passing ferries (Marine Accident Investigation Board (MAIB), 2000; Blunden, 2004).

*Decay* – A novel interpretation of wave height decay is presented. It has long been assumed that wave height decay was a function of lateral separation (in effect – propagation distance). It is believed that the rate of decay is a function of the number of wave cycles undergone, which is expressed in terms of the packet group celerity. Also, the limiting wave celerity in shallow water was used to show that the leading wave in a shallow water wake decayed in the same manner due to the packet-like nature of this single wave form. It is also believed that, at most slow to moderate speeds, a definitive decay relationship is impossible to accurately determine analytically and experimentally due to unpredictable and variable wave packet superposition.

**More developed**
A better understanding of deep and shallow water wakes is presented. For the deep condition, packet superposition makes wave wake analysis complex. The importance of understanding what is being extracted from a wave wake record and how that relates to the vessel and the wake is examined. Many of the features of superimposed wakes and how to interpret them are discussed. A more developed practical guide accounting for water depth when assessing wake waves is outlined.

# Section 1 – Introduction

*An alleged scientific discovery has no merit*
*unless it can be explained to a barmaid.*

*Ernest Rutherford*

## 1.1    Introduction

The original premise of this study was to build on past decades of experience in wave wake and develop a systematic method of predicting the environmental effects of operating high-speed craft in sheltered waterways. It would be useful for designers, operators and regulatory bodies to possess such a method, though an over-arching approach would always be limited by the accuracy of its underlying assumptions. At best, it would offer a degree of comfort to certification and regulation, but it would not be a substitute for a bespoke assessment. There are too many unknowns and too many variables to give guarantees.

Many of the techniques currently used to assess wave wake impacts are historical by nature. For instance, the height of the highest wave (termed the maximum wave) as an indicator of the intensity of a vessel's wave wake has long been used as a principal measurement, and its application can be found in the early work of Johnson (1957) and Lesleighter (1964). It could also be argued that the origins of the concept of the highest wake wave evolved from Kelvin's description of the Kelvin wedge (Kelvin, 1887) and Havelock's elucidation of wave transformation at the *cusp* (Havelock, 1908). The fascination with wave height remains to this day, as evidenced in the literature review of Section 2 and Appendix A. The adaptation of high-speed craft to sheltered and near-coastal waterways passenger transportation and the immediate repercussions that followed became the impetus for a substantial proportion of the scientific investigation, rather than the growing post-war prevalence of small craft.[4]

In modern parlance, regulation of a public or private activity that does not generate direct government income must be done on a *user pays* basis, or at a minimal cost to government. Publicly funded regulatory commissions, authorities and statutory boards with legislated powers to oversee commercial and private activities have been somewhat replaced with outsourced certification. The Australian commercial vessel sector is an example of this, with a degree of privatisation of certification in most states, a reduction or elimination of government-subsidised oversight, and a commensurate shift in fees paid. There are many examples of a move away from public regulatory oversight and certification in other industry sectors and the commensurate failures inherent in a philosophy so easily distorted by commercial self-interest.[5,6]

---

[4] Discussing the post-war growth of recreational craft ownership: https://case.edu/ech/articles/b/boating-recreational (last accessed 17th August, 2019).
[5] Self-certification by Boeing of its 737 Max 8 aircraft: https://www.washingtonpost.com/investigations/how-the-faa-allows-jetmakers-to-self-certify-that-planes-meet-us-safety-requirements/2019/03/15/96d24d4a-46e6-11e9-90f0-0ccfeec87a61_story.html?noredirect=on (last accessed 16th September, 2019).
[6] Problems of self-certification and privatised certification within the NSW building sector: https://www.abc.net.au/news/2019-08-19/building-report-author-says-she-wouldnt-buy-new-apartment/11421268 (last accessed 16th September, 2019).

Recreational boating in Australia has not yet been exposed to excessive regulation. Apart from areas of activity and or speed restriction, it is still possible to operate a recreational vessel almost anywhere with few restrictions and with a minimal level of certification and licencing.[7] In the Northern Territory, operator licencing is not required at all. Most Australian states now mandate practical (private) certification courses for new recreational boating licence applications, though these courses are only an introduction to recreational boating and there isn't necessarily the strong component of operator competency as there is with motor vehicle licencing. Existing recreational boating licences are grandfathered from additional competency requirements.

Recreational craft wave wake studies have grown to be the largest sector for research but without adequate funding. Recreational vessel activities are not a direct source of government revenue and so receive limited government attention. Passenger ferry environmental studies are mostly a reaction to community concerns about shoreline impacts. Where the service is private and or of a small scale, regulatory intervention is more prompt than when a service is government run and or of a large scale, implying a degree of public amenity and purpose to be protected. Coastal ferry wave wake analyses (mostly in Europe, but also in North America and New Zealand) were heavily funded in the 1990s because of direct or indirect government interest in interisland/interstate transport services, the substantial investments involved, and the potential dangers to the community. Subsequent service regulation, as well as economics (demand reduction and rising fuel costs), has relegated coastal ferry studies to a small, specialised industry.

Commercial vessel activities are more heavily regulated, especially those certified to carry passengers. The additional regulation may have the appearance of being double-edged; regulation for passenger safety is more stringent, but it may also be used for route licencing and potentially for exclusivity and or government subsidy. The former is the case for the tourist ferry services on the Gordon River in Tasmania, and the latter is the case for the Brisbane River CityCat service, which is subsidised by the Brisbane City Council.[8] The implication with government subsidy is an identified public need and an inherent desire to sustain the service; the further implication being a concerted effort to maintain the status quo even when operational problems such as environmental degradation become increasingly evident.

As the study progressed, it became clear that many of the fundamental techniques used to evaluate wave wakes lacked proper explanations as to their applicability and relevance. The historical nature of these techniques makes them vulnerable to perpetual recycling – retained for no other reason than their continual presence in the literature. Further progress towards a means of predicting the propensity to cause erosion would rely too heavily on empirical methods that may not be sufficiently rooted in fact to be of long-term value. Moreover, our understanding of the composition of shallow water wave wakes was itself shallow and in need of a better understanding.

A different approach was taken - one which returned to the fundamentals of wave wake, how we interpret them, and how they cause the problems they do.

---

[7] http://www.myboatinglife.com.au/get-onboard/boat-licences.
[8] The Brisbane City Council publishes online its annual reports of transport subsidies: https://www.brisbane.qld.gov.au/about-council/council-information-and-rates/news-and-publications/council-annual-plan-and-budget/annual-report-and-financial-statements (last accessed 2nd October 2019).

## 1.2 The Principal Determinants of Wave Wake Severity.

Much has been written about this and it must be one of the most misunderstood and misrepresented tenets of the wave wake story. It is accepted that at slower speeds ($Fr_L < 0.5$) wave wake can be influenced by many vessel design parameters, but at high speeds the two principal determinants are length and displacement. Macfarlane and Renilson (2000, Fig. 5-10), referring to the AMC's Wave Wake Database, showed that catamaran forms produced slightly lower maximum waves than monohulls but slightly longer corresponding wave periods, with the resulting wave energy being similar. That was shown using equivalent length and displacement for comparison, but it was noted that monohulls are generally longer for the same displacement and carrying capacity. This argument is developed further in Section 7, with practical examples in Figures 7.9 and 7.11. The increased length of an equivalent monohull necessary to offset their lack of deck area helps to offset the monohull form's higher wave heights by improving the slenderness ratio.

Slenderness ratio, defined as $L/\sqrt[3]{\nabla}$ and more colloquially referred to as *displacement-length ratio* (of which there are many variations of the formula; the numbers vary but the intent is the same), can give a simple indication of a vessel's wave wake intensity. Slenderness ratio has been demonstrated to be a primary determinant of high-speed wave wake height (Cox, 2000, among many), remembering it as a primary determinant of vessel wave drag. Slenderness ratios range from about *4* to *5* for small craft, up to *9* and above for lightweight river ferries. As vessel size increases, the slenderness ratio also creeps upwards (improves). That can best be explained by the argument of "*economies of scale*," or the ship design equivalent to the increase in system efficiency with increasing scale due to factors such as Reynolds number effects. As a simplified example, a *20 m*-long vessel with a *6 mm* aluminium bottom plate thickness scaled to *5 m* length would not have a scaled *1.5 mm* bottom plate thickness; it would be considered too light and too difficult to fabricate. The same scaling relationships can be developed for other weight parameters (machinery, fuel, passengers, outfitting, etc.). Bigger is almost always better.

Conversely, Froude scaling techniques from model to full scale dictate that wave period must be a function of $\sqrt{L}$. It is therefore obvious that longer vessels generate longer wave periods.[9] That then forms the dilemma that increasing length to improve the slenderness ratio and reduce wave height can also have the effect of increasing the commensurate wave period. Wave energy is a function of wave height and wavelength. In deep water, it devolves to become equally a function of wave height and period. The operational difficulty with skewing a vessel's wave energy from height towards period is that height decays with increased lateral separation but period does not. When the wave wake is generated super-critically in shallow water, reduced wave height can suppress the development of leading solitary waves in the super-critical wave, which is discussed further in Section 5. However, that is only delaying the inevitable, and whether that makes a service viable environmentally is highly dependent on the circumstances.

It may therefore seem contradictory that monohulls produce shorter wave periods (of the maximum wave) compared to catamarans of the same length, but that simplistic comparison ignores the effect of interference between the wave systems of a catamaran's demihulls. Catamarans may be the preferred passenger transport option with their demonstrable benefits of

---

[9] Assuming vessel speed is also scaled, so that period of the speed-dependent transverse wave system also increases. If speed is not scaled, the divergent waves still maintain a strong relationship to $\sqrt{L}$, even if the transverse system period is dependent only on speed. This is further discussed in Section 4.

increased deck area, stability and survivability, but they are not the only option, especially in developing countries where narrow monohull forms have practical local advantages. To be successful economically and environmentally, catamaran forms must be designed and constructed to lightweight standards to offset their (generally) increased structural area, and a poorly designed and constructed catamaran performs equally as inefficiently as a poorly constructed monohull. Moreover, developing countries may lack the technical capacity to build lightweight catamarans to the standard required to reduce environmental impacts. There is little point proposing expensive technology if the travelling public is unwilling or unable to pay the ticket price required for economic sustainability.

As will be shown, height and period affect the natural and built-up environment in different ways and sacrificing one for the other is not always a viable solution.


## 1.3     Wake Waves and Vessel Classes

The impacts of vessel wave wakes can be categorised broadly into three sectors of boating activity, with various sub-sectors:

*Recreational craft*:
a.  Small craft ($L < {\sim}6\ m$), usually trailerable. They may be used in specific roles (fishing, water skiing, jet skiing, and wake boarding, as examples) but often are multi-purpose, except that vessels used for jet skiing, wake boarding and wake surfing may have design and or equipment features specific to those sports;
b.  Large craft ($6\ m < L < 20\ m$), usually not trailerable, and with design features making them more suited to ocean passages and or having extensive live-aboard arrangements. They tend to have slenderness ratios similar to their small craft counterparts, with the additional displacement in the form of interior outfitting, inboard diesel engines, more complicated systems, and increased fuel capacity. Very large recreational craft ($L > 20\ m$) would be best considered as tourist vessels.

*Sheltered Waters Commercial vessels*:
a.  Slow speed vessels operating at $Fr_L < 0.5$ and most likely at $Fr_L < 0.4$, regarded as the displacement speed range;
b.  High-speed vessels operating at $Fr_L > 0.5$.

Within these two categories are three sub-categories of non-passenger vessels (work boats and commercial fishing vessels as examples), regulated passenger ferries, and tourist vessels. These vessels may or may not operate at depth super-critical speeds.

*Coastal ferries*:
Vessels having the same low and high-speed categories as sheltered waters commercial vessels but otherwise not delineated according to their ratio of passengers and vehicles. Their increased length can elicit shallow water effects, even when offshore.

Large ships in navigation channels are not considered in this study.

Recreational craft are easier to regulate because they are operated privately, and the activities are somewhat fragmented. They can be difficult to police because of their numbers and diffuse activities relative to enforcement resources. Direct government revenue from recreational

boating is small compared to the effort and resources necessary for licencing and policing. In a study of the economic impact of recreational boating in Virginia, USA (pop. *8.5 million*), Murray (2012) showed the contribution of state taxes and registration fees was only *1.7%* out of around *USD1.1B* total annual state-wide spending on recreational boating.

Wood *et al.* (2018) discuss the polarisation of voting patterns in Australia and the increasing numbers of single and small interest parties. That was evident in the 2019 NSW state elections, where the *Shooters Fishers and Farmers' (SFF) Party* gained an additional two seats in the Legislative Assembly (lower house) at the expense of the government, giving the SFF Party a coverage of around half the state's (largely regional, rural and remote) land area.[10] These boutique political parties give individuals undertaking fragmented, private pursuits an organised, political conduit through which to further their interests.

The wave wakes of many small recreational craft are sustainable with modest regulation, but those of ballasted vessels used for wakesurfing may not always be. The fragmentation of people's voting patterns and the rise in popularity of political interest groups has made it easier for a distortion of the science and public opinion. At least in their analysis, the wave wakes of small recreational craft respond well to simplified techniques using linear wave theory due to their higher h/L ratio and limited depth effects. The science is simpler; the politics less so.

Long vessels, which encompasses commercial passenger and tourist services, generate longer-period waves. At high speeds, divergent wave period is primarily a function of length and cannot easily be mitigated by design, as can wave height (Cox, 2000). Transverse wave period is a function of vessel speed, but the transverse system is depleted in shallow water or at a high speed in deep water. At slower (and depth sub-critical) speeds, the transverse system strength can be a cause of increased bank degradation where lateral separation and waterway width is restricted. In waterways restricted by depth and breadth, the long-period divergent waves cause damage to the built-up environment as much as the natural environment. They cause excessive wave runup that can scour beaches and seawalls. Longer period waves tend to cause onshore sediment transport, but where the sediment is entrained by the incoming wave and then the wave is reflected off a seawall, the sediment may be carried offshore and or in a longshore direction. In the case of Rich Passage, Washington State, it was noted that the long-period waves entrained the small diameter sediments between the gravel, causing the coarser material to become unstable (Golder Assoc., 2013).

Large coastal ferries have been mostly regulated using techniques of speed and course management, although there are still instances of wave wake issues reported (Soomere, 2007). They are not considered here, except that past incidents are better explained by the development of solitary wave components when operating super-critically in water considered to be very shallow for the vessel length, with accompanying high energy content as a percentage of the wave wake total. The past explanation has been that the leading deep-water waves were non-dispersive and therefore propagated with increased energy content. As will be discussed in Section 5, the "*non-dispersive*" description could be best regarded as highly over-simplistic, though there is truth in the statement of increased energy content. What has not been fully realised is the ability of high-speed vessels in very shallow water to generate leading solitary

---

[10] https://www.smh.com.au/nsw-election-2019/the-wunderkind-behind-the-rise-of-shooters-fishers-and-farmers-party-20190326-p517k6.html (last accessed 18th September, 2019). The article includes a photograph of Filip Despotoski, the SFF State Director, sitting next to an "*I fish and I vote*" poster.

waves at high depth super-critical speeds, and these waves can decouple from the wake and propagate independently at a depth super-critical celerity.

As has been noted in the literature, beachgoers and small craft operators have complained of large, often breaking waves arriving without any prior notice (Whittaker *et al*., 1999; Marine Accident Investigation Branch (MAIB), 2000; as examples), which would be a feature of decoupled solitary waves in very shallow water. Several fatalities caused by high-speed vessel wave wakes have been documented (Blunden, 2004). It is now commonplace in shoreside public areas in Europe for signage to warn of the potential dangers of waves from passing ships, though its usefulness is not guaranteed. It was noted in the investigation by Marine Accident Investigation Branch (MAIB) (2000) that the master of the affected vessel, who had held prior commercial seafaring certification, was unaware of a comprehensive public awareness campaign into the dangers of vessel wash undertaken some time before the described accident. Signage is necessary, but it may have limited effectiveness when the risks are not well defined and can be amplified by external factors (weather, tides and operator error, as examples).[11]

## 1.4     <u>Specific Environmental Impacts of Different Vessel Types</u>

### 1.4.1     Small recreational craft

Erosion is the primary problem, consisting of entrainment and offshore or longshore transport. Waves are modest but are longer and higher than the ambient climate. Banks with a scarp form predominate sheltered waterways whereas beaches are more limited in extent and are prone to accelerated erosion at their ends where the beach form changes to a scarp form. Undercutting of bank toes leads to instability. Changes in land use (removal of vegetation and changes to groundwater levels, for instance) and riparian vegetation depletion exacerbate the problem. There is much less of a problem with restricted channel effects (surge/drawdown). The effects on infrastructure, other vessels, beachgoers and surrounding residents would be best classed as a nuisance more than a threat to amenity or safety, though this nuisance factor has been known to initiate complaints of erosion (Macfarlane and Cox, 2003).

### 1.4.2     Large recreational craft

The modest or non-existent increase in slenderness ratio with increased size of recreational craft magnifies the wave wake problems of small craft. In addition, there may be increased impact on other waterway users from the steep waves (still dominated by height more than period) and fixed structures such as marinas.[12] Marina operators set speed limits, usually four knots, to minimise wakes within the marina environs, but that may not preclude waves from further beyond reaching the marina. In that case the more energetic, longer-period waves would be of concern, rather than shorter-period small craft wave wakes that would decay in height with distance.

Larger recreational craft use shaft propulsion almost exclusively, and the need to ensure sufficient channel depth for safe passage at speed helps to mitigate shallow water effects, including surge and drawdown.

---

[11] An example of the application and effectiveness of water safety signs in Australia, with legal case studies: https://www.royallifesaving.com.au/__data/assets/pdf_file/0014/4046/Water_Safety_Signs_-_Final_July_2008.pdf (last accessed 24th of September, 2019).
[12] The author has previously provided consultant wave wake and speed limit advice to the project engineers of a commercial marina development in Sydney Harbour. Speed limits provided a satisfactory solution.

### 1.4.3  Passenger vessels

Passenger ferries transiting at displacement speeds ($Fr_L < 0.399$) are only of concern when operating close to their displacement speed limit or into the depth trans-critical speed range ($Fr_h > 0.75$, assuming they cannot and do not operate into the depth super-critical speed range). Displacement speeds imply more traditional construction from steel and a design configuration more likely to be of monohull form, though not always. Catamarans operating at displacement speeds can experience notable constructive and destructive wave interference between demihulls (refer Lamb (2003): *Ch. 45 – Catamarans* (T. Armstrong), Fig. 45.17).

High-speed, "*low wash*," sheltered waters passenger ferries have, as their principal design feature, high slenderness ratios. The combination of long length and low displacement reduces wave height but with increased wave period. The long hulls reduce the effective *h/L* ratio, magnifying shallow water effects. Such vessels are known to cause excessive accretion of sediments in areas with beaches, caused by the long-period, low-height waves. Where seawalls are present, especially at the head of a beach or levee that may or may not be exposed at low water, incident waves are reflected and entrained sediment as well as newly entrained sediment at the toe of the seawall is reflected offshore, making an otherwise accretive process erosive. This erosion mechanism is discussed by Golder Associates (2013) in response to erosion in Rich Passage, Washington State.

Moreover, the long-period waves have a propensity to draw sediments from behind seawalls and cause sink holes. Seawalls not designed to be exposed to newly introduced incident wave parameters, mainly wave periods above ambient wind wave levels, may experience accelerated deterioration. That would be made worse by limited or no seawall maintenance.[13] The author's experience with waterfront property owners has been a reluctance to accept anything that may cause loss of land or reduction in property value. This is aggravated by the landowner's reluctance to accept that waterways are dynamic environments. Shorelines vary under natural processes, and anthropogenic intervention on both sides of the shoreline turns those natural processes into a constant aggravation. Vessel wash accelerates the otherwise natural processes as well as introducing new ones. The fact that the shoreline may have been several kilometres away *10,000* years ago means nothing when it's being monitored by an irate resident with a smartphone GPS.

In restricted channels where blockage becomes evident, speed would be limited by both depth effects and surge/drawdown. Even at depth sub-critical speeds, surge and drawdown can be intensive enough to destabilise scarp bank structures through the rapid variation in water pressure. Sediment is removed from the bank as the pressurised water flows laterally through natural fissures, eventually opening them up and causing large sections to slump. The only two operational remedies are to increase distance offshore and or reduce speed.

The need to meet tight service timetables increases the risk of exceeding wake-limiting speed and course conditions.[14] That becomes more so for commuter ferries where delays become cumulative when there are multiple stops. To make up time, operators have few options:

---

[13] As in "*I didn't build the seawall – I only bought the place!*" More rudimentary seawall and bulkhead construction on properties not regarded as *high-end real estate* may be barely adequate to protect against ambient conditions and natural processes, let alone the increased wave energy from passing vessels.

[14] An example of tight scheduling and subsequent complaints: https://www.brisbanetimes.com.au/national/queensland/maritime-union-believes-only-a-matter-of-time-before-serious-brisbane-ferry-crash-20170505-gvzfta.html (last accessed 19th September, 2019).

a. it may not be possible to increase the cruising speed between stops; commuter ferries operating long hours would use engines with commensurate duty ratings that may normally cruise at *90%* power, and the remaining available *10%* may give only a small increase in speed (around *5-10%* for a typical high-speed ferry normally operating at *80-90%* power, based on a typical commuter catamaran where installed power is proportional to $V^{2.3}$ approximately). For instance, increasing the transit speed from *25* to *27* knots reduces transit time by just *11* seconds per mile;

b. the vessel could accelerate faster, which is beneficial for reducing wave wake by limiting the transient effects that build up with slower acceleration. However, on the approach to a ferry terminus there may be the temptation to decelerate close to the jetty and quickly, which would bring the more damaging wake waves closer to the shore and infrastructure, as well as increase the risk of passenger injury (ashore and aboard) and collision with the jetty;[15]

c. the vessel could cut corners, risking increasing wave height by reducing lateral separation, or increasing energy of the leading waves by travelling super-critically in shallow water. Also, cutting corners implies cutting across the inside of a bend where wave wake energy is normally magnified anyway (conversely, energy is dispersed more widely on the outside of the bend). As with increasing already high speeds, cutting corners saves very little time.

Of these three options, only the first could be considered environmentally viable (in wave wake terms only) for a high-speed ferry. Wave wake height and energy tend to reduce with increased speed, provided the vessel is operating at higher length Froude numbers to begin with ($Fr_L > 0.5$, but preferably *0.6*) and water depth doesn't change. For that reason, the environmental impact of the wake waves at an already high speed should not worsen; however, engine emissions and economic viability would deteriorate. The only permanent solution is proper timetable scheduling and management.

### 1.4.4    Tourist vessels

Unlike passenger vessels that are bound by a timetable, tourist services are more flexible in their speed and route. Regulation of wave wake could be regarded as a simple process and undertaken as part of the normal vessel certification process. What is almost always lacking is a statutory requirement to undertake a route assessment before a vessel is introduced in service. The Gordon River services in Tasmania are examples of where high-speed tourist services in a sensitive riverine environment were curtailed and are now regulated (Cox and Macfarlane, 2019). Speeds are slow (in the order of five knots) to comply with threshold wave height and energy criteria established for the route. After initial resistance to regulation in the early 1990s, management has proved successful and the operators continue to grow their business with the steady introduction of purpose-built vessels.

Wave types, vessel types and their likely wave wake impacts are summarised in *Tables 1.1* and *1.2*.

---

[15] Ferry crashes are surprisingly common. Apart from excessive approach speed, modern electronic control systems have a habit of failing without warning. Their default failure mode is to return to an idle condition but that only reduces impact severity. https://www.theguardian.com/world/2013/jan/09/new-york-ferry-crash-50-injured and https://www.smh.com.au/national/we-were-going-too-bloody-fast-ferry-passenger-20050527-gdleey.html (last accessed 3rd October, 2019).

**Table 1.1** – *Parameterisation of vessel operations and effects on the environment.*

| Vessel type | Wake Parameters | | Operational Parameters | | | | Wave Wake and Operational Impacts | | | | | |
|---|---|---|---|---|---|---|---|---|---|---|---|---|
| | Wave type | h/L at generation | Route | Timetable | Regulation | Policing | Erosion | Surge and drawdown | Jetties and seawalls | Other small craft | Beachgoers | Noise |
| Recreational small | Deep | > 0.5 | Variable | Variable | Some | Difficult | Yes | No | Minor | Minor | No | Yes |
| Recreational large | Deep, trans, shallow | > 0.2 | Variable | Variable | Some | Some | Yes | Some | Some | Some[4] | Minor | Some |
| Passenger slow[7] | Deep to very shallow | > 0.075 | Fixed | Fixed | Yes | Yes | Some | Yes | Some | Some[4] | No | No |
| Passenger fast | Deep, trans, shallow | > 0.15 | Fixed | Fixed | Yes | Yes | Yes | Yes | Yes | Minor | Minor | No |
| Tourist slow | Deep to very shallow | > 0.075 | Partially fixed | Partially variable | Yes | Yes | Some | Yes | Some | Some[4] | No | No[2] |
| Tourist fast | Deep, trans, shallow | > 0.15 | Partially fixed | Partially variable | Yes | Yes | Yes | Yes | Yes | Some | Minor | No |
| Coastal slow[6] | Deep to very shallow | > 0.075[8] | Mostly fixed[1] | Fixed[3] | High | Yes | Some | Yes | Yes | Some[4] | Minor | No |
| Coastal fast[6] | Trans, very shallow | > 0.075 | Mostly fixed[1] | Fixed[3] | High | Yes | Some | Yes | Yes | Yes[5] | Yes | No |

1. Some variation may be possible in nearshore areas to mitigate wake effects.
2. Excluding party vessels.
3. But with some flexibility for weather, port traffic, etc.
4. Steep waves in deeper water.
5. Shoaling waves in very shallow water.
6. "Coastal" excludes large ferries transiting through restricted waters, regardless of depth.
7. Slow speeds allow for safe transit of very shallow and narrow areas, which may result in all wave types as well as surge effects.
8. Generally determined by draft/depth ratio and minimum under-keel clearance.

**Table 1.2** – *Wave type definition*

| Wave Definition | Water depth to vessel length ratio | Wave Appearance (refer Section 5, Figure 5.2 for a graphical description) |
|---|---|---|
| Deep | $h/L > 0.5$ | Wakes propagate with a deep-water form, with a more temporally symmetric packet envelope |
| Transition | $0.28 < h/L \leq 0.5$ | The leading waves become increasingly more prominent; packet envelope becomes asymmetric |
| Shallow | $0.15 \leq h/L \leq 0.28$ | The leading wave(s) dominates in size and energy content |
| Very shallow | $h/L < 0.15$ | With low slenderness ratio at super-critical speeds, the leading wave can have a solitary wave form if shallow enough |

### 1.5    Community and Environment

### 1.5.1    History

The earliest available record of the effect of vessel waves on shorelines was made by John Scott Russell around 1840 and recounted in detail by Kelvin (1887, p.471-473):[16]

> *"A spirited horse in the boat of William Houston, Esq., one of the proprietors of the works, took fright and ran off dragging the boat with it, and it was then observed, to Mr. Houston's astonishment, that the foaming stem surge which used to devastate the banks had ceased, and the vessel was carried on through water comparatively smooth with a resistance very greatly diminished."*

That led to the introduction of "fly boats" in Scotland, which were long, narrow boats (quoted as *60 feet* by *6 feet*) designed to be pulled by horses in very shallow canals at depth super-critical speeds (up to *9 mph*) where the resistance was greatly reduced. It must be said that the term "*devastate the banks*" may have meant *inundate the banks* in the language of the time; the canals were man made and their health was an economic concern, not an environmental one.

It is still quite uncommon even now for students of naval architecture to be lectured in detail about how their designs interact with the community and the environment. Boats do not exist in isolation and they do not float as an island on an endless sea. Waterways are a unique part of the landscape in that they are state owned and not privately owned, even if they pass through wholly privately-owned land. State ownership and control have long been recognised as necessary for the preservation of what could be best described as *communal commonwealth*.

It is important to understand waterway usage and how that concords/clashes with community aspirations and prejudices. Four examples are given, covering the landowner, regulator, researcher and vessel designer.

### 1.5.2    Landowners – Taylor (2013, p.131)

An example of the subtle contradictions (and subtle hypocrisy) of those who live with and complain about shoreline erosion is given by Taylor in "*A piece of paradise.*" It tells the story of Peter Bury and his life living on the Gippsland Lakes in south-eastern Victoria. Peter moved there as a young child, when his father gave up his job in Melbourne to move to the Gippsland Lakes and start a market garden business supplying fresh produce by railway to Melbourne.

Peter eventually started a business in the area and built a small slipway to service the local fishing and recreational vessel fleet. Some of his relevant observations include:

  a.  the decline in the ribbon weed beds since the early 1900s - the ribbon weed having grown "*over four feet high and out to a depth of ten feet*;"
  b.  the final decimation of the ribbon weed beds by a plague of millions of crabs in the late 1920s;
  c.  increased shoreline erosion at the time, caused by a gradual decrease in the reed swamps;

---

[16] Kelvin did not explicitly state which of Scott Russell's publications discussed the event, though mention was made of: Russell J.S. (1840). Experimental Researches into the Laws of Certain Hydrodynamical Phenomena. *Edin. Roy Soc Trans XIV*. 47-109 + plates I and III.

d.  rehabilitation attempts several decades ago by planting an imported wheatgrass. This was successful, except where eaten out by the large kangaroo population;

e.  an increase in salinity causing shoreline erosion, as well as other contributing factors such as land clearing and animal grazing.

He identifies "*the frequency and intensity of wash from passing motorboats*" as a significant contribution to erosion, though more recent by his own account, claiming "*they are always in such a bloody hurry when they go past.*" In his haste to lay blame on the passing vessel traffic, he forgets that:

a.  his father, having cleared the land for farming, contributed to degradation of the lakes by creating potential run-off and fertilizer leaching, and removing deep-rooted trees in favour of shallow-rooted crops allowed the water table to rise and salinity to increase;

b.  the slipway he built and operated would have required the removal of shoreline vegetation, as well as potentially contaminating the waterway with TBT and copper-based antifouling compounds;

c.  local land clearing, cattle grazing, and pasture cultivation allowed the kangaroo population to breed beyond a stable number, which then feeds on the shoreline vegetation when food becomes scarce;

d.  his livelihood potentially depends on the local vessel fleet.

It has become customary for those private landowners to, in effect, "*reset the clock*" from the time of their inhabiting the foreshore, and they regard past changes to the landscape as being not their concern. The fact that Peter can identify major erosion events long before boating became popular demonstrates how dynamic the shoreline is and how sensitive it can be to environmental change - even those changes regarded as indirect. That's not to say that Peter is the main cause or the only cause of ongoing erosion. He is not. But, similarly, the boating community may not be the primary source of erosion – just one of the sources that accelerates the degradation of an already stressed system. In fairness to Peter, who himself is a boatowner, he just wants them to slow down and not to be banned completely. There is always a regulatory middle path of compromise.

### 1.5.3    Regulators – Macfarlane and Cox (2003, 2005)

Between 2002 and 2004 site visits and field experiments were conducted on several rivers in S.E. Queensland by AMC Search Ltd. where erosion had been reported. These followed on from similar work on the Noosa and Brisbane Rivers in 2002. Extensive discussions with government officers formed part of that consultation process. Some are reported in Macfarlane and Cox (2003, 2005), but much of it was not reported at the time because of community sensitivity and the need to remain impartial. The discussion following is to be regarded as anecdotal.

*Mary River*

A barrage and associated irrigation works were constructed on the lower Mary River around *30* years ago. As with many Queensland rivers, flows were erratic and seasonal, varying from low flow conditions to floods. The barrage provided a consistent volume of water for nearby agricultural, horticultural and industrial use.[17] The need for the barrage to provide consistent levels for water extraction implies that water levels, excluding flood events, were previously lower, though the barrage itself is not high (estimated visually at around *3 m*).

---

[17] https://www.sunwater.com.au/schemes/lower-mary-river/ (last accessed 1st October, 2019).

Several sites upstream of the barrage had been identified where bank slippage and collapse had occurred. During the site visit, government officers provided anecdotes of their experiences and interactions with interested parties using the river:

a. water skiing and wakeboarding were the primary recreational boating activities but were limited to weekends/holidays and with limited numbers;
b. in some places where bank slumping was evident, the (high) banks were mostly denuded of vegetation. The land beyond was used for agriculture (primarily sugar cane and cattle);
c. slippage was evident on the very high banks to the east, but it was several metres above the water level (which was at the barrage level at the time) and well beyond the reach of vessel wakes;
d. cattle were seen grazing on the steeper banks. Apart from stripping the vegetation, they destabilise the bank structure.

It was concluded that although vessel wash may have been accelerating erosion in some places, the great majority was cause by land use issues and floods. During the 2011 floods, water in the Mary River rose to *20 m* above its normal level in places and even at the downstream end at Maryborough had risen more than *8 m*.[18] As catchment officer, Steve Burgess, explained: "*There are a lot of unstable places along the Mary, some of that is natural and some of that is the result of past activities and losing vegetation off the banks*."[19] Past activities in this case refer to gold mining, logging and agriculture, not recreational boating. The banks are known to be porous due to a predominance of sandy substrates.[20] Flood events are the single greatest cause of primary erosion. Recreational boating almost always does nothing more than aggravate an existing paradigm.

*Maroochy River*
As with the Mary River, the upper reaches of the Maroochy River pass through areas of intensive sugar cane cultivation, which in places has seen vegetation removed all the way to the river. At the time of inspection, a small number of residents used the river for water skiing, with numbers increasing somewhat during the holiday months. The sandy bank structure, largely denuded of vegetation, exhibited slippage and erosion in places. The banks could somewhat protect themselves against aggressive toe undercut by forming beaches from the slumped material, but this was complicated by the tidal range of the river (and therefore variable water level relative to the bank toe), and occasional flooding that scoured the river and any temporary, self-remediating features.

Local landowners blamed the water skiers for the erosion yet could not accept any blame themselves. It was pointed out that clearing the previously heavily wooded land and planting a shallow-rooted crop allowed the water table to rise, which destabilised the banks from the land side. As with residential waterfront landowners, the response was familiar: "*I didn't clear the land – I just bought the place.*"

[18] https://en.wikipedia.org/wiki/Mary_River_(Queensland) (last accessed 1st October, 2019)
[19] "Mary River battered by flood waters," ABC News Wide Bay, 26th January, 2011: https://www.abc.net.au/local/stories/2011/01/26/3122079.htm (last accessed 1st October, 2019).
[20] https://www.abc.net.au/news/2006-06-14/expert-raises-mary-river-dam-leakage-fears/1777430 (last accessed 2nd October, 2019)

### 1.5.4 Wave wake research community – Doctors *et al.* (2001, p.102)

The following quote has been selected as an example of the disconnect between vessel wave wake research and the effect it ultimately has on the community it serves. The authors are well regarded in the field for their successes in wave height amelioration through design.

Doctors *et al.* make a somewhat peculiar concluding observation:

> "*It should be added parenthetically here that the public frequently complains about the wave system generated by river vessels only when they travel at high speeds. This is despite the fact that the maximal wave heights are generally no higher at such speeds. Perhaps the answer to this riddle lies partly in the fact that the percentage of the wave system that can be associated with the divergent waves is greater.*"

It has been known since the $19^{th}$ century that the transverse wave system cannot be generated at depth super-critical speeds (Kelvin, 1887), and it has also been remarked that the transverse system becomes depleted at high speeds in deep water ($Fr_L > \sim 1$; refer Section 4). In almost all circumstances, high-speed river vessels would comply with one or both conditions that can negate the transverse system, and therefore the dominance of the divergent wave system would be absolute!

In the same paper, the authors dismissed the more intense transverse wave system of multihull vessels as being of lesser consequence for shoreline erosion compared to the divergent system (p.101, Sect. 5.1). That is not necessarily correct. Hill *et al.* (2002) describe the mechanics of transverse wave erosion in waterways restricted by width.

The peculiarity is this: acknowledging that wave height, which does not necessarily increase at high speeds in sheltered waters and can be manipulated by design, does not seem to correlate with the public's vociferous concerns, why didn't the authors investigate other wave parameters as possible causes of the consistently negative public response? Perhaps the answer to this riddle is *wave period*, which was not discussed at all by the authors and has never enjoyed the status and attention attributed to the more simplistic and visual wave parameter – *wave height*. Wave wake is a complex problem that cannot be solved in isolation.

### 1.5.5 Vessel designers – Conway (2019, p.32-35)

Conway provides an example of the continuing misinformation about what constitutes a *low wash* ferry. More disconcerting is that this example is of misinformation at the point where young engineers are learning and applying the science for the benefit of the community. The article reports on a (university) student design competition that forms part of the annual conference of the *Worldwide Ferry Safety Association* (WFSA). The 2019 competition theme was to design a ferry suitable for the Pasig River in Manila, the Philippines. Quite besides problems of waterway pollution and a travelling public unable to support the capital and operating costs of an advanced vessel design, the Pasig River is narrow at around *50 m* average width and shallow at around *4-6 m* average depth.[21]

The winning student design had a waterline length of *20 m*, lightship displacement of *25 t* (and a full load displacement of *36.1 t* based on the stated capacities, excluding the ballast system

---

[21] Murphy, D. and Anana, T. (2015). Pasig River Rehabilitation Program. Habitat International Coalition, http://www.hic-net.org/articles.php?pid=3362 (last accessed 28th August, 2019).

proposed as a solution for enabling passage under low bridges), and a service speed of *13 kn*. There are four points to be made:

a. the article states that: "*Designed to carry 100 passengers, M/V Pasig Express would incorporate a catamaran hullform to meet the low-wake requirement.*" It is quite likely that a catamaran design would be the most appropriate from the perspectives of stability and comfort (but definitely not for air draft and bridge clearance – passengers must be seated *above* a catamaran's hulls, not *in* them!), but the unsupported, generalised assumption that a catamaran form signifies an inherently low-wash vessel is incorrect (Cox, 2000). That is especially true in second and third-world countries where high-speed monohull river ferries are most common, largely because history and culture, and their innate design, construction and powering simplicity (refer Section 7, Figure 7.11);

b. the vessel's slenderness ratio at full load is about *6.1*, which compares to the Sydney Harbour Rivercat at *9.0* and the Brisbane River CityCat at about *8.0* (depending on the variant). The full-load displacement of the proposed design would have to be reduced by around *57%* to achieve the same slenderness ratio as the CityCat, which would be impossible. Alternatively, the waterline length of the proposed vessel could be increased to *26 m* to achieve the same slenderness ratio, but at the same time carrying *62* fewer passengers than the (second generation) CityCat and not accounting for the increased structural weight of the *6 m* longer hulls;

c. the length Froude number at the service speed would be *0.48*, which is at the worst specific resistance condition for a vessel (refer Figure 4.2 following). Moreover, low-to-medium speed catamarans are known to experience wave interference (positive and negative) that is strongly dependent on hull spacing and length Froude number [Lamb (2003): *Ch. 45 – Catamarans* (T. Armstrong), Fig. 45.17];

d. the depth Froude number at the service speed for the published average river depths would be in the range of $0.87 \leq Fr_h \leq 1.07$, which is around the depth-critical speed.

The last two points meet the criterion for the worst combination of depth and length Froude numbers (where $Fr_L = 0.5$ and $Fr_h = 1.0$), which occurs when $h = 0.25L$. The proposed design's $h/L$ ratio of *0.2* to *0.3* would be sufficiently shallow to be of concern (refer Section 5, Figure 5.18). Unfortunately, none of this was raised in the design analysis and instead the design was awarded first prize. After almost three decades of intense study and countless published papers on wave wake and its mitigation, little of it filters through to the next generation of designers and regulators.

# Section 2 – Literature Review

*If, with the literate, I am*
*Impelled to try an epigram,*
*I never seek to take the credit;*
*We all assume that Oscar said it.*

*Dorothy Parker*
*Life* Magazine, June 2, 1927

## 2.1    Introduction

Dorothy Parker's dictum, along with that of Richard Feynman in Section 4, reflect on how we describe wave wakes and the attendant dangers of engrained beliefs and facile generalisations. Although we are constantly immersed in waves of all forms (electromagnetic, light and sound, as if they are not enough) water waves are the only visible examples accessible to us that display their physical properties. Explanation is invariably accompanied by many of these generalisations, often conveyed with a wave of the hand to signify a clarity that requires no further explanation, when further explanation is *exactly* what is needed.

Similarly, we are all guilty of cherry-picking quotes that suit our narrative. This is no more evident than in the referencing of technical papers, where what might otherwise be considered as questionable becomes fact if repeated often enough. We absolve ourselves by only stating "so-and-so said", rather than "so-and-so said, and I agree." Agreement is implied by association and the failure to refute when it isn't advantageous to do so.

In past work in this field, the author was involved with several literature reviews within commercial documents released into the public domain (not formally published as such), as well as published papers on the subject. A good example is *Section 3* of Macfarlane and Cox (2003). Rather than continue with that traditional form of literature review, which often looks like little more than abstract summaries, a novel approach is presented.

Over the past thirty years there have always been three principal areas of wave wake investigation: recreational craft in sheltered waterways; commercial vessels (mainly commuter and tourist vessels) in sheltered waterways; large, high-speed ferries on coastal routes. Since the last major literature review prepared in 2003, many reports on wave wake and shoreline impacts have been published, but mostly on recreational craft. Nine of those reports were selected and critiqued in detail, rather than simply reviewing the themes and outcomes of each. Of the nine, eight are from the USA.

A common theme that has emerged is an effort to quantify erosion rates rather than only qualify them. So far, the results have remained site and vessel specific. Moreover, the understanding of vessel wave wake remains stagnant; stuck in the 1990's belief that wave height is the principal indicator of erosion potential. Other parameters such as wave period, energy and power are acknowledged, then largely forgotten. Where they are applied, their interpretation is poor.

Similarly, the science of vessel dynamics is poorly understood. All but one report (Bruno *et al.*, 2002) were completed by researchers with coastal engineering (or related) backgrounds, not with expertise in ship design. Maynord's 2005 study on vessel dynamics and wave wake is continually cited, even though it is substantially flawed.

**2.2   Summary of Reviewed References** (See Appendix A for full reviews)

**2.2.1   Bauer *et al*. (2002)** *- Estimating Boat-wake-induced levee erosion using sediment suspension measurements.*

This was by far the most useful and considered of the papers reviewed. The authors measured the wave wake and subsequent turbidity generated by a recreational vessel in a river. Additionally, experiments quantifying loss of sediment after multiple (i.e., up to *1,000*) vessel passes were conducted. Wave height was the principal focus and that provided a conundrum that was not addressed – that waves of the same height could create vastly different turbidity. The development of the turbidity and wave height relationship was most notable.

The authors made little attempt to quantify wake parameters in terms of vessel parameters. Whether that was deliberate or not is unclear, but it was favourable to the outcome in that questionable relationships were avoided. Consequently, none of the findings could be employed elsewhere, except as guidelines, though the paper must rank as a mandatory starting point for researchers in this field.

**2.2.2   Bruno *et al*. (2002)** *- Field and Laboratory Investigation of High-Speed Ferry Wake Impacts in New York Harbor.*

The premise of this investigation was the growth in high-speed passenger ferry traffic in the New York area and its impacts on shorelines and marinas/structures. Many shorelines away from the CBD and towards residential boroughs serviced by the ferries are not armoured.

The study was divided into two parts: field observations of existing vessels and model testing. The authors claim a degree of validation between the two, though provide no explanation of how this was achieved, considering the lack of any correlation between measurement techniques. The best that could be said is that waves were measured in both instances, but without the degree of standardisation of test procedures required for comparison.

As with many similar papers, the importance of wave period was stated at the outset, discussed in general and then generally disregarded in favour of discussion of wave height alone. The paper, as part of a larger study on behalf of the New Jersey Office of Maritime Resources, was of sufficient public interest to receive coverage in the print media.[22] Most surprising was the poor understanding of vessel dynamics – coming from an institution with a long history in this field.

**2.2.3   Hill *et al*. (2002)** *- Hydrodynamic Impacts of Commercial Jet-Boating on the Chilkat River, Alaska.*

The Chilkat River in Alaska is used principally by tourism operators and government vessels, with fewer recreational users. The tourism operators use open, flat-bottomed vessels of lengths around *6-10 m* carrying up to thirty passengers. They are propelled by jet outboards – a variation

---

[22] New York Times August 12, 2002*: Batten Down the Hatches! Commuters Ahoy!; Ferries Crowd the Hudson These Days, and There's No Speed Limit,* https://www.nytimes.com/2002/08/12/nyregion/batten-down-hatches-commuters-ahoy-ferries-crowd-hudson-these-days-there-s-no.html (last accessed 2nd May, 2019).

An interesting report related to this, written by a group of concerned marina owners, can be accessed at: http://www.iboatnyharbor.com/SLOW%20White%20Paper.pdf (last accessed 2nd May 2019).

of a normal outboard motor that has a pump unit rather than a propeller. The government vessels are smaller and lighter, but of similar form.

The authors are from the Department of Civil and Environmental Engineering at the Pennsylvania State University. Their understanding of the shoreline dynamics unfortunately exceeded their understanding of vessel wave wakes. No distinction was made between deep and shallow water wakes, except that critical speed zones based on length and depth Froude numbers were correctly identified. A most notable source of inconsistency was the variation in water depths at the sailing line and measurement points.

### 2.2.4    Maynord (2005) - *Wave height from planing and semi-planing small boats.*

Many wave wake experiments were conducted on several small craft to develop relationships between vessel parameters and the maximum wave height generated. Maynord was a noted researcher with the US Army Corp of Engineers in the field of erosion control, but not in the field of vessel dynamics. The techniques developed were a reasonable first attempt, but they were found to be lacking technically. For instance, the equations developed do not scale, even though a scaled example was within the stated limits of applicability.

As with many of these studies, wave period did not share equal status with wave height and was not developed as a primary wave wake parameter. Maynord's equations, though flawed, have become entrenched within the science.

### 2.2.5    Baldwin (2008) - *Impacts of Recreational Boating on River Bank Stability: Wake Characteristics of Powered Vessels.*

This report was commissioned by the Murray Catchment Management Authority to estimate the erosion potential of recreational vessel wave wakes on the Murray River. The author employed wave gauges at known boating sites to measure incidental wakes. Estimates were made of the erosion attributable to recreational vessels compared to existing riverine processes.

The report is unsound on several levels. Vessel dynamics are not understood at all and there are fundamental errors of judgement. Vessel wake energy was compared to wind wave and streamflow energy, with the conclusion that recreational vessels increased the total system energy by only *2%* to *5%*. Baldwin's use of energy density as the comparative measure was an incorrect approach because energy density ignores the effect of wavelength.

Consequently, this flawed report has been used by interest groups to justify the continued use of the Murray River for recreational boating without restrictions. As claimed by Brett Butler, owner of the Bundalong Tavern: [23]

> *"There is hard evidence that it is the flow of the river and floods that cause up to 95 per cent of the erosion and only 2 to 5 per cent is caused by boat wash."*

---

[23] As an example of many – *Murray River wakeboarding ban proposal blasted*:
https://www.weeklytimesnow.com.au/country-living/murray-river-wakeboarding-ban-proposal-blasted/news-story/e9c191fba546e18b1d89008b48531aef  (last accessed 24th June, 2019).

Those numbers were drawn directly from Baldwin's study and have been misrepresented in the statement. The evidence is neither "*hard*" nor correct.

### 2.2.6 Maynord *et al.* (2008) - *Boat-wave-induced bank erosion on the Kenai River, Alaska.*

The study was initiated by the local Kenaitze Indian tribe, who had concerns about bank erosion. Since the 1970s, the river has been a popular recreational salmon fishing area and lower parts of the river have experienced an increase in the permanent population, many of whom chose to live along the river. During the study, several hundred recreational boats were witnessed along the river per day during the peak fishing season. Most vessels were small open boats around *5 m* to *6 m* overall, often flat-bottomed and with a statutory engine power limit of *35 hp* (*26 kW*). The usual modus operandi was to run upstream at speed and drift fish downstream. The amount of vessel traffic led to considerable variations in speed and shoreline separation.

Apart from relatively high natural flow rates, the river is also subjected to occasional flooding. Flooding was identified as being the principal contributor to erosion and there was sufficient anecdotal evidence of this, not the least being that major erosive events were recorded outside of the recreational fishing season.

Once consideration not offered in the study is that the reason for the focus on boat wash may not only have been a concern about erosion, but also a concern about loss of amenity. The local indigenous population may have felt displaced by the population growth and the uncontrolled harvesting of a natural resource it utilised for food rather than entertainment, so sought to control this. It would be difficult in the US to control recreational fishing where the resource was not necessarily under threat and where there is an implied right to this activity in its laws and culture. Indirect control of the activity through environmental regulation may have been the better option.

### 2.2.7 Fonseca and Malhotra (2012) - *Boat wakes and their influence on erosion in the Atlantic Intracoastal Waterway, North Carolina*.

The subject of this report was Snow's Cut, a man-made canal joining the Intracoastal Waterway to the Cape Fear River. The canal had been planned since the early 1800s but was not completed until the 1930s. Erosion has been ongoing since the time of its construction. Constant bank instability, siltation and dredging has expedited remedial action.

The report used two sophisticated simulation methods that model wind wave and boat wave bottom shear stresses. These simulation methods use a GIS topographical model of the waterway in the wave transformation process. Based on logged information of passing vessels, two vessels were modelled: a *7 m* centre console and a *16.4 m* motor yacht. It was found that the smaller vessel exceeded the highest wind waves occasionally, but the larger vessel exceeded the highest wind waves by a substantial amount, except at the slowest speed.

There is a high reliance on past work that may be erroneous. The vessel wake model uses a wave height predictor from Sorenson (1967) for displacement hulls and a modified USACE model for planing hulls, assumed to be from Maynord (2005). Sorenson's model is quite old and from the very beginnings of wave wake understanding. Maynord's model has shortcomings and does not translate well beyond those vessels used to derive the relationships. Neither method appears to

have been published with an accompanying wave period prediction method, so it is unclear how the vessel wake model managed to achieve this.

As with other similar studies, the authors lack experience and credentials in vessel dynamics (one is an ecologist and one is a civil engineer).

### 2.2.8    Ozeren *et al*. (2016) - *Boat-Generated Wave and Turbidity Measurements: Connecticut River.*

A series of tests were conducted on the Connecticut River in New Hampshire and Massachusetts to determine correlation between wave wake parameters and measured erosion. The paper does not state if any active erosion on the river due to vessel wash had precipitated the study. The trials programme used a single recreational vessel to generate a wake. The principal wave parameters and subsequent turbidity were recorded. Data were collected in two ways. Firstly, data logging and cameras captured incidental wakes over a four-month period. This was discussed briefly but results were not reported at all. Secondly, controlled experiments were conducted at one site, measuring the waves and the subsequent turbidity caused.

This is possibly the best example of poor-quality research and analysis. Vessel dynamics were misrepresented, and the experiments were conducted in a poorly controlled manner. Wave height became the only wake parameter reported, even though wave period was mentioned as being of consequence. The conclusions of the report directly contradict the graphed data. Nothing of any value can be concluded.

### 2.2.9    Bilkovik *et al*. (2017) - *Review of boat wake wave impacts on shoreline erosion and potential solutions for the Chesapeake Bay*.

The report was instigated by the Chesapeake Bay Commission (CBC), which engaged the Scientific and Technical Advisory Committee (STAC) of the Chesapeake Bay Program (CBP) to study and report on the impacts of boat-generated waves and potential policy options. In general, the report relies heavily on past wave wake studies, many with questionable science, that have become self-perpetuating on the scientific literature merry-go-round. The report does, however, excel in the application of abbreviations and acronyms.

The scientific panel was extensive, with nine contributors, four external reviewers, and nine others providing some degree of assistance, yet none of those were listed with experience in naval architecture or related fields. This is a common thread in many similar reports, where assumptions are made and comments are given but without adequate academic background to either make informed statements or critically analyse referenced papers. It is *science by committee*.

## Section 3 – Waves

*Truth never triumphs—its opponents just die out;*
*or - Science advances one funeral at a time.*

*Max Planck*[24]

---

## Summary

Our understanding of how waves are interpreted needs to be modified. Although the concept of wave height decay is well known (though not well understood), what we might call a wave only exists in its measured form at one point in space and time. It is convenient to track a wave as it propagates, but that ignores the fact that it's not the same wave at every location. When viewed as one of a packet of waves, a wave viewed at one point in space and time evolves into another as the packet propagates: the packet widens and flattens due to dispersion, leading to an increase in the number of visible waves, each with constantly changing height *and* period.

The exception to this is the wave that exists at the packet envelope's maximum amplitude, which will have a constant wave period defined by the packet's group velocity. That wave is what we know as the maximum wave, or the highest wave in a propagating wave wake. Its traditional use at the single defining wave in a wake was almost certainly because of the preoccupation with wave height, but with the added benefit of a constant period. The relationships between the maximum wave, the propagating packet and the wave wake in general, have never really been explored properly in wave wake science.

Similarly, the weakening rate of dispersion of shallow water wave wakes is often misrepresented. The varying frequencies found in a shallow water wave wake packet mean that only part of the very first crest approaches a state of non-dispersion and not the whole first or several leading waves as has been claimed. The waves do disperse and transform into new waves within the packet as it propagates; slowly at the head of the packet where dispersion is weak but faster at the tail of the packet where the short waves are unaffected by depth and dispersion is strong.

Wave wakes are comprised of multiple wave packets that cause interference. Numerical examples are given to demonstrate how our understanding and quantification of wave wakes can be unduly affected by packet interference. Caution when interpreting wave wake records is required to avoid misrepresentation.

---

[24] The paraphrased version of: *A new scientific **truth** does not triumph by convincing its opponents and making them see the light, but rather because its opponents eventually die, and a new generation grows up that is familiar with it.*

Planck, M. (1948): Wissenschaftliche Selbstbiographie - Mit einem Bildnis und der von Max von Laue gehaltenen Traueransprache, Johann Ambrosius Barth Verlag (Leipzig), p. 22, as translated in: Scientific Autobiography and Other Papers, trans. F. Gaynor (New York, 1949), pp. 33-34.

## 3.1     Introduction

A different way of looking at wake waves is explained, rather than perpetuating the descriptions that are often little more than convenient. Some of this discussion might be regarded as too simple for a study such as this, but too often problems arise either because of the lack of a foundational philosophy to empirical measurements or the transition straight to a second-order partial derivative as if it were the basis for a rational explanation. There is a chasm between the science and its explanation to the general public.

Except for solitary waves (which are not periodic by nature), there is no such thing as a single, periodic, monochromatic (constant period) water wave. The existence of such a wave would require a singularity at its beginning and end. If (what appears as) a monochromatic wave existed in nature, it would require a small, superimposed group of waves of various frequencies to lead into and out of the monochromatic wave. Similarly, a train of pure monochromatic water waves cannot exist without additional frequencies to form the wave train's development to and from a steady-state condition.[25]  Kelvin (1887) recognised this.[26] In doing so, the waves can no longer be considered as monochromatic, since the apparently pure, monochromatic wave train would be contaminated with additional frequencies. They can be described mathematically, but only with the assumption that they have always existed and will always exist in a steady-state condition, which is convenient but unrealistic.

Similar examples can be found in flume tank experiments on waves assumed to be monochromatic. Such an experiment was reported by Newman (1977, Fig. 6.10) to explain the concept of group celerity. That is reproduced here as *Figure 3.1*. Although the wavemaker was programmed to produce monochromatic waves, it must produce multiple frequencies during its acceleration and deceleration, and it is these that give the packet its dispersive packet nature. Within the error of measuring (and Newman's annotated interpretation of the beginning and end of the packet), there is no discernible packet lengthening. The image is descriptive for demonstrating group celerity, though a packet of waves with varying frequencies would have been more descriptive of dispersion (refer to Figure 3.11 following).

In a dispersive medium such as water, waves only exist in groups, or packets. At times they may appear to be random, but random seas are only made up of many superimposed wave packets. That's where the problem of description begins. A group of waves is comprised of multiple frequencies. The lower frequencies travel faster, and the higher frequencies travel slower due to the dispersion relationship, even in shallow water. That causes the packet to stretch; the faster waves travelling ahead and the shorter waves falling behind. The packet length in deep water increases linearly with respect to time.

---

[25] Though transverse waves appear to come close, as discussed in Section 4.

[26] Refer to discussion on pages 462-466 of Kelvin (1887) on the development and maintenance of the transverse wave system, even if assumed to have existed for a long time. As Kelvin noted, even an apparently monochromatic, steady-state transverse wave system must have formed initially from shorter waves generated during the acceleration phase. Kelvin's 1887 lecture is quite unique as a foundational reference in that it is almost wholly narrative.

24

6.10

Sequence of photographs showing a plane progressive wave system advancing into calm water. The water is darkened with dye, and the lower half of the water depth is not shown. The wave energy is contained within the heavy diagonal lines, and propagates with the group velocity. (The boundaries of the wave group diffuse slowly with time, due to dispersion.) The position of one wave crest is connected in successive photographs by the light line, which advances with the phase velocity. Each wave crest moves with the phase velocity, equal to twice the group velocity of the boundaries. Thus each wave crest vanishes at the front end and, after the wavemaker is turned off, arises from calm water at the back. The interval between successive photographs is 0.25 s and the wave period is 0.36 s. The wavelength is 0.23 m and the water depth is 0.11 m.

**Figure 3.1** – *Fig. 6.10 of Newman (1977). The red-annotated sentence is discussed. In a sense it is a poor description of dispersion; the waves are implied as being monochromatic (wave period 0.36 s; wavelength 0.23 m), yet dispersion is a statement of the celerity/frequency relationship of waves and a dispersive group must contain waves of different wavelengths. The waves shown are dispersive - they are not purely monochromatic because of the acceleration/deceleration of the wavemaker. Water is a dispersive medium – purely monochromatic waves cannot exist. It is an unfortunate example of "wave-of-the-hand" explanations of wave mechanics that creates as much confusion as clarification.*

However, in doing so, the apparent number of waves within the packet increases with time. That phenomenon becomes critical to understanding how wake waves propagate. We make the simplification that waves can be viewed and measured discretely. This suits our view of the world around us, which has the appearance of a flow of discrete events - much in the same way as a cinematic film is a series of discrete images projected at *24* frames per second that are converted into an apparently continuous flow by our brain.[27]

Waves can be recorded temporally (fixed in space, variable in time), as in the case of a wave probe, or spatially (fixed in time, variable in space), as in the case of a photograph or a topographical map of the sea surface. There are notable differences between the two that are discussed following. An example of a mathematically generated, symmetrical wave packet is

---

[27] Interestingly, the traditional use of *24* frames per second in cinematography was for sound and not image clarity.

shown in *Figure 3.2*. Three waves are highlighted: the first visible wave; the highest wave (maximum wave); a short-period trailing wave. The asymmetry of the first wave is obvious, but further towards the tail the asymmetry becomes less obvious. The asymmetry is due to the variation in the instantaneous value of the period from the packet head to tail, which is in the form of an exponential decay. The exponential decay relationship is also evident in model and full-scale wave wake records, and it is not purely the result of the mathematical form used in the example. Towards the head, where the period decay is most rapid, the asymmetry is greater. The asymmetry of the first wave is further increased by the initial rapid increase in envelope amplitude, so that the first crest and trough, which sit on the envelope, are at substantially different elevations. The same occurs at the tail, but the amplitude asymmetry is tempered by the waves' shortness and slower decay of their periods.
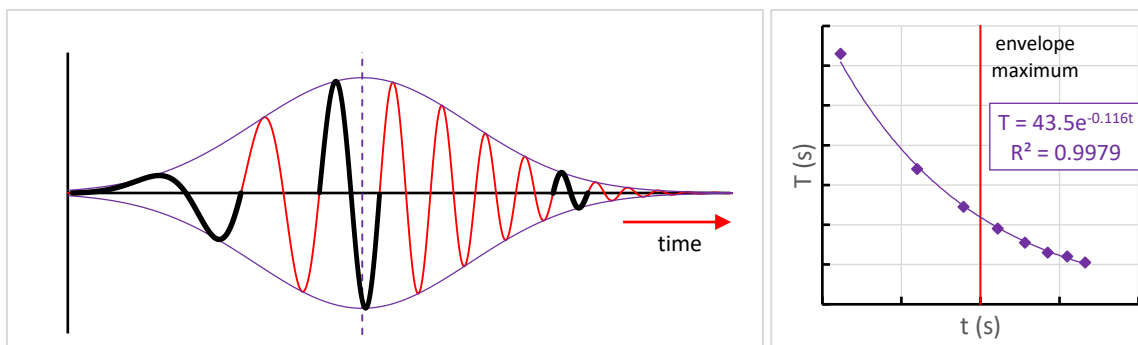


**Figure 3.2** – *Left: Generated wave packet (with symmetrical envelope for simplicity) showing how the decaying period from packet head to tail and changes in envelope shape cause asymmetry in the shape of individual waves. **Right**: Periods of each wave considered discretely, with time (t) taken as the mid-period (zero down-crossing in this case). The asymmetry of individual waves reduces as time passes.*

The implication of this is that the period we measure in the standard manner (between successive zero crossing points of the same sense – *up/up* or *down/down*) is only an average value and not the actual period. What is the actual period of the wave? It doesn't exist as a single number for the whole wave, only a single number that describes an increment of the wave as it existed at that instant. All we see is what is relevant only at that point in space and time. Move on, and the waves transform, with the parameters describing them changing as well. This also applies to the maximum wave, which can never exist perfectly at the envelope maximum.

A more abstract way of viewing waves in packets is not to think of them as a group of individual waves at all. Wake waves, as with most waves in engineering, are characterised by their height and period. In that sense it is better to visualise the wave group the way it's described mathematically, consisting of a travelling wave function in two parts. The first describes the envelope and how it evolves over time (the *signal wave*). The second is a period function that describes how the period varies from packet head to tail (the *frequency-modulated carrier wave*). The envelope is simple to visualise; the period function less so.[28] The more modern form of wave mechanics, embodied in the linear Schrödinger equation, is described in terms of a wave function $\psi$. This is discussed in Section 7, and Appendices B and C.

---

[28] Refer to footnote 30 following, which discusses research into the human obsession with shiny objects and the relationship to water. Height is easy to visualise; period much less so.

### 3.2    Wave Packet Representation

Wave groups exist within a boundary that can be described by one of several functions including Gaussian (common in physics due to its probabilistic descriptiveness), though there are non-Gaussian examples as well. Wave packets are described mathematically as the space where multiple wavelengths constructively interfere to describe a wave train; outside of which they destructively interfere in perpetual quiescence.

In water wave studies, envelopes are often described using solitary wave equations, hence the term *envelope soliton*. Solitons and their properties are discussed in Section 5.

### 3.2.1    Temporal versus spatial

A temporal representation of a wave field is relevant in practice; shorelines and maritime structures such as jetties and marinas are fixed in space and therefore experience incident waves that transform over time. Temporal representation is necessary to correctly model their response.

Historically, the highest wave has always been considered as the primary determinant of a vessel's wave wake characteristics, which in turn led to an unhealthy reliance on it as the *only* wave wake parameter worthy of comparative analysis (Cox, 2000). One of the earliest Australian studies of the effects of recreational boating and bank erosion was reported by Lesleighter (1964) in his study of speedboats on the Hawkesbury River in New South Wales. Most tellingly, the report does not have any references, probably because there weren't any relevant small craft wave wake studies available at the time, apart from texts on coastal and riverine engineering.[29] Given the lack of available literature, Lesleighter's work was surprisingly insightful and, in many ways, far better than some of the studies conducted nowadays.

Lesleighter (1964) makes several observations that are pertinent to this discussion:

> *"The waves are first felt as long and low; steepness increases and three or four higher waves pass followed by somewhat irregular small waves. The number of waves propagated by one pass seemed to vary between about four and fourteen, however in the majority of cases there are six to eight waves containing three to four pronounced waves in the middle of the train. It is thought that speed and distance from the recorder may have some bearing on the number of waves formed, however as this particular feature was unimportant for this investigation, the thought was not pursued."*

Lesleighter identified:
   a.   long period, low height leading waves;
   b.   a group of high waves at the centre of the wave train;
   c.   small waves following, of increasingly irregular form;
   d.   the relationship between the number of waves, vessel speed and lateral separation.

Lesleighter further states:
> *"The effect of the distance of travel of the waves is shown in Fig. 5. These graphs show that the waves flatten to some extent during travel – a feature which would be expected."*

---

[29] Havelock's 1908 paper on deep and shallow water effects may have helped, however all the vessels studied by Lesleighter were small recreational boats in water that was deep relative to vessel length.

Lesleighter's Fig. 5 is reproduced here as *Figure 3.3*. This is a statement of height attenuation with distance from the sailing line. Lesleighter also makes statements of relationships between wave height and vessel weight, wave period and vessel length, and vessel speed and maximum wave height, all of which are technically quite correct.
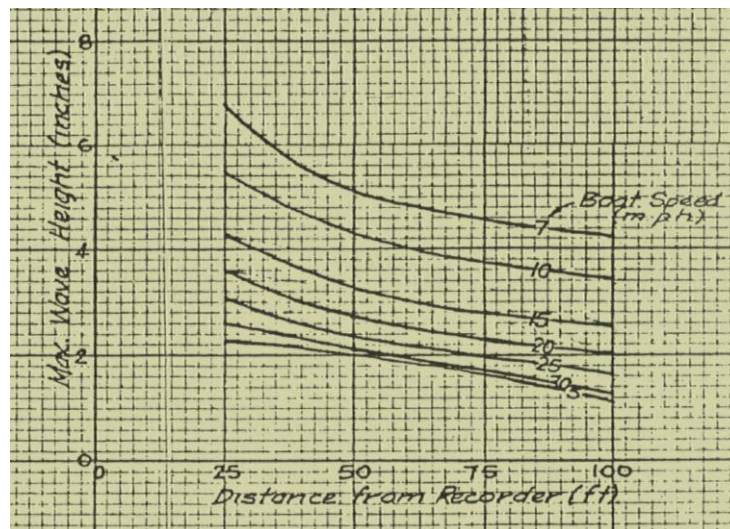


**Figure 3.3** – *Part of Fig. 5 from Lesleighter (1964), displaying the decay of the maximum wave (in inches), with lateral separation (in feet). Measurements were taken at 25, 50 and 100 feet from the sailing line and the manually drawn curves may not interpolate the data most accurately. Further analysis is discussed in Section 7 and shows that the measured decay rates are as expected. The vessel used was noted as being 13 feet overall length, 5 cwt weight (254 kg), and was fitted with a 35 hp outboard motor. The weight (assumed dry) is slightly questionable, which highlights a consistent problem with the enforcement of wave wake operability rules based on vessel dimensions.*

Lesleighter focussed mainly on the maximum wave height, which was identified as a distinct, reoccurring feature in both the measured waves and the wakes observed by the general public.[30] What has never properly been explained is why the maximum wave is such a consistent feature and why its period is stable in the far field. The only conclusion that could be drawn from the available literature for the constancy of this assumption is that the maximum wave, once formed, was stable and propagated as such (attenuation aside). However, that ignores the fact that deep water waves within a wake only exist with certain parameters at one instance in time, after which they disperse into a different arrangement, and essentially different waves. In a dispersive wave field, there is little point trying to track individual waves as they propagate.

To address this, six wave packet features are discussed, explaining how observed characteristics are predicted by theory. In this instance, what is important is to explain observations qualitatively and not to provide absolute answers.

---

[30] There is a whole branch of consumer psychology devoted to the choices we make. A study by researchers at Ghent University in Belgium (Meert, *et al.*, 2013) into the human preference for glossy and shiny objects found correlation with our primordial relationship with water, which is a particularly pertinent finding in this instance. Similarly, a commonly used political saying is "look over there – big shiny thing"; a retort at attempts to use psychology to divert political attention. These may explain the public's focus on the maximum wave, which is in effect the "big shiny thing" in a propagating wake. It is therefore regrettable that wave height has similarly maintained its prominence as the "big shiny thing" in wave wake science.

### 3.2.2 Consistency of the maximum wave – Figure 3.2

This is a function of the fact that the maximum wave is nothing more than a representation of the envelope maximum amplitude. As mentioned, it is better to consider propagating waves as having two parts; one that defines the height and one the defines the period. In a propagating, dispersing wave function, the wave function represents the carrier wave (though frequency modulated) and the envelope represents the signal wave that modulates (in the water wave case) the carrier wave amplitude. The maximum wave is the wave that occurs at the point in the packet where amplitude modulation is the least, i.e., at the envelope maximum amplitude. That is complemented by Section 3.2.3.

### 3.2.3 Constancy of the period of the maximum wave

The envelope soliton is defined according to its characteristic wavenumber, about which the envelope forms and propagates at a group celerity relative to that wavenumber. The intrinsic relationship in deep water between the packet group celerity and the phase celerity ($c_g = c_p/2$) means that the maximum wave will have a speed of twice the group celerity as it passes through the region of the packet maximum amplitude. That, plus the dispersion relationship between wave celerity and wavelength, gives the maximum wave a constant period.[31] The only assumption with this is that, in field measurements, the lateral separation is sufficient for packet waves to form clearly. Lamb (1895, p. 398) makes a similar observation with regards to a wave system downstream of a disturbance, which requires a finite distance to become fully established. Deep-water wave wakes have the added complexity of superposition of several divergent packets and the transverse wave train at slower speeds. Conducting tests at high speed ($Fr_L > \sim 1$) in deep water would effectively negate the influence of the transverse waves, operating in a speed range where they either cannot exist at all or cannot exist with any significance. This would be relevant to small craft, but maybe less so for large vessels.

### 3.2.4 Number of waves

This is a function of the packet length (occasionally referred to as packet width by some authors), which increases with propagation. As such, the number of observed waves is a function of the packet length and therefore the distance propagated. That correlates with Lesleighter's observations above. Peregrine (1983) shows that the number of waves is inversely proportional to the envelope soliton amplitude. In simplified terms, more waves are observed as distance from the sailing line increases. If a vessel passes very close to the shore or to another vessel, fewer waves of increased height are evident. If the vessel passes at a distance, greater numbers of smaller waves reach the shore. In the case of a large, high-speed vessel operating some distance from the shoreline, the combination of wave shoaling and an increased number of waves could result in extended periods of inconvenience or danger to shoreside occupants.[32]

---

[31] The relationship between group and phase celerity, and the dispersion relationship, can be found in Lighthill (1978), Newman (1977), or just about any text on waves.

[32] The reported incident at Chambers Island, Wisconsin, on September the 5th 2015 is an equivalent shallow water example, where the littoral combat ship *USS Milwaukee* passed by anchored recreational vessels, causing vessel damage and minor injuries. The vessel was travelling at speed approximately *2,400 m* offshore in an unknown water depth (but likely to be around *20 m* or more, giving $h/L \geq 0.18$). After propagating approximately *22L*, many waves estimated by onlookers at *1.5 m* height came ashore. The initial waves were insufficiently steep to break and engulfed the beach with run-up, a phenomenon associated with long-period waves. The shorter waves following tended to break. This would suggest the wake was moderately depth affected when generated. Most relevant articles are from news sites and many have expired: https://www.youtube.com/watch?v=8iYJpMLWZ6c (last accessed 12th of January, 2018).

Similarly, but not directly related, Peregrine (1983) also notes that there are twice as many waves evident when a packet passes a fixed point as there are when viewed at an instant in deep water due to the ratio of group to phase celerity. Stated simply, a trace recorded by a wave probe (spatially fixed; time varying: $f[0, t]$) would record twice the number of waves that a photograph would capture (spatially variable; time fixed: $f[x, 0]$). That may seem trivial and irrelevant but consider that deep-water wake patterns described by authors such as Kelvin (1887) and Havelock (1908) are fixed in time, not space. Conversely, shorelines are fixed in space, but not time.

Also, wake fields developed by potential flow theory may be fixed in time, such that wave cuts used to generate a numerical trace may not be the same as that generated by a wave probe. The maximum wave and accompanying period/wavelength might be exactly faithful, but other measures such as *wave range* (Doctors and Day, 2001), being the maximum elevation between any crest and trough in a wave cut, may not if the peak and trough of the range were not adjacent (if they were they would describe the maximum wave anyway).[33] Anything greater than near spatial location of the peak and trough would cause them to transform when measured temporally, made worse by packet interference. A shoreline, fixed in space, that experiences a crest, could not care less about the trailing trough defining the *wave range* if it laid several wavelengths offshore. By the time it reached the shoreline, that trough might be quite different.

### 3.2.5    Envelope shape – Figure 3.4 (upper envelope only)
A notable observation is that packets become asymmetrical with propagation when measured temporally in the field. This has two practical consequences. Firstly, the maximum wave tends to occur towards the head of the packet, which is important for model and field testing where the properties of the maximum wave are sought, and reflections contaminate the later parts of the record. In shallow water, where dispersion varies from zero at the wavefront to fully dispersive at some point further through the packet, the asymmetry becomes even more pronounced.[34] Secondly, it implies a considerable number of ever-decaying waves would follow long after a vessel has passed, which concurs with field observations.

### 3.2.6    Envelope evolution – Figures G5 and G6
Related to (d), this is of philosophical importance only. Vessel wakes are often considered as a burst of waves that travel away from the sailing line. Envelope mechanics show that the envelope soliton amplitude, when measured at a fixed point ($f[0, t]$) can never decay to zero. That implies that the wave packet grows from the sailing line but never leaves it behind. In very calm conditions, it is possible to visualise almost endless waves of gradually decreasing height and period growing from the sailing line, especially for high-speed vessels without a transverse system. These small, trailing waves account for only a tiny fraction of the total packet energy.

---

[33] Although the authors attempted to justify "*wave range*" as a valid (and preferred) alternative to the maximum wave, one possible reason for its introduction was its simple and rapid determination in a wake record, being nothing more than the combined maximum and minimum entries in a data set. The authors expressed no interest whatsoever in reporting wave period, which would be impossible with "*wave range*".
[34] It is not dispersion itself that defines the degree of asymmetry, but it defines the ratio of group-to-phase velocities which in turn determines the asymmetry. The value of $c_g/c_p$ ranges from 1 when non-dispersive to ½ when fully dispersive, and the fully dispersive condition would be reached practically when $\lambda/h < 2$.

### 3.2.7   Height attenuation and decay

This is an important feature that is afforded its own discussion in Section 7 and Appendices B and C. One important point to note for the maximum wave is that, provided a temporal measurement is compared to the equivalent point in space, the result will be *practically identical*. It can never be *exactly identical* – the very short time it takes a crest and following trough to pass through a wave probe allows for the maximum wave to transmute very slightly.
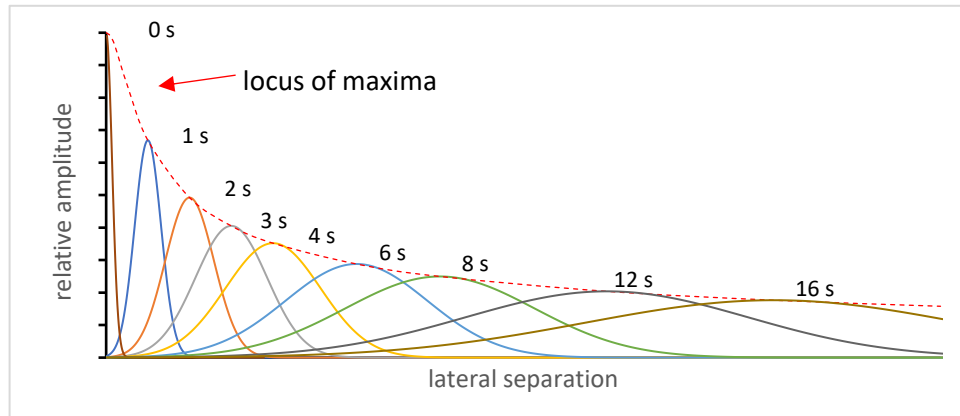


**Figure 3.4** – *Evolution of a packet envelope soliton (time fixed, spatially variable), as would be measured by a series of photographs through a wave flume. Each envelope soliton is defined by the characteristic wavenumber: the maximum value and its position relative to $(x, t)$ retain their consistency, but the envelopes spread symmetrically about the maximum. The locus of maxima is equivalent to the decay of the maximum wave with increasing lateral separation (refer Appendix B).*
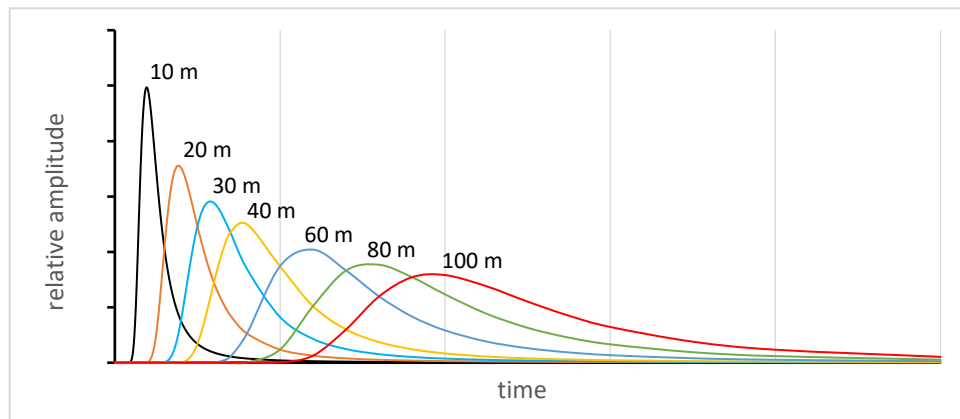


**Figure 3.5** – *Evolution of a packet envelope soliton (spatially fixed, time variable), as would be measured by a series of wave probes. Each envelope soliton is defined by the characteristic wavenumber: the maximum value and its position relative to $(x, t)$ retain their consistency, but the envelopes spread asymmetrically about the maximum. Also, the soliton tail never reaches zero amplitude, regardless of time.*
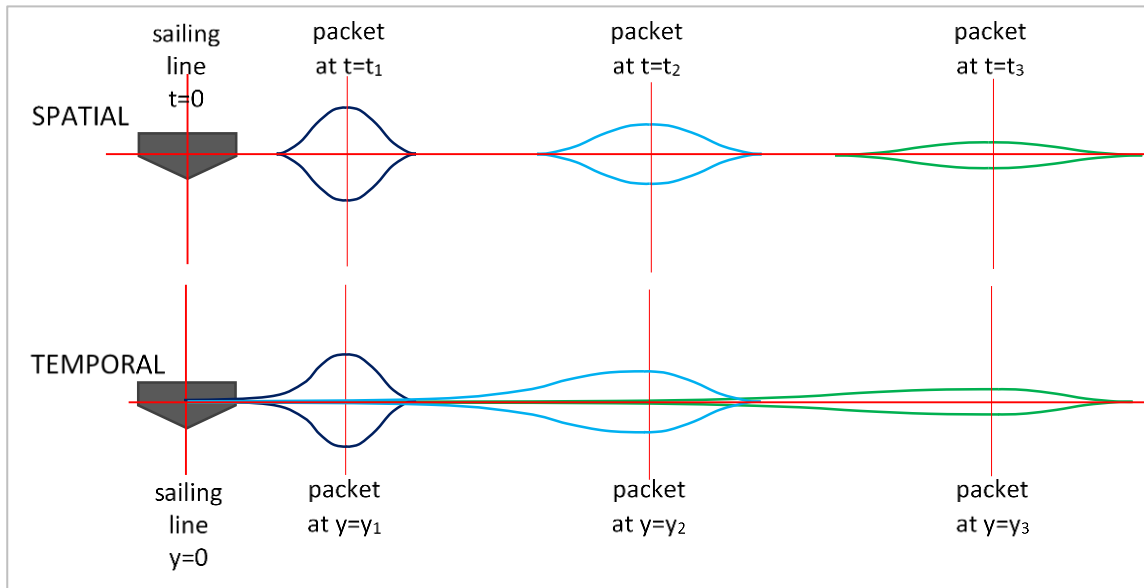
**Figure 3.6** – *Proposed schematic of how a single wave wake packet appears, depending on how it is recorded. The **upper** figure shows a packet recorded spatially at different time intervals, moving away from the sailing line and dispersing over time. This represents the $f[x, 0]$ condition that a photograph would record. The **lower** figure shows the temporal record, with the packet head moving away from the sailing line but the packet tail remaining at the origin and thereby making the envelope more asymmetrical over time. This represents the $f[0, t]$ condition that a wave probe would record. The asymmetry of the temporal envelopes may not be drawn exactly correctly, since the position of the maximum height may move (relatively) further from the head with propagation, especially when $Fr_L > 0.5$.*
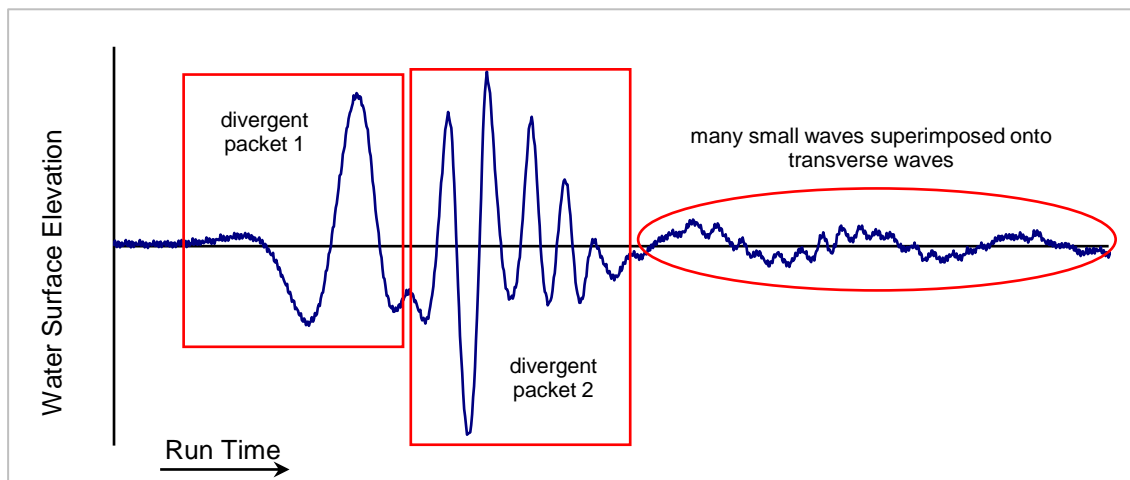


**Figure 3.7** – *Model AMC 99-17 wake trace at $y = 0.5L$ in deep water, showing the existence of a substantial number of very small waves following the divergent packets – so displaced in time as to be superimposed onto the transverse wave train. These short waves are too long to be capillary waves. It is also possible to see them on reflected waves crossing back through the probes. Such short waves could not be travelling with those longer-period reflections and could only be from the original radiating divergent packets. This model also displayed multiple divergent packets close in, with the peculiarity that the second packet maximum was higher than the first – something peculiar to monohulls (but much less energetic: refer Cox, 2000, Table 1).*

### 3.3 Measurement of the Maximum Wave

The maximum wave referred to in wave wake studies is essentially the wave closest to the envelope maximum amplitude. By definition, the packet propagates with a group celerity equal to that of the envelope maximum value, hence "*characteristic wavenumber,*" and since this wavenumber is constant the corresponding period must also be constant. In reality, the period does waver slightly about that given by the characteristic wavenumber, but that is because the individual packet waves move at their phase celerity through the packet as the packet itself propagates at the group celerity, so at any instant in time the maximum wave may be half a wavelength before or after the envelope maximum and so with slight period variance. There may be further contamination of the period of the maximum wave caused by the superposition of multiple wave packets and an underlying transverse wave system (if present).

*Figure 3.8* shows this schematically and *Figure 3.9* shows an experimental example. *Figure 3.9* is a practical example from experiments of the stability of the period of the maximum wave, with slight variations with lateral distance referred to above and in the discussion of *Figures G8* and *G9*. There is nothing new to this constant nature of the period of the maximum wave – it has long been held as one of the consistent features of deep-water wave wakes. Almost every past wave wake study has highlighted the desirability of recording the maximum wave. What has been consistently lacking is an explanation of why - more often than not reverting to a statistical explanation that can, in the extreme, degenerate into the engineering equivalent of "*just because.*"
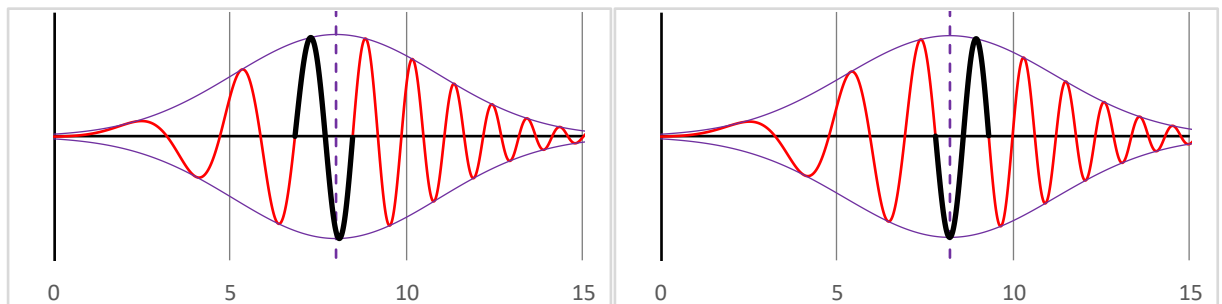


**Figure 3.8** – *Schematic example of how the position of the maximum wave can vary relative to the centre of the packet envelope, using a simple mathematical representation of a wave packet. The horizontal axis is in metres – they represent spatial (photograph) rather than temporal (wave probe) packets, which explains the packet symmetry These examples would equate to the waves of a ship model with $L \sim 2.4\ m$. The time difference between the two is only about 0.3 s. The position of the nominal maximum wave relative to the packet centre changes slightly, allowing it to flip from a zero up-crossing type (left) to a zero down-crossing type (right). This change shifts the maximum wave along the x-axis, from a longer to a shorter wavelength. The maximum wave height due to this change of position, after correcting for packet amplitude decay due to dispersion, is essentially unchanged, but the corresponding wavelengths in this schematic vary by 8% (1.635 m and 1.510 m), and the calculated linear theory wave energies also vary by 8% without accounting for (slight) height attenuation. This was also borne out in the study of how wave energy varied across a packet, with the most energetic wave fluctuating half a wave number (not wavenumber) about the maximum wave.*
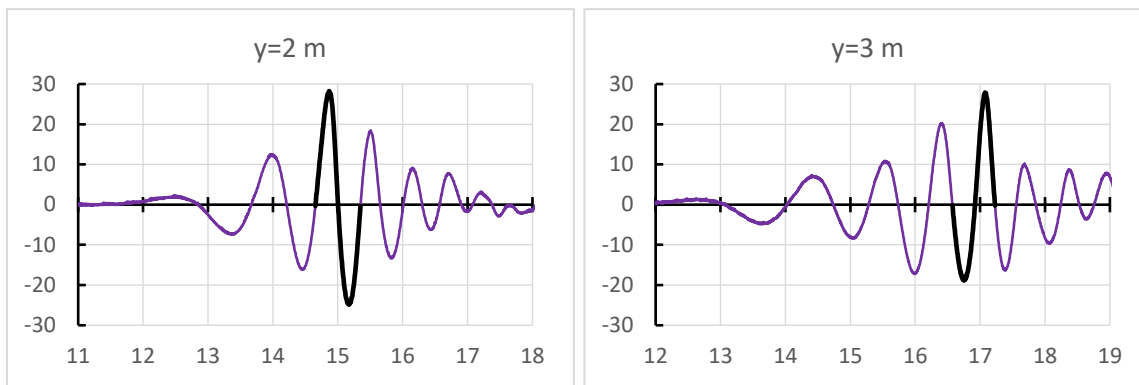
**Figure 3.9** – *Experimental example of maximum wave variation for model AMC 00-01, at $V = 3.5\ m/s$ and $h = 0.9\ m$ (depth super-critical; no transverse system) (x-axis: run time in seconds; y-axis: W.S.E in mm). The lateral separations equate to about $2L$ (left) and $3L$ (right). The maximum wave has flipped from up/up to down/down and moved from wave 3 to wave 4½ in the packet due to dispersion. The number of waves has increased from about six to about eight. The period of the maximum wave has decreased by 6% (due to minor positional variation of the maximum wave within the packet); the height by 12%; the energy by 31%: far more than the pure packet examples in Figure 3.8. This highlights the difficulty in measuring consistency at model/full scale due to packet interaction, with the packet to the right suffering obvious interference from the transverse waves from the acceleration phase passing through (around 17-19 s, where the crest and trough amplitudes are unsymmetrical).*
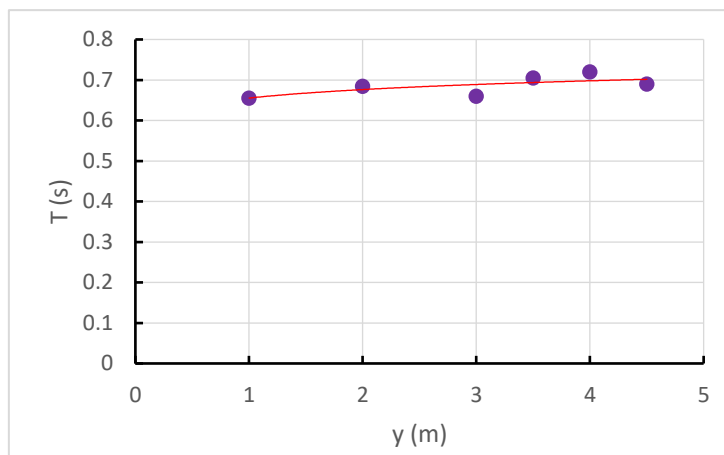


**Figure 3.10** – *Period of the maximum wave for AMC model 00-01 for $h = 900\ mm$, $V = 3.75\ m/s$. Once sufficiently dispersed, the period settles to a relatively constant value, with some of the variation caused by the slight packet-wise migration of the maximum wave about the envelope maximum amplitude. There are also other underlying causes for the variation, including the existence of multiple wave packets creating localised interference. At the tested speed the transverse waves would not exist ($Fr_h = 1.26$; $Fr_L = 1.17$), but there is always the possibility of transverse waves generated during the depth sub-critical, slow-speed acceleration phase reaching the outer wave probes, or contamination from reflections off the basin wall.*

## 3.4      Dispersion

Further mention must be made of dispersion, which in simple terms describes how waves can travel at different speeds and therefore spread out, especially when propagating as a group. The term is quite well understood as a concept in itself; what is less well understood (or explained well) is its effect on wake waves, how we measure them, and how we interpret them.

34

In deep water, where waves are fully dispersive, it is the measurement and interpretation of waves that is in question. The only waves in a packet that are consistent are the maximum wave, which propagates at the packet fundamental (or characteristic) wave number, and the first wave, which approaches asymptotically a terminal wave period in the far field. The study of the first wave in deep water becomes somewhat pointless given sufficient lateral separation, where its height and energy are greatly diminished. Also, the very first wave most likely comes from outside the Kelvin wedge (see Section 4.5). All packets that comprise a wave wake transmute, but our somewhat static interpretation of wake waves struggles to recognise that.

In shallow water, where waves become increasingly depth affected, our practical interpretation of dispersive effects also fails. As will be shown, it is common to regard at least the leading wave in a depth super-critical wake as being non-dispersive, since it propagates at the depth-limited celerity of $\sqrt{gh}$ that is no longer a function of wavelength.[35] It will be demonstrated that it is not the complete leading wave that is non-dispersive, but only a prominent feature of it.

To be absolutely pedantic, it is not unreasonable to say that there is no such thing as a fully non-dispersive wake wave in practice. A depth sub-critical transverse wave train behind a vessel in a steady-state condition has the appearance of being non-dispersive, since the waves are monochromatic with wavelengths only a function of vessel speed. As mentioned, it is not possible in practice for a transverse wave wake system, or any wave system, to be perfectly monochromatic and hence non-dispersive. A dispersive wake requires a range of component frequencies, described by Newman (1977) as being a "*narrow band of component waves, with nearly equal wavelength and direction*." That might be an over-simplification for the purposes of illustration, as the analysis of a wave wake packet would reveal a wide spread of frequencies.

The best illustration of this is a quote from Lighthill (1978, p. 270-271):

> *"In theory, there is a nondispersive case for ship waves: the 'long-wave' limit when all waves emitted are very long compared to the water depth h. In practice, however, the wavelength needs ($h < 0.07\lambda$) to be at least $14h$, and it proves impossible to operate on water of depth $h$ a ship so long that it generates only waves of length $14h$ or more!"*

A note is to be made of Lighthill's continual reference to $\lambda/h = 14$ as his definition of *fully shallow* (refer Section 5).

Divergent wave groups are comprised of many component waves (approximated mathematically as Fourier components), so that the waves we see at any instance is the result of how those component waves exist and relate to each other at that point in time. Move on in time and the number, size and disposition of the waves also changes. For that reason, only the crest of the very first wave in a shallow water wake could be considered as approaching a non-dispersive state, since it is the crest that conforms to the depth-limited celerity of $\sqrt{gh}$. A degree of dispersion occurs at all points behind the leading crest where the waves have not reached the celerity limit.[36] The only time the complete wake could be considered as non-dispersive is when the depth approaches zero and all waves in a propagating wake were fully depth affected, which is essentially impossible: no water - no waves! That is the alternative to Lighthill's quoted argument (reducing $h$ rather than increasing $L$).

---

[35] It is not uncommon to find reference to "*the leading waves*" (plural), as is discussed in Section 3.5.
[36] Also, in front of the leading crest, where there can be an underlying solitary wave component with celerity exceeding $\sqrt{gh}$ if the $h/L$ ratio is small enough (as discussed in Section 5).

Solitary waves can dominate wakes in shallow water under certain conditions (refer Appendices D, E, G and F), yet these waves should not be regarded as non-dispersive for two reasons. Firstly, the celerity of solitary waves is a function of their height, so they undergo amplitude dispersion, with the higher waves travelling faster. This is different to the frequency dispersion of periodic waves, but it is dispersion nonetheless. Secondly, a solitary wave remains steady and symmetrical in the first instance through a balance between non-linear depth effects that would otherwise cause the wave to steepen and break, and dispersion that would otherwise cause the wave to spread.[37] Within itself it is dispersing, and it was a lack of understanding of this counterbalance between dispersion and non-linearity that led the early theorists to believe that solitary waves were an impossibility.

*Figure 3.11* is a simple, graphic example of deep-water wave wake dispersion, discussed in the caption. *Figure 3.12* is an example of the leading wave of a depth super-critical wake that should be regarded as non-dispersive by the available literature on wave wakes, yet it is not.
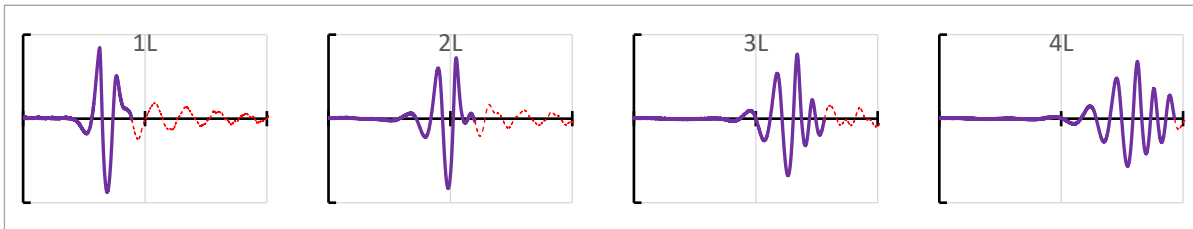


**Figure 3.11** – E*xample of deep-water wave dispersion from model experiments at four evenly spaced lateral locations relative to the vessel waterline length, $L$. At $1L$ (left), the divergent system (heavy, solid line) is contained within only a few high waves, followed by the smaller transverse waves (light, dashed line). With propagation, the divergent packet disperses - increasing the packet width, reducing the envelope height, and increasing the number of visible waves ($4L$, right). The only feature of the divergent system to remain (approximately) constant is the period of the maximum wave, which is defined by the fundamental (group) wavenumber. All other features vary with propagation. The scales are consistent.*

In wave wake studies, the deep-water dispersion example of *Figure 3.11* is a well understood, though that understanding is often quite superficial in how it manifests itself in practice. The shallow water example of *Figure 3.12* is not well understood and is often reported in a contradictory or confusing manner (see Section 3.5). Referring to Appendices C and D, it is only the first crest in this depth super-critical condition that propagates at $\sqrt{gh}$, and only under certain conditions where the underlying solitary wave component of the leading wave is not dominant.[38] The initial upswelling that precedes the first crest travels *faster* than $\sqrt{gh}$, which is only possible because of an underlying solitary wave component that comprises the first crest of super-critical wakes and becomes dominant with decreasing $h/L$ and slenderness ratios. The trough, and zero up-crossing that marks the end of the first wave, travel at speeds progressively less than $\sqrt{gh}$.

---

[37] The non-linear depth effects cause amplitude dispersion and a steepening of the front of the wave as the higher amplitude wave components run ahead. In contrast, frequency dispersion causes the shorter wave components to lag, creating a rearward shift in the position of the crest and a steepening of the back of the wave. In a solitary wave the two balance, resulting in symmetry.

[38] Which implies that the waves were generated in a depth super-critical state and not propagated from deep to shallow water.

Overall, the first shallow water wave is still dispersing, the reason being that it is not one wave but a packet of several waves (or at least that leading part of the wave function) that are almost fully depth affected and therefore weakly dispersive. The first wave has all the features of a wave packet: its height decays at a predictable rate with propagation; it widens with lateral separation; it becomes asymmetrical when recorded temporally. This is discussed in Section 5.
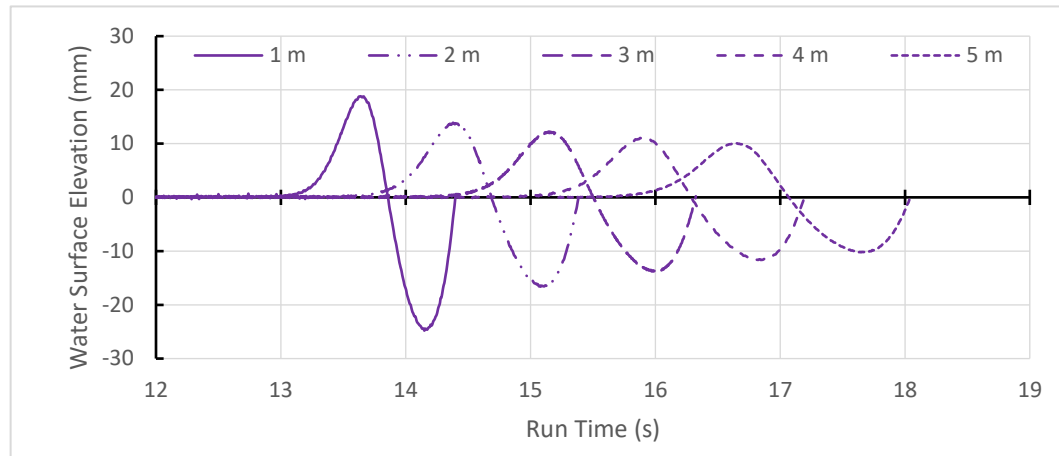


**Figure 3.12** *(reproduced from Appendix C, Figure C4) - The first shallow water wave for model AMC 00-01 ($V = 2.75\,m/s$; $h = 0.15\,m$; $Fr_h = 2.27$; $h/L = 0.144$) at five lateral locations. The height decays with propagation but the apparent period increases by about 75%. The leading wave crest conforms exactly to a celerity of $\sqrt{gh}$; the initial upswelling propagates at a celerity slightly (~6%) faster than $\sqrt{gh}$; the zero down-crossing and tail propagate at celerities less than $\sqrt{gh}$. Also of note are the disproportionate crest height at $y = 1\,m$ and the gradually reducing asymmetry between crest height and trough depth with increasing lateral separation, due largely to the faster decay rate of trough depth. Refer to Appendix C for a more detailed explanation.*

### 3.5    Dispersion Contradictions and Confusion

Examples of the contradictions and confusion can be found in Doyle, *et al.* (2001), who undertook a comprehensive (funded) project to study the shallow water wakes of large, high-speed ferries. Consider the following quotes from Doyle *et al.* (2001):

> *"In the super-critical region the long waves are non-dispersive and the wash pattern takes on a different appearance."*

The *long waves* (meaning long wavelength) are non-dispersive by the authors' reasoning, stated clearly as the first several waves and not just the first.

> *"Unfortunately when trying to characterise shallow water wake wash, considerable complications arise. The deep water decay rate is no longer valid and due to the divergence of the leading supercritical waves, the wave periods are not constant with distance from the sailing line."*

The wave periods are not constant due to the nature of the first wave being comprised of several depth-affected waves of gradually decreasing celerity across the group (and therefore increasingly dispersive). Rather than use the term "*dispersive,*" they invented a new term: "*divergence.*" How can several periodic waves that are non-dispersive, and are therefore by definition propagating at

37

the shallow water celerity limit of $\sqrt{gh}$, diverge? It cannot be due to amplitude dispersion, as their published wave wake traces show that the first wave is (generally) smaller or of similar amplitude to those following. The periods of these waves can only change if their wavelength changes, but what is driving that change?

> *"The low height decay rate in the leading super-critical wash for small h/L ratios, is attributable to the highest waves being largely non-dispersive in that energy is conserved in individual waves."*

The first quote claimed that the *long waves* were non-dispersive, yet now it is the *highest* waves that are *largely non-dispersive*, even though it refers to the shallowest of depths where the longest waves are the most depth affected (and the $H/h$ ratio would be insufficiently large to create anything other than almost inconsequential non-linearity – refer to Doyle *et al.*, 2001, Fig. 4). Even solitary waves need to reach a condition of $H/h \geq \sim 0.3$ for non-linear effects to be of consequence (Yamashita and Kakinuma, 2014, Fig. 3). Energy conservation due to weak dispersion or their assumed absence of dispersion is a symptom, not a cause. It is a combination of increasing weakness of the dispersion and the strength of a solitary wave component in the leading crest at reducing $h/L$ ratios that preserves energy and height (refer Appendix D).

A prior paper by Whittaker, *et al.* (1999), studying the same scenario, carries the same fallacious arguments:[39]

> *"Once the ship passes the critical speed energy is no longer pumped into a few transverse waves and the super-critical wash pattern is formed. It should be noted that these waves are not 'solitary waves' but are single non-dispersive waves, with crests and troughs and with energy conserved in each wave."*

This is another stated example of multiple, non-dispersive leading waves, but is patently not true. The waves are dispersive, but weakly dispersive. The wake pattern, which the authors offer as a schematic diagram (their Fig. 4), shows clearly that the leading waves are spreading out. It may be the mythical *divergence*, but it's certain to be *dispersion*.

Lastly, a question posed in the discussion following Gadd (1994) illustrates the importance of understanding the dispersive nature of wake waves:

> *". . . I would be grateful to hear of any suggestions about what one should try to minimize in any attempt to reduce the erosion damage caused by river vessels. For example, is it better to generate a large number of small waves or a small number of large waves?"*

To which the Gadd replied: "*I imagine (but do not know) that a small number of large waves might cause more erosion damage to river banks than a large number of small waves of the same total energy, because the rate of transmission of energy may perhaps need to exceed some threshold before significant damage occurs.*"

---

[39] And, worse, go on to contradict themselves by claiming that the first two waves in an observed ferry wake had a constant angle of *divergence* of around *10* to *12* degrees and were non-dispersive, though failed to explain how there could be a difference in crest angles when, by the very definition of *non-dispersive* as it applies here, both waves must have been travelling at the same depth-restricted celerity of $\sqrt{gh}$! They go on to clarify that "*In practice, the waves are not perfectly non-dispersive,*" yet carry the absoluteness of their non-dispersive argument further throughout the paper.

The answer is more insightful than what Gadd gave himself credit for. Though it is not obvious how a design could be manipulated to generate larger numbers of smaller waves, dispersion accounts naturally for increasing numbers of smaller waves with increasing lateral separation at a constant total energy. Wind waves are an example of small, persistent waves, and shorelines develop a stable profile over time to accommodate them (Cox, 2000). Section 8 develops the arguments for threshold conditions for erosion initiation and the wave parameters most likely to accelerate erosion. As with almost all discussion of wave wakes, the quoted question and response from Gadd (1994) are predicated on "*large*" meaning "*high*", with no mention of "*long*." Attention is drawn to the literature review (and predilection for wave height) in that regard.

### 3.6    Wave Packet Superposition Examples

To assist in the understanding of how different packets within the divergent wave system might interact and affect the measured result, several simulations have been performed using symmetrical packets with a decaying wave function. For comparison, experimental features are also discussed.

### 3.6.1    Experimental examples

*Experimental Example 1 - Bow and stern packets, slow speed – Figures 3.13 and 3.14*

Model AMC 99-17: $L = 1.824$ m; $V = 0.75$ m/s; $Fr_L = 0.18$; $h = 0.9$ m. Note the two distinct wave packets. At this speed, the model travels one waterline length in *2.43 s*, which is exactly the time separation of each packet (measured between maximum waves). It is suggested that the packets represent a bow and a stern divergent system. The consistent time separation also suggests that the packets have the same fundamental wavelength, $\lambda_o$. This is important, as it means the packets will not readily distance themselves; the time separation of the packet maxima being only an inverse function of vessel speed. Given sufficient propagation distance, the packets would begin to merge as the envelopes spread and overlap. The constant packet periods also have another important relationship – that these fundamental periods are a function of vessel length. The period of the transverse waves is *0.48 s*. These waves are clearly distinguishable as the first several waves following the second packet.
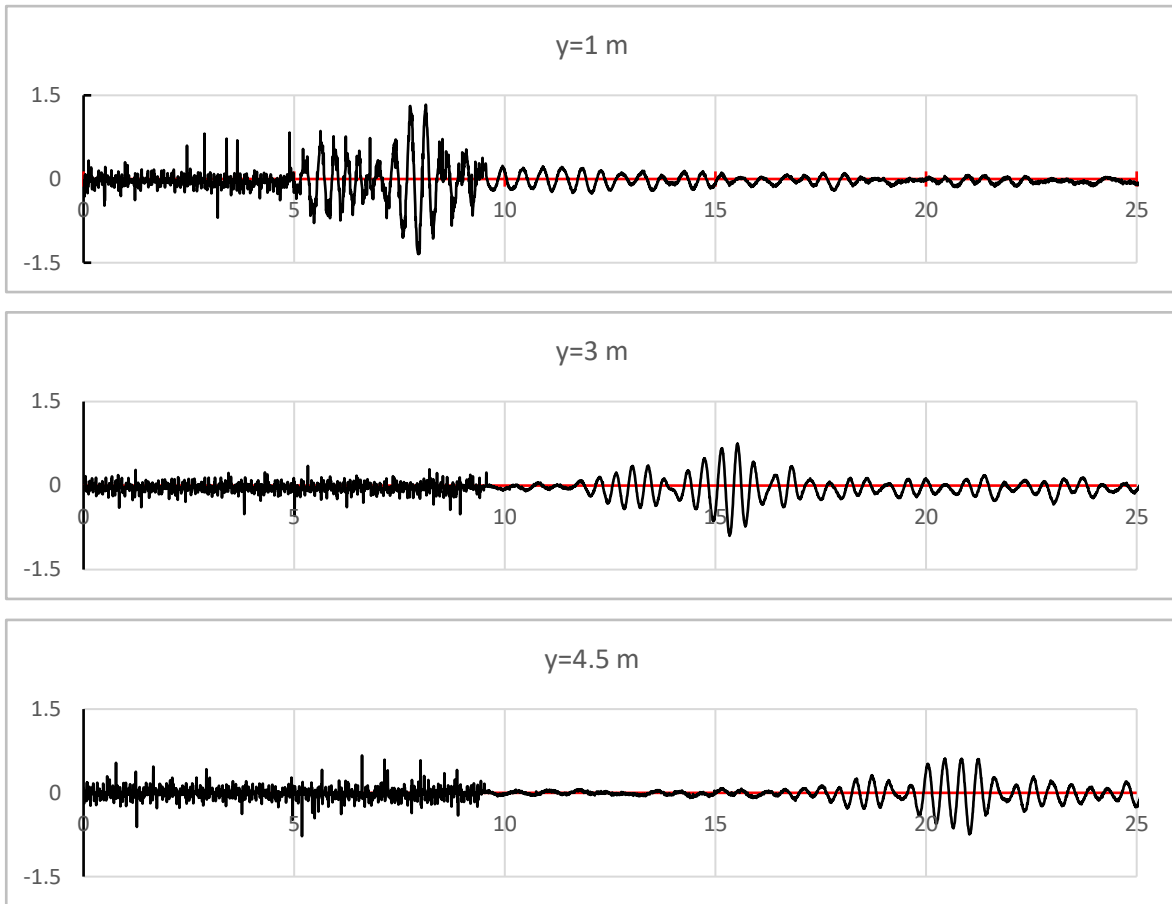
**Figure 3.13 (a, b, c)** – *Experimental results in Example 1 (x-axis: Run Time in seconds; y-axis: W.S.E. in mm).*
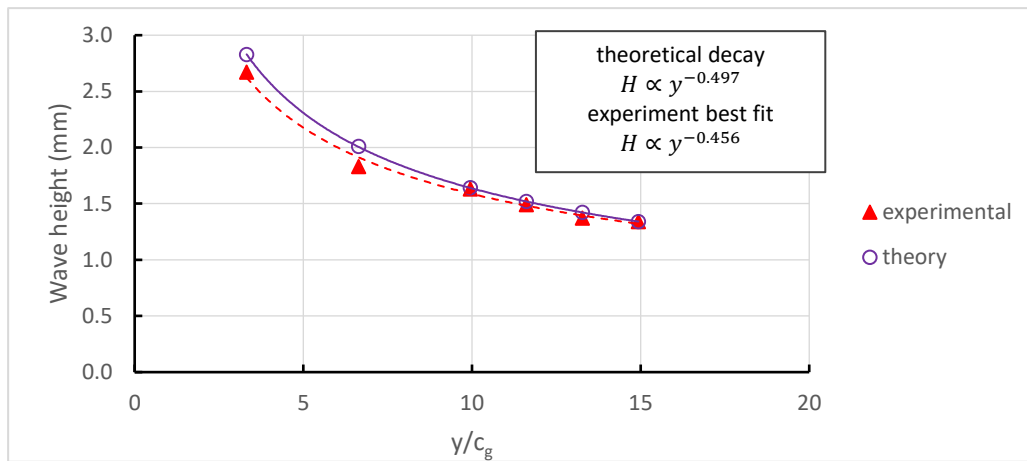


**Figure 3.14** - *Calculated and measured decay of the maximum wave of the second packet at $y = 1, 2, 3, 3.5, 4, 4.5\ m$ (refer Example 1, Figure 3.13). The theoretical heights were made relative to the measured value at the most distant probe ($y = 4.5\ m$; $y/L \sim 2.5$) – the theory will only give relative values. There is still the probability of some slight superposition of transverse waves, as well as the (known) presence of a third packet of shorter waves (more evident at higher speeds). The theoretical decay rate is based on the Schrödinger decay method (refer Section 7), which gives a variable decay rate as a function of the lateral distance relative to the number of group wave cycles. At slower speeds where the wavenumbers are larger, the decay exponent approaches the theoretical limit of -0.5. The equivalent power decay rates are curves of best fit, but with a decay exponent only relevant within the $y/c_g$ range shown. The more distant probes certainly follow the theoretical decay; the near-field probes are more likely to be affected by localised interferences.*

*Experimental Example 2 – Bow and stern packets superimposed at high speed – Figure 3.15*

*Model AMC 99-17:* $L = 1.824\ m$; $V = 1.75\ m/s$; $Fr_L = 0.41$; $h = 0.9\ m$. This represents the fastest speed at the tested depth to maintain all deep-water characteristics ($Fr_h < 0.75$). Note the waviness in the first packet crests and troughs ($t = 12 - 16\ s$) and the lumpiness of the very first small waves ($t = 9 - 12\ s$), indicating two packets on top of each other (refer to discussion in Section 4). Also note the emergence of the third, short-period divergent packet around $t = 17 - 19\ s$. As speed increases, this third packet becomes prominent in height, but with short periods. The total energy of this packet is much less than the first packet(s), even though it dominates visually at high speeds.
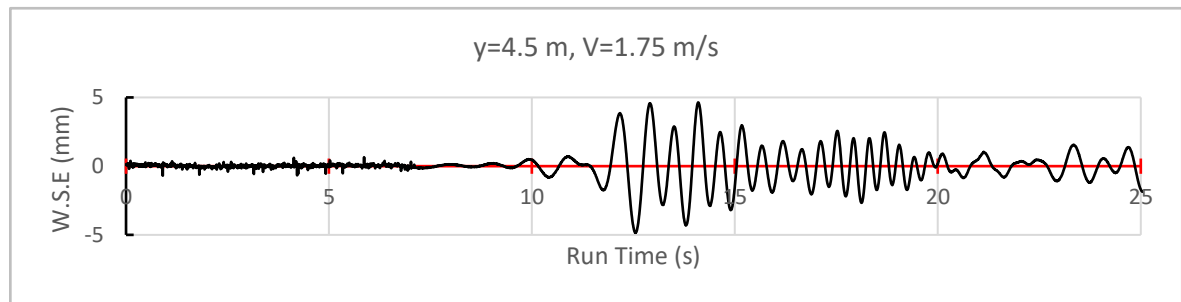


**Figure 3.15** – *Experimental results in Example 2. The waviness of the crest heights and trough depths is noted.*

*Experimental Example 3 – Scaled model test results at three different speeds – Figure 3.16*

These are scaled results from model test of monohull model AMC 99-17: $L = 36.54\ m$; $h = 88\ m$ (deep); $y = 0.3L, 0.5L, 0.7L, 1L, 2L, 2.5L$. The wave heights were taken for the first packet, which for this vessel was a composite of the bow and stern packets (otherwise indistinguishable). Note how at certain length Froude numbers the rate of height decay is either slow (*20 kn*) or initially varying between growth and decay (*10 kn*). Only at the non-displacement speeds does the decay rate tend to stabilise, but not absolutely or consistently. In general, decay rates in the near and medium fields are inconsistent, as they are at slower speeds.
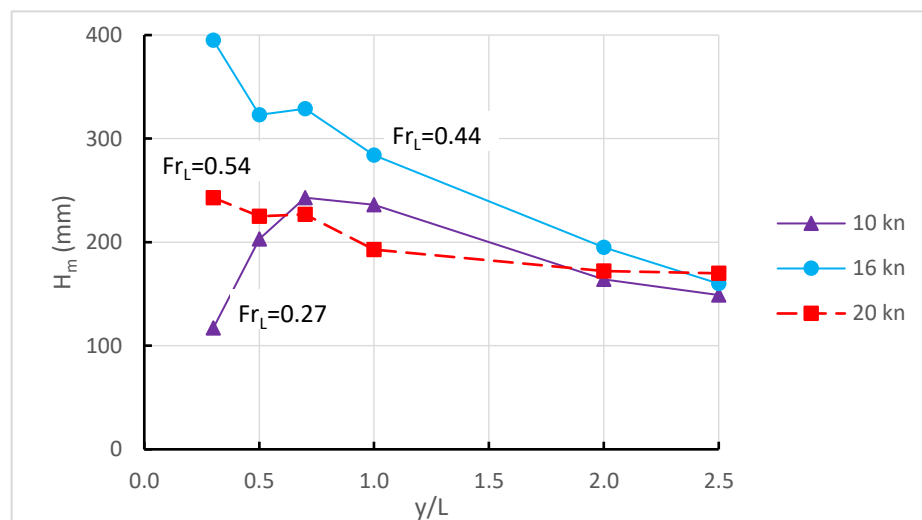


**Figure 3.16** – *Experimental results in Example 3.*

41

### 3.6.2 Simulated examples

*Simulated Example 4 – Two similar packets, slightly offset in time – Figure 3.17*

The result is a packet of almost the same height as one of the original packets, but with an initial lumpy region between $t = 20 - 25\ s$. The period of the maximum wave in the composite packet has also been shifted to a lower value. This, plus Section 3.6.3 following, would represent slow speed wave wakes where bow and stern divergent wakes of nearly equal parameters may interfere constructively or destructively, depending on their position relative to the sailing line and the vessel speed. They are practical examples of the variability seen in wave height decay at slow speeds.
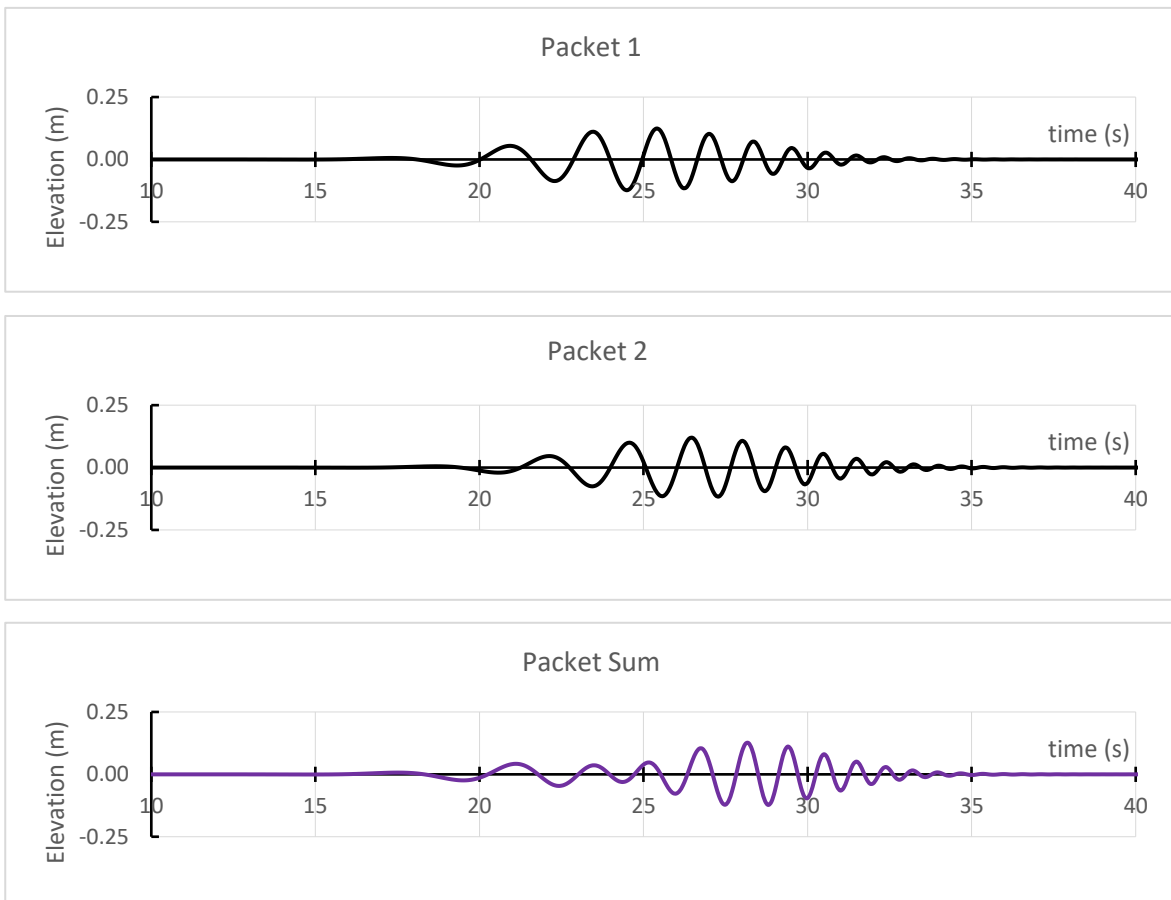


**Figure 3.17 (a, b, c)** – *Simulated results in Example 4.*

*Simulated Example 5 – Two identical packets offset in time to give constructive interference –*
*Figure 3.18*

If the time offset is sufficient, two identical packets can be made to constructively interfere almost perfectly, giving a composite with nearly identical overall packet length and fundamental periods, and around double the height of the component packets. The only feature of the composite packet that suggests it is a composite is the waviness at $t \sim 30\ s$, which distorts the envelope shape.
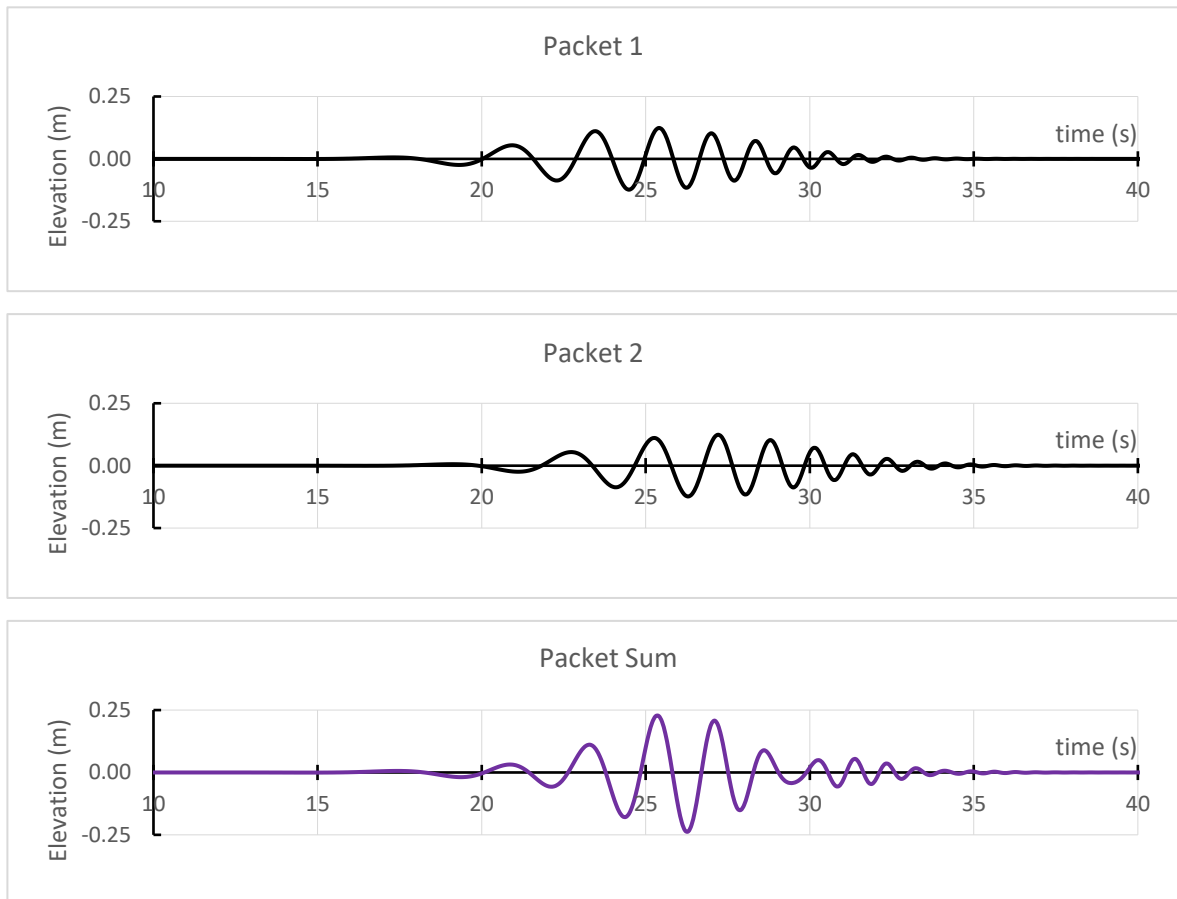


**Figure 3.18 (a, b, c)** – *Simulated results in Example 5.*

*Simulated Example 6 – Two similar packets, offset in time to destructively interfere – Figure 3.19*

This would give the appearance of rapid decay, at least at the point of measurement. Even worse, if this were a single probe measurement, the height would be misrepresented. As the packets in this simulation propagate at slightly different group velocities, the sum would change. That might explain what is often seen at slow speeds: near-field height increasing (or stable) before decaying in the far field, but not everywhere. It is often the case in full-scale trials at slower speeds that there can be great variation in wave height depending on the lateral separation (refer Figure 3.16), which is why the use of only a few wave probes can be misleading. This is discussed further in Section 7.3.4.
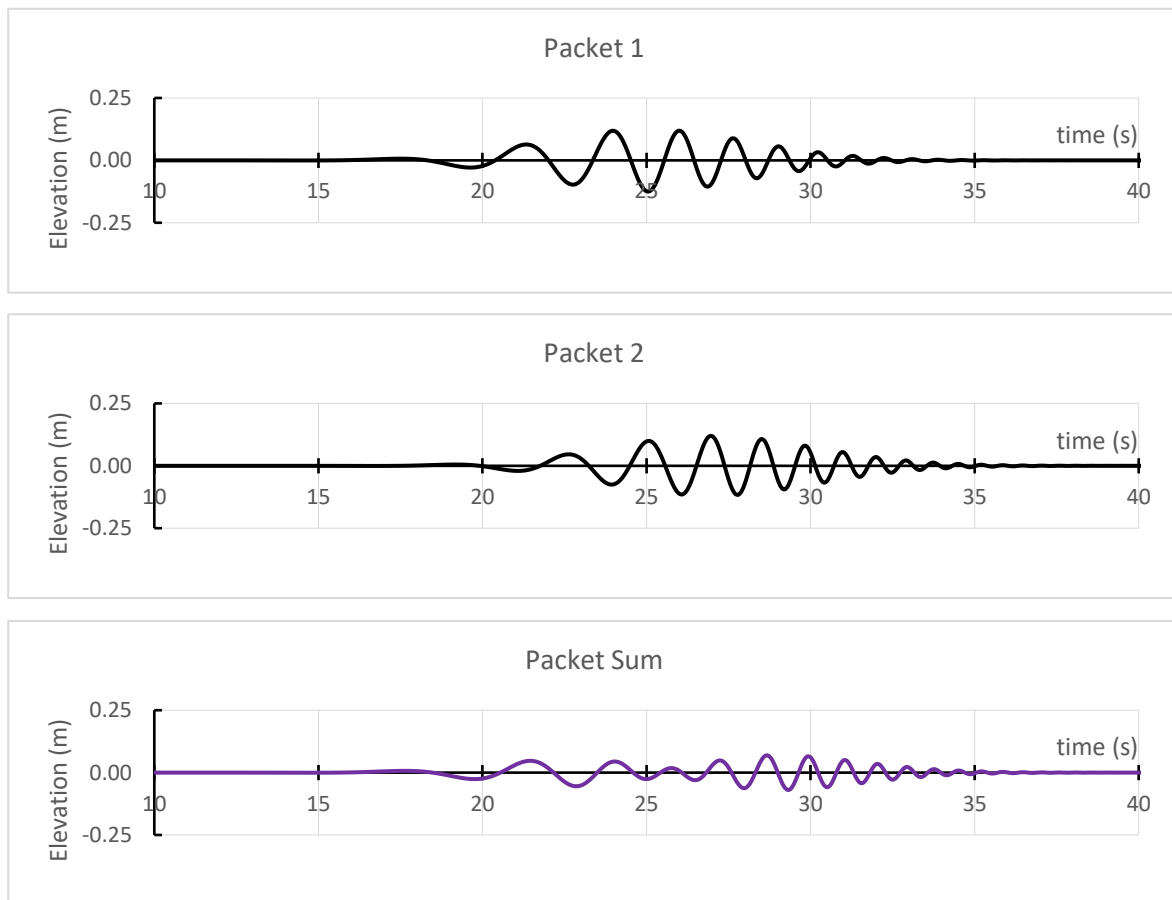


**Figure 3.19 (a, b, c)** – *Simulated results in Example 6.*

*Simulated Example 7 – Two packets, same height but very different periods – Figures 3.20 and 3.21.*

A normal divergent packet is superimposed onto a very long-period packet. The result is what is typically seen in the near field of a vessel travelling around the depth-critical speed, consisting of a very long surge followed by a drawdown and a decaying packet. If *Packet 2* consisted only of a solitary wave, the drawdown between the two packets would not occur. That suggests that the surge evident in a shallow, restricted channel at near depth-critical speeds is not wholly comprised of a solitary wave.
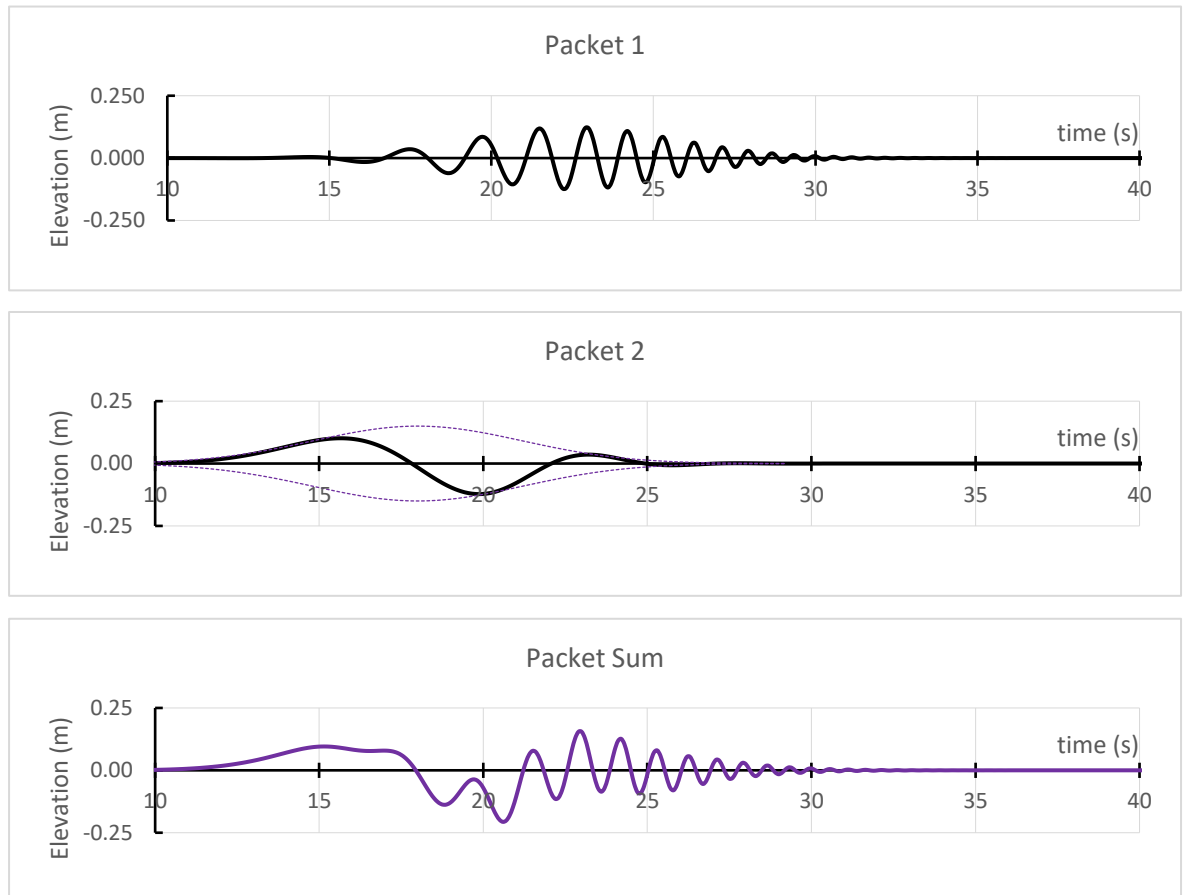


**Figure 3.20 (a, b, c)** – *Simulated results in Example 7.*
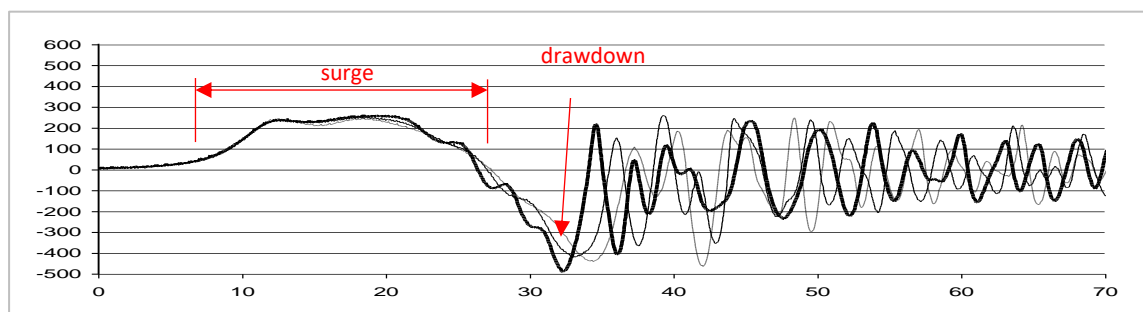


**Figure 3.21** – *Experimental version of Example 7 from Cox (2000, Fig. 11): model AMC 97-30 at full scale: $Fr_h = 0.95$; $Fr_L = 0.23$ (x-axis: Run Time in seconds; y-axis: W.S.E. in mm). Three near-field probe traces (**0.3L**; 0.5L; 0.7L) are shown. Note the surge with superimposed waves on top, similar to Figure 3.20c. The model test was conducted in the AMC towing tank and so reflections contaminate the trace after about 40 s.*

45

## 3.7    Wave Energy and Divergent Waves

As in coastal engineering, wave energy is described using linear theory or a variation of it, even in shallow water. That is largely because of the limited wave information available, which may only be height, period and water depth. For energy, the general equation of $E = \rho g H^2 \lambda / 8$ can be applied with reasonable engineering accuracy at any depth, provided the wavelength is known. The wavelength may be derived from a non-linear method, so in that regard the energy is a hybrid linear/non-linear relationship. In deep water, where the wavelength is determined by the simple relationship $\lambda = gT^2/(2\pi)$, the general equation devolves into $E = \rho g^2 H^2 T^2/(16\pi)$.

In very shallow water, when the Ursell number is greater than about *40* (refer to the Section 5), an appropriate non-linear theory must be applied to determine the wavelength correctly. Calculation of energy in shallow water is further complicated if the wave parameters are transposed from deep to shallow, with errors in transposed height and wavelength having a non-linear effect on the calculated energy. The only wave in a wave wake record that can be transposed is the maximum wave (the wave at the packet envelope maximum) because it is the only wave where its period is defined (and constant) everywhere and its height can be estimated with some accuracy. Other visible waves at one point in space and time will have evolved into something else at another point in space and time.

The usually repeated edict is that energy spreads along the length of the crest as a wave propagates, hence the attenuation in height. This is referred to in wave wake studies as diffraction. The origin is not clear, though it seems to have originated from Johnson (1957), who was an early wave wake researcher. Johnson was a coastal engineer, and the explanation would have appeared quite plausible in an ocean wave sense. Ocean waves, once generated, may propagate without additional energy input. If they propagated in isolated packets on an otherwise smooth sea, their energy would spread laterally as well as propagating forward. Wave fields consist of many wave packets that support each other laterally and eventually combine over time, which mitigates the lateral spreading.

The difference is that the energy input from the vessel (the generating source) is continuous when the vessel is travelling at a constant speed, unlike the wind energy input that creates water waves that propagate away. The waves being formed under the action of wind are termed *seas* and the residual waves that continue after the wind has died are termed *swell*. A vessel travelling at constant speed burns fuel at a constant rate per nautical mile and that energy directly relates to the resistance components, including wave energy.

For the divergent waves, energy doesn't spread along the wave crests; it spreads along (or across) the wave packet due to dispersion. The total energy in the packet per unit width (measured crest-wise) remains constant, but the energy is distributed across an increasing number of waves as lateral separation increases. In shallow water the effect is the same, except that the rate of dispersion changes non-linearly throughout the packet (non-dispersive at the leading crest at the head of the wake to fully dispersive at some point behind that). In the case of the transverse waves, which are trapped within the caustic boundaries of the Kelvin wedge, there is an argument for diffractive decay. This is further discussed in Section 6, where additional discussion of wave energy and wave power can be found.

# Section 4 – Deep Water

*Now, the next waves of interest, that are easily seen by everyone and which are usually used as an example of waves in elementary courses, are water waves. As we shall soon see, they are the worst possible example, because they are in no respects like sound and light; they have all the complications that waves can have.*

*Richard Feynman*
The Feynman Lectures on Physics[40]

## Summary

Wave wakes in deep water are often considered to have the least complicated structure, but the existence of multiple, interactive wave systems within the wake makes them the most difficult to assess. Much of the misunderstanding and misinterpretation of deep-water wave wakes stems from the difficulty in distinguishing between superimposed wave systems at the point of measurement. The shallow water condition has the benefit of the absence of the transverse system and more distinguishable divergent systems, though in a more complex format.

What constitutes *deep* for waves in general may not be the same for the vessel that creates them. That is because of the inconsistent relationship between vessel speed and the wavelengths generated within the different systems present.

The transverse wave system is comprised of waves with a speed-dependent wavelength, which implies that these waves might become depth affected even in relatively deep water if the vessel speed is sufficiently high. However, the transverse wave system dies away at high speeds ($Fr_L > \sim 1$). Conversely, at high speeds the principal waves in the divergent system have speed-independent wavelengths approximately equal to the waterline length. The combined effect leads to a condition where $h/L > 0.5$ is essentially *deep* in high-speed wave wake terms (though there may still be a minor hull resistance augment), and an even smaller ratio is possible at slower speeds. That is important, as the application of deep-water techniques can simplify the analysis of waves.

Most small craft have planing hull forms that introduce further dynamic complications into the relationship between vessel resistance and wave energy. Although they are the most common small craft form, their dynamics are often misunderstood and misrepresented in wave wake studies.

## 4.1    Introduction

In the field of water wave mechanics, the deep-water condition, devoid of the complications of depth, was the simplest to be considered. The initial understanding of wave mechanics was very much on a mathematical level; progressed by the likes of Airy and Stokes (among many) (Craik, 2004). At a practical level in the *19ᵗʰ* century, Scott Russell developed his wave line theory of hull design (Phillips-Birt, 1966), though it had as much to do with artistic flair as it did science. Similarly, Brunel's *Great Eastern* was built at the extreme length of *692 ft* (*211 m*) to make it

---

[40] Feynman, R.P., Leighton, R.B. and Sands, M. (1963). *The Feynman Lectures on Physics.* Boston, MA: Addison-Wesley. Volume I, Chapter 51-4.

47

longer than any known wave at sea (Dugan, 1953). That, too, had more to do with salesmanship than science. Scientific application of wave mechanics to ship design was only embraced in the late *19th* century, notably with the work of William Froude and the testing of HMS Greyhound (Brown, 2006). The deep-water condition progressed into the shallow water case, and only then was it realised that "*the more you know, the more you find you don't know,*" which is why the study of ship waves has progressed unendingly for more than *150* years.[41]

Boats are peculiar in that they produce waves that cannot be considered as random or unorganised regardless of how they may appear, unlike ocean waves or chaotic stream flows.[42] One of the unending problems of wave wake analysis has been the analysis of the waves and how they relate to the vessel and the environment. That appears regularly in technical papers, depending on the background of the researchers. The naval architects understand ship waves (though, more often than not, poorly!) and the coastal engineers understand the statistical nature of ocean waves, but neither really understands the other. Ship waves are not statistical entities; they are an inter-related, extended family emanating from a common origin.


## 4.2 What Constitutes Deep?

This is divided into two parts – the waves and the vessel.

### 4.2.1 Waves

For a wave, coastal engineers define deep water as the point where the wavelength is less than twice the water depth, or $\lambda/h < 2$. At that condition, a wave's celerity is *99.8%* of what it would be in infinitely deep water. There is engineering benefit in carrying the simple, deep-water linear wave equations through to modestly shallow water. This leads to the introduction of the term *practically deep*, which assumes the *approximately deep* condition of Lighthill (1978, p.216) when a wave's celerity is within *3%* of its deep-water value. The limit of this is when $\lambda/h \sim 3.5$ (or $h/\lambda > 0.28$ to be regarded as adequately deep, as preferred by Lighthill). Almost nothing is lost in the application of this extended limit, and there are very practical benefits when applied to small craft wave wake evaluation. A complementary term - *practically shallow* - is presented in Section 5; defined as the condition where a wave's celerity is within *3%* of the linear wave shallow water limit of $\sqrt{gh}$.

The Shore Protection Manual (Coastal Engineering Research Center, (CERC) (U.S.), 1984) Fig. 2-6 delineates linear wave theory equations into three depth zones: deep water ($\lambda/h < 2$); transitional water ($2 \leq \lambda/h < 25$); shallow water ($\lambda/h \geq 25$). The application of linear theory to anything beyond modestly transitional water ($\lambda/h \sim 7$, but certainly not more than $\lambda/h \sim 10$: refer Section 8) would incur increasingly erroneous results. For engineering calculations, where the uncertainly about the incident wave climate may be sufficiently large to tolerate moderate error in calculated wave parameters, application of linear theory is quick and simple. In an over-arching wave wake regulatory assessment, application of linear theory would be considered adequate.

---

[41] "*the more you know, the more you find you don't know*" has been attributed in various guises to Socrates, Aristotle, Einstein and Trump (@realDonaldTrump, 30th June, 2014), though in this post-fake-news world it's difficult for some to acknowledge who came first. Sad.

[42] In that regard a bore, or a rock in a shallow stream, could be considered as equivalent to a boat in that the waves produced are not random or chaotic.

### 4.2.2 Vessels

Generic vessel wave wake forms are covered in almost any textbook or paper addressing ship waves (Newman, 1977; Lighthill, 1978; Havelock, 1908, as examples).[43] Only those characteristics pertinent to this study are addressed in detail rather than the science in general. Height decay and wave dispersion are addressed separately.

Two wave systems are generated in deep water: *transverse waves* and *divergent* (diverging) *waves*. As is often necessary for the sake of colloquial explanation to a non-technical audience, these are further simplified to *stern waves* and *bow waves* respectively, ignoring the fact that divergent waves can be generated at several locations along the hull and not just at the bow. The two wave systems are quite different and, other than their interaction, are accounted for separately.

It has been a tradition to conduct high-speed vessel speed trials in water at least as deep as the vessel's waterline length to avoid shallow water resistance effects.[44] The transverse wave system accounts for the longest waves and has an intimate relationship with speed, such that $\lambda_T = 2\pi V^2/g$. Using the upper-limit definition of *deep* ($\lambda/h = 2$), the transverse waves would feel the bottom at $Fr_h = 0.56$; at the definition of *practically deep* ($\lambda/h = 3.5$), that would be reached at $Fr_h = 0.75$. For high-speed vessels, the transverse system gradually depletes at speeds above $Fr_L = 0.5$ and so the effects of the *practically deep* condition at high speed would apply more to the divergent waves, which are shorter.

Correction of trials performance due to water depth is widely reported, though most of the methods are only relevant to displacement speed vessels. The method reported in ITTC (1969) was based on the relationship where $h > 2.75\,V^2/g$. That has since been replaced by an equation based on Lackenby's method, which relates shallow water resistance augment to depth Froude number, midship section area, and depth (refer ITTC, 1969). Unlike the older methods, there is no direct correlation with vessel length in the Lackenby method. ***Figure 4.1*** shows graphically the limiting $h/L$ ratio for three different definitions of *deep* based on transverse wavelength/depth ratios. For higher speeds ($Fr_L > 0.5$), the gradual depletion of the transverse system reverts to the present rule-of-thumb of $h/L > 1$ being adequate. There is a difference between incremental resistance effects and wave wake effects as the depth begins to shoal – resistance changes having greater design and operational importance.

---

[43] Though often quite superficially and either littered with schematic over-simplifications or presented in a complicated manner that doesn't add to a practical understanding.
[44] From the author's industry experience.
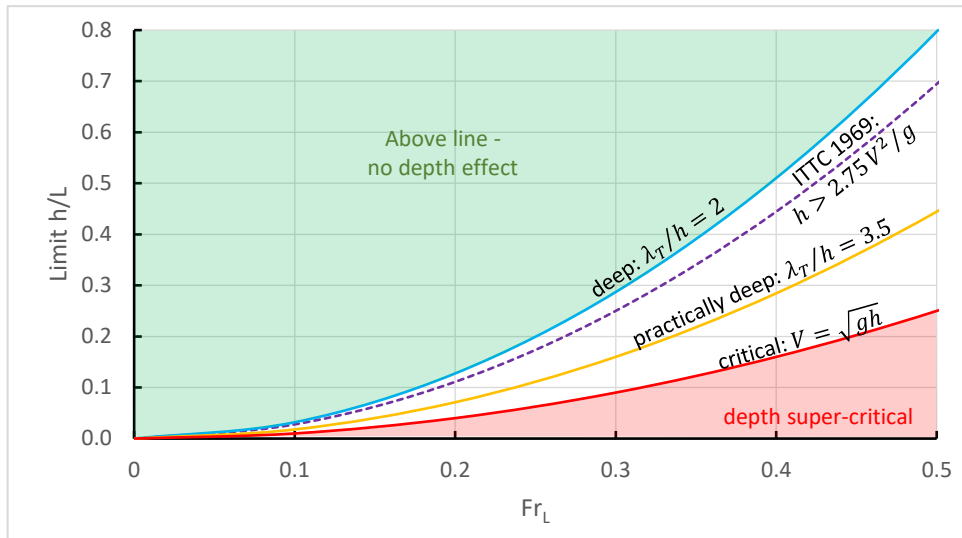
**Figure 4.1** – *Transverse wave limiting condition of $h/L$ ratio for $Fr_L \leq 0.5$, based on four depth definitions: deep; ITTC 1969; practically deep; linear theory critical depth. The ITTC curve relates to resistance augment; the limit being defined by the ITTC as a speed reduction of maximum 2% due to shallow water depth effects. This would be a more onerous condition than any significant variation in the wave wake, in which case the practically deep condition would be sufficient for all depth Froude numbers where the transverse wave system was present.*

The divergent system wavelengths are shorter and do not have the same intimate relationship with vessel speed (refer Figure 4.3 following). As an approximation, the dominant, deep-water divergent system waves have wavelengths in the order of $L$ (Lighthill, 1978, p.274). Macfarlane *et al.*, (2008, Fig. 3) confirmed this experimentally. In that case, the dominant divergent waves would not feel the bottom until $h/L < {\sim}0.5$ and would not be regarded as shallow water affected until $h/L < {\sim}0.28$ (and for speeds above $Fr_L {\sim} 0.5$ at $h/L < {\sim}0.28$, the transverse system would disappear due to depth criticality – refer Figure 4.1). Although the wave wake itself would have evolved into a depth super-critical system by that stage, the features of the divergent packet would be similar to those of a deep-water packet. With further shoaling, the divergent wave system gradually assumes the features of a very shallow water system where the leading wave begins to dominate the packet (refer to Section 5).

A minor complication is that dispersive wave packets are comprised of multiple wavelengths. Vessels generate multiple packets, and the leading packet with its longer wavelengths is the first to arrive in the far field. Not all waves within a packet, or the packets themselves, become depth affected at same time. As wave packets move into shoaling water, the leading (longer) waves are the first to become depth affected. The highest waves in deep water are found towards the middle of their respective packets where the wavelengths are shorter than at the packet head, so they do not become depth affected at the same time as the leading waves.

When the leading waves become depth affected, packet dispersion and the rate of cycling of energy through the packet changes. This slowing rate of energy cycling through the packet when the leading waves shoal may reduce the height of the maximum wave, even if it is not itself depth affected. That is discussed further in Section 5 and supported by experimental examples in Appendix D. It is only important if the maximum wave is measured in (marginally) deep water and the leading waves are already substantially depth affected.

### 4.3    Transverse Waves

At a steady-state vessel speed the transverse waves appear monochromatic: their celerity is equal to that of the vessel and therefore their deep-water wavelength ($\lambda = 2\pi V^2/g$) and period ($T = 2\pi V/g$) are functions of vessel speed. Consequently, they are easily discernible on a frequency spectrum and (if necessary) can be extrapolated across a deep-water wave wake trace and subtracted to show the approximate divergent-only wave pattern.[45]

The height of a transverse wave varies laterally along its crest and (counter intuitively) increases away from the sailing line towards the Kelvin wedge. This was shown by Havelock (1908) (though his approximation resulted in a singularity and infinite height at the Kelvin wedge) and confirmed by experiments (Bertenshaw, 2018). The crest height of a transverse wave on a nominal ray *12⁰* either side of the sailing line is increased *18%* over that at the sailing line. At larger angles the divergent system begins to dominate; the transverse system never reaches its theoretical height and ends up superimposed on the divergent system.

In rivers, the transverse system becomes trapped by the banks and therefore doesn't experience the height decay along the sailing line that would otherwise occur in open water. The transverse system is known to exist in width-restricted waterways long after the vessel generating it has passed. Eventually all the energy in the transverse system is expended at the shorelines, but the erosive mechanisms are slightly different to those of the divergent system. Rather than waves impinging at an angle to the shoreline as with a divergent system, the transverse waves create a shearing action from the orbital celerity component in the wave.[46] This is further discussed in Hill *et al*. (2002) (reviewed in Appendix A). Additionally, the bank structure can be weakened by the cyclic variation in pore pressure created by the passing waves, which gradually opens fissures as pressurised water is forced laterally through the bank material during the relatively short-period wave cycle.

The height of the transverse system is largely a function of hull draft and displacement (among other influences), but there is more to it than that. Catamarans are known to produce strong transverse systems; apart from the transverse system generated by each hull, the transverse system is complicated by the wave interference between the hulls and the travelling depression it produces. It is difficult to compare catamarans and monohulls on an equivalent basis, but in general catamarans tend be shorter for the same displacement (monohulls require increased

---

[45] Showing as a spiked peak, but in the analysis of model tests the frequency response of the transverse wave system is often spread due to the limited length of the steady-state condition at higher speeds (there is usually a period decay throughout the wavetrain as the shorter transverse waves generated in the acceleration phase are never far behind – refer Figure 4.9). The spiked peak feature can give the impression that the transverse waves are monochromatic, which they appear to be in the narrow window used to construct the Fourier analysis, but the train is comprised of multiple frequencies generated during the acceleration from rest (Kelvin, 1887): the longer the steady-state condition, the more peaked the response.

[46] Using linear theory, the horizontal and vertical orbital celerity components are $u = \omega A e^{ky} \cos(kx - \omega t)$ and $v = \omega A e^{ky} \sin(kx - \omega t)$ respectively, where $A$ is wave amplitude and $y$ is the mean distance from the free surface. The maxima occur when $y = 0$ and have the values of $u_{max}, v_{max} = 2\pi A/T$ (though out of phase by $\pi/2$). This is a slight simplification as it assumes a deep-water condition, which may or may not be the case depending on the bank geometry (scarp or beach) and the wavelength. A shallow water condition at the bank would be not dissimilar, but with an elliptical action (increased horizontal velocities) and wave refraction. Non-linearity causes the velocities to vary between crest and trough due to Stokes' Drift, being higher at the crest than the trough, though this is minor for small waves.

length to achieve the same deck area as catamarans) and with deeper hull draft. Low-wash catamarans are an exception, with their weight-minimising design features.

In deep water, the transverse system dies away at high speeds. It is not known whether the waves die away due to the intimate relationship between their wavelength and vessel speed, and the inability of vessels to generate very long waves, or if the waves do exist at high speeds but are too small to measure.[47] **Figure 4.2**, taken from Tuck and Lazauskas (1998, Fig. 1), shows the wave resistance ($R_w$) components of a Wigley monohull form and the contribution of the transverse and divergent (*diverging*) systems. The relative strengths are dependent on the hull form and its parameters. The drag of the transverse system reaches a maximum at $Fr_L \approx 0.48$, and at $Fr_L = 1.0$ (*13.7 m/s*) the drag of the transverse system has reduced to around *4%* of its peak value and just *1.5%* of the total wave system. Interestingly, a volumetric Froude number of ~3.35 (which is the defined point where a planing hull form is supported fully by dynamic lift) occurs at *18.5 m/s*, which is also the point where the transverse system is effectively depleted and the total wave resistance curve reaches a plateau. The Wigley hull is not a planing hull form.
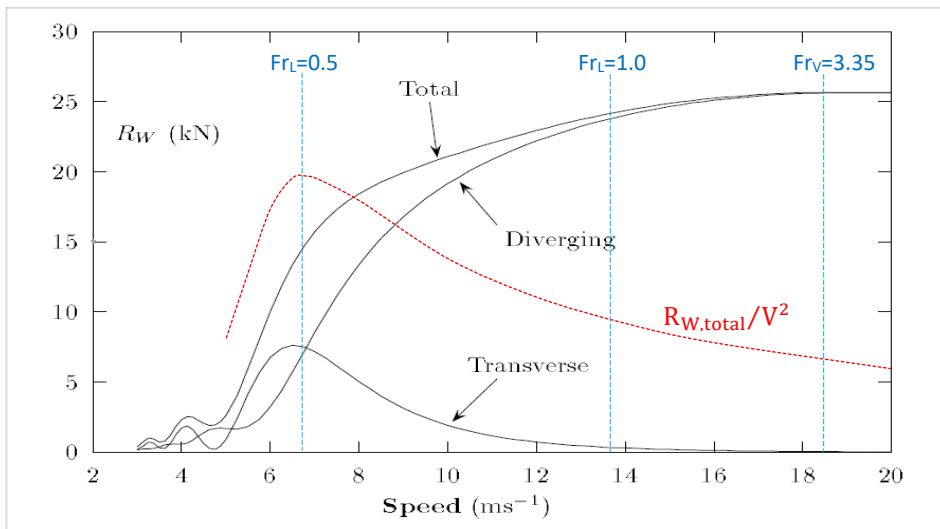


**Figure 4.2** – *Reproduced (embellished) from Tuck and Lazauskas (1998, Fig. 1): wave resistance components of a Wigley hull (L = 19.1 m; Δ= 31.25 t; T = 1.25 m; SR = 6.11; $Fr_L$ = 0.5 at 6.84 m/s). Superimposed is the curve of $R_{W,total}/V^2$ (without vertical scale), showing the peak at $Fr_L$ = 0.5 (refer to discussion of this in Section 4.4). The parameters of the maximum divergent wave w.r.t. speed reflect the wave drag coefficient, not the total wave drag.*

**Figure 4.3** shows the transverse wave parameters against length Froude number for a slender monohull with an unusually high slenderness ratio, which tempered the heights but not the overall distribution of each parameter with speed. The transverse wave periods have been calculated (using $T = 2\pi V/g$) and not measured, due to the difficulty measuring the periods experimentally for such small waves. Three points are of note:

---

[47] Reference is made to Gadd (1994) and the claim that vessels cannot generate *significant* waves longer than around $3L$. At $Fr_L = 1$, the transverse waves would have a wavelength of $2\pi L$, which is double this, or would have a wavelength of $3L$ at $Fr_L = \sqrt{3/(2\pi)} = 0.69$. Gadd may have been referring only to divergent waves, though didn't state as much. The wavelength of the significant divergent waves should be ~$L$.

a. The maximum height occurs at $Fr_L = 0.5$, as expected, and decreases rapidly with increasing speed;

b. Wave energy ($E \propto H^2 T^2$) at high speed mirrors the wave height curve (with the effect of reducing height offset by increasing period), but falls quickly at slow speeds (height and period both reducing with reducing speed);

c. Vessels can operate at speeds up to around three-quarters of their *hull speed* (hull speed defined as $Fr_L = 0.399$), and at high speeds $> Fr_L \sim 0.75$, without producing transverse waves with significant energy. However, energy is not necessarily the wake parameter than defines the erosion potential of transverse waves; the intensity of both erosion mechanisms previously mentioned (shearing action and pore pressure) are increased with reducing wave period (refer footnote 46).[48] The obvious diametric example of that is the negligible short-term erosive effect of a tidal range, due to the extremely long period and low inherent velocities.

The last point is of relevance to small craft studies; the point where the transverse system becomes negligible (or non-existent) occurs at lower absolute speeds. For instance, a recreational craft with a static waterline length of *5 m* would have a negligible transverse wave system at speeds above *14 kn*, which is likely to cover most recreational activities except for wakesurfing.
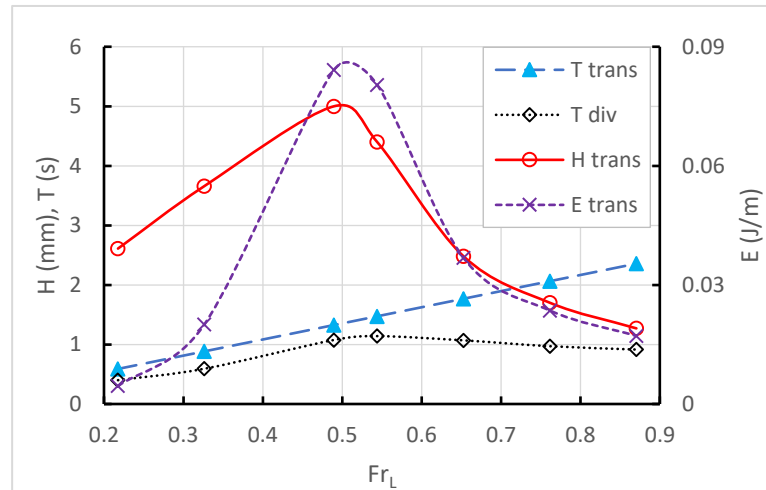


**Figure 4.3** – *Transverse wave parameters for a slender (high-speed) monohull model (AMC 99-17) measured at 0.3L from the sailing line on the first visible transverse wave. The transverse wave periods ($T_{trans}$) were calculated from the model speed. Although wave energy is low at slow speeds due to the short period, the height is not low, and the combination of moderate height and short period increases the orbital celerity and bank shearing action. The periods of the first divergent packet maximum wave at $y = 0.7L$ (noted as $T_{div}$) are shown for later discussion.*

---

[48] This is not an argument in itself. Transverse wave period is a function only of vessel speed and cannot be manipulated by design. A slower speed would reduce transverse wave period, inducing a faster scouring action and increasing the erosive potential, but it would also reduce the transverse wave system height below $Fr_L \sim 0.5$. One would tend to offset the other.

## 4.4    Divergent Waves

The divergent waves, which propagate obliquely from the sailing line, are probably the most studied but the least understood practically. Part of that lack of understanding is the complexity of the multiple divergent systems that all vessels produce, and part is their over-simplification (and often the perpetual misunderstandings). Some of the principal features of the deep-water divergent system are explained.

Vessels produce several packets of divergent waves; often three, emanating from the bow, stern and forward shoulders (or chine entry point, if pronounced). With sufficient lateral separation for the packets to disperse, more than three may be visible.[49] At first glance the bow and stern divergent systems can be very similar, but the others have different fundamental wavenumbers. That is a generalisation and cannot be applied everywhere. Vessels with more prominent transom sterns, such as planing craft, tend to produce similar bow and stern packets. Vessels with a streamlined aft end tend to produce dominant bow divergent packets and small transom divergent packets. The strength of the packet is a function of the strength of the disturbance. The presence of multiple, superimposed packets complicates wave wake analysis and is almost certainly the reason for the ongoing debate about wave height decay rates and standards for interpretation and measurement.

An apparent peculiarity of the curves in *Figure 4.2* is that the resistance due to the total wave system continues to increase above $Fr_L = 0.5$, yet this is known to be the point where the height, period and energy of the maximum wave reach their greatest values, and at speeds beyond which they reduce. The answer is that the wave resistance coefficient ($\propto R_w/V^2$) is reducing after reaching its maximum value at $Fr_L = 0.5$ (where the wave resistance coefficient's exponent of speed is exactly *2* in this example). That leads to the question of how the extra wave energy at high speeds, reflected in the increasing wave resistance, is entering the wave system and in what form. That extra energy is not reflected in the maximum wave parameters. If that is the case, is the regulatory premise that operating at a higher speed is preferable to operating at a moderate speed correct? That is another example where the quantity of energy delivered is less important than the form in which it is delivered.

Low-speed vessels (displacement hull forms), signifying those designed to operate at $Fr_L < 0.399$ rather than high-speed forms operating with low input power, operate in the very worst speed range for the satisfactory analysis of wave wake. Their speeds are too slow for the individual packets generated to combine into (almost) one, often leading to what appears as a very long and confused divergent packet due to the slower rate of dispersion resulting from the very modest wave periods. This is explained in the discussion following. The strong transverse system created by the displacement hull form at slower speeds has periods similar to the divergent waves, which causes localised constructive and destructive interference to the wake signature. Only at high speeds, when the transverse system periods increase and heights decrease, does this interference subside. *Figure 4.3* explains this: the divergent and transverse waves have similar wave periods and period variation with speed up to $Fr_L = \sim 0.5$, after which they diverge abruptly and

---

[49] Many packets are evident in this photo of a paddle steamer by Klaus Leidorf:
http://www.leidorf.de/components/com_zoom/www/view.php?popup=1&q={obfs:2252272082192242632752762862272152122652172232032632732762732862272152122652192092592242152192142632862272152122652202192082 63275} (last accessed 5th August, 2019).

markedly. The different wave systems strongly influence each other at slow speeds, especially in the near-to-medium field, but much less so at high speeds.

Model test results were analysed for their packet development, with an emphasis on high-speed vessel hull forms. At slow speeds in the near-to-medium field, the two main packets (assumed to be bow and stern divergent) are clearly visible in most cases. This is only the case before dispersion allows the leading (longer period) waves in the second packet to over-run the trailing (shorter period) waves in the first packet. When that occurs, it becomes difficult to separate the packets visually. *Figure 4.4* shows two model test examples (AMC 99-17) at low-to-medium speeds in deep water (deep relative to the divergent and transverse wavelengths generated).
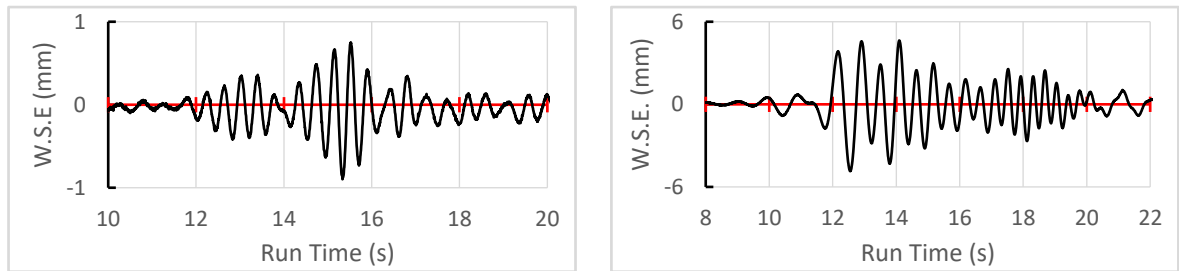


**Figure 4.4 (a): _left_; (b): _right_** – *Divergent wave packet development for model AMC 99-17.*

**Figure 4.4(a):** $L = 1.824 \, m; V = 0.75 \, m/s; Fr_L = 0.18; h = 0.9 \, m; Fr_h = 0.25, y = 1.64L.$
  Note the two distinct wave packets ($12 \, s < t < 14 \, s$ and $14 \, s < t < 16 \, s$). At this speed, the model travels one waterline length in *2.43 s*, which is exactly the time separation of each packet (measured between maximum waves). The packets represent bow and stern divergent systems. The consistent time separation viewed over several wave probes also suggests that the packets have the same fundamental wavelength. This is important, as it means the packets will not distance themselves readily; their time separation being only an inverse function of vessel speed. With time they will disperse; the packets will lengthen and spread over each other, but at a rate and lateral separation dependent on the speed-dependent fundamental periods. The constant packet periods also show another important relationship – that these fundamental periods are a function of vessel length. The period of the transverse waves is *0.48 s*. These waves are clearly distinguishable as the first several waves following the second packet.

**Figure 4.4(b):** $L = 1.824 \, m; V = 1.75 \, m/s; Fr_L = 0.41; h = 0.9 \, m; Fr_h = 0.59; y = 2.47L.$
  This represents the highest speed in the test programme at the tested depth to maintain all deep-water characteristics ($Fr_h < 0.75$). Note the waviness in the first apparent packet envelope ($12 \, s < t < 16 \, s$) and the lumpiness of the very first small waves ($9 \, s < t < 12 \, s$), indicating two packets with similar fundamental wavenumbers on top of each other but slightly offset in time. These features are simulated in Section 3 (Figures 3.17-3.19). Also note the emergence of the third, short-period divergent packet around $17 \, s < t < 19 \, s$. As speed increases, this third packet becomes prominent in height, but with short periods. The total energy of this packet is much less than the first packet(s), even though it dominates visually at high speeds.

*Figure 4.4(b)* requires further analysis and is shown below as *Figure 4.5*. The waviness of the crests and troughs may be caused (wholly or partially) by the underlying transverse wave system. The mid-height of each wave face and back are marked, through which an approximate curve can be fitted. This does have the appearance of a decaying transverse system and the first several crests approximate closely the transverse system period of *1.12 s*. By subtracting this underlying transverse wave system from the crests and troughs, the approximate envelope can be developed. Although it looks reasonable, there is some residual waviness in the envelope that might be from bow and stern divergent systems. The question then becomes – when we measure such a wave wake, what are we actually measuring?

A Fourier analysis was performed on *Figure 4.5*; shown in *Figure 4.6*. Three peaks are evident. The first correlates with the calculated transverse wave frequency. The second band corresponds to the average frequency at the envelope maximum in *Figure 4.5* (around run time *13.25 s*) and the third band corresponds to the short-period waves following the main group (run time *17 s* to *19 s*). The difficulty with a Fourier analysis is that it will only show the spread of frequencies and not the existence of multiple wave packets if those packets have similar characteristic frequencies. Whether or not the main divergent packet is comprised of one or more packets remains unknown. It may be possible to determine this by the temporal variation in the individual wave periods. If two similar packets were partially overlapped, resulting from the packets dispersing into each other, there may be a waviness in the resultant periods of consecutive waves in the packet. This was reviewed but the results were inconclusive.
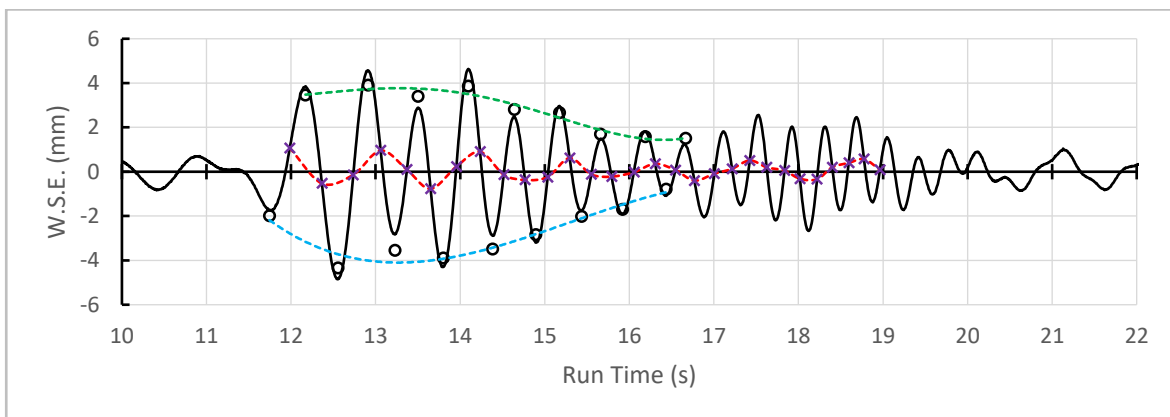


**Figure 4.5** – *Modified version of Figure 4.4(b). By taking the mid-point of every wave face and back (cross markers), an approximate underlying transverse wave system can be developed. It corresponds well to the calculated transverse system period of 1.12 s. Subtracting this wave from the crests and troughs of the main trace (hollow circles) gives an approximate envelope shape, which is indicative of a dispersing packet but with some residual waviness. That could indicate two similar divergent packets in close proximity (refer to Figures 3.17 and 3.18 in Section 3).*
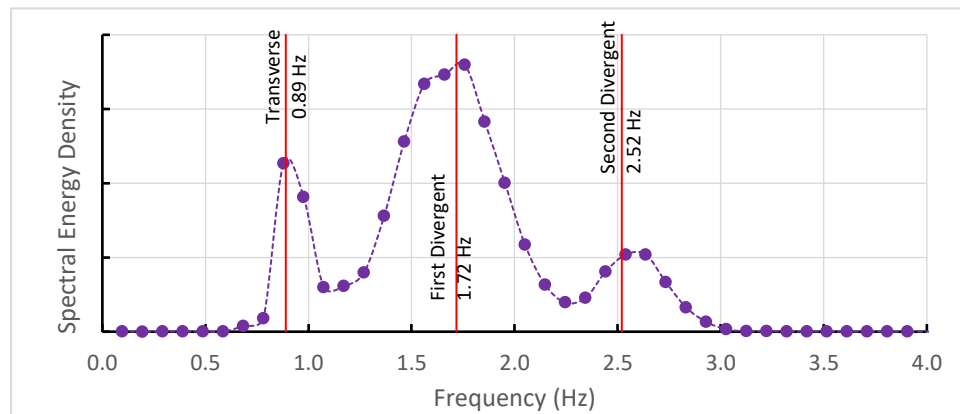
**Figure 4.6** – *Fourier analysis of Figure 4.5. The peaks correspond to those derived from the wave trace, but the composition of the main band in terms of the number of contributing wave packets remains unknown.*

At high speeds in deep water (at least $Fr_L > 0.5$ but more like $Fr_L > 0.6$ for consistent results), the appearance of the divergent wave wake begins to change:

- the various packets generated end up (mostly) on top of each other, leading to variability in the measurement of the principal wake features of height and period;
- the period of the maximum wave tends to become stable laterally and decreases only slightly with increasing speed;
- the height of the maximum wave also decays more consistently with lateral separation and decreases slightly with increasing speed. At the lower end of the high-speed range, packet superposition causes a degree of height instability laterally, which reduces somewhat as the transverse system becomes insignificant at $Fr_L > 1.0$ (refer Figures 4.2 and 4.3). For high-speed craft, which implies vessels with a higher slenderness ratio, the transverse system is usually less dominant to begin with.

*Figure 4.7* is a graphic example of deep-water wave wakes in two speed regimes: where the transverse system is strong (left figure) and where it is non-existent (right figure).
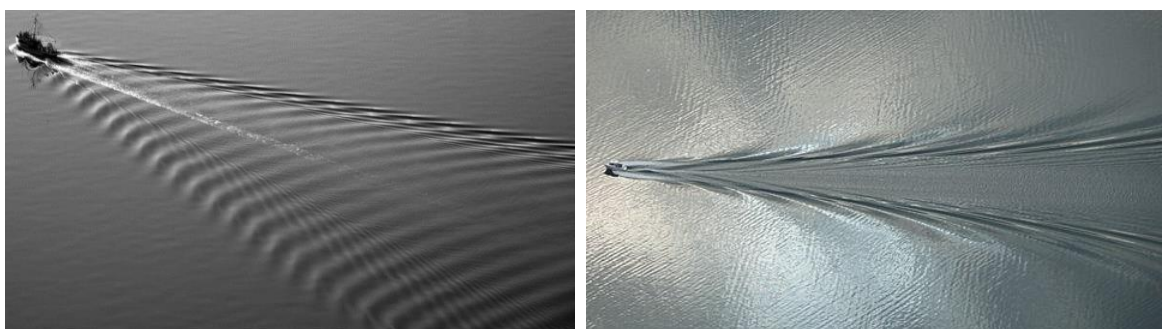


**Figure 4.7** – *Deep-water wave wakes. **Left**: Fishing boat wake with multiple divergent packets (at least two) and a strong transverse system, increasing in height towards the Kelvin wedge. The abrupt knuckle at the outer end of each transverse wave may be the true cusp, beyond which a phase shift between the transverse and divergent systems is expected (divergent lagging the transverse). (Photo courtesy Steff Abegg; www.stephabegg.com) **Right**: Small vessel ($L \sim 7\ m$) in very deep water (Preikestolen, Lyse Fjord, Norway; depth about 400 m). The transverse system is not evident, and the divergent system has the appearance of a shallow water wake, except that the waves are not absolutely long crested. (Photo by Edmont, https://commons.wikimedia.org/wiki/File:Fjordn_surface_wave_boat.jpg#/media/File:Fjordn_surface_wave _boat.jpg, CC BY-SA 3.0, last accessed 2nd August, 2019).*

### 4.5　The Wave Systems Relative to the Kelvin Wedge

It has long been known that wave wake records may not exactly represent the maximum values if the wave cut does not exactly correspond with the idealised intersection of the two systems at the Kelvin wedge (Johnson, 1957, as an example of many). The points of system intersection lie inside the Kelvin wedge, creating a phase shift at the wedge itself. At first reading there is apparent contradiction in the literature, though not necessarily. Newman states a *90°* (one-quarter) net phase shift at the Kelvin wedge (Newman, 1977, p.289), though between the transverse $(+\pi/4)$ and divergent $(-\pi/4)$ systems. Havelock and Lighthill both claim a $\pi/4$ phase shift at the Kelvin wedge (Havelock, 1908, p.423) (Lighthill, 1978, p.397), both using different methods. Havelock was describing a phase shift between transverse and *combined* systems, and Lighthill's explanation was in regard to single systems at caustic boundaries. Newman (double system) and Lighthill (single system) would concur, except that one phase is leading and one is lagging. The most important factor to note in its practical application is that there is a phase shift at the boundary and that the true "*cusp*" lies inside the Kelvin wedge.

Lighthill (1978, Fig. 97, p.390+) explains the localised reinforcement of a single system at a point inside a caustic boundary, its subsequent phase shift at the boundary and height decay beyond the boundary – all necessary to avoid the linearised singularity at the boundary. That localised point of reinforcement of Lighthill's *single* system decays with a -⅓ exponent, but only in a localised region inside the boundary. In ship terms, the caustic boundary becomes the Kelvin wedge. Beyond the wedge, each wave crest decays to zero exponentially. A simple schematic of this is shown in ***Figure 4.8***, based on the wave pattern of Newman (1977, Fig. 6.15) (refer to Figure 7.1 in Section 7 following). It explains several known features. Firstly, as noted by Hovgaard (1909) in field observations, the cusps form at an angle slightly narrower than the Kelvin wedge. Secondly, as noted by Newman (1977, Fig. 6.17) (refer Section 7, footnote 80), the wedge containing the waves appears to be shifted upstream about one boatlength. In that case it would contain *all* the waves, including those decaying beyond the wedge.

The importance for measuring wave wakes is that the very leading waves in a deep-water wave cut would be those decaying waves outside the wedge and may not reflect what is developing in the wave system as a whole.
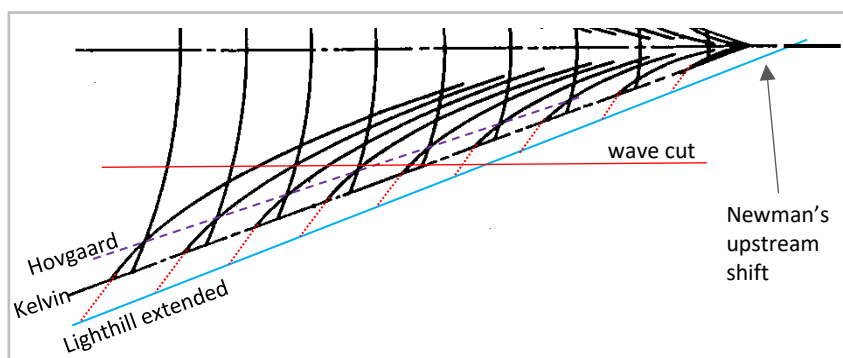


**Figure 4.8** – *Adapted from Newman (1977, Fig. 6.15), with reference to Lighthill (1978, Fig. 70). The phase shift at the Kelvin wedge leads to the apparent contraction of the cusp angle where interference between the systems is greatest. That concurs with Hovgaard's observations. Beyond the Kelvin wedge, waves exist and decay in height exponentially, explaining Newman's visual upstream shift of the wedge apex (Newman, 1977, Fig. 6.17). Note how a wave cut would record the extended waves as well as localised interference patterns. Recorded wave traces are never "clean", especially when the transverse system is present.*

A phase shift can be demonstrated experimentally, as shown in **Figure 4.9**, where the (extrapolated) transverse crest leads the Kelvin wedge and the highest divergent wave crest clearly lags the Kelvin wedge by at least one-quarter wavelength. The complication is that this divergent crest is not a pure divergent crest but a combined divergent/transverse crest. It could well be argued that the apex of the Kelvin wedge should not be the bow but some point slightly further aft where the vessel displaces enough water to initiate the wave system (refer Figure iii, and footnote 80 of Section 7). Also of note in **Figure 4.9** is the decay in transverse wave period experienced in model testing due to the limited length of the steady-state condition.
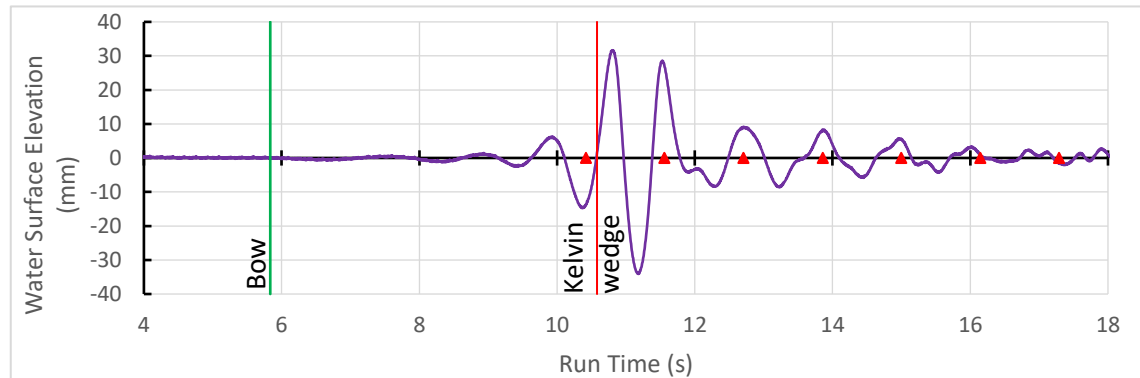


**Figure 4.9** – *Practically deep wake trace for AMC model 00-01: $h = 0.9\ m$, $V = 1.75\ m/s$, $y = 3.0\ m$ ($\sim 2.9L$), $Fr_L = 0.55$, $Fr_h = 0.59$. There is slight depth effect, but with only the very first wave long enough to be affected at all. The moderate vessel speed, which is below what would normally be considered as high speed, and the length Froude number close to the wave drag specific maximum value of 0.5, have the effect of concentrating the divergent packet into one with fewer waves but of greater intensity. In a high-speed vessel, this packet form would be seen much closer to the vessel. The red triangle markers indicate transverse wave crests ($\lambda_T = 1.96\ m$), which contract in period in the later stages as the shorter transverse waves generated during acceleration pass through. The (extrapolated) transverse crest leads the Kelvin wedge by about $+\pi/4$ (one-eighth of a phase) as defined by Newman (1977) and the maximum divergent wave crest lags, in this case by about a quarter phase. In fact, the maximum wave in this example is a "combined" wave (divergent and transverse, though possibly not perfectly cutting the "cusp") and the true position of the divergent system crest is difficult to define accurately. It is acknowledged that the line marked "bow" is its static position and so the Kelvin wedge would shift aft by 0.06 s per 100 mm of aftward shift in dynamic position (about double the thickness of the "bow" line).*

## 4.6     An Example of Confusion between Deep and Shallow Conditions.

Rich Passage (Puget Sound) in the USA has been a site of decades of high-speed ferry operation, environmental evaluation and litigation.[50] The route is somewhat unique in that the water depths are quite deep, and the seasonal wind-wave climate and currents are often more energetic than would be expected in sheltered/semi-sheltered waterways (Golder Assoc., 2013, p. 36). After the unsuccessful introduction of two large, high-speed catamarans (*38 m Chinook/Snohomish*), the government operator undertook several evaluations of suitable alternatives, including smaller, foil-assisted catamarans. The most evaluated of those was the *22 m* LOA *Spirit*.

---

[50] Wikipedia gives a comprehensive overview: https://en.wikipedia.org/wiki/Kitsap_Fast_Ferries (last accessed 1st August, 2019).

A comprehensive route study was presented by Osborne *et al.* (2009), where much of the discussion was premised on the need to avoid operation at depth-critical speeds. ***Figure 4.10*** (reproduced from Osborne *et al.*, 2009, Fig. 6) presents a diagrammatic interpretation of that analysis.[51] That analysis is, however, almost completely inapplicable to the vessel being studied (the *Spirit*), which has a stated waterline length of *20 m*. ***Table 4.1*** shows the various wave and vessel parameters that *Spirit* may encounter and none of them would correlate with ***Figure 4.10***. The water depth in Rich Passage (between Point White and Point Glover) is at least *24 m*. Osborne *et al.* (2009) note that Rich Passage is deep close to shore.

**Table 4.1** – *Parameter analysis for Rich Passage.*

| Wave Wake Condition | Criterion | Parameter Range | Complementary Parameter Range |
|---|---|---|---|
| *Transverse system depleted at high speed.* | $Fr_L > 1$ | $V > 27\ kn$ | $h > 20\ m$ to avoid any depth effects, even if small. |
| *Dominant divergent waves reach "deep" condition.* | $h/L \approx 0.5$ | $h > 10\ m$ | $V > 19.3\ kn$ to avoid any (minor) depth-critical speed effects (producing a deep-water-like wake) |
| *Dominant divergent waves reach "practically deep" condition.* | $h/L \approx 0.28$ | $h > 5.6\ m$ | $V > 14.4\ kn$ to avoid depth-critical speed (producing a super-critical wake). |

As a confirmation of this, ***Figure 4.11*** (reproduced from Osborne *et al.*, 2007, Fig. 5) shows the wave wake trials results of *Spirit*. The sailing line depth at trials was *84 ft* (*25.6 m*) and the depth at the wave gauge ($y \approx 4.3L$) was slightly deeper. The trials conditions are listed as $Fr_h = 0.91$ and $Fr_L = 1.08$; the length Froude number being incorrectly calculated using the vessel overall length and not the waterline length (correct value is $Fr_L = 1.15$). There are four points to consider:

a. the wave packet (Figure 4.11, upper) has the characteristics of a deep-water packet, with the maximum wave towards the middle of the packet and a well-defined, symmetrical envelope;

b. at such a high length Froude number the trace is devoid of an obvious transverse system;

---

[51] Osborne *et al.* (2009) state that: "*The speed at which H_{max} occurs is often referred to as the hump speed. The hump occurs when the ship produces a wake with a wavelength that is one-half the length of the ship.*" This is simply incorrect. The "*hump*" they are referring to occurs at $Fr_L \approx 0.5$ (refer Figure 4.2), when the transverse system wavelength is $\sim \pi L/2$ and the divergent wave system characteristic wavelength is shorter than the transverse waves (refer Figure 4.3 as an example). Using an idealised dipole hull model, the hump *would* occur at $Fr_L \approx 0.56$ when the bow (source) transverse and stern (sink) transverse systems constructively interfere. Vessels are not dipoles; their *effective length* is less than *L* and the hump always occurs earlier (refer Figure iii in *Definitions*). Note also the incorrect Eqn. 1 of Osborne *et al.*, where they substitute *L* for $\lambda$ into the linear wave celerity equation to claim that $V = \sqrt{(gL/\pi)tanh(\pi h/L)}$, which would only be correct when $\lambda = 2L$ and not $\lambda = L/2$ that they claim as the hump condition. Their understanding of the resistance hump is complicated by the fact that dynamically supported craft (planing craft in particular) may experience a different form of resistance hump, as discussed in Section 4.7. At higher speeds the dominant divergent waves have lengths of about *L* (Lighthill, 1978), but these waves do not have the intimate relationship with vessel speed that the transverse system has, and their celerity cannot be directly related to the vessel speed. Such incorrect basic assumptions and statements are, unfortunately, common throughout the literature.

c. the peak in the energy graph corresponds with the maximum wave and not the leading waves, which is an indication that the wake is a deep-water wake;

d. the period graph does not show any waves with periods longer than about *8 s*, confirming that the transverse system does not exist due to the high length Froude number, even though the depth Froude number is still sub-critical. The scattered long-period wave records following the main packet would include those transverse waves generated during the acceleration phase and eventually passing through the wave probe.
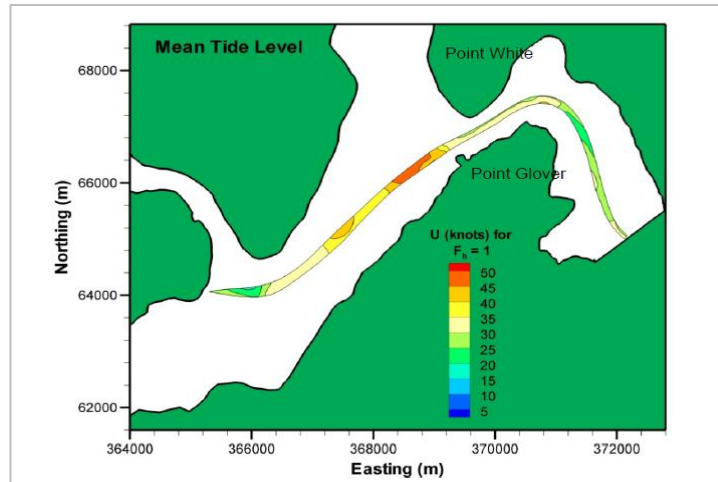


**Figure 4.10** – *Reproduced from Osborne et al. (2009), Fig. 6, showing a depth Froude number analysis of the Puget Sound high-speed ferry route. The most controversial site, Rich Passage, is between Point White and Point Glover. For almost all this route, the ferry under evaluation (the Spirit) would be too short to generate waves long enough to be depth affected, even though Spirit's operational speed of 30-35 knots would correlate with the depth-critical speed in Rich Passage.*
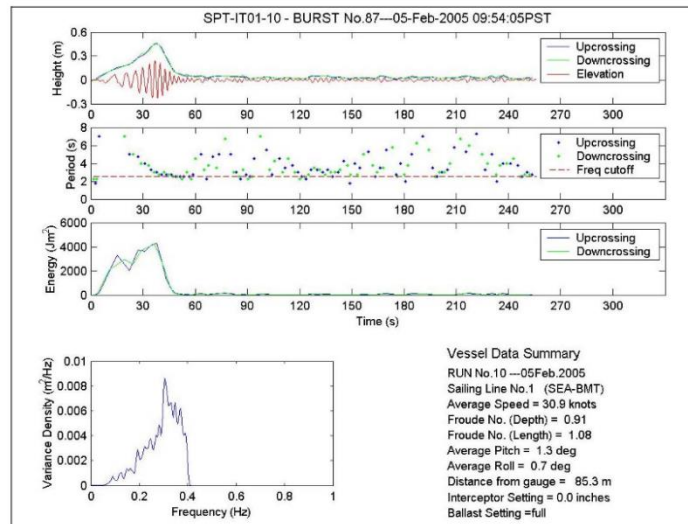


**Figure 4.11** – *Reproduced from Osborne et al. (2007), Fig. 5: Wave wake trials results for the vessel Spirit ($L = 20\ m$). The upper graph shows that the wake has a high-speed deep-water appearance, even though the vessel is close to the depth-critical speed. Wave energy peaks around the maximum wave, which is further confirmation of this. The lack of any transverse system is evident, even with the depth sub-critical speed - a result of the high length Froude number. Note that the period of the maximum wave is about 3.3 s; its corresponding wavelength of 17 m correlates with Lighthill's premise that the dominant divergent waves at high speed have a length $\sim L$.*

61

## 4.7     Planing Craft Dynamics in Deep Water

Special mention is made of planing craft dynamics in deep water, since small recreational craft make up a substantial proportion of vessels subjected to wave wake evaluation, the majority have a planing monohull form, and most operate in water sufficiently deep relative to vessel length to generate waves with deep-water characteristics. Planing hulls are configured with a shape that produces dynamic lift with increasing speed. This has the effect of lifting the vessel partly out of the water and reducing its wetted surface area and its dynamic immersed volume. As with all vessel forms operating at $Fr_L > 0.5$, specific wave drag decreases with increasing speed. Offsetting this is a resistance component from the lift generated (in effect, the hull's lift/drag ratio).[52]

The reducing wave wake intensity of planing craft at high speeds is often wrongly attributed to the reduction in their displaced volume as buoyancy is offset by dynamic lift. Laderoute and Bauer (2013) claim that:

> "*Speedboats generate the most turbidity and the largest wave heights, especially when there is a sequence of speedboats. This is especially true when the speedboats are used for water skiing and wake boarding because the speeds are slower and more water is displaced by the vessel hull, thereby yielding larger waves.*"

Similarly, Tan (2012) presents a definition of the planing condition as:

> "*Planing – The lift force supports the hull position with little contribution from buoyant force. The bow dips and wake size decreases since less of the hull contacts the water surface.*"[53]

In these examples the wave height is attributed to the dynamic displaced volume, for which there isn't a definitive relationship. High-speed displacement vessels exhibit the same relationship between wave height and speed, yet their displaced volume does not change dynamically by much, if at all. In the extreme, foil-borne hydrofoils produce wave systems even when the dynamic displaced volume of their foils is a few percent of the hull-borne total hull volume.

Dynamic planing effects change the way in which small craft wave wakes are categorised. The combination of the dynamic trim angle necessary to present the hull bottom at an angle of incidence to the water, as well as the bodily lift from the bottom pressure generated, has the effect of reducing the dynamic waterline length – substantially in some cases. Performance parameters based on static waterline length, such as length Froude number, lose their applicability at higher speeds. This is compensated by adopting volumetric Froude number, where

---

[52] As a general reference, discussion can be found in Savitsky (1964). Savitsky was far from the first to study planing craft; his contribution was to formalise methods to estimate resistance and planing dynamics. General planing hull dynamics are now considered to be quite generic and therefore sparsely referenced here, just as nobody would bother referencing William Froude when introducing Froude number.

[53] Similar comments are found throughout the US-sourced literature (another example being Fonseca and Malhotra, 2012, discussed in detail in the literature review). That is because of a vortex of circular referencing, with Maynord (2001, 2005) at the core. A good example of this is the definition of three operating modes (displacement, semi-planing and planing) defined by Maynord (2005, Table 1). The same table is replicated by Tan (2012), but with Maynord's erroneous (typographical) value for the planing regime of "$F_\nabla > 2.3$," which should be "$F_\nabla > 3.3$" according to the original reference from which the value was sourced. Typographical errors are excusable but not their perpetuation caused by a lack of proper review. Refer also to the second paragraph of the introduction to Section 2.

the length parameter is replaced with $\sqrt[3]{V}$, since the vessel weight in the form of displaced volume (which equates to lift from static buoyancy or dynamic forces, or a combination of the two) does not vary.

Larger vessels that operate at relatively slower speeds and with limited dynamic effects conform better to length-based parameterisation. Apart from the lower length and volumetric Froude numbers, their waterline length remains constant. That is especially so for catamaran designs. It is useful to correlate between volumetric Froude numbers and length Froude numbers for comparative purposes. Planing hulls go through four distinct phases from rest to the fully planing condition and understanding them will help to explain the relationship between planing craft and wave wake.[54] Almost all the literature refers only to three: displacement, semi-planing and planing. The four phases are characterised by the relative vertical position of the vessel's centre of gravity with respect to the still water surface, which is an indication of the relative ratio of buoyancy and dynamic forces. This is shown in **Figures 4.12** and **4.13**.

In the initial phase, when the hull support is dominated by hydrostatic forces ($Fr_L < \sim 0.5$), the centre of gravity sinks to its lowest point relative to the static condition: this is the *displacement mode*. As speed increases further, the centre of gravity begins to lift but remains below its static position: this is the *semi-displacement mode*. The centre of gravity recovers to its static vertical position at $Fr_\nabla \sim 1.75$ and continues to rise. Once above its static vertical position, the vessel is in the *semi-planing mode* with an increasing proportion of its weight supported dynamically. When the vessel reaches $Fr_\nabla \approx 3.35$, its weight is fully supported by dynamic lift: this is the *planing mode*. Further speed increase beyond this cannot bring greater lift; the total lift cannot exceed the total weight. Instead, the running trim reduces, and the vessel rises further to reduce its wetted area; the combined effect maintaining the overall lift. The reduced running trim immerses the forebody where the increased deadrise makes the lifting surface less efficient overall.



| Static | Semi-displacement | Semi-planing | Planing |
|---|---|---|---|
| V=0 | $Fr_\nabla < 1.75$ | $1.75 \leq Fr_\nabla < 3.35$ | $Fr_\nabla \geq 3.35$ |
| | CG below static | CG rising above static | CG above static |
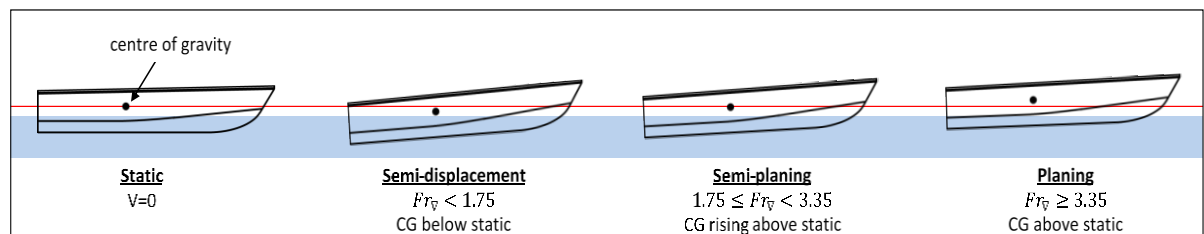
**Figure 4.12** – *Migration of the centre of gravity of a planing hull relative to its static position as speed increases.*

63
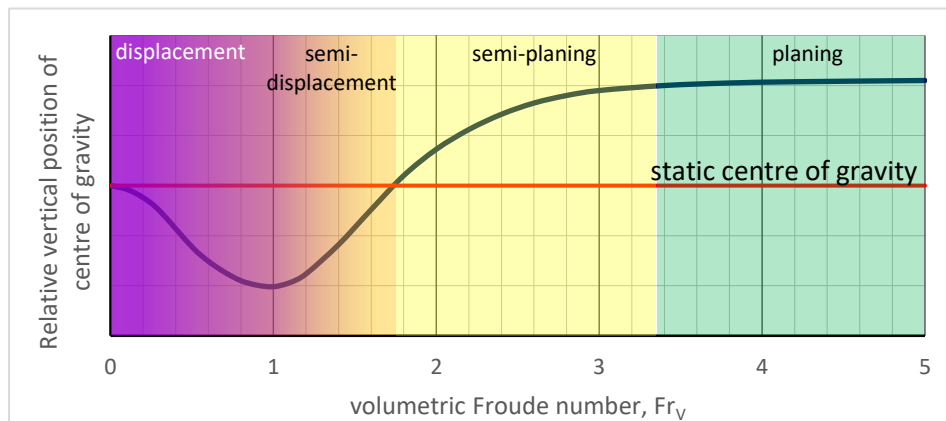
**Figure 4.13** – *Migration of the centre of gravity relative to its static vertical position as speed increases. The displacement and semi-displacement regions are not well defined using volumetric Froude number, hence the variable shading. The trough (maximum sinkage) occurs at around $Fr_L = 0.5$. The centre of gravity recovers to its static position at around $Fr_{\overline{V}} = 1.75$ (around $Fr_L = 0.8$ for typical recreational planing craft), which is the beginning of the point where the transverse wave system becomes depleted.*

Tan (2012, Fig. 56) graphs relationships between displaced volume and waterline length for three groups of published recreational vessel data. The slenderness ratios can be inferred from these, with averages of *5.68* to *5.88*. However, it is quite probable that the published data was the "*dry weight*" (approximately the lightship weight) of the vessels, excluding fluids, stores and passengers. **Figure 4.14** shows slenderness ratios for a (modest) sample of small craft at their operating condition. The average slenderness ratio is closer to 4.5.

The point of maximum specific resistance correlates with the condition where the centre of gravity has reached its lowest relative vertical position. The point where the centre of gravity recovers to its static vertical position occurs at around the point where the transverse wave system is almost depleted. That is particularly so for high-speed planing monohulls, which appear to have a less dominant transverse system than equivalent multihulls.[55] It has been observed by the author on full-scale trials that monohulls appear to lose their transverse system in deep water at a length Froude number around *0.8* to *0.9*, with catamarans slightly higher at *0.9* to *1.0* (approximately), though that may only be a visual impression (refer also to Ma *et al.*, 2016, who claim a general value of $Fr_L \sim 0.85$).
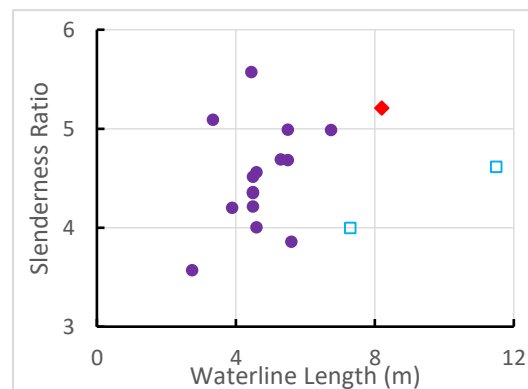


**Figure 4.14** – *Sample slenderness ratios for vessels reported in Macfarlane and Cox (2003). The solid markers are recreational planing monohulls. The diamond marker is a planing commercial vessel in a light condition (without passengers). The hollow squares are displacement vessels.*

---

[55] The transverse wave system of multihulls is strengthened by their increased hull draft and from the reinforcement of each demihull's wave system. This is a reasonably well-known phenomenon (refer to the discussion by Doctors appended to Gadd, 1994, and Doctors *et al.*, 2001, p.101).

**Table 4.2** – *Correlation between salient length and volumetric Froude number conditions for typical recreational planing craft. Bold values indicate the known features.*

| Condition | $Fr_L$ | $Fr_\nabla$ |
|---|---|---|
| Maximum specific resistance | **0.5** | ~1.0 |
| Centre of gravity recovers to its static position | ~0.8 | **1.75** |
| Fully planing | ~1.6 | **3.35** |

The fully planing condition has no specific length Froude number feature, except that it is of a value considerably higher than larger high-speed vessels operate at (refer Tables 7.1 and 7.2 in Section 7). Small recreational craft are able to operate at high relative speeds where their less-than-desirable slenderness ratios and potentially deleterious wave wake effects are offset by their greatly improved hull dynamics.

Given the traditional specific resistance peak at $Fr_L \approx 0.5$ and the planing hull specific resistance peak around $1.0 < Fr_\nabla < 1.75$, the relationship that $Fr_L = Fr_\nabla/\sqrt{SR}$ implies that the higher the slenderness ratio, the narrower the band of peaked wave wake parameters. For instance, a recreational planing craft with a slenderness ratio of *4* would see parity at $Fr_L = 0.5$ and $Fr_\nabla = 1.0$, whereas a lightweight passenger vessel with a slenderness ratio of *8* would see parity at $Fr_L = 0.5$ and $Fr_\nabla = 1.4$. The planing dynamics of the recreational planing craft would extend the increased wave wake parameters well above $Fr_L = 0.5$, whereas the lightweight passenger vessel's length and volumetric-based parameters are more centred. It is a minor and obscure point, but it means that the range of damaging speeds to avoid widens as slenderness ratio decreases.

Overall, planing hulls may have a wider speed range where increased wake height, period and energy is problematic. ***Figure 4.15*** shows curves of specific resistance (drag/weight) against volumetric Froude number. The left figure is taken from McVoy (1985), Ch. IV Fig. 13, showing the results for the *Series 62* hullform where only L/B ratio was varied. The growth in the pre-planing hump has been somewhat tempered by the *Series 62* LCG being further forward than would be the case for most recreational monohulls; the exception being inboard ski boats which have their engines amidships and crew forward. The right figure shows calculated specific resistance for a monohedron monohull with varying slenderness ratio only (varying only displacement). The LCG was configured at *39% L* forward of the transom. The hump growth is more consistent.

Although neither of these component graphs of ***Figure 4.15*** give an immediate indication of wave wake severity, they do demonstrate the variability possible with planing hull forms due to varying hull dynamics with changing hull parameters. The schematic shape presented by Maynord (2005, Fig. 1) may be more representative of small planing craft wave wakes. Use of dynamic trim control using trim tabs, interceptors, and outboard engine trim, or static trim control using weight movement, are known to reduce the severity of the resistance hump in most craft and the waves they can generate. It is the combination of increased running trim and displacement, and operational speeds around $1 < Fr_\nabla < 2$, that ballasted wake surfing boats seek to manipulate in the desire to increase wave wake height and steepness.
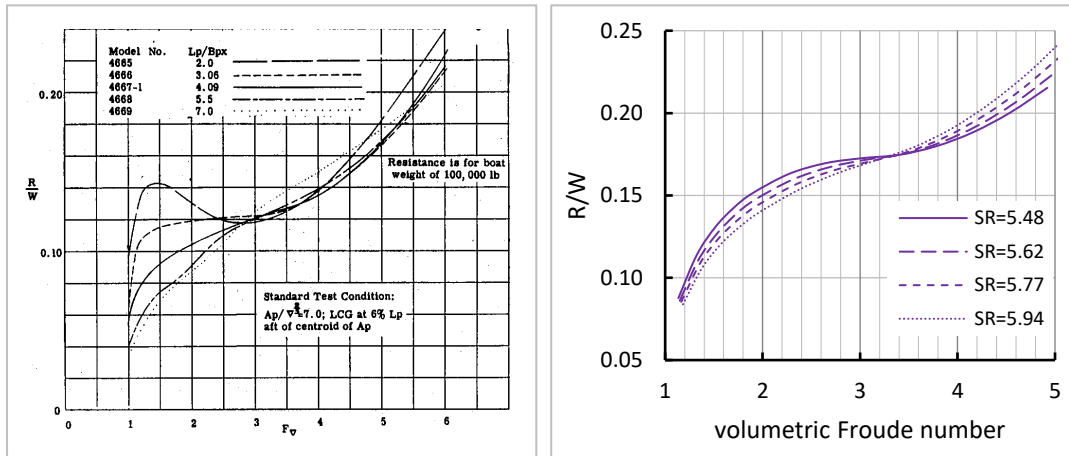
**Figure 4.15** – *Specific resistance (drag/weight) against $Fr_\nabla$ for planing craft.* **Left**: *taken from McVoy (1985), Ch. IV – Planing Craft (Edited by Dr. Daniel Savitsky), Fig. 13. These curves represent the Series 62 hullform with varying L/B ratios only. Of note is the increasing size of the resistance hump at $1 < Fr_\nabla < 2$ with decreasing L/B ratio and the invariance of specific resistance to L/B ratio towards the inception of the fully planing condition ($Fr_\nabla \sim 3$).* **Right**: *Calculated specific resistance for a generic monohedron monohull with varying slenderness ratio. All other hull parameters are held constant and only displacement is varied. For minimum resistance at fully planing speeds, optimising LCG and L/B ratio is as important as reducing displacement.*

# Section 5 – Shallow Water

## Summary

Wave wakes in shallow water are defined as those generated in shallow water and not deep-water wave wakes that propagate into shallow water. The distinction is important, as it is not possible to transform a deep-water wave wake into the form generated in shallow water simply by the action of shoaling, but it is possible to transform a shallow-water wave wake into a deep water form by increasing the depth and removing the depth/celerity restriction. A series of novel experiments demonstrated this.

A wave wake generated in shallow water is similar in composition to that in deep water, except that the shallow water celerity limit for periodic waves of $\sqrt{gh}$ forms a barrier that compresses the head of the propagating packet. Provided the water is not extremely shallow relative to vessel length, the crest (and only the very apex of the crest) of the leading wave propagates at $\sqrt{gh}$, and the other waves fall behind with progressively slower celerities. At the rear of the wake, the short-period trailing waves may not be depth affected at all. Consequently, dispersion varies across the packet from what appears to be a non-dispersive leading crest to a fully dispersive tail. In fact, all waves, including the leading wave, are made up of multiple frequency components. As propagation proceeds and dispersion transforms the packet, the multiple frequency components of the first wave disperse, causing the leading wave to stretch, or increase its wavelength, as the slower-moving components fall behind and are shed from the wave into the trailing waves. As with a deep-water wave wake, the number of waves in the shallow wave wake and their defining parameters change over time.

All shallow water wave wakes have a solitary wave component embedded within the leading wave, even at very high depth Froude numbers where solitary waves were thought not to exist. That causes the initial upswelling of the leading wave to propagate faster than $\sqrt{gh}$, so that the leading wave stretches both ahead of and behind the crest apex. If the water is shallow enough, this solitary wave component becomes dominant and propagates at a celerity compliant with solitary wave theory. The shallow-water wave wake wedge, previously defined by the linear shallow water celerity limit of $\sqrt{gh}$, is now defined by a solitary wave celerity greater than $\sqrt{gh}$. In extremely shallow water, this leading solitary component can energise itself and decouple from the trailing wake at all depth Froude numbers greater than unity. A number of novel model experiments have demonstrated the existence of solitary waves in depth-supercritical wave wakes, their relationship to vessel dynamics, and the mechanism by which they energise themselves at the expense of the trailing wake and decouple and propagate independently.

A table of depth-dependent operating regimes is proposed.

## 5.1 Introduction

In the study of wave wake, shallow water has consistently been regarded as the more complex of the two depth conditions. Whenever faced with multiple and difficult-to-qualify variables, engineers have a strong preference to simplify their understanding with approximations and linearised empirical relationships set in a matrix of design margins. Conversely, theorists relish the non-linearities which take them far from the over-simplification of a linearised world.[56] One seeks a workable, consensus outcome; the other seeks the (manicured) truth.

Deep water has the benefit of removing depth effects and the increasing non-linearity that comes with shoaling water. Anything that reduces the number of variables cannot be bad. The question with shallow water has always been "*how shallow?*" - the answer to which results in an almost infinite matrix of possible wave wake generation and propagation combinations. As discussed in Section 4, the analysis of vessels such as small, high-speed craft operating in restricted waterways can largely be done using deep water theories, which hold sufficiently for short waves at modest depths to be accurate in an engineering sense. Past small craft field studies such as Macfarlane and Cox (2003, 2005) have demonstrated the validity of that approach.

Fortuitously, there are two facets of shallow water wave wake analysis that at least delineate, if not simplify, the calculations. Firstly, the absence of a transverse wave system at depth super-critical speeds removes one of the unnecessary distractions of a deep-water wake system; unnecessary in that the environmental effect of the transverse system is normally not quantified in wave wake studies, yet it can have a strong influence on the measured divergent wave system parameters. Secondly, there is a celerity limit to shallow water waves of $\sqrt{gh}$ in the case of periodic waves or a little above that in the case of solitary waves that come to dominate depth super-critical wakes as $h/L \rightarrow 0$.

Regardless of these, the problem of quantification rather than qualification remains, made worse in a real-world setting by the continual variability of depth along a vessel's shallow-water route and how that affects the wake it creates. Empirical and statistical methods are probably the only long-term options for quantification of the environmental effects.

## 5.2 What Constitutes Shallow?

As with deep water there are two parts to this question, each with further subdivisions. These two parts describe how the waves are affected as they propagate and how they are generated.

### 5.2.1 Propagation (Transformation)

Coastal engineering already makes use of these conditions in the form of the Ursell number, though considering only the outcome (how waves appear) and not the cause (how they were generated). Ursell number[57] is defined as $U_R = (H\lambda^2)/h^3$, which is described by Fenton (1990) as:

---

[56] Yet preface their derivations with "*assume an inviscid, incompressible, irrotational, unbounded fluid….,*" otherwise described sarcastically by John von Neumann as "*the men who studied dry water.*" [The Flow of Dry Water, Richard Feynman lectures: http://www.feynmanlectures.caltech.edu/II_40.html (last accessed 7th of January, 2019)].

[57] Stokes (1847) had already discussed an almost identical form of this relationship and its importance to shallow water waves. Ursell repackaged it and put usable, real-world values against it.

$$U_R = \frac{H/h}{(h/\lambda)^2} = \frac{\text{"nonlinearity" } (measure\ of\ height)}{\text{"shallowness" } (measure\ of\ depth/length)}$$ [5.1]

A value of $U_R = 26$ marks the accepted line of demarcation between the linear and Stokes theories ($U_R < 26$), and non-linear theories ($U_R > 26$) (Le Méhauté, 1976). There is some dispute as to the appropriate value of this parameter, with Hedges (1995) suggesting a value of $U_R = 40$ better describes the boundary between Stokes and cnoidal theories. Interpretation of the shallowness parameter $h/\lambda$, which in practice also describes the degree of dispersion, may be the cause, compounded by appearing as a *square* in the denominator.

The same variance of interpretation can be said of waves that are interpreted as *fully shallow*. Lighthill (1978) notes (in part) that a value of $h/\lambda = 0.07$ (or $\lambda/h \approx 14$) represents the condition where a wave's celerity is within *3%* of its shallow water limit of $\sqrt{gh}$, which we can refer to as *practically shallow* (as opposed to *practically deep*).[58] Newman (1977) refers to a shallow water limit of $h/\lambda_o < 0.06$ (note that this is referenced to the wave's deep-water wavelength, $\lambda_o$). Dean and Dalrymple (1991) refer to a value of $\lambda/h = 16$.[59] The Shore Protection Manual (SPM) (Coastal Engineering Research Center (U.S), 1984) uses a value of $h/\lambda < 0.04$, which is possibly the depth-corrected definition of "*very shallow water*" of $h/\lambda_o < 0.05$ used by Munk (1949), who refers to a US Navy Hydrographic Office document that pre-dated the SPM.[60]

Fenton (1999) reviews the work of Iwagaki (1968) and Hedges (1995) (among others) and shows that a value of $\lambda/h = 16$ is a sufficiently accurate starting point for the application of shallow water theories. The model tests conducted here concur, with the non-linear wake waves becoming dominant at a higher Ursell number of $U_R \sim 52$. This higher value (*30%* greater than that of Hedges) may appear significant but can be achieved with about an *8%* reduction in water depth – an approximation assuming $H$ and $\lambda$ remain constant. The value of $\lambda/h = 16$ is therefore used in this study as the point of inception of dominant, shallow-water wave-wake effects. ***Figure 5.1*** (Appendix E), reproduced from Fenton (1999), outlines the areas of applicability of cnoidal and Stokes shallow water wave theories, which is slightly different from the well-known graph of Le Méhauté (1976), as shown in Section 8, Figure 8.1. Note that references in ***Figure 5.1*** to "*solitary*" and "*Nelson H/d=0.55*" mark only maximum breaker depth indices for waves.

Lastly, Dingemans (1997) denotes shallow water slightly differently, proposing the relationship $T\sqrt{g/h} > 20$. The use of wave period '$T$' in place of wavelength '$\lambda$' is a clever, practical alternative; period remains constant, yet the wavelength continually changes in shoaling water. The limiting celerity of a shallow water wave gives the simplified relationship $\lambda = T\sqrt{gh}$, which reduces Dingeman's relationship to $\lambda/h > 20$ (which is a very close approximation, since $\sqrt{gh}$

---

[58] Lighthill refers to the finite depth dispersion equation $c = \omega/k = [gk^{-1}tanh(kh)]^{\frac{1}{2}}$, which approaches its deep and shallow celerity limits at large and small values of $kh$ respectively. Lighthill adopts a deep/shallow approximation when the celerity is within 3% of its deep/shallow value. For the deep case, $[tanh(kh)]^{\frac{1}{2}} = 0.97$ when $\lambda/h \approx 3.5$; for the shallow case, $c = 0.97\sqrt{gh}$ when $kh = 0.44$, so $\lambda/h \approx 14$.

[59] Applying footnote 58, $c = 0.975\sqrt{gh}$ when $\lambda/h = 16$.

[60] As the depth decreases, a wave's celerity slows to the shallow water limit of $\sqrt{gh}$ asymptotically and eventually to the absolute non-dispersive condition, but at $h = 0$. In all reality, whole periodic waves never quite reach a fully non-dispersive state, only a relative one, the reason being that individual waves are comprised of multiple frequencies and are not monochromatic, which is only a simplification. Applying footnote 58, $c = 0.99\sqrt{gh}$ when $\lambda/h = 25$. It seems unusual that the SPM, which is full of empirical, engineering relationships, would be so pedantic about removing all but the last traces of dispersion. Refer to the discussion following regarding the unsuitability of linear theory in shoaling water.

would represent only the celerity of the periodic wave's crest and not the whole wave, as will be shown later). The two (minor) weaknesses of Dingeman's approach is that solitary waves, which are commonly used as the basis for breaking wave studies, do not have a well-defined period and their celerity always exceeds $\sqrt{gh}$.
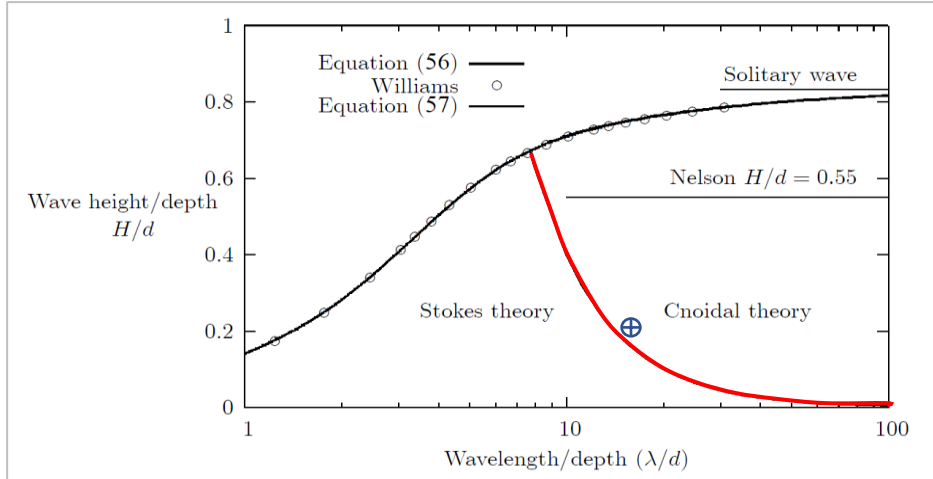


**Figure 5.1** (Appendix E) - *Reproduced from Fenton (1999), Figure 2, with reference to Hedges (1995). Note that $d \equiv h$. The line of demarcation between cnoidal and Stokes theories is shown at an Ursell number of 40 (red line). The value of $H/h = 0.206$ and $\lambda/h = 16$ proposed here gives an Ursell number of about 52, shown as a crossed marker, which moves the Fenton/Hedges line fractionally higher.*

In summary, ***Table 5.1*** shows the $\lambda/h$ delineations used in this study. In a practical sense, the relationship to local wavelength $\lambda$ rather than the deep-water wavelength $\lambda_o$ is an added complication for wave wake evaluation. Small recreational craft usually manage to satisfy the *practically deep* definition, at least for their maximum wave, but larger vessels cannot, and the local wavelength must be calculated from the water depth, wave height and wave period using an appropriate shallow water wave theory. The often-quoted linear (Airy) wave theory equation used to estimate local wavelength for waves not too long relative to depth is given by [5.2].

$$\lambda = \frac{gT^2}{2\pi} tanh\left(\frac{2\pi h}{\lambda}\right) \qquad [5.2]$$

The relationship must be solved iteratively for $\lambda$. Although the Shore Protection Manual (CERC, 1984, Fig. 2-6) shows this as being valid for all waves in its *transition range* ($0.04 < h/\lambda < 0.5$), the relationship will become increasingly unreliable for longer waves in shallow water when $U_R > 40$. A far better alternative is [5.3] from Fenton and McKee (1990), which is valid for all values of $\lambda/h$ and does not require iteration:

$$\lambda = \frac{gT^2}{2\pi}\left[tanh\left(2\pi\sqrt{h/g}/T\right)^{3/2}\right]^{2/3} = \lambda_0\left[tanh(2\pi h/\lambda_o)^{3/4}\right]^{2/3} \qquad [5.3]$$

**Table 5.1** – *Wavelength/depth relationships used in this study.*

| Condition | $\lambda : h$ relationship |
|---|---|
| *Deep* | $\lambda \leq 2h$ |
| *Practically Deep* | $\lambda \leq 3.5h$ |
| *Transition* | $3.5h < \lambda < 14h$ |
| *Practically Shallow* | $\lambda \geq 14h$ |
| *Shallow* | $\lambda \geq 16h$ |

### 5.2.2   Generation

Operating at a depth super-critical speed does not necessarily guarantee a wake comprised of waves with shallow water properties. For instance, a high-speed small craft with $L = 5\ m$ operating at *9.9 m/s* in *10 m* water depth would be operating at the depth-critical speed ($Fr_h = 1$), yet its transverse wave system would become indiscernible at $Fr_L \sim 0.85$ (Ma *et al*., 2016), or around *6 m/s*. The highest (maximum) wave in its divergent system would have wavelengths of about $L$, so would be insufficiently long to feel the bottom (refer Table 5.1). This is what simplifies the analysis of small craft, but complicates the analysis of large craft, in sheltered waterways.

Here we consider only the depth super-critical case at the sailing line and therefore at the point of generation, where the leading waves carry most of the wake energy and are also depth affected. This is different to deep-water waves propagating into shallow water, which is treated as a *transformation* and not *generation*. The wavefront, represented by the leading crest, propagates at the shallow water celerity limited by $\sqrt{gh}$ if comprised of periodic waves, or at a slightly super-critical celerity if comprised of a solitary wave, and successive waves propagate at progressively slower speeds determined by dispersion – weak near the leading crest but strengthening away from it. In the deep-water generation condition, where the wake is fully dispersive, and celerity is limited only by wavelength, the longer waves propagate ahead from the time of their generation. In shallow water, where the wake is comprised of waves varying from non-dispersive at the head to fully dispersive at the tail, waves that could otherwise run ahead in deep water become trapped by the depth-imposed celerity limit and agglomerate at the head. The leading crest therefore appears to become increasingly dominant as depth decreases, as more wake energy accumulates at the head of the wake.

Solitary waves are a known feature of wakes around a depth Froude number of unity. The results of model experiments presented in Appendices D to H demonstrate that the very head of a depth super-critical wake has a solitary wave form, which becomes increasingly stronger and more prominent as the depth decreases. In the extreme case, when $h/L \to 0$, the leading wave is transformed into a solitary wave capable of detaching itself from the trailing wake and propagating independently. This extreme condition has particular relevance to the operation of large high-speed craft in coastal waters but less so for small craft. Although a question of semantics, some authors use the term *decouple* rather than *detach* to describe the phenomenon of a solitary wave breaking from its trailing wake. Both terms are considered the same here, though it's not known if the solitary waves do actually decouple. As an example, the moon and earth are *detached* but not *decoupled*. The difference is subtle.

As a guide, if the divergent wavelengths are in the order of the waterline length, the limit of *deep* water would be at $h/L = \sim 0.5$ and the limit of *practically deep* would be at $h/L = \sim 0.28$. The longer leading waves may be more depth affected, but they are often less significant (or even insignificant) in terms of their height and therefore their energy relative to other waves in the

71

wake. That is not wholly the case though. If the leading waves are substantially depth affected and dispersion is suppressed, the cycling of packet energy is reduced and the waves still in deep water may be slightly depleted compared to a fully deep condition (refer Appendix D). This can generally be ignored, provided the bathymetry variation is gradual.

As water shoals further to $h/L \sim 0.15$, the leading shallow water wave may dominate to the point where it may contain more than *50%* of the total wake energy if the slenderness ratio ($SR$) is low enough (refer Appendix E), increasing rapidly as sailing line depth shoals further. The relevance of $h/L \sim 0.15$, derived from model experiments, applies here to small recreational craft, which have an operating slenderness ratio around *4* to *5*. Vessels with a higher slenderness ratio would require shallower water for the same effect to be felt. Compounding this leading wave energy dominance is the increasing strength of a leading solitary wave component of the wake, which becomes dominant when $H/h > \sim 0.2$, where $H$ in this case is the crest height above still water (refer Appendix E). Since wave wake height is strongly a function of displacement-length ratio (Cox, 2000) and therefore displacement for a given length, this dominant solitary wave can be tempered, but not eliminated, by reducing displacement and hence increasing slenderness ratio. Reducing displacement reduces the leading wave height, but not its period.[61]

### 5.2.3    Example of wave wake development with decreasing depth
*Figure 5.2* provides a descriptive example of how a wave wake develops as the water depth at the sailing line is varied. The wave traces were taken from model tests at four different $h/L$ ratios ranging from deep (or *practically deep*, since the deepest $h/L$ ratio is less than *1.0*), through to a depth condition that could be regarded as almost un-navigable for small craft, but possible for large, coastal craft (refer to examples in Doyle *et al*., 2001). The scales are consistent between graphs (water surface elevation *±30 mm*, run time *6 s*).

As previously noted, the divergent waves would not become depth affected to any extent until $h/L < \sim 0.5$, and even then, the effect would be minimal. In the second graph of *Figure 5.2*, at $h/L = 0.288$, the wave wake is not materially different from the deepest condition, except for the obvious growth of the leading wave height.

As discussed in the Section 6, the energy of the first wave grows from a small value in the deep condition to become about *90%* of the total wake energy in the shallowest condition.

---

[61] Or period of its components, as will be discussed.

**Figure 5.2** – *Wake records for AMC model 00-01 recorded at $y = 2\ m\ (\sim 2L)$ at $V = 3\ m/s$ and at different water depths; top to bottom:*

1. *$h = 0.90\ m, h/L = 0.864$;*
2. *$h = 0.30\ m, h/L = 0.288$;*
3. *$h = 0.15\ m, h/L = 0.144$;*
4. *$h = 0.10\ m, h/L = 0.096$;*

*Depth Froude number varies from 1.01 (top) to 3.03 (bottom). Elevation is in mm and time is in seconds. Scales are consistent.*

*Several salient features are noted:*

a. *The progress of the packet envelope from a Gaussian form dominated by the maximum wave to one dominated by the first wave as depth reduces;*
b. *The (approximate) constancy of the period of the first wave, reinforcing the notion that the principal wake periods generated are not a function of depth but of speed and vessel parameters such as length;*
c. *The gradual increase in the height of the first wave and commensurate decrease in height of the maximum wave to the point where is becomes indistinguishable from other trailing waves in very shallow water.*
d. *The dominance of the first wave as water shoals and the prominence of a leading solitary wave form.*
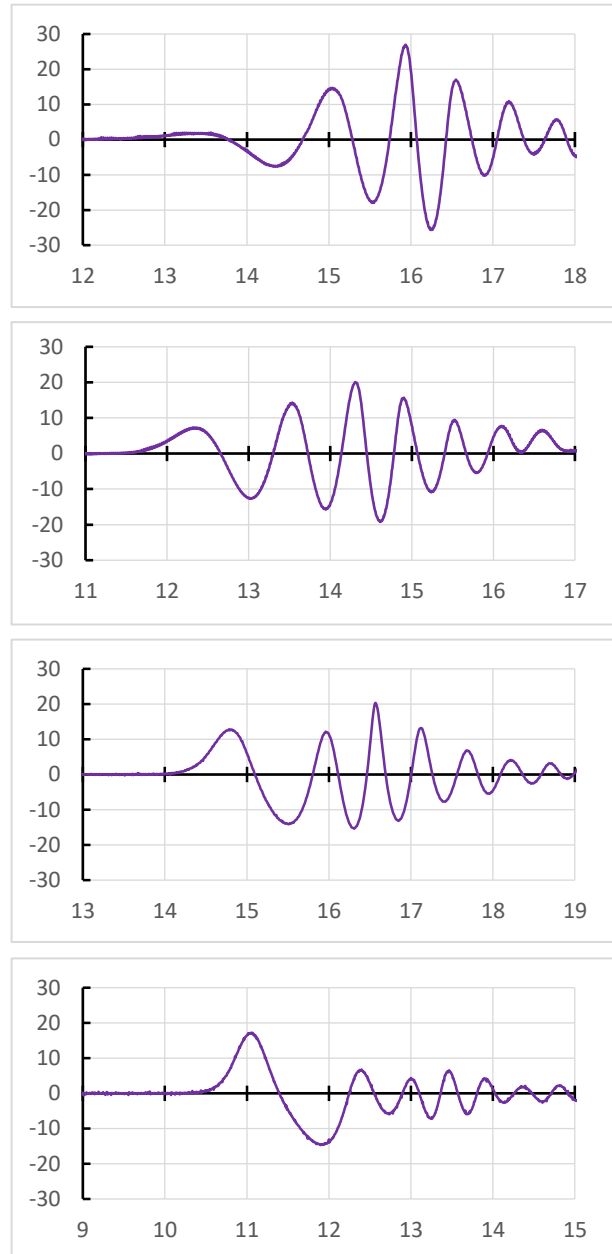


### 5.3    Channels Restricted by Width and Depth

There is a relationship between the transverse wave system, which tends to become depth affected first because of its (generally) longer wavelengths, and the point at which surge and drawdown become apparent and substantial (refer Figure 3.2.1). The wavelength of a deep-water transverse wave is related only to vessel speed by $\lambda = 2\pi V^2/g$. Taking the defined limits of *deep* ($\lambda/h = 2$) and *practically deep* ($\lambda/h = 3.5$), the limiting vessel depth Froude numbers can be calculated as $Fr_h = \sqrt{(1/\pi)} = 0.56$ in the *deep* condition and $Fr_h \approx \sqrt{(3.5/2\pi)} \approx 0.75$ in the *practically deep* condition. **Figure 5.3** shows (scaled) model and full-scale results of surge and drawdown in width and depth-restricted waterways. The monohull results were from model tests and the catamaran results were from full-scale tests. The surge does not become apparent until $Fr_h > \sim 0.8$, which coincides with the *practically deep* condition above. The drawdown becomes

apparent much earlier: $Fr_h > \sim0.6$ for the monohull and $Fr_h > \sim0.5$ for the catamaran. That concurs with the *deep* condition above. The explanation for the earlier occurrence of the catamaran drawdown may be found in its more dominant transverse system.

In this example and in others, control of drawdown warrants greater attention than control of surge. Gadd (1995) remarks that "*in very shallow canals it seems quite likely that the main problem may arise from the shallow water troughs . . .  rather than the radiated waves.*" Gadd then goes on to claim that "*I am not sure that there would be a lot of scope for ameliorating the problem by detailed changes of hull shape, because the shallow water trough seems to be largely a function of displacement only.*" This is an interesting but peculiar statement, as it was not qualified with speed or speed-related parameters. Drawdown is known in practice to be a localised phenomenon in shallow, open waterways, but in depth and width-restricted channels its lateral severity can be supported by the proximity of a nearby riverbank in the same way that a solitary wave becomes more pronounced under the same conditions. Further discussion is found in Cox (2000), who included an example of varying channels with the same cross-section and hydraulic radius but with increasingly negative influence when width was restricted, even if depth was increased:

> "*Scott (1971) presents an interesting discussion regarding blockage and its causes.  Scott's aim was to compare the resistance measurements of a series of well-tested models in different towing tanks to derive a more accurate blockage estimation method.*
>
> "*Two important points were raised, of which one was somewhat controversial.  Firstly, for speeds sufficiently below the depth-critical speed, tank width was far more important than tank depth, such that a model towed in a towing tank of  4' x 4'  (1.2m x 1.2m) cross-section required three times the blockage correction of an 8' x 2' tank  (2.4m x 0.6m), even though the model and tank cross-sectional areas and the hydraulic radii are the same.*"
>
> "*a) Vessels should attempt to maintain a separation of at least 1L from either shore or shallow water with depth less than its draught at speeds up to $F_d$ = 0.75 ($F_d \equiv Fr_h$).*
>
> "*b) Depth-Froude number should be limited to 0.75 in 3m depth, 0.8 in 4.5m depth and 0.85 in 6m depth, provided blockage correction from Equation 1 (Section 7.2.1) is less than 4% (i.e. $U_1/U \leqslant 1.04$).  Operation at higher depth Froude numbers will require verification by model testing.*
>
> "*c) The total surge should be limited to 100mm height, assuming the associated drawdown will be of similar magnitude.*"

At high speed (depth-super-critical speeds) the surge and drawdown effect become part of the radiating wave wake and, as much as their severity may reduce from that of the depth-critical condition, they could not be regarded as environmentally benign (refer Cox, 2000, Fig. 11). Gadd (1994) draws the same conclusion.

For the sake of this study, the recommended approach would be to limit depth Froude number in restricted channels to $Fr_h \leq 0.75$. This may be increased if channel depth increased, but that would require specific assessment. A modest depth increase may bring only a fractional increase in transit speed, and the practical risk of criterion exceedance due to irregular bathymetry may not warrant the extra validation effort in deeper channels.
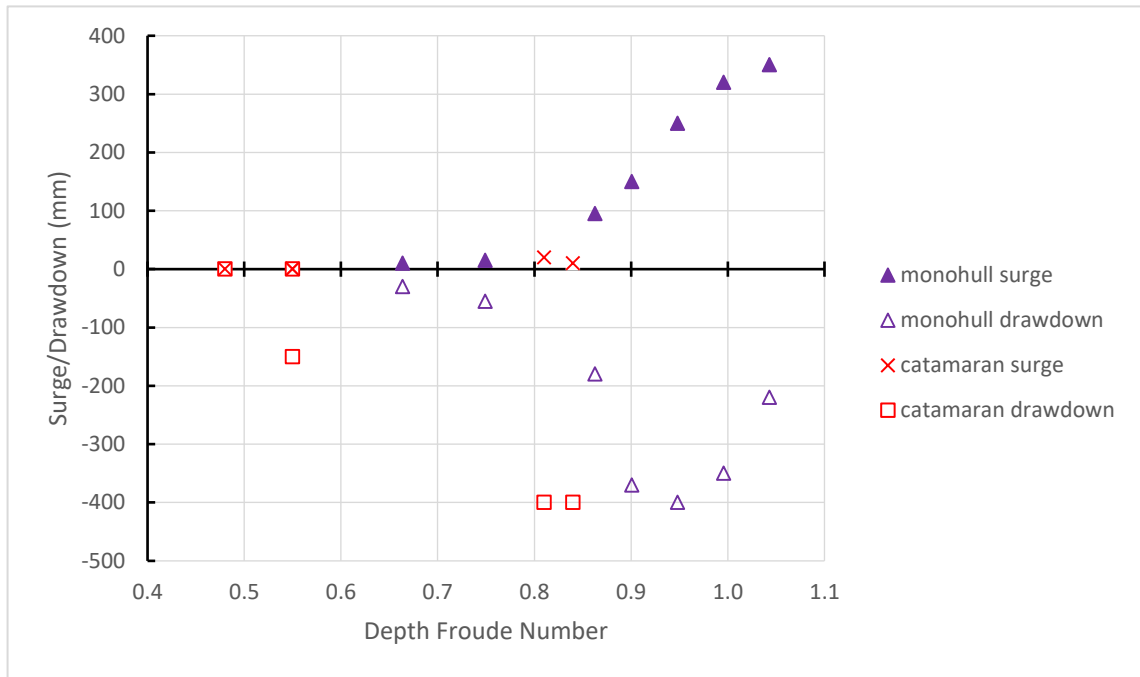
**Figure 5.3** – *Surge and drawdown with varying depth Froude numbers for a long, slender catamaran vessel (full-scale field trials) and a slender monohull model scaled to $L = 49\ m$ in water restricted in depth and width. The catamaran's measurements were taken at about 0.6L lateral offset (0.5L demihull lateral offset) in a river where the depth, width and cross-section varied due to tidal fluctuations (in general, increasing with increasing $Fr_h$), with blockage varying from 2.3% to 1.6% accordingly. The monohull was tested in the AMC towing tank, with blockage of 1.8%, recorded at 0.5L lateral offset. Of note is how neither vessel produced appreciable surge, provided $Fr_h < 0.8$. The monohull only produced appreciable drawdown at higher depth Froude numbers than the catamaran, though this may have been partly a function of the differences in bathymetry between the towing tank (rectangular) and the river (U-shaped centre channel flanked with shallow, submerged levees in an inverted top hat form). The field observers noted the shoreline impact of the catamaran's 400 mm drawdown as "severe;" the shoreline being only ~0.75L from the sailing line. They also observed "material being sucked out of the bank" at every drawdown.*

## 5.4    Composition of Depth Super-Critical Wakes

There is a tendency in the literature for the sub and super-critical speed conditions to be portrayed as two totally independent phenomena separated by a boundary at the critical speed that must be crashed through, somewhat analogous to breaking the sound barrier. Certainly, Havelock's often-replicated Fig. 8 (wave angle against $Fr_h$) would give that impression, having a singularity and hence a sharp peak at $Fr_h = 1$ (Havelock, 1908; Robbins, 2013, Fig. 20; Macfarlane 2012, Fig. 2.4; Kofoed-Hansen *et al.*, 1999, Fig.5; Whittaker *et al.*, 1999, Fig. 2). Similarly, the often-published wave wake patterns in the sub-critical, critical and super-critical conditions would complement that (Havelock, 1908, Fig. 9 as an example).

In reality, the underlying waves generated by the vessel in the deep and shallow water may not be materially that different. Certainly, the transverse system may not be present in shallow water[62],

---

[62] "*may*" not "*would*" – it depends on the definition of *shallow* (refer to the discussion in Section 5.2.2). For instance, a *100 m* ferry with a *4 m* draft in an *8 m* deep channel would have $h/L$ and $T/h$ ratios regarded as *shallow,* yet would be capable of creating a transverse wave system up to the depth-critical speed of *17 kn*.

but what may change with the divergent system is not the energy, but how the different waves manifest that energy in the depth-restricted conditions imposed at their generation.

The impetus for the comparison between deep and shallow wave wakes came from the shallow water model experiments of AMC 00-01. As noted, it is a particularly useful model because of its short length (increasing relative lateral separation at each wave probe) and low slenderness ratio (simulating small craft but also intensifying wave features, especially height). As $h/L$ decreased, the maximum (highest) wave migrated towards the head of the wave wake until a point was reached where the first wave was the highest (Figure 5.2). It became obvious that the first wave in shallow water decayed in height with lateral separation, but its period increased dramatically. That is not normally the case for the maximum wave, which usually reflects the packet's group celerity and therefore has a constant period. The increasing period can be seen in *Figure 3.12*. *Figure 5.4* shows the first wave at three lateral positions, with relative scales maintained.

The only wave wake feature that decays in height but stretches spatially/temporally with propagation is a packet envelope. It was therefore surmised that the first wave was not a single wave, but a packet of waves that had formed at the sailing line, had similar frequencies, but were unable to quickly diffuse due to the depth-imposed weak dispersion. As lateral separation increased, the slightly higher frequency waves fell behind and gradually fell out of the packet itself, causing the height decay and the apparent increase in period (or increase in packet envelope length).

Of course, this explanation is in the form of a discrete wave approach, rather than the more correct continuous wave function approach. In that case it's not whole waves that are being shed as they fall away, but a continuous release of higher frequencies and corresponding energy that results in a smooth height decay and gradual period change. Appendix C explains how the first wave, when analysed as a packet, has a group celerity approximated by $\sqrt{gh}$, which is also the phase celerity in a fully shallow condition. In fact, the group celerity is not constant across the packet (first wave), since the whole packet (first wave) is not everywhere non-dispersive. Only the crest is non-dispersive and propagates at $\sqrt{gh}$; the head has a solitary wave component and so undergoes amplitude dispersion, and the tail gradually becomes weakly (frequency) dispersive. The evolution of the solitary component of depth trans and super-critical wave wakes is discussed in detail later.

Robbins (2013) concluded that the height of the leading wave in a super-critical wave wake was a more consistent parameter than the traditional *highest* (maximum) wave, which may occur later in the wake. However, he didn't offer any explanation for why that may be the case. The reason for its consistency is explained by the fact that the first wave is a packet and so has the timbre of a deep-water condition, albeit with different parameters.
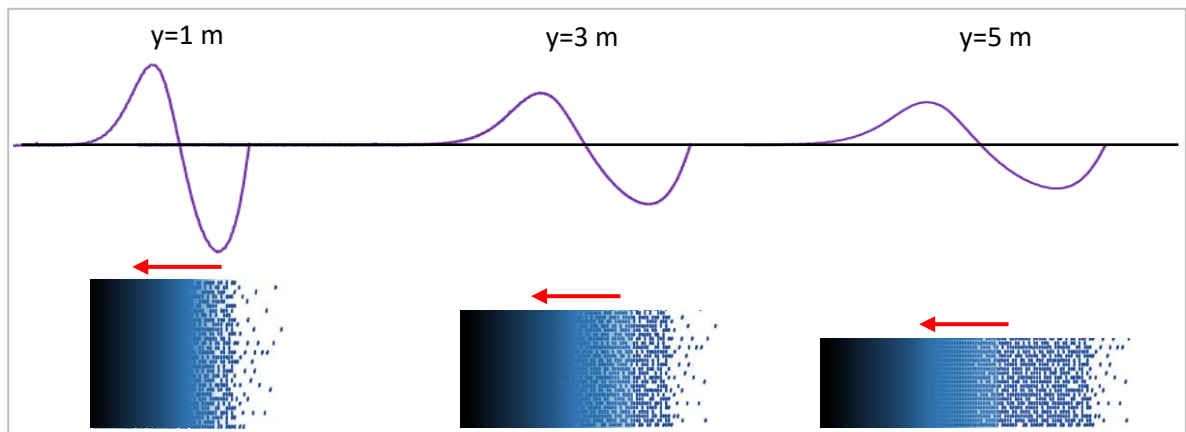
**Figure 5.4** – *Graphic representation of the propagation and decomposition of the first shallow water wave with relative scales (y-axis: water surface elevation; x-axis: time) maintained (see Figure 3.12). The first wave acts as a wave packet, comprised of what would have been several waves in a fully dispersive environment (deep water). At intermediate shallow water depths, the first crest propagates at a celerity of $\sqrt{gh}$ (dark shade), with local celerity throughout the trailing tail slowly decaying after that. This causes the first wave to spread and reduce in height as the slower (higher frequency) components, unable to keep up, fall to the back of the wave and are gradually shed. Energy is therefore gradually shed into to waves following. The wavefront has a solitary wave component of increasing strength with decreasing water depth, which travels faster than $\sqrt{gh}$ and causes the wavefront (preceding the crest) to spread (but slowly).*

To further study this, a Fourier analysis was performed on the first wave. It must be stated at the outset that taking discrete segments of a wave trace can exaggerate the results and cannot be used to derive absolute values such as energy. The FFT (Fast Fourier Transform) response of a wave packet has the shape of a skewed normal Gaussian spread over a wide range of frequencies, in comparison to a monochromatic wave which exhibits only a narrow, peaked frequency response. If the first wave were a packet, it would contain energy over a broad range of frequencies.

*Figure 5.5* shows an example of one such analysis for the leading wave at five lateral positions. It exhibits the expected response – a skewed normal Gaussian distribution (*figure item 1*) showing that the first wave has the form of a wave packet. Importantly, it shows that after the initial propagation phase, the far field low-frequency components exhibit steady energy levels across a range of low frequencies ($y \geq 3\ m$) (*figure item 3*), but the far field high-frequency components slowly die away (*figure item 2*), which is the equivalent of the schematic in *Figure 5.4*. Also, the spectral density of the lowest frequency component from the analysis, which is the best measure of the strength of an underlying solitary component at the head of the wave, remains perfectly constant (*figure item 4*). *Figure 5.6* overlays a *first wave* Fourier analysis with a *whole packet* Fourier analysis to show that the approach is a satisfactory approximation (but with caution).

To test the hypothesis that the first shallow-water wave was comprised many waves, a unique model experiment was devised. If the first wave was indeed a packet of waves speed limited by the water depth, removing that speed limit and allowing full dispersion would allow the first wave to break into its components.

To achieve this, the AMC model test basin was arranged with a built up, shallow water area along the sailing line and deeper water in the far field. The model, AMC 00-01, would create waves in

shallow water and those waves would propagate into deeper water. The transition between depths at $y = 1.5\ m$ abreast of the sailing line was abrupt rather than a gentle slope, which was unavoidable with the basin geometry. In previous experiments in the reverse, with the vessel in deep water and the waves propagating into shallow water, an abrupt depth transition did not seem to create enough reflection to be significant. In any case, the experiment was intended to be mostly qualitative. The results were not only as anticipated, but strikingly so. Reference is made to a more complete discussion in Appendix H.
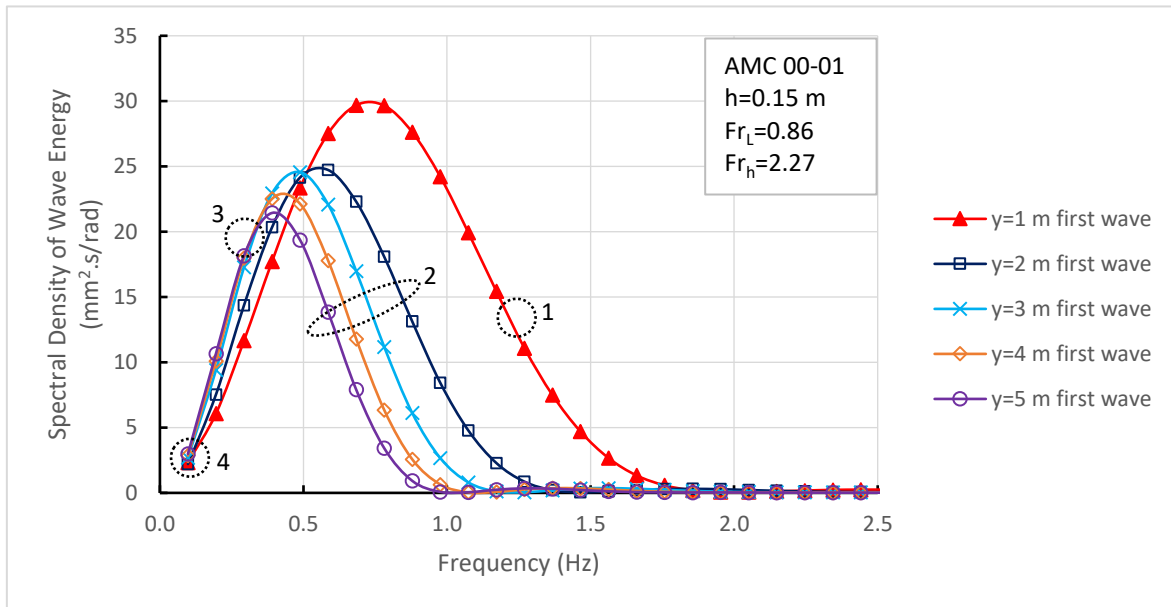


**Figure 5.5** – *Fourier analysis of the first wave at a depth super-critical condition for model AMC 00-01 at five lateral positions. Of note is the consistency of the leading slope at low frequencies at $y = 3\ m$ and beyond, and the gradual dispersion of the higher frequencies (narrowing of the frequency range) - dropping out of the packet as they are unable to travel with the wavefront at $\sqrt{gh}$. The overall shape and very consistent spread of frequencies demonstrates that the first shallow water wave is not a wave, but a packet.*
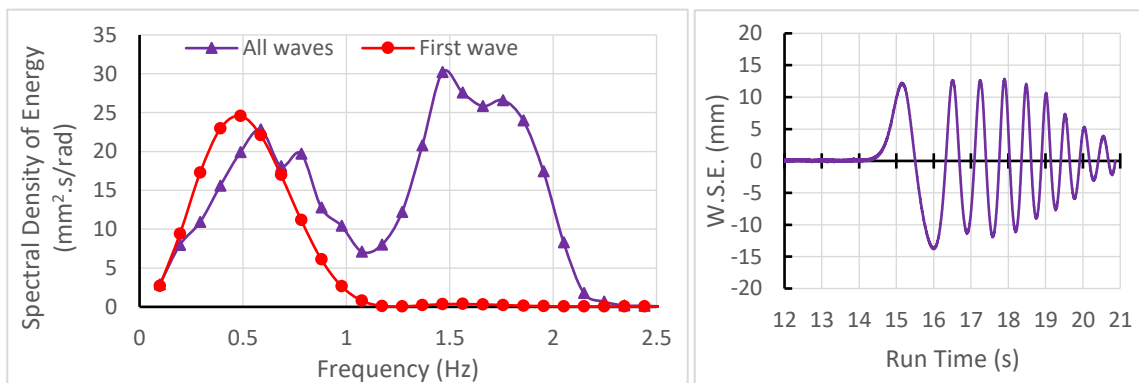


**Figure 5.6** – *Fourier analysis for model AMC 00-01 at $y = 3\ m$ lateral separation corresponding to Figure 5.5. The analysis of the first wave is compared to all waves, showing that the low-frequency hump is reasonably approximated. The wave trace is shown to the right. Note that the low-frequency hump (left hump) would encompass only the first wave and the high-frequency hump (right hump) would account for all the other waves.*

78

*Figure 5.7* (Figure H2 of Appendix H) shows clearly the disintegration of the first wave into multiple component waves once deep water was reached at $y = 1.5\ m$. The first wave is circled with the dashed blue line and the first of the trailing waves is circled in red. The position of the first trailing wave (circled red), taken mid-wave as its zero down-crossing, is almost linear with time at each wave probe ($R^2$=0.9967) and its height decays with a decay exponent of -0.412. An analysis of the energy of the of the decomposing first wave, taken as the summation of each discrete component wave (within the blue dashed area), shows that it propagated consistently to within ± *2%*. Another feature of the total energy was that the waves, once fully dispersive in the deeper water, began to cycle energy back at a faster rate to those waves still in the shallow water. Compared to a constant shallow water condition (without depth change), the trailing waves still in the shallow water experienced a height increase once the leading wave had begun to disperse in the deeper water (Davis, 2018). This is the opposite of what was measured in deep-to-shallow experiments (Drobyshevsky, 2017). These two phenomena, where part of the wave wake is in water of substantially different depth to the wave probe, can cause error in the recorded wave heights (reduction of height at a deep-water probe if the leading waves are in shallow water; increase in wave height at a shallow-water probe if the leading waves are in much deeper water).
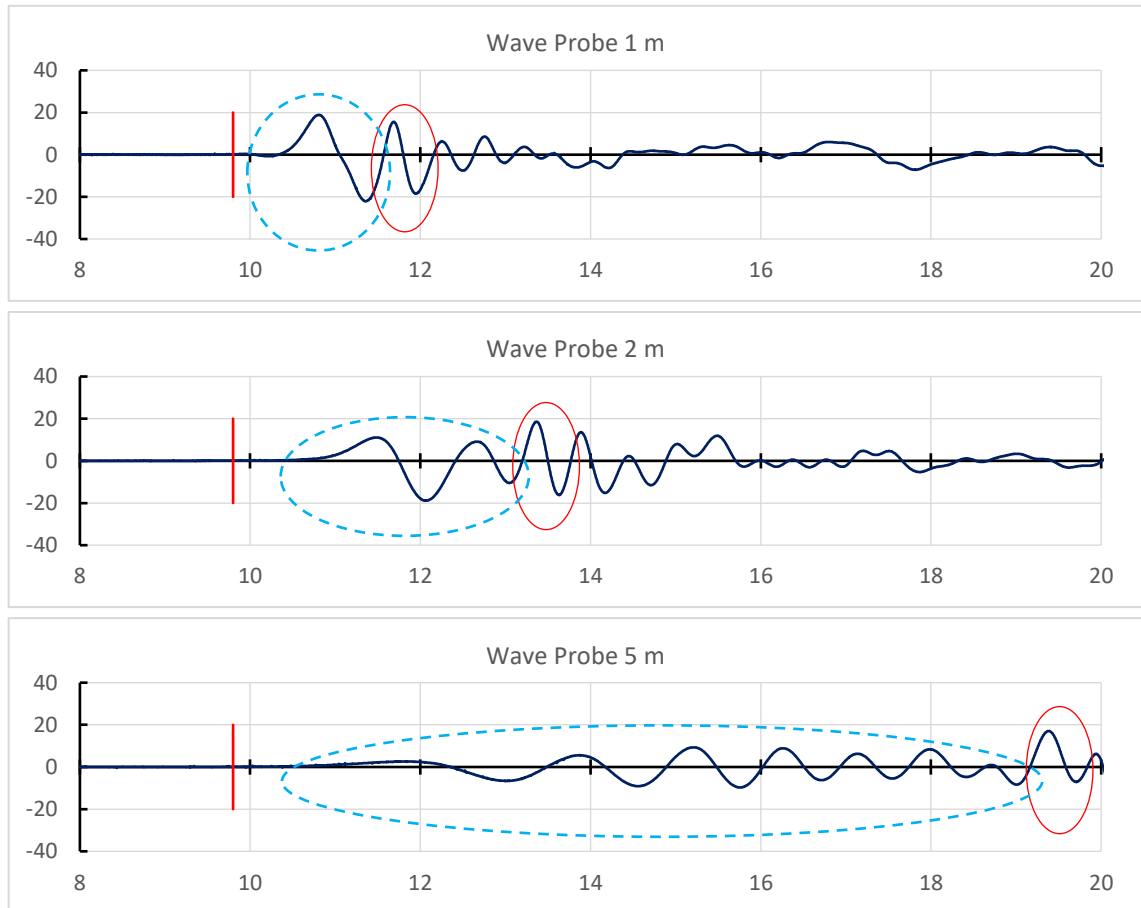


**Figure 5.7** – *Traces for $V = 2.75\ m/s$; $Fr_h = 2.27$ – shallow (150 mm) to deep (900 mm). Water surface elevation is in millimetres and run time is in seconds. The 1 m probe (top) was in shallow water and shows the expected undular bore form. The 2 m probe (centre) was the first deep water probe (depth transition at 1.5 m) and shows the first wave beginning to decompose. The 5 m probe (bottom) was the furthest deep-water probe and shows that the first wave has decomposed into a deep-water packet form, with envelope evident around 10 s to 19 s. The bow crossing is marked at 9.8 s. The decomposing first shallow water wave is circled by the dashed blue line and the first of the more dispersive trailing waves is circled in red.*

### 5.5    Shallow Water and Solitary Waves

### 5.5.1    History

It would be worthwhile to recall briefly the history of the solitary wave. Its discovery in the sense of a formal description is attributed to John Scott Russell in 1834, though the phenomenon in canals was already known to the Dutch (Champneys, 2018). Although Scott Russell went on to conduct his own privately funded studies and publish the results, his findings were largely greeted with scepticism, particularly by the mathematicians of the day. George Airy, the Astronomer-Royal and eminent wave theorist, read Scott Russell's findings (published in 1837, 1840 and 1845), to which he concluded "*We are not disposed to recognize this wave as deserving the epithets 'great' or 'primary' ...*" (Rayleigh, 1876).[63] Airy was unconvinced that such a wave could exist at all, primarily because its very existence discorded with his mathematics.[64] Instead, Airy suggested that the wave observed by Scott Russell was nothing more than a very long periodic wave, which itself is a specious and even ludicrous explanation, given the impossibility for a single periodic water wave to exist, let alone remain in an apparently permanent state.

George Stokes, who initially also agreed that such a wave could not exist (though stated as much far less aggressively than Airy), later believed that such a stable wave was possible by expanding the number of terms in his wave equation. The problem with the available theory was the stability of the wave and how non-linearity caused by the relatively large $H/h$ ratio suggested the wave should steepen and break. Expansion of the wave terms introduced sufficient internal dispersion to counterbalance the steepening, therefore forming a stable crest. Non-linearity causes amplitude dispersion, where celerity is dependent on height rather than frequency. Moreover, the higher parts of a wave travel faster than the lower parts, leading to wave steepening and breaking. In a solitary wave this is balanced by internal dispersion, which would otherwise cause the wave to spread. In the basic form of the KdV equation $u_t + u_{xxx} + uu_x = 0$, the second term $u_{xxx}$ is the dispersive term and the third term $uu_x$ is the non-linear term. The solution to the KdV equation with the dispersive term ignored is a breaking wave; the solution with the non-linear term ignored is a decaying, widening crest that devolves into a dispersive, periodic tail which, given time, acquires the appearance of a shallow water wave wake.

By now it was forty-five years after Scott Russell's first observations. Stokes conveyed his findings to Lord Kelvin in 1879, who wrote back that he disagreed (Champneys, 2018).[65] Neither of them

---

[63] Russell, J. S. (1837). Report of the Committee on Waves, appointed by the British Association at Bristol in 1836. *BA Reports VI*. 417-468 + plates 1-8.
Russell J.S. (1840). Experimental Researches into the Laws of Certain Hydrodynamical Phenomena. *Edin. Roy Soc Trans XIV*. 47-109 + plates I and III.
Russell, J.S. (1845). Report on Waves. *York 1844 BA reports*. 311-390 + plates 47-57.

[64] And, his ego it would seem. Airy had form in that regard, having dismissed the calculations of a junior mathematician as to the possible cause of the erratic orbit of Uranus and missing the opportunity to discover Neptune (not ideal for the Astronomer-Royal!), as well as his role in killing off Babbage's analytical engine project, which he described as "*absolutely useless*" (Filippov, 2000). Had it gone ahead (and worked, of which sub-sections constructed years later appeared to do), it would have pre-dated the earliest Turing-complete electronic computer by about a century. No doubt Airy slept well at night.

[65] The great men of scientific and social status strike again! Kelvin's dismissal discords with his almost sycophantic praise of (the deceased) Scott Russell eight year later in his 1887 lecture (Kelvin, 1887). These men were not alone as products of their time. In 1878, a young Max Planck enquired about a career in physics. A well-regarded physicist, Philipp von Jolly, questioned his choice - "*In this field, almost everything is already discovered, and all that remains is to fill a few unimportant holes.*" Black ones, possibly.

realised that in 1876 Lord Rayleigh had already shown the validity of the solitary wave solution, and that Joseph Boussinesq, using an entirely different approach, had achieved the same five years before Rayleigh, which vindicated Scott Russell's observations (Champneys, 2018). Given the instrumentation limitations of the time, Scott Russell's description of the relationship between the wave celerity and $\sqrt{g(H+h)}$, and therefore its amplitude dispersion in contrast to the frequency dispersion of Airy's waves, are notable.

The solitary wave was termed "*soliton*" in 1965 because of its increasing relevance to particle physics (Filippov, 2000). There is no precise definition of what a soliton is, though there are three principle properties ascribed to it: it is of permanent form; it is localised within a region; it can interact with other solitons and emerge from a collision unchanged, except for a phase shift. The last of these properties, and the phase shift in particular, gives rise to its relevance to particle physics, though the existence of the phase shift was not realised until around *120* years after Scott Russell's initial observation. It is also the last property – emerging from a collision unchanged – that disqualifies solitary waves in water as being true solitons, and they are instead termed *near solitons*. Mathematicians had proposed the shedding of a tail of periodic waves after a collision, which was only described experimentally in very recent years (Craig *et al*., 2006, among others). In all cases here the ambiguous term *soliton* is avoided when describing individual waves unless used in context by a referenced author or when describing a wave packet envelope, and only the term *solitary wave* is used.

John Scott Russell was not a mathematics novice, but as a Scotsman and a shipbuilder from a lowly background he was up against the scientific and social establishment from the start, especially with his reliance on frivolous experimental and empirical *hobbies*. Although an Irishman, Stokes fared better because of his irrefutable mathematics, and it was only mathematics that counted.[66] Scott Russell had the vision but not the highest level of pure mathematics, or social status, necessary to realise it. Airy had the mathematical ability – the positive application of which is diminished for someone who cannot see.

### 5.5.2  Solitary wave theories
In this study, reference is made to different solitary wave theories. There are four in common application: Korteweg de Vries (KdV) – being the shallow water limit of cnoidal wave theory; Boussinesq (Bq) – which describes a solitary wave as an independent entity; Improved Boussinesq (iBq) – which corrects minor errors in Boussinesq's original derivation affecting the width of the wave form; Benjamin Bona and Mahoney (BBM) – a more recent approach that can be regarded as a hybrid result. Further reading can be found in Dingemans (1997, p. 705-707). The general first-order equation for a solitary wave is:

$$\zeta(x,t) = H \operatorname{sech}^2\left(\frac{x-ct}{\Delta}\right)$$

[5.4]

where the wave celerity $c$ and the width $\Delta$ are shown in ***Table 5.2***. The width $\Delta$ is the inverse of the wavenumber $k$ and therefore the nominal wavelength of a solitary wave is $2\pi\Delta$.

---

[66] Class and mathematics were seemingly used as means of keeping the empirical *riff raff* out of science. As a self-educated scientist and empiricist from a low-class background, Michael Faraday was forced to act as butler and valet to his mentor, Sir Humphrey Davy, during scientific excursions to Europe, which included tending to his clothes and emptying his chamber pot [Voss, D. (Ed.) (2016). This month in Physics History. *APS News, Vol. 25,* No. 3, American Physical Society].

As a vessel progresses from a depth sub-critical speed towards a depth critical speed, the transverse waves, which are travelling at the vessel speed, increase in height and reduce in wavelength. Also, the rate of dispersion (assuming the dispersive, real condition of a vessel having accelerated from rest and not the constructed, infinitely steady-state condition) reduces, causing the tail of the wake to propagate at almost the vessel speed ($c_g/c_p \rightarrow 1$). A point will be reached where the primary components of the wave wake appear coalesce into a single (or a few) significant waves, which are commonly (and erroneously) termed *solitons*. This forms the end condition described by the Korteweg de Vries equation, moving from a sinusoidal form in a deep condition to a solitary form at the shallow limit.

**Table 5.2** – *Parameters for first-order solitary wave equations (from Dingemans, 1997, p. 707). Also refer to Appendix E.*

| Solution | celerity, c | width, Δ |
|---|---|---|
| Korteweg de Vries, **KdV** | $\left(1 + \dfrac{1}{2}\dfrac{H}{h}\right)\sqrt{gh}$ | $\sqrt{\dfrac{4h^3}{3H}}$ |
| Boussinesq, **Bq** | $\sqrt{g(h+H)}$ | $\sqrt{\dfrac{4h^3}{3H}}$ |
| Improved Boussinesq, **iBq** | $\sqrt{g(h+H)}$ | $\sqrt{\dfrac{4h^3}{3H}\left(\dfrac{c}{\sqrt{gh}}\right)}$ |
| Benjamin Bona Mahoney, **BBM** | $\left(1 + \dfrac{1}{2}\dfrac{H}{h}\right)\sqrt{gh}$ | $\sqrt{\dfrac{4h^3}{3H}\dfrac{c}{\sqrt{gh}}}$ |

### 5.5.3 Solitary waves at trans-critical speeds

McCowan (1894) showed that a solitary wave could be generated by a bore in a super-critical flow provided the flow's depth Froude number was less than *1.25*. Benjamin and Lighthill (1954) remarked that the value may be slightly less (~*1.21*), necessary to balance the energy released at the bore. They also state that "*For it is known that, for every Froude number between 1 and some limiting value, a uniform supercritical stream may form without frictional effects into a solitary wave.*" **Figure 5.8** (from Appendix G, Figure G4) compares the crest heights and trough depths of the first wave of three models at a lateral offset of about *1 m* in shallow water. Crest amplitudes and trough depths have been divided by slenderness ratio to provide a degree of normalisation. Two models are monohulls and one is a slender catamaran form. The crest heights peak at a vessel depth Froude number conforming to the limiting super-critical flow condition of McCowan and Benjamin/Lighthill for a bore. In this case the wake of the vessel, operated at varying depth sub and super-critical speeds, becomes the analogue of the bore. Conversely, the troughs reach a maximum depth around the critical speed, except that the catamaran exhibits an extended range.

When considering wave generation and wave height, a vessel operating at depth super-critical speeds just above the critical speed realises the worst condition. It might be expected that vessel residuary resistance would peak at or about the same super-critical speed as the wave height, or at least at the critical speed where $Fr_h = 1$. At the same time the angle between the sailing line

and the rays containing the waves would be expected to reach *90 deg.* as the wavetrain reached a *non-dispersive* condition at $Fr_h = 1$ (Havelock, 1908, Fig. 8).[67] This is actually not the case. Both a vessel's residuary resistance and subtended wave angle are known to reach maximum values at $Fr_h \sim 0.9$ (for the vessel), beyond which they decrease as the transverse waves transform. This is discussed in detail by Robbins (2013), who provides examples, including his Fig. 20. However, in demonstrating what has been a reasonably well-known phenomenon, Robbins (2013) attributes these premature maxima to *non-linear viscosity effects*, which is most likely not the case. They are known to occur at model and full scale (inferred from Kofoed-Hansen *et al*., 1999, Fig. 3), and that alone should disqualify viscous effects as a cause.

In a depth sub-critical condition and as vessel speed approaches $\sqrt{gh}$, the waves in the wave system will become increasingly depth affected. For some of the component waves in the system, a point will be reached where $\lambda/h$ approaches a fully shallow condition. Benjamin and Lighthill (1954) make the comment that weak undular bores evolve into a train of sinusoidal waves and strong undular bores evolve into a train of solitary waves. Grimshaw (2011) confirms this, adding that the effects become pronounced as $t \rightarrow \infty$. Although the vessel may be in a depth-sub-critical condition, components of the wake representing solitary waves, present at the non-dispersive head of the undular bore, will reach criticality. That is important to overcome the observation of Benjamin and Lighthill (1954), that a train of cnoidal waves may have the appearance of an undular bore, but alone cannot form an undular bore in a uniform flow. Wave wakes formed in deep water and transitioning to shallow water cannot have the same form as those generated at depth super-critical speeds in shallow water to begin with. In the case of the shallow water vessel wave wake, the leading solitary component would be in existence from the time of generation. Further reading can be found in Wu (1987, p. 86).

Wu (1987) explains it clearly, though in relevance to solitary waves (termed by some as *precursor solitons*) formed in the traditional sense of $Fr_h < \sim 1.2$:

> *"Generally speaking, its physical significance can be attributed to a well-balanced interplay between the nonlinear and dispersive effects. In this transcritical speed range, the dispersive effect is weak, so the velocity of propagating mechanical energy away (by means of radiating long waves) from the forcing disturbance is about equal to the velocity of the moving disturbance. The local wave will therefore grow as the energy acquired by local fluid at the rate of work by the moving disturbance keeps accumulating. When the local wave reaches a certain threshold magnitude, the increase in phase speed with increasing amplitude (due to the nonlinear effects) will be sufficient to make the wave break away from the disturbance, thus 'born free' as a new solitary wave propagating forward with a phase velocity appropriate to its own amplitude. The process is then repeated over a new cycle."*

It can be shown readily that a long wave, having reached a defined (or nominated) *fully shallow* condition, would achieve a (wave) depth-critical celerity at a critical vessel depth Froude number

---

shown in [5.5] and [5.6], assuming the relevant solitary wave parameters in **Table 5.2**.[68] At vessel depth Froude numbers above this critical condition, the long waves have transformed to a depth super-critical condition, which reduces drag. In generic terms, this critical vessel depth Froude number is:

**KdV form** $$Fr_{h,crit} = \left[1 + \frac{8\pi^2}{3(\lambda/h)^2_{shallow}}\right]^{-1}$$ [5.5]

**iBq form** $$Fr_{h,crit} = \left[1 + \frac{1}{3(\lambda/h)_{shallow}/\pi^2 - 1}\right]^{-\frac{1}{2}}$$ [5.6]

where $(\lambda/h)_{shallow}$ describes the point where the waves could be considered as *shallow (*in terms of *deep, transition and shallow)*. **Table 5.3** shows how the vessel critical depth Froude number varies with different definitions of *shallow* (refer Table 5.1 and discussion).

**Table 5.3** - *Calculated vessel depth Froude number at which residuary resistance and wave angle reach their maximum, for different definitions of shallowness.*

| | | KdV | iBq |
|---|---|---|---|
| **Shallowness Definition** | $(\lambda/h)_{shallow}$ | **Vessel $Fr_{h,crit}$** | **Vessel $Fr_{h,crit}$** |
| Lighthill | 14 | 0.882 | 0.875 |
| Fenton; Dean & Dalrymple; (Cox) | 16 | 0.907 | 0.891 |
| Dingemans | 20 | 0.938 | 0.914 |
| Shore Protection Manual | 25 | 0.960 | 0.932 |
| Limit | $\lambda/h \to \infty$ | $Fr_{h,crit} \to 1$ | $Fr_{h,crit} \to 1$ |

Two important results of [5.5] and [5.6] are that wave height cancels out and water depth appears only in the definition of *shallow*. Experimental examples are presented in Appendix E, where restricted channel width and water depth did not seem to change the depth Froude number at which the peak wave drag coefficient occurred; they only influenced its magnitude. This concurs with the findings of Robbins (2013) and the apparent disjuncture between wave angle and shallowness in terms of depth relative to vessel length at the peak condition. Dand (2002, Fig. 1) concurs in relation to model-scale residuary resistance coefficients of a catamaran and its demihull variant, with the resistance peak occurring at $Fr_h \approx 0.9$ for both $h/L = 0.047$ and $h/L = 0.125$.

The question then becomes which of these two wave forms is correct (or more correct). Based on shallow water experiments conducted for this study (discussions following), the iBq form is more likely to be correct, but not initially. The experiments conducted here showed that solitary waves formed from undular bores are only able to detach and propagate independently once they achieve an iBq wave profile – the iBq profile being fuller than the KdV profile and therefore having greater energy. The experiments and numerical comparisons of Lee *et al.* (1989, Fig. 10b) would confirm this, though it was not observed by the authors: wherever the leading solitary crest

---

[68] Derived using the relationships for KdV and iBq solitary wave celerities and widths in Table 5.2, knowing that $\lambda = 2\pi\Delta$ and assuming a limiting shallow water condition of $(\lambda/h)_{shallow}$ has been achieved.

appears to propagate independently (without trailing trough below the free surface), the experimental crest aligns temporally with the numerical Boussinesq crest, and wherever the leading solitary crest appears to propagate dependently (with trailing trough below the free surface), the experimental crest aligns temporally with the numerical KdV crest (i.e., not fully energised). Regardless, there is little practical difference between the two forms, provided the longest component waves are sufficiently close to a non-dispersive state to trap energy cycling through the packet from the trailing waves. Further discussion can be found in Appendix E.

Knowing that undular bores will form into solitary waves given sufficient time (Grimshaw, 2011), it is also quite possible that, given enough time, solitary waves would be shed from a model at even lower vessel depth Froude numbers than shown in *Table 5.3*. It would never happen at full scale due to bathymetry and speed variability, but it has been witnessed at model scale. There may be a lower critical limit, but it may simply be that present model test facilities are insufficiently long to allow solitary waves to form and shed at reduced sub-critical conditions. The non-linear model of Lee *et al.* (1989) showed that a moving disturbance could create solitary waves down to $\sim Fr_h = 0.2$ (inferred from Lee *et al.*, Fig. 6), but with greatly diminished amplitudes that may not be detectable below $\sim Fr_h = 0.6$ in practice (Lee *et al.*, Fig. 3). The solitary waves must reach a critical energy level to shed and the rate of transfer of energy between the trailing waves and the solitary waves is a function of the degree of dispersion – the greater the dispersion in the wake, the slower the accumulation of energy in the leading solitary waves. That would best be investigated using an extremely short model in extremely shallow water (time scales with $\sqrt{L}$), but with attendant errors due to speed and depth stability at the small scale.

Although *Table 5.3* shows variability in what may be considered as the wave supercriticality transition point, Lighthill's $\lambda/h = 14$ is the lowest value defining *shallow* noted in the literature and therefore could be considered as a practical lower bound. The value of *0.875* for Lighthill's definition of *shallow* is less than *3%* lower than the value *0.9* quoted experimentally. Extended discussion of this condition, with experimental and numerical examples, can be found in Appendix E.

Lastly, the limit condition where the wave angle at least would concur with the theoretical angle (*90 deg*.) calculated by Havelock (1908) can only be so when the wavelength is infinitely long, or the water depth is infinitely shallow, and the waves become truly non-dispersive (refer footnote 67). That returns us to a previous comment: "*no water, no waves*." It mirrors the fact that the group and phase velocities converge but never meet in shallow water. As with the definitions of $(\lambda/h)_{shallow}$ in *Table 5.3*, there may be cause here for a *practically non-dispersive* definition, along the lines of "*within 3%,*" as favoured by Lighthill.

There is an analogy between the criticality of a generated solitary wave at slightly sub-critical vessel speeds and the development of shock waves. In aerodynamics, the term *critical Mach number* ($M_{crit}$) refers to an aircraft's Mach number when the accelerated flow over its wings reaches a Mach number of unity and shock waves form. Variables such as compressibility, planform and sectional shape can vary $M_{crit}$ considerably (and complicate the analogy for compressible and incompressible flows), but a commonly stated value for the (non-lifting) fuselage is around *0.9*, which concurs with the value calculated here. In that case the aircraft is in

a subsonic condition but some of the flow around it has accelerated to supersonic. In this analogy, $M_{crit}$ is the equivalent of $Fr_{h,crit}$.
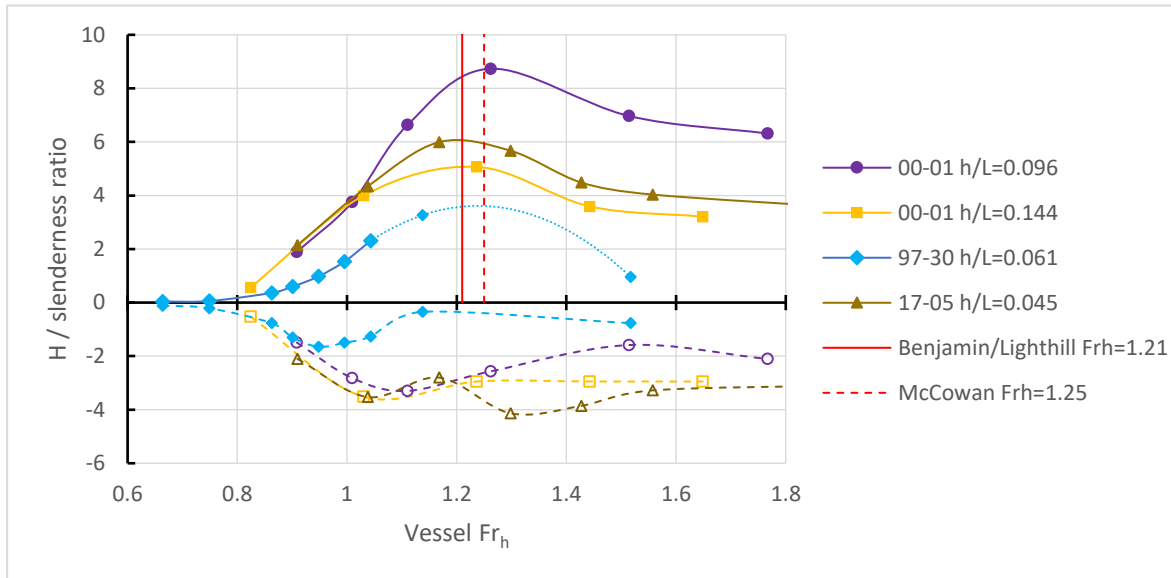


**Figure 5.8** – *Amplitude of leading crest (solid lines) and depth of the following trough (dashed lines) against depth Froude number for three models at different $h/L$ ratios and at $y{\sim}1L$. Models 00-01 and 97-30 are monohulls, and 17-05 is a low-wash catamaran. Amplitudes/depths have been normalised by the slenderness ratio – the traditional non-dimensional parameter relevant to wave height. In all cases the leading crest peaks around $Fr_h{\sim}1.25$, as predicted by McCowan (1894). The trough minimum occurs earlier, except for the catamaran which exhibits an extended range. Similar trends were evident at wider lateral positions. Although $Fr_h{\sim}1$ has long been considered the worst wave wake case for vessels in restricted waterways, a higher value would be warranted for vessels in open, shallow water.*

### 5.5.4  Solitary waves at super-critical speeds

A comprehensive review of available literature does not provide any reference to solitary waves in vessel wakes at speeds well beyond the critical speed condition. One of the most recent depth critical speed studies is that of Robbins (2013), whose *Wash Characterisation Summary Table* (Robbins, 2013, Table 7, p. 109) notes that *solitons* are only evident in one condition, "*Shallow Water Critical* ($Fr_h \cong 1.0$)," and not at other conditions. That is a peculiar statement as it conflicts with the study's text, where *solitons* had been noted in the range $0.9 < Fr_h < 1.2$ (refer Robbins, 2013, p. 49 and the discussion of the findings of Ertekin [19]).

As discussed, the work of Benjamin and Lighthill (1954) and McCowan (1894) showed that solitary waves cannot be generated in a uniform stream of greater depth Froude number than about *1.25*. In McCowan's case the limiting condition also corresponded to the maximum amplitude of the solitary wave at that depth Froude number, which became the commonly quoted breaker depth index of $H_b/h = 0.78$ (sometimes denoted as $H_b/h_b$). Advances since McCowan's time have increased the breaker depth index slightly, but rarely are values above $H_b/h = 0.83$ reported, which extends the limiting depth Froude number up to almost *1.3* (Fenton, 1990; Yamashita and Kakinuma, 2014). Conversely, values around $H_b/h = 0.55$ have also been recorded (Fenton, 1999). In the field of ship waves, reports of solitary waves at $Fr_h > {\sim}1.2$ are not recorded and are regarded as not possible (Robbins, 2013). At least, until now. Again, we must differentiate

between the depth Froude number limit of the wave and the depth Froude number limit of the vessel when generating solitary waves. There is an upper limit for a solitary wave in terms of limiting celerity in a given water depth, but not for the vessel generating it.

During shallow water model experiments conducted for this study, certain phenomena kept appearing. The model used, AMC 00-01, has a slenderness ratio in its heavy test condition of *4.75*, which is typical of the vessel type it represents (small to medium recreational craft) but less than most commercial passenger ferries. A reduced slenderness ratio has the effect of amplifying wave wake effects, particularly wave heights. At low $h/L$ ratios, in this case *0.144* and lower, the leading wave became the dominant wake wave. Moreover, its period continually increased with lateral separation, increasing *75%* over just four boatlengths of lateral separation. The crest/trough asymmetry also reduced in that time. That can be seen in ***Figure 3.12***.

To investigate the period change, salient temporal features of the first wave were plotted spatially, as they would be around the critical speed for studying crest positions (refer Appendix D). Lighthill (1978, p.466) refers to the initial upswelling of a solitary wave as being the point where the local amplitude is *3%* of the crest amplitude; the method describing the wave's notional wavelength. This condition is shown in ***Figure 5.9***. The lateral variation of the initial upswelling was compared to the crest and the calculated wavefront based on the maximum wave celerity of $\sqrt{gh}$ (Havelock, 1908). Interestingly, while the crest followed the Havelock wavefront perfectly, the initial upswelling subtended an angle several degrees more than the Havelock wavefront and with a very consistent straight-line form away from the model. That suggested there was a component of the first wave able to travel faster than $\sqrt{gh}$, and the only wave capable of that is a solitary wave. It was premised that the leading wave of a shallow water wake has at least a component solitary wave buried within it. That also led to the discovery that the first shallow water wave is not a wave, but a packet of waves of similar (but slowly increasing) frequencies that are formed at the sailing line but are unable to spread quickly because of the weak dispersion. They are trapped in the first apparent wave and only leak out slowly with propagation as the higher frequencies gradually fall behind.
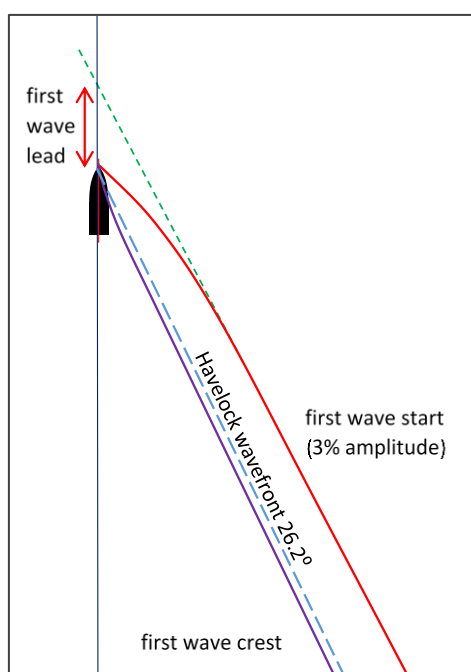


*Figure 5.9* (*Appendix D, Figure D6*) *– Wake pattern of the initial upswelling and first wave crest at super-critical speeds for model AMC 00-01 at $h/L = 0.144$, $V = 2.75\ m/s$ and $Fr_h = 2.27$. The figure is drawn to scale, with the vessel length representing the model's static waterline length of 1.04 m. The first wave crest corresponds to the calculated Havelock wavefront based on the limiting celerity of $\sqrt{gh}$..*

*The angle of the initial upswelling is 27.9° and its celerity is approximately 6% faster than $\sqrt{gh}$. Increased celerity of a periodic wave at depth super-critical vessel speeds should decrease the wavefront angle – a strong indicator that the initial upswelling is due to a solitary wave component, which is the only wave form that can propagate faster than $\sqrt{gh}$. As shown in Appendix M, the angular uncertainty is ±0.3°.*

To further magnify the shallow water effects, another experiment was conducted in very shallow water ($h/L = 0.096$). That produced an even stronger solitary component of the first wave – sufficient in strength that the leading crest angle exceeded the classical Havelock wavefront angle. It was shown that the crest celerity conformed to that of a solitary wave of KdV form and the wavefront angle using the celerity of the solitary crest in place of $\sqrt{gh}$. This is shown in **Figure 5.10**. Trailing the leading crest was a periodic tail resembling an undular bore.
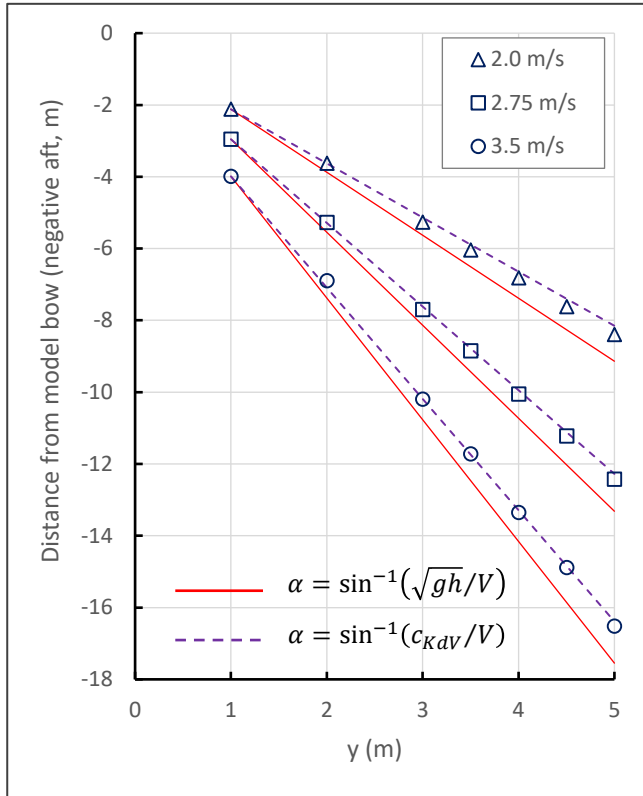


**Figure 5.10** – *Positions of the first crests of Model AMC 00-01 at three super-critical speeds in 0.1 m water depth. This is considered as an extremely shallow depth, with $h/L = 0.096$. The depth-critical speed is 0.99 m/s.*

*The solid (red) lines show the classical Havelock wavefronts based on $\sqrt{gh}$, and the dashed (purple) lines show the Havelock wavefronts based on the KdV solitary wave celerity given in Table 5.2. The Boussinesq form of the solitary wave celerity would give marginally slower wavefronts, lagging slightly behind the KdV wavefront.*

*The consistency of crest positions with the solitary wave form of the Havelock wavefront is demonstrated. Note that the axes are scaled differently for clarity. Wavefronts are notionally aligned to their respective crest positions at $y = 1\ m$.*

### 5.5.5   Very Shallow Water – Depth Transition (Appendix G)

The lack of any published information on the existence of solitary waves at the vessel depth super-critical condition ($Fr_h > {\sim}1.2$) required an alternative approach. Considerably more information was available on hydraulic jumps and bores, and the wave wake in shallow water had similarities to the bore released at a hydraulic jump (R.G.H. Grimshaw 2017, pers. comm., 7th November). In the analogue proposal, the solitary wave leading the wake would create the hydraulic jump and the trailing periodic waves would form the bore, even though it is not exactly the same as the traditional case where the water is moving and the cause of the hydraulic jump (usually a bottom step) is fixed. If similar outcomes between the two cases could be demonstrated, there was better chance of finding explanations in the hydraulic engineering literature where such processes have been studied extensively. The experimental setup, shown schematically in **Figure 5.11**, allowed the wake formed in shallow water to propagate into even shallower water, forcing a transformation.

The purpose of the experiment was four-fold:

a. to force the undular bore formed at the $h = 0.1\ m$ condition to become unstable (turbulent or breaking), demonstrating that the very shallow water wake does conform to general bore relationships;
b. to determine qualitatively how the bore changes when the parameters causing it change;
c. to observe changes to the leading solitary waves on transition;
d. to determine if the leading solitary wave component of the wake is able to fully disassociate itself from the trailing periodic wake and propagate independently.
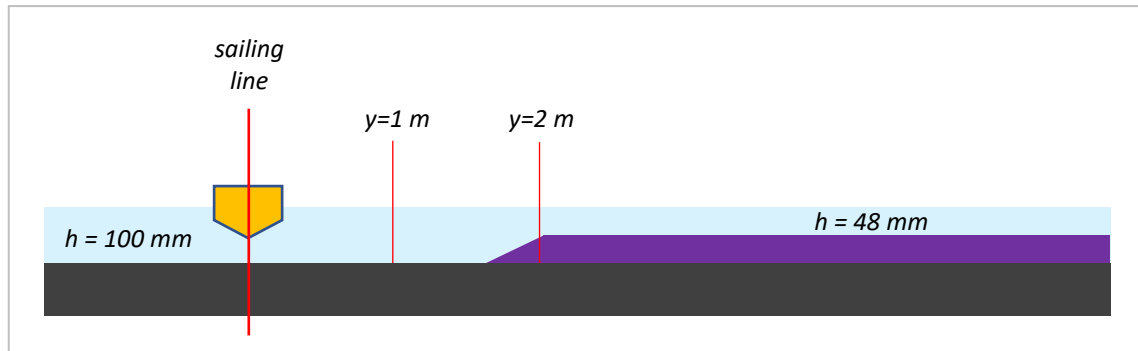


**Figure 5.11** – *Sectioned schematic of shallow water transition experimental setup (not to scale).*

Transmission and reflection over the step are discussed in Appendix G. There isn't a simple method to estimate transformed heights where the waves are not perfectly plane (in the true definition of a plane wave) and are not propagating normally to the step, but that was not the purpose of the experiments.

The results were quite conclusive. ***Figure 5.12*** shows salient features of this experiment. Firstly, as predicted, the stable undular bore (periodic waves following the solitary leading crest) became unstable some distance into the shallow water. The waves could never form into a cohesive, single *breaking bore*, but the waves could break individually. Secondly, the leading solitary wave transformed in several ways. It reduced in height and shed a secondary solitary wave to maintain its stability. It also experienced an apparent change of form with increasing lateral separation (discussed following). Thirdly, and most importantly, the leading solitary wave began to detach (decouple) itself from the wake and propagate independently. This is shown in ***Figure 5.13***. That has relevance in explaining how the wave wakes from large, high-speed ferries operating on near-coastal routes have at times created dangerous wakes. It is known that the leading shallow-water waves were to blame, but the mechanism has never been properly explained.

The change of form is consistent. If the solitary component is weak or still attached to the trailing periodic wake, it has a KdV profile. The KdV solitary wave profile is narrower than the fuller iBq profile. With increasing propagation, the solitary wave becomes fuller; initially in the leading part of the wave (before the crest) and eventually all the wave. At the time of detachment and propagation independent of the trailing wake it has increased to the volume predicted by the iBQ equations. The energy of a solitary wave is proportional to the area under the crest and so the wave appears to be energising itself prior to detachment. This energy can only come from the trailing periodic waves due to the (weak) dispersion. In essence, energy that normally cycles through the packet from tail to head and back again becomes trapped by the non-dispersive

solitary wave.[69] If the solitary wave is weak (insufficient strength caused by water too deep or insufficient amplitude), it may take many cycles for enough energy to be tapped slowly from the trailing wake. Examples of this are shown in Appendix G and Appendix F.
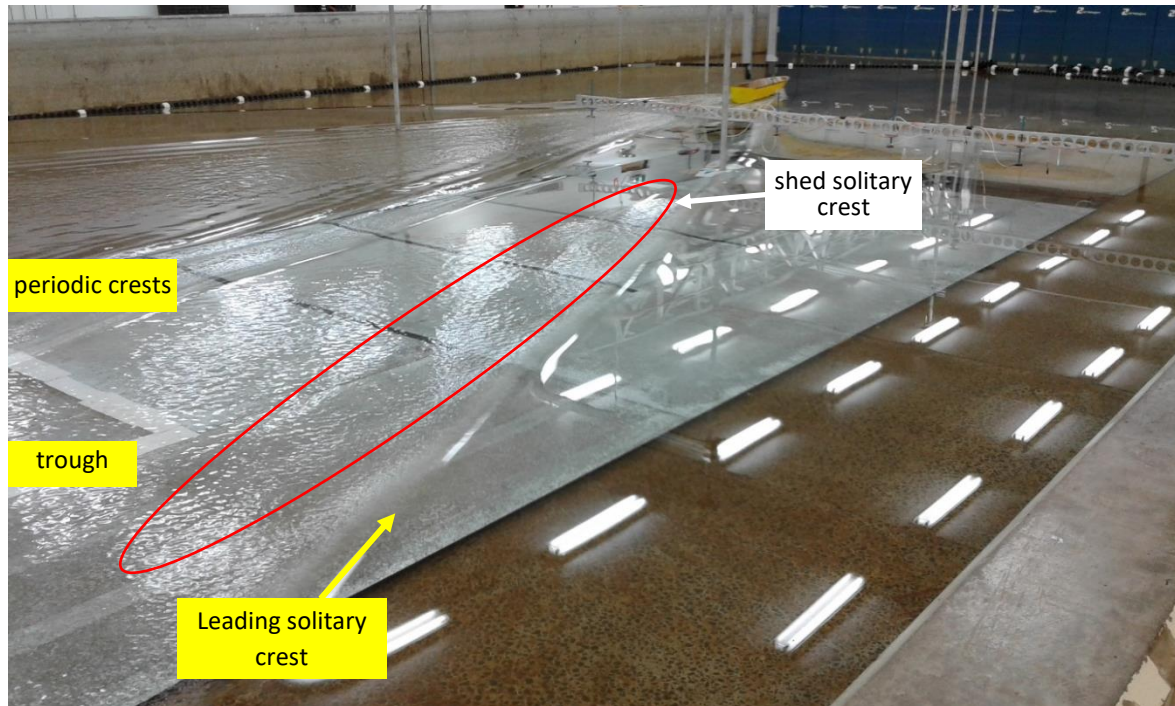


**Figure 5.12** – *Test at 3.25 m/s ($Fr_h = 3.28$ at the sailing line). The very shallow section (silver colour) extended just beyond the measurement area but was later widened to study the leading crest propagation. It is possible to see the small solitary wave shed by the leading solitary crest (more readily visible at larger scale). There is also turbulence evident in the trough after the leading crest but commencing only about 1.0 m after the depth transition. Before this trough turbulence, the trough is glassy. Note also the leading crest/trailing waves in the background at a constant depth on the opposite side of the sailing line (top of photo).*
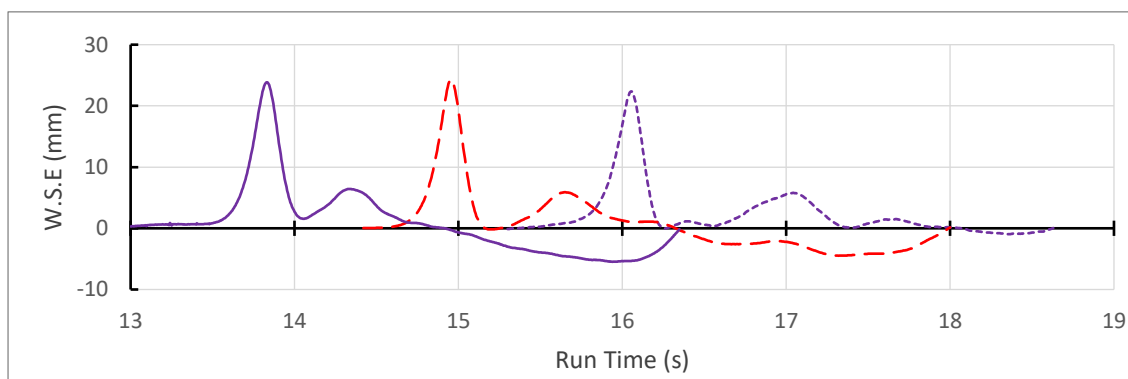


**Figure 5.13** – *Leading crest and trailing trough at a model speed of 3.0 m/s, $h = 48\ mm$ (at the probes), for the 4, 5 and 6 m probes. The 6 m trace has been truncated due to reflections. Note the stable amplitude of the shed solitary wave at around 7 mm. The first trough after the leading crest does not dip below the still water level, showing that the leading crest is a solitary wave in the process of decoupling itself from the rest of the wake.*

---

[69] Non-dispersive in frequency terms as the head of a shallow water packet and not in terms of internal dispersion within the solitary wave itself. Its internal dispersion is a closed system.

### 5.5.6 Extremely shallow water (Appendix F)

Experiments on model AMC 00-01 were conducted at a water depth of *52 mm*. The model has a static draft of about *60 mm* at the standard (laden) test displacement, and to accommodate this the model was fixed in heave and trim at an attitude that approximated its shallower dynamic planing waterline. The dynamic trim and midships draft normally vary with speed - both decreasing with increasing speed. It was expected that the fixed attitude would give about the same combination of displaced volume and dynamic lift to the free-trimming tests in slightly deeper water. In reality, that was probably not quite the case at all speeds, so the results should be viewed qualitatively only. The fixed heave and trim attitude would only be relevant to the highest speeds; at lower speeds where planing lift was lower, the vessel would normally sit deeper and trim more, which would increase wave height.

It was again confirmed that there is a relationship between the solitary wave height and its super-criticality; the maximum height occurring at $Fr_h \sim 1.25$ where McCowan (1894) predicts the limiting condition to be, even though the fixed experimental setup had a shallower planing attitude than would occur at this pre-planing speed. Another peculiar result from the transition test (Appendix G) was also confirmed but is not explained in the available literature. As the (leading) solitary wave propagates away from the sailing line, its profile changes from the slimmer KdV form to the fuller iBq form. Examples are shown in ***Figures 5.14*** and ***5.15***. The rate and the completeness of this transformation depends on $Fr_h$ and lateral separation; increasing both improves the transformation. The volume under a solitary wave is a measure of its energy (Munk, 1949) and therefore the iBq form would be more energetic. As shown in Appendix F, the relationship between spatial volumes of the two forms is $\nabla_{iBq}/\nabla_{KdV} = \sqrt{(H+h)/h} = Fr_{h,iBq}$. Moreover, only when the far-field crest assumed an iBq profile did it appear to detach from the trailing wake and propagate independently – defined as being *without trailing trough*. The premise is that a solitary wave needs to attain a certain energy level for it to detach, with (weak) dispersion throughout the group causing energy to be trapped in the non-dispersive head (the solitary crest), energising it at the expense of the trailing waves. An analogy is with boiling water and the latent heat required for the phase change.
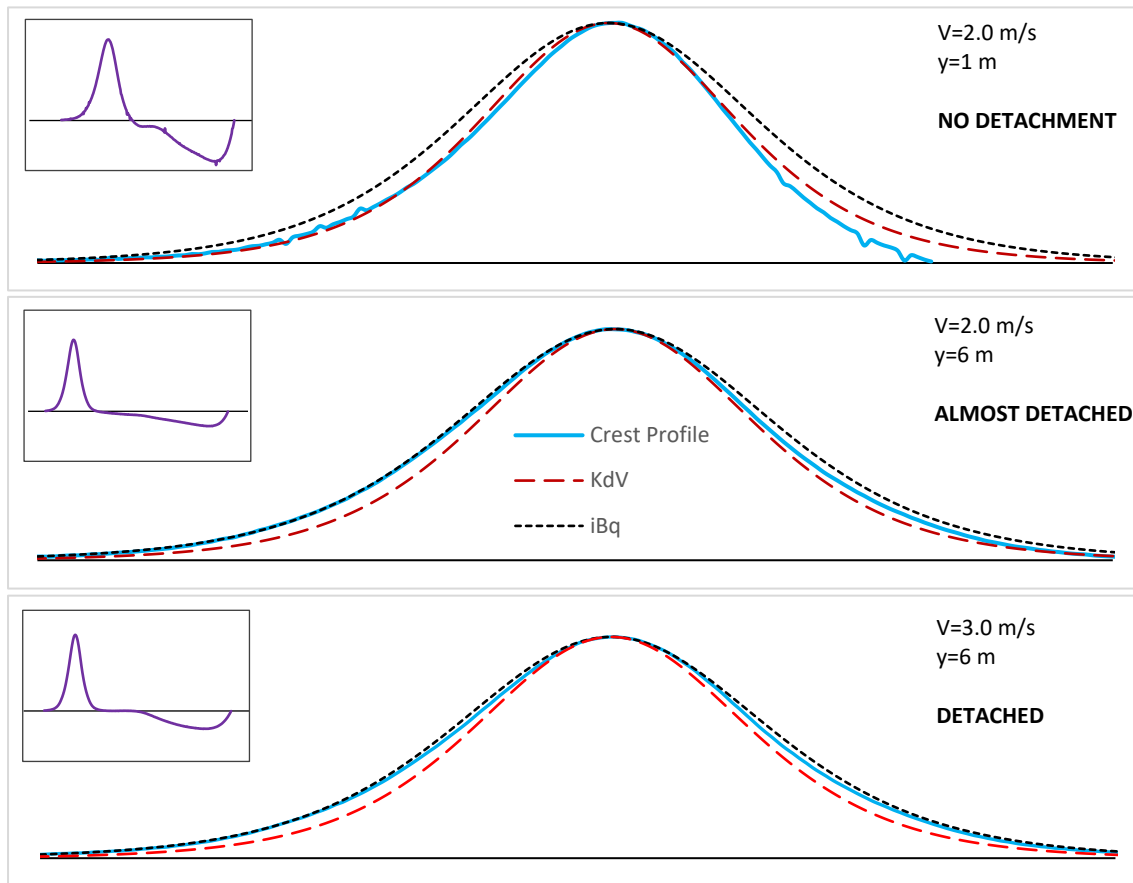
**Figure 5.14** – *(Figure F3, Appendix F) Evolution of the leading solitary crest at different lateral positions and model speeds (wave propagation right to left). The top two figures at $V = 2.0\ m/s$ show the change in profile from a KdV to iBq form with propagation from near field ($y = 1\ m$; ~1L) to far field ($y = 6\ m$; ~6L), demonstrating an increasing volume and therefore increasing energy content relative to height. The lower figure at a higher speed in the far field shows an almost complete agreement with the iBq form. Refer to Figure 5.15 following and the partial/full detachment of the solitary crests in the far field in this case.*
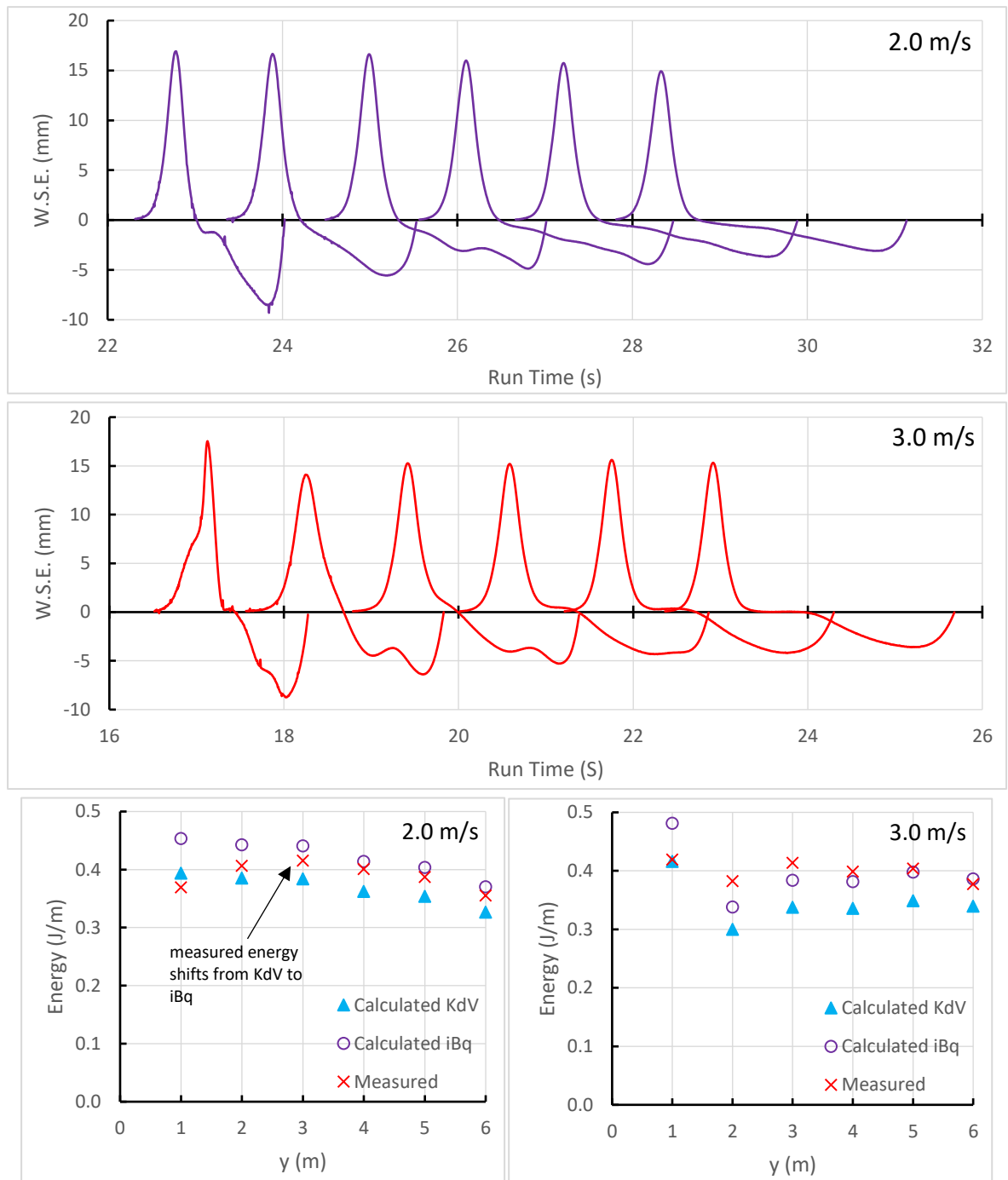
**Figure 5.15** – (Figure F4 – Appendix F) *Solitary wave energy comparison for two extremely shallow test conditions (h = 52 mm) for model AMC 00-01 with six wave probes at $y = 1\,m \rightarrow 6\,m$ ($\sim 1L \rightarrow \sim 6L$). Only the first crests and troughs are shown. Most notable is how the leading solitary wave energy evolves from a KdV value in the near field to an iBq value in the far field. The 2.0 m/s results are most descriptive in that regard; the 3.0 m/s crests have irregularities (possibly from model spray at the higher speed) that change the volume.*

### 5.5.7    Propagation of solitary wave – depth transition (Appendix H)

An additional feature of the shallow-to-deep experiments was the propagation of the leading solitary component of the first shallow water wave. Once into deep water, the solitary component was able to propagate at its unrestricted speed, though it did tend to disintegrate quickly in the deeper water where it could not remain stable (too much dispersion and too little non-linearity). *Figure 5.16* shows the first wave crest for different speeds in two different depth transitions: *100 mm* to *850 mm* and *150 mm* to *900 mm*.[70] At the slower speeds, the first crest began to catch up to the model before disintegrating; at the higher speeds, it lagged. At a vessel speed around *2.5 m/s* the leading crest remained perpendicular to the sailing line in the deeper water. Taking the model speed and the deep-water depth, the depth Froude number at that speed was just below *0.9*, which is around the speed where shallow water resistance peaks and the wave angle reaches *90 deg*. This further supports the discussion on solitary waves at trans-critical speeds and concurs with the explanation as to why resistance and wave angle peak before $Fr_h = 1$. It also supports the proposal that the waves generated in shallow and deep water are one in the same but manifest themselves differently at different water depths.

Ertekin and Wehausen (1986) present numerical modelling of *solitons* in different conditions (the reference found *after* conducting these experiments). One of those studied was a *soliton* propagating from a shallow shelf to deeper water over a slope (Ertekin and Wehausen, 1986, Fig. 12). It was noted that the single *soliton* generated in the shallow water devolved into a wave train upon reaching the deeper water, which was predicted by Johnson (1973).[71] Ertekin and Wehausen make the following comment: "*However, although the leading wave in the deeper region appears to be a part of a wave train, its velocity is supercritical and we assume that eventually a soliton will develop from it.*" As was noted in the discussion accompanying Ertekin and Wehausen's paper, computer limitations (in 1986!) cut short the simulation. In the model tests reported here, the leading solitary wave crest did retain its supercriticality in the deeper water but died away very quickly. The re-formation of a solitary wave at the head of a trailing undular bore is discussed by Grimshaw (2011) but would only happen where the undular bore was described as strong (bore strength defined as $\beta = (h_1 - h_0)/h_0$). It may be not be so in the case presented by Ertekin and Wehausen, which is similar to the reason why the solitary wave in the experiments described here collapsed in deep water. Lee *et.al* (1989, p. 580 and Fig. 3) also note the subsidence of waves trailing a leading solitary wave, though offer no explanation.

These experiments reported here demonstrate the reversible condition of a shallow water wave wake. In the case of the wave wake in transition from shallow to very shallow, the leading solitary wave experiences increased non-linearity and shallowness. The solitary wave draws energy from the trailing waves, causing them to collapse (Figure 5.12). Conversely, in the case of the transition from shallow to deep, the leading solitary wave experiences reduced non-linearity and shallowness once it reaches the deeper water. The solitary wave sheds energy into the trailing waves, causing it to collapse (Figure 5.7).

---

[70] For simplicity, the structure forming the shallow area was maintained and the basin water depth was varied.

[71] Johnson's paper refers to the observations of near-solitary waves from the Severn Bore moving into deeper water and forming rounded waves. That observation was made by V. Cornish and published in 1910. As with the paper by Ertekin and Wehausen (1986), Johnson's paper was only found *after* the experiments reported here were conducted.
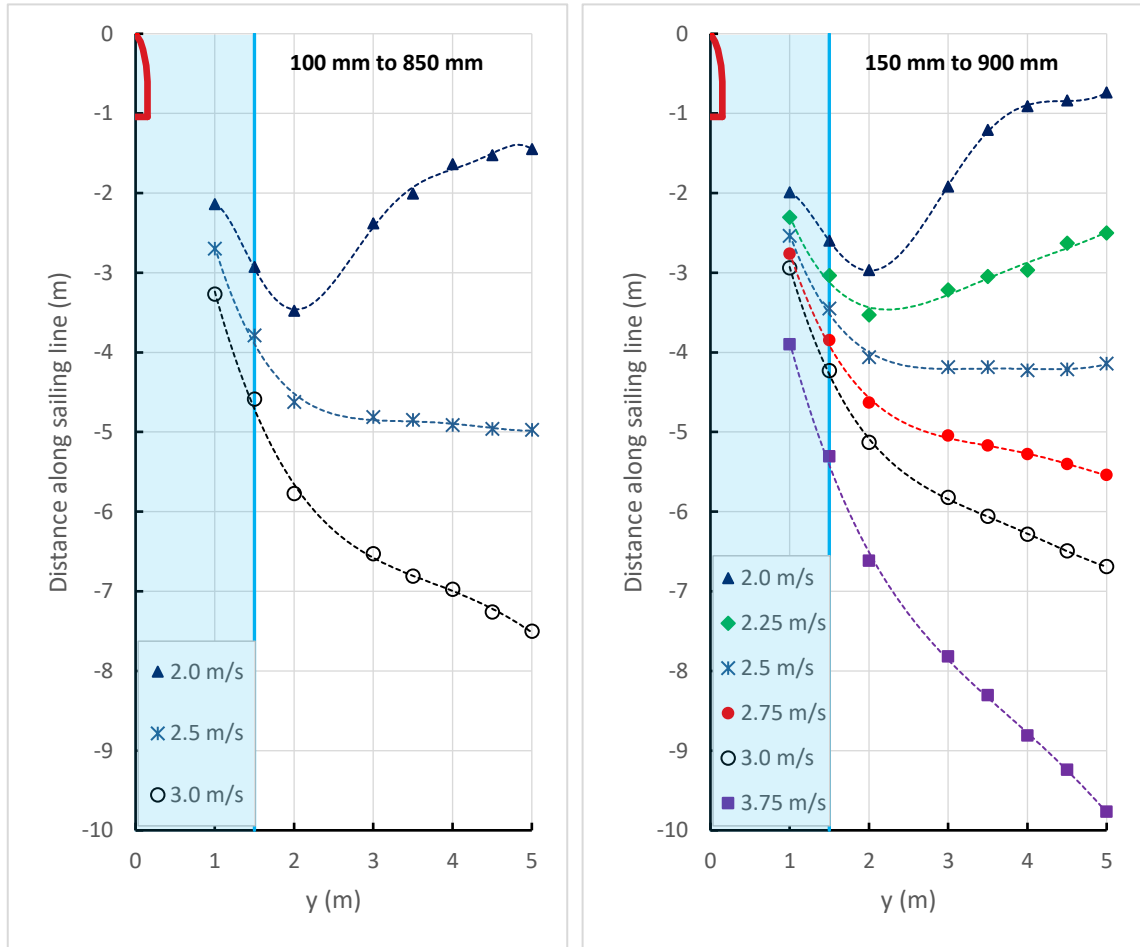
**Figure 5.16** – *Relative positions of the first wave crests in shallow-to-deep tests. The model is at depth super-critical vessel speeds in the shallow water region, marked in blue. The left figure is at $h = 100mm$ to $850\ mm$ and the right figure is at $h = 150mm$ to $900\ mm$. The vessel is shown, and the figures are to scale. Note that the 90-deg. wave angle occurs at $Fr_h \sim 0.9$ (or just before, at about 0.86), calculated using the vessel speed but the deeper water depth (even though the vessel is in shallow water). This concurs with the presented theory of solitary waves becoming "critical" at this point. By the time the first crest reached the most distant probe it was considerably depleted.*

## 5.6     Speed Regimes

Based on the findings of this study, four distinct, depth-related speed conditions are proposed, rather than just the three conditions (sub, trans and super) plus the critical speed special case found in most references.

Macfarlane and Cox (2003), describing speed regimes for practical applications in speed management, list three conditions: sub-critical ($Fr_h \leq 0.8$); trans-critical ($0.8 < Fr_h < 1.2$); super-critical ($Fr_h \geq 1.2$). Continuous vessel operation in the trans-critical range was considered untenable and therefore wave phenomena in that range were regarded as scientific peculiarities – interesting in themselves but having no practical regulatory application. Reference was made to a fourth condition, critical ($Fr_h = 1.0$), which is a special case within the trans-critical range.

Doyle *et al.* (2001) refer only to three conditions: sub-critical ($Fr_h < 1$); critical ($Fr_h = 1$); super-critical ($Fr_h > 1$). A note is made that $Fr_h < 0.6$ is a deep-water condition (an approximation of

$Fr_h = \sqrt{\pi^{-1}} = 0.56$; the condition where the transverse wavelength is twice the water depth) and the deep-water wave pattern starts to change at around $Fr_h = 0.7$.

Cox (2000) refers to the range $0.75 < Fr_h < 1.25$ as being unsuitable for continuous operation, except that the lower limit could (in certain circumstances) be extended to *0.85* with model and or full-scale validation. As was noted, an increase in the lower limit would only apply with increasing water depth (noted as $Fr_h = 0.75$ at *3 m* depth, $Fr_h = 0.80$ at *4.5 m* depth, and $Fr_h = 0.85$ at *6.0 m* depth) and without width restrictions. Nineteen years on, the transient operating range of $0.75 < Fr_h < 1.25$ concurs with this study.

Macfarlane (2012) delineates operating speeds into four conditions: sub-critical ($Fr_h < 0.75$); trans-critical ($0.75 < Fr_h < 1$); critical ($Fr_h = 1.0$); super-critical ($Fr_h > 1$).

Robbins (2013) presents a *Wash Characterisation Summary Table* (Table 7, p. 109). The table provides the author's summary of wave wake parameters across four operational zones: Deep Water ($Fr_h < 0.5$); Shallow Water Sub-Critical ($0.5 < Fr_h < 1.0$); Shallow Water Critical ($Fr_h \cong 1.0$); Shallow Water Super-Critical ($Fr_h > 1.0$). When delineating operating zones, the term *shallow water* should not be attributed to the vessel, but to the waves it generates. It is known that a vessel operating in water deeper than its waterline length will produce a deep-water wave pattern, regardless of speed. At that condition, where $h = L$, a speed would be reached where $Fr_h = Fr_L = 1.0$, but the transverse system becomes depleted in the range $0.85 < Fr_L < 1.0$ (depending on vessel form) and so there is no depth effect of consequence (refer Section 4 and Figure 4.2). For instance, a *10 m* (waterline length) vessel operating in *20 m* water depth would reach the depth-critical speed at *27 kn*, yet it would not be depth affected – the transverse system would be depleted, and the waves of the divergent system would be too short to feel the bottom. That is important, as it the premise for the evaluation and operation of small craft in sheltered waterways.

Also, the upper limit of for deep water of $Fr_h = 0.5$ is probably too low. As noted, the longest waves in deep water, the transverse waves, only begin to feel the bottom at $Fr_h = 0.56$ and are still regarded as being in a *practically deep* condition up to $Fr_h = 0.75$ where depth effects are inconsequential. ***Table 5.4*** explains the proposed operating regimes.

**Table 5.4** – *Proposed operating regimes*.

| Proposed Condition | Operating Range | Notes |
|---|---|---|
| *Sub-critical* | $Fr_h \leq 0.75$ | Similar wave wake conditions to deep water. The longest waves (transverse waves) are at their *practically deep* limit of $\lambda/h = 3.5$ at $Fr_h \approx 0.75$. |
| *Trans-sub-critical* | $0.75 < Fr_h \leq 0.9$ | Transition phase prior to developing super-critical features. Increasing surge and drawdown effects. The long components of the wave wake make the transition to supercriticality at $Fr_h = {\sim}0.9$. |
| *Trans-super-critical* | $0.9 < Fr_h \leq 1.25$ | Development of critical speed wave features. Maximum resistance at $Fr_h = {\sim}0.9$. At $Fr_h = {\sim}1.25$ the vessel can no longer generate and shed solitary waves of the form seen around the critical speed. |
| *Super-critical* | $Fr_h > 1.25$ | Stable super-critical, shallow water regime. |

**Note**: *An additional $h/L$ limiting criterion is to be applied, above which wave wakes could be considered as insufficiently depth affected to be termed "shallow".*

Whether or not it is worthwhile exchanging the "*0.9*" value for "*1.0*" is questionable. Values of the vessel depth Froude number between *0.9* and *1.0* would not normally be considered as *super-critical*, which is by definition reserved for $Fr_h > 1$, but the question is whether it is more important to consider just the depth Froude number of the vessel or to include the waves it may generate. Regardless, continuous operation around the depth-critical speed is always to be discouraged and the range of $0.75 < Fr_h < 1.25$ regarded as a transient operating condition only.

Lastly, ***Figure 5.17*** summarises the speed regimes discussed.
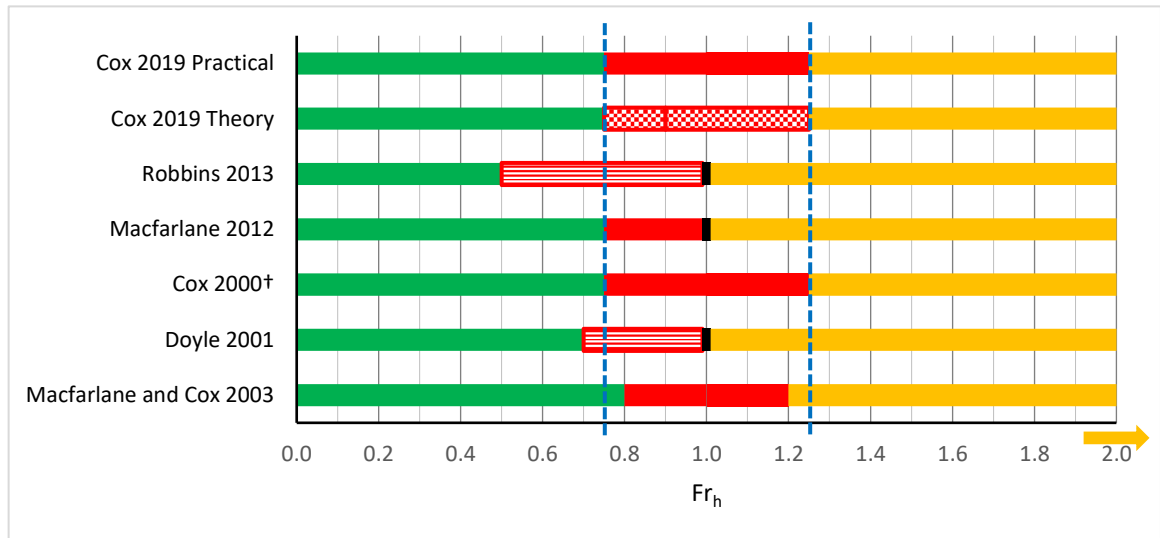


**Figure 5.17** – *Summary of depth-related operating zones. Green indicates unlimited (but with further assessment), solid red indicates transient operation only (not continuous), hatched red indicates restrictions were noted but not specified, and yellow indicates operation is possible subject to further assessment (and extending beyond $Fr_h = 2$). Further assessment would depend on other parameters such as $h/L$, slenderness ratio, waterway width and shoreline sensitivity. The vertical dashed lines indicate the limit of "practically deep" ($Fr_h < 0.75$) and McCowan's upper limit for solitary wave generation in super-critical flows ($Fr_h{\sim}1.25$). † Lower limit is dependent on blockage effects.*

## 5.7 Shallow Water Operational Guideline Summary

Absolute statements of operating limits in shallow water are complicated; the permutations of waterway depth and width conditions in restricted waterways, along with variations in vessel design parameters, ensure this. Generalised guidelines are as follows, with reference to ***Figure 5.18***:

a. when the $h/L$ ratio is above *0.5*, the wake will exhibit very modest shallow water effects can be treated as if in a deep condition;

b. avoid speeds around $Fr_L{\sim}0.5$ where specific residuary resistance reaches its maximum. Notionally, the range show in in ***Figure 5.18*** is $0.45 \leq Fr_L \leq 0.55$, but practically may need to be expanded to $0.4 \leq Fr_L \leq 0.6$ to provide a speed control buffer;

c. speeds below $Fr_h = 0.75$ are generally safe for operation, if difficulties with maintaining operation at the limit when depth, and speed control in vessels with a high power-to-weight ratio, are recognised;

d.  continuous speeds in the range $0.75 < Fr_h < 1.25$ are to be avoided. Acceleration and deceleration through this range is to be completed as quickly as is practicable;

e.  speeds above $Fr_h = 1.25$ generate increasingly deleterious effects as $h/L$ ratio decreases, and a greater percentage of the total wave wake energy is carried by the leading wave. The effects are magnified by decreasing slenderness ratio;

f.  operation at combined conditions above $Fr_h = 0.75$ and below $h/L = 0.15$ should be regarded as untenable. The leading wave may approach a solitary form, allowing it to draw energy from the trailing wake and potentially propagate independently. If the waterway laterally beyond the sailing line was deep and wide, the generated wake may degenerate. If, as is most likely the case, the waterway beyond the sailing line shoals, the deleterious wave wake would be magnified further.
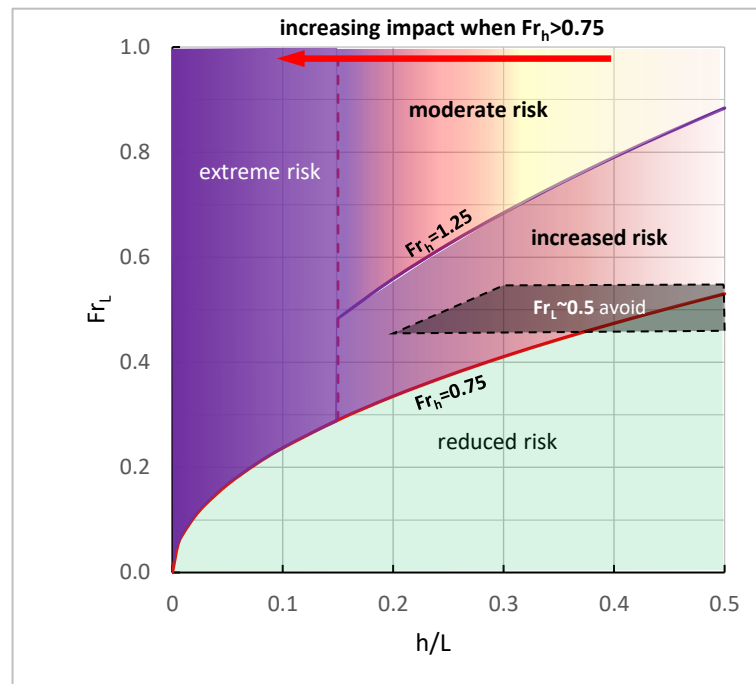


**Figure 5.18** – *Generalised operational zones in shallow water (Cox and Macfarlane, 2019, Fig. 3).*

# Section 6 – Wave Energy and Power

## Summary

The most common variable used to characterise a vessel's wave wake is wave height, even though
its direct, simplistic relationship to any subsequent shoreline erosion is questionable. Wave
energy and wave power offer alternative means of quantification, though they too can be
misleading if misinterpreted.

This section investigates how wave energy and power, which are composite parameters derived
from the principal parameters (height and period/wavelength) of discrete waves, are represented
within a propagating wave wake. As waves change in form with propagation, so does their energy
and power, which in turn changes how energy and power are distributed through the wave wake.
The question remains: if the total wake energy per nautical mile of sailing line remains essentially
constant but the energy of the principal waves reduces with propagation as the packet spreads,
why does increasing sailing line distance from the shore reduce the risk of erosion when the same
total quantity of energy reaches the shore? The answer is that the form in which energy is
delivered rather than its quantity is a principal determinant of the propensity to cause erosion.

The packet-wise variance of wave energy and wave power are studied, leading to interesting
conclusions about constant relationships in those parts of a packet before and after the maximum
wave. These may help to explain environmental responses to wave wakes.

## 6.1    Introduction

The need for composite parameters such as wave energy and wave power to describe the
intensity of wave wakes came from the coastal engineers, not the naval architects. As has already
been discussed, the early modern researchers of wake waves and the environment were coastal
engineers (Johnson, Sorensen and Lesleighter, as previously quoted). Prior to that, naval
architects were active in the field (J. Scott Russell as one, plus a small number referenced in
Johnson, 1957), but the interest seemed as much academic as practical. Ships are self-contained
entities, and naval architects are trained to think of them as such – only interacting with the rest
of the world at the jetty.

It seems peculiar that the naval architects would not embrace holistically the relationship
between wake waves and their energy content; after all – the energy in the wake has a direct

relationship to the resistance of the hull and the fuel consumed, which are principal concerns for the ship designer. Wave wake analysis had long been used as a means of estimating vessel resistance (Ward and van Hooff, 1976, as an example) but for the purpose of improving transport efficiency only. Instead, wave height has been the dominant parameter for assessing wakes, even when its correlation with erosion was erratic or inconclusive. That seemed to matter less than demonstrating the ability to manipulate wave height by design.

## 6.2     Energy and Power, and their Relationship to Erosion

The perennial question in wave wake analysis has been which wake parameter is the most descriptive of, or most relevant to, the potential for erosion. Von Krusenstierna (1990) sought correlation between many wave parameters, both single (height and period) and composite (such as power and energy), as well as between individual wave parameters (of the maximum wave) and averaged parameters (significant wave values). There were trends, but none of the parameters could be judged as having a substantially better correlation than the others. In a related paper, Nanson *et.al*. (1994) make the following insightful observations regarding the Gordon River program (taken from Macfarlane and Cox, 2003, Section 4.6.1.1):

> *"The wave characteristics used in this study as predictors of bank erosion and sediment entrainment fall into two groups. Firstly, there are those that describe the wave train as a whole (mean period, mean wavelength, significant wave height and significant wave power) and secondly, those that describe only part of the wave train (maximum wave height, peak wave power and maximum wave steepness).*

> *"It might seem logical that the wave characteristics which describe the wave train as a whole would give a better measure of erosive potential than those that only describe part of it. As Renilson and Lenz (1988) point out, the maximum wave height may not be a good measure of the erosive energy in a wave train as some trains contain only one pronounced peak whereas others have a series of peaks close to the same height. For this reason significant wave height and significant wave power were used as variables in this study. However, it is also possible that the erosive energy of a wave train is concentrated in a small part of the train, with the remaining waves having little effect. It is not possible here to solve this problem conclusively as not enough data were available. However, the relatively high correlations between erosion rates and the variables describing only part of the wave train indicates that the erosive potential of a wave train may well be concentrated in, and reflective of, its maximum components."*

In response to the safety concerns of wakes from large, high-speed ferries on coastal routes, Kofoed-Hansen *et al*. (2000) proposed an equation limiting the parameters of the maximum wave in *3 m* water depth. The equation is effectively a constant wave power equation, allowing for any combination of height of the maximum wave and corresponding wave period provided the threshold value of power was not exceeded. As the statement of a threshold, it returns us to the conundrum of how much of any shoreline degradation is acceptable if a threshold proves to be so low as to exclude all vessels, or at least high-speed vessels of any type. That constant power equation was quoted in many subsequent studies, even if its transposition to other operating environments was questionable (sheltered rather than coastal routes). The problems being addressed by Kofoed-Hansen *et al*. (2000) were not principally related to shoreline erosion, but more towards beachgoers and recreational craft that might encounter long-period shoaling waves

from passing coastal ferries. A wave power equation and its relationship to wave shoaling in shallow water may be most appropriate in that instance. For sheltered waterways erosion, it may not be.

Another erosion equation that has been used in analytical wave wake studies is from Abbott and Price (1994, Fig. 17.2, p. 217). Their equation (taken from the *Shore Protection Manual*) has a power relationship ($H^2T$) in linearised form and the equation is almost certain to be specific to (or influenced strongly by) the data from which it was derived. They note that the equation does not always work for individual inputs but works best over a long period of time. That would reduce its efficacy when used with ship waves.

It is also questionable whether an equation or methodology requiring detailed inputs such as incident wave angles and beach profiles are useful or may be unnecessarily complicated. In coastal engineering, there is an identifiable need to predict sediment entrainment and transportation, but the incident wave climate cannot be controlled unless mitigative structures are built. Conversely, vessel regulators have the options of modifying sailing lines or eliminating the source altogether.


## 6.3     Height Decay due to Diffraction and Dispersion

The argument of *height decay due to diffraction*, or the spreading of energy laterally along the wave crest, has found its way into wave wake theory in general, applied equally to the divergent system as well as the transverse system.[72] A cursory glance at any ship wake would show that this cannot be the case for the divergent system.

*Figure 6.1* presents Kelvin's original published wave pattern. The divergent crests are drawn as being long-crested, but the reality is that divergent waves at slower speeds always appear to be short crested (refer Figure 4.7).  At high speeds in deep water, the divergent waves have the same long-crested appearance as depth super-critical wakes. How would these apparently continuous divergent wake crests decay by diffraction if their crest lengths lengthened by the rate at which the source (vessel) moved and with fresh energy?

Wave system energy is constantly being transferred from the vessel – crest-wise in case of the divergent system and longitudinally in case of the transverse system. If a transverse system is trapped between parallel shorelines, the energy is also trapped and is released only by interaction with the bottom or the banks. Between the caustic boundaries of the Kelvin wedge, the transverse system crests lengthen. The transverse wave height decay expressed by Havelock (1908) along any ray emanating from the vessel concords with the transverse energy spreading crest-wise within the wedge, in which case there is an argument for diffractive height decay.

The constant input of energy to one end of the divergent system ensures that the total divergent system energy that goes ashore per mile of sailing line is effectively constant (bottom and internal friction aside). Divergent wakes decay due to dispersion; their total wake energy per unit crest

---

[72] Refer Section 7 for further discussion.

length remains constant but is continuously being distributed *across* a packet with an increasing number of waves. Reduce the dispersion, such as in the leading waves in shallow water, and the energy depletion (height decay) of individual waves is also reduced. Eliminate the (external) frequency dispersion, as is the case with solitary waves, and the decay is also eliminated as energy is conserved.

A wave cut through the divergent system of Figure 6.1 shows the lengthening packets with increased lateral separation, but it does not show properly the increasing numbers of waves within the packet due to dispersion. Diagrams such as these are only ever schematic.
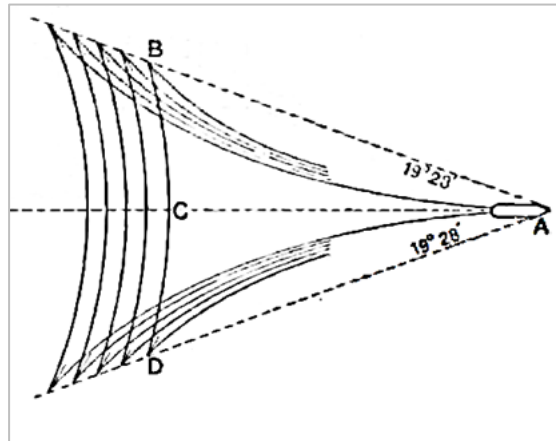


**Figure 6.1** – *Kelvin's original wave diagram (Kelvin, 1887, Fig. 48). Accuracy of some features, such as his proposed congruence of crest angles at the cusps, may have suffered from drafting limitations.*

Taking the discretised approach of looking at individual divergent waves at an instant, it is easy to show that the total divergent wave energy remains approximately constant with increasing lateral separation. The results are never perfect due to packet interference and the fact that temporal records imply that the discretised waves measured in one location with varying time do not all belong to the same packet parameters (the packet having evolved with time as it passes through the fixed wave probe position). There are some interesting points to consider:

a.   wave energy (and power) reach a peak value slightly before the envelope maximum, implying that the maximum wave may not necessarily be the most energetic. The peak occurs at around half to one wave before the envelope maximum. The graphic reason for this is that the slope of the envelope, representing the wave height, varies only slightly around the maximum, but the wave period from the envelope maximum to the packet head increases at an increasing rate;

b.   in mathematically generated examples (such as that of Figure 3.2) where relative energy can be approximated from the instantaneous values of wave period and height, the point of maximum energy migrates slightly towards the packet head as the packet disperses and the number of visible waves increases. In the case of Figure 3.2, the maximum energy occurs at about the crest of the maximum wave (marked by the heavy black line);

c.   in an analysis of discretised model test wake waves, the maximum wave power also peaked around half a wave before the maximum wave;

d.   the trailing waves carry very little of the total packet energy. In the case of Figure 3.2, the first six and a half waves contribute about *99%* of the total packet energy.

The importance of this is further explained in Section 8, but a brief comment is warranted here. It has long been known that increasing lateral separation is beneficial environmentally, allowing the waves to attenuate in height. That recommendation is a feature of every guidance document on vessel operations and their wave wake impacts on the environment. If wave energy is conserved within the packet and wave energy was the assumed measure of erosive potential, why should greater lateral separation be important? The energy of the maximum wave would decrease with increasing lateral separation, but the total wake energy would not. Some energy would be lost

102

due to bottom friction and an almost negligible amount would be lost due to internal friction, but the majority would make it ashore. Moreover, decreased wave height would be offset by an increased number of waves, maintaining total packet energy

The reason lies with the form in which energy is delivered rather than the quantity, erosion thresholds, and rates of erosion when thresholds of both wave height and period are exceeded. That forms the basis of Section 8.

## 6.4　　Relationship Between Vessels and their Wave Energy/Power

Wave wake intensity is a function of vessel residuary resistance, which itself is a function of hull parameters. There is direct correlation between a hull's resistance, the power required to drive it and the fuel required to generate the power. Logic suggests that wave power is a function of engine power, and engine power must correlate directly with the wave wake intensity. That is true, but it doesn't define the parameters of the wake in terms of wave heights and periods. It also ignores the relative influence of residuary and frictional drag for different hulls.

As an example of the application of wave energy techniques, it has become a common practice to compare incident wave wake energy to ambient wind wave energy on an annualised basis; the premise being that a modest increase in total wave energy is unlikely to cause accelerated erosion. Pattiaratchi and Hegge (1990) studied high-speed ferries on the Swan River in Perth and used an annualised energy approach. However, their report was unable to achieve any correlation between the wave wakes measured and the recorded shoreline erosion (which was not particularly prevalent anyway, even with a long history of commercial vessel operations on the river). Moreover, Pattiaratchi and Hegge calculated threshold wave parameters of *65 mm* height and *1 s* period, above which offshore sediment transport was possible, yet the ambient wind waves often exceeded this (especially in summer) in what could be regarded as a dynamically stable environment.

Acceptance of the basic premise of threshold wave parameters negates the usefulness of annualised wave energy comparisons. In a dynamically stable environment, most if not all the wind waves (excluding extreme weather events) would fall below the threshold parameters. Any systematic exceedance of the thresholds would render the environment dynamically unstable, in which case the introduction of vessel wake waves would accelerate erosion rather than initiate it. That is often the case in inland waterways and rivers where land use practices and flow regulation initiate bank erosion and (mostly recreational) vessels exacerbate it. Regulating the vessel traffic may only slow the shoreline recedeance; it may not halt it.

The question proven to be difficult to answer is: *in what form are wake waves most erosive*? The almost unanswerable question then becomes: *how much of that form is acceptable*?

In referring to wave energy being a composite parameter made up of wave height and period, Cox (2000) commented that "*if energy alone is used as an indicator of the probability of erosion, information regarding the magnitude of each of these variable components is lost.*"[73] That statement was borne out of the results of Nanson *et al*. (1994), who developed simple criteria for

---

[73] Without acknowledgement, Doyle *et al*. (2001) make the almost identical statement that "*Nevertheless, if energy alone is used as an indicator of the magnitude of vessel wake, important information regarding the individual components of wave height and period is lost.*"

103

determining erosion conditions on the Gordon River in Tasmania. For the protected shorelines investigated, subjected to a wind wave climate only until the introduction of tourist vessels, there were thresholds of significant wave height and period below which erosion rates were constant and above which erosion rates increased. The values at the threshold were *0.25 m* significant wave height and *2.7 s* significant wave period. When plotting the data, no attempt was made by Nanson *et al*. to maintain relationship between data pairs of height and period, and consequently the threshold parameters may not have related to the same wave.

It is suggested that the magnitude of energy (or equivalent parameter) is less important than the form in which it is delivered. This concurs with the existence of thresholds and the findings of Section 8. Two analogies are offered; analogies being useful when presenting to general community forums. The first describes the annualised energy from dropping a small coin from a height of *50 mm* every second for one year, which would be analogous to the effects of wind waves. That annualised energy as a single event would be equivalent to dropping a *1-tonne* vehicle from a height of about *4.5 m*. One could be regarded as inconsequential and the other catastrophic, yet both have the same energy.

The second, originally presented by Cox (2000), is an example of electrical power. At *240 V*, a current of just *30 mA* will cause electrocution. At *12 V*, a current of *0.6 A* would cause a jolt, but nothing more. Both have the same electrical power, yet one is fatal. Cox (2000) goes on to state:

> *"Just as voltage represents potential and current the flow rate, it may be said that wave period represents the potential to cause erosion and wave height defines the rate of erosion for an introduced wave regime with energy levels beyond the natural regime. Under a varying wind wave climate, wave period (the potential) varies slightly while wave height (the rate of erosion) varies significantly more. Provided the potential remains low, the overall erosion will be low. Shorelines subjected to wind waves in particular change according to the incident height and period, armouring themselves under wave action by increasing beach slope. Should the wave period increase further to a point well beyond the average, nett erosion may occur in an attempt to secure a new dynamic equilibrium condition."*

It is as relevant now as it was when it was first written. Macfarlane and Cox (2003) introduced the concept of *energy per unit wave height*, where $E/H \propto HT^2$ (in linear, deep-water form). The parameter had as good a relationship to measured erosion as wave power, yet it avoided some of wave power's limitations and apparent discrepancies. Use of the parameter has been continued throughout this study, where appropriate.

## 6.5    Wave Packet Energy and Power Analysis

To assist with the understanding of how the composite parameters of wave *energy*, *power* and *energy per unit wave height* are distributed within a propagating wave packet, a mathematically generated packet has been analysed. It consists of a symmetrical envelope (Gaussian) representing the signal wave, which was used to modulate a sine carrier wave with decaying period. This approach allows for a continuous and discretised analysis. This is shown in **Figure 6.2**. The analysis is intended to be purely qualitative.
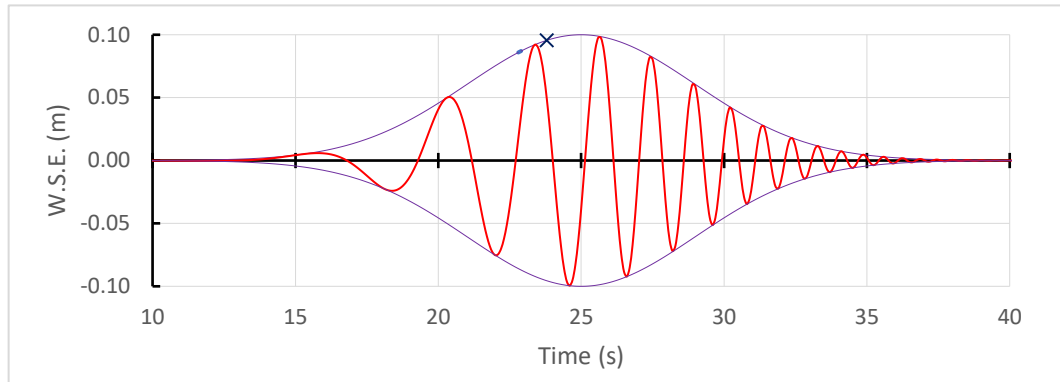
**Figure 6.2** – *A wave packet consisting of a (symmetrical) envelope (signal wave) that modulates a simple sine wave (carrier wave) with decaying period. This form allows for continuous and discretised analysis of the packet. The cross on the upper envelope marks the peak of continuous energy at 23.9 s (calculated using the instantaneous period and envelope height). Continuous energy per unit wave height peaks at 22.6 s and always leads peak energy and power. Continuous power peaks at 24.4 s and always fractionally lags the other two parameters.*

The packet-wise distribution of the three principal composite parameters of power, energy and energy per unit wave height can be compared by calculating each parameter using the instantaneous values of wave height (in this case, twice the envelope amplitude) and wave period (based on a continuous period function). The distribution of each is shown in *Figure 6.3 (left)*. The maximum value of each parameter peaks before the envelope amplitude peaks. By the time the envelope maximum has been reached (signifying the maximum wave position in a discretised analysis), *59%* of the total power, *67%* of the total energy, and *73%* of the total energy per unit wave height has passed through. *Figure 6.3 (right)* shows the discretised version of this. The magnitude of the results has been manipulated for a clearer qualitative presentation.
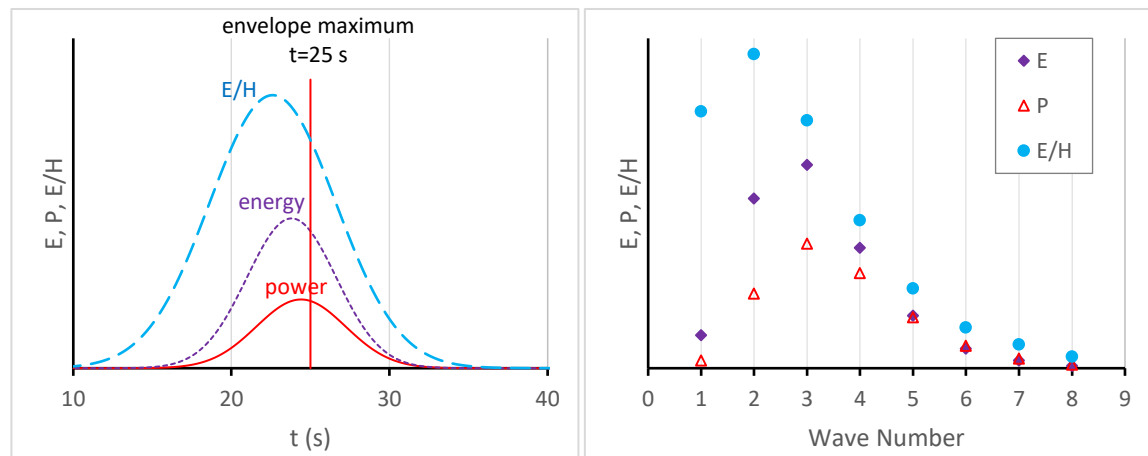


**Figure 6.3** – *Comparison of continuous and discrete interpretations of the symmetrical wave packet in Figure 6.2. The vertical axes are not to scale. **Left**: Power, energy and energy per unit wave height using the instantaneous values of height (twice the packet envelope amplitude) and period. By the time of the highest wave (envelope maximum), 73% of total E/H, 67% of total E and 59% of total P have passed. **Right**: Discretised version of Figure 6.2, taken as individually numbered waves. Wave 3½ would be judged as the maximum wave. The same parameter shift towards the packet head is seen.*

Keen observers may have expected an asymmetrical distribution of energy and power in **Figure 6.3** *(left)* - skewed towards the head of the packet where the periods are longer, as is seen in the discrete interpretation in **Figure 6.3** *(right)*. This is only a matter of interpretation created by considering the instantaneous energy as being a function of the instantaneous packet envelope elevation and the corresponding instantaneous period. The asymmetry is represented by the distribution of the area under the curve around the packet maximum, which is clearly skewed towards the head, and not the shape of the curve itself. Similarly, taking **Figure 6.3** *(right)*, which is in terms of *wave numbers*, and converting it to run time, would remove most of the skew (stretching the leading waves and compressing the following waves). Analysis of field data shows that to be the case.

The packet-wise distribution of wave power compared to wave height is interesting, with an example in **Figure 6.4** *(left)*. This is not an innate dependency (effectively plotting *x against x*), as each wave consists of paired values of height and period, and the relationship between period and height is variable. The *leading* waves – those before the highest wave or most energetic wave, and the *following* waves, exhibit close relationships. It will be shown that these relationships have relevance in explaining how wave wakes interact with the natural and built environment. Also, the last of the *leading* waves is usually marked by the most energetic wave, which may or may not be the highest wave. The most energetic wave can occur slightly before the envelope maximum by around half to one wave cycle. The variation in discretised wave period is shown in **Figure 6.4** *(right)*.
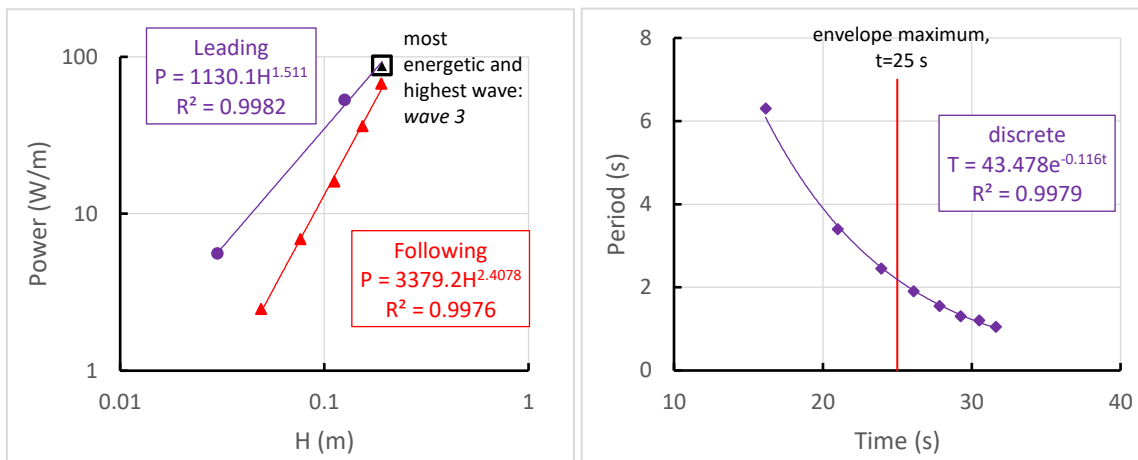


**Figure 6.4** – *Parameters of the discretised waves of Figure 6.2. This discretisation process reflects how we measure waves in real life. Each data marker refers to a discrete wave. **Left**: The wave power as a function of wave height has two distinct sectors – leading (before the maximum wave) and following (after the maximum wave). The log-log variation is quite linear. The equation exponents show that the leading waves are approaching a constant energy per unit wave height state ($a = 1.5$), and the following waves are approaching a constant wave steepness ($a = 2.5$) – refer to Table 6.1. **Right**: The decay of the discretised wave period is almost perfectly exponential. The "time" for each wave is taken at the centre of the wave cycle (zero downcrossing point), which occurs slightly more than T/2 through each wave due to packet-wise period decay.*

## 6.6    Packet-wise Wave Energy Distribution and the Effects of Water Depth

### 6.6.1    Generation as opposed to propagation

Somewhat peculiar to boats is their capacity to generate waves in shallow water as opposed to propagating waves from deep to shallow, which is the case with ocean waves. The transformation of deep-water waves in shallow water is reasonably well understood; the only complication for wake waves being their well-defined packets (complicated by packet superposition) and how they transmute during the shoaling process. Small craft wave wakes with their modest periods respond well to transformation, but the wave wakes of larger craft are more complex.

Examples of the packet-wise distribution of energy and its relative strength are examined. The vessel used was model AMC 00-01, whose parameters resemble those of recreational craft. The energy of the wake was calculated using linear theory ($E = \frac{1}{8}\rho g H^2 \lambda$), with wavelength calculated using the most appropriate linear or non-linear theory (linear, Stokes or hyperbolic).

### 6.6.2    Energy variation within individual waves as water shoals

*Figure 6.5* describes how the energy of individual waves changes with reducing $h/L$ ratio at the time of their generation. Each wave (from packet head) is numbered. Cox and Macfarlane (2019) note that the condition where waves becomes substantially depth affected (transition) occurs at $h/L < {\sim}0.28$, which would concur with the increasing growth of the energy of the leading wave. Conversely, the very short waves *4* and *5* experience no effect at all above this depth/length ratio. All waves following the leading wave experience a depletion of energy in very shallow water as energy is increasingly trapped at the head of the packet. The first wave in the shallowest condition has about the same energy as the maximum wave in the deepest condition, yet it is delivered with *2.7* times longer period (and coincidentally *2.7* times longer wavelength). The variation in shallow water wave periods is discussed in Section 5.

### 6.6.3    Packet-wise energy distribution

*Figure 6.6* *(left)* demonstrates the packet-wise variation of energy as the water depth shoals. In the deepest condition ($h/L = 0.863$), the wake has a deep-water form though is devoid of a transverse wave system ($Fr_h = 1.01$ but more importantly $Fr_L = 0.94$). The highest waves are the most energetic. As the depth reduces, energy becomes increasingly trapped in (shifted towards) the head of the packet. At $h/L \sim 0.3$, the leading waves have equivalent energy. Increasing shallowness moves that energy into the packet head.

*Figure 6.6* *(right)* shows the energy of the first wave as a percentage of the total wave wake energy. In extremely shallow conditions, the leading wave may contain almost all the wave wake energy. Such shallow depths relative to length are not easy for small craft to achieve in practice but are possible for larger vessels. The relative energy content of the leading wave changes with lateral separation due to dispersion; the further away from the vessel the greater the spread of energy across the widening wave packet. In shallow water where dispersion is suppressed, the lateral change in energy distribution within the packet slows. That has direct consequences for vessels generating depth super-critical wave wakes in waterways of restricted width.

Although wave height may not deteriorate as water depth decreases, changes in apparent shallow water wavelength and how that changes with lateral separation becomes the determinant for packet-wise wave energy distribution. Section 5 explains how the leading wave is not a wave but a packet of waves that disperse very slowly due to their depth-limited celerity.
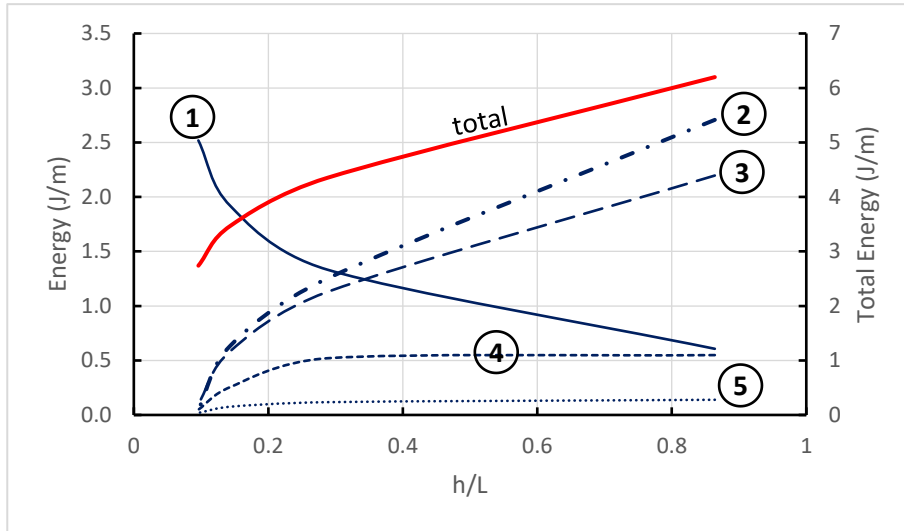
**Figure 6.5** – *Model AMC 00-01 ($y = 2\ m$; $V = 3.0\ m/s$). Change in wave energy of individual packet waves (as numbered) as depth decreases. The total wake energy decreases with decreasing water depth, and the energy contained within the leading wave accelerates at $h/L < {\sim}0.28$, as expected. At very shallow depths, most of the energy is contained within the leading wave.*
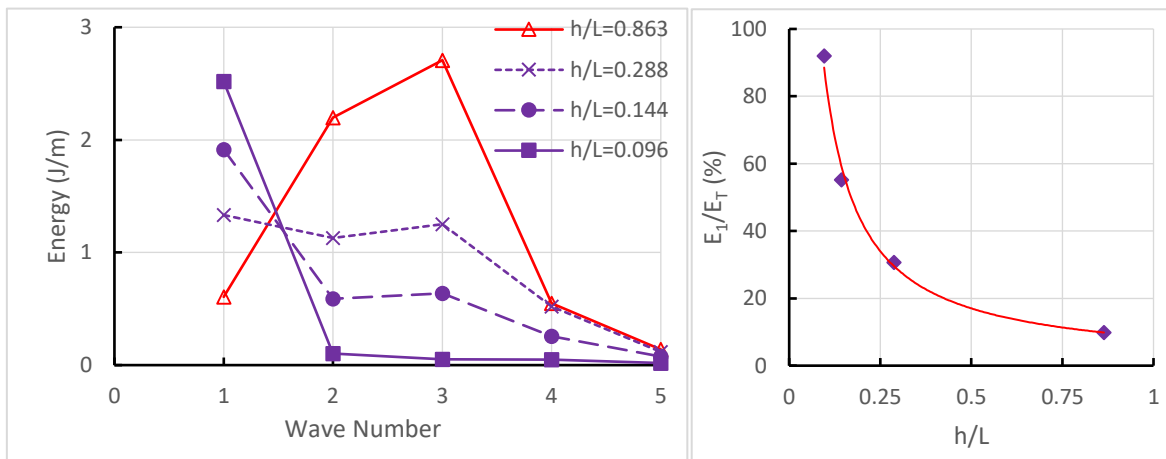


**Figure 6.6** – *(conditions as per Figure 6.5)* **Left***: Change in energy distribution in the wave wake as depth decreases. At very shallow depths relative to vessel length, the first wave contains most of the total energy.* **Right***: The energy of the leading wave as a percentage of the total wake energy. The percentage will change as a function of dispersion, depending on where the wave cut is taken.*

## 6.7     Wave Power

### 6.7.1    Analysis

Wave power has been largely derogated from wave wake assessment standards between vessels on the premise that vessel wakes are best regarded as event-based and not statistical time-based phenomena (Macfarlane *et al.*, 2008). However, across an individual wave packet that may be different; the importance of wave power within a wave packet may be justified knowing that the transmission of energy through a wave packet is a function of the group celerity, which also describes the transmission of wave power.

When plotting the value of wave power as a function of wave height for individual waves in a trace, including both zero upcrossing waves (whole wave numbers) and zero downcrossing waves (half wave numbers), waves preceding the maximum wave, termed the *leading waves*, exhibited a different relative power relationship to those succeeding the maximum wave, termed the *following waves*. Further investigation showed that the cross-over point was likely to be either the most energetic or most powerful wave and not the maximum wave. There is insufficient data to make an absolute statement, but it would appear from the analysis of many packets that the most energetic wave and not the most powerful wave is the cross-over point (by a very small margin of difference), though it is almost certainly not the maximum wave or, if it is, it would be coincidental. That is not an unrealistic assessment, since the proposition of the maximum wave being the definitive wake wave is based on the very simplistic measure of *highest wave*, which ignores the importance of wave period. Practical examples follow.

### 6.7.2 Variation of wave power with other wave parameters

It would be the case that other wave parameters such as wave period, wave energy and wave steepness would have an expected relationship with wave power, the only variation being the strength of the relationship.

There are potential relationships of interest, depending on the exponent of the deep-water *Power-Height* relationship, but some of which would be meaningless in practice. Defining a generic relationship that $P \propto H^a$ and knowing that $P \propto H^2 T$ gives $H^{(2-a)}T = const$ in deep and near-deep conditions. Examples of different values of the exponent $a$ and the relationships derived are shown in **Table 6.1**. Comparisons using *energy* and *energy per unit wave height* against wave height yield similar relationships but with different exponents.

**Table 6.1** – *Relationships implied by varying the Power-Height equation ($P \propto H^a$) exponent.*

| Exponent, $a$ | Relationship | Physical quantity |
|---|---|---|
| 3 | $T \propto H$ | No identified quantity |
| 2½ | $T \propto \sqrt{H}$ | Constant wave steepness, $H/\lambda$ |
| 2 | $T = const.$ | Constant period, $T$ |
| 1½ | $T\sqrt{H} = const.$ | Constant energy per unit wave height, $HT^2$ |
| 1 | $HT = const.$ | Constant energy, $H^2T^2$ |

The general exponent range for leading waves is from $1 < n < 2$ and for following waves from $2 < n < 3$. Refer to **Figure 6.4** *(left)*. For both wave types (*leading* and *following*) it is practically impossible to reach these upper and lower limits, requiring a vessel of disproportionate displacement and length. It would, however, not be impossible to test some of the limits at model scale, though the accuracy may be questionable, especially when a very long and unusually light vessel was required to achieve the outcome. Analysis of the results of a small sample of vessels suggested that the exponents in **Table 6.1** have modest dependency on slenderness ratio, with the exponent increasing with increasing slenderness ratio.[74]

---

[74] At high speeds, taken to be (well) above $Fr_L = 0.5$, wave height is strongly a function of slenderness ratio, and wave period is strongly a function of $\sqrt{L}$ (Cox, 2000). From $P \propto H^2 T$ it follows that $P = f(L^{5/2}/\nabla^{2/3})$. Plotting the leading and following wave power equation exponents against $(L^{5/2}/\nabla^{2/3})$ for a small number of samples showed reasonable correlation for the leading waves ($R^2 \approx 0.87$) and good correlation for the following waves ($R^2 \approx 0.98$).

This analysis may seem trivial, but it has direct relevance to how the natural and built environments react to wave wakes. The leading waves (those before the maximum wave) build gradually in energy and power but have a relatively constant (or similar) energy per unit wave height, even in shallow water. The propensity for erosion may therefore be instigated by the leading waves, of which the maximum wave is an indication of their erosive potential. Similarly, the following waves, which have much reduced energy, power and energy per unit wave height values, approach a state of constant wave steepness in their shorter wavelength, deep-water guise. That could initiate synchronous rolling in moored and anchored vessels, especially with the wave period decaying at a slower rate in the following waves. Anyone who has observed casually the induced roll motions of a small yacht on a mooring would have noted that the initial waves cause mild rolling but the many short waves that follow can cause quite violent roll motions. That is obviously a function of the natural roll period of the vessel. Yachts, which have a low VCG, have increased stiffness and therefore reduced roll periods.

# Section 7 – Wave Height Decay

> Reporter: *"They say you are one of only three people in the world who understand Einstein's Theory of Relativity."*
>
> Arthur Eddington: *(after a long pause) "I'm trying to think of who the third person is!"*[75]

## Summary

It is acknowledged that wave height decay is a contentious subject, though doesn't have to be. The history of various assumptions about, and estimations of, height decay are given, along with how they may have been misinterpreted.

The measurement of wave height at different locations is fraught with uncertainty. The existence of multiple wave systems and the possibility of wave superposition from multiple wave packets can lead to incorrect assumptions about height decay rates. Experimental results show conclusively that decay rates derived from just a few wave cuts can give wildly varying results, especially in deep water, depending on the relative locations of the measurements.

The traditional understanding of wave height decay is that it is a function of the lateral separation from the sailing line. Using different techniques, it is proposed that the decay rate is a function of group celerity: at any given lateral location, those waves having undergone more wave cycles (due to a slower group celerity) will decay faster than those having undergone fewer cycles. Using maximum wave height as the preferred measure of wave wake intensity suggests that packet dynamics is most important, since the maximum wave is little more than a representation of the packet maximum amplitude. Moreover, the relationship between height decay and group celerity also holds in shallow water for the height decay of the leading wave due to its packet-like structure, which propagates with a consistent group celerity approaching $\sqrt{gh}$.

When applied to generic techniques used to determine vessel operability in a given waterway, conservative estimates of decay rate must be applied to avoid the over-estimation of wave height decay.

## 7.1    Introduction

The decay of the height of wake waves as distance from the sailing line increases has been a contentious subject for decades. The reasons for the contention are unclear, though (as is usual in science and engineering) it may have had more to do with interpretation rather than apparent misrepresentations of wave theory.

The complexity of the subject means that there will probably never be a simplified method of estimating wave decay. With the wave climate in the medium to far field consisting of multiple,

---

[75] A sometimes quoted but incorrect account of the exchange. The (reportedly) correct version took place during a lecture by Eddington, who gave his considered reply after being goaded by an acquaintance in the audience who mistook the long pause for modesty. Nevertheless, the embellished version suits the narrative nicely.

superimposed wave trains emanating from different areas of the hull, complicated by waterway bathymetry, even model or full-scale assessment at certain speeds can give conflicting results.

The need for estimating wave decay is to provide the basis for assessment of wave parameters at a point away from the sailing line where the propagating waves may conflict with other vessels, structures or the shoreline. In deep water, it is only wave height that varies with lateral separation; wave period remains constant for the maximum wave and the spread of wave periods across a propagating packet remain consistent, even if individual waves (other than the maximum wave) at a particular instant have varying periods as the packet contents transform.

Model or full-scale testing gives the greatest certainly, but with commensurate cost and time constraints. Full-scale testing is fraught with difficulty at all sizes. Small craft wakes can be small, as witnessed in the work of Lesleighter (1964) where the recorded far-field wake waves were as small as *1.2 inches* (*30 mm*). Similarly, full-scale trials of large craft imply more open water that is deeper and wider, which comes with attendant wind wave contamination, depth influences and instrumentation issues. There are mitigating circumstances.

Firstly, large commercial craft proposals would have the increased luxury of sufficient development budget to conduct model-scale experiments. As a percentage of the overall project cost, wave wake experiments would be modest and would provide the proponent, regulatory bodies and financiers some comfort as to the outcome. Probably the most notable example of the failure to do this was the BC Ferries PacifiCat project in Canada, where *C$460M* of taxpayer money was invested into the construction of three high-speed catamaran passenger/car ferries, which were soon turned into *C$19.4M* at a disposal auction due, in part, to the failure of the proponents to assess the potential for wave wake impacts.[76]

Secondly, small craft operate at higher speeds where decay becomes more stable. As much as the science of hydrodynamics is based on relative speed, the reality is that absolute speed is still used by industry and the general public to compare vessels. A *120 m* catamaran car ferry is classed as a high-speed vessel at *40 knots*, even though its length Froude number of $\sim$0.6 places it barely outside the displacement speed range.[77] A recreational boat operating at *30 knots* is considered to be nothing exceptional yet would be equivalent hydrodynamically to the *120 m* catamaran ferry operating at *115* to *150 knots* (depending on whether length or volumetric Froude number was used as the basis for comparison). Consequently, recreational craft operating at even moderate speeds generate wave patterns that are more consistent and predictable. The transverse system often no longer exists at the higher speeds (depth limitations aside) and the multiple packets of the divergent system are less prone to variable interactions.

It has always been assumed that wave height is in the form $H = \gamma y^n$, where $\gamma$ is a variable dependent on speed and the vessel, and $n$ is the exponent of the power relationship.[78] The value of $\gamma$ is inconsequential when estimating how waves decay with lateral separation, provided the height is known at one location. Attempts to quantify $\gamma$ numerically have proved quite fruitless, as there are too many variables to be accounted for. Instead, it has been quantified by an empirical analysis of model and full-scale wave wake tests (Macfarlane, 2012). The burning question is the

---

[76] Wikipedia is not always the best reference, but it is the most comprehensive in this instance. https://en.wikipedia.org/wiki/Fast_Ferry_Scandal (last accessed 31st January 2019).

[77] And in terms of the hydrodynamics of truly high-speed craft would be considered as almost banal.

[78] Note the later substitution of $H = \gamma y^a$ as the generic equation to avoid conflict with Havelock's use of '$n$' to signify individual crests.

value of the decay exponent $n$. In this text, analytical height decay exponents are notated as fractions and numerical/empirical exponents are notated as decimals.

## 7.2    <u>History</u>

### 7.2.1    Kelvin and Havelock

Probably the earliest comprehensive study of wake wave decay is that of Havelock (1908), who derived decay relationships for transverse waves and the combined transverse/divergent system at the cusp defined by Kelvin (1887). Taylor (1943) made estimates of relative heights at various points in the wave system and, although it was stated as conforming to the work of Lord Kelvin (with various references offered), it is only presented as a finished figure (Taylor's *Fig. 36*) without explanation. Havelock assumed point sources and made other assumptions that meant the relationships were indicative but not necessarily exact. Part of the problem was that the method collapsed due to singularities at the extremes (the sailing line and the Kelvin wedge for the divergent system, and at the Kelvin wedge for the transverse system), but this was later partly overcome (and partly ignored!) in Havelock's development of the approximation.

Havelock showed (by his approximate method) that the transverse system decayed according to $\overline{\omega}^{-\frac{1}{2}}$, where $\overline{\omega}$ is the distance along the sailing line aft of the origin. The innate relationship between the wavelength of the transverse system and vessel speed also means that $\overline{\omega}$ can be represented by individual crest positions. Havelock did not bother to remove the singularity at the Kelvin wedge for the transverse system, possibly due to the presence of the divergent system in that area and the pointlessness of the exercise.

For the divergent system, Havelock developed two relationships. Firstly, he resolved the singularity at the sailing line (which he termed *axis*) and Kelvin wedge, and showed the diverging system amplitude to be proportional to $(2n + \frac{1}{4})^{-\frac{1}{2}}\left[3cos\alpha - \sqrt{9cos^2\alpha - 8}\,\right]^{\frac{1}{2}}$ along any ray, where $\alpha$ is the angle of the ray to the sailing line and $n$ is a positive integer describing successive wave crests along the ray.[79] The equation is only valid up to the Kelvin wedge, beyond which the term $9cos^2\alpha - 8$ becomes negative.[80] The use of a polar co-ordinate system does not invalidate the general decay power relationship between height and lateral separation. Further, it can be shown that this amplitude proportionality reduces to a decay exponent approaching *-½* along any ray as $n \to \infty$, and is less than *-½* in the near field (but not substantially).[81]

It will be shown later that the recurring decay exponent of *-½* seen in the transverse and divergent systems has both mathematical and practical validity. Sorensen (1973) made a case for the *-½*

---

[79] *And axis* and *central line*. The rays forming the Kelvin wedge are referred to as *radial boundary*, *outer boundary,* and *outer end of each diverging crest*. For all its cleverness, Havelock's 1908 paper is the worst example of confusing terminology. That is besides the typographical and graphical errors in Eqn. 100, Table II and Fig. 6.

[80] Lighthill (1978) refers to this as a *'caustic' boundary* (in the geometric sense of the term) but points out that the waves do exist beyond the wedge, though decaying exponentially. Newman (1977) makes the comment that "*Figure 6.17 also shows a commonly observed feature, namely that the apex of the sectors containing the Kelvin waves is displaced upstream from the ship's bow by an amount typically as large as one ship length*". Newman's Fig. 6.17, an aerial photograph of a ship wake with the Kelvin wedge superimposed, shows this, but erroneously. The wedge drawn encloses *all* of the wave system, including that beyond the *'caustic' boundary* of Lighthill, so must be displaced upstream to do so. Had the wedge apex been positioned at the ship, the boundary rays may have concorded with the actual cusps.

[81] The decay exponent is about *-0.459* between the first two crests.

113

transverse wave decay exponent based on the linear theory relationship between energy density, energy conservation and wave height.

Havelock (1908) then developed a relationship valid at the Kelvin wedge, or cusps, where the divergent and transverse systems viewed independently have the same instantaneous phase and propagation angles. Combining the two systems eliminated the singularity of the transverse system at the Kelvin wedge but didn't necessarily provide a solution to it. It also resulted in a $\pi/2$ phase shift, as shown graphically in **Figure 7.1**.

Havelock's equation (Havelock, 1908, Eqn. 98) for the amplitude of successive cusp crests, $\zeta_{mc}$, is:

$$\zeta_{mc} = \frac{3g}{2^{5/6}\Gamma(\frac{2}{3})\left(2n + \frac{3}{2}\right)^{1/3}\pi^{1/3}c^4\rho} \qquad [7.1]$$

where $c$ is the velocity of the source, $n$ is a positive integer representing each successive cusp crest, and the value of the gamma function is ≈1.354. It is easy to show that the decay exponent for the combined wave system described by [7.1] approaches -⅓ as $n \to \infty$, but it does so extremely slowly. For the first two crests, the decay exponent in terms of $H \propto y^a$ is only -0.217, and for the first ten crests it is only -0.263.[82] The decay exponent only approaches -⅓ beyond 20 crests along the Kelvin wedge (and ignoring the first 19 crests). This is interesting, as it has been noted by Kofoed-Hansen et al. (1999) that the -0.33 decay exponent appeared only to apply in the near field, yet by Havelock's method it would be speed dependent (speed increasing the cusp wave spacing and therefore the lateral separation) and only valid close to the vessel at slow speeds. For instance, at *hull speed*, when $Fr_L = 0.399$, twenty crests and above ($n = 20$) would be around 7L lateral separation and beyond, which would normally be considered as well into the far field. At half the *hull speed*, twenty crests and above would be beyond about 1.75L laterally. As will be discussed, the wave height decay rate varies with vessel speed, measurement position and number of wave cuts taken, and it is probably not a pure power relationship relative to lateral separation.

Stoker (1957, Eqn. 8.2.40), presents a similar result but without the sleight of hand used by Havelock to remove an (apparently) troublesome relationship between wave amplitude and velocity.

---

[82] Using '$a$' as the generic exponent value rather than the usual '$n$' because of its alternative use by Havelock to signify successive crests.
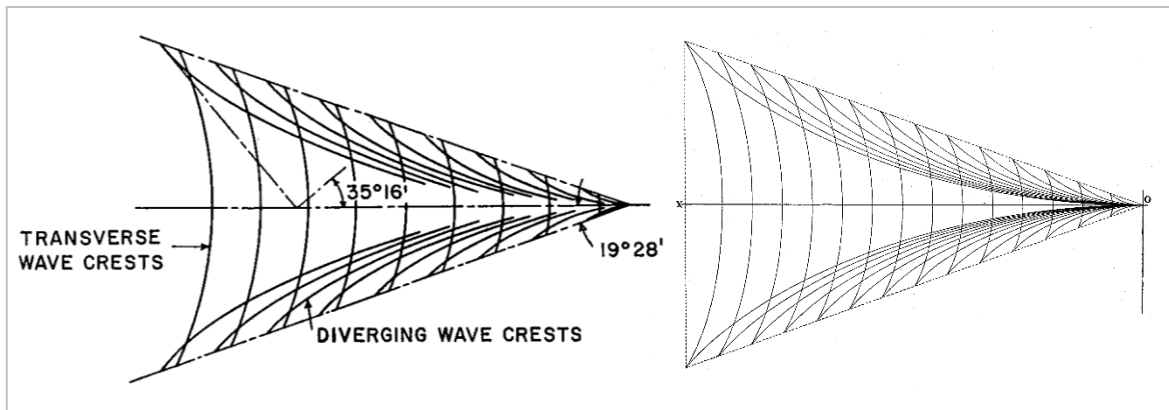
**Figure 7.1** – *Detailed (and rather idealised) versions of the deep-water Kelvin wave wake pattern.* **Right:** *(taken from Taylor, 1943, Fig. 37) – Taylor's interpretation of Kelvin's original wave pattern, showing how the (theoretical) waves meet in phase at the Kelvin wedge as true cusps, which by definition is where curves meet and terminate rather than just intersect. In the real world the boundary is not purely caustic, and the waves systems do cross over.* **Left:** *(taken from Newman, 1977, Fig. 6.15) – the revised version showing the phase shift at the Kelvin wedge, so that the actual points of intersection of the two systems lie inside the wedge. This concurs with Hovgaard (1909), who observed that the slow-speed wedge angle was often less than the theoretical value. Keen observers will note that, in real life, divergent waves appear short-crested in the far field at $Fr_L < \sim 0.5$. These wave pattern diagrams are only ever simplified schematics.*

### 7.2.2 Johnson, Sorensen and the early days of environmental assessment.

As history progressed, there was a growing need for the practical application of wave wake theory. The increasing utilisation of inland waterways for commercial and recreational purposes conflicted with environmental sustainability and the growing sense of community involvement in maintaining the surrounding environment (as well as a growing sense of entitlement!). After WWII, recreational boating was made available to the growing middle class, along with high-powered engines and cheap fuel. The need to understand the environmental consequences became pressing.

Many studies, such as those of Johnson (1957) and Sorensen (1967, 1973), firstly noted the mathematical treatments of Kelvin and Havelock, but then went on to conduct model and full-scale trials. Water depth was accounted for, as well as craft primarily designed to operate at high speed, as opposed to a displacement or semi-displacement vessel form powered beyond normal limits. At that point it was realised that there was a lot more involved that the simplified, single point source solutions of Kelvin and Havelock. Although they address wave decay in detail, neither Johnson nor Sorensen (or others around that time) arrived at a definitive solution or explanation.

Lesleighter (1964) did not specifically study wave decay in itself but did conduct a series of field trials at three lateral separations on a small recreational vessel over a wide range of speeds. The potential for contamination from wind waves was great, given the very modest wave heights recorded were as small as 30 mm, but the consistency is commendable. The vessel used was a *4 m* recreational planing craft with an outboard engine. Wake measurements were taken in deep water (relative to vessel length) at lateral separations of *7.6 m*, *15.2 m* and *30.5 m* (*25 ft.*; *50 ft.*; *100 ft.*), equating to *2.2L, 4.4L* and *8.8L* respectively. The height of the maximum wave was extracted.

Re-configured results are shown in **Figure 7.2**, with heights converted into decay exponents over the range of length Froude numbers tested (based on an estimated static waterline length of *3.5*

*m*). To demonstrate how the measurement process itself can affect the decay exponent, the decay was determined at three combinations of the three lateral measurement point: near and mid; mid and far; near and far. A fourth condition – all three locations – gives the same result as the near-and-far case (due to a quirk of three-point curve fitting where the goodness of fit is at a maximum when the fitted curve passes through the extreme points).
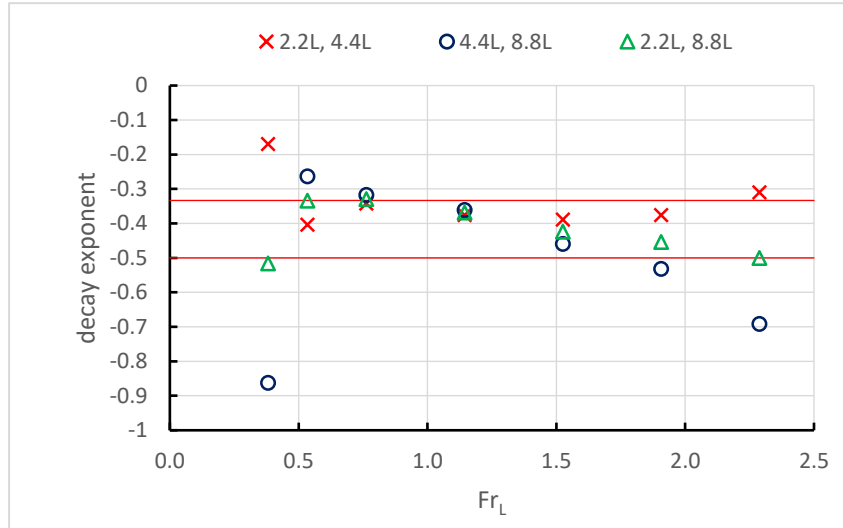


**Figure 7.2** – *Power decay exponents derived from Lesleighter (1964, Fig. 5), with wave heights recorded at three lateral separations. Different combinations of those lateral separations can produce different decay exponents in deep water, particularly at displacement speeds. A fourth variation – all three measurement locations – gives the same results as the 2.2L/8.8L data. As discussed following, commercial high-speed ferries fall into the range $0.5 < Fr_L < 1.0$ where the decay exponent is consistent at around -0.33.*

There are very profound conclusions to be drawn from ***Figure 7.2***:

a. the decay exponent is highly dependent on where the measurements are taken;

b. at the slowest speed, which is at $Fr_L = 0.389$ and close to *hull speed*, the decay exponent varies wildly from *-0.17* to *-0.86*, depending on where it is measured. That is simply a consequence of the interaction of multiple wave systems and the strength of the transverse system at slower speeds;

c. very high speeds also result in wildly varying decay exponents; the instability decreasing with an increasing number of wave cuts;

d. measurements closer to the vessel are more stable, with exponents around *-0.2* to *-0.4* across a wide speed range. This correlates with Macfarlane (2012), who analysed a large database of model and full-scale wave wake records, with the model-scale wave heights recorded up to a maximum of around *4.5L* from the sailing line (conforming to the near-to-mid range here);

e. at very high speeds, the decay exponent derived from all three lateral separations approaches *-0.5*, though recognising that the trend is not asymptotic.

f. as will be further highlighted, there is a speed range ($\sim 0.5 < Fr_L < \sim 1.2$) where the decay exponent is quite consistent at about *-0.33*, regardless of how it is measured, and that concurs with the typical operating range of high-speed commercial vessels.

### 7.2.3 The advent of high-speed commercial craft.

The advent of high-speed commercial vessels, passenger and car ferries in particular, shifted wave wake from being a nuisance to a threat to the environment. The early adoption of high-speed passenger craft was sporadic, though due regard is given to the extensive network of river hydrofoils in the former Soviet Union.[83] A notably busy high-speed passenger route is the Hong Kong to Macau service, made popular with the introduction of Boeing Jet Foils in the 1970s and the subsequent addition of high-speed catamarans soon after. That was largely an open water service, though services later expanded into the sheltered waterways of the Pearl River Delta.

The successes in more open waters led to the push to introduce (relatively) fast craft into sheltered waterways as a means of opening new public transport routes, alleviating land-based transport cost and infrastructure constraints. In parallel with this was the introduction in the early 1990s of high-speed car/passenger ferries on coastal services and the attendant problems they eventually created.

Although the mathematics of depth super-critical and high-speed sub-critical conditions were (reasonably) understood by the late 19th, early 20th century, there were several facets that were not recognised until shipbuilding made high speed transport possible many decades later.

The first was the high-speed, deep water condition, where the transverse wave system and its intimate connection between wavelength and vessel speed meant the system could no longer exist. It is known that the transverse system becomes essentially inconsequential (undetectable) at $Fr_L \sim 1.0$, and even earlier for shallow-bodied vessels with weaker transverse systems, principally monohulls. Dand *et al*. (1999), in their study of high-speed catamaran hydrodynamics in shallow water, make the comment that "*at super-critical speeds the effect of depth disappeared and the resistance coefficients assumed a constant value independent of speed and depth. Interestingly the deep-water high-speed coefficients were virtually the same as those obtained in shallow water at super-critical speeds*." That is a further indication that the transverse system plays no part at high speeds.

The second, also in the deep-water condition, was that the Kelvin wedge contracted at increasing speeds beyond $Fr_L \sim 0.5$. It is a phenomenon obvious to those studying high-speed craft wakes but has only been formally described in the past decade (Rabaud and Moisy, 2013; Ma *et al*., 2016, as examples). There is slight misrepresentation of this contraction, as noted by Darmon *et al.* (2014). The Kelvin wedge does retain a constant angle at all speeds, but the wedge of waves of maximum height contracts away from the Kelvin wedge with increasing $Fr_L$. The contraction would have an obvious effect on the work of Havelock (1908), whose decay formulae are relevant to the classical interpretation of the cusp location. As noted, Johnson (1957) points out that Hovgaard (1909) had already commented on the contraction of the Kelvin wedge at low speeds, noting that "*The observations here recorded show that this is not the case, the obliquity of the waves being greatly influenced by speed and form of the ship, and being not ever the same for all waves in the same ship at a given speed.*" Reference is again made to **Figure 7.1**. Hovgaard's statement concurs with Lighthill (1978, p. 390-395), who shows that the point of maximum amplitude lies close to the *caustic boundary* and not necessarily on it.

---

[83] The author has made many attempts over the years to determine if wave wake studies were conducted by Soviet authorities, such as the Hydrofoil Central Design Bureau, but to no avail. Joseph Stalin didn't exactly leave an enduring legacy of *community and stakeholder consultation*.

The third was the dominance of the leading wake waves in shallow water and how there is potentially a link between the deep and shallow water wakes: the two are not necessarily independent entities separated by a barrier at the depth-critical speed. Furthermore, the solitary wave may have remained as a mathematical novelty except for its use in coastal engineering (refer Munk, 1949; Keller, 1949). Dand *et al.* (1999) comment that "*the research into such waves has been sporadic since their discovery by Scott Russell and much of this has been directed toward its use as an analogue for breaking waves in shoaling water.*"

At some point in the process the -⅓ decay exponent of combined waves at the Kelvin wedge was transformed into a -⅓ decay exponent of the divergent waves, giving rise to the commonly stated relationships that transverse waves decay according to $y^{-1/2}$ and divergent waves decay according to $y^{-1/3}$. Some authors have been quick to point out that this is a misinterpretation (refer Doctors and Day, 2001), yet there are three mitigating factors that show this is not completely wrong.[84]

Firstly, as discussed, the -⅓ decay exponent represents what Havelock (1908) describes as "*the amplitude of the cusped waves,*" implying the combined divergent and transverse systems at the Kelvin wedge.[85] The transverse system along any ray almost to the Kelvin wedge decays according to a -½ exponent, so the divergent system cannot also decay at the same rate otherwise the combined system would also decay with a -½ exponent. There lies an apparent contradiction, because Havelock also shows that the divergent system alone also decays with an exponent that approaches -½ in the far field and is nearly that in the near field (as discussed). How the combined systems result in a -⅓ decay exponent is explained by Lighthill (1978): in his terms, "*healing the wound*" caused by the *caustic boundary* allows waves to exist beyond the boundary and avoids infinite coefficients (from a straight caustic boundary, with zero curvature). [86,87] The existence of a phase shift between the two systems at the cusp and not the perfect alignment proposed by Kelvin means that the combined system at the wedge boundary is not a perfect superposition.

Secondly, referring again to Lighthill's term "*healing the wound*" caused by the singularity at the caustic boundary using a ray method (equivalent to the Kelvin wedge in ship waves), he shows that amplitude decay with an exponent in the order of -⅓ is valid near the boundary, or just before it. Just before this localised reinforcement to subdue the singularity at the caustic boundary, the decay rate reverts to -½. Most importantly, this applies to single wave packets, and equally to light and water waves. It is therefore not a requirement to have combined wave systems to create the -⅓ decay exponent, as Havelock's method required.

Based on a cursory interpretation of Havelock's work, it was not unreasonable to surmise that a depleted transverse system at high speed would not change the decay rate at the boundary, and therefore the dominant divergent system would assume the decay rate of the combined entity. Certainly, Havelock may have been unaware in 1908 of the probable depletion of the transverse

---

[84] Yet in their haste to point out the apparently flawed logic of others, offer quasi-empirical decay rate examples using just two wave cuts derived from numerical ship models with no logical basis in ship design and without any detailed explanation. Refer Doctors and Day (2001), Fig. 5(b). A similarly unrealistic comparison is made by Tuck and Lazauskas (1998), but they acknowledge the potential for that.

[85] This in itself is problematic, as the reference to *amplitude* assumes the wave crests and troughs are symmetrical about the still water level, which they are quite often not.

[86] *Caustic* defining a boundary where waves are intensified but beyond which waves cannot penetrate by ray theory. In reality, they can. Refer to Section 4.5 and also to Kelvin (1887) and his discussion of the existence of ship waves outside the Kelvin wedge.

[87] Lighthill (1978) p. 395 and Eqn. 394. The $\pi/4$ phase shift is discussed on p. 397.

system at high speeds in deep water. The fastest vessel in the very late 19$^{th}$ century (1897), Charles Parson's *Turbinia*, could just achieve a length Froude number of *1.0*.

In fact, the depletion of the transverse system should not in itself be a cause of a change in decay rate. In the absence of the transverse system, the dispersive divergent system would still undergo Lighthill's localised reinforcement at the boundary. There are two phenomena that conflict when explaining why the decay rate at high speeds ($Fr_L > \sim 1$) settles back towards -½: the wavelengths are at their longest and the *apparent* Kelvin wedge contracts, but the chances of cutting exactly where the waves are at their maximum *increases* with contraction, remembering that it's not the Kelvin wedge that contracts, but the locus of the highest waves that contracts. Lighthill (1978, Fig. 70) shows the point where the -⅓ decay rate applies is narrow and the chances of cutting exactly at that point are limited. Experimental values of wave height decay at high speeds fall somewhere between -⅓ and -½, hence the quoted experimental values of *-0.2 to -0.45* (which includes shallow water conditions as well) (Macfarlane, 2012). Model testing limitations make it difficult to measure far-field, deep-water waves much above $Fr_L = 1$.

Thirdly, it had been noted by many researchers, acting independently, that the decay rate at high speed in deep water where the divergent system dominated was approximated by *-0.33*, but most certainly in the near-to-mid field less than about *4L* from the sailing line (Macfarlane and Renilson, 1999, among others). This is based solely on model and full-scale testing, and without regard to validating theoretical estimates. It also concurs with ***Figure 7.2***, which is another credible, independent result.

Referring to ***Figure 7.3***, Kofoed-Hansen *et al*. (1999) report the interpretation of the -⅓ exponent as belonging to the divergent system only, as well as the results of full-scale testing. They also observe that the decay exponent in the near field is about *-0.33* but in the far field is about *-0.55* (which could be interpreted as close enough to *-0.5* with the full-scale error involved).
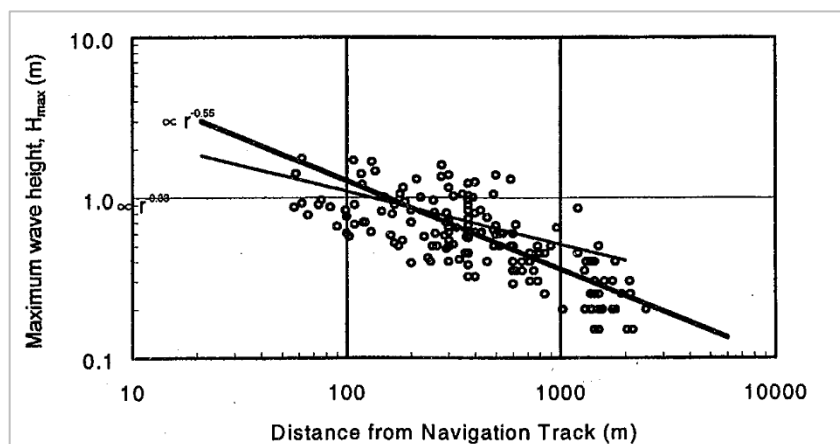


**Figure 7.3** – *Reproduced from Kofoed-Hansen et al. (1999, Fig. 4) representing the wave height measurements from field trials of large, high-speed catamaran ferries. The depth range is stated as 10-30 m, but it is unclear if this was at the point of generation or at the point of measurement. The authors claim that depth effects would be minimal and the range of possible Ursell numbers would support that. Two decay exponents are shown: the flatter (thin) trend line representing the near-field ($< 3L$) decay exponent of -0.33; the steeper (thicker) trend line representing the far-field decay exponent of -0.55. Although these results conveniently concur with others, the goodness of fit would have to be regarded as poor given the scatter, remembering that this is drawn at log-log scale which has the tendency to tighten the data spread visually.*

### 7.3    Complications in Determining Decay Rates

A consistent feature of the literature is the statement of how the analysis of a point source is tidy mathematically but doesn't really represent a ship. A cursory glance at an aerial photograph of a low speed ship wake reveals many components to a wake and not just the two shown in **Figure 7.1**. The following complications must be considered.

### 7.3.1    Wave superposition
All vessel will create at least two and possibly four (or more) wave systems, comprised of transverse waves (which become inconsequential at $Fr_L > \sim 1$, or non-existent at depth super-critical speeds), bow divergent, stern divergent, and possibly a forward shoulder (or chine entry point) divergent system. Some authors (Whittaker *et al*., 1999 and Kofoed-Hansen *et al*., 1999) note that large ferries can create very steep, short-period waves that are likely to be fully dispersive in shallow water and therefore arrive at the shore much later and in large numbers, but with minimal shoreline impact. Whittaker *et al*. (1999) attributes these to the *plunging plumes* (jet efflux) behind waterjet-propelled vessels, but they are known to be present in the distant wakes of conventionally-propelled vessels as well.

The multiple divergent packets may give rise to wake decay rate variations closer to the sailing line, as has been noted in the discussion prior. In deep water and with sufficient lateral separation, dispersion allows the leading waves of the trailing packet to overtake the trailing waves of the leading packet. Depth restrictions on celerity and dispersion in shallow water reduce the propensity for individual packets to overlap. Section 3 shows examples of packet interactions and how this affects the composite wake.

### 7.3.2    Transverse system presence
Lighthill (1978) makes the argument that the dominant waves in a wake will have wavelengths that approximate the length of the vessel. At slower speeds the transverse system will dominate and at higher speeds the divergent system will dominate as the transverse system either becomes inconsequentially small or the wavelength so long as to make the wave steepness small. When the vessel speeds are depth super-critical, or $Fr_L > \sim 1$ (and most importantly, $Fr_L > \sim 0.5$), decay rates become more predictable. For slow speed vessels ($Fr_L < \sim 0.5$) of low slenderness ratio and or low $B/T$ ratio, the transverse system dominates (and similarly the unpredictability of wave superposition dominates). The same effect occurs with slow speed catamaran forms due to the increased relative strength of the transverse system with the double hull arrangement and interference effects at displacement speeds.

### 7.3.3    Lateral separation
The variation of theoretical decay rates of divergent and transverse systems with lateral separation have been discussed. That correlates with model and full-scale observations, where decay rates are often faster with increasing lateral separation (attention is drawn again to **Figure 7.2** and the variation of decay rate with measurement position). Apart from the influence of localised superposition, there is also a group celerity effect that will be discussed following. In essence, the decay of the maximum wave may be time-dependent, so that for a given lateral separation the wave groups with a higher group celerity will appear to decay slower, having progressed through fewer wave cycles for the same distance propagated.

### 7.3.4    Examples
A compelling example of all three complications is shown in **Figure 7.4**, which compares experimental deep-water decay rates at two model speeds depending on different combinations

of wave heights from the six wave probes used. The slower speed is at the upper end of the displacement speed range where the transverse system is prominent, and the combination of wave superposition, a strong transverse system and variation of wave cut locations render accurate prediction of far-field wake almost impossible. The high-speed condition is at a speed where the transverse system is depleted and where multiple divergent packet superposition is less prominent, but different wave cut combinations still create uncertainty.

| Wave probes used | Decay exponent n ($H \propto y^n$) | |
| | 1.25 m/s $Fr_L=0.39$ | 2.75 m/s $Fr_L=0.86$ |
|---|---|---|
| All probes (y=1 to 4.5) | -0.08 | -0.36 |
| All but y=1 (y=2 to 4.5) | -0.23 | -0.45 |
| y=1 and y=3 | +0.01 | -0.30 |
| y=3 and y=4.5 | -0.41 | -0.55 |
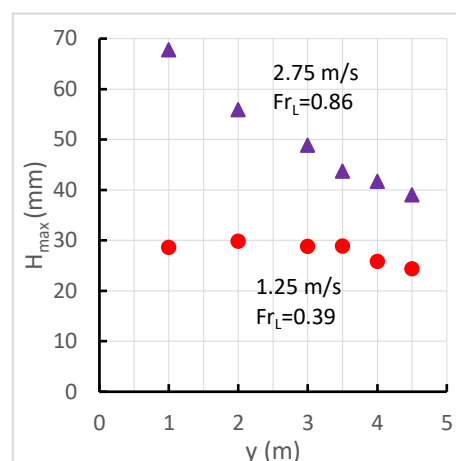


**Figure 7.4** – *Variable decay rates in two deep-water speed conditions for model AMC 00-01. It is not unusual to discard the results of the very near-field probes where local interference can be strong. Use of all probes excluding the first gives the most consistent results but not necessarily the correct result at speeds below $Fr_L = 0.5$. Consistency improves with depletion of the transverse system at higher speeds. The use of just two wave cuts can give wildly varying results.*

Another issue raised by this comparison is the limitations of model testing to determine accurate decay rates. Accuracy would only come with increased wave cuts and lateral separation, of which the latter is often not possible in test facilities. Larger test facilities may afford greater lateral separation, but that may be offset by the temptation to use larger models, as well as limitations on achieving a reasonable length of steady state speed relative to the increased lateral separation.

## 7.4    Traditional Explanation for Height Decay

As discussed in Section 3, the reason offered for the decay of wave height with lateral separation is due to diffraction, or the spreading of energy along the wave crest. This is almost certainly not true in the case of the divergent system. The earliest reference to this would appear to be by Sorensen (1973), a coastal engineer.[88] The observation may appear true when viewed in the context of ocean waves but cannot be true for ship waves. It implies that wave energy is being dispersed over an ever-increasing crest length relative to the sailing line, further implying that the total energy that reaches a distant shore would be depleting in terms of Joules per metre of shoreline parallel to the sailing line. A vessel travelling in a steady-state condition burns a given amount of fuel per metre travelled, part of which becomes divergent wave energy that is delivered into the system at a constant rate. Ignoring bottom friction and internal losses, that

---

[88] The 1973 text is the most commonly cited, but there are related papers from earlier years.

total divergent wave energy per metre of sailing line must eventually go ashore. In contrast, an ocean wave entering a bay would experience diffraction, such that its fixed energy content is spread over a longer shoreline.

In a similar example, a stone dropped into a pond causes radiating waves. The waves decay due to two mechanisms: decay due to dispersive effects as the packet propagates from the source - the packet lengthens and the number of waves in the packet increases; decay due to the ever-increasing diameter of the rings. The stone is a single impulse, not a continuous source. A continuously oscillating sphere would produce different results to a single impulse.

The linear Schrödinger equation used to define the packet decay in Section 7.7 following is a one-dimensional equation in terms of $u(x, t)$, where $u$ is the surface elevation. It exhibits the requisite decay over time, even though it is only one dimensional. A two-dimensional analysis is not required, provided the vessel speed is steady.

## 7.5    Numerical Example of Height Decay

One of the few examples of systematic wave wake decay analysis using numerical methods is presented by Doctors and Day (2001). Six variants with modified Wigley hullforms were modelled numerically – three catamarans and three monohulls – all at a constant displacement of *60 t* and a constant draft of *1.5 m*. The monohulls had a fixed beam of *2 m* and the catamaran had a *10 m* overall beam and *1 m* demihull beam. To maintain the requisite constant displacement, an adjustable parallel midbody was included. The overall (and waterline) lengths were fixed at *24 m*, *30 m* and *36 m*.

Doctors and Day presented their results in terms of absolute speed ($U$) rather than relative speed ($Fr_L$), reproduced as **Figure 7.5**. That would seem to be peculiar given the variation in model length and the technical preference for comparison based on non-dimensional parameters. Consequently, **Figure 7.5** has been re-drawn in three parts, shown as **Figures 7.6, 7.7 and 7.8**.
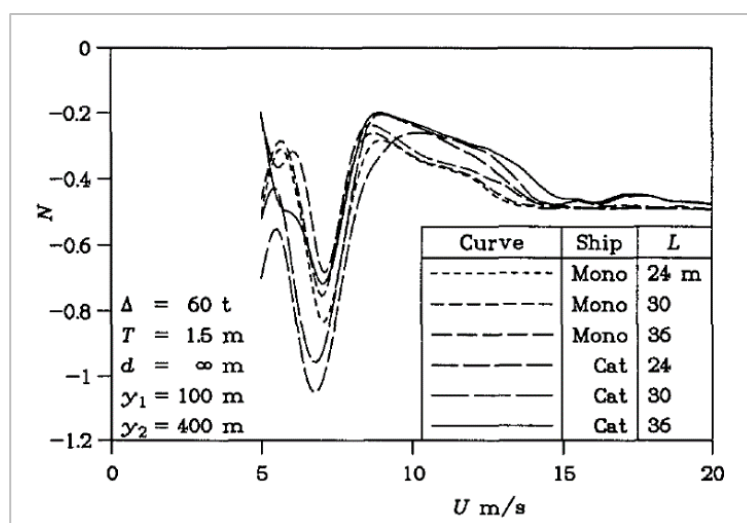


**Figure 7.5** – *Fig. 5(b) of Doctors and Day (2001) (see Appendix B, Figure B5). Here, $N \equiv n$, $U \equiv V$ and $d \equiv h$.*

Comments are as follows:

a. It must be stated strongly from the outset that at no point was there any attempt to discuss or quantify wave period, even though it is a primary determinant of wave energy and erosive potential. Minimising wave height often comes at the expense of increased wave period.

b. As discussed (referring to Kofoed-Hansen *et al.*, 1999, and analysis of Lesleighter, 1964), the decay exponent can vary between the near and far fields, and it can be exaggerated by varying the positions of the wave cuts; markedly so at slow speeds. Doctors and Day chose two wave cut locations at *100 m* and *400 m* lateral separations rather than multiples of the waterline length. There is some practical validity to choosing fixed distances and it is quite common for a wave wake height criterion to be stated at a fixed distance, but for a technical analysis the use of relative lateral offsets may have been more relevant.

c. Whilst it is true that the catamarans produced smaller wave heights than the monohulls (Doctors and Day, 2001, Fig. 5a), the comparison is not wholly fair for two reasons (and assuming that the proposed models were intended to be passenger vessels). Firstly, monohulls are almost always longer than catamarans for the same passenger capacity (refer Figure 7.9); the extra length being required to offset the limited deck area, and the limited stability in a multi-deck arrangement. As Doctors and Day noted, the longer vessels always produced smaller waves.[89] Secondly, at typical high-speed passenger vessel service speeds ($\sim 20 \; kn < V < \sim 30$ kn), the monohulls produced higher waves but exhibited faster wave height decay rates. For instance, at around *10 m/s*, the monohull near-field waves were about *30%*



**Figure 7.9** – *Comparison of catamaran and monohull passenger capacity against waterline length using published vessel data. The quantity of data is limited, but the trend is clear. There are exceptions, depending on service area type. Note the identical slopes of the trend lines, which suggest similar variations in L/B ratio but with the monohulls missing an overall 'slice' of breadth.*

higher than the *equivalent* catamaran, but after decay correction the difference would reduce to about *15%* in the far field. The energy would be further tempered by the fact that catamarans tend to produce longer-period maximum waves than monohulls of the same length (Macfarlane and Cox, 2007). A modest increase in the length of the monohull to offset passenger capacity limitations may eliminate the far-field wave height difference altogether.[90]

---

[89] Though without a requisite qualification about displacement or slenderness ratio. Taken at face value, their statement could imply that length increase at *any* cost is worthwhile, which it may not be.
[90] This has relevance to passenger vessel design in developing countries, where the construction of ultra-lightweight catamarans is difficult due to technology and or capital constraints. A casual review of any second or third world sheltered waterway passenger ferry service would note the almost exclusive use of monohulls, often with high to extreme L/B ratios. Figure 7.11 shows an example. The premise is usually not a wake concern, but a need to minimise engine size and fuel consumption at the lowest capital cost. Modest wave wakes come as a direct consequence.

d.  As discussed following, the representative decay exponent of *-0.33* in the speed range of *8 m/s* to *13 m/s* (*16 kn* to *25 kn*) actually correlates perfectly with the expected speed range of sheltered waterway commuter ferries. Moreover, analysis based on length Froude number rather than absolute speed gives the same result.

e.  Catamaran resistance at low speeds ($Fr_L < 0.5$) is known to be highly sensitive to hull spacing, and the hull spacing and demihull beam used in the analysis would not be representative of most catamarans. Only the *36 m* catamaran variant would be considered as close to representing a full-scale vessel.

f.  There is undue focus on the exponent of *-1.06* as an apparent justification of the use of catamarans. ***Figure 7.10*** offers a graphic example of how different decay exponents alter the far field wave height over the range of decay exponents presented by Doctors and Day. It is questionable whether an extreme example such as *-1.06* is realistic, as it is not commonly recorded in model or full-scale experiments. Certainly, the use of multiple wave probes at model scale would remove any anomalies arising from relying on only two wave cuts. Also, it can only be a function of wave superposition, and the reliance on only two wave cuts does not guarantee that the decay rate is consistent everywhere at that speed. Transverse and divergent wave systems are different by nature. Referring to Figure 4.2, the waviness in the total resistance curve is caused by constructive/destructive interference in the transverse systems, which is purely a function of ship length and speed. It is not caused by any predictable interference between transverse and divergent systems. For those reasons it should be treated as an anomaly and not a credible design target.
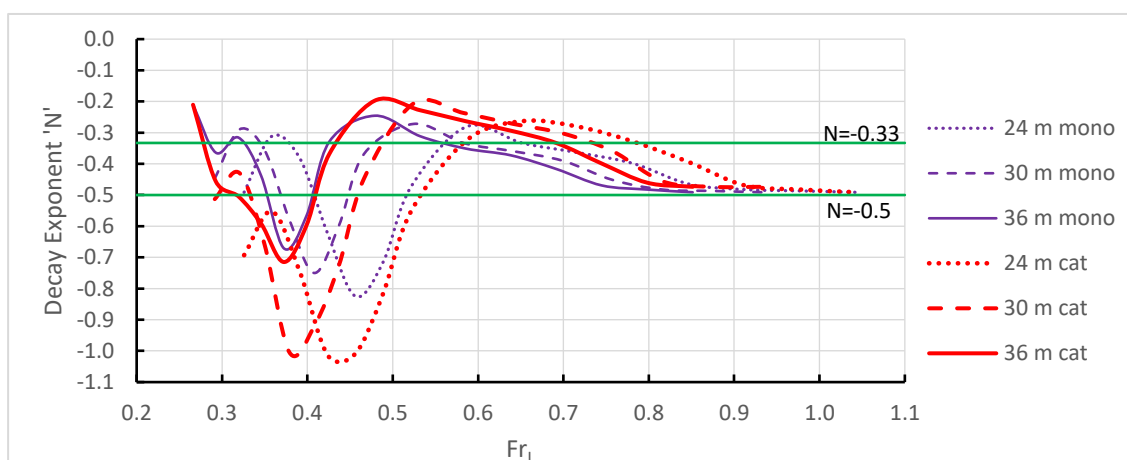


**Figure 7.6** – *Figure 7.5 reproduced with abscissae non-dimensionalised by length Froude number.*
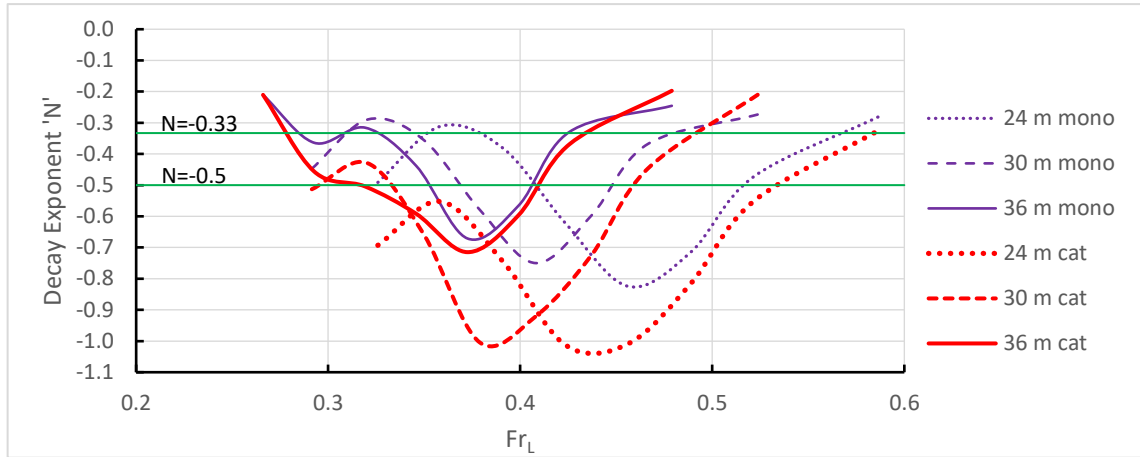
**Figure 7.7** – *Low-speed segment of Figure 7.6. The peaks and troughs of the decay exponent show a tendency to align according to length and with increased variability as slenderness ratio decreases.*
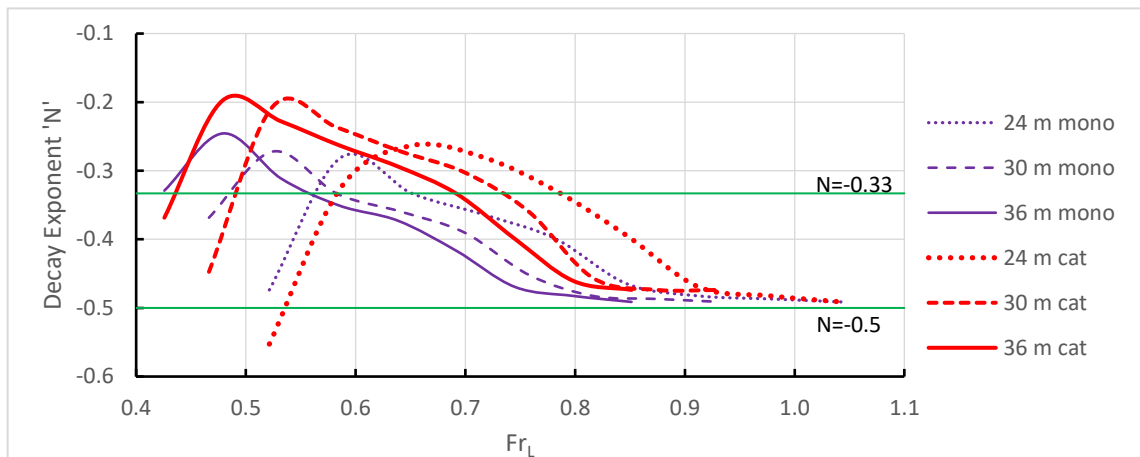


**Figure 7.8** – *High-speed segment of Figure 7.6. The catamaran forms exhibit delayed improvement in decay exponent, probably resulting from their stronger transverse systems. The high-speed decay exponents of all hullforms devolve to that of a single wave packet ($N \equiv n = -0.5$).*

It is agreed that a systematic variation of vessel parameters often results in models that could be considered as practically unrealistic but is otherwise useful in determining the effects of parameter variation. An analysis regime that maintains a constant displacement of *60 t* whilst varying length should have been balanced with the analysis of constant length but varying displacement, given that length and displacement are the two primary vessel parameters determining wave wake. The basis for the analysis of Doctors and Day would appear to be the *Rivercat* ($L \approx 36\ m$; $\Delta \approx 60\ t$; $B = 10.5\ m$, demihull beam $1.0\ m, T \approx 1.3\ m$), on which the authors had previously published. The other five variants would be considered as increasingly unrepresentative of actual, or viable, vessel designs.

The presentation of results in ***Figure 7.5*** in terms of absolute speed is a *neat* way of aligning the humps and hollows, but the authors did not provide comment on why that should be so. The extreme hollows in the decay exponent curves all align at around the same speed, which is an interesting outcome. Divergent wavelength is known to correlate with waterline length (Lighthill, 1978; Cox, 2000). It is the transverse system wavelength that is purely a function of vessel speed

125

and not of other vessel parameters. This and the increased relative transverse system strength of catamarans (Doctors *et al.*, 2001, p.101) are most likely the causes of the extreme humps and hollows at low speeds. It is unfortunate that this was not commented upon by the authors, as it is an outcome requiring further exploration.

When speed is non-dimensionalised, the low-speed results of **Figure 7.7** are quite variable, but two features are obvious. Firstly, the extremes in the decay exponent variation are tempered by increasing slenderness ratio and reduction in number of hulls (change of hullform). Secondly, the strong relationship between the transverse system and wave interference in highlighted, knowing that catamarans produce stronger transverse systems. Whether any of these factors could be incorporated into a useful design is questionable.

Although slow-speed vessels are less likely to create wave wake environmental concerns, other design considerations are likely to prove more fruitful than chasing extreme wave height decay rates in narrow speed ranges through hull configuration. For instance, slow-speed passenger vessels are often constructed from steel, which may offer reduced construction costs, a more robust structure and, in the case of monohulls, increased displacement to offset the limited stability of a multi-decked vessel.[91] A change in form from monohull to multihull (to remove the stability limitation) and construction from aluminium or composites would be more beneficial overall than any attempt at decay exponent optimisation within a narrow operational window.

Lastly, the high-speed condition of **Figure 7.8** confirms observations from past model and full-scale tests:

a.  the strength of a catamaran's transverse system delays improvement in the decay exponent with increasing speed, shown as a rightward shift of the catamaran curves;
b.  high-speed commercial vessels tend to operate in a length Froude number range where a decay exponent of *-0.33* is the most appropriate;
c.  at very high speeds, the decay exponents of all variants devolve to the simpler, single packet decay rate of *-0.5*. Interestingly, the monohulls reach this point at $Fr_L \approx 0.85$, which corresponds to a transverse wavelength of $\sim 4.5L$. That concurs exactly with the lower bound of the high-speed range of the reduced monohull Kelvin wedge angle of Ma *et al.* (2016).

---

[91] The low cost of steel construction is somewhat of a myth. Steel is around one-fifth the cost of aluminium but around three times the weight, and the scantlings are never comparable. When the costs of the additional steel cutting, handling and finishing processes (sandblasting) are added in, along with the increased maintenance costs, the cost difference between the two materials is not that great and can be quickly recovered in fuel savings. In their extremes, each material has unique advantages and disadvantages: robust steel hulls can have a very long life but at the expense of maintenance and fuel/machinery costs; very lightweight aluminium vessels can have low running costs but at the expense of construction cost/complications and fatigue life. In some ways this explains the different design approaches in first, second and third-world shipbuilding.
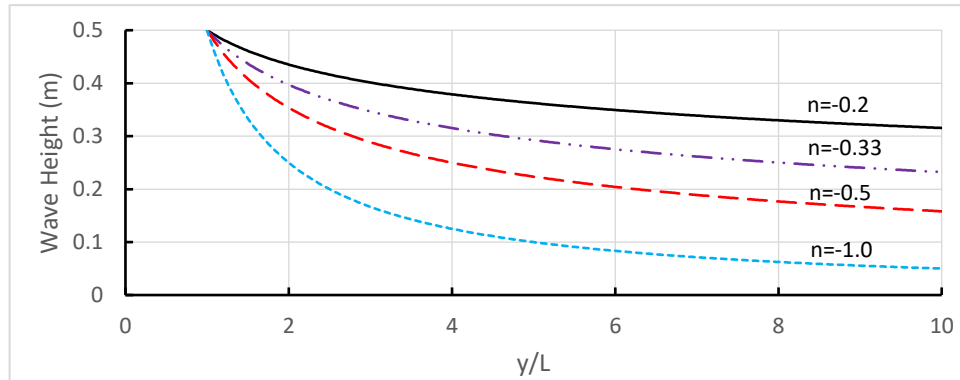
**Figure 7.10** – *Visual expression of decay rates with lateral separation, assuming an initial nominal value of* $H = 0.5 \, m$ *at* $y/L = 1$.



**Figure 7.11** – *An extreme example of a monohull river ferry (Rio Napo, Peru). The approximate dimensions are:* $L_{OA} = 33 \, m$; $B_{OA} = 2.6 \, m$; $B_{WL} = 2.0 \, m$; $\Delta = 10 - 12 \, t$ *(laden),* $SR = \sim 13.5$. *The service speed of 16 knots is achieved with three outboard motors of 170 kW total power. Passenger capacity is 70 persons. Construction is of thin galvanised steel sheeting with simple bench seating and canvas superstructure. Propulsion with outboard engines is not the most efficient at the service speed, but they are capital cost-effective, easy to service, simple to replace, and easy to refuel in remote locations. Photos courtesy of James Langner, Fibrecon Marine, Lima.*

## 7.6    Decay Rate and Vessel Operating Speed Range

It is relevant to consider the anticipated speed ranges of vessels operating in sheltered waterways. In the high-speed condition, these can be separated into three likely groups: small recreational craft; large recreational craft; commercial vessels including passenger ferries.

*Small recreational craft*: with waterline lengths ranging from around *2.5 m* to *6 m* (jet ski to large ski boat), the length Froude number would exceed *1.0* at speeds of around *9 kn* to *15 kn* respectively. *Table 7.1* shows relevant speeds for different vessels and activities.

127

**Table 7.1** – *Recreational craft speed ranges.*

| Activity | Speed Range (kn) | $Fr_L$ L = 4 m | L = 5 m | L = 6 m |
|---|---|---|---|---|
| Wakesurfing (amateur / pro) | 8 / 11 | 0.66 / 0.91 | 0.59 / 0.81 | 0.54 / 0.74 |
| Wakeboarding | 18 to 20 | 1.48 to 1.64 | 1.32 to 1.47 | 1.21 to 1.34 |
| Water skiing - adult | 15 to 21 | 1.23 to 1.72 | 1.10 to 1.54 | 1.01 to 1.41 |
| Water skiing - child | 11 to 14 | 0.90 to 1.15 | 0.81 to 1.03 | 0.74 to 0.94 |
| High-speed transit | 20 to 30 | 1.64 to 2.46 | 1.47 to 2.20 | 1.34 to 2.01 |

*Notes*:

1.  Any vessel less than $L = 4\ m$ used for anything other than wakesurfing or other unballasted activity would have a wake regarded as almost inconsequential in anything other than the most sensitive waterway.
2.  Speed ranges (except high-speed transit) were taken from www.evo.com and www.usawaterski.org (last accessed 9th January 2019).

Based on *Figure 7.8*, wakesurfing activities would fall into the speed range where decay rates are modest. All other activities would tend towards the high-speed range where high-speed decay rates are at the maximum of *-0.5*. This is a common theme in small craft environmental assessment: high-speed transit is preferable to medium or slow speeds, but with the caveat that wave period does not exceed threshold values (refer Macfarlane and Cox, 2003, Sections 4 and 6).

*Large recreational craft*: This is taken to be from $6\ m < L < 15\ m$. To achieve $Fr_L > 0.9$, which (according to Figure 7.8) would maximise the decay rate, would require a minimum speed of *13 kn* to *21 kn* respectively. That would be easily achievable in most instances, though would come with a wave height that may be untenable, regardless of decay rate. Large recreational craft are known to have lower slenderness ratios and therefore higher wakes.

*Commercial craft*: This is where the widespread adoption of the *-0.33* exponent is justified. *Table 7.2* shows the operating length Froude numbers for passenger vessels with history of sheltered waterway operation and environmental assessment. Excluding the highest and lowest values (*First Fleet Class* and *Red Jet 7*), the length Froude numbers range from $0.6 \leq Fr_L \leq 0.9$ and the average is $Fr_L = 0.73$. All but two vessels have catamaran hullforms. From *Figure 7.8*, this average length Froude number would correlate to a catamaran hullform decay exponent of *-0.33*.

Designers of high-speed commercial craft are well aware of the necessity to avoid unfavourable speed regimes, hence the generic definition of high speed being $Fr_L > 0.5$.[92] Similarly, speed is expensive and commercial operation at $Fr_L > \sim 1.0$ is uncommon. Those working in the field of the environmental assessment of ferry operations were also aware of the fairly narrow range of length Froude numbers, which is the reason why the decay exponent of *-0.33* was a continual feature of model and full-scale studies. It was not a misunderstanding of the theory; it was the result of a model and full-scale testing, and the need for a generic decay exponent.

---

[92] The IMO High-Speed Craft Code refers to a minimum definition of high speed as $V > 3.7\nabla^{0.1667}$, which is a volumetric Froude number relationship ($Fr_\nabla \sim 1.2$) and relates roughly to a length Froude number of around *0.5*. The paucity of published vessel displacement data makes assessment on $Fr_\nabla$ difficult.

**Table 7.2** – *Length Froude numbers of a selected range of passenger ferries.*

| Vessel | Fr$_L$ | Operating area |
|---|---|---|
| Sydney Rivercat | 0.63 | Parramatta River, Sydney |
| Brisbane CityCat | 0.82 | Brisbane River, Brisbane |
| Incat 74 m Wavepiercer | 0.71 | Inter-Island Service, New Zealand (Condor 10) |
| Mestral Class (Albayzin) | 0.60 | Inter-Island Service, New Zealand |
| Sydney First Fleet | 0.36 | Sydney Harbour, inner and outer harbour |
| Sydney Emerald Class | 0.72 | Sydney Harbour, inner and outer harbour |
| Sydney Jet Cat | 0.90 | Sydney Harbour, outer harbour |
| Rottnest Ferries Star Flyte | 0.73 | Rottnest Island via Swan River, Perth |
| Isle of Wight Red Jet 7 | 1.01 | Southampton to Isle of Wight, UK |

*Note: all these vessels and or service routes have been the subject of environmental wave wake reporting.*

Those involved in environmental reporting are obliged to apply what has become known as the *Precautionary Principle*, which is summarised as: "*When an activity raises threats of harm to human health or the environment, precautionary measures should be taken even if some cause and effect relationships are not fully established scientifically.*"[93] In effect, in the face of unknowns, estimates should be conservative by nature. In that case, the use of the *-0.33* decay exponent would be regarded as appropriate. Use of an exponent of *-1.06*, as was shown theoretically possible by Doctors and Day (2001) under certain narrow conditions for specific hullforms, would be regarded as unviable and certain to be struck down in an environmental assessment.

## 7.7    Decay Rates

It must be accepted that, in all reality, a simple solution probably does not exist because the cause itself is not simple. The best that can be achieved are guidelines for decay rate approximations based on water depth and length Froude number.

### 7.7.1    Deep water decay – slow speed (Fr$_L$ < 0.5)
It must be accepted that a systematic method for determining the wave height decay at slow speeds does not exist, and the chances of developing a simple method of calculation would be difficult, if not impossible. In the displacement speed range ($Fr_L < 0.399$), the transverse wave system is quite active.[94] Figure 4.3 of Section 4 shows how the periods of the divergent and transverse systems are more closely aligned at slower speeds and that, combined with the presence of several divergent packets, leads to interference and instability.

---

[93] Known widely as the final statement of the *Wingspread Conference*: a meeting of academics in Racine, Wisconsin, in January 1998.

[94] Though only approximate by nature. This nominal condition is where the transverse wavelength is the same as a vessel's waterline length ($\lambda_T = L$, so $V/\sqrt{gL} = (2\pi)^{-\frac{1}{2}} = 0.399$) with the common analogy that the vessel must "*climb over its own bow wave*" to go faster (convenient for a lay audience, but not exactly correct). There is no special relevance in this point, except that it concurs with a region where resistance increases rapidly.

Mitigating this instability are the more moderate wave periods and the rapid change in wave wake parameters with speed – small changes in speed bringing large changes to wakemaking resistance. **Figure 7.12** shows an example, taken from full-scale trials of an *8.2 m* WL monohull tourist ferry *Everglades Waterbus* (Macfarlane and Cox, 2003). The wave wake heights were measured at *2.8L* (*23 m*) abreast of the sailing line in water considered to be *practically deep*. The initial growth in wave height (and wave period, which is ignored here but follows a similar trend) is steep and mirrors the very marked growth in wave drag in the slow speed range ($Fr_L < 0.5$). The right side of **Figure 7.12** is in two parts and is based on an assumed wave height of *0.2 m* at *2.8L* and a decay exponent of *-0.33*. That would correspond to *0.16 m* wave height at *5.6L*. The curve "*height*" shows how a *0.2 m* initial height at *2.8L* would transform at a lateral separation of *5.6L* (twice the initial distance) with differing decay exponents. The curve "*speed*" shows how the vessel operating speed could be varied to achieve the same far field wave height of 0.16 m with $n = -0.33$ if the actual decay exponent proved different. For the most commonly quoted decay exponent range of $-0.2 \leq n \leq -0.5$, speed could be varied just 0.7 kn ($\pm\sim5\%$) for the same far field wave height outcome with different decay exponents.
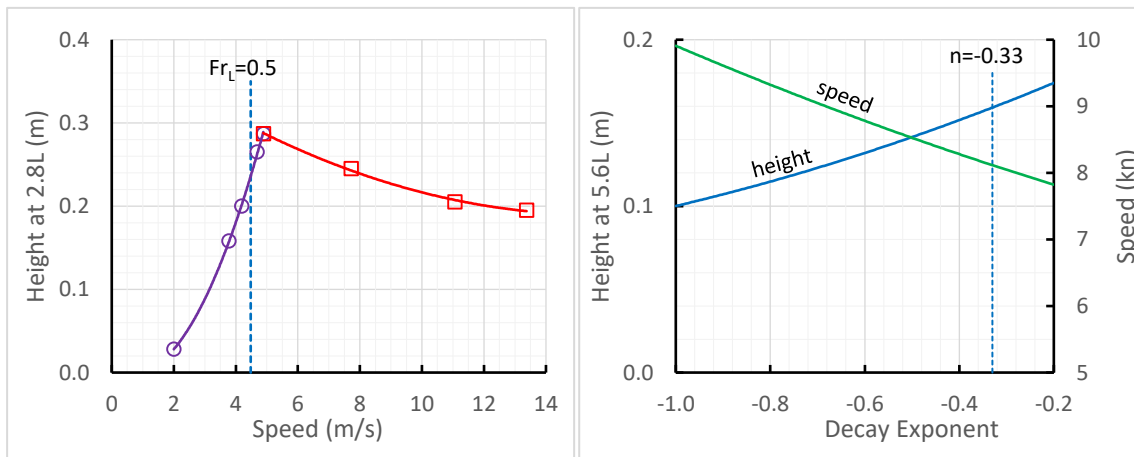


**Figure 7.12** – *An example of how the assumed decay exponent at slow speeds ($Fr_L < 0.5$) has limited effect on outcome. The values are from full-scale trials of an 8.2 m WL monohull vessel. **Left**: height of the maximum wave measured at a lateral separation of 2.8L, showing the very steep initial growth with increasing speed. **Right**: How an assumed 0.2 m wave height at 2.8L would transform at 5.6L for different decay exponents. The second curve "speed" shows which speed the vessel could be operated at to achieve the same wave height at 5.6L under decay exponents different to an assumed exponent of -0.33. In other words, how much faster or slower could the vessel be operated if the actual decay exponent was different to -0.33, and still achieve the same far field wave height outcome. Wave period variation is ignored, though it reinforces the argument further.*

So, the rapid change in wave height with speed in the slow speed range means the exact decay exponent is of lesser importance because can be compensated with a minor speed change. If an energy criterion was also applied, the possible speed variation would be even smaller. If the decay exponent in service proved better than expected and allowed a higher operating speed for the same far-field height requirement, there would be a commensurate steep increase in wave period. Any allowable speed increase from a better-than-expected height decay rate to the *-0.33* assumed would be quickly dampened by increased wave period and the effect it has on energy, not the least reason being that the period of the maximum wave does not decay with lateral

separation. Conversely, any required speed decrease for a worse-than-expected height decay rate to the *-0.33* assumed would benefit from reducing wave period. Arguments about low speed height decay exponents get lost in the fact that, for high-speed vessels operating at slow speeds, these percentage speed changes reduce to a nudge on the throttle.

In the absence of experimental or applicable statistical data, the most prudent approach at slow speeds would be to adopt a cautionary approach and use the commonly quoted decay exponent value of *-0.33*.

### 7.7.2    Deep water decay – high speed ($Fr_L > 0.5$)

Appendix B details a different approach to deep water decay, though in itself it is not a solution. It develops an argument for a decay rate approximation based on a one-dimensional linear Schrödinger wave equation, which results in a decay rate that is a function of group celerity. The method describes how a wave packet envelope, termed a packet soliton, changes as it propagates.[95] The amplitude extremes of a packet envelope propagate with the characteristic packet wavenumber, which remains a constant value. That is analogous to the maximum wave in a propagating wave wake, which propagates with constant wave period but varying height. This is the explanation of why the maximum wave is the most consistent feature to measure in a wave wake, though it's never discussed as such. The reason for adopting the highest wave as the principal measure of wave wake has more to do with psychology and perception than reality. Lesleighter (1964) made a similar observation and commented on the public's tendency to over-estimate size visually (a phenomenon also well known in ocean wave observations), and Section 3 (especially footnote 30) expands the argument with further examples. Science was always playing catch-up with human nature.

The most usual form of non-dimensionalising lateral separation has been to express lateral separation in terms of boatlengths (taken always as static waterline lengths). In some ways this would seem logical, but only if the waves generated by a vessel could be directly related to waterline length. That is not untrue at high speeds, but the relationship is far more complex at displacement speeds. Rather than relate the waves to the source, there are methods that relate the waves to the principal wave parameters.

The parameter $yk$, which is the product of the lateral separation $y$ with wavenumber $k$ ($= 2\pi/\lambda$), has been used in wake surveys for the estimation of wave resistance (Ward and van Hooff, 1976). In that instance the wavenumber was based on the wavelength of the transverse system, which has a fixed relationship with vessel speed. If used to non-dimensionalise the divergent system, it would have to be based on the characteristic packet wavenumber, which is the wavenumber of the maximum wave (designated as $yk_o$). That is at least convenient. The parameter $yk_o$ is also non-dimensional. In practical terms, it represents the number of wave cycles completed up to a given lateral separation – the greater the number of completed cycles, the faster the decay.

As discussed, the method detailed in Appendix B is based on group celerity, which was the basis for Kelvin's original ship wake studies (Lamb, 1895). The proposed decay equation is:

$$u(y,t)_{max} \propto \left[ 1 + 4\left(\frac{y}{c_g}\right)^2 \right]^{-\frac{1}{4}}$$

[7.2]

---

[95] Refer to the discussion in Appendix B. The envelope that describes the bounds of a wave packet has the properties of a soliton.

where $u$ is the packet maximum relative amplitude (1 at the origin, approaching zero towards infinity) and $y$ is the lateral separation. Amplitude in absolute terms is not possible with this method. When described as a power law decay, the decay exponent varies from *0* at the sailing line to *-0.5* in the very far field. The decay exponent would only be around *-0.33* within one boatlength from the sailing line, beyond which it quickly approaches *-0.5*. The decay rate is time dependent, hence the reliance on group celerity. This equation signifies the relationship between the propagation time of the packet to reach a given lateral separation and the decay it experiences. The higher the group celerity, the shorter the time to reach a given position and the slower the rate of decay. One obvious problem is that the value $y/c_g$ is not non-dimensional and has the dimension of *seconds*. The reason for that comes from its derivation and certain assumptions made (refer Appendix B). By making it relative between two locations and not absolute, that problem is removed.

Another consequence of the dimensional nature of [7.2] is that is does not scale. The lateral separation $y$ scales with $L$ but $c_g$ scales with $\sqrt{L}$, so that decay rates at model scale would be different to full scale. The actual difference in calculated decay exponents is not large at all and is only discernible in the near field where wave height is always difficult to measure due to local interactions. As an example, a *30 m* vessel with a characteristic wave period (period of the maximum wave) of *5 s* would have a single wave packet decay exponent at *2L* of *-0.5*; a *1:20* scale model would record a decay exponent of *-0.478*.[96] The difference is well within a normal range of variation.

Any effort to rationalise wave decay using the wave parameters would only be relevant to the decay of a single wave packet. The decay analysis presented by Havelock (1908) shows that the transverse and divergent waves decay with a power law exponent approaching *-½* in the far field when viewed individually (and not at the Kelvin wedge where the relationships experience a singularity), but the combined systems at the cusp decay with a *-⅓* power law exponent in the far field. The individual systems are similar in that regard to [7.1], but the combined systems are not. Therefore, we can expect the decay exponent may approach *-½* only where a single system is present.

**Figure 7.8** is a telling example of this. It focuses only on the high-speed condition ($Fr_L > 0.5$). The constancy of the decay exponent at high length Froude numbers is evident – in the speed regime where the transverse system is expected to be inconsequential. There may be multiple divergent systems, but they seem less likely to interfere if the speed and or the lateral separation is sufficiently high. In this condition, the wake is approaching the pure form of a single wave packet, with theoretical far-field decay exponent of *-½*.

### 7.7.3   Shallow water - transition speed

At the depth-critical speed, crest height decays approximately linearly with lateral separation. **Figure 7.14** (following) shows an experimental example of this. If a transitional condition were to be established and remain stable for some time, it is likely that the linear variation would change as the crest length grew and the crest height near the vessel reached a practical upper limit. The height measurements at model scale are clearly of a linear and linearly decaying nature laterally but only because of the limited time to form a steady-state condition.

---

[96] Based on the conventional decay relationship $H \propto y^n$.

Height decay in this speed regime is of academic interest only. Vessel operators should be actively discouraged from operating continuously at the depth-critical speed.

### 7.7.4   Shallow water - supercritical speed

Reference is made to the appendices accompanying this section and to Section 5, which have more detailed analyses.

Shallow water wake decay is complex. Doyle *et al*. (2001) comment that "*unfortunately when trying to characterise shallow water wake wash, considerable complications arise. The deep water decay rate is no longer valid and due to the divergence of the leading supercritical waves, the wave periods are not constant with distance from the sailing line.*" They go on to note that decay exponents of *-0.25* have been observed in field measurements (their *Fig. 2*) at $h/L \sim 0.1$ and at high speeds, and the same design tested in shallower water at model scale recorded a decay exponent as low as *-0.2*.

Reference is made to Section 5 and its relevance to the discussion of shallow water wave wake decay. Ongoing analysis leads to the conclusion that the decay rate of a single divergent wave packet is a function of group celerity or, more appropriately, the rate of dispersion. Havelock (1908) refers to Lamb (1895) and his comment that Kelvin's original ship wave analysis was based on a group celerity approach. The deep water, single packet relationship proposed in [7.2] shows this, but it cannot be applied generally in shallow water as it assumes a fully dispersive environment (i.e., where $c_g/c_p = 0.5$). There is a specific example in shallow water where it appears to have some validity – that being the decay of the first wave if the water is sufficiently shallow.

The envelope soliton (which defines the maximum wave) in a fully dispersive, single wave packet from a continuous source decays with a power exponent that approaches *-0.5* in the far field. At the other extreme, where the system is fully non-dispersive, the height of a solitary wave does not decay at all.[97] As is noted in Sections 5 and Appendices D, E, F, G and H, vessel wave wakes generated in shallow water at depth super-critical speeds have a leading solitary wave component that eventually dominates if conditions are conducive (increasing $H/h$ ratio created by a reduced vessel slenderness ratio at a reduced $h/L$ ratio). These extremes set the bounds of the decay exponent.

If the decay rate is a function of the ratio between phase and group celerities, and the lateral separation, the question becomes whether decay is dependent on time or distance. The premise is that the decay of the packet will depend on how many *cycles* it has undergone. This was a simpler concept to understand if the alternative decay parameter $yk_o$, which defines the number of wave cycles the maximum wave has been subjected to by the time it reaches a given lateral separation. In a depth-affected condition when $0.5 < (c_g/c_p) < 1$, it takes longer for waves to cycle from the tail to the head of the packet relative to how far the packet propagates (or in what time). That seems to be the mechanism that determines the decay rate. As discussed in Section 5, there is no such thing as a fully non-dispersive wake or wave for that matter; only the very leading part of the first crest can be regarded as non-dispersive.

Energy cycling through a shoaling packet at a reduced rate, energy shed into the trailing packet by the components of the first shallow water wave unable to propagate at $\sqrt{gh}$, and cycling packet

---

[97] Non-dispersive in the classical sense that its celerity is no longer a function of wavelength; ignoring amplitude dispersion and internal dispersion mechanisms of solitary waves.

energy that becomes trapped in a dominant solitary wave at the head of a very shallow water wake all add to make shallow water decay the most complex of problems. That is before consideration of multiple divergent packets and packet interaction are considered. It is often the case that there is no obvious single maximum wave in a shallow water packet and therefore no clear group celerity to adopt. It is also quite possible that non-linearities in shallow water may cause the group celerity to change gradually with propagation as the wave wake is transformed.

Some of the experimental results of Doyle *et al.* (2001) have been reconfigured as **Figure 7.13**. It is assumed that the high speed, deep-water decay exponent would apply at $h/L \geq {\sim}0.45$, as explained in Section 5, and that appears to support the general trend in the decay exponents.[98] In the extreme, once $h/L > 1$ the vessel's divergent wake would be regarded as being in the *deep* condition and, at high speeds ($Fr_L > 0.85$ for a monohull, or $> 1$ in general; refer Figure 7.8), would return a decay exponent of *-0.5*. However, as discussed, few passenger ferries operate at sufficiently high speeds for that to occur, and wake waves do not always exist as single packets where the decay exponent is *-0.5*. The trend shown in **Figure 7.13** as $h/L \rightarrow 1$ may not strictly be correct.
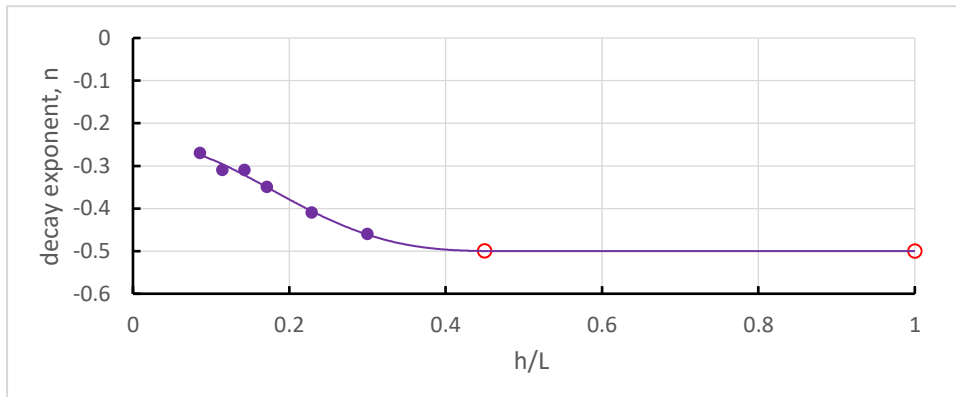


**Figure 7.13** – *Depth super-critical wave height decay at high speed, using data from Doyle et al. [2001, Fig. 3(a)]. These are from model tests of a large monohull ferry. The solid markers are from Doyle et al., and the hollow markers are projections based on the decay of a single packet subject to minimal depth effects. The wave measured was the highest in the first (most energetic) group, but groups become increasingly indistinguishable as $h/L$ decreases and there is the same risk seen in deep water of the highest wave at each lateral position being exposed to superposition.*

### 7.7.5    First wave in shallow water - supercritical speed

The first wave in a shallow water wake is a special case. As discussed in Section 5, the first shallow water wave has the features of a wave packet and not a single wave. This becomes more evident as the $h/L$ ratio reduces, and the first wave becomes dominant. It is known that the leading crest propagates at $\sqrt{gh}$, but the initial upswelling propagates slightly faster (due to the presence of a leading solitary wave component) and the trough/tail of the first wave lags the crest at a speed less than $\sqrt{gh}$. The non-linear, amplitude-dispersive upswelling and the lagging trough/tail cause the first wave to *disperse* with lateral separation.

---

[98] Assuming the divergent wavelengths are in the order of the waterline length and taking the limit of *practically deep* as $\lambda > 3.5h$, shallow water would become significant at $h/L < {\sim}0.45$.

The group celerity in a non-dispersive wave is equal to $\sqrt{gh}$. That simplifies the analysis of the first wave as a group. However, the whole of the first wave (or any periodic water wave in practice) is not non-dispersive, and there is weak dispersion of increasing strength from head to tail. The group celerity of $\sqrt{gh}$ is therefore an approximation for the wave as a whole. This approximation worsens as the $h/L$ ratio increases, and the first wave is a smaller wake feature to the point where a decay rate estimation based on group celerity approach becomes unreliable. Certainly a $h/L$ ratio of *0.3* was inconclusive and had to be reduced to about *0.15* before the approach was reasonably consistent. The decay of the first shallow water wave therefore becomes:

$$u(y,t)_{max} \propto \left[1 + 4\left(\frac{y}{\sqrt{gh}}\right)^2\right]^{-\frac{1}{4}}$$

[7.3]

The decay of the first shallow water wave has practical applicability in certain conditions because of the first wave's increasing percentage of overall packet energy as $h/L$ reduces. In extreme conditions, the first wave can account for more than *90%* of the overall wake energy (refer Section 6).
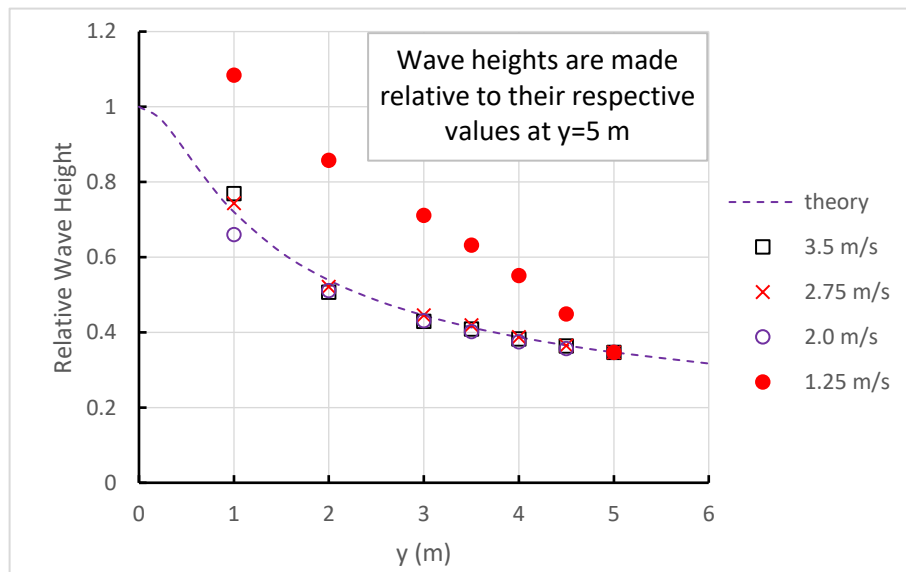


**Figure 7.14** – *Shallow water first wave height decay comparison for model AMC 00-01 ($h = 0.15\ m$) (Appendix C, Figure C6). The depth-critical speed is $V_{crit} = 1.213\ m/s$. In general, all results follow the linear Schrödinger theory described by [7.2], except around the depth-critical speed where the wave form and propagation are different. The close fit, even for the near-field location, is due to the shallow water depth, the increasing strength of the first (apparent) wave relative to the rest of the wake as depth decreases, and the first wave group celerity approaching $\sqrt{gh}$ as water depth decreases.*

# Section 8 – Severity of Erosion

> *In M. Mitchell Waldrop's article "Spontaneous order, evolution, and life" (Research News, 30 Mar, p. 1543), he "roughly paraphrased" the Second Law of Thermodynamics as "you can't unscramble an egg." An egg can be unscrambled, and the Second Law violated, by feeding it to a hen.*
>
> *Leonard Hayflick*
> *Science* 15 June 1990:
> Vol. 248, Issue 4961, p. 1281

## Summary

A novel way of calculating the degree to which a wave may cause erosion is proposed. It is known that waves create shear stress as they interact with the bottom, and the extent to which sediment is entrained is a function of the bottom shear stress relative to the threshold entrainment value. Analysis of past (unrelated) experiments shows that the determination of threshold shear stress correlates well with measured turbidity.

The novel determinant of erosion severity is derived from how much excess shear stress exists above the threshold value. Normalisation in terms of multiples of the threshold value simplifies calculation. The results demonstrate what has been previously observed and measured experimentally – that the initial exceedance of the threshold causes a disproportionately large amount of turbidity, and further excess shear stress results in a more linear progression.

Quantification of this method can only be done experimentally when the sediments are fine enough to permit the use of turbidity as the appropriate indicator of erosion. Methods to account for the vertical location of the turbidity sensor relative to the bottom are developed. It is shown that the application of linear wave equations are not unreasonable for the determination of threshold values, though non-linear wave equations give the closest correlation. An equation and a table of constants for ranking waves is derived from the analysis. It is acknowledged that further experimental work is required to confirm the results and give correlation to actual erosion rates; the experiments cited here were not designed to quantify the method proposed but were designed to study erosion from wave wake in general.

## 8.1    Introduction

The difference between an erosion threshold and a defined erosion rate must be acknowledged if vessel regulation is to be successful. Thresholds can be quite low – an example being those derived from the 2004 Gordon River experiments (*Appendix K*), where wakes with parameters of the maximum wave of $H_{0.5} = 114\ mm$, $T = 1.1\ s$ and $E = 30\ J/m$ at $h = 0.5\ m$ did not generate turbidity. In fact, it could be argued that even those waves complying with the criteria at the nominal turbidity measurement depth would generate turbidity in shallower water, especially during the breaking phase. Only the very shortest of waves could be considered as being completely free of turbidity generation potential - far shorter than the ambient wind waves.

The Noosa River study of Macfarlane and Cox (2003, Fig. 4.2), re-working the data presented by von Krusenstierna (1990), demonstrated this by grouping von Krusenstierna's erosion data into groups of *low*, *moderate* and *high* based on erosion pin measurements. The threshold was deemed to be the upper limit of *low*, at *30 J/m* energy. That value corresponds exactly with the 2004 Gordon River results using elevated turbidity as the erosion measure in a completely different experimental arrangement. The significance of this correlation is that fine sediments, which remain suspended in the water column for some time after initial entrainment, are best characterised by turbidity, but coarse sediments that settle quickly are best characterised by direct erosion measurements (such as erosion pins). It is proposed that correlation of either measurement method with the proposed methodology would qualify all sediment types.

Predicting thresholds of erosion, and the wake waves that might satisfy those thresholds, is not difficult if the relativity of the threshold is recognised. What is far more complex is determining erosion rates where the threshold is exceeded and whether different vessels may or may not be allowed to operate. An attempt is made to qualify the severity of erosion of a wave that propagates from deep to shallow water, to the point of breaking. The methodology could be extended to include waves formed initially in shallow water, though it may require knowledge of wavelength and not simply wave period. Wavelength could be estimated from wave period, wave height and water depth, but with error that increases as the ratio of $h/L$ decreases and the composition of the leading wave becomes more complex to assess.

The premise for the method is that the degree of sediment entrainment beneath a shoaling wave is an indicator of the degree of erosion, and the degree of sediment entrainment is a function of the intensity of the bed shear stress beneath a wave. Furthermore, the summation of this shear stress from the point of initial sediment entrainment, in this case a true threshold, through to the point of breaking, is related to the severity of erosion. The breaking condition itself is not considered.

In this regard, erosion is defined as entrainment of sediment, so may also mean accretion. As a generic term, it is defined as sediment entrained and therefore susceptible to transportation away from its initial location (Bauer *et al.*, 2002).

## 8.2    Wave Theories

Linear (Airy) wave theory is preferred in coastal engineering because of its relative simplicity. Fig. 2-6 of the Shore Protection Manual (Coastal Engineering Research Center (CERC) (U.S.), 1984) lists variants of linear wave theory from fully deep to fully shallow for use in engineering calculations. Wave parameters can be readily calculated directly or with simple iteration. As waves become steeper (period short relative to height), or more importantly as waves move into shallow water, linear wave theory can no longer be applied with confidence. Its usefulness can extend at least to $\lambda/h \sim 7$, but certainly not more than $\lambda/h \sim 10$. In the extreme it tends to estimate wavelengths shorter than may be experienced and therefore the error in shallow water wave height (due to shoaling) increases. The growth of these discrepancies is consistent beyond the linear theory applicability limits and there is no obvious jump in parameters. This makes it both appealing - because the numbers still appear credible and workable, but also misleading - lacking an obvious indication of discrepancy that a discontinuity would provide.

*Figure 8.1* shows the approximate ranges of suitability of the linear and non-linear wave theories (Le Méhauté,1976, reproduced in US, 2006). The relatively narrow area of applicability of linear theory is noted. The Stokes theories extend as high as 5$^{th}$-order, beyond which higher order solutions may be unwarranted (US, 2006, p. II-1-58). Cnoidal theory extends in a wedge between the nominal breaking limit (see later) and an *Ursell number*, $U_R$, equal to *26*.

As discussed in the Section 5, Hedges (1995) suggests the line of demarcation between Stokes and cnoidal theories to be in the order of $U_R = 40$. This apparent fluidity in the boundaries of wave theory applicability complicates the assessment of sediment movement and entrainment, since bottom shear stress is a function of bottom celerity, which itself is a function of wavelength.

Also of interest is the *shallow water Ursell number $U_s$*. By substituting the limiting shallow water wavelength, $\lambda = T\sqrt{gh}$, the shallow water Ursell number becomes $U_s = gHT^2/h^2$ which has the familiar theme of proportionality to $HT^2$.

Cnoidal theory is particularly complex to apply, and its application within a generalised wave wake calculator would be optimistic at best; impossible at worst. Isobe (1985) presents a simplified method of calculating first-order cnoidal wave parameters, though even this would be complicated to incorporate into a desktop wave wake solution. This is not unique, as Isobe (1985) states:

> *"Although there has been much progress in describing highly nonlinear waves (e.g., Fenton, 1972; Schwartz, 1974; Cokelet, 1977; Nishimura et al., 1977), the linear wave theory is still commonly used in studies of nearshore currents, sediment transport and so on."*

Similarly, many papers, including those of Komar and Miller (1973) and Cox *et al*. (1996), make use of bottom shear stress equations based on linear theory.

Superimposed onto *Figure 8.1* are the relative values calculated for four waves used in this analysis, from the depth of the threshold of sediment entrainment to breaking: two at *0.1 m* and two at *0.2 m* deep water wave height, with two being short waves of *1 s* period and two being much longer waves of *6 s* period. The shorter period waves, being steeper and not subject to shoaling to any great extent, are best described by higher order Stokes equations. The longer period waves generally conform best to cnoidal theory, or the more simplified *hyperbolic theory*, best described by Fenton (1999) as the *Iwagaki 5$^{th}$-order approximation*, where the computationally-difficult elliptical functions of the cnoidal theory are replaced by a series of hyperbolic functions with very small loss of accuracy (remembering that real-world waves don't follow wave theories with absolute accuracy anyway).

Of note in *Figure 8.1* is the tendency of calculated wave parameters to pass between several wave theories, such as *2 s* period waves that pass from Stokes II to Stokes III to hyperbolic theories as they propagate from deep water through to breaking. Also of note is the tenuous boundary of wave breaking, nominally set at a $H_b/h_b$ (*breaker depth index*) limit of *0.78*. The classic definition of the wave breaking, as described by Stokes, is the point at which the speed of a water particle at the crest exceeds the wave celerity and hence the wave form becomes dynamically unstable. There are other definitions, such as the point where the tip of the crest moves ahead of the wave face. In reality, the exact point of wave breaking is not easily defined or identified. Fenton (1999) gives examples of several un-related, practical experiments where the

maximum breaker depth index achieved was just *0.55*, demonstrating the imprecision in describing the wave breaking condition.

The definition of wave breaking has a large effect on the integration of the bottom shear stress from entrainment threshold through to breaking. As will be demonstrated, most of the integrated shear stress occurs just before breaking, such that any deviation in definition of breaking could have a disproportionate effect on the integration. In that case it was decided to adopt a consistent breaker depth index value of 0.78 for all wave cases. If it is wrong, it is better to be consistently wrong.

The case of the *0.1 m*, *1 s* wave in **Figure 8.1** demonstrates the fragility of wave transposition into shallow water, particularly the variability of wavelength calculation. Fenton (1990) makes two particular observations: firstly, that cnoidal theory tends not to converge for waves of low amplitude (which may cover most sheltered waters vessel wake waves); secondly, that just about all theories (except for Fourier approximation methods) tend to become unreliable at the limits of wave steepness, made worse by the fact that the accepted theoretical limits for wave steepness also fall short in practice (Fenton, 1999). The Iwagaki approximation tends to over-estimate wavelength near to the practical limit of $U_R = 26$, to the point where the calculated shallow water wavelength could exceed the deep-water wavelength. The ratio of $\lambda/\lambda_o$ should never be greater than unity, even if the ratio of $c_{g(h)}/c_{g(o)}$ (ratio of group celerity at intermediate depth $h$ to group celerity in deep water) briefly increases above unity as a wave begins to feel the bottom. Some of the minor discrepancies in the following computations come from discrepancies in wavelength calculation between the theories and the strong effect that wavelength has on sediment entrainment.
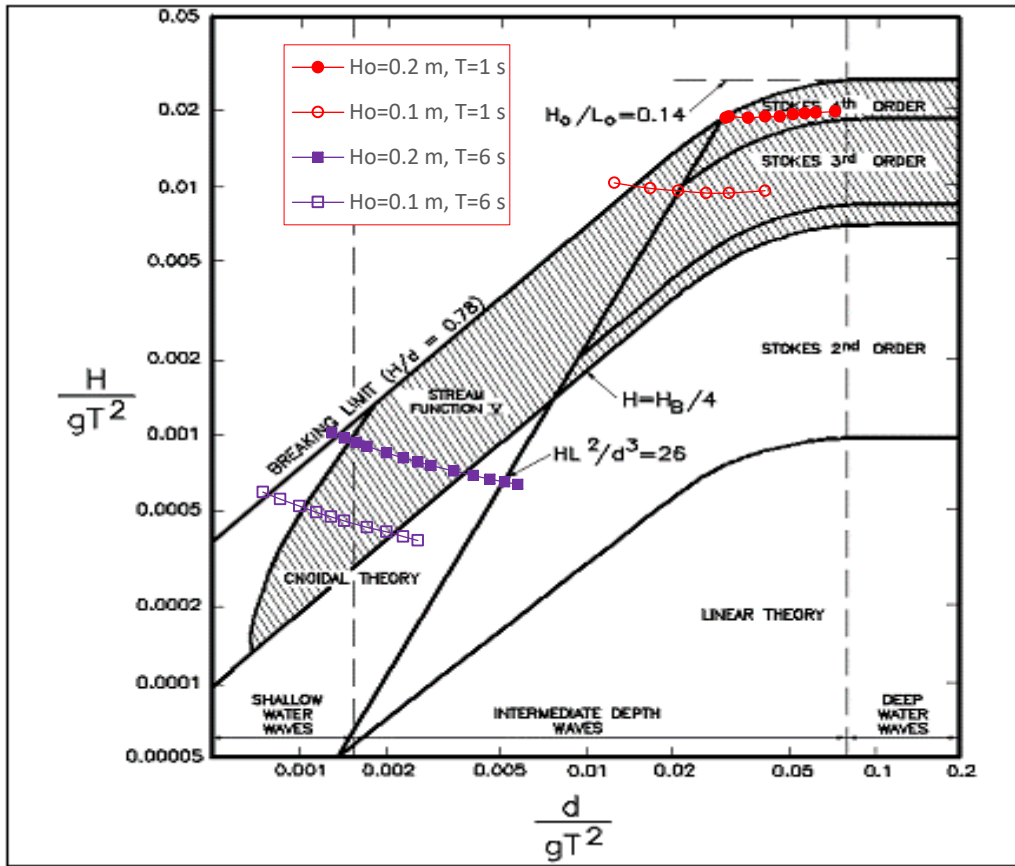
**Figure 8.1** – *Applicable areas of various wave theories, originally from Le Méhauté (1976), with parameters $L \equiv \lambda$ and $d \equiv h$. The various lines of demarcation have been shown to be somewhat arbitrary. Le Méhauté's line of demarcation at $U_R = 26$ is lower than the presently accepted value of $U_R \sim 40$ (refer Section 5). Superimposed are the results for four waves over a depth range from the threshold of sediment entrainment to breaking.*

## 8.3  Premise for the Severity of Sediment Entrainment

The work of Komar and Miller (1973) extended the work of Shields (1936) to produce an equation for the threshold relative stress beneath a wave. The Komar-Miller equation is:

$$\frac{\rho u_m^2}{(\rho_s - \rho)gD} = 0.30 \left(\frac{d_o}{D}\right)^{1/2} \qquad [8.1]$$

where $\rho$ is the water density, $\rho_s$ is the sediment density, $u_m$ is the near-bottom celerity, $D$ is the diameter of sediment grains, and $d_o$ is the orbital diameter of wave motion.

The Unified Soil Classification System (USCS) for sand size is shown in **Table 8.1**. Sediment greater than *0.075 mm* diameter is termed *sand*, and sediment less than *0.075 mm* diameter is termed *silt*.[99] It is assumed that the sediment is unconsolidated, without any degree of cohesion.

---

[99] *ASTM D2487-11, Standard Practice for Classification of Soils for Engineering Purposes* (Unified Soil Classification System), ASTM International, West Conshohocken, PA, 2011. www.astm.org

**Table 8.1** – *Unified Soil Classification System designation for sand sizes.*

| Designation | Diameter |
|---|---|
| very fine | $\frac{1}{16}$ to $\frac{1}{8}$ mm (0.063 to 0.125 mm) |
| fine | $\frac{1}{8}$ to $\frac{1}{4}$ mm (0.125 to 0.25 mm) |
| medium | $\frac{1}{4}$ to $\frac{1}{2}$ mm |
| coarse | $\frac{1}{2}$ to 1 mm |
| very coarse | 1 to 2 mm |

Sediment will move whenever the left-hand side of [8.1] (normalised actual shear stress, $S$) exceeds the value of the right-hand side (normalised threshold shear stress, $S_t$). Two additional relationships required in [8.1] are:

$$d_o = \frac{H}{\sinh\left(\frac{2\pi h}{\lambda}\right)}$$
[8.2a]

*and*

$$u_m = \frac{\pi d_o}{T}$$
[8.2b]

The initial application of these equations to identify thresholds used the simplified relationship between deep and shallow water wavelength shown in Section 5 [5.3], as proposed by Fenton and McKee (1990). However, rather than rely on an equation that has a strong link to linear theory, wavelength has been calculated using the appropriate wave theory as per *Figure 8.1*. The assumption in this case is that the waves have moved from deep water into shallow water and were not generated in shallow water to begin with, so both height and wavelength (and wave celerity, as will become important as well) vary according to water depth.

Initially, a wave propagating from deep water, over a gradually shoaling bottom and through to breaking, would initiate sediment movement at the threshold depth and that would increase in intensity until the wave breaks. This is shown schematically in *Figure 8.2*.
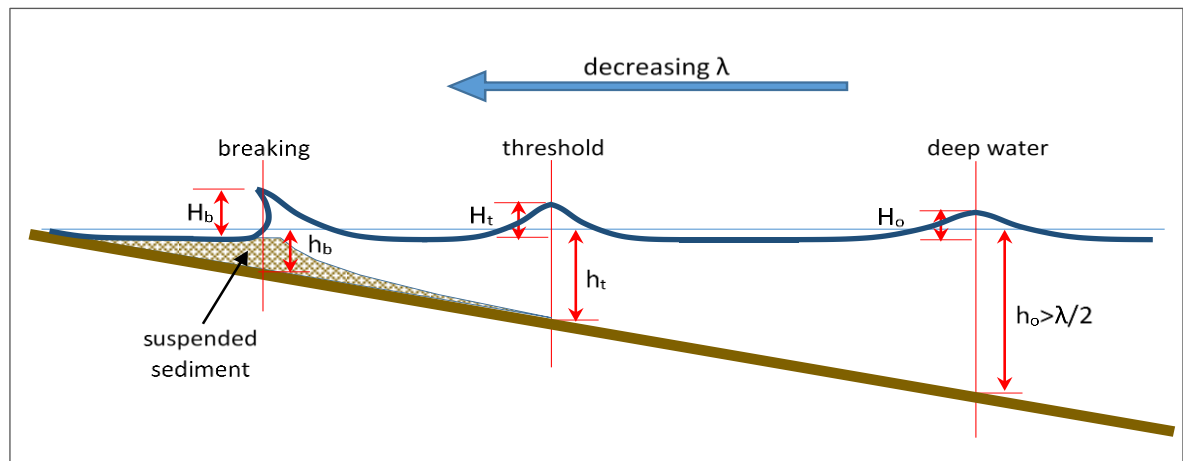


**Figure 8.2** – *Schematic representation of a wave moving from deep water through to breaking. The subscripts 'o', 't' and 'b' denote deep water, threshold and breaking, respectively.*

At any point shoreward of the sediment movement threshold depth, the rate of sediment entrainment will increase as the bottom shear stress increases with reducing depth and increasing orbital celerity at the bed. It is proposed that the severity of entrainment, and therefore the severity of erosion (by the generic definition proposed earlier), is a function of the increasing shear stress as the water shoals.

The relationships in [8.1] - the *actual shear stress S* and the *threshold shear stress* $S_t$ - are used to derive a third parameter $S'$, termed the severity of entrainment (a measure of excess shear stress above the threshold) and defined as $S' = S/S_t$; in other words – by how many times the actual bottom shear stress at any point exceeds the local threshold shear stress. As will be demonstrated, the severity of entrainment is a more useful parameter, with a threshold shear stress condition of $S = S_t$ giving a value of $S' = 1$.

As an example, ***Figure 8.3*** (linear) and ***Figure 8.4*** (log-log) show these normalised bed shear stresses (actual, threshold and severity) as a function of shoaling water depth from threshold to breaking for one set of deep-water wave parameters: $H_o = 0.2\ m$ and $T = 2\ s$. The salient features of ***Figure 8.3*** are:

a. the relatively slow growth in the threshold shear stress $S_t$ as depth initially decreases;
b. a considerably faster growth in the actual shear stress $S$ but accelerating almost exponentially towards the point of wave breaking;
c. a similar, but more modest, growth in the quotient of actual and threshold values ($S'$).

The log-log plot of ***Figure 8.4*** exhibits an almost straight-line relationship for all three variables, indicating a power relationship. The irregularity of the lines is largely due to differences in wave theories. The sample wave moves between three wave theories, commencing with Stokes second order in deep water, moving to Stokes third order at around *0.6 m* depth, and then to hyperbolic theory (*Iwagaki 5th-order approximation*) from *0.5 m* depth through to breaking. There is some discontinuity in the calculated wavelengths at the boundaries of each theory, and with sediment stress strongly a function of wavelength it is not unreasonable to assume that the waviness of the curves is largely due to this.
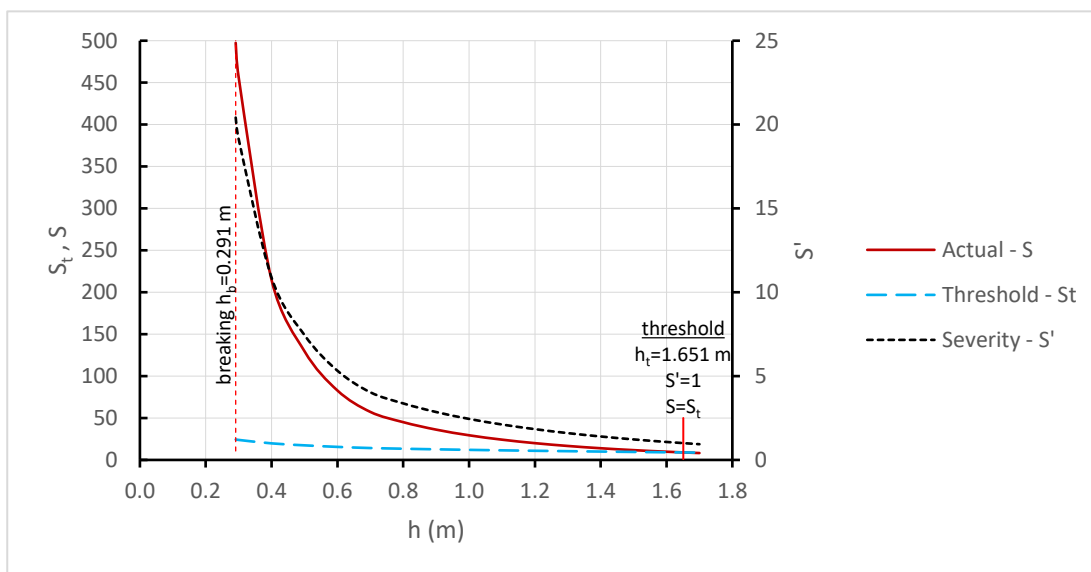


***Figure 8.3*** *– Normalised actual shear stress (S), normalised threshold shear stress ($S_t$) and the severity of entrainment ($S' = S/S_t$) for a wave of 0.2 m deep water wave height and 2 s period as it shoals through to breaking. The nominal sediment diameter D is 0.075 mm (very fine sand/coarse silt).*
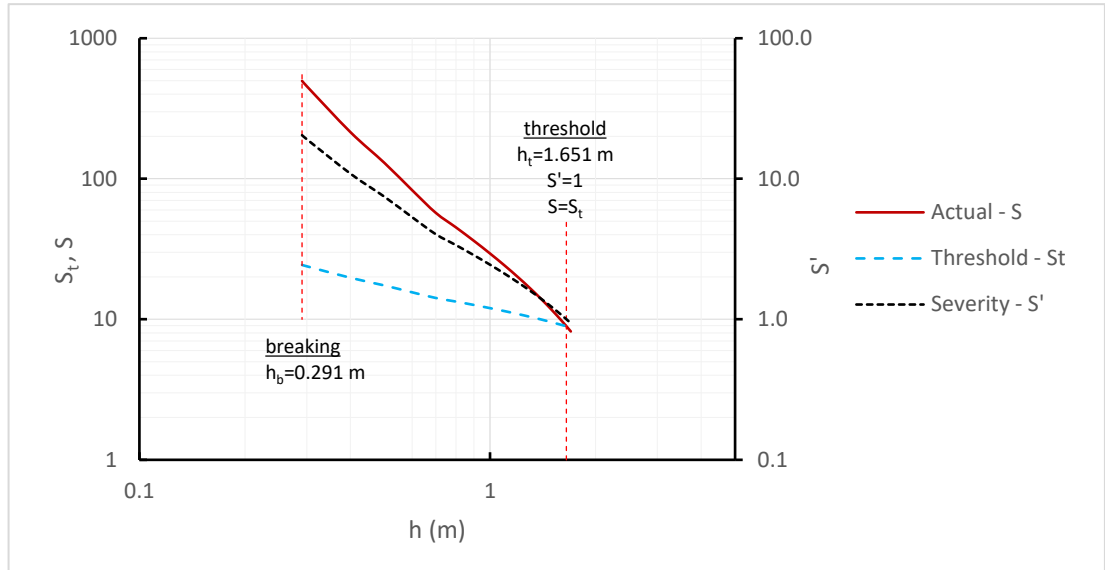
**Figure 8.4** – *Figure 8.3 as a log-log graph, showing near-straight line (power) relationships.*

From this point, the next fundamental question is whether the measure of severity of entrainment $S'$ should be a function of distance (from threshold to breaking), time or both distance and time as celerity. Although there are intimate relationships between these parameters, when applied to shoaling waves the change of some of these parameters in shallow water, wave celerity in particular, is somewhat complex to work with. For this reason, the measure of severity was arranged as a function of depth.

Depth and distance are also related by bottom slope, $m$. In this initial formulation it was assumed that bottom slope was not known, or not needed. If it is to be accounted for, severity is assumed to be a function of distance between the beginning and end depths $h_t$ and $h_b$, therefore a function of $1/m$. The only flaw in this assumption is that the breaker depth index is known to be a function of bottom slope and the breaker depth index has been taken at a constant value of *0.78*.

**Figure 8.5** shows schematically how the severity of sediment entrainment, $S'$, varies as depth changes from $h_t$ (threshold of sediment movement) to $h_b$ (breaking). The benefit of this approach of using $S'$ is that it automatically accounts for the different threshold stress at each water depth. **Figure 8.3** demonstrates that the threshold stress is a function of water depth (or more correctly as a function of parameters such as wavelength and wave height that are themselves functions of water depth). Defining severity as the quotient of actual and threshold stress (as functions of depth) simplifies the calculation and analysis.

Using **Figure 8.5**, two areas under the $S'$ curve are measured. The total area, $A_{total}$, is defined as the full area under the $S'$ curve from $h_t$ to $h_b$ and vertically from $S' = 0$ to $S'(h)$. The point $S' = 0$ should correspond (approximately) to $h = \lambda/2$, a depth beyond which the wave is not feeling the bottom. The nett area[100], $A_{nett}$, is defined as the area under the $S'$ curve from $h_t$ to $h_b$ and vertically from $S' = 1$ to $S'(h)$. In simplified terms:

$$A_{total} = \int_{h_b}^{h_t} S'dh \qquad\qquad [8.3a]$$

---

[100] The term "nett" rather than "net" is preferred. *Net* has a specific meaning in maritime terminology.

*and*

$$A_{nett} = \int_{h_b}^{h_t} (S' - 1)dh \qquad\qquad\qquad \text{[8.3b]}$$

*giving*

$$A_{nett} = A_{total} - (h_t - h_b) \qquad\qquad\qquad \text{[8.3c]}$$
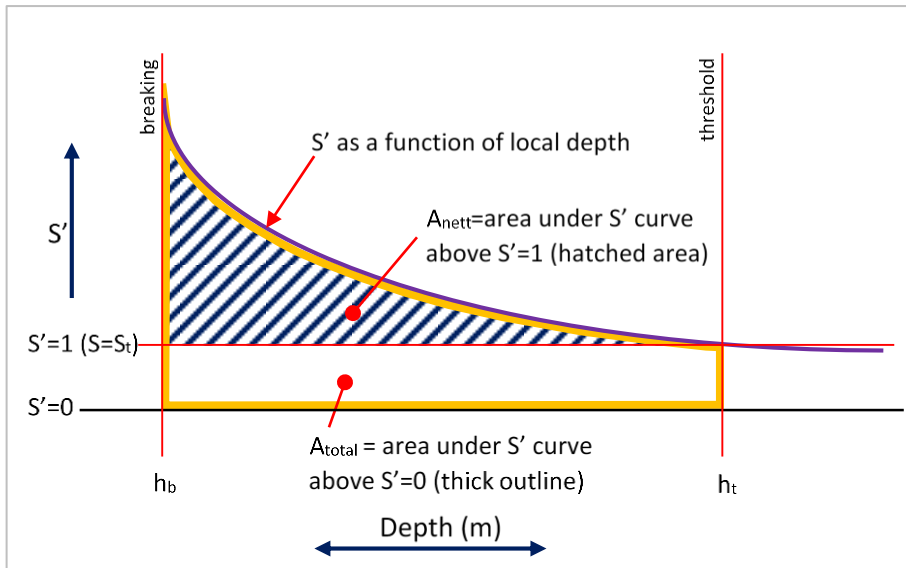


**Figure 8.5** – *Schematic for the calculation of total and nett areas under the $S' = f(S, S_t, h)$ curve from entrainment threshold depth ($h_t$) through to wave breaking depth ($h_b$).*

When calculating $S'$ by considering only depths ranging from $h_t$ to $h_b$ and therefore ignoring bottom slope, the horizontal distance between threshold and breaking becomes inconsequential to the calculation. However, it could be argued that a wave shoaling from threshold to breaking over different bottom slopes acts over different distances according to the slope, possibly meaning more turbidity if the slope was more gradual (and therefore the distance between threshold and breaking was greater). If the independent variable was taken as a horizontal distance instead of depth and $S'$ was therefore a function of that distance, the severity would vary according to $1/m$, with $m$ being the bottom slope. This could only be tested by developing an intrinsic relationship between sediment suspension rate and $S'$, which is not possible with the data available. That would also raise the question of whether an over-arching, simplified erosion prediction method would warrant, or benefit from, the inclusion of an increasing number of parameters such as bottom slope, given how variable bottom slope can be in both the longshore and cross-shore directions.

Some of the error in calculating $S'$ can arise from the way in which the wave parameters themselves are calculated. The method is iterative, requiring an estimate of wavelength at the selected depth and period (which remain constant) to calculate a wave height, which is then used to calculate a new wavelength, and so on. Convergence comes with just a few iterations, but for

certain waves – steep waves in shallow water in particular – there can be variance in wavelength without change to the wave height but with considerable change to the value of $S'$.

As an example, a wave with parameters $H_o = 0.2\ m$, $T = 1\ s$ and $h = 0.4\ m$ returned the following ranges of depth-corrected parameters using Stokes third-order theory: $H = 0.185\ m$; $\lambda = 1.571\ m$ to $1.649\ m$ (a *5%* variance); $S' = 2.561$ to $2.880$ (a *12.5%* variance). The variability has greatest influence on short-period waves in shallow water, explaining in part the minor inconsistencies encountered in calculating the quotient $S'$.

## 8.4    <u>Discussion Examples</u>

Two deep-water wave height conditions were examined for consistency and to extract relationships: $H_o = 0.1\ m$ and $H_o = 0.2\ m$ deep water wave heights, with periods ranging from $T = 1\ s$ to $T = 16\ s$. The *12 s* and *16 s* periods are unrealistic for sheltered waterway vessel waves, but they were included to assess trends and consistency at extreme values. The selected sediment diameter was *0.3 mm* - being mid-way between a fine silt and a coarse beach sand. The material was assumed to be quartz with a specific gravity of *2.65*. An additional condition with *0.075 mm* diameter sediment was considered, with similar results. Fresh water was assumed, remembering the density difference between fresh and salt water is almost inconsequential when compared to the assumptions of sediment density and its variability in real life. The assumption of fresh water allowed for correlation with past river trials.

### *Example 1 – $H_o = 0.1\ m$*

***Figure 8.6*** shows the relationship between normalised stress $S'$ and water depth for seven wave periods from *1 s* to *16 s*, from $S' = 1$ (threshold) to breaking (defined as $H_b/h = 0.78$). The curves are similar in form, showing the extremely non-linear development in $S'$ from threshold to breaking and the spreading of the horizontal extent of the curves with increasing wave period. Assuming a constant bottom slope, this increase in horizontal extent would be analogous to increasing lateral distance between threshold and breaking. This is further discussed in ***Example 2***.

***Figure 8.7*** is the log-log plot of ***Figure 8.6***. The curves do not quite exhibit a straight-line form, so do not have a constant power relationship (in terms of $y \propto x^n$). This is different to when linear wave theory is applied, as discussed later.

### *Example 2 - $H_o = 0.2\ m$*

***Figure 8.8*** is essentially similar to ***Figure 8.6*** ($H_o = 0.1\ m$) but with increased values. The $T = 1\ s$ curve demonstrates a peculiarity at breaking. There are two wave breaking criteria: *depth limited,* and *steepness limited*. The depth-limited criterion and its practical limitations have been discussed, but the accepted, standardised value for breaker depth index is *0.78*. The linearised wave steepness limit in shallow water from Miche (1944), described in the CEM (United States, 2006), is:

$$(H/\lambda)_b = 0.14\ tanh(2\pi h/\lambda)_b \qquad\qquad [8.4]$$

where the subscript *b* denotes breaking. This equation assumes that limiting wave steepness is a function only of depth, but it is known to also be a function of bottom slope. As with breaker depth index, the wave steepness limit can vary wildly in practice, which is why it is most common to find standardised values of *0.78* for breaker depth index and *0.142* for limiting wave steepness, regardless of the existence and influence of other parameters. Over the range of wave parameters used in this study, only one condition ($H_o = 0.2\,m, T = 1\,s$) invoked the steepness limit.

## 8.5    Variation of Excess Shear Stress with Height, Period and Depth

***Figure8. 9*** shows how the area under the $S'$ curve changes with period for the two deep-water wave heights investigated. Reference is made to ***Figure 8.5*** for definitions of the two area parameters: $A_{total}$ and $A_{nett}$. Also, the area under the $\{H_0 = 0.2\,m, T = 1\,s\}$ curve assumes depth-limited breaking to make it consistent with the other wave conditions, otherwise it would be truncated by the steepness limit. It must also be noted that if the steepness-limited breaking condition is applied to this particular wave, the area values at $H_o = 0.2\,m$ are similar to those at $H_o = 0.1\,m$ ($A_{total}$ increases by *17.7%* and $A_{nett}$ increases by *14%* when wave height is doubled) suggesting that, at the very short periods typical of sheltered water wind waves, the erosion is not being driven by height. In contrast, at longer wave periods where the steepness limit does not apply, doubling the wave height more than doubles the areas $A_{total}$ and $A_{nett}$ for a given wave period. For now, the depth-limited breaking condition for the ($H_0 = 0.2\,m, T = 1\,s$) wave is retained for consistency.

At short wave periods, $A_{total}$ and $A_{nett}$ grow quickly, but the growth rate tapers off at longer periods to the point where area becomes almost unaffected by period. In reality, though, this is at wave periods far longer than of interest, and the range of $T = 1\,s$ to $T = 6\,s$ is the one of any real consequence in sheltered waters. The area under the $S'$ curve has no immediate correlation to erosion rates and should only be used as an indication of relativity.

***Figure 8.10*** is of interest for assessing sensitive waterways, showing the range of depth from $h_t$ to $h_b$ as a function of $T$ for a shoaling wave with $H_0 = 0.2\,m$ and $D = 0.3\,mm$. At very short periods the depth range is small but increases quickly with period. Although the relationship tempers at longer periods, most sheltered waters vessel wake waves would fall within the range of $1\,s \le T \le 6\,s$ and wind waves with short fetch and modest wind speeds would have wave periods largely less than *1 s*. The reactivity of sheltered waterways to long-period waves is further demonstrated by this.

## 8.6    Rate of Growth of Excess Shear Stress from Threshold to Breaking

**Figure 8.11** has bearing on the selection of the wave breaking criterion. The rate of accumulation of $A_{nett}$, or area under the $S'$ curve as a percentage of the total (such as those in Figure 8.6) is shown. Almost *40%* of the accumulated shear stress comes in the last *10%* of propagation between the entrainment threshold depth and wave breaking. The breaker depth index, known to vary from around *0.55* to *0.83* (Fenton, 1999), would change the value of $A_{nett}$, which is the measure of erosion severity.
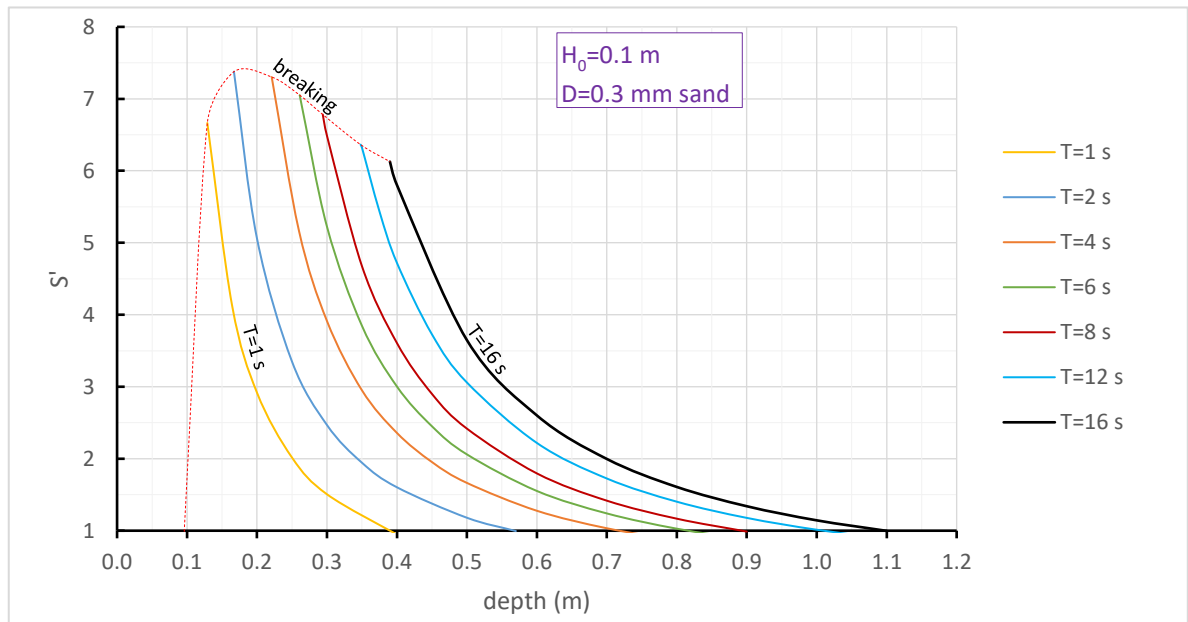
**Figure 8.6** – *Curves of severity of entrainment (S' = S/S_t) at 0.1 m deep water wave height over a range of wave periods. The lower limit (S' = 1) corresponds to the sediment movement threshold. All waves break due to depth, not steepness. A wave with a period less than 0.636 s would not entrain sediment before breaking. A wind wave meeting this threshold would arise from a 44 kn windspeed over a 32 m fetch, which is not practical. Wind waves under ambient, steady-state conditions (windspeed, say, 10 kn), would require a very long fetch (approaching 1 km) to exceed the sediment entrainment threshold.*
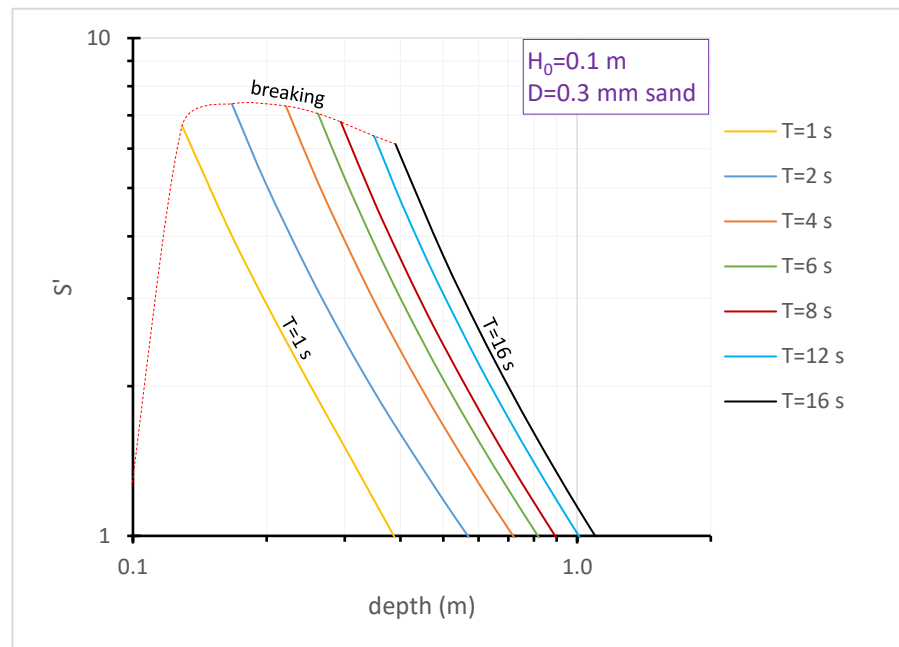


**Figure 8.7** – *Log-log plot of Figure 8. 6, showing that the curves do not have an exact power relationship.*
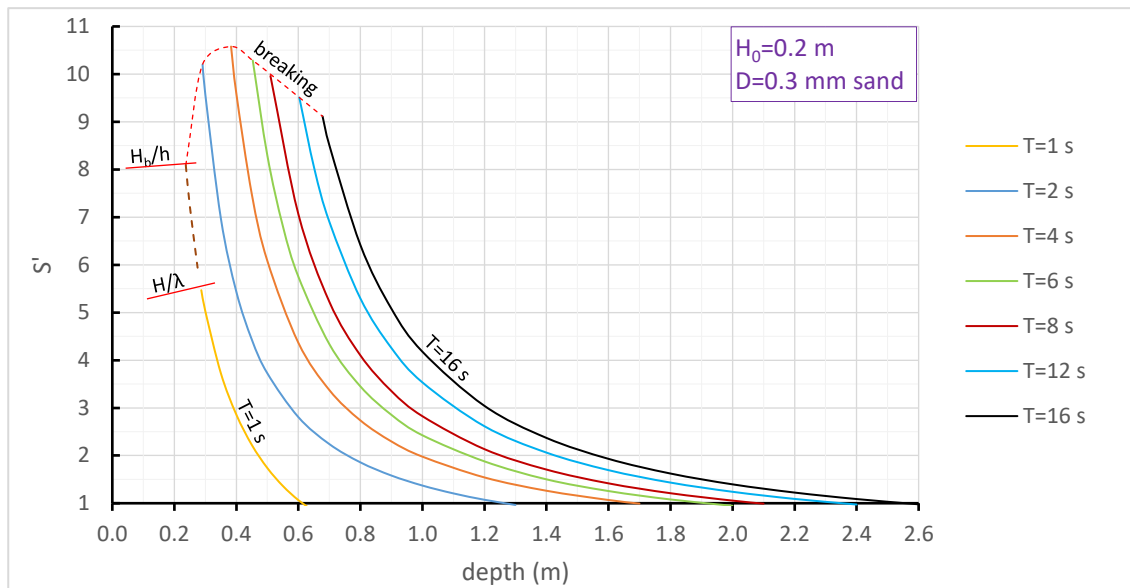
**Figure 8.8** – *Curves of severity of entrainment ($S' = S/S_t$) at 0.2 m deep-water wave height over a range of wave periods. Note the wave steepness ($H/\lambda$) breaking for waves with $T < 2$ s. Such steep waves would be rare in nature (steady windspeed around 50 kn over a 150 m fetch) but possible for small craft (short and heavy, near hull speed) to generate.*
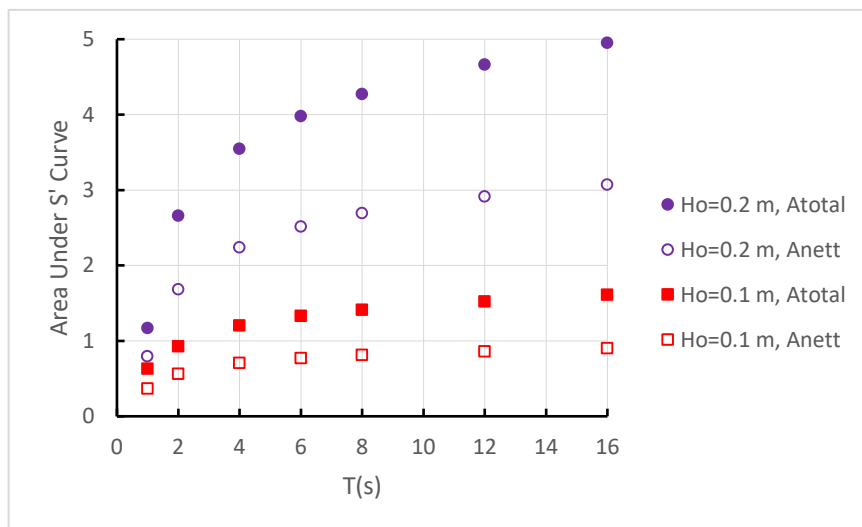


**Figure 8.9** – *Area under the $S'$ curves of Figures 8.6 and 8.8 – both the total area and nett area (refer Figure 8.5). The $H_o = 0.2$ m and $T = 1$ s data points assume breaking due to depth, not steepness. Note that the total and nett area curves are similar in form. Of importance is how small initial increases in period greatly accelerate the accumulated shear stress, with decreasing effect at very long periods (that are impractical anyway). The increase in deep-water wave height has a similar, but continually increasing, influence.*

The minor discrepancy at T=1 s is due to different breaking criteria. The dashed line is breaking at the wave steepness limit (breaking earlier); the solid line is breaking at breaker depth index limit ($H_b/h=0.78$). All longer period waves (T<2 s) conform to the breaker depth index limit.
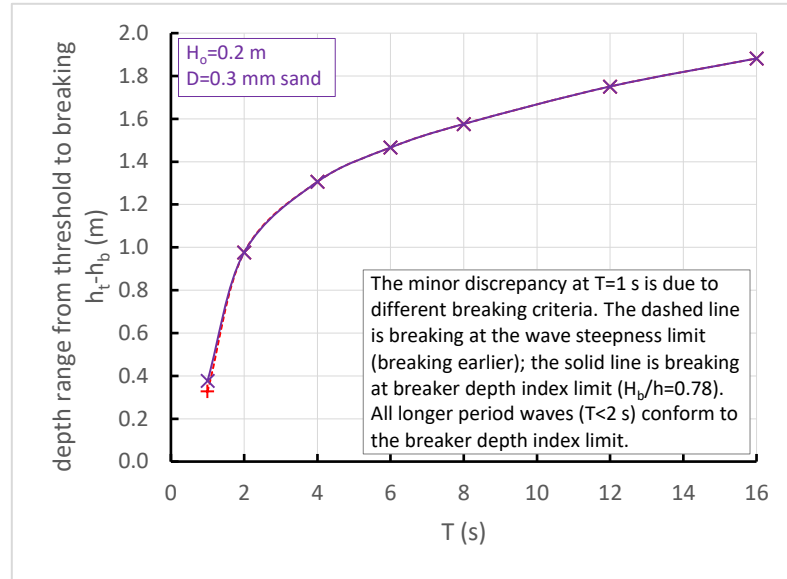
**Figure 8.10** – *Depth range $(h_t - h_b)$ over which sediment is entrained at 0.2m deep-water wave height and over a range of wave period. The correlation between the entrainment depth range and the area under the S' curve (Figure 8.9) is evident.*
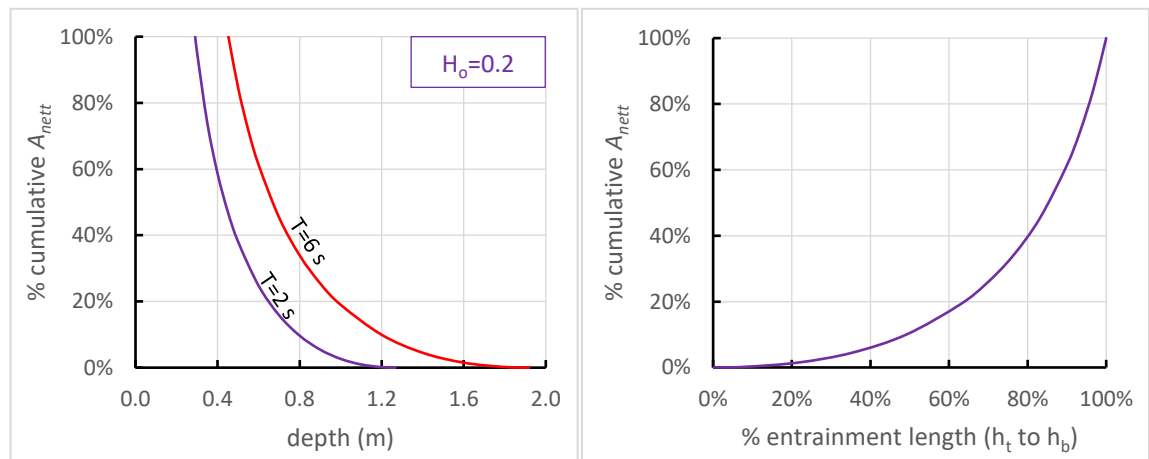


**Figure 8.11** – *Examples of the rate of accumulation of $A_{nett}$ (area under the S' curve) from threshold through to breaking $(D = 0.3\ mm$ sand). **Left**: examples of different periods for the same initial deep-water wave height. **Right**: entrainment length, taken from the threshold (0%) to breaking (100%), shown as a percentage. The right curve is identical for all values of period when the abscissae are expressed as percentages. It shown that the last 40% of the severity of erosion comes with the last 10% of entrainment. This is important when considering the breaking condition.*

## 8.7    Relationship Between $A_{nett}$ and Energy per unit Wave Height ($E/H$)

Energy per unit wave height ($E/H$) is taken as the default parameter for assessing waves because of its demonstrated correlation with the elevated turbidity measured at past field trials. $E/H$ takes the dimensional value of $J/m^2$, being *Joules per metre of wave height per metre of crest length*. Wave energy, taken per unit crest length, is effectively a force (*Nm/m*), meaning $E/H$ would be equivalent to a distributed load (*N/m*).

149

The area under the $S'$ curve has the linear units of *metres*, since $S'$ is dimensionless. Similarly, $S$ and $S_t$ (the left and right sides of the Komar-Miller sediment stress equation [8.1]) are also dimensionless through a separate normalisation process, even though they are regarded as *shear stresses*. If the severity of erosion was derived directly from the un-normalised $S$ and $S_t$, which it could but with increased computation (refer to *Figures 8.3* and *8.5*), the area under the $S'$ curve would have the units of "*stress-metres*", or *N/m*, which are the same units as $E/H$. This is an indication that the area under the $S'$ curve and $E/H$ may be related.

To test this hypothesis, the quotient of $A_{nett}$ and $E_o/H_o$ (the deep water variant of $E/H$) was plotted against $T$, as shown in **Figure 8.12** (for $H_o = 0.1\ m$) and **Figure 8.13** (for $H_o = 0.2\ m$), for $D = 0.3\ mm$ sand. Somewhat surprisingly, the relationship is almost perfectly linear in log scale and the equation exponent is essentially the same for both vales of $H_o$, with only the constant changing. There is a discrepancy for the $(H_o = 0.2\ m, T = 1\ s)$ condition, which falls short the expected value, but this may be explained by the limiting wave steepness rather than breaker depth index truncating the accumulated shear stress early. Also, non-linear wave theories are unable to accurately predict the shoaling of such small, steep waves in very shallow water.[101] Provided the waves are realistic, the relationship between $A_{nett}$ and $E_o/H_o$ is robust.

The surprisingly close relationship between $A_{nett}$, $E_0/H_0$ and $T$ is due to the intimate relationship between $A_{nett}$ and $T$, since $E_o/H_o \propto T^2$. There is no reasonable explanation of why the area under the $S'$ curve should be so closely related to wave period, particularly given the different wave theories used to derive the results. The variability of certain parameters such as shoaling wave height, which can increase up to $3H_o$ before breaking at $T = 16\ s$ yet reduce to around $0.9H_o$ at $T = 1\ s$, against the robustness of the results for short to very long wave periods, gives comfort that there is a consistent relationship.

The importance of this relationship is in the simplified application of this to operational guidelines for vessels. The calculation of $S'$ as a measure of erosion severity is tedious, but calculation of energy per unit wave height is simple. Even if linear wave theory is used to calculate energy per unit wave height where the waves were measured in water less than truly deep, the error may not be enough to disqualify the method as an indicator of erosion potential.

---

[101] A wave with parameters $H_o = 0.2\ m$ and $T = 1\ s$ would even fall outside our assumed sheltered waterway hindcast wind wave climate, requiring unrealistic conditions in the order of *25 m/s* wind speed and *150 m* fetch to generate it.
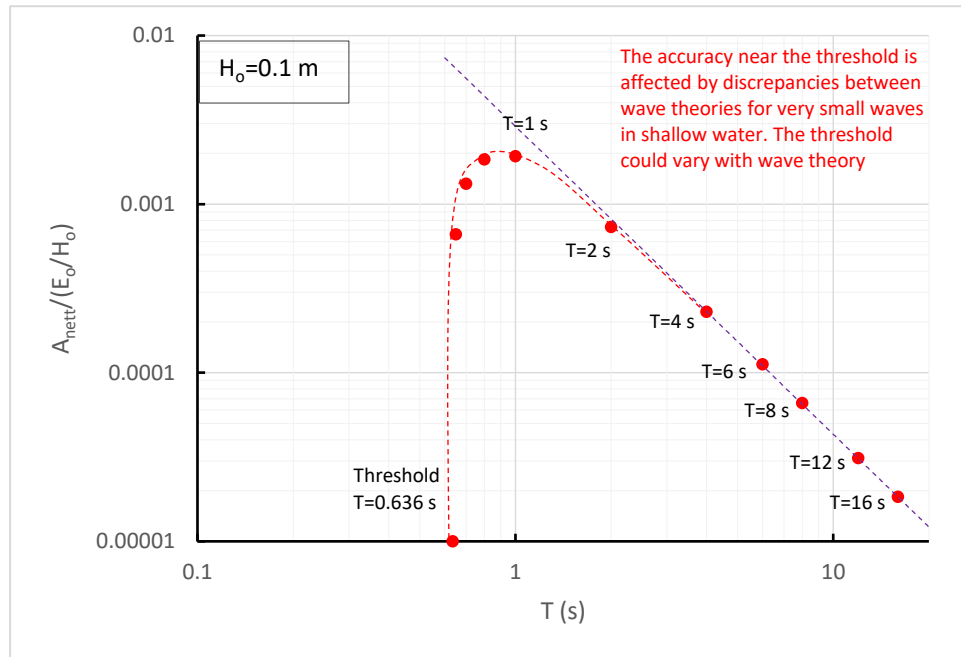
**Figure 8.12** – $A_{nett}/(E_o/H_o)$ as a function of period, for $H_o = 0.1\ m$ ($D = 0.3\ mm$ sand). The threshold condition, where the wave breaks before entraining sediment, is $T = 0.636\ s$ at $H_b = 0.096\ m$. This ignores the dynamics within the broken wave, which are complex at best. The relationship is remarkably robust at $T \geq 2\ s$.
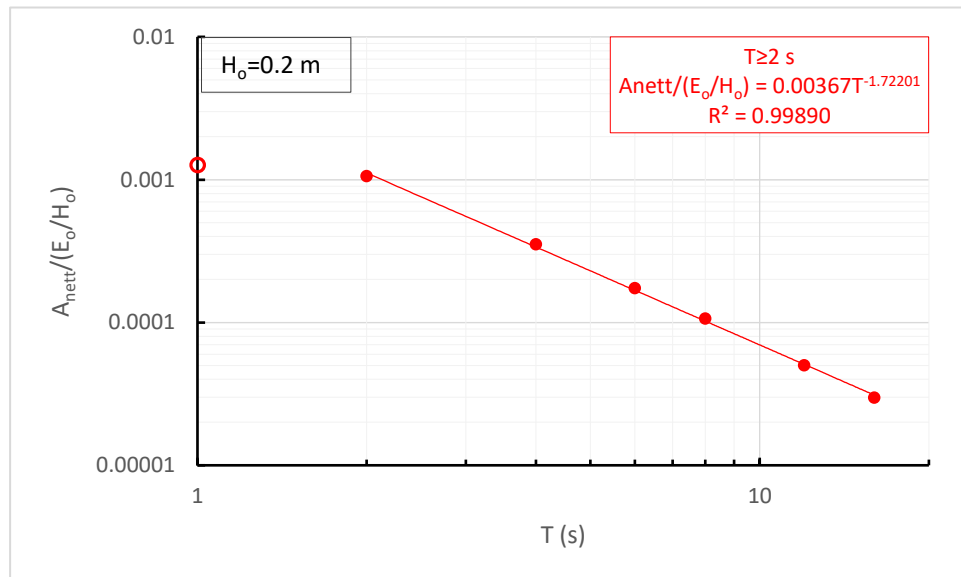


**Figure 8.13** – $A_{nett}/(E_o/H_o)$ as a function of period, for $H_o = 0.2\ m$ ($D = 0.3mm$ sand). The data set $T \geq 2\ s$ (solid markers) isolates the discrepancy at $T = 1\ s$ (circle marker).

## 8.8    Severity of Erosion – Comparative Measure

### 8.8.1    Introduction

A comparative measure of the erosive nature of waves is necessary in order to compare the relative impact of waves from different vessels and under different operating conditions. Such a measure would be considered as a composite parameter, being made up of some of the principal wave wake parameters that can be defined for every vessel.

Such a comparative measure must be relatively generic in its derivation without its robustness being compromised by simplicity. If the measure was overly specific to particular vessel features such as L/B or B/T ratios, or to shoreline characteristics, it would become pointless in an over-arching approach. In developing the comparative measure based on severity of erosion, only the simple wave wake parameters of maximum wave height and corresponding wave period are used to describe the vessel wake; both these parameters being easily related to simplified vessel parameters such as length, displacement, speed and distance off. Deep water parameters are assumed, which may require shallow water wave height (and indirectly wavelength) to be depth corrected. At the shoreline, basic parameters of sediment size (fine, medium-fine and medium) and bottom (beach) slope are required. The effects of vegetation and consolidation are not accounted for – even if present, they are unlikely to be present everywhere and the worst case of unconsolidated sediments must always be considered.

The problem also becomes one of relating erosion to vessel wake waves and not just waves in general. ***Figure 8.14*** shows schematically how a vessel's wake may be linked to erosion. With these parameters, the method could be applied by any sufficiently trained person to gauge relative erosivity. An approach more detailed would require site-specific and vessel-specific testing and monitoring by qualified staff, which is beyond the intent of this study. Appendix J addresses correlation between shear stress parameters and sediment entrainment, with interesting and consistent results.
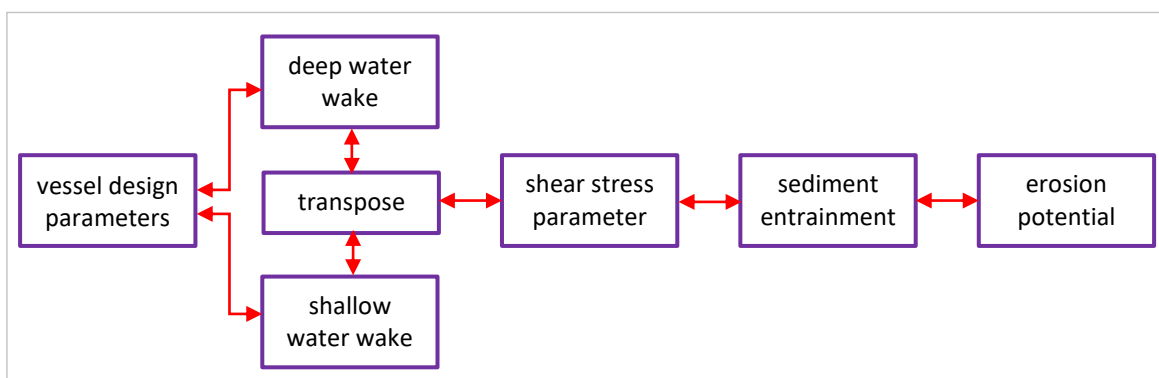


**Figure 8.14** – *Schematic of the development and inter-relation between elements linking vessels to the wake created and the measure of their erosive potential. The process must be reversible if operational restrictions and design variations are to be assessed for new and existing routes*.

### 8.8.2    Threshold conditions – no entrainment before breaking

For every value of deep-water wave height $H_o$, there is a corresponding value for the wave period that would cause a wave to break due to excessive wave steepness before it begins to entrain sediment. Once broken, it is assumed that the wave would continue to propagate as a bore and not re-form into a wave of reduced height. A re-forming wave would be possible under certain conditions but would require very short-period waves such that the deep-water Iribarren number $\xi_o$ was much less than *0.5* (signifying a spilling condition). The Shore Protection Manual (Coastal

Engineering Research Center (U.S.), 1984, p.4-49) notes that spilling waves (such as sheltered waters wind waves) are less effective at transporting sediment. Spilling waves should be considered as difficult to replicate with vessel wake waves in the medium to far field, though they are usually present close to the sailing line where the divergent wave packets have insufficient distance to disperse and the waves are steep. *Figure 8.15* shows this clearly, though for waves spilling due to steepness before sufficient dispersion has occurred rather than due to shallow water.



Crests breaking on the first few divergent waves where steepness is high

**Figure 8.15** – *Vessel travelling at $Fr_L \sim 1.0$ in deep water ($h \geq L$). The first divergent waves are steep, and their crests break periodically close to the sailing line. Breaking can also occur due to near-field interactions between bow and stern divergent packets. The near-field wake turbulence is caused by the water jet efflux.*

As an example, and referring to *Figure 8.12*, the threshold period for $H_o = 0.1\ m$ is $T_t = 0.636\ s$. As the maximum wave in a vessel wake, such a wave could only be generated from a very short vessel at slow speeds close to the shore, which is unlikely to have any measurable environmental impact. Similarly, a hindcast wind wave with these parameters would come from a *15 m/s* wind speed and a *50 m* fetch, which would be considered a rare condition. Varying the sediment size varies the depth at which entrainment is initiated. *Figure 8.16* shows how the steepness threshold period changes with deep-water wave height. The slope of the curve exhibits the correct relationship for wave steepness ($T \propto H^{½}$). These steepness thresholds are therefore of little more than academic interest for wake waves, which are almost always longer for a given height.
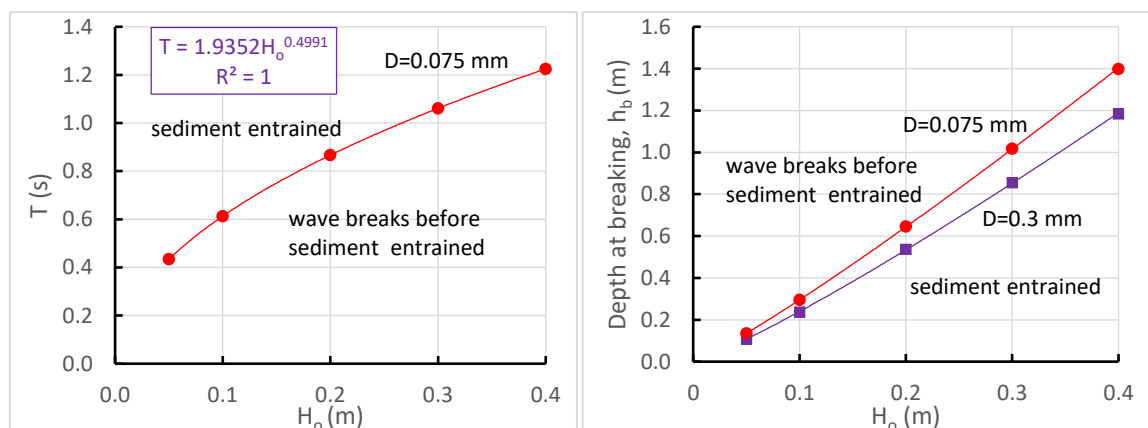


**Figure 8.16** – *Left: Threshold (entrainment and breaking) values of wave period against deep water wave height based on maximum wave steepness and threshold of sediment entrainment. Right: Changing sediment diameter changes the threshold entrainment depth. A wave with period below the curve on the left and at a depth above the curves on the right would break before exceeding the bed shear stress threshold.*

### 8.8.3   Use of $A_{nett}$ as a comparative measure of the potential for erosion

$A_{nett}$, being the cumulative total of the excess shear stress beneath a wave from the threshold of sediment movement through to wave breaking, is an attempt to quantify the energy being transferred from the wave to the bed sediment by shear stress. The analysis of the Gordon River turbidity experiments (Appendix K) has qualified the relationship between the excess shear stress and elevated turbidity at one measurement depth, and the postulation that the relationship is valid wherever there is excess shear stress gives the basis for the validity of $A_{nett}$. These, combined with the observation of Ozeren *et al.* (2016) of a linear relationship between turbidity level and suspended sediment concentration, form the basis of $A_{nett}$ as a comparative measure between waves and for different sediments. The method for calculating $A_{nett}$ allows for bathymetry to be readily accounted for.

Its relationship to deep water wave height has been quantified for a range of deep-water wave heights from $0.05\ m \le H_o \le 0.8\ m$ and for wave periods from $1\ s \le T \le 16\ s$. In addition, three sediment sizes were used: $D = 0.075\ mm, 0.15\ mm$ and $0.3\ mm$. These represent a typical sediment range from very fine sand (*0.075 mm*) through to a medium sand (*0.3 mm*). Mud is considered equivalent to very fine sand and is assumed to be unconsolidated, without cohesiveness or clay content.

***Figure 8.17*** shows graphically how $A_{nett}$ varies with $H_o$ and *T*. To clarify it further, ***Figure 8.18*** shows how it varies with wave period for two wave heights. Both graphs are for a sediment diameter of $D = 0.3\ mm$.
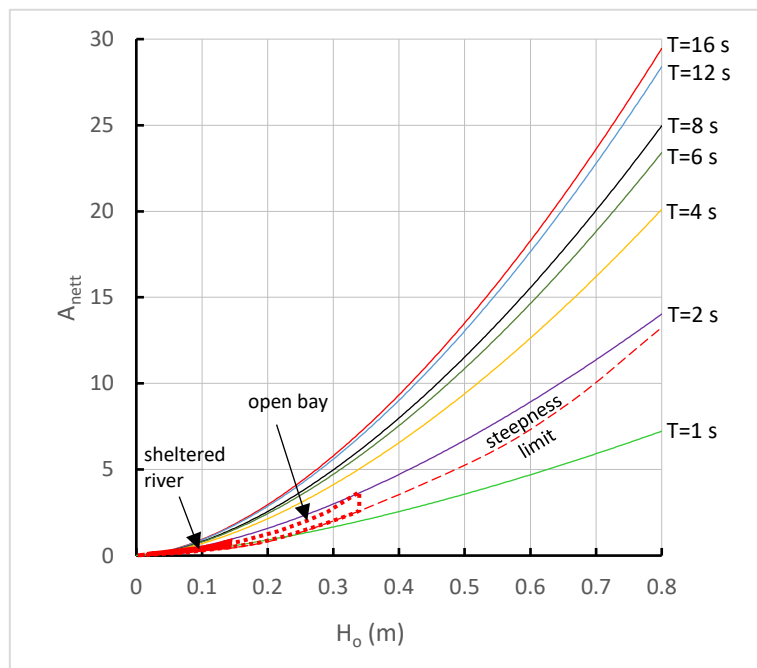


**Figure 8.17** – *Variation in the accumulated excess shear stress ($A_{nett}$) with deep-water wave height ($H_o$) and wave period (T) for $D = 0.3\ mm$. The curve for $T = 1\ s$ is shown for clarity but would otherwise be truncated at a low wave height by the steepness limit. Very long wave periods were included in the analysis to validate the consistency of the trend well beyond anticipated wave periods. The nominal wind wave values for sheltered rivers (up to 500 m fetch and wind speeds to 5 m/s), and open bays (up to 3,000 m fetch and 10 m/s wind speed), are delineated by the solid and dashed red wedges respectively.*

For discussion, three example hindcast wind wave scenarios are noted in **Table 8.2**.

**Table 8.2** – *Example hindcast wind waves ($H_{max}$, $T_{max}$).*

|  | fetch (m) | wind speed 5 m/s | wind speed 10 m/s |
|---|---|---|---|
| very sheltered river | 100 | 0.026 m, 0.50 s | 0.062 m, 0.66 s |
| sheltered bay | 500 | 0.059 m, 0.84 s | 0.138 m, 1.13 s |
| open bay | 3,000 | 0.142 m, 1.48 s | 0.336 m, 2.03 s |

***Discussion: Figure 8.17*** – The threshold steepness limit would truncate the short period wave curves, but the curve for $T = 1\,s$ is shown in full for clarity. $A_{nett}$ increases non-linearly with increasing wave height and wave period, though the relationship to wave period has a growth exponent less than unity. When viewed in respect of sheltered waterways, the existing wind wave climate impact (shown as red wedges) is minor, even after accounting for the exaggerated wave height (to *0.8 m*) and period values (to *16 s*).

***Discussion: Figure 8.18*** – This gives a better explanation of the growth in erosion potential for small waves. For both wave heights shown (*0.1 m, 0.2 m*), but more visible with the *0.2 m* height, the initial growth in $A_{nett}$ with increasing period is rapid, followed by decreasing rates as period increases further.
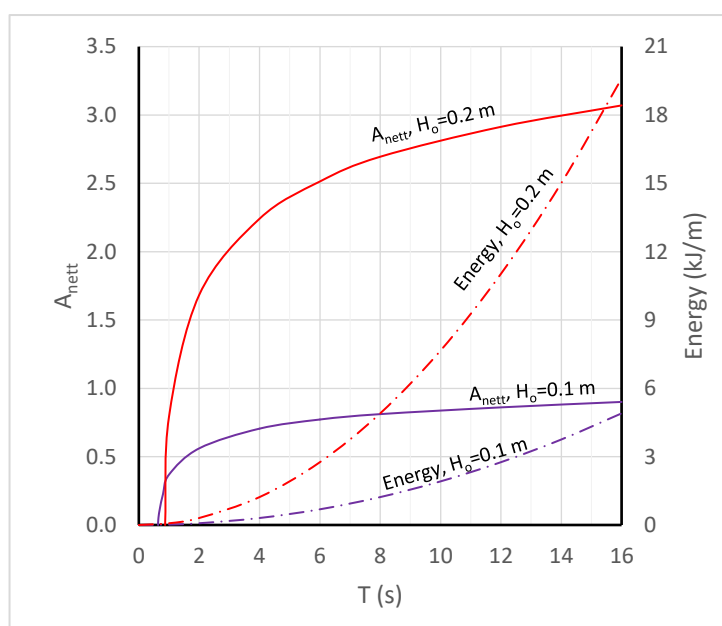


**Figure 8.18** – *$A_{nett}$ against wave period from two different deep-water wave heights of 0.1 m and 0.2 m for $D = 0.3\,mm$ sand. The corresponding deep-water wave energy is also shown. The threshold period increases with increasing deep-water wave height due to wave breaking. That ignores the turbulent effect of the broken wave itself.*

Also shown in **Figure 8.18** is the deep-water wave energy which, for a fixed value of deep-water wave height, increases quadratically. The relationship between $A_{nett}$ and $T$, and $E_o$ and $T$, would appear to contradict the Gordon River analysis (*Appendix K*), which demonstrated that excess shear stress ($S'$) had a strong linear relationship to $E_o$ at a particular depth (*Figure 8.19*). If $A_{nett}$ is the summation of excess shear stress from threshold of sediment entrainment to breaking, it too

155

should exhibit the same linear relationship with $E_o$; i.e., if $E_o$ is increasing quadratically with wave period, so should $A_{nett}$.

This isn't a contradiction, just a sleight of hand. The energy scale of **Figure 8.19** extends from *0-800 J/m*; the scale of **Figure 8.18** extends from *0-21,000 J/m,* courtesy of the extreme range of wave periods*.* The Gordon River paired wave parameters of height and period land at the very left-hand side of **Figure 8.18**, where there is a stronger correlation with the growth of energy. The right-hand side of **Figure 8.18**, where the $A_{nett}$ curve is flatter to the point of increasing at a slowing rate with increasing energy, is untested by field data. That does not invalidate the assumed relationships, since sheltered waters vessels are unlikely to be capable of producing maximum waves with periods longer than about *8 s* in the extreme, or *5 to 6 s* in most recorded instances.

There may be a desire to use **Figure 8.18** as justification for increasing allowable wave period, provided wave height is low. This is the inherited argument of those seeking to reduce wave height alone through design, which in turn can result in an increase in wave period.[102] Increasing wave height certainly increases $A_{nett}$ at a faster relative rate (*>linear*) and it is true that increasing wave period from, say, *6 s to 12 s* at $H_o = 0.2\ m$ increases $A_{nett}$ by just *16%* against a four-fold increase in energy, but it ignores the fact that the damage has already been done. The greatest reduction in overall sediment entrainment comes with a substantial, and probably impossible, reduction of wave period rather than just a reduction in wave height. This is what is mirrored in the environment by wind waves – small changes bring environmental change, but changes to wave period are the immediate determinant of the accelerated entrainment after threshold exceedance. **Figure 8.19** shows a practical example of this, though of a sub-trans-critical wake rather than a pure divergent system. The extent of the turbid water does not change with successive waves and the immediacy of the turbidity correlates with the thresholds and turbidity growth of **Figure 8.18**.

---

[102] Inherited, since design efforts to reduce wave height achieved their aim without consideration of wave period at all but came as a consequence of the method used - being an increase in slenderness ratio that partially shifted wave energy from height to period.
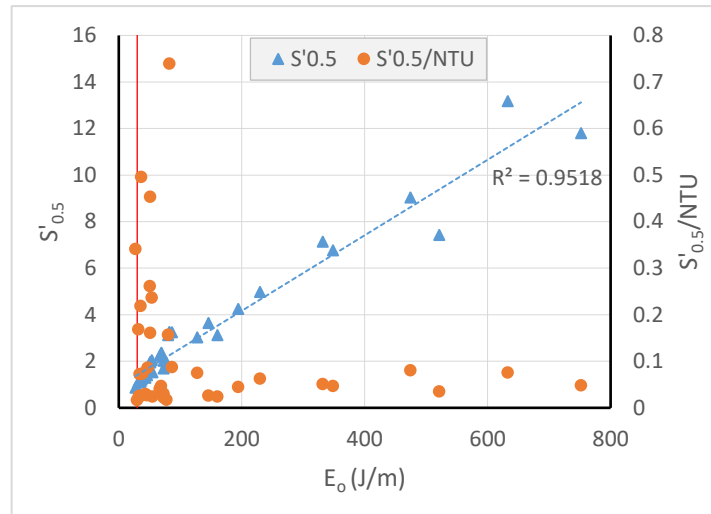
**Figure 8.19** – *Variation in excess bed shear stress S' at $h = 0.5\ m$ with deep-water wave energy from the Gordon River trials (Appendix K) (triangle markers, left axis). The strong linear relationship is evident. Also shown is the excess bed shear stress divided by the recorded elevated turbidity in NTU (round markers, right axis). With initial sediment entrainment, $S'_{0.5}$/NTU has high values (due to small turbidity relative to shear stress), but eventually falls to approximately constant values. Note the energy scale (0-800 J/m). The nominal Gordon River threshold energy of 30 J/m is shown.*
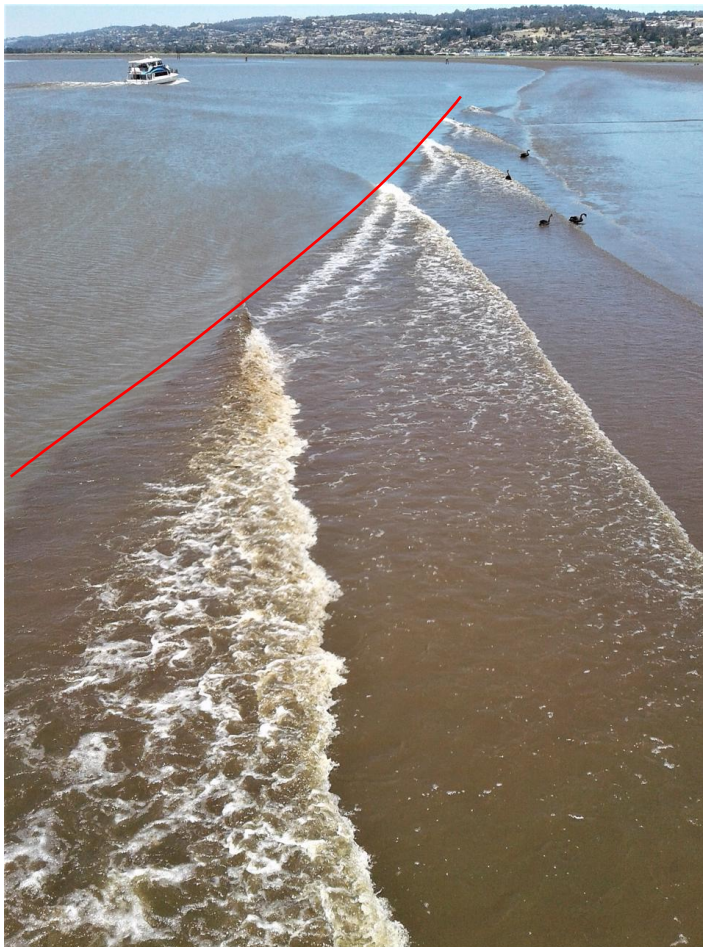


**Figure 8.20** – *Turbidity caused by a passing vessel. The vessel is operating in a sub-trans-critical condition, signified by the crest angle approaching 90 degrees to the sailing line and the lack of a defined divergent system.*

*The waves in this instance, being strongly a function of the transverse system, appear more monochromatic than would a divergent system. They are also undergoing considerable refraction. The bank slope steepens quickly beyond the broken waves such that shoaling is only visible just before breaking.*

*Note how the turbid region barely grows with successive waves, if at all, and it is closely related to wave breaking. This would concur with Figure 8.18, where substantial turbidity is initiated once the threshold period is exceeded.*

157

## 8.9　　Relationship to Energy per unit Wave Height and Energy

Energy per unit wave height was found to closely mirror the actual elevated turbidity thresholds of the 2004 Gordon River trials (*Appendix K*). Energy did also, but to a lesser extent. In both cases the energy used was the deep-water wave energy, being easy to calculate (or at least calculate for waves transposed between shallow and deep water). Provided shoaling is not substantial, as was demonstrated for the short-period waves in the Gordon River tests, deep-water wave theory gives a quick and sufficiently accurate answer and so is suitable for small craft evaluation. It doesn't work well, however, for longer waves from larger craft.

For the relationships presented here, where $A_{nett}$ is related to wave period, it is inconsequential if $A_{nett}$ is correlated with $E_o/H_o$ or $E_o$, since the correlation is done for fixed values of deep-water wave height and hence the difference between $E_o/H_o$ and $E_o$ is only the value of the constant (equal to $H_o$). Energy per unit wave height in deep water is maintained as the preferred measure due to its relevance to other erosion mechanisms, notably wave run-up.

## 8.10　　Proposed Comparative Measure

### 8.10.1　Development
*Figure 8.12* represents an example of how $A_{nett}/(E_o/H_o)$ varies with wave period for a fixed value of deep-water wave height. As noted, the variation with $E_o$ in the denominator is the same, with a shift in the value of the constant (since $H_o$ is a constant). As discussed, there is a very robust, straight line response (in log-log format) that proves to be quite consistent for other values of $H_o$. At a particular value of wave period, the relationship falls away; this representing graphically the rapid initial growth of turbidity once a threshold of excess shear stress has been achieved.

The straight-line response is in the form:

$$\frac{A_{nett}}{(E_0/H_0)} = CT^{-n}$$

[8.5]

where the parameter $C$ is a function of wave height and sediment diameter (sediment is always assumed to be unconsolidated sand).

The exponent, $n$, corresponding to the steady-state segment of *Figure 8.12* (log-log) and *Figure 8.21* (linear)**,** was calculated for each value of deep-water wave height. This exponent is shown in *Figure 8.22*. At higher values of wave height, the exponent settled at a constant value of about *1.705*. There does appear to be some minor inconsistency in this, though the actual variation is only in the order of *±0.75%* (keeping the vertical scale of Figure 8.22 in mind). It was possible to vary the exponent value by increasing the number of points in the numerical integration of $S'$ from initial sediment entrainment to breaking and changing the integration methods used (Simpson's one-third rule, Simpson's three-eighths rule and trapezoidal rule). Most importantly, the relative consistency was maintained at very long wave periods.

The relationship between $S'$ and $D$ for a given wave height is such that $S' \propto \sqrt{D}$, which was used to greatly reduce computation time for $A_{nett}$. When varying sediment diameter, $S'$ varies according to this relationship and the depth of wave breaking is the same; all that changes is the threshold depth of entrainment, which becomes deeper for the smaller sediments.

158

The values of the parameter *C* are shown in **Figure 8.23**. The most interesting feature of this is the consistency of the trend with increasing wave height and lack of the inflexion experienced by exponent *n* in **Figure 8.22**.
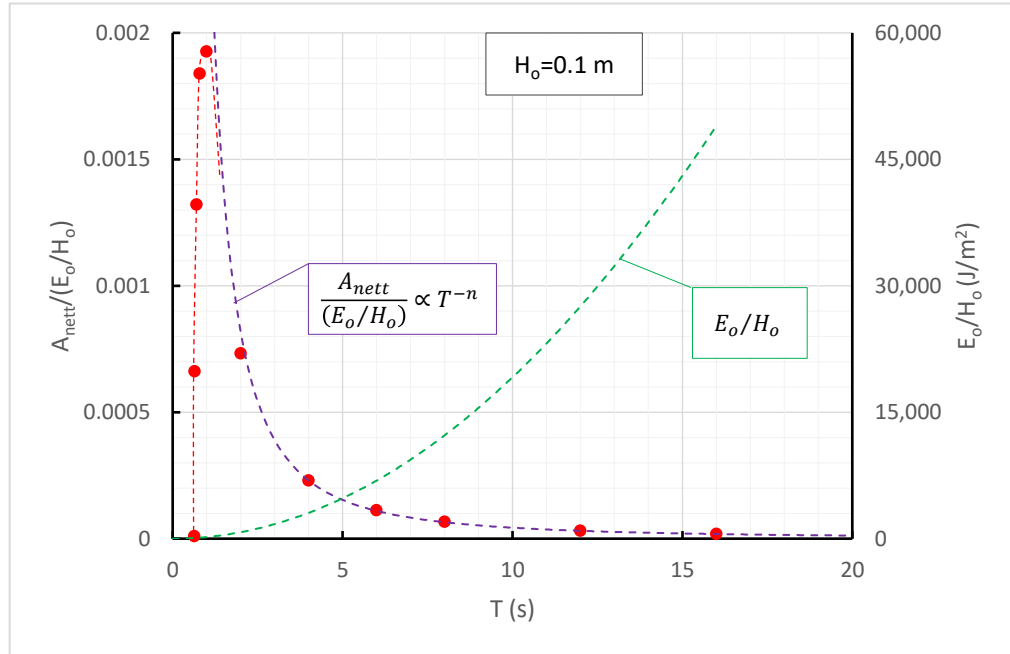


**Figure 8.21** – *Linear plot of Figure 8.12. Of note is the rapid initial growth in excess shear stress once the bed shear stress threshold is exceeded, with only a fractional increase in accompanying energy per unit wave height and therefore energy, since $H_o$ is constant. $A_{nett}/(E_o/H_o)$ peaks at $T \approx \pi\sqrt{H_o}$ and the beginning of departure between initial values of $A_{nett}/(E_o/H_o)$ and the proportionality to $T^{-n}$ occurs at $T \approx 2\pi\sqrt{H_o}$, or when $H_o/\lambda_o < 0.016$. This is consistent for all wave heights.*

Values of the parameter *C* and exponent *n* in [8.5] are shown in **Table 8.3**. It would be possible to derive relationships for parameter *C* and exponent *n* for any value of sediment diameter *D* and wave height, but for a generalised approach this is considered unnecessary. It is suggested that three values of sediment size would give sufficient coverage of probable values in sheltered waterways. Moreover, it is unlikely that anyone using this as a comparative measure as part of a regulatory assessment would measure sediment diameter.
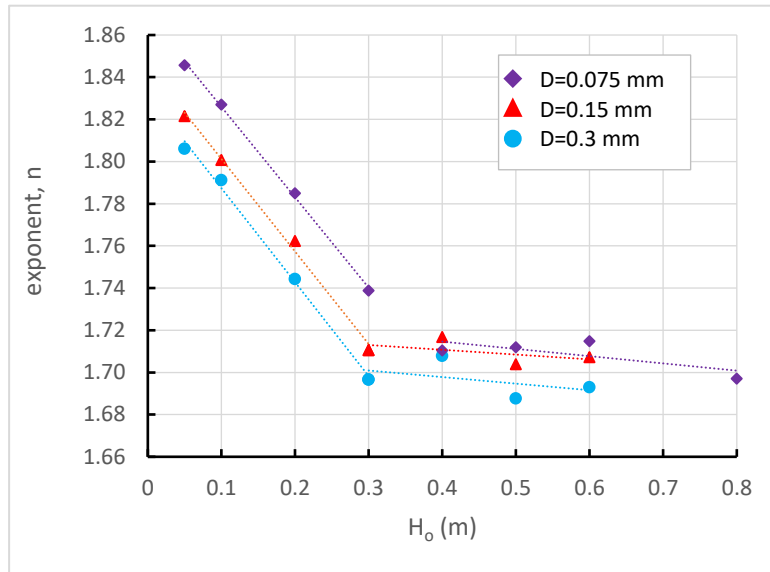
**Figure 8.22** – *Variation in the value of the exponent n with deep water wave height for three values of sediment diameter. Note the scale of the vertical axis, which could exaggerate the perception of goodness of fit.*
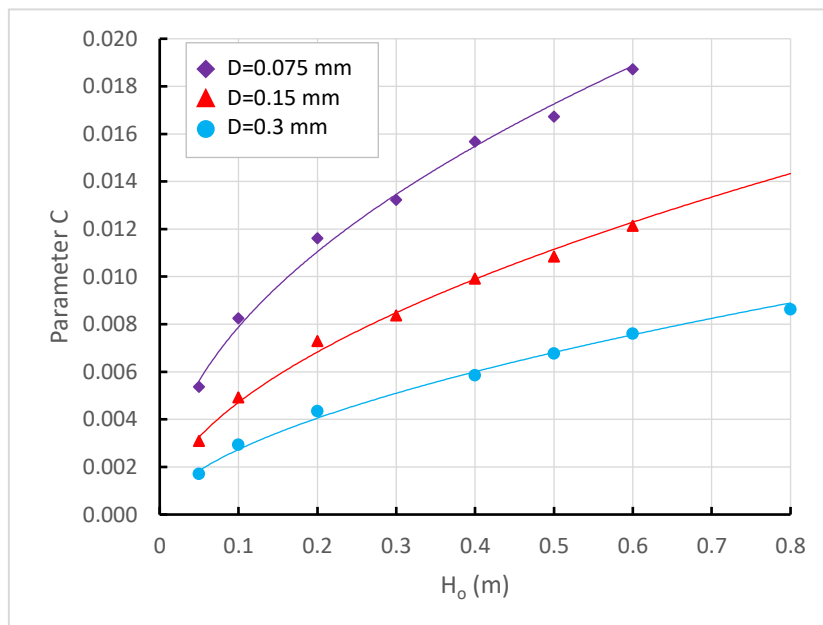


**Figure 8.23** – *Variation in the value of the parameter C with deep water wave height for three values of sediment diameter.*

**Table 8.3** – *Coefficients used to calculate $A_{nett}$.*

| D (mm) | C | n | | | |
|--------|---|---|---|---|---|
| 0.075 | $0.0242H_o^{0.487}$ | $0 < H_o \leq 0.285$ | $n = 1.832 - 0.446H_o$ | $H_o > 0.285$ | $n = 1.705$ |
| 0.15 | $0.0161H_o^{0.534}$ | $0 < H_o \leq 0.320$ | $n = 1.845 - 0.439H_o$ | $H_o > 0.320$ | $n = 1.705$ |
| 0.3 | $0.0101H_o^{0.567}$ | $0 < H_o \leq 0.382$ | $n = 1.869 - 0.429H_o$ | $H_o > 0.382$ | $n = 1.705$ |

### 8.10.2 Accounting for the effect of bottom slope

Previously, bottom slope was removed from the calculation by integrating the excess shear stress on a depth scale from threshold depth of sediment movement (assumed to be the threshold of entrainment) through to depth of wave breaking. It is a simple task to re-introduce bottom slope to the final equation and convert the integration of excess shear stress from a depth-based summation to one based on shoaling distance. In that case, [8.5] can be re-written as:

$$\frac{A_{nett}}{(E_0/H_0)} = \frac{1}{m} CT^{-n}$$

[8.6]

or fully expanded:

$$A_{nett} = \frac{\rho g^2 C}{16\pi m} H_o T^{(2-n)}$$

[8.7]

where *m* is the bottom slope, expressed as a fraction. In these relationships, there is no allowance for bottom friction, which only becomes significant over long distances. King (1972) calculates the loss in wave height due to bottom friction for a *6 s* period wave over a *1:10* bottom slope as less than *1%*. Also, $A_{nett}$ does not attempt to make allowance for the effects of the wave bore after breaking, which is widely regarded as a substantial source of nearshore turbidity but extremely complex to quantify.

This also correlates with how shorelines react to natural changes in the incident wave climate. Both beach slope and grain size are indicators of incident wave energy (Coastal Engineering Research Center, 1984). Increased slopes indicate larger grain size and lower wave energy. Shallow slopes indicate greater wave energy. This corresponds with [8.7], since a decrease in bottom slope *m* would increase $A_{nett}$. As a comparison, $A_{nett}$ has been calculated for the extreme condition (20 knot) wind waves in **Table 8.3**, for two different bottom slope/sediment diameter combinations. This is shown in **Table 8.4**. If $A_{nett}$ is the comparative measure of the severity of erosion, increased slope would mitigate an increase in wave energy and/or wave height and period.

**Table 8.4** – *Example Calculation of $A_{nett}$ using [8.7].*

| $H_o$ (m) | T (s) | $E_o$ (J/m) | $A_{nett}$ | |
|---|---|---|---|---|
| | | | D=0.3 mm, m=1/4 | D=0.075 mm, m=1/20 |
| 0.097 | 0.90 | 14.6 | 1.96 | 28.21 |
| 0.138 | 1.13 | 46.5 | 3.55 | 50.12 |
| 0.336 | 2.03 | 890.5 | 17.01 | 225.07 |

Interestingly, for a given slope and sediment diameter, the values of $A_{nett}$ vary proportionally to about $\sqrt{E_o}$. The Shore Protection Manual (Coastal Engineering Research Center, 1984), referring to the work of King (1972) makes the comment:

> "Analysis by King (1972, p. 330) suggests that slope depends dominantly on sand size and also significantly on an unspecified measure of wave energy."

King (1972) does appear to specify a correlative measure between beach slope (King uses the term $Z$ for beach slope, not $m$) and incident wave energy, such that $m = (\text{const.} -\log E)$, though the relationship is somewhat extrinsic but holds if the grain size is held constant. If, in the examples of **Table 8.4**, $E_o$ and $D$ are held constant and slope is varied to give the same value of $A_{nett}$, the subsequent relationship between $E_o$ and beach slope follows a power law ( $m \propto \sqrt{E_o}$ , approximately). The power law relationship is a close fit ($R^2 \approx 1$ for an exponent of *0.527*, indicating an intrinsic relationship), but the log relationship suggested by King is also not unreasonable ($R^2 = 0.937$), considering King's log-law relationship was based on field observations.[103]

King (1972) also makes the comment that:

> *"The minimum gradient is associated with the finest material and the maximum value of wave energy or fetch. These are fine-sand beaches exposed to long swells in exposed situations. The greater wave length in these areas helps to reduce the beach gradient. At the opposite extreme are the steepest beaches where the size is greatest and the energy lowest. The beaches are in sheltered positions where waves will be short and hence the equilibrium grade steeper."*

There is some minor conflict with the Shore Protection Manual (Coastal Engineering Research Center, 1984), which largely attributes slope changes to wave height (increased wave height results in reduced beach slope), with limited mention of wave period.

Past wave wake studies, such as the Noosa River study (Macfarlane and Cox, 2003) and the early Gordon River study (von Krusenstierna, 1990), made it clear that any relationship between incident wave energy and subsequent erosion was most likely non-linear, in that double the energy wouldn't result in double the erosion. The energy of different wake waves can vary by orders of magnitude, yet the rate of environmental decay doesn't follow directly. Similarly, beach profiles do not (and cannot) change linearly with wave energy but by a tempered amount.

Moreover, the results of **Table 8.4** appear to demonstrate that $A_{nett}$ is qualitatively related to sediment entrainment and sediment movement, since the largest value of $A_{nett}$ is also associated with the highest wave energy and lowest bottom slope, and vice versa, as stated by King (1972) and the Shore Protection Manual (Coastal Engineering Research Center, 1984).

### 8.10.3 Turbidity sensor vertical position

Further analysis of the 2004 Gordon River trials (*Appendix K*) shows the limitation of relying on a test programme utilising just a single turbidity sensor and how those results may be affected by the testing procedure. Two turbidity meters were used in the Gordon River trials, one at half depth in *0.5 m* of water and one at half depth in *2.0 m* of water, though quite close together. The results for the deeper sensor proved to be somewhat misleading, since it showed similar thresholds of height and period, which could clearly not be the case given the four-fold increase in water depth. **Figures 8.17** and **8.18** show that the degree of sediment entrainment is very non-

---

[103] With all coastal engineering fieldwork, a statistical analysis of an offshore wave climate yielding parameters such as significant wave height and period is the only reasonable representation of the incident wave climate. It is essentially impossible to measure responses of individual ocean waves, or even to quantify them.

linear once the threshold is exceeded, and this is a possible interpretation of the apparent discrepancy.

Setting the sensors at half depth would have offset the recorded turbidity. Initially, the slight misalignment between the predicted threshold and the measured turbidity threshold was believed that this was due to a wrong assumption of sediment size (which was not recorded at the time of testing), knowing that an increased sediment size would move the threshold mostly to the right, but slightly upwards. A sediment diameter of *0.3 mm* would more closely suit the turbidity data. Also, the vessel data was taken as those recorded at the wave probe in *4 m* depth, without transposition to *0.5 m* depth. The (reasonable) justification for that was the very minimal change in transposed wave heights for such short-period waves.

Referring to **Figures 8.29** and **8.30** (following), the calculated threshold curve is derived from wave conditions where sediment begins to move at the bed. Such threshold wave conditions would not cause turbidity at half depth, so the threshold conditions recorded by the nephelometer at half depth would imply an already developed shear condition at the bed. That would have the effect of moving all of the vessel turbidity data points to the left, closing the "zero" discrepancy between the calculated threshold and the measured turbidity. Alternatively, the threshold curve could be adjusted to a *mid-depth* condition, moving the curve mostly to the right. This is an easier method of correction.

Another factor that may have contaminated the elevated turbidity measurement at half depth is the cumulative effect of subsequent waves in the incoming wake. Analysis is premised on the maximum wave being the characteristic wave, yet the leading, long-period waves would initiate sediment entrainment before the maximum wave passed. **Figure 8.24** demonstrates this, looking at individual packet waves for the *QG Cowan* (*L=6.75 m, V=31.88 kn*) and the *Large Ski Boat* (*L=5.3 m, V=7.78 kn*) (taken from Macfarlane and Cox, 2003, Fig. B3 and B4). Packet waves with whole numbers start with a zero up-crossing and those with half numbers start with a zero down-crossing.

It is interesting to note that the first one or two half-waves do not have sufficient height to initiate bed shear threshold exceedance, as do the final packet waves. Also of note is that the maximum value of *S'* (ratio of actual to threshold shear stress) is about *20%* of the cumulative packet total $(E_{max} \approx 0.2 \sum_{packet} E)$. This exactly matches the energy of the maximum wave which is also about *20%* of the cumulative packet energy $(S'_{max} \approx 0.2 \sum_{packet} S')$. These relationships would only be relevant at one lateral offset: at other lateral offsets the energy of the maximum wave would vary with dispersion, but the packet total should remain constant.

The relationship was consistent for both vessels, which were operating at different relative speeds (*$F_{rL}$=2.0*: high speed; *$F_{rL}$=0.56*: transition). Additionally, the cumulative sum of *S'* up to the maximum wave was *67%* of the cumulative packet total for the *QG Cowan* and *60%* for the *Large Ski Boat*, the difference possibly due to the different length Froude numbers. By the time the maximum wave has passed, most of the bed shear stress has been exerted.

**Figure 8.24** would confirm the observations of Bauer *et al*. (2002):

> *"The first 3–5 wave half-cycles (crests and troughs) entrained progressively more sediment, and maximum concentrations were typically achieved after the third wave crest of the primary wave packet. Thereafter, turbidity levels remained high for periods of 40–80 s and then de-creased to background levels within three to five minutes."*

Consider also that the wave packets generated by Bauer *et al*. (2002) were less dispersed, such that the third crest of the primary packet was essentially (or close to) that of the maximum wave. Once turbid, the settling rates would be slow for fine sediments; the return to background conditions promoted by fluvial flows and not settling.
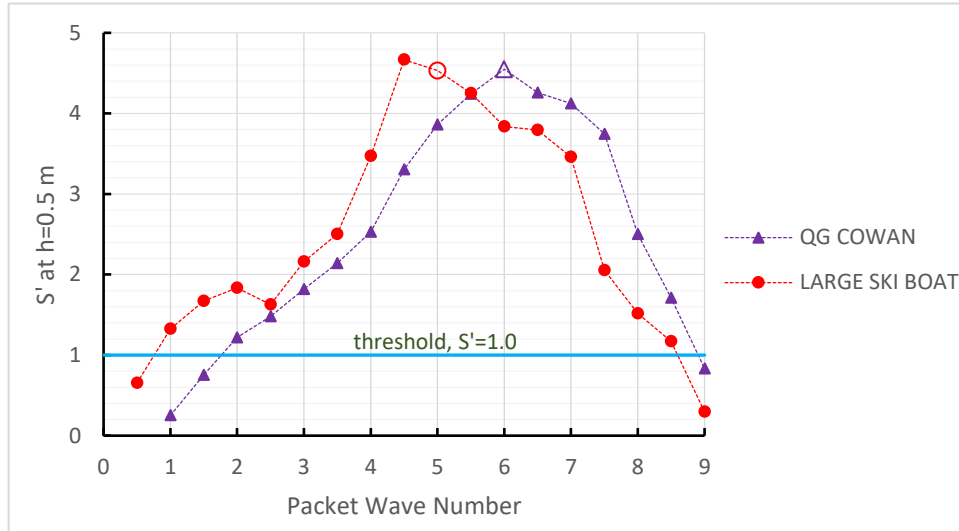


**Figure 8.24** – *Variation in normalised shear stress, S' (actual bed shear stress/threshold bed shear stress) in 0.5 m water depth across wave packets for two vessels: the QG Cowan operating at $Fr_L = 2.0$ and the Large Ski Boat operating at $Fr_L = 0.56$. The sediment is assumed to be unconsolidated sand, D=0.3 mm and the wave wake at generation is considered to be a deep-water wake (h/L > 0.5). The term 'Wave Number" is not to be confused with "wavenumber." The two data sets are of similar shape, with the high-speed condition tending to delay the onset of bed shear above threshold. Data points represent discrete events but are joined for clarity. The maximum waves are shown as hollow markers.*

When discussing the lack of recorded turbidity at locations further offshore (in deeper water), Bauer *et al*. (2002) also make the observations:

> "This implies that either erosion was negligible (i.e., the water was too deep to be influenced by short surface waves) or these outer instruments were positioned too high in the water column to sense near-bottom suspension plumes. More importantly, the absence of a turbidity signal at these offshore instrument locations also suggests that very little sediment was dispersed from near-bank sources toward the center of the channel."

There are two important points. Firstly (and obviously), measured turbidity will be dependent on the vertical positioning of the sensors relative to the bed. This may be explained schematically in **Figure 8.25**. **Figure 8.26** demonstrates this further, showing how the relative shear stress $S'$ grows as a wave shoals. The implication is that wave parameters yielding a threshold turbidity (i.e., NTU in the range of *2-5* units) at half depth have already exceeded the threshold at the bed, such that any subsequent inshore measurement might be in the form of:

$$(turbidity)_{bed} = (half\ depth\ turbidity)_{h=0.5\,m} + f(S'_{0.5}) \qquad [8.8]$$

or

$$(turbidity)_{bed} = (half\ depth\ turbidity)_{h=0.5\,m} + f(S - S_t)_{threshold\ wave} \qquad [8.9]$$

Quantitative determination of the shift in zero by measuring turbidity elsewhere in the water column but at the bed itself would involve complex experimentation. The nature of the vertical dispersion of entrained sediment plumes beneath a wave may render experiments untenable – the exact height of the plume may be impossible to measure and the likely reliance in laboratory experiments on (apparently) monochromatic waves would lead to contamination by successive waves.

Secondly, sediment mixing along the orientation of the wave propagation (sense independent, so may be onshore or offshore) would be minimal if the findings of Bauer *et al*. (2002) are correct. For this reason, any assessment of the cumulative impact of shoaling waves cannot be made with a single turbidity sensor.
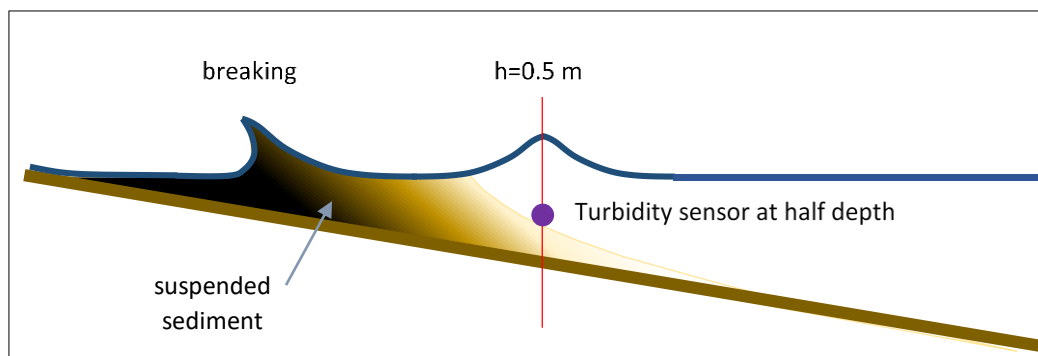


**Figure 8.25** – *Schematic representation of the degree of turbidity beneath a shoaling wave and how the vertical positioning of the turbidity sensor would result in a relative and not absolute measurement.*
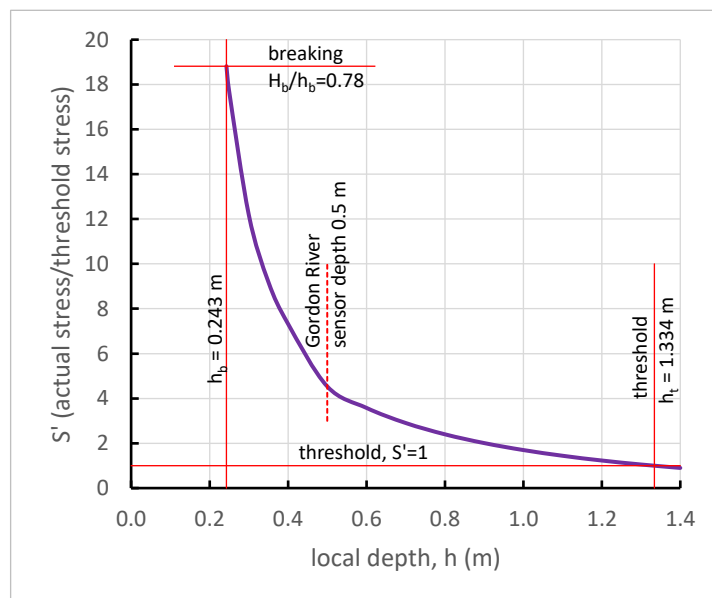


**Figure 8.26** – *Example of the variation in S' (actual stress/threshold stress) for the maximum wave of the Large Ski Boat in Figure 8.24, for a sediment size of D=0.075 mm. At a water depth of 0.5 m the bed shear stress has already reached a value of 4.53, or an actual bed stress of 4.53 times the local threshold stress. The degree of relative bed stress at 0.5 m depth sufficient to create a sediment plume higher than half depth is unknown, so that this "zero error" in also unknown unless accompanied by field tests to determine the wave that generates a turbidity threshold at half depth.*

### 8.10.4 Adjusting for the vertical position of the turbidity sensor

If the parameters of the threshold wave, defined as the most energetic wave at a depth that just begins to initiate bed sediment entrainment ($S = S_t$, or $S' = 1$), were known, it would be possible to apply a correction to other waves. Of the two equations proposed, equation [8.9] is the most reasonable form, since it describes the mid-depth threshold in terms of the excess shear stress at the bed ($S - S_t$). Equation [8.8] is less reasonable since the threshold bed stress calculated for the threshold wave parameters will not be the same as the threshold bed stress for other wave parameters, so the correction would incur a relative error. It can be shown that, provided the wave period is not long (less than *3 s*), the corrected thresholds using equations [8.8] and [8.9] are very similar. For the sake of accuracy, only equation [8.9] is used.

In the example of the Gordon River tests (*Appendix K*), the threshold wave was determined separately. That threshold wave, with wave height and period derived from a specific wave and not determined individually (and therefore incorrectly), had the principal parameters of $H = 114\ mm$ and $T = 1.1\ s$, though with minor variation of around *5%*.[104] ***Figure 8.27*** shows how parameters of the threshold wave was determined. Each of the height/period combinations has an associated turbidity record. Using the composite parameter $E_o/H_o$ aggregates the data points into a trendline, onto which the turbidity (the third of the three dimensions) can be projected. This is reproduced as ***Figure 8.28***.
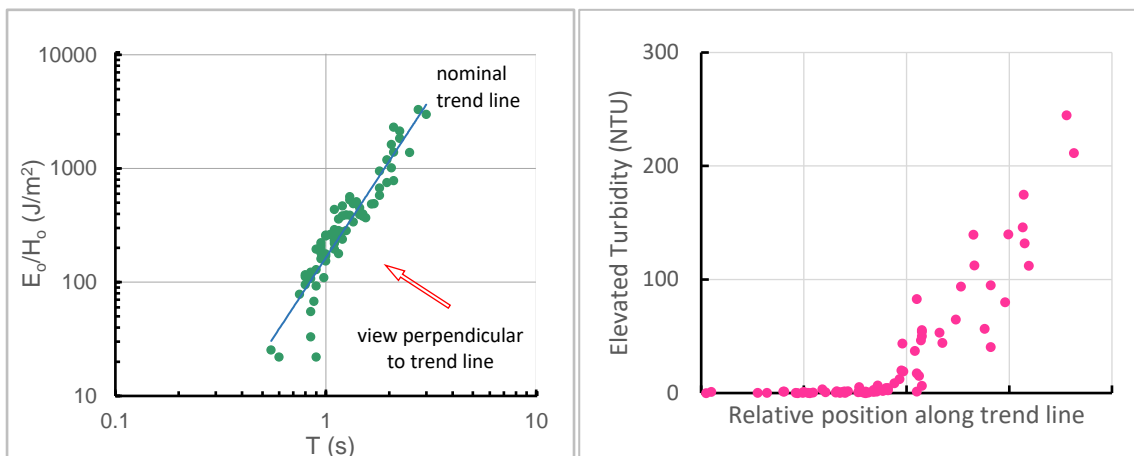


**Figure 8.27** – *2004 Gordon River data used to determine a true threshold wave.* **Left**: *Rather than plot height against period, the composite parameter $E_o/H_o$ was plotted against period. Not only does this aggregate the data along a trend line, $E_o/H_o$ has a close relationship to the entrainment threshold such that the threshold wave identified would be a true threshold wave. Each of the data points in the left figure has an associated turbidity record.* **Right**: *The elevated turbidity record relative to each data point in the left figure, shown in terms of the relative position along the trend line of the left figure. The composite of these two figures as a 3-D chart is shown in Figure 8.28.*

---

[104] It is tempting to plot elevated turbidity against wave height and wave period separately, from which a threshold height and period can be determined. That method is incorrect. Many waves have one of their two principal parameters below their respective thresholds, but exhibit turbidity. Only a 3-dimensional analysis, with height, period and turbidity on the same graph, would indicate a threshold wave, remembering that there are infinite combinations of turbidity threshold wave heights and periods. The use of a composite parameter such as *E/H* helps to tighten the data spread.
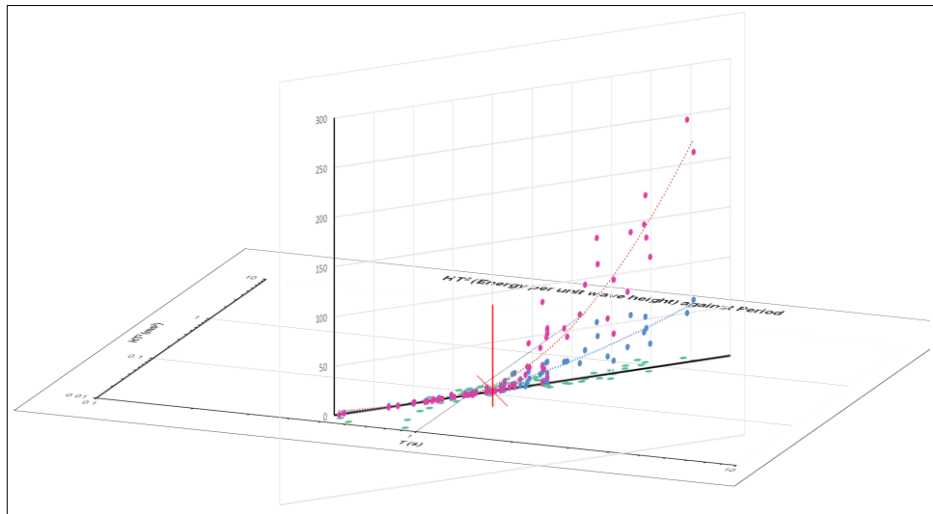
**Figure 8.28** – *Composite plot of the two 2-D graphs of Figure 8.27: energy per unit wave height ($E_o/H_o$) against period (horizontal plane) and turbidity relative to position along horizontal trend line (vertical plane), taken from the 2004 Gordon River data. This method of analysis produces combined threshold wave height and period, rather than thresholds determined separately.*

The parameters of the threshold wave were used to generate **Figure 8.29**, which is the sediment threshold curve with two corrections. Firstly, the threshold is corrected for the mid-depth sensor position, moving the uncorrected threshold curve slightly to the right. Secondly, the wave parameters from the vessel trials, having been measured in *4 m* water depth, were transposed into *0.5 m* water depth. This essentially shifts the data points depending on the wave period. Below $T \approx 2.2\ s$ the waves decrease in height with decreasing wave period, reducing in height by *5%* at $T = 1\ s$. Above $T \approx 2.2\ s$ the waves increase in height with increasing period, increasing in height by *14%* at $T = 3.0\ s$.

**Figure 8.30** shows how transposing the wave heights from the probe position and measurement depth of *4 m* to the turbidity sensor position and depth of *0.5 m* has almost no effect on the shorter period waves but moves the longer period waves slightly to the right (increased height). Except when shoaling is expected to be significant, the effort in this adjustment is probably not warranted.

With **Figures 8.29** and **8.30**, the uncertainty in the nephelometer was *3 NTU*. Recordings of *0-1 NTU* were taken as indicating no turbidity; *2-5 NTU* as threshold turbidity; *>5 NTU* as definite turbidity (NTU readings are rounded to whole numbers).

Overall, the ability to predict sediment entrainment is quite robust.
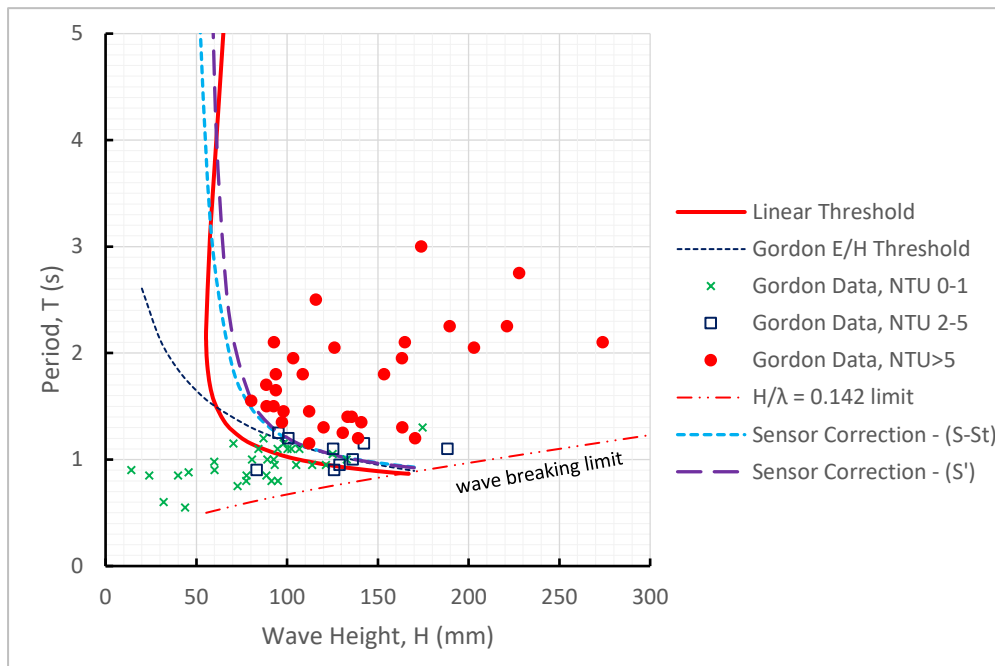
**Figure 8.29** - *Sediment threshold curves at D=0.075 mm and h=0.5 m, overlaid with the Gordon River test data. The linear theory (uncorrected for sensor depth) is shown for comparison. The two correction methods using non-linear wave theory are compared (according to eqn. [8.8] and [8.9]). For most of the waves around the threshold, either correction would be viable. The E/H parameter threshold shows remarkable consistency in predicting threshold wave conditions.*
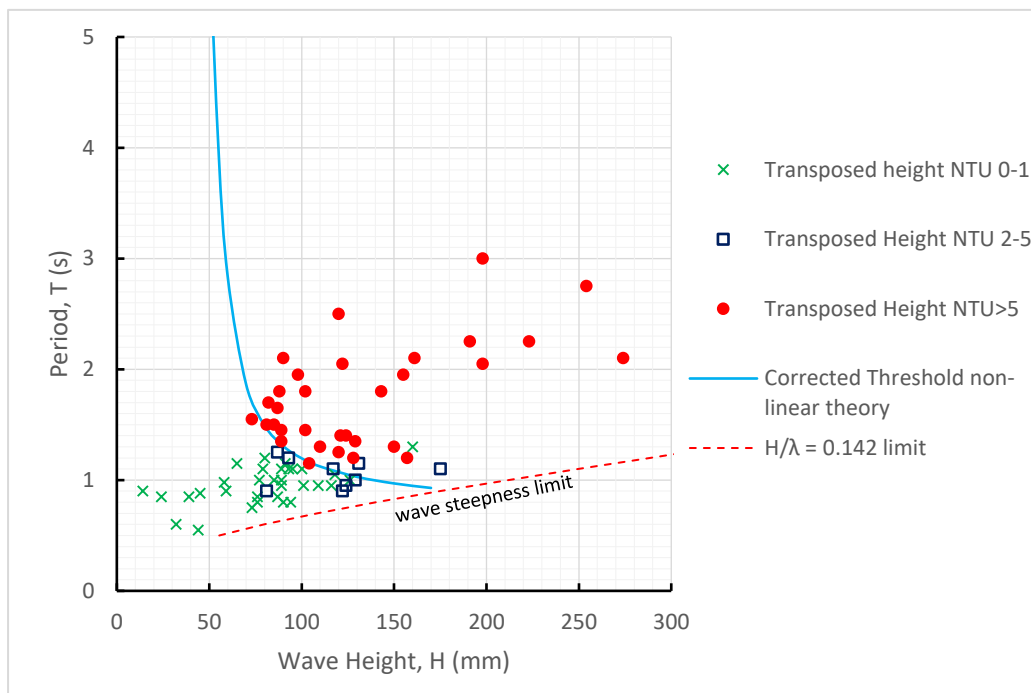


**Figure 8.30** – *Figure 8.29 but showing only the sensor depth correction using [8.9] and with the 2004 Gordon River wave data transposed from the 4 m wave measurement depth to the 0.5 m turbidity measurement depth. That has the effect of moving the longer period waves (2-3 s) to the right, but most of the shorter-period waves (<2 s) are unaffected. The threshold shown is the depth-corrected, non-linear wave theory variant.*

### 8.11    Application to Vessel Wave Wakes

Although the proposed method of determining the ability of waves to initiate erosion correlates with existing field data, more tests would be required to validate the robustness of the method and determine the relationship between the parameters in [8.5] and [8.6], and the extent of erosion, if not the erosion rate.

Additional experiments under controlled conditions (variable but known vessel condition, speed, and lateral offset), measuring the effects of incident waves in terms of turbidity at several offshore locations as well as erosion pin techniques, would satisfy the validation proposal. This is essentially what has been done in the past (Bauer *et al*., 2002, and the 2004 Gordon River tests of *Appendix K*, as examples), except that the experiments need to be better controlled to avoid variability.

$A_{nett}$ is a relative parameter only. Doubling its value does not mean a doubling of the expected erosion severity. As discussed in Macfarlane and Cox (2003), erosion from vessel wave wake is highly non-linear, and it steps between conditions in orders of magnitude. That in itself indicates a power relationship ($\propto x^n$). The means of ranking $A_{nett}$ requires formalisation.

In a desk-top assessment, the procedure would be:

  a.  Use the existing AMC Wave Wake Database (WWDB) to identify the likely principal wave parameters given the vessel parameters;
  b.  Where necessary, transpose these parameters. The proposed $A_{nett}$ calculation is related back to the deep-water condition. The wake parameters for vessels large enough to be depth-affected may need to be transposed back to deep water.
  c.  Calculate $A_{nett}$ and rank according to other vessels or a perceived limiting condition for the waterway.

It would be a relatively simple task to work in the opposite direction; knowing what the waterway could stand in terms of a threshold or modest erosion condition and determining the vessel and or operating limits necessary to meet those conditions.

Wake waves generated in shallow water, as opposed to shoaling waves, may have one or a few waves containing substantial amount of the total wake energy, depending on the $h/L$ ratio at the time of generation. The leading wave, which was shown in Section 5 to act as a packet of waves and not a single wave, may nor may not correlate to the severity of erosion method proposed here. That would have to be the subject of additional field work, complicated by the practical limitations of testing at very low $h/L$ ratios.

For operating conditions outside this, such as those experienced in width-restricted waterways at or near the critical speed condition, further experimentation is not really required. Determining environmental impact under conditions that are obviously untenable is to be viewed as a pointless waste of limited resources.

It is acknowledged that the method presented here only accounts for wave wakes of a deep-water form shoaling and dissipating on a beach of unconsolidated composition. Additional conditions are discussed in Section 9.

Further elaboration is found in Appendices J and K.

169

# Section 9 – Conclusions and Further Work

*Those are my principles.*
*If you don't like them, I have others.*

*Groucho Marx*
*(unattributed!)*

## 9.1    Conclusions

### 9.1.1    Introduction

One conclusion that can be drawn from this study is that a practical appreciation of wave wake generation and propagation is far from universal. Some standards for the measurement and interpretation of wave wakes have been proposed over the past few decades, but without an international body to formalise them they are open to interpretation and manipulation. That has led to improperly qualified claims about design capability and operational suitability. Progressing with an algorithm to evaluate the sustainability of vessel operations without proper, justifiable foundations was pointless.

Vessels are of widely different forms and operate over almost infinite combinations of speed, depth and dynamic conditions. The foundations for the subject must be based on how the waves are generated, how they propagate and how they interact with the natural and built-up environment. The story is the sum of many complex and complicated parts.

### 9.1.2    Section 2 – Literary Review

The misinterpretation and misrepresentation of wave wakes, as opposed to what could be just difference of opinion, are now so entrenched within the literature that they have reached a critical mass permitting self-perpetuation. Fundamental lack of understanding of vessel dynamics is at the heart of the problem; made worse by the fact that students of naval architecture are not adequately instructed on how vessels interact with the environment and the mitigative/ameliorative design and operational measures required for a sustainable solution.

Although there are many technical documents and section of book chapters on the subject, there isn't a (known) single published book or treatise that addresses wave wakes and the environment in full. A comprehensive guidance document would certainly help to allay much of the present confusion and conflict.

### 9.1.3    Section 3 – Waves

Our static view of waves inhibits our ability to interpret them as they change over time. Vessels are known to produce multiple wave packets that interfere with each other as they propagate. That makes it difficult to interpret wave wake records and narrow down the principal parameters of each wake. The only deep-water wave to remain consistent is that occurring at the peak of the propagating wave packet envelope, otherwise regarded as the maximum wave. Other packet waves before and after the maximum wave transmute; changing in height and period as well as increasing in number. It is therefore only appropriate to consider waves as they exist at a point in space and time, beyond which they become something else.

The potential problems of wave wake interpretation have been highlighted, using simulated examples to show how easy it is for wave packet interaction to disguise the true nature of the principal wake parameters. It is possible to extract the parameter of the maximum wave from wave traces using simple algorithms, but with the risk of incorrect interpretation of the true

characteristics of the record. An algorithm can always be used to identify and record the parameters of what is believed to be the maximum wave, but it should always be verified manually.

### 9.1.4    Section 4 – Deep Water

Although traditionally regarded as the easiest condition to study, it can create complex wave systems and interactions. The presence of the transverse wave system brings the greatest complexity, though some high-speed vessel forms are known to generate multiple divergent wave packets of similar strength and they can also cause confusion.

The transverse system has been shown to die away at high speeds in deep water, which helps to explain why wave wakes recorded at high length Froude numbers tend to have more stable characteristics. To simplify wave wake analysis, wakes recorded at a water-depth-to-vessel-length ratio ($h/L$ ratio) of *0.5* or above can be considered as deep-water wakes, with only the first few waves (leading part of the divergent wave packet) affected by depth. That is a necessary simplification to the analysis of waves, the practical recording of which can be difficult in deep water field trials.

The difference between temporal and spatial interpretations of wave wakes is a point of differentiation between experimental and numerical results. Shorelines experience wave wakes temporally and that must be the basis of the relationship between the waves and their impacts.

Recreational craft almost universally have planing monohull hull forms. The understanding of the dynamics of planing hulls and how that is represented within the wave wake generated is critical to the correct interpretation of small craft waves and their interaction with the environment. There are several design-related stages in the evolution of wake waves across the operating speed range and it is unwise to simplify them or ignore them altogether.

### 9.1.5    Section 5 – Shallow Water

Although long thought to be a complex collection of phenomena difficult to qualify let alone quantify, the complications brought by the wide range of $h/L$ ratios compared to the almost singular condition in deep water is somewhat offset by the linear celerity limit of $\sqrt{gh}$. Additionally, the depletion of the transverse wave system in shallow water removes the confusion it can create.

Until now, it has been customary to assess shallow water wave wakes in the same manner as deep-water wakes, but they are not exactly the same. A shallow water wake consists of what would have been several deep-water waves agglomerated by the depth/celerity restriction into a single leading wave, followed by increasingly dispersive trailing waves. As the wake propagates, the leading wave loses energy as its higher frequency components slowly fall behind. Overall, all shallow water wave wakes are dispersive to some extent and the concept of non-dispersive leading waves is a misnomer. Only the leading crest travels with a celerity of $\sqrt{gh}$, and those parts of the leading wave than follow the crest travel at reducing celerities.

The leading shallow water wave becomes dominant within the wake as $h/L$ and slenderness ratios reduce, to the point where it becomes the dominant wave. Also, it propagates and decays as if it were a wave packet, which is important for predicting its evolution. The leading wave is comprised of an underlying solitary wave component that becomes increasingly dominant in very shallow water. Those parts of the leading wave that travel ahead of the crest travel faster than $\sqrt{gh}$ due to the presence of the underlying solitary wave component. Overall, these two

171

mechanisms of a leading solitary wave component and weakly dispersive tail cause the leading wave to stretch over time.

It was also demonstrated that vessels can produce solitary waves at depth super-critical speeds well above what was previously thought possible. In suitable conditions of very shallow water and low slenderness ratio, the leading solitary waves at high depth Froude numbers become so dominant that they can trap energy slowly cycling through the trailing wake, energise themselves and detach (decouple). That helps to explain past accidents caused by the waves from large, high-speed ferries operating in very shallow coastal waters.

The proposed wave height decay model predicated on group celerity rather than vessel length provides a unique description of the leading shallow water wave, since its depth-limited celerity and therefore its depth-limited group celerity is approximated by $\sqrt{gh}$.

A new set of shallow water operational guidelines is proposed, based on the findings of this study that correct and extend past work into shallow water wave wakes.

### 9.1.6    Section 6 – Wave Energy and Power

These composite wave parameters are slowly overtaking wave height as principal determinants of erosion potential but are lacking in a fundamental appreciation of how they represent it. It is not yet fully understood how the energy of a wave wake evolves as it propagates and how that changes the wake's severity. It is known that the energy within the divergent system is largely maintained as it propagates, but the energy of the maximum wave reduces as the total energy is spread amongst an increasing number of waves. The question remains as to why a shoreline can tolerate a total energy in one form (many small waves) but not another form (fewer, more energetic waves).

Inherent relationships between packet waves and how wave power is distributed across the packet lead to the understanding that different parts of a wave packet present different challenges to waterways. A packet's leading waves are the ones with the higher erosion potential, but the following waves may cause synchronous rolling of moored vessels.

### 9.1.7    Section 7 – Wave Height Decay

Wave height decay retains its position as the most controversial and least understood of the wave wake phenomena. We must accept that a definitive solution probably doesn't exist because of the propensity for unaccountable interactions between wave packets and wave systems, even when the wave field is well defined. The number and location of wave cuts can vary the outcome to a substantial extent.

Although there has been some misinterpretation of past wave height decay studies, it has not necessarily influenced the outcome. It can be shown that a single wave packet envelope decays in height consistently and predictably; what cannot be shown is what happens when there are several such packets propagating through each other. It becomes a matter of interpretation. The presence and strength of the transverse wave system appears to be the greatest cause of decay variability, causing localised highs and lows in decay rate parameters. The nature of vessel operations and the variability of operating speeds would caution against proposing a *low wash* service within one of those narrow speed windows where wave heights decayed faster.

Using an existing, comprehensive numerical analysis of the wave wake decay of different vessels, it was shown that the existing decay parameters in common usage are relevant within the normal

speed range of sheltered waterways passenger vessels. At higher speeds where the transverse system is depleted and the divergent packets become more defined, the decay parameters settle to those of a single propagating wave packet. In shallow water, decay rates are complicated by the decreased rate of dispersion and its variability between the head and tail of the propagating wake.

Following on from the very original work of Kelvin (1887) in describing the classical wave wake pattern based on a group celerity relationship, an alternative method of describing the height decay of a wave packet was derived from a common form of a linear Schrödinger wave equation. It shows that group celerity, or the number of wave cycles the packet waves undergo as they propagate, determines the packet envelope height decay. Applying this to the finding that the first wave in shallow water has the properties of a wave packet, and therefore propagates at approximately the linear wave celerity limit in shallow water of $\sqrt{gh}$, the height decay of the first shallow water wave is quite predictable using the group celerity method.

Regardless, wave system interactions mean there isn't a perfect answer. Applying this in a regulatory environment requires the use of the precautionary principle, where a conservative condition is assumed. In that case, in lieu of a comprehensive vessel testing and route-specific certification process, the widely accepted decay exponent of *-0.33* is proposed as the only viable value.

### 9.1.8    Section 8 – Severity of Erosion

There is the requirement to quantify the erosive effects of different waves. Conducting experiments and plotting measured erosion against wave parameters does not provide an explanation as to why shorelines react differently.

Bottom shear stress is known to initiate sediment movement and entrainment, and by summing the amount of shear stress above the threshold value through to the point of breaking is a novel means of ranking erosion potential. Comparison with a limited number of past field trials has shown promising correlation. Moreover, the method shown how changing the wave parameters of height and period influence the entrainment process. Most importantly, it confirms what has long been known – that the erosion process is a highly non-linear phenomenon. Doubling composite wave parameters such as wave energy does not double the erosion rate.

There are other erosion mechanisms to be explored but require further field trials. This is discussed in *Further Work*.

The quantification of erosion severity was also used to quantify erosion thresholds, which correlated very well with previous experiments on the Gordon River. Establishing the validity of erosion thresholds poses the unanswerable conundrum – *by how much can an erosion threshold be exceeded and still be sustainable*? Neither science nor the community can answer that with certainty.


## 9.2     Where Does That Lead Us?

The intent was to increase our understanding of the principal tenets of wave wakes that govern their generation, propagation and shoreline impacts. Sections three to eight describe this in detail and with fresh perspectives. There is a real risk of proposing corrective measures that have a tenuous scientific basis and may only be relevant within a specific set of circumstances. Improving

173

the foundations of the subject was necessary for maintaining relevance with advancement, otherwise the science would be lost in a sea of empirical relationships and regression analyses with little or no basis in the principles of ship design and hydrodynamics other than *lines of best fit*.

Except for specific cases, further model testing is possibly not required; it may not increase our understanding much further. What is required from this point forward is greater attention to the environmental impacts. There was scope within this thesis to expand the erosion mechanisms to include the effects of long-period waves on beaches (the *wave runup* mechanism) and waves on scarps (transverse and other waves in sheltered rivers), but field experiments for these conditions didn't exist and there was no way to validate proposed methods. Proposed ongoing experiments are discussed in *Further Work*.

The present method of ranking the erosion potential of waves should be satisfactory for small craft in its present form. However, what is lacking is quantification of erosion rates above the thresholds and how they may or may not be acceptable, which is the question that cannot be easily answered.

The question of the increased wave wake from manoeuvring and the concentration of waves on the inside of turns has been avoided. It is discussed briefly in *Further Work*. It can be quantified for vessels on regular routes, but not for the random manoeuvres of recreational craft.

## 9.3    Further Work

### 9.3.1    Erosion – limitations and scope for extension

The erosion ranking method of Section 8 has been predicated on two conditions: the shoreline is represented by a beach such that the waves shoal and break (without reflection), and the waves were generated sub-critically (or at least in water *not too shallow*). The field experiments used for correlation came either from small craft in water deep enough for the wake to be classed as *deep*, or from large vessels travelling at slow speeds. There have not been any erosion field experiments conducted using a high-speed vessel in shallow water ($h/L < 0.5$).

As noted, the effect of shallow water at the time of wave wake generation is to cause the wave energy to aggregate in the head of the propagating wake. The maximum wave may or may not be representative of the wake. If the $h/L$ ratio is low enough, the first wave dominates and that may be representative of the wake as a whole, but at moderate ratios of $h/L$ the first wave would be energised but not dominant (refer Figure 5.2). Shallow water wave wakes may correlate better by quantifying the change in energy distribution using Fourier analyses; most importantly the area under the response peaks (representing packet energy) and the moments of those areas. That would be an unfortunate complication; almost every wave wake study to date has been predicated on maximum wave values, and Fourier analyses would be time consuming and complicated. That defeats the purpose of a simplified methodology

An additional erosion mechanism identified applies to long-period waves and wave runup on sloping beaches. This could be mostly ignored for deep water; long-period waves could only come from long vessels, and it is not common to find sheltered waterways sufficiently deep for a long vessel to create a deep-water wave system. A shallow water solution would be the primary aim.

When the shoreline approaches a scarp form, which is a common form on inland rivers, the shoreline becomes increasingly reflective. The bank material may be more consolidated, which is necessary for stability. An example of low consolidation and subsequent ongoing erosion is found in the Snow's Cut study of Fonseca and Malhotra (2012). Also, transverse wave systems can become a primary erosion mechanism, as discussed in Hill *et al.* (2002), with its orbital shearing action and cyclical pore pressure. This must be further quantified. The extreme pore pressures generated by surge and drawdown of large vessels operating at high blockage conditions close to banks can be addressed by regulation. It is not the purpose of this study to quantify what is clearly unviable.

Most importantly, the condition of waves that are shallow from the time of their generation and whether modelling them as individual waves is appropriate is to be investigated.

### 9.3.2    Shallow water test programme

There are two ways to achieve this. Neither is perfect.

*Small Vessel*

A small, high-speed vessel could be used to generate shallow water wakes. That would be a direct analogue of small craft in very shallow rivers. For a nominal *5 m* static waterline length, the following displacements and slenderness ratios in ***Table 9.1*** would apply:

**Table 9.1** – *Required parameters of a 5 m (WL) vessel for field trials.*

| Slenderness Ratio | Displacement (kg) | Represented class of vessel |
|---|---|---|
| 4 | 2,000 | Wake boat (heavy recreational boat) |
| 6 | 590 | Medium (20-25 m) tourist vessel |
| 8 | 250 | Low wash ferry (Brisbane CityCat) |

The necessary minimum $h/L$ ratios to achieve would be preferably *0.15* ($h = 0.75\ m$), or at least *0.2* ($h = 1.0\ m$): the longer the vessel being modelled, the lower the $h/L$ ratio to be applied.

The complication would be to achieve the necessary combination of wave heights and periods to satisfy all shallow water wave wake conditions. A *5 m* (WL) recreational vessel could be ballasted to operate at *2,000 kg*, but the period of its maximum wave would only be around *1.5 s*. That is not going to model the very long wave periods of a larger vessel. It may also be difficult to operate a small vessel safely in water as shallow as *0.75 m* (unless fitted with a waterjet). A small recreational vessel could not be expected to meet the low weight requirements to satisfy the higher slenderness ratios of *6* and *8*, quite besides the problem of scaling sediment size.

*Large Vessel*

The only way to achieve the combination of high slenderness ratio and long-period waves would be to trial a suitable vessel at full scale. This would be a complicated experiment to initiate and co-ordinate.

It might be possible to use a small vessel of lightweight construction in shallow water and test it in a location with extremely fine sediments. The sediment diameter could then be scaled, but not perfectly. The method presented in Section 8 showed that sediment size could be accounted for, so it may not be a concern. It is certainly easier to conduct testing in areas of fine sediments that respond well to turbidity measurements, rather than sand for which entrainment is more difficult

175

to quantify. It is also extremely difficult to find suitable locations to conduct scaled experiments such as these. *Figure 9.1* shows past wave wake field trials of a similar vessel with slenderness ratio of *8.7* (reported in Cox, 2000).



**Figure 9.1** – *Tests of a 7.375 m (LOA) self-propelled 1:8 scale model in water of approximately constant depth (no beach) conducted on the Hunter River in 1999. **Left**: A location was selected that dried at low water, allowing the course giving the most consistent depths to be chosen (and hazards identified). That also varied the h/L ratio naturally over the course of the tidal cycle. As flat as the bottom was, moderate depth variability at scale is acknowledged. **Right**: Testing in shallow water down to as little as 0.3 m depth ($h/L \sim$0.05), which was only possible with waterjet propulsion.*

### 9.3.3    Link between deep and shallow wakes

It would be beneficial to explore further the relationship between a vessel's deep and shallow water wave wakes. Deep water has a more definite meaning, unlike shallow water in which depth is a variable. Connection between the two would give researches and regulators a means of assessing a vessel's potential shallow water wave wake properties by only conducting deep-water experiments.

### 9.3.4    Increased lateral separation

The AMC's model test basin is limited in width to *12 m*. Even with an offset sailing line, the maximum lateral separation achievable is about *4.5 m* without risk of excessive reflections from the basin walls, or slightly more (up to *6 m*) if only the first wave is to be recorded (as is the case in very shallow water).

An alternative was to construct a very short model of around *0.5 m* waterline length to effectively increase the $y/L$ ratio. To ensure waves of sufficient height were generated, a very low slenderness ratio of about *3.5* was proposed. A model has been constructed with a flat-bottomed punt form, having a nominal waterline length of *0.505 m*, draft of *0.032 m*, displacement of *3.5 kg* and slenderness ratio of *3.326*. It is recognised that such a full form (block coefficient *0.866*) may not give a representative wake at slower speeds ($Fr_h <$ 0.5, or *1.1 m/s* in this case), but it would satisfy the premise that wave wakes at high speed are primarily a function of vessel length and displacement, and not of vessel form.

This model would effectively double the lateral separation achieved with model AMC 00-01 and give further insight into divergent wave packet propagation in the far field (up to about nine boatlengths).

Another advantage of the short model is the extended scaled speed range. The AMC's model test basin has a maximum depth of *900 mm* and maximum model speed of *3.75 m/s*. The waves of the shorter model would not be depth affected at all ($h/L > 1$), and the transverse system will be depleted much earlier (from around *2 m/s* and above), giving a wider speed range free of contamination from the transverse system.



**Figure 9.2** – *New model for future work, shown in the AMC towing tank accelerating to 2 m/s in 50 mm water depth ($Fr_h = 2.8$). A strong leading solitary wave was formed, which will be of benefit in future testing.*

### 9.3.5    Shallow water testing and solitary wave generation

The newly-constructed model was intended for use primarily in solitary wave generation at high depth super-critical speeds. The short model's increased lateral separation would further improve understanding of how solitary waves decouple from the trailing wake and what effect that has on them. The benefits of the flat bottom punt form are the capacity to run in very shallow water without grounding and their general lack of spray that may otherwise contaminate the wave wake (spray being a function of local deadrise angle and magnified by the incorrect Weber number scaling at model scale).

Preliminary tests were run in the AMC towing tank, with the model ballasted to *3.5 kg* and with a water depth of *50 mm* (Figure 9.2). Even with just *18 mm* of static underkeel clearance, the model did not ground during the acceleration phase when a substantial solitary wave was formed, even

with the extreme running trim. The model's exceptionally low slenderness ratio enabled the formation of a large solitary wave at high super-critical speed.

### 9.3.6 Composition of high-speed wave wakes

As noted in Section 4.4 and referring to Figure 4.2, the parameters (height, period and energy) of the maximum wave peak at $Fr_L = 0.5$ and reduce thereafter. That has led to the belief that operating at higher speeds is preferable to operating at moderate speeds where the parameters of the maximum wave are at their greatest. Figure 4.2 shows that a vessel's wave resistance continues to increase above $Fr_L = 0.5$, which reflects increased wave wake energy. If that increased energy is not being reflected in the maximum wave parameters, where is it entering the system? There are possibly more waves, or the additional energy is being spread through the packet ends and doesn't show at the packet peak.

There are two avenues for investigation. The first would be to summate individual wake wave energies across a speed range to see if it approximates the increasing wave drag decay of Figure 4.2. The benefit of higher speeds would be the reducing influence of the transverse system. The second would be to compare Fourier analysis responses; principally the areas under the spectral density curves and their mean frequency values.

### 9.3.7 Accelerating, decelerating and manoeuvring

It is known that wave wakes intensify on the inside of turns and spread on the outside. There has been very limited work in this area, with Macfarlane and Cox (2005) attempting rudimentary field experiments to measure the effects.

For small craft, measurement of waves in very tight turns may not result in consistent results if the local maxima/minima of crests and troughs were not recorded. These localised waves would pass through each other and propagate away from the turn, which is a further complication. For vessels large and small on a meandering course, the simplest way to estimate the effect would be to intensify the energy according to the simple geometry of the turn (Figure 9.3). How the wave height and period vary is a matter to be explored, as accounting for energy alone may not explain how the shoreline reacts.

Acceleration and deceleration recommendations would best be qualified with generic guidelines due to the complex nature of the transient effects and the complication of quantifying them relative to the vessel, route and bathymetry.
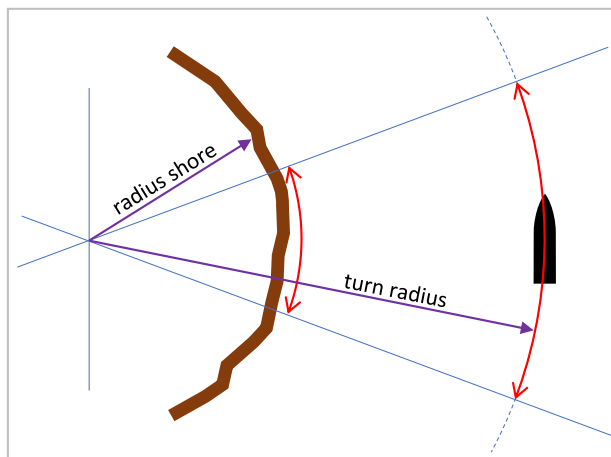


**Figure 9.3** – *Simplified method to account for the magnification of wake waves on the inside of bends. The energy reaching the shore is intensified by the ratio of the turn radius to the shoreline radius. If the maximum wave is used as the energy measure, it may need to be corrected for decay as well. The wake waves on the outside of the turn would be diffracted in the same manner.*

I wondered how many people there were in the world
who suffered, and continued to suffer,
because they could not break out from their own web
of shyness and reserve, and in their blindness and folly
built up a great distorted wall in front of them
that hid the truth.

*Rebecca*,
Daphne du Maurier, 1938

# References

Abbott, M.B. and Price, W.A. (1994). *Coastal, Estuarial and Harbour Engineers' Reference Book*. London: E&FN Spon.

Baldwin, D. S. (2008). Impacts of Recreational Boating on River Bank Stability: Wake Characteristics of Powered Vessels. Report for the Murray Catchment Management Authority. Murray-Darling Freshwater Research Centre, Wodonga, Victoria.

Bauer, B. O., Lorang, M. S. and Sherman, D. J. (2002). Estimating Boat-Wake-Induced Levee Erosion using Sediment Suspension Measurements. *Journal of Waterway, Port, Coastal, and Ocean Engineering*, *Vol. 128*, No. 4. 152-162.

Benjamin, T.B. and Lighthill, M.J. (1954). On cnoidal waves and bores. *Proceedings of the Royal Society of London. Series A, Mathematical and Physical Sciences Vol. 224*, No. 1159. 448-460.

Bertenshaw, T. (2018). *Quantification of vessel-generated transverse waves in deep water* (Unpublished undergraduate research project). University of Tasmania, Launceston.

Bilkovic, D., Mitchell, M., Davis, J., Andrews, E., King, A., Mason, P., Herman, J., Tahvildari, N. and Davis, J. (2017). Review of boat wake wave impacts on shoreline erosion and potential solutions for the Chesapeake Bay. STAC Publication Number 17-002, Scientific and Technical Advisory Committee of the Chesapeake Bay Program, Edgewater, MD.

Blunden, A. (Ed.) (2004). UK MAIB issues reports on two wash related accidents. *Fast Ferry International May 2004*. 31-36.

Bradbury, J., Cullen, P., Dixon, G., and Pemberton, M. (1995). Streambank erosion, revegetation and management of the lower Gordon River, Tasmanian Wilderness World Heritage Area. *Environmental Management Vol 19*. 259-272.

Brown, D.K. (2006). *The Way of a Ship in the Midst of the Sea: The Life and Work of William Froude*. Penzance: Periscope Publishing.

Bruno, M.S., Fullerton, B.J., Datla, R. and Rogowski, P.A. (2002). Field and Laboratory Investigation of High-Speed Ferry Wake Impacts in New York Harbor**.** Center for Maritime Systems, Davidson Lab., Stevens Institute of Technology, Hoboken N.J. [reproduced in Bertram, V. (Ed.) *Proc. 4th Intl. Conf. on High Performance Marine Vehicles* (*HIPER '04*)].

Chabchoub, A., Kimmoun, O., Branger, H., Hoffman, N. Proment, D., Onorato, M. and Akhmediev, N. (2013). Experimental Observation of Dark Solitons on the Surface of Water. *Phys. Rev. Lett. Vol. 110,* 124104.

Champneys, A. (2018). Westward Ho! – Canal Dreams. Musing on Mathematics and Mechanics. *Mathematics Today,* April 2018. 59-63.

Coastal Engineering Research Center (CERC) (U.S.) (1984). *Shore protection manual*. Fort Belvoir, Va.: U.S. Army Coastal Engineering Research Center.

Conway, M. (Ed.) (2019). Safety in numbers. *Ship and Boat Magazine May/June 2019*. London: Royal Institution of Naval Architects. 32-35.

Cox, D.T., Kobayashi, N. and Okayasu, A. (1996). Bottom shear stress in the surf zone. *Journal of Geophysical Research*, *Vol. 101*, No. C6. 14 337-14 348.

Cox, G. (2000). Sex, Lies and Wave Wake. *Proceedings of the International Conference on the Hydrodynamics of High Speed Craft – Wake Wash and Motions Control (HHSC 2000)*.

Cox, G. and Macfarlane, G. (2019). The Effects of Boat Waves on Sheltered Waterways – Thirty Years of Continuous Study. *Australasian Coast and Ports 2019 Conference*, Hobart.

Craig, W., Guyenne, P., Hammack, J., Henderson, D. and Sulem, C. (2006). Solitary water wave interactions, *Physics of Fluids, Vol. 18*, 057106.

Craik, A. D. D. (2004). The origins of water wave theory. *Annual Review of Fluid Mechanics*, *Vol. 36*. 1–28.

Daily, J. W. and Stephan, Jr., S. C. (1952). The Solitary Wave: Its Celerity, Profile, Internal Velocities and Amplitude Attenuation in a Horizontal Smooth Channel. *Coastal Engineering Proceedings*, No. 3, P. 2. 13-30.

Dand, I. W. (2002). The effect of water depth on the performance of high speed craft. *Proceedings of the High Performance Yacht Design Conference, Auckland*, *2002*.

Dand, I.W., Dingham-Peren, T.A., King, L. (1999). Hydrodynamic Aspects of a Fast Catamaran Operating in Shallow Water. *Proc. International Conference on Hydrodynamics of High Speed Craft*. London: Royal Institution of Naval Architects.

Darmon, A., Benzaquen, M., Raphael, E. (2014). Kelvin wake pattern at large Froude numbers." *J. Fluid Mech.*, *Vol. 738*, R3.

Davis, J.R. (2018). Effect on Vessel Wave Wake of Wave Propagation from Shallow to Deep Water (Unpublished undergraduate research project). University of Tasmania, Launceston.

Dean, R. G. and Dalrymple, R. A. (1991). Water wave mechanics for engineers and scientists (2nd printing with corrections). Singapore: World Scientific.

Demirbilek, Z., Bratos, S.M. and Thompson, E.F. (1993). Wind Products for Use in Coastal Wave and Surge Models. *Miscellaneous Paper CERC-93-7*, U.S. Army Engineer Waterways Experiment Station, Vicksburg, MS.

Dingemans, M. W. (1997). *Water Wave Propagation over Uneven Bottoms: Part 2 - Non-linear Wave Propagation*, Volume 13 of Advanced Series on Ocean Engineering. Singapore: World Scientific Pub. 967.

Doctors, L. J. & Australian Maritime Engineering Cooperative Research Centre (1994). Experiments on the resistance of a catamaran in restricted water. Australian Maritime Engineering CRC Ltd, [Sydney, N.S.W.].

Doctors, L.J. and Day, A.H. (2001). The generation and decay of waves behind high-speed vessels, *Proc. 16th Intl. Workshop on Water Waves and Floating Bodies (WWWFB 2001)*. 33-36.

Doctors, L.J., Phillips, S.J. and Day, A.H. (2001). Focussing the Wave-Wake System of a High-Speed Marine Ferry. *Proc. 6th Int. Conf. on Fast Sea Transportation (FAST 2001), Vol 1*. 97-106

Doctors, L. J., Renilson, M. R., Parker, G., Hornsby, N. (1991). Waves and Wave Resistance of a High-Speed River Catamaran. *Proc. 1st Int. Conf. on Fast Sea Transportation (FAST '91)*. 35-52.

Doyle, R., Whittaker, J.T. and Elsäßer, B. (2001). A Study of Fast Ferry Wash in Shallow Water. *Proc. 6th Int. Conf. on Fast Sea Transportation (FAST 2001)*. 107-120.

Drobyshevsky, D. (2017). *An investigation on the vessel wave wake generated in deep water and propagating to shallow water across a slope* (Unpublished undergraduate research project). University of Tasmania, Launceston.

Dugan, J. (1953). *The great iron ship*. London, UK: Hamish Hamilton.

Ertekin, R.C. and Weihausen, J.V. (1986). Some Soliton Calculations. *Proc. 16th Symposium on Naval Hydrodynamics*. 167-185.

Fenton, J. D. (1972). A ninth-order solution for the solitary wave. *J. Fluid Mechanics, Vol. 53*. 257-271.

Fenton, J.D. (1990). Nonlinear Wave Theories. In B. Le Méhauté & D.M. Hanes (Eds.), *The Sea – Ocean Engineering Science, Part A, Vol. 9* (pp.3-25). New York: Wiley.

Fenton, J. D. (1999). The cnoidal theory of water waves. In J. B. Herbich (Ed.), *Developments in Offshore Engineering, Gulf, Houston, chapter 2* (pp. 55-100).

Fenton, J. D. & McKee, W. D. (1990). On calculating the lengths of water waves. *Coastal Engineering, Vol. 14*. 499-513.

Filippov, A.T. (2000). *The Versatile Soliton*. Basel: Birkhauser. 261.

FitzGerald, D., Hughes Z. and Rosen, P. (2011). Boat wake impacts and their role in shore erosion processes, Boston Harbor Islands National Recreation Areas. *Natural Resource Report NPS/NERO/NRR-2011/403*, National Park Service, Fort Collins, Colorado.

Fonseca, M. and A. Malhotra. (2012). Boat wakes and their influence on erosion in the Atlantic Intracoastal Waterway, North Carolina. NOAA Technical Memorandum NOS NCCOS #143.

Gadd, G. E. (1994). The Wash of Boats on Recreational Waterways. *Trans. Royal Institution of Naval Architects Vol. 136,* Pt. B. 261-280.

Golder Associates Inc. (2013). Rich Passage Wave Energy Evaluation - Beach Response to In-situ Testing of Rich Passage 1. Project 113-93490.003, on behalf of Kitsap Transport, Seattle, USA.

Grilli, S.T., Svendsen, I.A., Subramanya, R. (1997). Breaking criterion and characteristics for solitary waves on slopes. *Journal of Waterway, Port, Coastal and Ocean Engineering, Vol. 123*, Issue 3. 102-112.

Grimshaw, R. (2011). Transcritical Flow Past an Obstacle. *ANZIAM J. Vol. 52*. 1-25.

Grimshaw, R. H.J, Zhang, D.-H. and Chow, K. W. (2009). Transcritical Flow Over a Hole. *Studies in Applied Mathematics*, *Vol. 122*. 235-248.

Grimshaw, R.H.J; Zhang, D.-H.; Chow, K.W. (2007). Generation of solitary waves by transcritical flow over a step. *Journal of Fluid Mechanics*, *Vol. 587*. 235-254.

Havelock, T.H. (1908). The propagation of groups of waves in dispersive media, with application to waves produced by a travelling disturbance. *Proc. Royal Society of London*, *England*, Series A. 398-430.

Hedges, T. S. (1995). Regions of validity of analytical wave theories. *Proc. Inst. Civ. Engnrs, Water, Maritime and Energy, Vol. 112*. 111–114.

Hill, D., Beachler, M. and Johnson, P. (2002). Hydrodynamic impacts of commercial jet-boating on the Chilkat River, Alaska*. Pennsylvania State University Report on behalf of the Alaska Department of Fish and Game, Habitat and Restoration Division.

Hovgaard, W. (1909). Diverging Waves. *Trans., Inst. of Naval Architects*, *Vol. 51*. 251-261.

Ippen, A. T.; Kulin, G. (1954). The Shoaling and Breaking of the Solitary Wave. *Coastal Engineering Proceedings*, No. 5, Part 4. 27-47.

Isobe, A. (1985). Calculation and application of first-order cnoidal wave theory. *Coastal Engineering, Vol. 9*, Issue 4. 309-325.

ITTC (1969). Guide for Measured Mile Trials. *Rep. of Perf. Comm. Proc. 12th ITTC, Rome*.

Iwagaki, Y. (1968). Hyperbolic Waves and Their Shoaling. *Coastal Engineering Proceedings, Vol. 1,* No. 11. 124-144.

Johnson, J. (1957). Ship Waves in Navigation Channels*. Coastal Engineering Proceedings, 1(6)*, 40. 666-690.

Johnson, R.S. (1973): "On the development of a solitary wave over an uneven bottom." *Proc. Cambridge Phil. Soc.*, *Vol. 73*. 183-203.

Keller*, J. B. (1949). The solitary wave and periodic waves in shallow water*. Annals of the New York Academy* of *Sciences*, *Vol. 51*. 345-350.

Kelvin (1887) – see Thompson, W.

King, C.A.M. (1972). *Beaches and Coasts* (2nd ed.). London: Edward Arnold (Publishers) Ltd.

Kirkegaard, J., Kofoed-Hansen, H. and Elfrink, B. (1998). Wake wash of high-speed craft in coastal waters. *Coastal Engineering 1998.* Reston, VA: ASCE. 325–337.

Kofoed-Hansen, H., Jensen T., Sorensen, O.R., and Fuchs, J. (1999). Prediction of Wake Wash from High-Speed Craft in Coastal Areas. *Proceedings of the International Conference on the Hydrodynamics of High Speed Craft*.

Kofoed-Hansen, H., Jensen, T., Sorensen, O.R., and Fuchs, J. (2000). Wake Wash Risk Assessment of High-Speed Ferry Routes – A Case Study and Suggestions for Model Improvements. *Proceedings of the International Conference on the Hydrodynamics of High Speed Craft – Wake Wash and Motions Control (HHSC 2000)*.

Komar, P.D. and Miller, M.C. (1973). The threshold of sediment movement under oscillating water waves. *Journal of Sedimentary Petrology, Vol. 43*, No. 4. 1101-1110.

Laderoute, L. and Bauer, B. (2013). River bank erosion and boat wakes along the Lower Shuswap River, British Columbia. Final Project Report submitted to Regional District of North Okanagan Fisheries and Oceans Canada.

Lamb, H., Sir (1895). *Hydrodynamics*. Cambridge, UK: University Press.

Lamb, T. (Ed.) (2003). *Ship design and construction*. Jersey City: Society of Naval Architects and Marine Engineers.

Lee, S. J., Yates, G. T. and Wu, T. Y. (1989). Experiments and analyses of upstream-advancing solitary waves generated by moving disturbances. *J. Fluid Mech. Vol. 199*. 569-593.

Le Méhauté, B. (1976). *An introduction to hydrodynamics and water waves*. New York: Springer Verlag.

Le Roux, J.P. (2007). A simple method to determine breaker height and depth for different deepwater wave height/length ratios and sea floor slopes. *Coastal Engineering, Vol. 54*, Issue 3. 271-277.

Lesleighter, E. J & Maritime Services Board of New South Wales (1964). Hawkesbury River - the effect of speedboat activities on bank erosion. Report No. 106, Dept. of Public Works, Harbours and Rivers Branch, Manly Hydraulics and Soils Laboratory, Manly.

Li, Y. and Raichlen, F. (2001). Solitary Wave Runup on Plane Slopes, *Journal of Waterway, Port, Coastal, and Ocean Engineering Vol. 127*, Issue 1. 33-44.

Lighthill, J., Sir (2001). *Waves in fluids*. Cambridge, UK; New York: Cambridge University Press.

Longuet-Higgins, M. (1974). On the Mass, Momentum, Energy and Circulation of a Solitary Wave. *Proceedings of the Royal Society of London. Series A, Mathematical and Physical Sciences, 337*(1608), 1-13.

Lyakhovitsky, A. (2007). *Shallow Water and Supercritical Ships*. Fair Lawn NJ: Backbone Publishing Company.

Ma, C., Zhu, Y., Wu, H., He, J., Zhang, C., Noblesse, F. (2016). Wavelengths of the highest waves created by fast monohulls ships or catamarans. *Ocean Engineering 113*. 208-214.

Macfarlane, G.J. (2002). *The measurement and assessment of sub-critical vessel generated waves* (Unpublished Master of Philosophy dissertation). University of Tasmania, Launceston.

Macfarlane, G.J. (2012). *Marine Vessel Wave Wake: Focus on Vessel Operations within Sheltered Waterways* (Unpublished Doctor of Philosophy dissertation). University of Tasmania, Launceston.

Macfarlane, G.J. and Cox, G. (2003). Vessel Wash Impacts on Bank Erosion – Noosa River Between Lake Cootharaba and Lake Cooroibah – Brisbane River Kookaburra Park to the Bremer River Junction. *Report Number 01/G/18*. AMC Search Limited, Launceston.

Macfarlane, G.J. and Cox, G.L. (2005). Vessel wash impacts on bank erosion – Maroochy River. *Report for the Moreton Bay Waterways and Catchments Partnership, 04/G/18*. AMC Search Ltd, Launceston.

Macfarlane, G.J. and Cox, G. (2007). An introduction to the development of rational criteria for assessing vessel wash within sheltered waterways. IMarEST *Journal of Marine Design and Operations*, Part BII.

Macfarlane, G.J., Cox, G. and Bradbury, J. (2008). Bank erosion from small craft wave wake in sheltered waterways. *RINA Transactions, Part B: International Journal of Small Craft Technology 150*. 33-49.

Macfarlane, G.J. and Renilson, M.R. (1999). Wave Wake – a Rational Method for Assessment. *Proc. Conference on Coastal Ships and Inland Waterways*. London: Royal Institution of Naval Architects.

Macfarlane, G.J. and Renilson, M.R. (2000). When is Low wash Low Wash? - An Investigation Using a Wave Wake Database. *Proc. International Conference on Hydrodynamics of High Speed Craft - Wake Wash and Motions Control*. London: Royal Institution of Naval Architects.

Marine Accident Investigation Branch (MAIB) (2000). Report on the investigation of the man overboard fatality from the angling boat 'Purdy' at Shipwash Bank, off Harwich on 17 July 1999. MAIB Report 1/10/194. 23.

Maynord, S. (2001). Boat waves on Johnson Lake and Kenai River, Alaska. Technical Report ERDC/CHL TR-01-31, U.S. Army Corps of Engineers, prepared for the Alaska Department of Fish and Game.

Maynord, S. T. (2005). Wave height from planing and semi-planing small boats. *River Research and Applications 21*. 1–17.

Maynord, S.T., Biedenharn, D.S., Fischenich, C.J. and Zufelt, J.E. (2008). Boat-wave-induced bank erosion on the Kenai River, Alaska*.* Engineer Research and Development Center TR-08-05, US Army Corps of Engineers, Vicksburg.

MCA (2001). A physical study of fast ferry wash characteristics in shallow water. Technical Report Research Project 457, the Maritime and Coastguard Agency, UK.

McCowan, J. (1894). On the highest wave of permanent type. *Phil.Mag Series 5, Vol. 38*. 351-358.

McVoy, J.L. (Ed.) (1985). Modern Ships and Craft. *Naval Engineers Journal, Vol. 97* (2).

Meert, K., Pandelaere, M. and Patrick, V. (2014). Taking a shine to it: How the preference for glossy stems from an innate need for water. *Journal of Consumer Psychology*, *Vol. 24*, Issue 2. 195-206.

Mei, C.C. (1989). *The Applied Dynamics of Ocean Surface Waves*. New York: Wiley Interscience.

Miche, R. (1944). Mouvement ondulatoires de la mer en profondeur constante ou decroissante. *Annales des Ponts et Chaussees, Vol. 114*. (1) 26-78, (2)270-292, (3) 369-406.

Munk, W. H. (1949). The solitary wave theory and its application to surf problems. *Annals of the New York Academy of Sciences*, *Vol. 51*. 376-424.

Murray, T.J. (2012). Assessment of the Economic Impacts of Recreational Boating in Virginia. Marine Resource Report No. 2012-12*,* Virginia Institute of Marine Science.

Nanson, G.C., Von Krusenstierna, A., Bryant, E.A. and Renilson, M.R. (1994). Experimental Measurements of River Bank Erosion caused by Boat-Generated Waves on the Gordon River, Tasmania, *Regulated Rivers, Research and Management Vol. 9*. 1-14.

Newman, J.N. (1977). *Marine Hydrodynamics*. Cambridge, MA: MIT Press.

Orszaghova, J., Borthwick, A.G. and Taylor, P.H. (2012). From the paddle to the beach - A Boussinesq shallow water numerical wave tank based on Madsen and Sørensen's equations. *J. Comput. Physics, Vol. 231*. 328-344.

Osborne, P. D., Hericks. D. B., and Cote. J. M. (2007). Full-Scale Measurements of High Speed Passenger Ferry Performance and Wake Signature. *OCEAN 2007*. 1–10.

Osborne, P.D., Cote, J.M., and MacDonald, N.J., (2009). Impact Studies and Criteria for High Speed Operations with Foil-Assisted Catamarans in a Wake Sensitive Area. *Proceedings of the 10th International Conference on Fast Sea Transportation*. 885-896.

Ozeren, Y., Simon, A. and Altinakar, M. (2016). Boat-Generated Wave and Turbidity Measurements: Connecticut River. *Proc. World Environmental and Water Resources Congress 2016: Hydraulics and Waterways and Hydro-Climate/Climate Change*. 390-398.

Palais, R. (2008): Published in two versions:

   *Short version (excluding examples and extended discussion):*

   Gowers, T. (Ed.) (2008). *The Princeton Companion to Mathematics*. Princeton NJ: Princeton Univ. Press. 234-239;

   *Extended version (principal reference)*:

   An Introduction to Wave Equations and Solitons, published online at Univ. Ca, Irvine: http://vmm.math.uci.edu/PalaisPapers/ (last accessed 8th September, 2018).

Parnell, K. and Kofoed-Hansen, H. (2001). Wakes from large high-speed ferries in confined coastal waters: management approaches with examples from New Zealand and Denmark. *Coastal Management, Vol. 29*. 217–237.

Pattiaratchi, C. and Hegge, B. (1990). Impact of Ferry and large Vessel Traffic on Swan River Foreshore Erosion. Centre for Water Research Report WP 452 CP, University of Western Australia, Perth.

Pauli, W. (1973). *Pauli lectures on physics*. Cambridge MA: MIT Press.

Peregrine, D, H. (1983). Water Waves, Nonlinear Schrödinger Equations and their Solutions. *Journal of the Australian Mathematical Society,* Ser. B25. 16-43.

Pelinovsky, E.N., Shurgalina, E.G. and Rodin, A.A. (2015). Criteria for the Transition from a Breaking Bore to an Undular Bore. *Izvestiya, Atmospheric and Oceanic Physics, 2015*, *Vol. 51*, No. 5. 530-533.

Phillips-Birt, D. (1966). *Sailing Yacht Design*. London: Coles.

Rabaud, M. and Moisy, F. (2013). Ship wakes: Kelvin or Mach angle*? Phys. Rev. Lett. 110*. 214503.

Rayleigh, L. (1876). On Waves. *The London, Edinburgh, and Dublin Philosophical Magazine and Journal of Science, Vol. 1:4*, 257-279.

Robbins, A. (2013). *Shallow Water Catamaran Wash – Simple Characteristics for a Complex Problem* (Unpublished doctoral dissertation). University of Tasmania, Launceston.

Ruprecht, J.E., Glamore, W.C., Coghlan, I.R. and Flocard, F. (2015). Wakesurfing: Some Wakes are More Equal than Others. *Australasian Coasts and Ports 2015 Conference*, Auckland.

Savitsky, D. (1964). Hydrodynamic Design of Planing Hulls. *Marine Technology, Vol 1*, No. 1. 71-95.

Schaper, H., and Zielke, W (1984). A Numerical Solution of Boussinesq Type Wave Equations. *Coastal Engineering Proceedings*, *Vol. 1*, No.19. 1057-1072.

Scott, J.R. (1971). On Blockage Correction and Extrapolation to Smooth Ship Resistance. *Transactions of the Society of Naval Architects and Marine Engineers, Vol. 78*. 288-326.

Shields, A. (1936). Anwendung der Ähnlichkeitsmechanik und der Turbulenzforschung auf die Geschiebebewegung. *Mitteilung der Preussischen Versuchsanstalt fur Wasserbau und Schiffbau*. 26.

Soomere, T. (2007). Nonlinear Components of Ship Wake Waves. *Trans. ASME, Applied Mechanics Reviews, Vol. 60*. 120-136.

Sorensen, R.M. (1967). Investigation of ship-generated waves. *Journal of Waterway, Harbors and Coastal Engineering Division*, 93. American Society of Civil Engineers. 85-99.

Sorensen, R.M. (1973). Water waves produced by ships. *The Journal of the Waterways Harbours and Coastal Engineering Division, Proceedings of the American Society of Civil Engineers, Vol. 99* (WW2). 245-256.

Stoker, J.J. (1957). *Water Waves*. New York: Interscience Publishers Inc.

Stokes, G. G. (1847). On the theory of oscillatory waves. *Transactions of the Cambridge Philosophical Society, Vol. 8. 441–455.*

Stumbo, S., Fox, K.; Dvorak, F. and Elliot, L. (1999). The prediction, movement and analysis of wake wash from marine vessels. *Marine Technology, Vol. 36,* Part 4. 248–260.

Taylor, D. W. (1943). *The speed and power of ships: a manual of marine propulsion*. U.S. G.P.O.

Taylor, L. (2013). *Through their eyes: glimpses of a changing Australia*. Burleigh Heads, Australia: Brigalow Press.

Taylor, P.H. (2016). A Simple Approach for Shallow-Water Solitary Wave Interactions." *Proc. 20th Australasian Fluid Mechanics Conference*, Perth, Australia.

Tan, S.W.S. (2012). Predicting Boat-Generated Wave Heights: A Quantitative Analysis through Video Observations of Vessel Wakes. Trident Scholar Project Report No. 409, United States Naval Academy, Annapolis, USA.

Thomson, W. (Lord Kelvin) (1887). On ship waves. *Proc. of the Institute of Mechanical Engineers*. 409-433.

Tuck, E. O., and Lazauskas, L. (1998). Optimum hull spacing of a family of multihulls. *Ship Technology Research-Schiffstechnik*, *45*(4), 180.

United States. (2006). *Coastal engineering manual*. Washington, D.C.: U.S. Army Corps of Engineers.

von Krusenstierna, A. (1990). *River Bank Erosion by Boat-Generated Waves on the Lower Gordon River, Tasmania* (Unpublished Master of Science dissertation). University of Wollongong, Wollongong.

Ward, L. W. and van Hooff, R. W. (1976). The Effect of Probe Location on a Model Wave Resistance Survey Along a Longitudinal Cut**.** *Journal of Ship Research, Vol. 20,* No. 1. 7-21.

Whittaker, T.; Bell, A., Shaw, M. and Patterson, K. (1999). An investigation of Fast Ferry Wash in Confined Waters. *International Conference on Hydrodynamics of High Speed Craft*.

Wei, G. and Kirby, J.T. (1998). Simulation of Water Waves by Boussinesq Models. *Research Report No. Cacr-98-02*, Center for Applied Coastal Research, Ocean Engineering Laboratory, University of Delaware, Newark. 202.

Wood, D., Daley, J. and Chivers, C. (2018). Australia Demonstrates the Rise of Populism is About More than Economics. *The Australian Economic Review, Vol. 51*, No. 3. 399–410.

Wu, T.Y. (1987). Generation of upstream-advancing solitons by moving disturbances. *J. Fluid Mech. Vol. 184*. 75-99.

Yamashita, K., & Kakinuma, T. (2014). Properties of Surface and Internal Solitary Waves. *Coastal Engineering Proceedings, Vol. 1*, No. 34.45. 1-15.

# Appendix A – Detailed Literature Review

Note: the format of each review reflects the format of the paper being reviewed. There is variation.


## Appendix A1 - *Estimating Boat-wake-induced levee erosion using sediment suspension measurements.*

Bauer, B. O., Lorang, M. S. and Sherman, D. J. (2002). Estimating Boat-Wake-Induced Levee Erosion using Sediment Suspension Measurements. *Journal of Waterway, Port, Coastal, and Ocean Engineering*, *Vol. 128*, No. 4. 152-162.

The study was a comprehensive attempt to correlate between vessel wave wake and rates of erosion. Several approaches were used to quantify the rate and there was satisfactory correlation. One of the weaknesses of the study was, in some ways, a strength. There was little attempt to quantify the wave wake in terms of vessel parameters and the results are site and vessel specific. Conversely, it could be argued that it was better to avoid correlation between vessel parameters and the wakes they produce rather than publish the type of flawed comparison that commonly finds its way into the literature (and becomes difficult to expunge).

a. The chosen site had several notable features:
   - a vertical scarp above the water, making the bank relatively reflective;
   - a subaqueous levee consisting of consolidated clay and silt; the consolidation suggesting a normally stable levee and a deposition from extreme events such as recent floods, vessel wash or upstream erosion;
   - although having a small tidal range, the flow was considered fluvial (one-way) and not tidal (two-way). Entrained sediments re-settled elsewhere;
   - little vegetation.

b. Only one vessel was used, and all tests were completed within a very short timeframe. There was no focus on repeatability, collecting wide-ranging data, or testing different vessels. That would suggest that, from the beginning, there was no intention of trying to relate the erosion mechanism to wake parameters, or no clear thought on how to achieve it. It is also possible the authors thought that vessel was would be simple to quantify in the same manner that wind wave parameters can be estimated from windspeed and fetch.

c. Current meters were used to record bed velocities, and this avoided the need to be particular about how the waves were measured. It avoids the need to apply wave transformation equations in shallow water, but it also meant potential loss of the benefit of correlating between the waves and the near-shore parameters (waves measured in deep water and then transposed into shallow water provides correlation between the two depth conditions, but direct measurement of the shallow water parameters such as bed celerity eliminates the need to transpose waves back to a deep-water condition). Wave height was transposed from the probe to the shallow water measurement point EM5 (approx. *0.5 m* depth). There was no mention of height attenuation.

189

d. Table 1 from the reference (reproduced below as Table A1.1) shows the boat passage parameters. There were just seven runs. The vessel length was noted as *7.5 m*, giving a waterline of around *6* to *6.5 m*. This would be regarded as a large vessel for a sheltered river. Using the bathymetry in Fig. 2 and guessing a channel depth of around *5 m*, the depth Froude number was sub-critical for runs *4* and *5* (*6 knots*), near-critical for runs *1* and *2* (*12* and *15 knots*) and supercritical for the rest, though "*deep super-critical*" (having the appearance of a high-speed, deep-water wake). The ratio of $h/L$ would put the generated maximum waves in the "deep" category (>*0.5L*). Some of the leading waves would have been depth-affected at high speeds.

**Table A1.1** – *Bauer et al. (2002) Table 1.*

**Table 1.** Summary of Boat Passage Parameters and General Hydrodynamic Conditions at EM5

| Run | Time | Boat parameters | | | Wave parameters | | |
| | | Speed (knots) | Direction | Water depth (m) | $U_d{}^a$ (m s$^{-1}$) | $V_d{}^a$ (m s$^{-1}$) | Height[b] (m) |
|---|---|---|---|---|---|---|---|
| 1 | 6:48:42 | 12 | Downstream | 0.32 | 0 | 0.04 | 0.18 |
| 2 | 7:03:34 | 15 | Downstream | 0.29 | 0.01 | 0.08 | 0.21 |
| 3 | 7:11:10 | 18 | Upstream | 0.27 | 0.02 | 0.08 | 0.18 |
| 4 | 7:22:27 | 6 | Downstream | 0.24 | 0.01 | 0.07 | 0.07 |
| 5 | 7:29:35 | 6 | Upstream | 0.22 | 0.01 | 0.06 | 0.06 |
| 6 | 7:38:41 | 23 | Downstream | 0.20 | 0.01 | 0.07 | 0.12 |
| 7 | 7:48:04 | 23.5 | Upstream | 0.18 | 0.01 | 0.07 | 0.12 |

[a] $U_d$, $V_d$ refer to mean drift (river) velocity assessed from preevent segment of time series prior to boat-wake event. Positive values indicate onshore ($U_d$) and downstream ($V_d$).
[b] Wave height was calculated using linear shallow-water theory with maximum orbital velocity in onshore direction.

e. Other tests were performed, including running a vessel repeatedly (*500* and *1,000* passes) past the bank at an unfavourable speed to simulate a regular incident wave field. The total erosion was measured and the average erosion per pass calculated. That is useful in a practical sense, but it doesn't help to correlate between the wave wakes of different vessels and the erosion they may cause. It would not provide a basis for approving new vessels or variations in recreational or commercial activities.

f. For an assumed waterline length of maximum *6.5 m*, the length Froude numbers ranged from *0.39* at *6 knots* to *1.51* at *23.5 knots*. Except for runs *4* and *5*, the tests would be considered as "*high speed*." Calculated parameters are shown in **Table A1.2**.

**Table A1.2** – *Calculated run parameters.*

| Run | 1 | 2 | 3 | 4 | 5 | 6 | 7 |
|---|---|---|---|---|---|---|---|
| Speed (kn) | 12 | 15 | 18 | 6 | 6 | 23 | 23.5 |
| Fr$_h$ | 0.88 | 1.1 | 1.32 | 0.44 | 0.44 | 1.69 | 1.73 |
| Fr$_L$ | 0.77 | 0.97 | 1.16 | 0.39 | 0.39 | 1.48 | 1.51 |
| H$_m$ (mm) | 180 | 210 | 180 | 70 | 60 | 120 | 120 |

g. The wake traces of Fig. 5 (high-speed, super-critical) show features of a super-critical wake trace, but in relatively deep water; to the point where it could almost be considered as a deep water, high-speed trace. The leading wave period is around *4.1 s* and the period of the maximum wave is around *2.4 s*. This corresponds to the equations that the leading wave period is around $1.53\sqrt{L}$ (*3.9 s*) and the period of the maximum wave is about *60%* of this (*2.3*

*s*) (Macfarlane *et al.*, 2008). The slightly longer leading wave may suggest a shallow water influence.

h.  Fig. 7 is interesting. It shows the sediment suspension time for each of the seven runs. Run *1*, *6* and *7* have particularly long elevated suspension profiles. Runs *4* and *5* (at *6 knots*) show very minimal profiles, even though the length Froude number is approaching hull speed. Most interestingly, runs *2* and *3* (*15* and *18 knots*) are similar but notably lower than runs *6* and *7* (*23* and *23.5 knots*). However, runs *2* and *3* have maximum wave heights of *75%* and *50%* respectively higher than those of runs *6* and *7*, suggesting that wave height alone is not an erosion mechanism. This is further reinforced by Table 4 of Bauer *et al.* (2002), which shows the two erosion estimate methods. Taking run *3*, it has similar or slightly lower calculated erosion rates than runs *6* and *7*, yet the wave height in run *3* was *50%* higher than in runs *6* and *7*. Run *2*, which has the highest wave height (*175%* that of runs *6* and *7*), shows higher predicted erosion rates. Similarly, run *1* has the same wave height as run *3*, yet it has more than double the predicted erosion rates. Clearly, wave height is not an indicator of erosion rates.

i.  There is the note that some of these erosion processes may be accretive by nature, but because the erosion results in turbidity and there was a background current, the sediment ended up somewhere else before it settled. Erosion is therefore taken to mean movement away from the initial position. Boat traffic would be approximately even in both directions and therefore any longshore movement would average to zero over time. The exception would be at the start and end of speed zones. Longshore drift and accounting for the obliqueness of the incident waves may not be important to consider.

j.  **Figure A1.1** highlights two points relevant to small craft and to erosion:

   a.  **Figure A1.1 Left** – $H_m$ against $Fr_L$: note that the height of the maximum wave peaks well above the usual position of $Fr_L = 0.5$. Planing craft experience a peak in specific resistance in the transition between semi-displacement and semi-planing speeds, or around $Fr_\nabla \sim 1.5$. For typical recreational vessels with slenderness ratio about *4.5* to *5*, that would give $Fr_L \sim 0.67$ to $0.70$. This must always be considered when small craft are being evaluated, though in practice it makes little difference with their wide speed range. The vessel used in the test was not identified, except that it was *7.5 m* overall length. If the laden displacement was an estimated *2.5 t*, the peak in wave height would correspond with the semi-displacement/semi-planing regime.
   b.  **Figure A1.1 Right** - $H_m$ against erosion rate: As with the Gordon River elevated turbidity trials, wave height is a poor indicator of propensity to cause erosion. All that can be said is that there is a general trend towards increased erosion with increasing wave height.
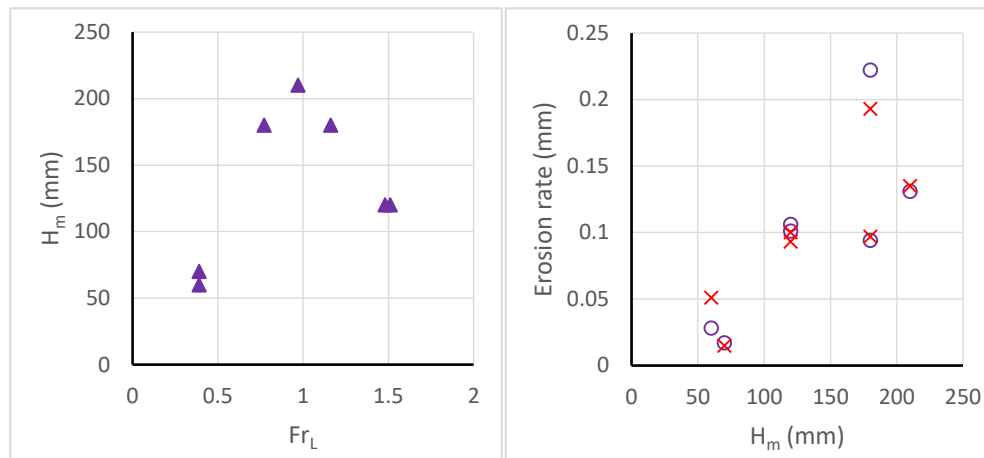
**Figure A1.1** – *Test parameters derived from Bauer et al. (2002). The two data sets in the right-hand figure represent different erosion rate calculation methods.*

**Appendix A2** - *Field and Laboratory Investigation of High-Speed Ferry Wake Impacts in New York Harbor.*

Bruno, M.S., Fullerton, B.J., Datla, R. and Rogowski, P.A. (2002). Field and Laboratory Investigation of High-Speed Ferry Wake Impacts in New York Harbor. Center for Maritime Systems, Davidson Lab., Stevens Institute of Technology, Hoboken N.J. (reproduced in *The Proceedings of Hiper '04*).

The premise of this investigation was the growth in high-speed passenger ferry traffic in the New York area and its impacts on shorelines and marinas/structures. Many shorelines away from the CBD and towards residential boroughs serviced by the ferries are not armoured.

The study was divided into two parts: field observations of existing vessels and model testing. The authors claim a degree of validation between the two, though provide no explanation of how this was achieved, particularly in light of the lack of any correlation between measurement techniques. The best that could be said is that waves were measured in both instances, but without the degree of standardisation of test procedures required for comparison.

As with many similar papers, the importance of wave period was stated at the outset, discussed in general and then generally disregarded in favour of discussion of wave height alone.

### Section: Field Observations

*Test 1 – July 2002*

This consisted of setting up two pressure gauges, one in *11 m* water depth approximately *100 m* seaward of a pier head and one in *4 m* water depth inshore of the pier head, nearby to a ferry terminal. Records were taken over an eight-day period and presented as eight-day graphs of water surface elevation and a corresponding histogram of wave periods, grouped into half-second increments. Of note:

a.  wave height peaks corresponded with traffic peaks, as would be expected;
b.  a comment regarding increased wave heights at the inshore gauge was made: "*the inshore gauge typically recorded wave heights between 5% and 10% higher than the offshore gauge, likely because of the effect of shoaling and/or wave reflections from the shoreline.*" Even if the shoreline was *100%* reflective, it is unlikely that increased wave heights in the shallow water would be due to reflections. Any waves undergoing reflection would have also undergone height attenuation, so the reflected waves passing the inshore gauge would have to be lower in height than initially recorded at the offshore gauge. It is also unclear whether the reflected waves would have consistently passed through what remained of any incident waves and consistently positively superimposed. A *0.3 m*, *3 s* period wave in *11 m* water depth would initially lose *5%* of its height in *4 m* water depth before increasing due to shoaling in shallower water. That is common for all waves, which initially attenuate due to a slight increase in group celerity as they move to transitional depths. What was not explained is that New York Harbour has a *2.5 m* tidal range, so it is possible that the water depth at the inshore gauge could have been as low as *1.5 m*. Even then, *3 s* period waves would not shoal appreciably;
c.  the discussion highlights a consistent wave wake analysis problem of reporting wave heights and wave periods, but not necessarily for the same wave. Averaged or maxima of wave height and period are misleading in an analysis if they do not correspond to the same wave;

193

d.  a comment was made regarding correlation between wave period and the effects of wave wakes on infrastructure and marinas. Wave period was further described for *Test 2*, then never discussed in quantified terms. It was only once discussed in (unqualified) terms in the laboratory analysis.

### Test 2 – July 2004

This was similar to the first test - near a ferry terminal in an unknown water depth. As with *Test 1*, water surface elevations were corrected for tidal fluctuations, but the actual water depth during the recording period remains unknown.

It is noted that some of the records involve superposition of multiple vessel wakes. Both sets of field observations highlight known deficiencies in this style of analysis, in that incidental wake measurements are essentially useless for understanding wave wakes, given that vessel parameters, vessel speeds, lateral separation between vessels and gauges, water depth at the vessels and gauges, wake signatures for individual vessel, and conditions of acceleration/deceleration/manoeuvring were not reported. The only use for such records is in defining a time-delineated climate of all wave sources at a particular location, making the records site-specific and therefore not transferable to another location.

Lastly, a comment was made that "*a computer modelling effort is underway to examine the wake generation characteristics of each vessel type under the observed speed and water depth conditions.*" This is an unusual statement. The sentence prior, describing a one-hour wave height/period/energy record (Fig. 4 of the paper), claimed "*the figure does not indicate the type and speed of the ferry in each instance, although those records do exist.*" How would the computer modelling model "*observed speeds*" that were not observed and, even worse, could be expected to be non-steady-state in and around a ferry terminal? The rhetoric and the methodology do not coincide.

### Section: Laboratory Studies

This is the point where useless field observations are backed with useless model tests.

The wave wakes of four vessels were tested at the Davidson Laboratory High-Speed Towing Tank, which is similar in size to the AMC's towing tank. The four vessels were models of actual ferries and proposed vessels. Wave wakes were recorded at fixed lateral separations of *3 ft* and *5 ft*, corresponding to approximately *0.5-0.57LOA* and *0.85-0.95LOA* respectively (only "*length*" was recorded, which from a literature survey of the fleet is most likely to be the overall length). Additional tests were conducted with dynamic trim control to model the effects of running trim at transition and high speeds.

Model wave wake records in the very near field (*<1L*) are known to be fraught with problems relating to local interactions, lack of sufficient packet dispersion (in deep water), and model-scale spray contamination. That would certainly be an increased risk with planing monohull forms. Except in specific circumstances, the AMC does not conduct wave wake experiments in its towing tank and has not done so to any degree since the model test basin was established in 2001.

In at least one case, vessels were incorrectly identified (with reference to a non-existent *71 ft Monohull "Sea Otter"*). Almost four pages of tabulated run/speed/wake heights were presented, but corresponding periods were not tabulated.

## Section: Results and Discussion

The discussion claimed that "*the wake heights and periods found in the field measurements agree qualitatively with what was observed during the physical model tests,*" yet results were not offered in either comparable qualitative or quantitative form. How is it possible to compare field test wave heights when distances off could have varied several hundred percent, speeds were not recorded, depths were not recorded, and vessel parameters were not recorded? How is it possible to compare the statistical representation of a histogram of wave periods over an eight-day timeframe against near-field, model test wave periods that were not presented?

Comments were made about peaks in wave energy at dynamic transition speeds (assumed around $Fr_L = 0.5$) and how transit times through this speed range were to be minimised. This is well-known advice. However, it was also stated that wave energy reduced at high speeds, with the inference that operation at high speeds was desirable and probably acceptable; but ignoring the fact that wave energy is shifted into longer-period waves, and it is these waves that cause problems for shorelines and structures.

The comment "*the largest amount of wake energy created per unit time occurs during the transition from displacement to planing mode*" is a statement of wave power, yet there is no quantification or qualification of the use of wave power anywhere else in the document. Also, it is incorrect to attribute the peak in wave energy in the transition range from slow to high speeds to a transition from displacement to planing mode, since all vessels will exhibit this tendency to a degree, regardless of hull form. Planing hull dynamics can exaggerate the effect, but that is a mechanism that must be considered separately since it doesn't necessarily occur at the same non-dimensionalised speed. All vessels experience a specific resistance peak at $Fr_L = 0.5$, but planing craft can experience an additional resistance increase in the pre-planing condition $\sim 1.0 < Fr_{\nabla} < \sim 2.0$.

"*Wave shoaling is taking place during at least some stages of the tide in the shallowest areas of the shorelines, some of which contain marinas. Deepening (dredging) these specific areas has the potential to reduce wave heights by 30% in some of the shallowest regions. Deepening by itself will not completely mitigate any wake problem in this harbor, but should be considered part of the total approach.*" It would be expected that marinas would be in water deeper than around *2 m* at low water, so a wave of *0.3 m* height would need a corresponding wave period in the order of *5 s* for shoaling to be evident at this depth. That underlines the problem of reporting wave heights and wave periods separately. Except in exceptional circumstances, dredging could never be considered as a viable means of mitigating wave height. The concurrent economic, environmental and regulatory constraints make it a highly unattractive option.

Comments regarding overly-reflective shoreline structures are noted. Similar comments were made in the Puget Sound studies of the *POFF* (*passenger-only fast ferry*)[105], where much of the shoreline erosion was attributed to landowners building reflective seawalls to delineate their land

---

[105] Golder Associates Inc. (2013).

195

from the beach/tidal zone, maximising land area and hence utility. The incident waves entrained beach material and the reflected waves carried it offshore.

The difference between the wakes and the individual waves were incorrectly identified by the statement "*the length of ferry wakes is in general significantly longer than the length of wakes associated with even larger, slow-moving (displacement-mode) vessel operating in the Harbor. It is this large wavelength . . .*" The "*wake*" describes all waves and so referring to the "*length of ferry wakes*" would describe the time record of the propagation of all waves in a wake, not individual waves.


**Section: Recommendations**

"*Assign the most efficient hull forms to the most wake-sensitive areas.*" Apart from lack of a quantitative definition of what a "*wake-sensitive area*" is, there is no corresponding definition of what is an "*efficient hull form.*" Rather than promote "*efficient hull forms*" as a solution, it would have been better to define how to achieve it. The principal feature of an efficient hull form is one with the lowest laden displacement, which in turn encourages design features such as multihulls (to maximise deck area and stability while minimising weight) and lightweight construction. The models tested were typical of traditional New York ferries and would not be regarded as lightweight or efficient by Australian standards. The paper has a strong and increasing inclination towards mitigating wave height, and if that becomes the driver of efficiency it will ignore the shift in wave energy to longer-period waves.

A recommendation was made against blanket speed restrictions, on the basis that it could increase the height of wakes from vessels intended to operate efficiently at high speeds. That partly acknowledges the fact that speed restrictions should be relative to length, but it ignores the wave period generated at high speeds.

Overall, the paper adds almost nothing to the discussion and the science, and in some instances, it sets them back.

Hill, D.; Beachler, M.; Johnson. P. (2002) "*Hydrodynamic impacts of commercial jet-boating on the Chilkat River, Alaska.*" Pennsylvania State University Report on behalf of the Alaska Department of Fish and Game, Habitat and Restoration Division.

The Chilkat River in Alaska is used principally by tourism operators and government vessels, with fewer recreational users. The tourism operators use open, flat-bottomed vessels of lengths around *6-10 m* carrying up to thirty passengers. They are propelled by jet outboards – a variation of a normal outboard motor that has a pump unit rather than a propeller. The government vessels are smaller and lighter, but of similar form.

The authors were from the Department of Civil and Environmental Engineering at the Pennsylvania State University. Their understanding of the shoreline dynamics unfortunately exceeded their understanding of vessel wave wakes. No distinction was made between deep and shallow water wakes, except that critical speed zones based on length and depth Froude numbers were correctly identified. A most notable source of inconsistency was the variation in water depths at the sailing line and measurement points, varying from *0.45 m* to *1.5 m* and *0.3 m* to *1.1 m* respectively.

## Section: Report Conclusions.

Several of the conclusions warrant comment:

*"Turbidity measurements at the banks clearly demonstrate that boat wakes are capable of dislodging sediments from the banks. Peak values of suspended sediment concentration far outweigh the ambient load of the river and are found to increase with increasing wake height."*

Although wave period was measured and discussed in reasonable detail, there was no attempt at correlation between wave period and measured erosion.

*"Boat wakes are found to increase in amplitude with increasing boat size. Measurements suggest that the wake train of the largest commercial boat studied contains roughly 10 times the energy of that of the smaller ADFG boat studied."*

The first statement is very simplistic; a longer but lighter vessel may contradict this. The energy comparison has been invalidated by the lack of consistency in measurement. The installed power of the smallest vessel was *50 hp* and the largest vessel was *300 hp*. Engine power should be somewhat representative of the wave energy. The probable reasons why it appears not to be are the failure to record actual power at trials (as opposed to nominal engine rated power) as well as properly account for differences in water depth, lateral separation and vessel speed. For the largest vessel, *COM32*, calculated total wave energy ranged from *580 J/m* at *26 mph* and *5,440 J/m* at *14 mph*, at different displacements. How the total wake energy of the largest vessel could be judged as containing "*roughly 10 times the energy of that of the smaller ADFG boat studied*" is unclear when there was a ten-fold energy variance for the *COM32* vessel alone.

*"While there is a well-known dependence upon boat speed (confirmed by the controlled measurements), boats navigating the upper Chilkat River tend to travel in a fairly narrow band of speed. This is largely due to the necessity of keeping the boats 'on-plane', or 'on-step'. Given the*

197

*shallow water depths, these speeds (15 – 25 mph) correspond to high depth- and length-based Froude numbers. This is beneficial in minimizing wave heights at the banks."*

By the time of report preparation in 2002, critical depth and length speed zones were well understood, and the authors had referenced several past papers highlighting that (Parnell and Kofoed-Hansen, 2001; Stumbo *et al*., 1999; Kirkegaard *et al*., 1998). What was also known at the time, but apparently ignored, were the detrimental effects of shallow water wave wakes. That may be partly due to the fact that many shallow water ferry studies were concerned with navigation and wave safety issues, and not necessarily erosion - the exception being the New Zealand studies of Parnell.

Test Series *5* was conducted for one vessel in water just *0.45 m* deep at the sailing line, giving $h/L\sim0.1$. Such an extreme condition would result in most of the wake energy (as much as *90%*) being contained in the first wave, and the linear wave theory used to calculate the wave energy would not be entirely accurate.

*"Boat wakes are found to decrease in amplitude with sailing line-to-bank distance. An equation is obtained which allows for the prediction of expected wave height at the bank as a function of boat size and sailing line distance. If a maximum allowable wave height at the bank is specified, this allows for the calculation of a minimum sailing line distance."*

The first statement is poorly worded – the decrease in amplitude comes with increasing lateral separation and has nothing to do with the bank position. The same effect will occur in an unbounded waterway.

The equation derived to predict wave height as a function of boat size and sailing line distance is questionable. Firstly, the equation was derived from Fig. 6.3, reproduced below as ***Figure A3.1***. Apart from the high degree of data scatter, the authors noted from Nanson *et al*. (1991) "*that bank impact increases significantly beyond the threshold of $H_{max}$ ~30 cm*." The difference between estimated and recorded wave height is up to around *50%* in some instances, which is hardly ideal when working to thresholds.



Figure 6.3: Non-dimensional maximum wave heights, as function of non-dimensional distance from sailing line to shore.
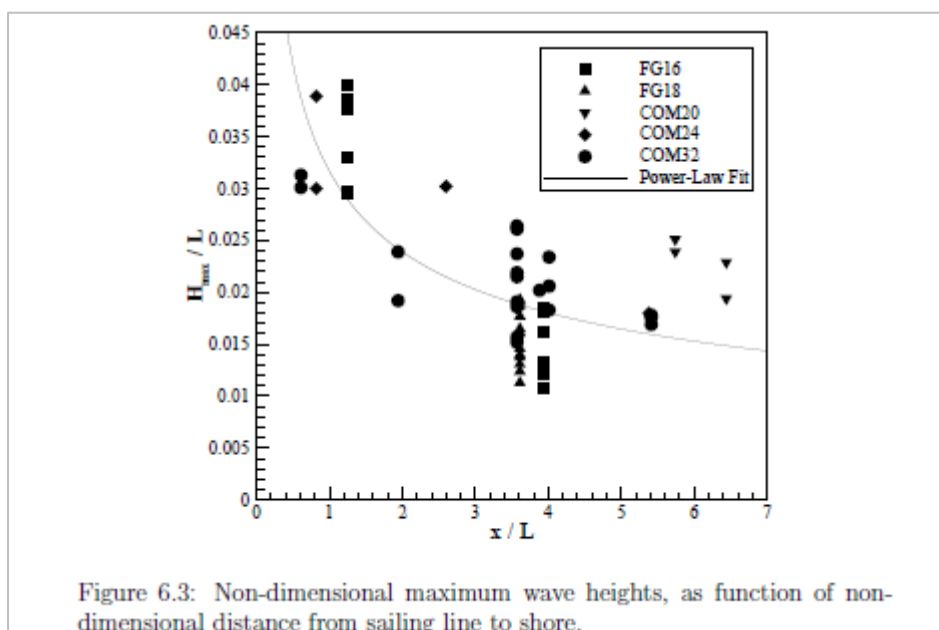
**Figure A3.1** *– Fig. 6.3 reproduced.*

198

Secondly, the scatter would suggest the relationship used to normalise the data, in this case $H_{max}/L$, may not be the most appropriate, or even relevant. This is further demonstrated in Fig. 6.2, reproduced below as **Figure A3.2**. No reasonable engineering conclusions could be drawn from these diffuse patterns.



Figure 6.2: Non-dimensional maximum wave heights, as functions of depth- and length-based Froude numbers, for all boats studied.
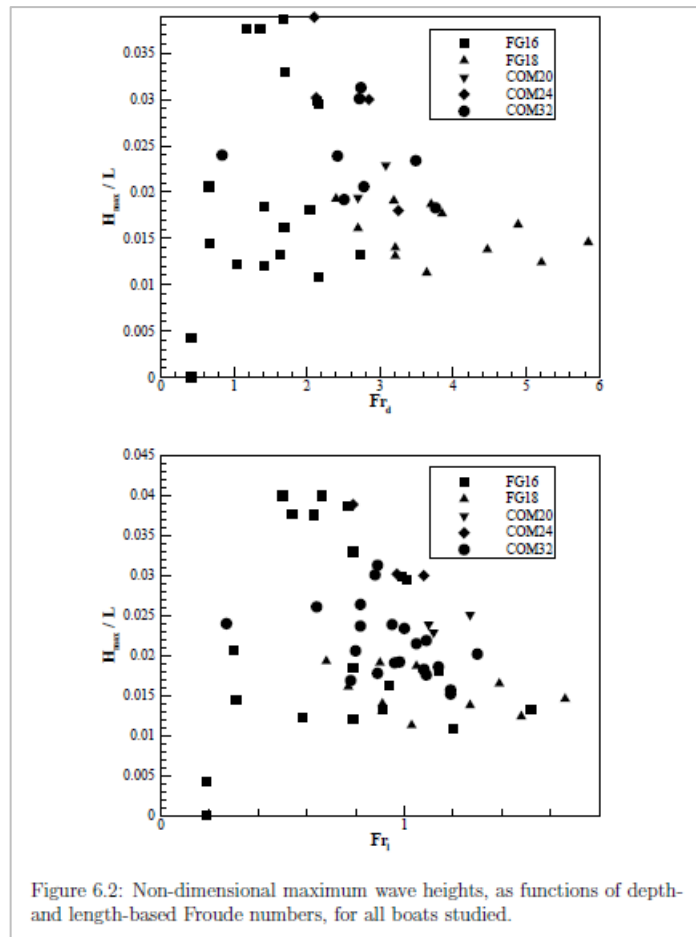
**Figure A3.2** – *Fig. 6.2 reproduced*.

**Section: Recommendations**

The report recommendations can be summarised as:

- stay as far as possible from shorelines to minimise wave height at the shore, even though it was recognised that this was not always possible due to navigational constraints;
- avoid depth and length critical speed regimes;
- when the water level is low and the lower banks (beneath the consolidating vegetation root mat) are exposed, further operational consideration is required (but not specified).

These are quite simplistic, to say the least. There are no specific recommendations pertaining to vessel dimensions, maximum displacement or correlation with wave period, vessel dimensions and erosion potential.

One interesting point of discussion is the relative influence of vessel wakes on the erosion of vertical banks. A simplified method of analysis was proposed based on laminar flows, where the

199

vertical velocities of standing waves produced at impact were converted to a shear stress on the bank. This was then compared to the shear stress induced by the streamflow itself and was found to be of the same order of magnitude where streamflows were more energetic, and two orders of magnitude higher in low energy reaches. When the turbulent boundary layer of the vessel wave impact was accounted for, the shear stress was said to increase by thirty times, in which case the effect of vessel waves would be greater than that of the streamflow, even if the wake duration was shorter.

The simplified method would have some applicability to sheltered rivers in Australia often not subjected to large or regular flood events and with cross-sections of a U-shaped profile.

Maynord, S. T. (2005). Wave height from planing and semi-planing small boats. *River Research and Applications, Vol. 21*. 1-17.

Stephen Maynord worked for the US Army Corps of Engineers, which has sponsored similar investigations in the past. This 2005 paper includes the results of a previous study published in 2001. A series of *400* full-scale tests were conducted on small craft to develop relationships between principal vessel parameters (length, displacement, speed, deadrise and lateral separation) and the wave wakes produced.

## Section: Boat Wave Characteristics

Although the author has a distinguished background in coastal engineering, the title of the paper clearly limits the focus to wave height alone. Certainly by 2005 it was well understood that wave parameters other than just wave height were important to the overall understanding of wave wake effects. Wave period is first mentioned in the context of vessel wave characteristics, where it is defined as "*the time it takes for two successive wave crests to pass a given point*." In coastal engineering, where mean water levels in a wave field are impossible to determine accurately, measuring crest to crest may be reasonable. For vessel wake waves, measurement is best taken between corresponding zero crossing points rather than crests, since successive crest elevations usually vary and superposition of different waves (divergent and transverse) can exaggerate crest elevation.

Maynord's Fig. 2 gives detailed packet-wise wave period variation at three different lateral separations. This is the only presentation of wave period data and there is no subsequent discussion or analysis. Four comments can be made:

a.  the period of the maximum wave is constant, as would be expected of a propagating deep-water packet where the maximum wave represents the envelope maximum, which propagates at the characteristic wavenumber (hence constant wave period). This was not commented on;
b.  the first graph of Fig. 2 (at $y = 9.1\ m$) clearly shows several waves that are most likely part of the transverse system, with constant period. The speed was not recorded, but must have been sufficiently modest to allow the formation of transverse waves;
c.  it becomes increasingly difficult to accurately delineate the long-period leading waves at increasing lateral separations, especially from field trials;
d.  although Maynord provides a specific definition of wave period as being between successive crests, he chose to measure half wave periods from trough to crest and vice versa, even though the exact positions of crests and troughs are ill-defined compared to zero crossing points. It may seem a pedantic point but creating and following consistently standardised measurement techniques is important for the integrity and future application of the study conclusions.

The two height parameters selected for analysis are MAXPOW – the wave height generated at the maximum power of the motor, and MAXWAV – the maximum wave height measured at any speed over the operating speed range. Superficially, both would appear reasonable parameters to

measure, but even modest consideration would suggest they are misleading and potentially useless.

MAXPOW was intended to be representative of the maximum wave height at high speed, but under the limiting engine power condition imposed on vessels operating on the Kenai River in Alaska. That condition was imposed for safety reasons, not environmental reasons, though does demonstrate the limited effectiveness of speed limits (helmsman controlled) as opposed to design limits (through power limits) unless speeds are strictly policed. Speed limits are nominal; power limits are absolute.

There are, though, positive and negative consequences of limiting power. The positive consequence is that owners are more likely to opt for a smaller, lighter vessel to achieve better performance, which in turn is more likely to result in smaller waves (though not always). The negative consequence is that owners willing to sacrifice speed for a larger, heavier vessel risk operating at speeds barely into the high-speed range and therefore generating higher wake waves. From the *35 hp* engine power limit noted by Maynord and vessel particulars provided (though not necessarily for Kenai River vessels), the lengths and weights would appear to be well in excess of what would be expected with just *35 hp* installed power. Maynord claims that some of the larger vessels tested at the power limits of *35* and *50 hp* were potentially operating in a semi-planing mode, though the results presented show that all were able to operate in a fully planing condition, even with reduced power.

In discussing vessels and wave wake mechanics, Maynord makes statements that are misleading:

*"Diverging waves form at the bow and stern of the boat at an angle that depends on the vessel length Froude number."*

This is misleading, in that the shape of the classical Kelvin wave pattern is independent of vessel form and speed. Rabaud and Moisy (2013) demonstrated that the Kelvin angle does contract at high speeds, at least when describing the highest waves, but their paper was published a decade after Maynord's.

*"Planing boats operate in three modes as shown in Figure 1."*

Maynord's Fig. 1 (reproduced as Figure A4.1) overlays the usual speed-dependent maximum wave height curve with planing hull dynamics. This common misconception is also found in other references, such as Ozeren *et al.* (2016), who also managed to mesh this misconception with depth effects as well. Any hull form, whether planing or not, will produce a maximum wave height relationship with speed the same as Maynord's Fig. 1. Planing dynamics have specific definitions and should not be directly substituted with length Froude number dynamics, even if the effects are similar.

Maynord refers to the wave height peak (Fig. 1, point A) as the *hump*, which is a term often used to describe the transition mode between displacement, semi-planing and planing regimes. Again, this is a mix of normal hull dynamics with planing hull dynamics. This is demonstrated by the statement that "*MAXWAV is difficult to measure and MAXWAV data have considerable scatter.*" The difficulty of measurement and the data scatter suggests strongly that there are several distinct hull dynamic mechanisms involved, and they don't always coincide at the same speed.

Figure 1. Wave height versus speed trends in small planing boats
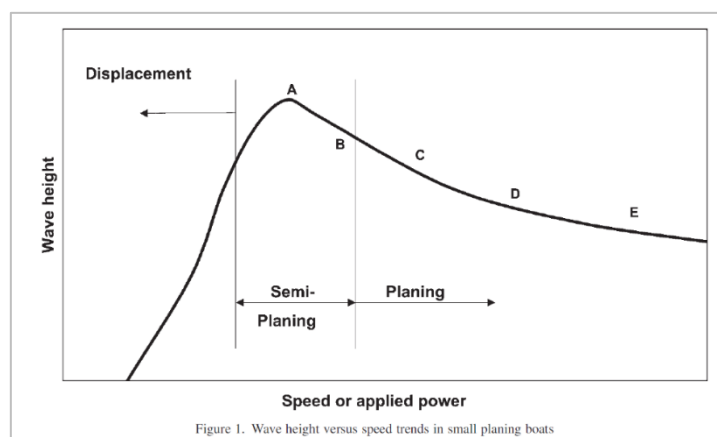
**Figure A4.1** – *Fig. 1 reproduced*.

*"Figure 1 shows the general trend of maximum wave height versus boat speed (equivalent to applied power)."*

As a simplified statement intended for an audience with limited technical understanding, such as marine regulatory authorities, most vessel designers and the general public, this is reasonably descriptive. As a technical explanation it is flawed. The implication is that increasing engine power to increase vessel speed will result in smaller waves and hence fewer environmental problem. The flaw in the argument is that the overall wake energy may not decrease as much and taking just one component wake wave and measuring with just one parameter does not reflect the overall effect. In conclusion to their experiments, Ozeren *et al.* (2016) stated that *"At planing speeds, even though the maximum wave height is lower than the critical value, the measured turbidity increased."* Reducing the maximum wave height by operating at higher speeds does not necessarily lead to reduced environmental impact overall – all it does is reduces the impact compared to other damaging speed regimes ($Fr_L \sim 0.5$, $Fr_h \sim 1.0$).

**Section: Previous Studies**

Maynord presents the results from past studies, including those of Zabawa and Ostrom (1980). Fig. 3 shows a basic lack of understanding of ship design, with the maximum wave heights for different vessels at different lateral separations plotted against vessel speed, ignoring scale relationships. Apart from a general statement of trends, the fact that the equations for the seven curves shown have different constants and exponents is a principle failing of Maynord's later approach, in that regression analyses are pointless if the resulting equations are specific to particular vessels and particular conditions.

Maynord's eqn. (3), taken from Bhowmik's 1975 paper, shows the importance of non-dimensionalising parameters such as lateral separation, though vessel speed is absolute. All of the quoted studies attempt to derive equations for wave height, but without consistent methods and definitions the equations remain specific to the vessels tested and cannot be applied to other vessels.

## Section: Summary of Results for Wave Height

Throughout the document there are several statements about the relationship between vessel length, wavelength and water depth, as well as the importance of conducting experiments and measuring waves at a depth at least half the vessel's static waterline length. That would concur with the calculation that wave measurements down to around $0.5L$ are equivalent to deep water.

Six results from the field trials are summarised. Five warrant comment (the numbers correspond to those in the paper):

(2) MAXPOW (wave height at maximum engine power) was different for all four vessels tested and the ranking (WP, KF, KL and LW) confirms that slenderness ratio is the principal wave height parameter at high speeds. Also, differences were greatest at the lowest engine power (*35 hp*) – a result expected since the larger, heavier vessels were more adversely affected by insufficient engine power than the smaller, lighter vessels. It was unfortunate that neither of these findings were related back to the science and were stated as though they were new findings rather than confirmations of known relationships.

(3) MAXPOW and MAXWAVE decrease with increasing distance from the boat. It is unclear why this was even stated in a technical paper.

(4) MAXPOW decreases with decreasing load. This is a recycled version of item (2).

(5) MAXPOW decreases with increasing power for the three largest vessels but was insignificant for the lightest vessel. Increased power meant increased speed and that resulted in the expected trend of reducing wave height with increasing speed. The lightest vessel operated at the highest volumetric Froude number where increased speed resulted in minimal changes to wave height.

(6) The V-hull boats (WP and KL) caused larger MAXPOW than the flat-bottomed boats (KF and LW). That contradicts item (2), where deadrise was not prominent in the MAXPOW results. It's possible that the intended message was that, for equivalent length and weight, V-hull boats produce higher waves than flat-bottomed boats.

The general summary was therefore reduced to a confirmation of known relationships, conflicting arguments and over-simplifications of the science.

## Section: General Equation for Boat Wave Height

From this point forward, the analysis degenerates into a regression analysis. Although regression analysis is a common technique in ship design, it is one that should be used cautiously as the underlying implication of its application is a limited understanding of the science. Poorly considered parameters for analysis can result in relationships between variables and outcomes that are inconsistent with what may otherwise be expected.

For instance, Maynord states that hull draft was eliminated as it varied along the hull (due to running trim) and varied with speed. Instead it was "*reflected in $\nabla$.*" That is true, but what is not reflected in this approach is deadrise angle. As a crude example, a flat-bottomed boat would have about half the draft of a V-bottomed boat at the same displacement if the V-bottomed boat's chines were at the waterline. Maynord's eqn. (3) and (4), reproduced from past papers by Bhowmik (both of which are well referenced in the field), show a strong relationship between wave height and vessel draft – linear at displacement speeds and non-linear (exponent of *0.355*)

204

at higher speeds. Even in the high-speed case, doubling the draft according to Bhowmik would increase wave height by *28%*. Maynord later proposes a deadrise correction that would increase the wave height of a V-bottomed hull by *22%* compared to a flat-bottomed hull but does not define how the correction varies with deadrise.

It is also interesting to note that slenderness ratio is noted, yet never features in the analysis even though it has been shown to be a principal determinant of wave height at high speed. Instead, Maynord elects to eliminate length and beam by developing equations for each individual boat based only on speed, displacement and lateral separation. That becomes the fundamental flaw of the paper, as there is nothing that links all four vessels in such a way that a general equation could be applied to all vessels. It may be that a single equation of sufficient accuracy does not exist and increasing the number of parameters may only increase the data scatter. The equations are in the form of:

$$\frac{H_{max}}{\nabla^{\frac{1}{3}}} = const.(Fr_\nabla)^{exp1}\left(\frac{y}{\nabla^{\frac{1}{3}}}\right)^{exp2} \hspace{2cm} \text{[A4.1]}$$

For the four vessels tested, the constant varied from *0.71* to *1.08*, $exp1$ varied from *-0.46* to -*0.795* and $exp2$ varied from *-0.39* to *-0.44*. Only $exp2$ was reasonably consistent. The others demonstrate that the equations are vessel specific and otherwise difficult to apply elsewhere.

Maynord takes an interesting approach to lateral separation by using $\nabla^{\frac{1}{3}}$ rather than static waterline length to non-dimensionalise it. This is a technique borrowed from planing hull dynamics, where waterline length can vary substantially with increasing speed but displaced volume (inter-related with lift when dynamic) remains constant. It would be interesting to see if this approach worked with other collected data for planing craft.

In an attempt to unify the results for all craft into a single equation, Maynord uses the derived equation for each vessel to produce a set of wave height curves for a fixed vessel displacement and lateral separation, with the independent variable being displacement Froude number.



Figure 9. Comparison of Kenai River and Boston Whaler boat wave equations versus displacement Froude number at same distance from boat and same total boat weight
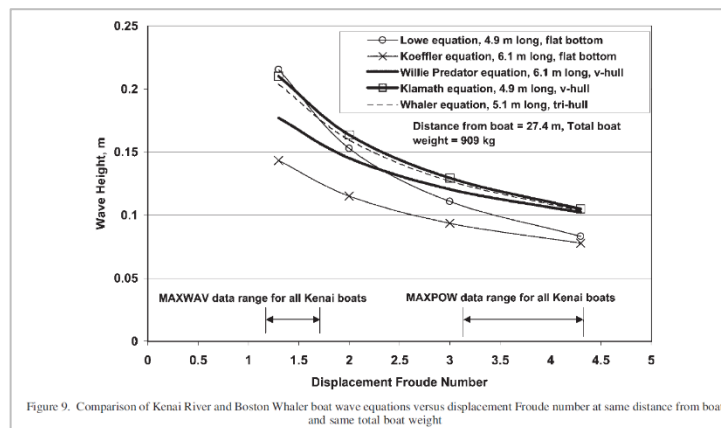
**Figure A4.2** – *Fig. 9 reproduced*

In this figure, data from Zambawa and Ostram (1980) was used (the *Boston Whaler* vessel), though data for the *Uniflight Cruiser* from the same report was discarded as it was considered to be too different from the nominal boat weight of *909 kg*. It's quite probable that, after correction, the data never followed the same pattern.

Maynord makes an observation for vessels in the planing mode that "*boat length has a lesser effect than hull shape on planing boats, with the 6.1 m boats producing slightly smaller waves than the 4.9 m long boats*." That directly conflicts with item (2) of the *Summary of Results for Wave Height*, where the longer (and heavier) vessels were said to produce the highest waves. It is known that the resistance of planing craft operating at fully planing speeds ($Fr_\nabla > 3.35$) becomes insensitive to length, with shorter hulls becoming progressively more efficient at higher speeds (though due to running trim and wetted area dynamics).

If the data in Fig. 9 (Figure A4.2) were corrected for $y/L$ rather than $y/\nabla^{1/3}$ (hence a constant, since the assumed lateral separations and displacements are constant), the curves would be further scattered vertically. A single equation is offered (Maynord 2005, Eqn. 16), in the form:

$$\frac{H_{max}}{\nabla^{1/3}} = C(Fr_\nabla)^{-0.58} \left(\frac{y}{\nabla^{1/3}}\right)^{-0.42}$$

[A4.2]

The coefficient $C$ accounts for deadrise and varies from *0.82* for flat-bottomed boats to *1.00* for V-bottomed boats, though with undefined deadrise. The equation is applied to past data and quite reasonable correlation is demonstrated, the only deviation being due to possible influence of shallow water during some tests. Moreover, the wave height in [A4.2] varies according to $H \propto \nabla^{0.57}$ and $H \propto V^{0.58}$. The relationship between height and vessel speed may be reasonable, but the relationship between height and displaced volume contradicts previous findings. Cox (2000) showed that wave height was directly proportional to displacement (or displaced volume) for model *AMC 99-17*, taken from deep-water tests with a *50%* variation in displacement. The deviation from linearity was a maximum of *2%*.

In its basic form, the test for [A4.2] is that it should remain valid when scaled from model scale to full scale. In that case, $\nabla^{1/3}$ can be replaced with $L$, $Fr_\nabla$ is constant and so the equation scales properly.

However, there remains the fundamental problem with all regression analyses that they are only applicable to the data from which they were derived and may not transpose to other vessels. To test this, [A4.2] was applied to model tests for the Rivershuttle at various speeds in deep water, as a more extreme example. The model satisfied all of the applicability criteria, yet wave heights are at least *50%* over-predicted. This is shown in ***Figure A4.3***.

In summary, apart from the inconsistencies and contradictions, the paper is a reasonable attempt. It falls down in three places: lack of proper consideration of wave period (and energy), the lumping together of several different resistance and wave wake regimes into planing mechanics, and its reliance on regression analysis that ultimately derives a predictive equation for wave height which is almost certainly specific to the vessels from which it was derived. This would further justify the statistical, scaled approach of the wave wake database as an alternative, predictive method.
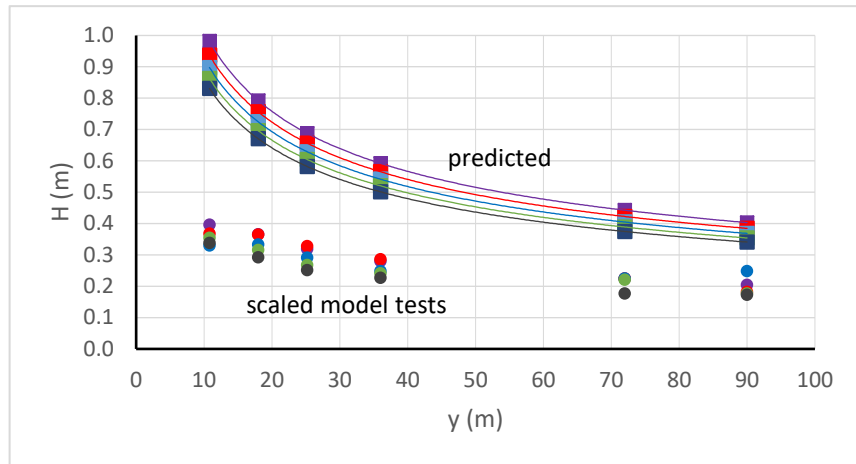
**Figure A4.3** – *Comparison of scaled model test results and predicted results based on [A4.2] for model AMC 99-17. The vessel parameters are within the stated applicability range for [A4.2] ($h/L = 1.22 : 0.66 < Fr_L < 0.88 : 2.21 < Fr_{\bar{V}} < 2.95 : 1.90 < C_v < 2.53$). The predicted wave heights assume $C = 0.82$ (a flat-bottomed boat) and would be 22% greater if the Rivershuttle deadrise of 14 degrees was accounted for. This demonstrates that [A4.2], although dimensionally correct, does not scale.*

**Appendix A5 - *Impacts of Recreational Boating on River Bank Stability: Wake Characteristics of Powered Vessels.***

Baldwin, D. S. (2008). Impacts of Recreational Boating on River Bank Stability: Wake Characteristics of Powered Vessels. Report for the Murray Catchment Management Authority. Murray-Darling Freshwater Research Centre, Wodonga, Victoria.

This report was commissioned by the Murray Catchment Management Authority to estimate the erosion potential of recreational vessel wave wakes on the Murray River. To achieve this, wave probes were set up at four sites along the river with known boating activity, in water depths that would otherwise be considered as very shallow ($0.35\ m \leq h \leq 0.69\ m$). Turbidity readings were taken just below the surface at locations *1 m* and *4 m* from the bank.

Although wakes were recorded and measured, the relationship between wakes and turbidity rested on a visual correlation between wave height and elevated turbidity. The energy of the erosive wakes was compared to the streamflow energy and wind waves. As with other wave wake erosion studies, it was found that the vessel wakes accounted for around *2%* to *5%* of the total energy in the system. Also, the calculated sediment load caused by wave wakes was shown to be a small fraction of the total fluvial load. Consequently, it was concluded that the effect of recreational vessels on erosion rates was minimal.

The report is divided into two parts: determination of wake and turbidity, and estimation of erosion rates. Both would appear to depend on over-simplifications, parameters averaged to the point of incoherence, and questionable logic.

Darren Baldwin has degrees in science and law, and a PhD in chemistry.[106] His principal areas of interest are in changes in carbon and nutrients in aquatic ecosystems. As with many reports on this subject (examples: Fonseca and Malhotra, 2012; Maynord *et al.*, 2008], the investigator lacks a background in naval architecture.

**Section: Executive Summary**
*"The purpose of the current study was to estimate the potential of powered recreational boats to increase bank erosion along the Murray River near Echuca-Moama. In particular the study considers whether wake boats substantially increase the rate of erosion relative either to other boat types or other factors than lead to erosion in this section of the river."*

Wake boats are not necessarily a specific design. Their form is essentially no different to other similar types of recreational craft with planing hull forms, such as ski boats. What makes them different is they have added-on equipment, such as ballast bags and or hydrofoils, that act to increase the displacement (statically or dynamically) and the running trim, and towing points set high to increase the dynamic trimming moment and hence the running trim.

Ruprecht *et al.* (2015) also claim that wakes can be increased through modifications to the hull design, but without providing details or references. Generally, there is little that can be done to the hull design to increase wake heights without affecting performance, form or function

---

[106] https://loop.frontiersin.org/people/93590/bio (last accessed 6th February, 2018)

elsewhere, and changes would be limited to deadrise and length/breadth ratio.[107] The identification of wake boats is discussed further.

The reference to other erosion factors gives the appearance that the study is multi-faceted. Several other erosion mechanisms are mentioned, yet only two are quantified – fluvial flow and wind waves.

*"The amount of sediment suspension caused by boat traffic varied with location and was estimated at between 0.45 and 3.6 kg/ metre of bank/hour in the Echuca region. In comparison, based on background turbidity levels, the total suspended solid load passing a given point in the river was estimated to be 25.4 tonnes/hr."*

This does not compare like-with-like. It implies that the background flow is eroding *25.4 tonnes per hour* when in fact it could be just *25.4 tonnes* passing through from further upstream, or a lesser amount being eroded and in a dynamic exchange, such that turbidity is maintained. This is discussed further in response to the calculation method.

**Section: Introduction**
*"The wake characteristics produced by a vessel will depend on a number of interrelated factors including the displacement of the vessel, the length of the vessel in contact with the water (e.g. whether or not the vessel is on the plane), the speed of the vessel, the shape of the hull and so on (Maynord, (2001; 2005)."*

Maynord is not the best source to extract comments about relationships between vessel wave wake and vessel parameters. Maynord's expertise is in erosion control on a large scale; not necessarily vessel dynamics. Phrases such as "*and so on*" imply the quote has been plucked from the literature without understanding, as though statement alone signifies proof. It would have been far more useful to discuss how the most relevant parameters (length, displacement, speed, water depth and distance off) influence wave wake, but to do that would require the author to have an intimate understanding of these parameters, which he appears not to have. The fact that water depth is not listed here is testament to that, being one of the most influential of the primary wave wake parameters.

*"How much energy is transferred from each boat passage to the bank will depend in turn on how close the boat is to the adjacent shore and the relationship between the wave characteristics produced by the boat passage and the topography of the river bottom (Maynord, 2005)."*

Wave energy is dissipated by internal friction and bottom friction, but both rely respectively on substantial timeframes (several hundred wavelengths) and a generous interaction with the bottom, which itself is dependent on wave height and wavelength. In a riverine environment, almost all a vessel's wave wake energy will dissipate at or near the shore; it cannot magically disappear. What is most important is the form in which the energy is delivered. Energy is a composite parameter. Two waves having the same energy can have different erosion potential.

---

[107] Wake heights have the strongest correlation with displacement and waterline length. Trailerable boats cannot be heavy by design, hence a wake boat's reliance on ballast bags or dynamic means to increase wake height without increasing road weight.

*"This is especially true for newer, high-speed recreational boat designs (wake boats) that, contrary to normal design principles, attempt to maximise the wake produced by the vessel so that a person towed behind the vessel can (potentially) use the enhanced wake for aerobatic tricks."*

Wake surfing seeks to generate high, steep waves. At high vessel speeds, especially in shallow water where speeds are depth super-critical, the waves generated are of a reduced height and steepness. High speed is therefore not a requirement of wake surfing boats. Wake boarding, which is similar to water skiing except that the skier rides a board, does require higher speeds. Moreover, water skiers prefer flatter water and ski in calmer waters behind the vessel where the waves are small or have a long wavelength that reduces their steepness. It is impossible to satisfy all three sets of criteria by vessel design alone, which is why wake surfing boats use ballast and dynamic devices to increase their near-field wake heights.

**Section: Methods**

*"Site 1 was in a no-skiing zone downstream of the Victoria St boat ramp, Site 2 was in an unrestricted boating zone approximately 5 kilometres downstream of Echuca, and Sites 3 and 4 were in zones where vessels speed were restricted to less than 8 knots (≈ 14.5 km/hr)."*

This is one glaring point that is not discussed further in the report. An *8-knot* speed limit is almost certainly going to result in the most energetic wake for a small recreational craft. This would normally occur when $Fr_L = 0.5$ (the point where all vessels experience a peak in specific resistance) and when $Fr_h = 1.0$ (the depth-critical speed that magnifies vessel resistance), but also when $Fr_\nabla \sim 1.75$ for planing craft. The river is described as having "*maximum depths not much greater than 2 metres.*" A typical wakeboarding boat (similar to the report cover photograph) with a static waterline length of around *5.3 m* would experience a peak in resistance and wave wake energy at a speed of *7.0 kn*. The depth-critical speed would be *8.6 kn* in *2 m* water depth and *10.5 kn* in *3 m* water depth. The pre-planing resistance peak would occur at around *11 kn* to *12 kn*. Overall, the speed range to avoid would be about *7 kn* to *12 kn*. Operating just under *8 kn* in *2 m* water depth is going to create substantial wake energy.

Where a blanket speed restriction is recommended, a speed of *5 kn* is likely to be more sustainable in this instance, based on Macfarlane and Cox (2003). A "no wash" restriction is universally accepted as *4 kn*. Part of the problem would appear to be incorrect speed management by the authorities.

*"Wake boat – a boat which was either designed or retrofitted for wake boarding. In the current study any boat fitted with a wake-tower (see cover photo) was classed as a wake boat."*

It doesn't matter what the boat looks like or what accessories it's fitted with; what is important is how it's being used. Wake boarding and wake surfing vessels achieve their aim through passive or active weight and or trim changes. These modifications cannot be visually detected and could be fitted to any vessel, including the paddle steamers.

*"Ski boat - a boat which was designed specifically for towing a water skier. In the current study, any boat (other than a wake boat) that had a rearward facing seat adjacent to the forward steering position (for an observer, a legal requirement for towing people behind a boat) was classified as a ski boat."*

210

It would be better to class a ski boat as a boat actually towing a skier! There are two parts to the wave wake story. The first is the vessel itself and how it is arranged. The second is the operating parameters: vessel speed, water depth, distance off, manoeuvring and acceleration/deceleration. Whether or not it's towing a skier or just transiting the river makes very little difference to the outcome. The skier or wake boarder has its own wave wake, but it is inconsequential compared to the towing vessel (Macfarlane and Cox 2005).

*"Aluminium fishing dingy (also called a tinnie) – Aluminium vessel typically from 10 – 16 ft long fitted with a small outboard motor. Although capable of planning, generally they are run on the semi-plane or in non-planing mode."*

In wave wake terms, a firm high-speed condition for a *10-16 ft* dinghy would be in the range of *10-13 kn* based on length Froude number ($Fr_L > 1.0$) or around *16-19 kn* based on volumetric Froude number ($Fr_\nabla > 3.35$ when fully planing). These speed ranges are easily achievable with modest engine power. Maynord (2005) erroneously merged several distinct wave wake mechanisms with planing craft dynamics, and the interminable citing of his work has meant those errors have become entrenched within the literature.

*"Vessel speed was then categorised as either slow (less than about 15 km/hr), moderate (from about 15 to about 40 km/hr) and fast (greater than about 40 km/hr)."*

In vessel design terms, speed is not absolute. It is always relative to length. A ski boat operating at *7 kn* will generate its most energetic wake in deep water, yet a large ship would generate a small wake at the same speed (blockage aside). This is the primary reason why blanket speed restrictions don't work well. If they are set for a vessel too large, the small craft may operate at their worst wave wake condition. If set too low, the large craft are penalised.

It is most likely that the 8-knot speed limit is an historical navigational limit set for the commercial paddle steamers. These vessels, noted in the report as being around *30 m* in length, would be operating at a length Froude number of $Fr_L = 0.24$ at a speed of *8 kn*, which is quite within the displacement speed range of $0 < Fr_L \leq 0.399$. Operation at speeds up to about *75%* of the displacement speed, or $Fr_L < 0.299$, will incur modest wake waves (Macfarlane and Cox, 2005). The depth effect, however, would remain and would be significant (blockage in the range of *1-3%*, or more in extreme conditions). Although depth effects were known about, it was only with the publishing of Havelock's 1908 paper that the science was formalised. Even so, few operators and regulators understand the science, even today.

**Section: Data Analysis**
The wave train analysis is quite questionable. A lot of the analysis is reminiscent of the approach reported by Nanson *et al.* (1994), which was based on the work of von Krusenstierna (1990) on the Gordon River. Averaging wave parameters is now regarded as being less representative of wakes, if for no other reason than it uses compounding approximations.

As an example, the upper part of Baldwin's Fig. 2 shows a wave trace. Taking the start and end of the trace to be *57.11'* to *57.55'*, the average wave period would be *2.11 s*, yet the period of the maximum wave is *1.60 s*. The very first wave has a period around *5 s*, though not easy to define accurately. If all waves in the trace were included (*57.11'* to end of sample), the average period

211

would be *1.67 s*, which is very close to the averaged value. The maximum wave ($H_m = 0.16\,m, T_m = 1.60\,s$) has a total (linearised) energy of exactly two orders of magnitude more than each of the final thirteen small waves ($H = 0.021\,m, T = 1.20\,s$), so the logic for including these small following waves in the parameter averaging is questionable. Parameter averaging can only be considered remotely viable when subjective reading of the wake trace is removed.

The wake form is what would be expected of a vessel operating at depth super-critical speeds but in water not too shallow. Under these conditions, most of the waves in the trace would not experience any shoaling, except just before breaking.

It is not clear why Baldwin chose energy density and power as the defining parameters. Energy density is essentially *wave action*. The equations quoted were taken from Hill *et al.* (2002), yet Hill *et al.* state "The amount of energy, per unit horizontal area, contained in a wave is given by $E = \rho g\,H^2/8$. To calculate the *actual* amount of energy in a wave, this figure must be multiplied by the wavelength of the wave and by the breadth of the wave." Note the authors' use of italics for "*actual.*"

Hill *et al.* (2002) recognised the need to use energy density in context by converting it to the energy of the actual wave. Baldwin appears to have cherry-picked the science, but without understanding what it meant. As an example of the comparative limitations of energy density, consider that a tsunami wave may have an initial height of *0.16 m*, hence the same energy density as the maximum wave example of Baldwin's Fig. 2. However, its wavelength of several hundred kilometres would give the tsunami immense total energy, compared to the approximately *3 m* wavelength of the maximum wave in Baldwin's Fig. 2 (assumed measurement depth of *0.5 m*). Similarly, the Boxing Day tsunami of 2004 had an initial wave height of *0.5 m*, hence an energy density about eight times that of the wake boat!

Baldwin's use of wave power (Eqn. 2) is correctly applied to the whole wave, with wave celerity being a function of wavelength and water depth. It would have been more appropriate if the term "*specific power per unit length of a wave*" were more correctly described as "*power per unit crest length*," or "*crest width*" as it is sometimes referred to, and not erroneously implied as per unit wavelength. Note that Hill *et al.* (2002) uses the correct terminology "*The power, P, in watts, per unit breadth of wave crest . . .*"

It is not unreasonable to suggest that Baldwin's methodology is not a satisfactory comparative basis. It only *sort of* works because the vessels of interest (excluding the paddle steamers and houseboats) are approximately of the same type, length and speed. In the case of the paddle steamers and houseboats, the longer period waves their longer hulls can produce at high speeds are tempered by their low installed power and hence slower operating speeds.


### Results: Boat Wake Characteristics
*"Total energy density of the wave train produced by wake boats, particularly wake boats that are towing skiers (or their equivalent) was also higher than other vessels in the study (Figure 5)."*


The implication in this statement is that the wake of a boat is increased due to the skiers it is towing, which is essentially incorrect. The AMC has field-tested ski boats with and without skiers and the difference in wake was immeasurable. The following was reported in Macfarlane and Cox (2005) from full-scale trials:

It is most likely that any differences measured by Baldwin would have been due to variations in speed or distance off, neither of which were controlled conditions.

Taking the wake trace in Baldwin's Fig. 2 (upper), the maximum wave ($H_m = 0.16\ m$; $T_m = 1.60\ s$) would be classed as a Stokes second order wave at all the measurement site depths ($0.35\ m \leq h \leq 0.69\ m$). As such, its wavelength is only a function of water depth and wave period, not wave height. The calculated celerity of the highest wave in a wake trace is strongly a function of period, hence vessel speed and waterline length, as is shown in **Figure A5.1** below (Fig. 4 of Macfarlane *et al.*, 2008). Of note is how the period of the maximum wave varies with length Froude number, but stabilises at high speeds.

It is most likely that Baldwin's celerity calculations are skewed by not knowing the relative speeds of the vessels and therefore the comparison is pointless. The report states that "*approximate speed*" was recorded for each passing vessel, but the data was not presented or (apparently) used in the analysis. Also note that "*The wavelength of waves from both wake boats and ski boats that were towing skiers etc (3.1 ± 0.4 and 3.2 ± 0.3 respectively) was shorter than for those vessels without tows.*" When combined with energy density, the peak power of wake boats with and without tows is similar. That further demonstrates that the use of energy density as a parameter for comparison is misleading.
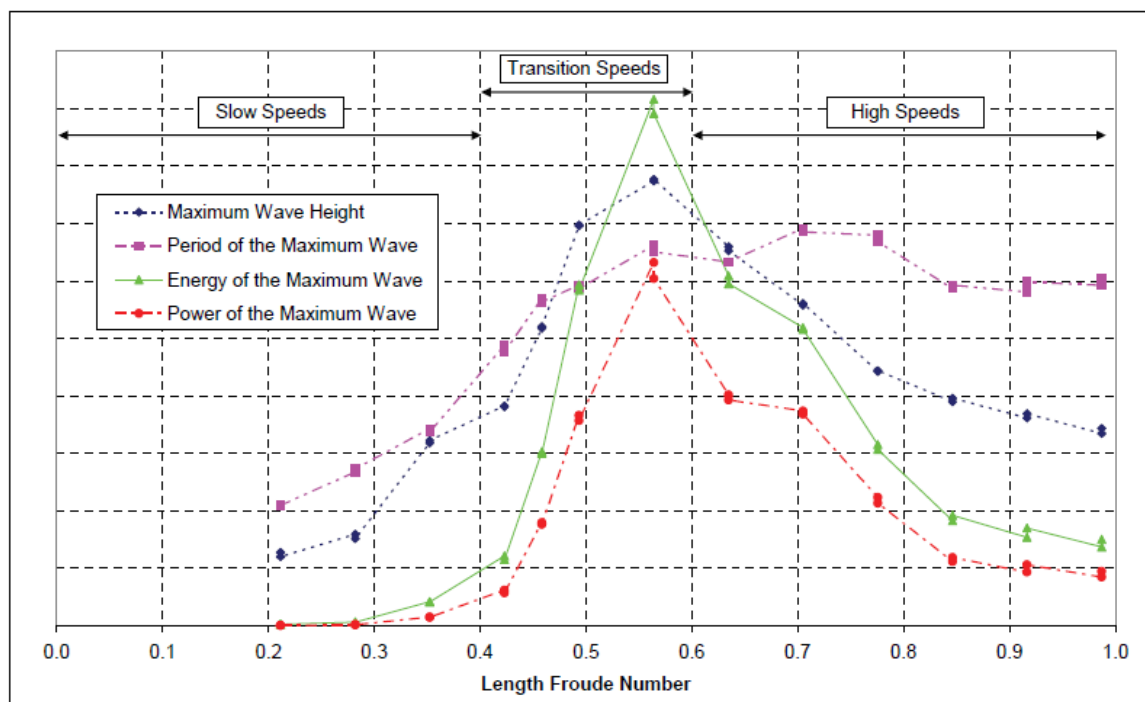
**Figure A5.1** – *Typical vessel wave wake parameters at different length Froude numbers (Macfarlane et al., 2008, Fig. 4). Note the peaks around $Fr_L \approx 0.5$. Note also how the height of the maximum (largest) wave decreases at high speed, yet the period remains constant. Travelling at high speeds reduces wave energy but delivers that energy in a wavelength that is much longer than sheltered waterways would normally experience.*

### Section: Wind Generated Waves

Wind waves are often used in wave energy calculations to compare annualised ambient and vessel wave environments, the premise being that the effect of energy on erosion rates is cumulative. It is now considered to be a flawed approach. It is not necessarily the quantity of energy, but form in which it is supplied.

There are concepts of thresholds, below which turbidity and erosion are negligible. Over extended periods sheltered waterways adapt to the ambient conditions and react accordingly. The introduction of wave energy in a form not experienced before is what causes erosion. Floods are a good example of this, even though the energy of a flood event may be no different to the summated ambient energy between flood events.

### Section: Sediment Remobilisation

*"Individual boat passages increase the turbidity in the water immediately adjacent to the shore line (Figure 9) and there is some indication, at least at Site 1 (Figure 9 A) that the resultant turbidity is positively correlated with Hmax."*

This is an example of selective analysis. Waves are described by several parameters, not just wave height. The fact that increased turbidity occurred just after the passage of large waves does not necessarily show correlation if other parameters associated with those waves also increased. It could also be said that the boats causing the large waves were painted white, therefore there was a positive correlation between hull colour and maximum wave height.

214

A review of Bauer *et al*. (2002), a commonly quoted wave wake erosion study, shows that a direct link between wave height and turbidity is tenuous. As one of many examples, Table 4 of Bauer *et al*. (2002) shows that run 1 had the same wave height as run *3*, yet it had more than double the predicted erosion rate. The same tenuous correlation was discussed in Macfarlane *et al*. (2008) (Fig. 5 and 6), where the wave producing the second-highest elevated turbidity reading had the same wave height as a wave generating no turbidity at all.

*"If it assumes that the turbidity plume extends 2 metres from the bank, to a depth of 0.2 metres then this equates to sediment loads of between 0.45 kg/l metre of bank/hour at Site 2 to 3.6 kg/m/hr at Site 3. In comparison, based on the background turbidity levels (about 50 NTU) and flow in the river at the time of the study (about 8100 ML/day) the total suspended solid load passing a given point in the river would have been about 25.4 tonnes/hr."*

There are several flaws in the logic. Firstly, taking the highest vessel wave wake sediment load reading of *3.6 kg/m/h* and estimating a flow velocity of *0.275 m/s*, the resulting sediment load would be *7.1 t/h*, which is not inconsequential compared to the river total of *25.4 t/h*. The *25.4 t/h* figure is, though, not directly comparable with the wave wake erosion rate calculated. The form of the calculated results is also misleading; the vessel wave wake results are presented in kilograms per metre per hour, yet the background sediment load is quoted in tonnes per hour. The fact that the river has a measured sediment load does not mean that the load came from that part of the river. In an idealised system, the river would start with zero turbidity and pick up sediment over time. At some point the river would reach dynamic equilibrium, or a saturation point relevant to the system energy and sediment characteristics. Further on, there would be a dynamic exchange as some material fell out of the water column and some was re-suspended, maintaining the overall load relevant to system energy. It is quite likely that only a fraction of the river's calculated background sediment load actually came from the study area.

Also, vessel wave wakes can form a mechanism for other forms of erosion, such as bank undercutting and slumping, which greatly accelerate the amount of material removed. These would not necessarily show in the format of the calculation used by Baldwin.

### Section: Discussion – Wave Characteristics
*"For this study, probably the most important wave characteristic was wave height, because of its relationship to both wave energy and wave power."*

Baldwin's Eqn. 1 shows the linear equation for energy density as $ED = \rho g H^2/8$ which, convenient to his arguments, is only in terms of wave height. Rearranging this equation into the linear form for energy of whole wave gives $E = \rho g^2 H^2 T^2/(16\pi)$. This assumes deep water, though the same linear equation would be of a similar form in shallower water (transitional water relative depth and wavelength, as was the case in the report with $\sim 4 < \lambda/h < \sim 10$) but with depth-modified wavelength. The important difference is that height and period have a similar bearing on wave energy. To ignore wave period in the discussion overstates the relevance of wave height.

*"However, the Ptot produced by a wash determines how much material can be moved by the wave (ref) while the Ppeak determines what size particles can be moved – the higher the power the large the particles that can be resuspended."*

A reference was not given for this claim. It is an over-simplification of the process!

215

*"This study has shown that different bank materials can produce different amounts of bank erosion. The highest turbidities were observed were at Site 3. Site 3 was in an area where speeds were restricted to less than 8 knots and was subjected to passages from boats with low wash characteristics (paddle steamers and aluminium fishing dinghies). However the bank material consisted of easily dispersed clays. Conversely, the lowest observed turbidities were at Site 1, which although was in an unrestricted speed zone and subjected to many high speed boat passages, had a sandy bank."*

Firstly, paddle steamers and aluminium dinghies don't have low-wash characteristics. Wave wake is relevant to vessel parameters, which can usually be simplified as length, weight and speed. The paddle steamers have modest wakes because their speed relative to length is low. Given enough power, they would produce the largest wakes of all the vessels on the river.

Secondly, the statement of turbidity differences is not an indication of preference for one bank material over another, but a statement of the limitations of turbidity as an erosion measure. Coarse-grained materials such as sand are more difficult to entrain and to keep entrained than silt. Turbidity is not normally used as an indicator of erosion when sand is present.

*"Therefore, if the mean observed power per wind-generated wave is multiplied by the number of waves produced per unit time, a value of the total energy expended on the bank by wind generated waves can be estimated; in one hour this is equivalent to 115 J per metre of bank."*

Hindcast wind wave parameters for the quoted wind speed and fetch would be $h = 0.037\ mm$ and $T = 0.7\ s$, though highly dependent on the effects of vegetation. These would give an energy density of $\bar{E} = 1.67\ J/m^2$, as against *1.7* calculated by Baldwin. However, Baldwin's recorded wind waves have a much lower mean wave, suggesting that the banks are not really exposed to the wind speed and fetch quoted, but are sheltered by the surrounding vegetation and topography. Baldwin's energy value of *115 J/m* per hour would be equivalent to *~10^6 J/m* annually. At this energy level and with the height and period parameters generating that energy, the banks could be considered as being in a dynamic equilibrium, with minimal long-term effects.

In comparison, *10^6 J/m* would be the energy of a single deep-water wave off the East Coast with parameters of $h = 2.5\ m$ and $T = 9\ s$, which are typical, year-round values. The work of von Krusenstierna (1990) specifically identified thresholds of various parameters, such as energy, height and period, below which erosion was essentially zero. More recent work correlating wave parameters and turbidity measurements on the Gordon River confirm the existence of thresholds. ***Figure A5.2*** shows this graphically. Increasing wave height does not necessarily lead to sediment entrainment immediately offshore, provided the corresponding wave period remains low. This is the mechanism that describes wind waves, which grow in height at a far greater rate than they grow in period for a given increase in wind speed. Height growth comes with increasing wind speed; period growth comes with increasing fetch.
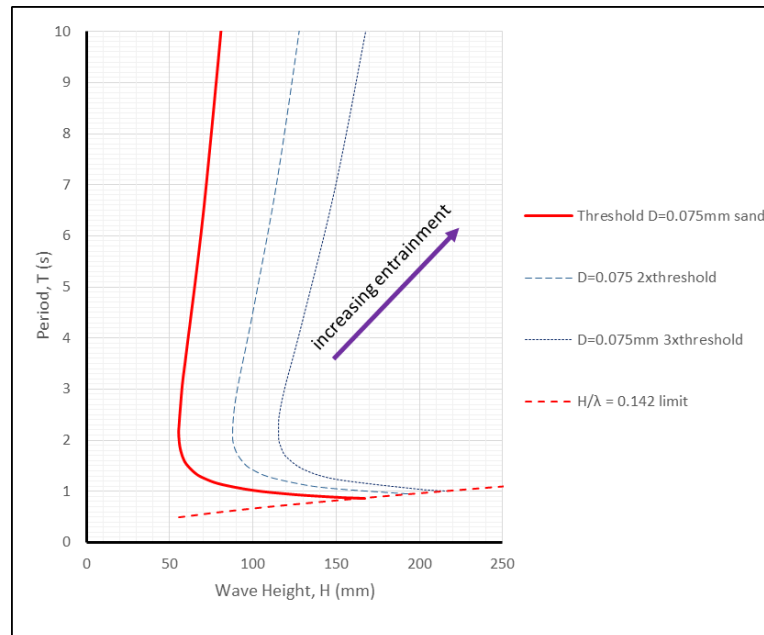
**Figure A5.2** – *Threshold values of wave height and wave period required to initiate sediment entrainment for 0.075 mm diameter (very fine) sand in 0.5 m water depth, based on linear wave theory. Note how wave height does not influence entrainment provided the period is short.*

*"Although the energy vector is different for waves generated by boats (approximately perpendicular to the shore) and river flow (approximately horizontal to the shore) nevertheless, near shore flows in the Murray River contain substantially more energy than individual boat passages."*

This statement ignores the limitations of energy alone as an indicator of the propensity for erosion. It is not the total energy as such, but the form in which it is delivered. For that reason, comparison of annualised energy levels is pointless.

*"This is consistent with other studies that have estimated that wave energy produced by boats is between 2 and 5% of the total energy dissipated against banks in large rivers (Hill et al., 2002: Maynord et al., 2007)."*

The Chilkat and Kenai Rivers are not directly comparable. Even though the energy produced by boats was calculated to be much less than other riverine processes, there was sufficient anecdotal evidence to suggest that there had been an acceleration of erosion with the advent of recreational boating. Vessel wake wakes are in themselves not the primary cause, but they can exacerbate existing causes of erosion and intensify the effects.

217

Maynord, S.T., Biedenharn, D.S., Fischenich, C.J. and Zufelt, J.E. (2008). Boat-wave-induced bank erosion on the Kenai River, Alaska*. Engineer Research and Development Center TR-08-05, US Army Corps of Engineers, Vicksburg.

The study was initiated by the local Kenaitze Indian tribe, who had concerns about bank erosion. Since the 1970s, the river has been a popular recreational salmon fishing area and lower parts of the river have experienced an increase in the permanent population, many of whom chose to live along the river. During the study, several hundred recreational boats were witnessed along the river per day during the peak fishing season. Most vessels were small open boats around *5* to *6 m* overall, often flat-bottomed and with a statutory engine power limit of *35 hp*. The usual modus operandi was to run upstream at speed and drift fish downstream. The amount of vessel traffic led to considerable variations in speed and shoreline separation.

Apart from relatively high natural flow rates, the river is also subjected to occasional flooding. Flooding was identified as being the principal contributor to erosion and there was sufficient anecdotal evidence of this, not the least being that major erosive events were recorded outside of the recreational fishing season.

Once consideration not offered in the study is that the reason for the focus on boat wash may not only have been a concern about erosion, but also a concern about loss of amenity. The local indigenous population may have felt displaced by the population growth and the uncontrolled harvesting of a natural resource it utilised for food rather than entertainment, so sought to control this. It would be difficult in the US to control recreational fishing where the resource was not necessarily under threat and where there is an implied right to this activity in its laws and culture. Indirect control of the activity through environmental regulation may have been the better option.

### Section: Managing Wave Impacts (numbering refers to the report)

*"1. Vessel design. Hull form is the primary means of managing wakes with vessel design. This approach has been adopted by some Alaska state agencies in their adoption of flat bottom boats partially as a result of Maynord (2001) studies showing reduced maximum wave height with flat bottomed boats compared to v-hull boats. PIANC (2003) notes that one factor that generally cannot be reduced by hull vessel design is wave period, which is important in determining shoreline impacts."*

There are many selective arguments here. Hull form can help to manage wakes but, in most cases, it has a very limited effect. Displacement is probably the greater determinant of wave height. Maynord's 2001 study was summarised in Maynord (2005), and although the flat-bottomed hulls did produce lower wave heights than the equivalent length v-bottomed hulls, they were also lighter by around *20%*, depending on loading. This weight difference is not unexpected. A v-bottomed hull would be designed and built to operate in waves, so would have a higher structural weight and potentially larger engines.[108] Maynord did note the weight difference in the *Results*

---

[108] Engine power was limited on the Kenai River, but vessels could use larger engines that had been "*de-tuned.*" It is possible that some of the larger vessels may have had this arrangement and "*re-tuned*" to their original power outside of the Kenai River area. Engines may therefore have been larger and heavier for use elsewhere.

*and Discussion* but does not make the connection between this and why the flat-bottomed boats were preferred.

Maynord's reference to PIANC, wave period and its importance to shoreline impacts is very relevant. It's unfortunate that Maynord's 2005 paper did not attempt any correlation between wave period and erosion.

*"2. Operational measures from PIANC (2003) that might be applicable to the Kenai River:"*

A list is provided; relevant to the coastal ferry operations the PIANC document was written around more than recreational boating. Most of Maynord's recommended measures involve operator training, scheduling and route navigation.[109] Unlike commercial ferry operations, recreational boating is a relatively un-regulated activity; operators may have no formal training, and operational restrictions are often limited to crude speed zones. Without on-going and effective policing, mitigating recreational boating wave wake impacts through training and regulation would most likely fail.


**Section: Results and Discussion**

It is interesting that only waves greater than *0.25 ft* (*75 mm*) were considered – the *75 mm* threshold being one of the operational limits applied to the Gordon River. None of the relevant Gordon River references appear in the report, except for Nanson *et al.* (1994) that preceded the application of this threshold on the Gordon River.

*"1. Use flat bottomed boats. Based on Maynord (2005), maximum wave heights are 22 percent higher with a v-hull boat with all other factors such as boat speed, length, and weight being equal. Using the boat wave equation from Maynord (2005), the v-hull WP at 3170 lb with six people traveling at 20.6 mph produces a 42 percent larger wave than the flat bottom KF at 2650 lb with six people traveling at 22.4 mph. It is not known if flat bottom boats are generally lighter and faster than v-hull boats used on the Kenai River."*

Maynord (2005) derived a wave height equation (eqn. 16) that included a coefficient accounting for deadrise. The difference in coefficient value between flat-bottomed and v-bottomed hulls was *22%* (*0.82* against *1.00* respectively), though without definition of what constituted "*v bottom.*" The reference to a *42%* higher wave for the v-bottomed hull is based on the derived equation that is technically flawed on several levels, and so unreliable. Flat bottom boats are generally lighter for reasons previously discussed and would generally travel faster for the same installed power, since planing hull resistance is a function of deadrise angle (in simplistic terms).

*"2. Allow use of 50 hp."*

Once into the high-speed range, it is well known that wave height reduces as speed increases. The power limit of *35hp* was mandated for safety reasons; though not detailed, they were probably safety of navigation and collision avoidance. Another possible reason is the ease with which lightweight, flat-bottomed hulls can be flipped during turns at high speed. What is not reduced at high speed is wave period, which remains approximately constant. Maynord attributes the

---

[109] When applied to recreational boaters in more remote areas, it is best described in colloquial terms – *good luck with that!*

reduction in wave height with speed to "*the boat drafting and/or trimming less,*" which is at best a great oversimplification of the relationship between planing hull dynamics and wave drag.

"*4. Reduce boat weight. One advantage of the flat-bottomed boats tested in the 2000 study was their lighter weight.*"

That is true, but none of Maynord's published documents made the connection between hull forms (v bottom or flat bottom), their relative weights and subsequent wave heights. There is contradiction between the findings based on hull form and those based on weight, as discussed in the review of Maynord's 2005 paper.

"*Flat bottom boats generally have to slow down more than v-hull boats when wave conditions are present. The net result is that flat bottom boats will be traveling slower and, because of their slower speed, causing waves closer to the wave height from the v-hull that did not have to slow down as much in wave conditions.*"

This is pertinent, as it highlights the limitations of focusing only on one vessel parameter (hull form) in reducing wave height. The answer is never simple.

Maynord provided discussion of correlation between bank types and erosion rates, noting that banks naturally armoured with a cobble bench or with vegetation were less susceptible to erosion. However, Maynord also provided evidence that major flood events can over-ride this correlation and cause erosion at stable sites. Shoreside anglers were also identified as a cause of bank damage in a similar manner to grazing cattle (refer to the review of Fonseca and Malhotra, 2012, photograph 3).

### Section: Summary

"*An attempt was made to correlate boat wave energy with bank recession rates; however, no relationship was found.*"

This is not unexpected. Correlation between wave parameters and erosion potential is a complex enough problem, but correlation between wave parameters and actual rates of erosion is elusive. Apart from a problem of lack of urgency, hence adequate public funding, the number of variables involved, and the difficulty replicating both polychromatic vessel wakes and bank structure/materials in flume tank laboratory experiments suggest that it will remain elusive. As an alternative, threshold conditions of sediment entrainment can be predicted, but their application would cause a severe curtailing of many recreational and commercial boating activities.[110]

"*The relative contribution of boat wakes and river currents was also evaluated by comparing energy at the shoreline from boat waves and energy at the shoreline from streamflow.*"

This was not dissimilar to the approach used by Hill *et al.* (2002) in their Chilkat River study – comparing shear stresses due to waves and streamflows. Maynord noted that vessel wave energy

---

[110] This leads, in effect, to the "*Masai*" conundrum – how to regularly bleed the living animal, in the case of the Masai for their sustenance, without actually killing it. The threshold condition would be consistent with "*don't bleed the animal at all.*" Beyond the threshold condition, how much erosion is tolerable without undue environmental damage and how is "*undue damage*" quantified?

on the Kenai River ranged from *5%* to *59%* of the streamflow energy at the shoreline. Whether or not that equates to erosion potential is questionable – streamflows result in a streamwise direct shear stress that may or may not entrain and transport sediment whereas vessel waves create a more orthogonal shear stress with both longshore and cross-shore components. For small craft waves with shorter periods, the process is more likely to be erosive and the cross-shore component is more effective in entraining turbid water into the main streamflow. In effect, vessel waves would move greater amounts of sediment further.

*"The conversion from wave height to boat wave energy expended on the shoreline used herein is based on wave height alone with no variation due to wave period. This assumption is generally justified because the largest waves in the wave train tend to have the same period regardless of distance. Only those smaller waves preceding the maximum wave tend to have periods greater than the peak wave. These waves are generally small enough to not have wave height that exceeds 0.25 ft."*

Maynord developed an energy equation that used the wave height prediction equation of his 2005 study. He rightly determined that the period of the largest wave (maximum wave) remains approximately constant at high speeds (though fails to qualify it applicability as being at "*high speed*"). In deep-water linear terms, $E \propto H^2 T^2$ and so $E \propto H^2$ when $T$ is constant. That is not unreasonable, but what is not made clear is how to compare between vessels or determine the cumulative energy, since $T$ varies between vessels. It could be justified if all vessels were similar in length (which they are in this case), but the bounds of applicability would have to be clearly stated.

There would also have to be a decay relationship for this approach to be of any use. The total wave energy does not change but gets spread across an increasing number of waves as the wake propagates and disperses.

Also, dismissing the leading, long-period waves as being of no consequence is also misleading, as they are responsible for other erosion mechanisms that contribute to the overall problem. This form of analysis depends on waves being of a deep-water form, or at least experiencing limited depth effects. The wave measurement probes were mounted on shoreside structures, limiting their reach to around *1.0-1.5 m* from the bank. Depths at the probes varied, but were as shallow as *0.3 m* and typically not more than *0.5-1.0 m*. This can lead to an inability to correctly categorise the waves, as well as contaminates traces with reflections.


A final comment should be made about wave wakes, energy levels and erosion in general. Much attention is given to relatively modest changes in wave heights and periods; the nett effect being a percentage change in energy. Past studies (Macfarlane and Cox, 2003, and sections of this study) have demonstrated that changes come with order-of-magnitude variations in energy, not percentage variations. The same can be found with naturally-occurring wind waves, where the energy difference between a normal climate and a storm climate is one or two orders of magnitude. As is often the case, it's not just the quantity of energy, but the form in which it comes and the method of delivery (Cox, 2000).

221

**Appendix A7** - *Boat wakes and their influence on erosion in the Atlantic Intracoastal Waterway, North Carolina.*

Fonseca, M. and Malhotra, A. (2012). Boat wakes and their influence on erosion in the Atlantic Intracoastal Waterway, North Carolina. NOAA Technical Memorandum NOS NCCOS #143.

The subject of this report was Snow's Cut, a man-made canal joining the Intracoastal Waterway to the Cape Fear River. The canal had been planned since the early 1800s but was not completed until the 1930s (UNCW[111]). It is noted by UNCW as being *1.75 miles* (*1.52 nm*) long, average depth around *12 ft* (*3.6 m*) deep, though shallower in places and requiring ongoing dredging.[111] It is *85 m* wide at its narrowest point (noted as "*100 ft*" in some sources[111,112]), though up to around *120 m* in other places. Since the time of its construction, erosion has been ongoing. Constant bank instability, siltation and dredging has expedited remedial action.

The report used two simulation methods. The first, WEMo, is a wind wave method that models wave height, wave energy and shear stresses beneath the shoaling waves. The second method, BoMo, models vessel wake waves (based on the maximum wave), their propagation to the shore and the shear stresses they create. These simulation methods use a GIS topographical model of the waterway in the wave transformation process.

Based on logged information of passing vessels, two vessels were modelled: a *7 m* centre console with a displacement of *2 t*, and a *16.4 m* motor yacht with a displacement of *34 t*. Three speed conditions were modelled for each vessel: *3*, *10* and *20 knots*. It was found that the smaller vessel exceeded the highest wind waves occasionally, but the larger vessel exceeded the highest wind waves by a substantial amount, except at the slowest speed.

As with many previous vessel wave wake studies, there is a high reliance on past work that may be flawed. The BoMo model uses a wave height predictor from Sorenson (1967) for displacement hulls and a modified USACE model for planing hulls, assumed to be from Maynord (2005). Sorenson's model is quite old and from the very beginnings of wave wake understanding. Maynord's model has shortcomings and does not translate well beyond those vessels used to derive the relationships. Neither method appears to have been published with an accompanying wave period prediction method, so it is unclear how the BoMo models of Fonseca and Malhotra managed to achieve this.

As with other similar studies, the authors lack experience and credentials in vessel dynamics. Mark Fonseca is an ecologist, and Amit Malhotra is a civil engineer specialising in GIS and remote sensing.

**Section: Methods**
Table 1 of Fonseca and Malhotra (2012) describes the vessels modelled, but in terms of "hull length" (assumed to be $L_{OA}$) and not actual waterline lengths. This is particularly important if the dimensions were taken from published manufacturer data, as they often include hull appendages

---

[111] University of North Carolina Wilmington, Barrier Island Ecology, 2015: https://sites.google.com/site/barrierislandecology2013/coastal-and-barrier-island-ecosystem-factors/snow-s-cut-1 (last accessed 19th January, 2018).

[112] It's not impossible that the original cut was *100 ft* wide by *12 ft* deep, though the stability of a canal with these dimensions cut through mostly unconsolidated sand would be very questionable. It was most likely *300 ft* wide by *20 ft* deep, given the width at the old bridge revetments is about *280 ft*.

such as marlin boards to increase the apparent length and therefore sales appeal. Similarly, the draft of the larger vessel is most probably to the bottom of the propellers and not the hull itself.

The three speeds chosen for modelling were the same for each vessel and not relative to length. Consequently, the non-dimensionalised speeds are shown in **Table A7.1** below:

<u>Table A7.1</u> – *Non-dimensionalised speeds and their relationship to planing dynamics.*

| Speed (kn) | 7 m Vessel ($L \approx 6.0\ m$) | | | 16.4 m Vessel ($L \approx 14.8\ m$) | | |
|---|---|---|---|---|---|---|
| | $Fr_L$ | $Fr_\nabla$ | Regime | $Fr_L$ | $Fr_\nabla$ | Regime |
| 3 | 0.20 | 0.44 | displacement | 0.13 | 0.28 | displacement |
| 10 | 0.67 | 1.47 | semi-displacement | 0.43 | 0.91 | displacement |
| 20 | 1.34 | 2.98 | semi-planing | 0.85 | 1.83 | just semi-planing |

Regimes for planing hulls – ***displacement***: $Fr_\nabla < \sim 1.0$; ***semi-displacement***: $1.0 < Fr_\nabla \leq 1.75$; ***semi-planing***: $1.75 < Fr_\nabla < 3.35$; ***planing***: $Fr_\nabla \geq 3.35$. The fully planing speeds for these vessels, when hull weight is fully supported by dynamic lift, would be *22.5 kn* for the *7 m* vessel and *36.5 kn* for the *16.4 m* vessel.

The authors described the speeds as "*planing*" (*20 knots*), "*plowing*" (*10 knots*) and "*slow*" (*3 knots*). The slow speed descriptor is acceptable, but "*plowing*" is not a technical description and "*planing*" is a dynamic regime relative to speed and displacement (assuming the vessel has a hull shape capable of generating dynamic lift in the first place). If speed regimes were absolute and not relevant to vessel dimensions, a container ship at service speed would be considered as "*planing.*"

When comparing length and volumetric Froude numbers for these vessels, the disparity between the two becomes apparent. Based on length Froude number, the peak in specific wave drag and subsequent wave wake comes at $Fr_L = 0.5$. For a typical range of planing craft this is equivalent to a volumetric Froude number of $Fr_\nabla \sim 1.0$; inexact due to the disparity between length and volumetric Froude numbers. With the definition of planing being the point where a hull is fully supported by dynamic lift, which for most normally configured planing hulls occurs when $Fr_\nabla \geq 3.35$, the equivalent length Froude number would be $Fr_L \geq 1.68$, which is at least double what is usually considered as being "*high speed.*" This only serves to highlight one point: planing hull dynamics and high-speed vessel dynamics are not necessarily the same thing, even though they are often confused in the literature.

*Figure A7.1* shows the regions of planing dynamics graphically and how the centre of gravity migrates vertically relative to its static position. The boundaries of each zone are not absolute and can vary with vessel parameters, especially those in the displacement and semi-displacement zones where volumetric Froude number is not the best parameter for the non-dimensionalisation of speed.

"*Based on an assumption of fine sand throughout the area (0.015 mm average grain diameter) we also computed whether sediment on the seafloor would move and potentially erode (erosion here is considered to be when sediment is moved from its original position) under those conditions.*"

The average grain diameter for a fine sand is *0.125-0.25 mm* according to the Unified Soil Classification System (USCS).[113] The stated value of "*0.015 mm*" is probably a typographical error

---

[113] *ASTM D2487-11, Standard Practice for Classification of Soils for Engineering Purposes* (Unified Soil Classification System), ASTM International, West Conshohocken, PA, 2011.

(*0.15 mm*), of which there are several in the paper. The definition of erosion as sediment moved from its original position is a standard theme in shoreline erosion papers and one adopted here. It is important for all sediment types, but particularly more so for silts that can leave water turbid for extended periods and in locations far from the original source.
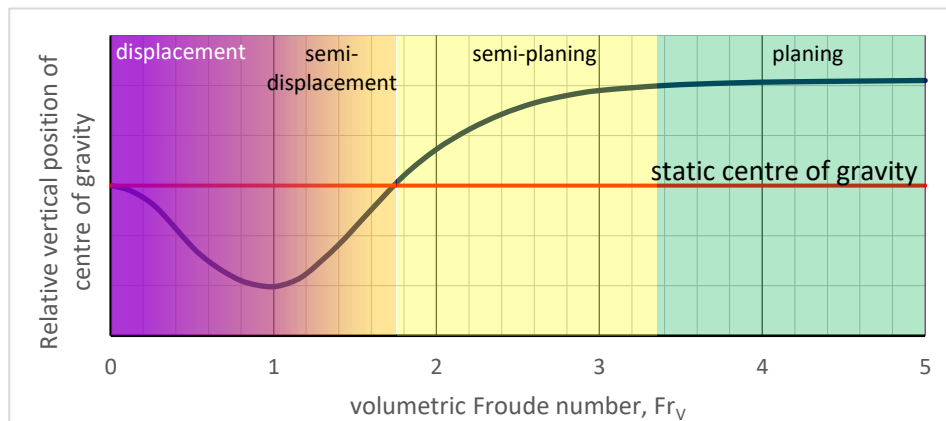


**Figure A7.1** – *(Figure 4.13, Section 4 reproduced) Relative position of the centre of gravity of a planing vessel at different speed regimes.*

## Section: Results

"*At planing speeds, wave heights have diminished to within the range of wind events revealing the comparatively (to plowing) lower displacement of the hull for vessels of this size when on plane*"

The authors erroneously correlate the displaced volume of water with the wake height. If that were the case, how would this logic explain two phenomena. Firstly, high speed displacement hull forms, such as high-speed catamarans, exhibit the same effect even though their displaced volume changes little. Secondly, hydrofoil vessels would displace very little water at high speeds, accounted for only by the immersed volume of their foils, yet they can still generate waves? The generation of waves depends on a travelling disturbance. Whether that is in the form of a hull displacing water or a travelling pressure source (planing hull, hydrofoil or hovercraft) is immaterial to the argument. Different sources may produce the same effect to differing degrees, but wave height is not in the form of a linear relationship with displaced volume.

(referring to the 16 m vessel) "*Even on plane, vessels of this size do not rise sufficiently onto the water surface to displace less water than as seen for the 7 m vessels; vessel speeds would have to be considerably greater to lift the bulk of the vessel onto the water surface; such speeds have not been observed in our video reconnaissance of the AIWW (see above: **Context: Boat wakes in the AIWW**). However, at planing speeds, wakes were diminished as compared with plowing speed conditions.*"

Firstly, the *16 m* vessel never reached fully planing speeds (refer to Table A7.1 above). Secondly, the first sentence implies that there is a direct relationship between the displacement of water and the wave heights produced, lamenting the fact that the *16 m*, *34 t* vessel could not rise sufficiently to have less displaced volume than the *7 m*, *2 t* vessel (short of growing wings). How such a huge reduction could ever happen in practice is unclear. Thirdly, a vessel able to travel "*at the water surface*" is not a guarantee of reduction of wave height, since hovercraft will also produce wakes courtesy of the travelling depression beneath the skirt. Lastly, at "*planing speeds,*

224

*wakes were diminished as compared with plowing speed conditions*" – wakes were diminished because the reduction of wave height is a function of length Froude number and has no direct relationship with planing dynamics. The same effect is evident in high-speed displacement craft.

"*Although wave heights describe energy distribution at the water surface, sediment movement only occurs if waves enter sufficiently shallow water to transfer energy to the seafloor.*"

Wave height partly describes energy distribution at the water surface. There is also an equivalent dependency with wavelength, described more commonly by wave period. Wave period was apparently considered in the BoMo and WEMo models, but otherwise ignored in the report. Also, the depth of the orbital motion beneath a wave is substantially a function of wave period and not wave height, so a reference to wave height may be misleading. The standard parameter defining interaction between waves and the bottom is $h/\lambda$ (or $\lambda/h$ as an alternative) with wave height more of a factor determining the strength of the orbital motion and less so its vertical extent.

"*Given that most of the channel margins are composed of sand at the angle of repose, waves did not cause erosion until very close to shore, giving the appearance in the figures of this being shoreline erosion; all erosion forecasts here are for areas of submerged seafloor only.*"

The wave height algorithm within the BoMo method is assumed to be from the work of Maynord (2005). Fig. 4 of the report is consistent with the equation developed by Maynord (2005). If that is the case, only the divergent waves were considered here. Many vessels, especially larger vessels, may have transited Snow's Cut at depth sub-critical speeds. That, combined with the deep transom immersion of a planing hull form at slower speeds, would have induced fairly long transverse waves. Transverse wavelengths could vary from *18 m* to *37 m* in average depths from *3 m* to *6 m*, making them sufficiently long to initiate entrainment if the water was at the shallower end of the range. That entrainment would lead to longitudinal displacement along the Cut and may have exacerbated the siltation recorded at the entrances to the cut. Similarly, there would be plenty of scope for transit around the depth-critical speed which, according to Fig. 3 of the report, would range from around *10.5-12.9 kn* in places to *12.9-14.9 kn* in the deeper sections (though tide dependent).

To demonstrate this, ***Figure A7.2*** taken from UNCW (refer footnote 111) shows an aerial photograph of a large cruiser transiting the old swing bridge (replaced by the present fixed span bridge slightly to the east, which would be in the foreground). Notable are the transverse waves behind the vessel, formed at the time between when it was stationary and waiting for the bridge to open, and when it reached its depth super-critical speed as it passed through the bridge opening. Note that this section of the Cut remains the narrowest part of the Cut as the banks had been armoured to protect the old bridge approaches against the expected erosion. The extent of the erosion may be gauged by considering that: the Cut was man-made and most certainly of an approximately constant width; the old bridge revetments possibly represent its original width; the photo pre-dates the construction of the new bridge in 1962. It is likely that revetment maintenance was ongoing and there are noticeable differences in the reinforcing material.
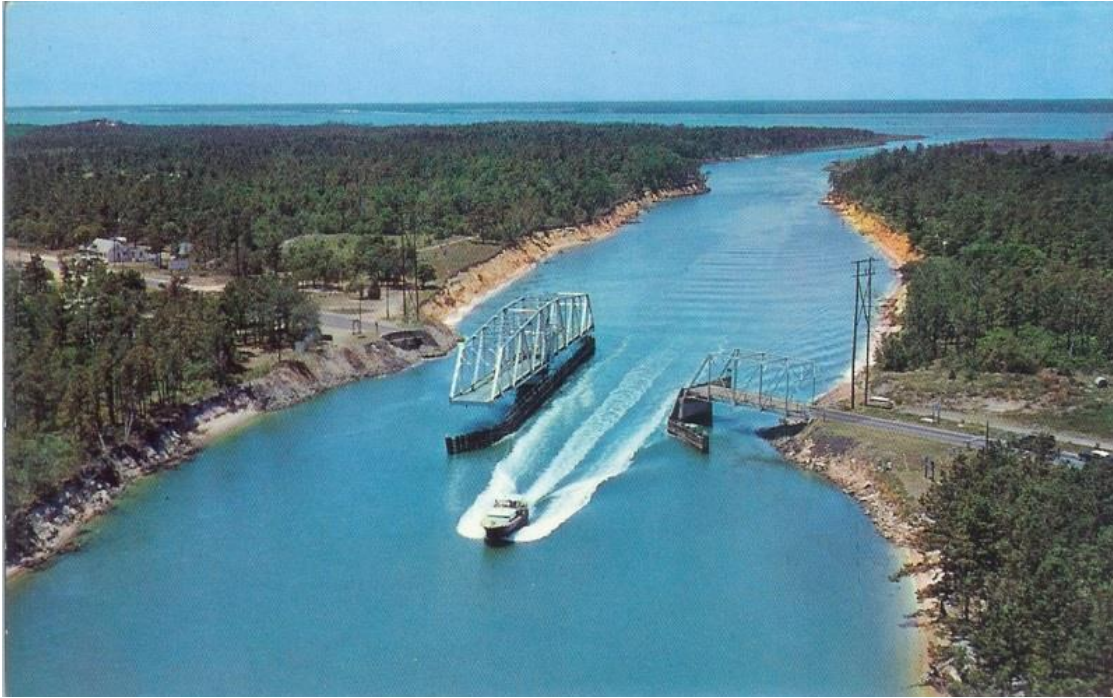
**Figure A7.2** – *Historical photograph of a large recreational vessel (estimated overall length of 15 m) transiting the old swing bridge across Snow's Cut. Notable are the transverse waves formed as it accelerated from rest (waiting for the bridge to open) to depth super-critical speeds, the large divergent waves, the exposed sand cliffs and the extent of bank retreat compared to the width at the bridge revetments. Refer footnote 111 for reference.*


**Additional Comments**

Maynord (2005) recommends that the ratio of water depth to vessel length ($h/L$) be greater than *0.5*, or at least *0.35*, for the use of his predictive equations. If the BoMo software uses Maynord's equations, the larger vessel would not satisfy this criterion for almost all of its transit of Snow's Cut. That would have affected assumptions regarding wave height and propagation angle. There is little point having a vessel wave wake "*forecasting tool*" employing an "*artificial neural network*" and "*non-linear Boussinesq models*" if the input is wrong and the types of waves described by the algorithm do not match those being generated in the actual waterway.

In Fig. 8 and 9 of the report, there are wind wave erosion sites that are not replicated by the vessel wash erosion predictions. The predominant erosive wind direction is from the north-east, yet there are areas on lee shores where erosion was predicted.

Three knots is a very slow speed for recreational vessels. Some may struggle to maintain steerage at that speed, and larger, high-powered vessels would have an idle speed greater than this.

Two notable comments come from local news reports:[114]

- "*Medlock said a driving force for the project is to protect federally owned land from being eroded away. 'The more land that erodes the more land we lose,' he said*." Jim Medlock is the project manager of the Snow's Cut erosion mitigation project with the Army Corps of

---

[114] http://www.starnewsonline.com/news/20170919/snows-cut-erosion-control-project-to-start-soon (last accessed 19th January, 2018).

226

Engineers. This is a common concern for waterfront landowners, where no allowance is made for changes to waterfront boundaries due to coastal processes – natural or otherwise;

- "*On the north side of Snow's Cut, New Hanover County has no plans in the works to address erosion at its park, said Tara Duckworth, the county's parks and gardens director. 'We've kind of known since the inception (of Snow's Cut) that Mother Nature was going to take it back eventually,' Duckworth said.*"

Additional photographs from the news report (see footnote 114) are shown below.



**Figure A7.3** - *Southern bank, looking west. The old swing bridge was in the background, in way of the power poles. Some shoreline areas have what appears to be consolidated substrate, which would tend to reduce the rate of erosion. Compare this to Figure A7.3.*



**Figure A7.4** - *Northern bank, 300 m to the east of the new bridge. Access for fishing does not help but is not a primary source of erosion.*

**Figure A7.5** - *Southern bank, about 50 m to the east of the new bridge, looking east-northeast. The north-easterly sea breeze would come almost directly down the Cut.*

**Appendix A8 - *Boat-Generated Wave and Turbidity Measurements: Connecticut River***

Ozeren, Y., Simon, A. and Altinakar, M. (2016). Boat-Generated Wave and Turbidity Measurements: Connecticut River." *Proc. World Environmental and Water Resources Congress 2016: Hydraulics and Waterways and Hydro-Climate/Climate Change*. 390-398.

A series of tests were conducted on the Connecticut River in New Hampshire and Massachusetts to determine correlation between wave wake parameters and measured erosion. The paper does not state if any active erosion on the river due to vessel wash had precipitated the study. The trials programme used a single recreational vessel to generate a wake. The principal wave parameters and subsequent turbidity were recorded. Data were collected in two ways. Firstly, data logging and cameras captured incidental wakes over a four-month period. This was discussed briefly but results were not reported at all. Secondly, controlled experiments were conducted at one site (poorly!), measuring the waves and the subsequent turbidity caused.

**Section: Abstract and Introduction**

The abstract states that "*wave height, wave period and turbidity level were investigated*," but three sentences later it all came down to this comment: "*Especially high-speed vessels are capable of producing sufficiently high waves that can cause damage to the riverbanks (MacDonald, 2005).*"

It goes on to say: "*in situ field experiments were carried out to quantify the relationships between boat speed, boat wave properties, and the turbidity levels along the beach.*" All this rhetoric is compressed into Fig. 8 (reproduced here as Figure A8.1), which is in two parts. The first is a graph of turbidity against wave height (height of the maximum wave). The second is a graph of boat speed against wave height. That is the limit of the analysis and attempted correlation between waves and turbidity.

**Section: Field Sites and Instrumentation**

The wave probe was set up in just 0.36m water depth, described with "*the objective to measure the boat-generated waves near the shore before they shoal and break.*" The vessel had a static waterline length of about *4.75 m*, so the period of the maximum wave would be about *1.4 s* at high speed (based on equivalent vessels from Macfarlane and Cox, 2003). Depending on the wave height measured, which varied between about *0.1 m* to *0.3 m*, the wavelength would vary from about *2.3 m* to *2.86 m* at the measured depth and period. These waves just fall into the lower end of "fairly long waves," which means they were moderately depth-affected. The *0.3 m* wave must have been at the point of breaking ($H/h = 0.83$). However, the short period means the depth effects would be limited. This supports the argument that small craft wakes are more like deep-water wakes.

Fig. 3 shows the test arrangement. Two turbidity sensors were set up with one at the wave probe (*0.36 m* water depth) and one in *0.14 m* of water depth (within the breaker zone, as noted). The authors state that the turbidity measurements at the shallow water sensor were not included in the figures, quite possibly because they caused data scatter within the breaker zone that could not be made sense of. What is most important is to determine the thresholds of sediment entrainment.

229

The sailing line was not controlled and only recorded as a GPS track. The lateral distance for the controlled experiments varied from *15 m* to *30 m*, or about *3.2L* to *6.3L*. This is discussed later. The authors decided to only compare results where the lateral distances were similar. It apparently didn't occur to them to mark a sailing line. The two most difficult factors to control in small craft trials are course and speed.

The water depth on the course was *3 m*. The authors discuss "*subcritical and supercritical range,*" though don't clarify this with "*depth subcritical . . .*" The longest wave would have a period around *3.3 s* at high speeds and a little longer at the transition (from semi-displacement to semi-planing). For a wave height range from *0.1 m* to *0.3 m*, the wavelength at the *0.36 m* measurement depth would vary from about *6.6 m* to *8.3 m*. That would make the longest wave fully depth-affected (calculated $\lambda/h > 18$), but not the maximum wave. At the *3 m* sailing line depth, with $h/L = 0.63$, the longest divergent wave would have a wavelength around *14 m* and so would be slightly depth affected. It's quite likely that none of the waves generated in the *3 m* depth would have appeared as substantially depth super-critical. With a waterline length around *4.75 m* and assuming a vessel can operate to depths down to around *0.5L* and still generate wakes that look like deep water wakes, the waves at *3 m* were most likely close enough to deep.

Looking at Fig. 1, which is a photograph of the test vessel at what appears to be high speed, the waves immediately behind the vessel are long crested. In the foreground can be seen the remains of the transverse waves at the time of acceleration, as well as short-period, fully-dispersive divergent waves.

## Section: Data Analysis
The data analysis is comprehensive, but the lack of fundamental understanding of vessel dynamics and wave wake parameters renders it largely meaningless. The authors define each wave as being between two successive zero down-crossings. Being coastal engineers, the authors would possibly consider a wave to start with a trough, followed by the crest, rather than the other way around.

## Section: Results and Discussions
Fig. 5 shows a frequency analysis of the incidental wakes, with the highest wave marked. The accompanying period seems to be around *1.6 s* to *1.7 s* average, which suggests a longer vessel than the test vessel. Sample wave height records are shown, with amplitudes varying from *30 mm* to *120 mm* (*60 mm* to *240 mm* height). It would be impossible to draw firm conclusions from these waves without knowing details of how they were generated.

There is discussion of the four measurement sites and sailing line distance, which varied between *50%* to *100%* due to poor control of the experiments. At the controlled test site (WLOG1), where sailing lines were tracked by GPS, comparison was made of runs with similar lateral offset but different vessel speeds. It was concluded that "*the errors due to wave dispersion is much less than the changes in the wave properties at different boat speeds.*" Dispersion would lengthen the wave packets, increase the number of waves and promote height decay.

The discussion of the first plot of Fig. 8 (turbidity against wave height) is limited to the comment that "*turbidity increases with increasing maximum wave height.*" The discussion of the second plot, which is wave height against boat speed, has this confusing commentary: "*In all three sets of experiments, the wave height increases with the increasing boat speed in the sub-critical non-*

*planing range. When the boat planes, the maximum wave height starts decreasing with a milder slope compared to the increasing trend. The peak is the critical speed and corresponds to Froude number equal to unity.*"

There is obvious confusion between vessel dynamics and depth dynamics. At the *3 m* water depth at the sailing line, the depth-critical speed would occur at *10.5 kn*. The two peak data points are at about *12.2 kn*, though there are insufficient points close enough either side to know if this was the peak. The depth Froude number at *12.2 kn* is *1.16*, which is over unity. The length Froude number at *12.2 kn* is *0.92* based on the static waterline length, and the dynamic waterline length was most likely less than the static, increasing the length Froude number. The peak in planing vessel hump resistance occurs at approximately $Fr_\nabla = 1.75$, which is the point where sinkage is at its maximum, and that occurs at about *11.7 kn*. It is quite clear that the peak measured and the relationship in general, relates more to the vessel dynamics and not the water depth. With $h/L = 0.63$, critical speed depth effects would be small to the point of being indeterminate.

Both parts of Fig. 8 have just twelve data points, appearing to be six double runs. It is possible to identify the same test point on the two graphs (shown below, red and blue). One noticeable point on the height/turbidity graph (Fig. 8 – left) is the very left-hand point, which is at around *7 mph*. It has the same corresponding wave height as another data point at a speed of about *28 mph*, yet totally different turbidity was recorded. That would suggest that wave period is playing a role as well, but there is no comment whatsoever about period beyond the single mention in the introduction.
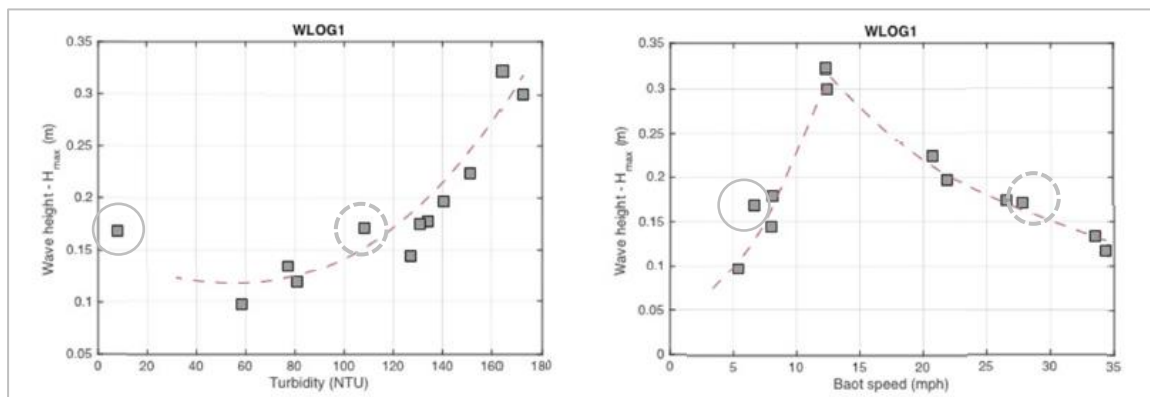


**Figure A8.1** - *Fig. 8 reproduced, showing identical data points on different graphs (circled) and the contradictory relationship between turbidity and wave height. Both waves have the same recorded height (right) but cause very different turbidity (left). Note that the y-axis scales are not identical.*

The main comment about Fig. 8 is that "*the turbidity increases with maximum wave height.*" That takes the science back *25* years and adds nothing. There is no further discussion or analysis, or results presented.

### Section: Conclusions and Further Work
"*At planing speeds, even though the maximum wave height is lower than the critical value, the measured turbidity increases.*" Compare that to the main discussion finding "*the turbidity increases with maximum wave height.*" Do they not contradict each other? They suggest that another parameter is influencing the relationships – that parameter being wave period. There is no discussion at all of wave energy or any other composite parameter.

231

One final comment is that *"previous laboratory experiments with the same instruments in mixtures of water and silty sediments at various concentrations showed that there is a linear relationship between the turbidity level and suspended sediment concentration."* That is important for correlating between predicted turbidity and the amount of sediment entrained.

Bilkovic, D., Mitchell, M., Davis, J., Andrews, E., King, A., Mason, P., Herman, J., Tahvildari, N. and Davis, J. (2017). Review of boat wake wave impacts on shoreline erosion and potential solutions for the Chesapeake Bay. STAC Publication Number 17-002, Edgewater, MD.

The report was instigated by the Chesapeake Bay Commission (CBC), which engaged the Scientific and Technical Advisory Committee (STAC) of the Chesapeake Bay Program (CBP) to study and report on the impacts of boat-generated waves and potential policy options. In general, the report relies heavily on past wave wake studies, many with questionable science, that have become self-perpetuating on the scientific literature merry-go-round. The report does, however, excel in the application of abbreviations and acronyms.

The scientific panel was extensive, with nine contributors, four external reviewers, and nine others providing some degree of assistance, yet none of those are listed with experience in naval architecture or related fields. This is a common thread in many similar reports, where assumptions are made, and comments are given without sufficient academic background to either make informed statements or critically analyse referenced papers.

*"Boat wake energy is event-dependent and is influenced by the vessel length, water depth, channel shape, and boat speed (Sorensen 1973, Glamore 2008)."*

And displacement? Also, wake energy is usually positively influenced by water depth, since most vessels require less power to travel at particular speeds in shallow water (i.e., depth super-critical). It's not the energy per se that becomes a problem in shallow water, but the form in which it is delivered and the way it propagates.

*"Wakes are most destructive in shallow and narrow waterways because wake energy does not have the opportunity to dissipate over distance (FitzGerald et al. 2011)."*

A close reading and a keyword search of FitzGerald *et al.* (2011) could not find this statement. It would appear to be a composite of several un-related ideas. Shallow water wakes are destructive because of the agglomeration of energy at the head of the wake (into one or a few waves) and not necessarily the lack of dissipation. The total wake energy doesn't change, but its distribution in the wake does.

*"Although boat wakes are periodic disturbances, in comparison to wind waves, they can be a significant source of erosive wave force due to their longer wave period and greater wave height, even when they represent only a small portion of the total wave energy (Houser 2010)."*

This is more insightful. It's not the quantity of energy that's important, but its quality and the form in which it is supplied. Comparison with wind wave energy is now believed to be pointless.

*"Our review of the literature demonstrated that even small recreational vessels within 150 m (~500 ft.) of the shoreline are capable of producing wakes that can cause shoreline erosion and increased turbidity (e.g., Zabawa and Ostrom 1980)."*

Apart from the report of Zabawa and Ostrom being *37* years old and pre-dating much of the more recent (about *25* years) surge of scientific interest, this statement is highly selective in its

arguments and lacks proper qualification. For instance, there was no qualification of vessel speed or water depth, or what constitutes "*small recreational vessels.*" There was also no qualification of the type of waterway, shoreline or sediment, except that the mention of "*turbidity*" suggests a component of mud or silt and therefore a quite sheltered waterway. Past fieldwork by the AMC would suggest that attempts to measure the wakes of small recreational craft at lateral separations in excess of thirty boatlengths (assuming $L \sim 5\ m, y = 150\ m$) against the background wind wave climate that could existing in a waterway at least *300 m* wide, would be pointless in many cases.

This statement is an unfortunate example of many reports on this subject, where insufficient rigour is attached to statements plucked from past studies lacking robust, critical appraisal.

"*The cumulative result is that each boat passage generates a complex series of waves known as a wave train, which propagate away from the sailing line at an angle that is dictated by hull shape and vessel speed.*"

Although not referenced, this was probably taken from Maynord (2005). It is simply incorrect. As is known now (but was not reported in the literature at the time of Maynord's 2005 study), the deep-water Kelvin angle defining the large divergent waves does contract at high speeds but is independent of hull shape. In shallow water the propagation angle is a function of speed and water depth, but not hull shape. At slower speeds ($Fr_L < \sim 0.5$), the angle is constant.



Figure 2. Pattern of vessel-generated waves in deep water. Diagram from Sorenson 1973. Photo by Edmont - Own work, CC BY-SA 3.0, https://commons.wikimedia.org/w/index.php?curid=6920796
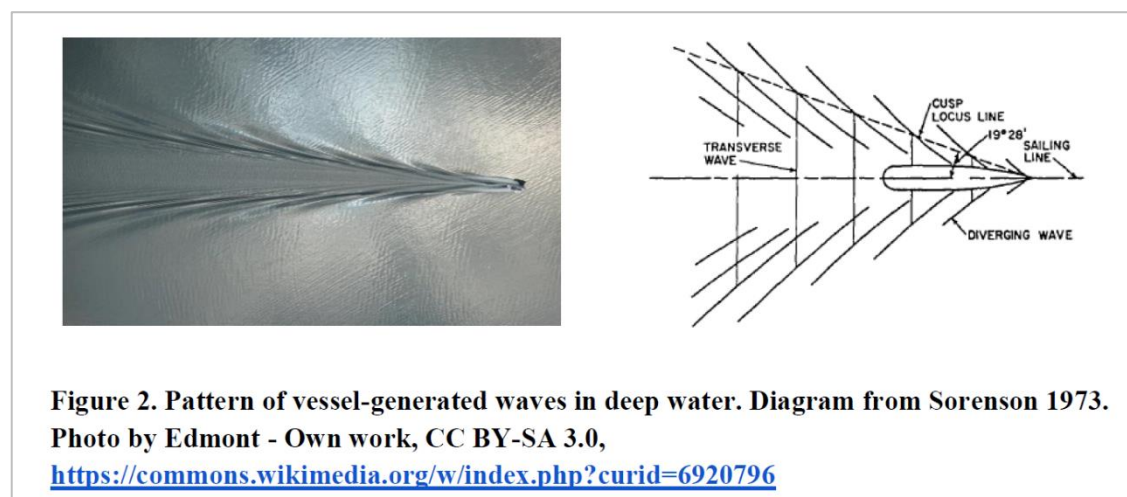
**Figure A9.1** – *Fig. 2 of Bilkovik et al. (2017) reproduced*.

This photograph in the report does not best represent a deep-water condition. It is nothing like the schematic on the right, which exhibits transverse waves, much shorter-crested divergent waves and a constant Kelvin angle. The schematic is also incorrect in several details, as is common with the Kelvin wake pattern. The photograph is of a small vessel at very high-speed relative to length, taken on the Lyse Fjord in Norway, which is a very deep body of water. (Refer Figure 4.6, Section 4).

"*Waves that travel in water that is deeper than 1/2 of their wavelength (the distance between two successive wave crests) are referred to as deep water waves. The motion of deep-water waves do not penetrate the full depth of the water column, thus these waves have little impact on the bottom sediments (Sorenson 1997, Hill et al. 2002).*"

234

If the motion of deep-water waves does not penetrate to the full depth of the water column, should they not have no impact on bottom sediments? There is also an implication that once waves begin to feel the bottom they start to entrain sediment. This also is not true. Depending on the sediment size and composition, the water must be much shallower than half the deep-water wavelength for sediment to be entrained. For instance, for a typical small boat maximum wave of $H_o = 0.2\ m$ and $T = 2\ s$, the deep-water wavelength would be $\lambda_o = 6.24\ m$ and sediment movement would not be initiated until around $h = 2.3\ m$ for a fine silt ($D = 0.075\ mm$) or $h = 1.27\ m$ for a medium sand ($D = 0.15\ mm$). The water would have to be even shallower before the movement is sufficient to form a plume and very shallow for that plume to reach the surface and be visible.

 "*As a result, waves of low amplitude and long wave-length that seem trivial in deep water, may result in large plunging breakers when they reach the shoreline.*"

The reference for this statement was Parnell and Kofoed-Hansen (2001), who were discussing the shoaling of very long-period waves from large ($L \sim 100\ m$), high-speed coastal ferries. The comment is quite misleading in the context of small recreational craft.

"*All other factors being equal, a positive correlation exists between the size of a vessel and the size of its wake (Hill et al. 2002, Fonseca and Malhotra 2012).*"

This statement is misleading. Firstly, what parameter defines "*size of a vessel*"? The whole premise of the "*low-wash vessel*" is that by holding parameters such as displacement and speed fixed, making the vessel longer will reduce the size of its wake, assuming size to imply wave height. If a smaller vessel size were desirable, why does the report discuss jet skis negatively in several areas? The authors partly explain this by noting that jet skis can operate in very shallow waters ($h \sim 1\ m$) and therefore very close to shorelines. They elected not to point out that jet skis are also considered a noise and navigation nuisance.[115]

"*As wave energy increases with wave height squared, wave height provides a reasonable proxy for erosive force.*"

And wave period doesn't provide a reasonable proxy for erosive force, since wave energy increases with wave period squared (at least in deep water)?

There are other misleading statements, such as those of Maynord that incorrectly attribute wave parameters and operating regimes at high speed to planing hulls and not all high-speed vessels in general.

The report goes on to address shorelines characteristics and erosion issues, but in a quite comprehensive and robust manner. That reflects the expertise of the review committee. The low standard of discussion of vessel wash may mean that future recommendations regarding mitigation, largely through boating and speed regulation, may be based on flawed beliefs.

---

[115] In comparison to an average *1.6* fatalities per year involving jet skis (riders, passengers and bystanders), the fatalities in Australia from shark attack averaged *1.1* per year for the past *20* years:

> National Coronial Information System – Jet Ski Deaths 2000-2012: http://www.ncis.org.au/wp-content/uploads/2014/01/Jetski-fact-sheet-Australian-data-only-December-2013.pdf. (last accessed 16th January, 2018).

> West, John G. (2011). Changing patterns of shark attacks in Australian waters. *Marine and Freshwater Research* **62**. 744-754. (John West studying sharks – you can't make this stuff up!)

# Appendix B – Deep Water Wave Height Decay

## B.1 Introduction

This has long been a contentious subject, complicated by the arguments for the deep-water condition spilling over into the shallow-water condition where the boundaries overlap. The theoretical studies of Kelvin (1887) and Havelock (1908) led to the understanding of deep-water wave height decay on the so-called cusp between the transverse and divergent wave systems. The heights decay could be approximated by a simple power law, with $H \propto y^n$, though the original method of Havelock (1908) was presented in terms of the decay between successively numbered crests. Havelock's exponent for transverse waves can be inferred as $n = -\frac{1}{2}$ along any ray; for the combined divergent and transverse systems it can be inferred as $n = -\frac{1}{3}$, but only at the point of intersection between the two systems. It must also be recognised that these exponents in terms of $H \propto y^n$ are not absolute everywhere; $n$ becomes asymptotic to $-\frac{1}{2}$ and $-\frac{1}{3}$ respectively only in the far field. The shallow water condition is far more complex and can yield greater *apparent* decay rates if the power decay law is applied.

The application is somewhat more disquieting. With the growth in passenger vessels operating in sheltered waters came a growth in the science, along with commercial and other opportunities. It became almost obligatory to label any design intended for passenger service in sheltered waterways as "*low wash*", without qualification of what that meant or how it was justified. Moreover, catamaran designs especially were (and still are) given that label without qualification.[116] The public's preoccupation with wave height as the principal determinant of environmental operational viability was reflected in the responses of designers, builders and most researchers, whose primary, and sometimes only, drive became the reduction of wave height through design.[117,118] Wave height was seen to decrease with distance from the vessel, implying that potential wave impacts were dissipating as well. That, along with misrepresented wave decay rates, gave the impression of waves and their accompanying energy almost magically disappearing, provided the requisite design or design philosophy was adopted.[119] Of course, total wave energy does not decay at all, internal and bottom friction excepted; it's only transferred into waves of different and changing forms as the packet propagates.

Macfarlane (2012) presents a summary of deep-water wave decay studies. The use of a decay exponent of $n = -0.33$ is a convenient engineering approximation based on the analysis of model and full-scale data. The work of Kelvin (1887) and Havelock (1908) quite possibly formed the foundation for wave decay investigations, but it can be said with confidence that the determination of the exponents has largely come from experiments. As a retort to the widespread

---

[116] As a most recent example, refer to: "Safety in Numbers – A plan for the Pasig," Conway (2019). The design was proposed to operate in a narrow river at $Fr_L \sim 0.48$ and $Fr_h \sim 0.87 - 1.07$, but was justified as "*low wash"* solely by adopting a catamaran design.

[117] And the public's inability to accurately judge wave height, as discussed in Section 3 and with reference to the observations of Lesleighter (1964, p. 10).

[118] As highlighted in the literature reviews of Appendix A, where wave height was studied *ad nauseam*, yet wave period was given only a cursory review or not discussed at all.

[119] Decay exponents in excess of *-1.0* in deep and shallow water have been published, yet without strong qualification of their narrow applicability. Refer to the comprehensive computational example of Doctors and Day (2001, Fig. 5) in Section 7.

use of $n = -0.33$ for divergent waves, being the most prevalent waves in wave wake studies, Doctors and Day (2001) made the comment: *"In the past, it has been suggested by some persons concerned with the damage caused by the waves behind river vessels, that the wave height varies with the inverse cube root of the transverse offset from the track of the vessel. This misconception presumably has its origins in a misunderstanding of the work of Wehausen and Laitone (1960, p. 487, Equation (13.42b)) and of Stoker (1966, p. 242, Equation (8.2.40))."*

Macfarlane (2012) reports a deep-water decay exponent ranging from $-0.2 \le n \le -0.45$; similar to Doctors and Day (2001) who suggest $-0.33 \le n \le -0.5$ in the high-speed range. Various reasons are quoted for the variation in decay exponent, such as vessel speed, the influence of design, the fact that vessels are not point sources, and interactions between wave systems. The most plausible reasons for the variation are wave packet interactions, which are mostly dependent on speed and lateral separation, and that height decay has been premised on the flawed argument that it based on a power relationship with a fixed exponent for a given condition, which is almost certainly is not. The power decay relationship was possibly nothing more than convenient.

In this analysis, there is a cross-over between a true deep-water condition and a depth super-critical condition. In the case of the latter, a vessel travelling fast enough in water not too deep relative to its static waterline length would be capable of reaching a nominal depth super-critical condition. That can often occur when the water depth is in the order of the static waterline length. The wake in that condition has the appearance of a deep water, high speed wake. Depth only has a significant effect when the $h/L$ ratio becomes small.

## B.2 <u>Schrödinger Wave Packet Equations and the Normalisation of Lateral Separation</u>

The simplest way to confirm mathematically what is observed experimentally is by using an analytical form of a wave packet in a dispersive medium. There are many forms of the wave function, but the one most commonly used nowadays is a linear form of Schrödinger's wave equation, which is a Gaussian form derived from his time-dependent wavefunction used in quantum mechanics.[120] Although the equation is described at the quantum level, it can describe relative relationships at the macro level by setting the mass $m$ and reduced Planck's constant $\hbar$ as

---

[120] *Derived* is possibly the wrong word. Schrödinger's equation cannot necessarily be derived from anything; yet is regarded as one of the basic tenets of physics. The physicist Richard Feynman said:
 *"Where did we get that from? Nowhere. It's not possible to derive it from anything you know. It came out of the mind of Schrödinger, invented in his struggle to find an understanding of the experimental observations of the real world."* Feynman, R.P., Leighton, R.B. and Sands, M. (1963). *The Feynman Lectures on Physics.* Boston, MA: Addison-Wesley. Volume III, Chapter 16-5.

The development of the equation by Schrödinger has a colourful storyline:
"*A few days before Christmas, 1925, Schrödinger, a Viennese-born professor of physics at the University of Zurich, took off for a two-and-a-half-week vacation at a villa in the Swiss Alpine town of Arosa. Leaving his wife in Zurich, he took along de Broglie's thesis, an old Viennese girlfriend (whose identity remains a mystery) and two pearls. Placing a pearl in each ear to screen out any distracting noise, and the woman in bed for inspiration, Schrödinger set to work on wave mechanics. When he and the mystery lady emerged from the rigors of their holiday on Jan. 9, 1926, the great discovery was firmly in hand.*"
From "*The Lone Ranger of Quantum Mechanics*" by Dick Teresi, The New York Times, Jan. 7 1990 (last accessed 15th July, 2019), reviewing: Moore, W. (1989). *Schrödinger. Life and Thought*. Cambridge, NY: University Press.

unity, recognising that these are dimensional quantities. Defining the initial condition for a one-dimensional wave packet at the origin as:[121]

$$\psi(x, 0) = u(x, 0) = \sqrt[4]{2/\pi}\, e^{(-x^2 + ic_g x)} \tag{B1}$$

the general form of Schrödinger's linear, one-dimensional, time-dependent wave equation satisfying the initial condition becomes:

$$u(x, t) = \frac{\sqrt{2/\pi}}{\sqrt{1 + 4t^2}} e^{\frac{-(x - c_g t)^2}{1 + 4t^2}} e^{i\frac{1}{1 + 4t^2}\left[(c_g + 2tx)x - \frac{tc_g^2}{2}\right]} \tag{B2}$$

where $t$ is time, $x$ is the spacial position (equivalent to lateral separation $y$ in wave wake terms), $u$ is the elevation as a function of position and time, and $c_g$ is characteristic group celerity; equal to the group celerity of the packet maximum about which the packet spreads. The first exponential function of [B2] describes the signal wave (packet envelope) and the second exponential function of [B2] describes the frequency-modulated carrier wave (time series elevation).

The packet envelope is defined by the probability density function:

$$|u(x, t)|^2 = \frac{\sqrt{2/\pi}}{\sqrt{1 + 4t^2}} e^{\frac{-(x - c_g t)^2}{1 + 4t^2}} \tag{B3}$$

The value of $|u(x, t)|^2$ in [B3] reaches a maximum when $x = c_g t$, with a maximum relative amplitude of:

$$u(x, t)_{max} \propto \left[1 + 4\left(\frac{x}{c_g}\right)^2\right]^{-\frac{1}{4}} \tag{B4}$$

As will be shown, this method could never provide absolute values of the packet maximum amplitude (and therefore the height of the maximum wave existing within the packet); it can only indicate the relative change in the packet maximum amplitude (with $u$ ranging from unity at the sailing line and approaching zero towards infinity). This limitation is the same as with the commonly quoted power relationship $H = \gamma y^n$, which devolves to $H \propto y^n$ due to the inability to quantify $\gamma$ analytically for all vessel types. Both methods only allow for the transposition of a known wave height from one location to another and not the estimation of the wave height of a vessel in the first instance. That could only be determined by model or full-scale testing, or from a statistical or empirical estimate.

## B.3    Normalisation by Wavenumber

To normalise lateral separation and to provide correlation to the more common lateral separation normalisation of $y/L$, the lateral separation could be multiplied by the fundamental wavenumber, such that $H_{rel} \propto yk_o$. Coincidentally, a similar method was reported by Ward and van Hooff (1976), who normalised lateral separation in the same manner, but using $k_o = g/V^2$, which is effectively $k_o = 2\pi/\lambda_T$, where $\lambda_T$ is the wavelength of the transverse waves and not the

---

[121] See Pauli (1973), p. 3-8.

maximum divergent wave. At displacement speeds, the close relationship between transverse and divergent systems makes the argument valid. High speeds become a problem, since high-speed vessels have weak or non-existent transverse systems, and the relationship between divergent and transverse system wavenumbers at high speeds is not simple to define (one is a function of speed only; the other is a function of vessel parameters, especially length).

The adoption of $yk_o$ for the divergent system aids in the understanding of height attenuation with distance in its alternative form of $2\pi y/\lambda_o$ (since $k_o = 2\pi/\lambda_o$). Lateral separation would be defined by the number of wave cycles undergone up to a particular point, which is a concept more directly relative to the waves and the dynamics of their packets rather than their source (the vessel).

As much as the strengths of normalisation by wavenumber are its non-dimensionality and hence scalability, its weakness is its inability to work in all shallow water conditions. Shallow water wave wakes often don't have identifiable characteristic wavenumbers, and the packet-wise variability in the dispersion strength negates the stability of the packet characteristics centred around the packet maximum. Moreover, depending on the $h/L$ ratio, the position of the maximum wave could vary between the first wave and another wave in the weakly dispersive packet following. Applying the traditional decay rate equation of $H \propto \gamma y^{-n}$ to shallow water wakes can result in widely varying decay exponents, which may be much smaller than $-\frac{1}{2}$ or $-\frac{1}{3}$.


## B.4     Normalisation by Waterline Length

The traditional normalisation using $y/L$ would appear to be not unreasonable, as it would allow for scaling between model and full scale, as well as comparisons between vessels. An adoption of $yk_o$ would provide a relationship to $y/L$. Experimental results scaled from model to full scale follow Froude scaling laws, such that wave periods scale according to $T \propto \sqrt{L}$. Therefore $y/L$ is equivalent to $y/T^2$, and since $yk_o$ is equivalent to $y/T^2$, the relationship $y/L$ is maintained. Similarly, Cox (2000) noted that at high speeds the period of the maximum wave is strongly a function of $\sqrt{L}$ based on the analysis of experimental data, which closes the logic chain here. *Figure B1* demonstrates this graphically, where the results of many full-scale field trials show how the period of the maximum wave at high speeds ($Fr_L > {\sim}0.75$) collapses to a narrow, constant band when normalised by $\sqrt{L}$. The consistency at higher length Froude numbers is greatly improved by the depletion of the transverse wave system.

The obvious drawback of $y/L$ is the variability of dynamic waterline length for certain high-speed vessels, particularly small craft which are often the subject of wave wake environmental investigation. High-speed vessel dynamics are more usually defined by volumetric Froude number rather than length Froude number, even for high-speed displacement forms not experiencing any variation in dynamic waterline length with speed.
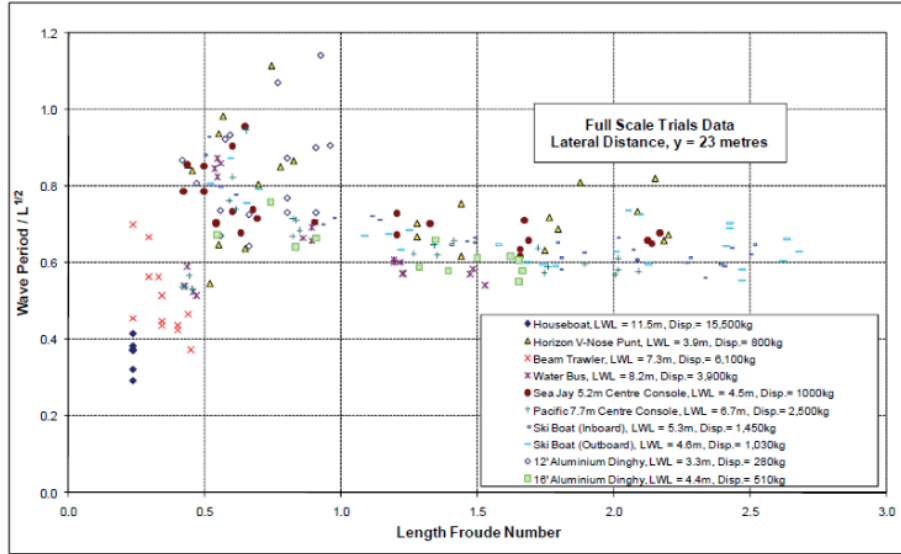
**Figure B1** – *Reproduced from Macfarlane et al. (2008, Fig. 3), showing how the period of the maximum wave normalised by $\sqrt{L}$ collapses to a consistent band at high length Froude numbers. The results are from field trials of small craft at full scale, with inherent variability caused by external factors.*

## B.5  Normalisation by Group Celerity

This is the basis of the Schrödinger linear equation, but it is not without complication. The parameter $y/c_g$ is dimensional, having the units of seconds. This has been explained (by setting some of the wave function constants to a value of unity, since we are interested only in macro-scale relative values), but only by making assumptions about how relationships at a quantum level are maintained at a macro level.

In qualitative terms, the parameter becomes the time taken for the packet to reach a given point, which in turn is used to describe how the packet has dispersed relative to a previous position and time. Decay comes with time; the shorter the time between measurement points, the lesser the extent of the packet envelope spreading and therefore height decay. Between two fixed points, waves travelling faster (i.e., with a higher group celerity) would have less time to decay and so the decay rate would be slower.

Regardless of which form of normalisation is used, those relating lateral distance to wave parameters would appear more reasonable than the traditional method of relating lateral distance to the wave source parameters. Normalisation by group celerity can be equated to normalisation by wavenumber, except that the relationship is $y/c_g \equiv y\sqrt{k_o}$, which is not the non-dimensional relationship considered by Ward and van Hooff (1976).

## B.6  Proposed Deep-Water Decay Rate

*Figure B2* shows comparison between the linear Schrödinger (LS) packet maximum amplitude decay given by [B4], two model test conditions for model AMC 00-01 satisfying (approximately) one or both conditions for neutralising the transverse wave system, and the height power decay based on $H \propto y^{-\frac{1}{3}}$. The experimental and power decay wave heights were made relative to their respective values at the most distant probe ($y = 4.5\ m$; $y/L = 4.32$; $y/c_g \sim 8.4\ s$) to correlate

240

with the relative wave heights of the LS equation; the most distant probe representing a more stable packet state.
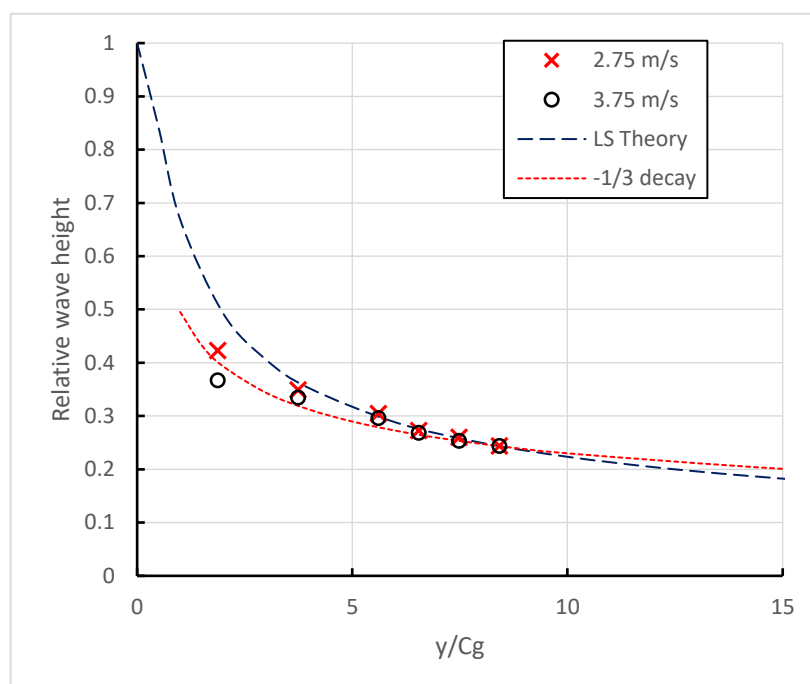


**Figure B2** – *Wave height decay relative to normalised lateral separation. The two experimental conditions for model AMC 00-01 (2.75 m/s and 3.75 m/s) were devoid of transverse waves, which are known to contaminate divergent wave height measurements. The periods of the maximum waves were identical in both cases therefore the packet group velocities were also identical. The model test wave heights and the $-\frac{1}{3}$ exponent decay are made relative to the most distant probe ($y = 4.5\ m$), shown at $y/c_g \sim 8.5$. Six probes spaced at $y = 1.0, 2.0, 3.0, 3.5, 4.0, 4.5\ m$ are evident, relative to a model static waterline length of $L = 1.042\ m$.*

These two speed conditions have essentially the same fundamental wavenumber and hence group celerity – a feature of high-speed vessel wakes where the period of the maximum wave becomes largely independent of vessel speed. Their consistency in the far field is evident, as is the inconsistency in the near field. The wave height clearly decays according to the LS theory once sufficiently separated from the sailing line and not the largely accepted fixed exponent power relationship.

## B.7     Slow Speed Comparison

As previously discussed, it has long been known that wave wake measurements close to a vessel are quite inconsistent due to localised interactions. At displacement speeds ($Fr_L < \sim 0.4$), the most significant cause in the near to medium fields is the interaction between the transverse and divergent systems. In this speed range, the heights and periods of the transverse waves of high-speed hull forms are closer in proportion to those of the divergent waves. Reference is made to Figure 4.2 of Section 4.

241

**Figure B3** extends **Figure B2** to include two slow speed conditions ($V = 1.0, 1.25 \, m/s$; $Fr_L = 0.31, 0.39$). There are several salient features:

a. slower vessel speeds imply larger wavenumbers and lower group velocities, shifting the data to the right;
b. the wave heights in the near-to-medium fields are inconsistent. This was most likely due to the strength of the transverse system. **Figure B4** shows an example of one wake trace ($V = 1.0 \, m/s$; $y/L = 0.96$), with the strength of the transverse system evident;
c. the periods of the maximum waves, which define the packet group velocities, were consistently robust and did not exhibit the inconsistency of the wave heights. This is most likely due to the difference in relative steepness to the two wave systems and the fact that the transverse waves were two to three times longer than the maximum divergent wave, further compounded by the difference in relative wave angles unless measured exactly at the Kelvin wedge (which is not true anyway due to the phase shift at the wedge;
d. the four most distant probes at each speed are quite consistent with the LS envelope decay rate. A power decay with the standard exponent of $n = -\frac{1}{3}$ is shown, made relative to the LS value at $y/c_g = \sim 8.4$ (as per Figure B2). Visually, the $n = -\frac{1}{3}$ exponent is less consistent with the more distant results.
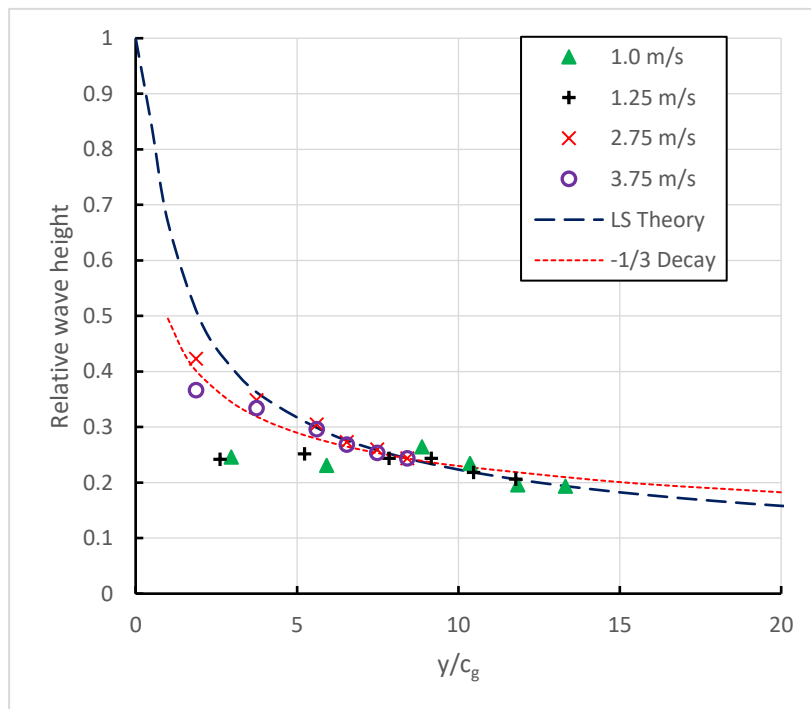


**Figure B3** – *Figure B2 reproduced with two additional slow speed conditions ($V = 1.0$; $1.25 \, m/s$). The length Froude numbers range from 0.31 to 1.17. Note how the lower group celerity at slower speeds shifts the data to the right. Also note the general inconsistency of wave height measurements close to the vessel but increasing correlation with the LS decay rate further from the vessel. Similarly, consistency improves with increasing speed due to the depletion of the transverse wave system. An additional power decay with $n = -\frac{1}{3}$ has been added for comparison (correlated with the LS curve at $y/c_g = \sim 8.4$, which was the middle probe location). Near field deviations excepted, the overall correlation with the proposed decay rate is clear.*
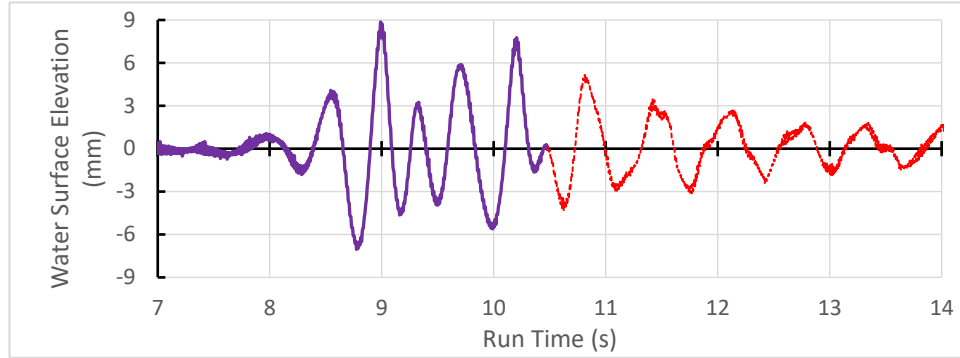
**Figure B4** – *Sample slow speed wave wake trace for Model AMC 00-01 at:* $y = 1.0\ m;\ y/L = 0.96;\ V = 1.0\ m/s;\ Fr_L = 0.31;\ Fr_h = 0.34$. *The divergent system (purple line left) is evident around 8-10 s, with the transverse waves following (red dashed line right). The transverse waves are large in comparison to the divergent waves and result in a substantial interference, evident by the uneven nature of the divergent wave peaks and troughs.*

## B.8 Comparison using Aggregated Data.

The robustness of [B4] is demonstrated in **Figure B5**, which combines model and scaled model results on a single decay graph. Conditions include slow and high speeds, as well as deep and shallow conditions (where the leading shallow water wave is not dominant).

Some of the near-field probe ($y \leq 2L$) results are shown and they almost always defy the general trend due to localised packet interactions. The scaling discrepancy caused by the dimensional nature of the parameter $y/c_g$ is not evident.
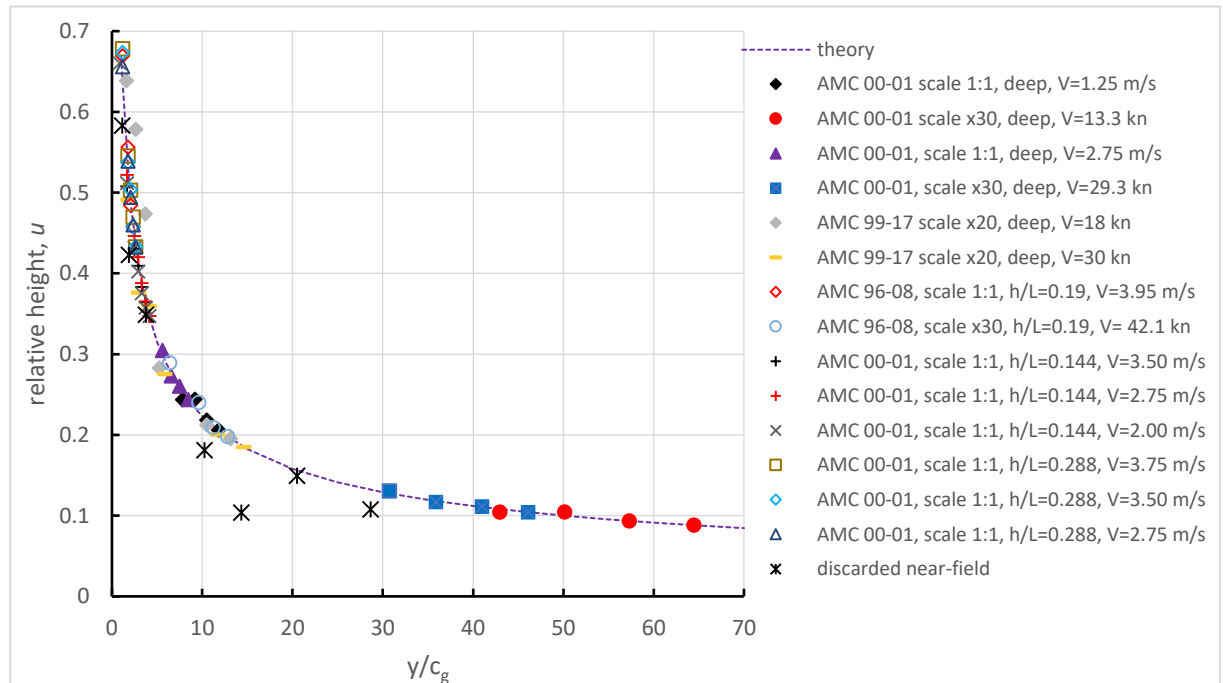


**Figure B5** – *Combined data from model scale and scaled model results for deep and shallow water (first wave in shallow water only). For each vessel condition, the most distant probe is given the relative height value according to [B4] and from that the heights at the intermediate probes are used to calculate the intermediate values of u. The calculated values compare well with the theoretical value. It also shows that the dimensionality of the $y/c_g$ parameter has little effect on scaled wave wake results. The near-field ($y < 2L$) data are shown to highlight that the method cannot account for localised packet interactions.*

243

## B.9 Approximations of Decay Exponents Relative to the LS Equation

To explain observed and reported decay rates, the LS curve was delineated into the lateral ranges commonly used to describe a high-speed wave wake field, and a power decay was fitted within each range. These ranges are not absolute and do vary according to interpretation. The assumed ranges are summarised in **Table B1** and shown graphically in the form of approximations in terms of $y/c_g$ in **Figure B6**.

**Table B1** – *Lateral field ranges and corresponding approximated power decay exponents ($H \propto y^n$)*

| Range | y/L | n |
|---|---|---|
| Very near | <1 | -0.322 |
| Near | 1 to 2 | -0.472 |
| Medium | 2 to 4 | -0.493 |
| Far | >4 | -0.499 |
| Extreme | →∞ | -0.500 |
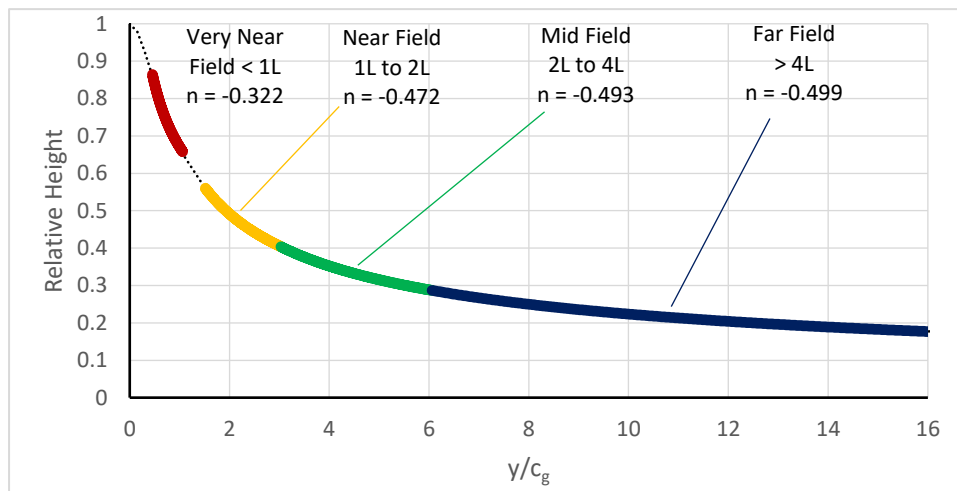


**Figure B6** – *Approximate delineation of the LS decay curve with commonly used high-speed ($Fr_L > 0.5$) wave field ranges (refer Table B1). Power relationships in the form $H \propto \left(y/c_g\right)^{-n}$ were fitted to each field range to derive the local decay exponent, for correlation with the commonly quoted wave decay equation $H \propto y^{-n}$. For a particular vessel and speed, the group celerity would be constant and so $H \propto \left(y/c_g\right)^{-n}$ devolves to $H \propto y^{-n}$. That would not be the case where the speed and or vessel varied.*

The *very near field* range ($y < 1L$) was included as it represents the location of historical wake measurements from model tests in towing tanks, where restrictions on lateral separation and tank wall reflections limited the scope. Many of the early experiments at the AMC were conducted in this way. Another example of such techniques can be found in Bruno *et al*. (2002), and discussion of the problems measuring wave wakes in towing tanks can be found in Macfarlane (2012, Section 4.2.1). The *very near field* also represents the location where the power decay exponent is close to the traditional value of $n = -\frac{1}{3}$ (Figure B6).

The decay exponent varies from zero at the sailing line to $-\frac{1}{2}$ at infinite lateral separation, with a practical range of about *-0.3* to *-0.5* where wave wake experiments are typically carried out. This

would correlate reasonably with the previously mentioned experimental results obtained by Macfarlane (2012) of *-0.2* to *-0.45* and the computational analysis of Doctors and Day (2001) of -*0.2* to *-0.5* when $Fr_L > 0.5$. In both those instances the measurements were of wakes comprised of multiple wave packets and not an individual wave packet.

There are two practical observations from this. Slow speed vessels generate short divergent wavelengths and therefore large fundamental packet wavenumbers, hence small group velocities. This would shift the wave decay exponent into the very far field range where the decay rate approaches its maximum, particularly for a large vessel such as a merchant ship. It is commonly observed that large ships can travel at moderate speeds (say, *8 kn*, but $Fr_L < 0.1$) in restricted waterways, yet the wake appears almost non-existent at *1L* laterally (blockage effects excepted). Conversely, smaller vessels such as passenger ferries operating at high speed in deep water would have long divergent wavelengths, hence small fundamental packet wavenumbers and high group velocities. Their divergent waves are quite visible several boatlengths laterally, as their waves initially fall into the lower decay rate range due to the reduced time available for decay and the fewer elapsed wave cycles.

The extreme deep-water decay rate of *-1.06* from Doctors and Day (2001) needs further mention. It represents the wave decay of a catamaran vessel of length *24 m*, displacement of *60 t* and at a speed of *6.7 m/s* (*13.0 kn*). A similar design exists on Sydney Harbour – the Sydney Ferries First Fleet vessels operated by Harbour City Ferries.[122] The design has a waterline length of *25 m*, a published displacement of *83 t* (but in an unknown condition) and is capable of *12 kn* in a light condition. The design was originally intended to be *30 m* long but was cut down for manning reasons. The fleet was also to be used on the Parramatta River service (assumed to be the lower Parramatta River) but could not due to the wash created. That would seem to conflict with the numerical findings of Doctors and Day (2001), which is another reason why computational analysis can only ever have credibility when validated by model and or full-scale trials, of which the First Fleet vessels were.[7] One of the First Fleet vessels was wake tested at full scale by the AMC but with insufficient probes to make a formal assessment of wave decay.

### B.10    Variability in Decay Rates

Variation in decay rates can be caused by interpretation of a wake trace. Three features dominate the variations: near-field effects (a loosely defined but convenient term); wave packet interference; superimposed transverse waves. Vessels are not perfect point sources, and localised wave interactions and depressions are known to exist near to the vessel. Wave cuts taken closer than $y = 1L$ from the sailing line are difficult to assess consistently, more so at slow speeds.[123] Wave cuts closer than $y = 2L$ should be considered as unreliable. Examples of interactions are provided in Section 3.

---

[122] http://www.afloat.com.au/afloat-magazine/2009/june-2009/Sydney_Public_Ferries#.XGOejFwzY2w and http://sydneyferry.blogspot.com/2014/10/the-story-of-first-fleet-ferries.html (last accessed 13th February, 2019).
[123] At slow speeds, the bow and stern packets are more discernible and separated in time by approximately one waterline length of travel. The possibility of constructive/destructive interference is greater. At high speeds, the two packets are more likely to be closer and the overall result is nearer to that of a single packet. Refer to examples in Section 3.

Similarly, buried beneath the divergent wave systems are (generally) smaller transverse wave systems. The transverse system decays at an apparently faster rate, yet superposition contaminates the divergent wave height results in the near field where the transverse system is more evident.

There are two ways to neutralise the transverse system. The first is to operate super-critically, such that the transverse waves depth restricted and they are unable to travel with the vessel. Provided $h/L > \sim 0.66$ in this depth super-critical condition, most of the divergent waves would not be depth affected and so the maximum divergent wave would approximate to a truly deep-water condition, but without the transverse waves present.[124] The second is to conduct experiments at $Fr_L > \sim 1$, when it is commonly observed that the transverse wave system is so small as to be immeasurable, or possibly even non-existent. At that point, $\lambda_T = 2\pi L$, which is longer than a vessel is thought capable of generating.[125]

---

[124] This, however, is a slight over-simplification. It can be shown that, although the maximum wave may not be depth affected, the waves preceding it in the packet are depth affected and there can be a reduced amount of energy recycled rearwards due to the weakening dispersion of the depth-affected leading waves. (Drobyshevski, 2017). It is very minor if the depth is constant, but can become substantial if the depth changes quickly, with the leading waves in very shallow water but the maximum wave still in deep water. The height attenuation of the maximum wave under those conditions could be in the order of *20%*.

[125] Gadd (1994) claims that vessels cannot generate *significant* waves longer than about *3L*, but for the transverse system that would occur at $Fr_L = \sqrt{3/(2\pi)} = 0.69$, which is questionable. Gadd did not differentiate between wave types, though was probably referring to the divergent system.

# Appendix C – Shallow Water Wave Height Decay[126]

## C.1    Introduction

The developed wave decay equation is based on the decay of the envelope of a packet propagating at a group celerity. The decay cannot be applied to any wave within the group, since a wave at one instance in time is not the same wave at another time. The wave decay equation, which describes the decay of the packet envelope, in effect describes only the decay of the maximum wave in the packet. The envelope soliton changes as it propagates, but it is always the same envelope soliton and so the decay relationship is valid.

The shallow water case would appear to be complicated by the fact that waves are weakly dispersive, with the degree of dispersion varying across the recorded wave packet according to the relative wavelengths and water depth. Just as the deep-water envelope soliton has the form of a Gaussian distribution, the shallow-water envelope soliton has the form of a skewed Gaussian distribution, with the degree of skewness increasing as the depth decreases. There is no simple definition of group celerity in that instance, as there is in the deep-water case. However, the first shallow water wake wave (or *apparent* wave, as it turns out) is different. It propagates at close to the depth-restricted speed of $\sqrt{gh}$ and so at a condition where the group and phase celerities converge. The first wave crest propagates at $\sqrt{gh}$ and hence forms the Havelock wavefront, with requisite angle to the sailing line determined by the water depth and vessel speed, but other parts of the first wave, such as the initial upswelling and the trough following the crest, do not travel exactly at $\sqrt{gh}$.[127]

The first wave in a shallow water wake is not a single wave, but the superposition of several waves that are unable to disperse much. There is in fact weak dispersion, as there is in the rest of the wake following, with the shorter period components of the wave function eventually falling behind and out of the nominal first wave. The apparent stretching of the period of the first shallow water wake wave with increasing lateral separation is evidence of this. As a group, these component waves would have features of a packet, but with the appearance of a single wave. That becomes the premise for this analysis.

## C.2    Shallow Water First Wave Form

Fourier analysis is helpful in assisting with the understanding of the form of the first apparent shallow water wake wave and its component frequencies. In a qualitative assessment, the interpretation of the Fourier analysis is important. A simple, monochromatic wavetrain would exhibit a very peaked response about its fundamental frequency; the sharpness of the peaked response reflecting its monochromaticity. In wave wake terms, such a feature would describe the transverse waves, where their period was a function of vessel speed only.[128] A dispersing wave packet would exhibit a range of frequencies; skewed by a lengthening tail of higher frequencies

---

[126] There are no references for this section. The explanations within are unique.

[127] The first crest conforms to a Havelock wavefront provided the water is not extremely shallow, where the first wave is dominated by the solitary wave embedded in all depth super-critical first waves.

[128] The transverse system cannot be purely monochromatic and must have component frequencies that describe the vessel acceleration/deceleration phases.

where greater numbers of smaller, shorter waves were appearing. **Figure C1** shows a graphic example. The energy of the packet peaks at a point ahead of the packet maximum (which defines the packet's fundamental wavenumber), typically by around half to one wave (the more waves in the packet, the more the energy peaks towards the packet head).

**Figure C2** shows the shallow water Fourier analysis of the first wave at five lateral locations from model tests (refer to Figure C4 following). The analysis demonstrates that the first visible shallow water wave is not a single wave, as would be the case with the solitary waves formed around the depth-critical speed but is actually a series of waves visible as a spread of frequencies.[129] This is not comparable to the peaked Fourier transform of a monochromatic solitary wave or the transverse wave system.
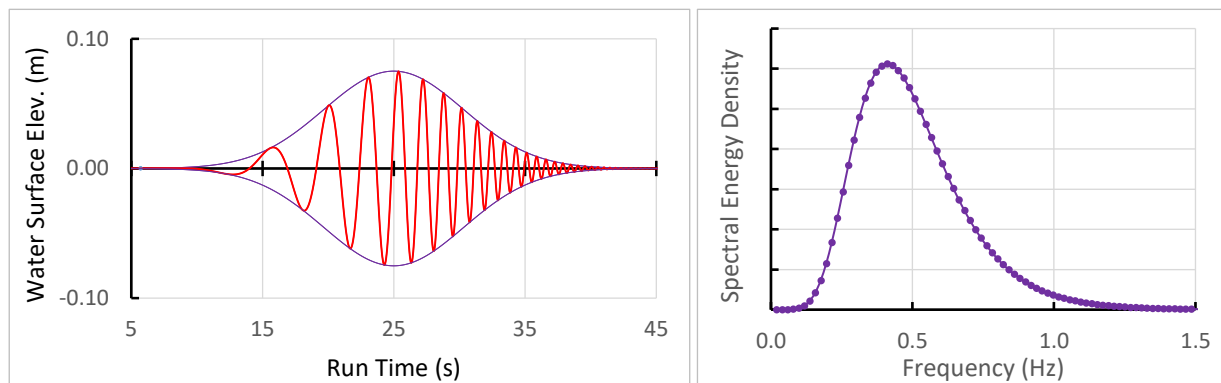


**Figure C1** – *Sample Fourier analysis (right) of a spatially-generated wave train (left), based on a simple Gaussian envelope and a sine function with exponential decay [$f(0, t)$]. Of interest is the shape of the asymmetrical frequency distribution, equivalent to a Rayleigh distribution, exhibiting the spread of frequencies inherent in a propagating wave packet. The degree of skewness (asymmetry) is an indication of the strength (or weakness) of the packet dispersion. The energy peaks at around $T = 2.44\ s$ (~$0.41\ Hz$) and the measured period of the maximum wave (as a discrete entity) is $T_m = 2.17\ s$. This is expected: the peak in the energy distribution occurs before the peak in the envelope (represented by the maximum wave). Note also the lack of energy at low frequencies – there being no underlying solitary component in this generated example.*

---

[129] Solitary waves do not have a defined period but become increasingly evident in a Fourier analysis at the lowest frequency. This can be noted in Figure C1, where the generated packet does not have a solitary wave component and therefore the response at low frequencies tends to zero.

248
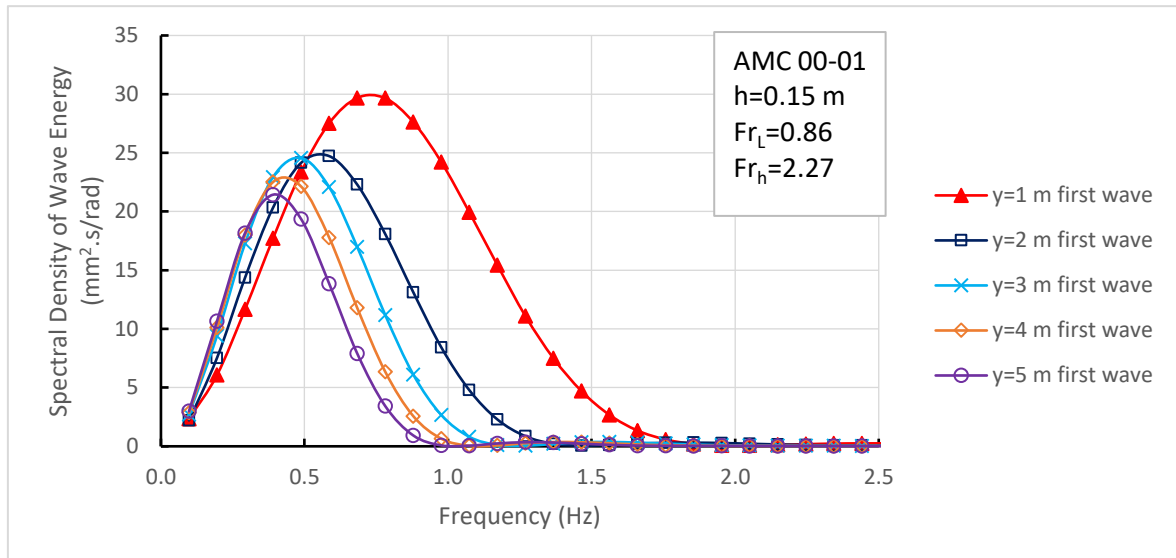
**Figure C2** – *Fourier analysis of the first wave at a depth super-critical condition for model AMC 00-01 at five lateral positions. Of note is the consistency of the leading slope at low frequencies at $y = 3\ m$ and beyond, and the gradual dispersion of the higher frequencies (narrowing of the frequency range) - dropping out of the packet as they are unable to travel at $\sqrt{gh}$. The overall shape and very consistent spread of frequencies demonstrates that the first shallow water wave is not a wave, but a packet. Note also the constancy of the energy density at the lowest frequency, which represents the embedded solitary component.*

There are several notable points of discussion for **Figure C2**:

a. the very consistent and smooth shape of the energy distribution is evident, identical to that of **Figure C1**. If conditions are very controlled (either mathematically in the case of Figure C1 or by the experimental depth/celerity limits of Figure C2), the response is more regular;

b. propagation leads to a narrowing of the frequency band. The wave function making up the first (apparent) wave would have a celerity limit of $\sqrt{gh}$, but not for all frequencies describing the function. There would be components of the first (apparent) wave propagating at "*near $\sqrt{gh}$*"; better described as the weakly dispersive components. They fall behind as the first wave propagates, leading to the stretching of the apparent period with increasing lateral separation (refer to Figure C4 following);

c. it has been shown that there are non-linear components of the first wave that travel ahead of the crest at a celerity slightly greater than $\sqrt{gh}$ (refer Appendix ZE, ZF). This is likely due to a solitary wave embedded within the first apparent wave (or packet) that travels at a depth super-critical celerity, otherwise representing one of the end conditions of the Korteweg de Vries equation that defines the components of this first wave. Such a solitary wave would be generated as the vessel accelerated through the depth-critical speed and remains in some form at depth super-critical speeds. The wake formed at the sailing line is initially packed into an infinitely short space. Stability in the very initial upswelling is reached at several boatlengths from the vessel, which appears to be related to point where the longest component in this first wave has travelled about one wavelength. **Figure C2** shows that the initial (leading frequency) slope of each spectral density curve stabilises at around $y \geq 3\ m\ (\sim 1\lambda)$, and further propagation results in the same leading frequency slope remaining constant but the trailing frequencies falling

away. This is what would be expected, as the weakly dispersive components fall out of the first packet and into the wave train following;

d. there is a very small, emerging peak at around $f \sim 1.0 - 1.5 \, s$; the frequency decreasing with lateral separation. Although the Fourier analysis in **Figure C2** was conducted only on the first apparent wave, which ends at a zero up-crossing, this (apparent) first wave does not exist independently and its wave function is part of a larger wave function describing the whole wavetrain. Analysing the full wake shows that this small peak occurs at the same position as that of the spectral response of the wake following the first wave, and so can be considered as the emerging "*link*" within the wave function that maintains the continuity of the wave function across the whole wake.
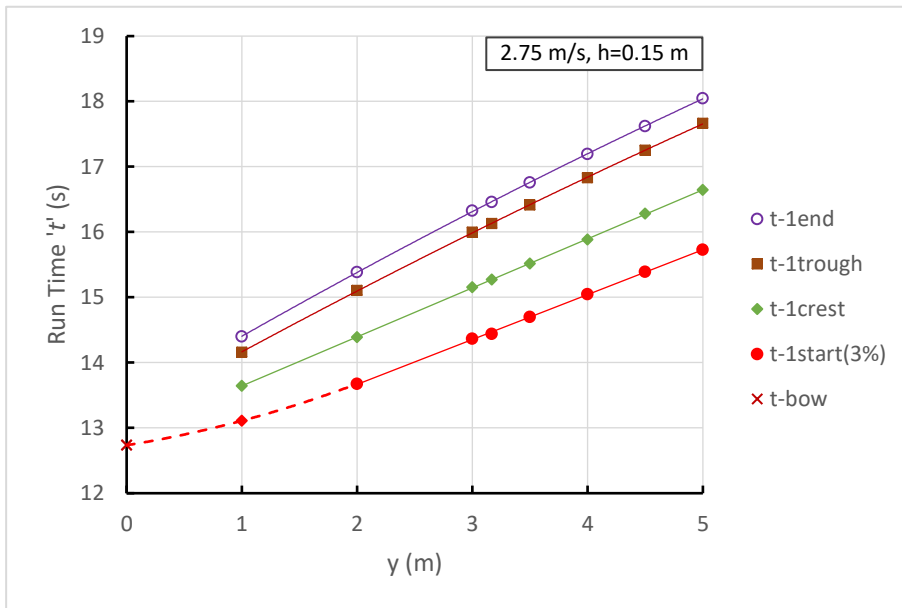


**Figure C3** – *Time/position plot of the shallow water first wave features for model AMC 00-01 ($L = 1.04 \, m$; $V = 2.75 \, m/s$; $h = 0.15 \, m$), including the initial upswelling (at 3% of the first crest amplitude), crest, trough and first wave end (zero up-crossing). The initial upswelling time is linear with lateral separation in the medium-to-far field, but not in the medium-to-near field (dashed line). The point of linearity commences at around $2 \, m < y < 3 \, m$. This correlates with the constant initial slopes of the Fourier responses in Figure C2.*
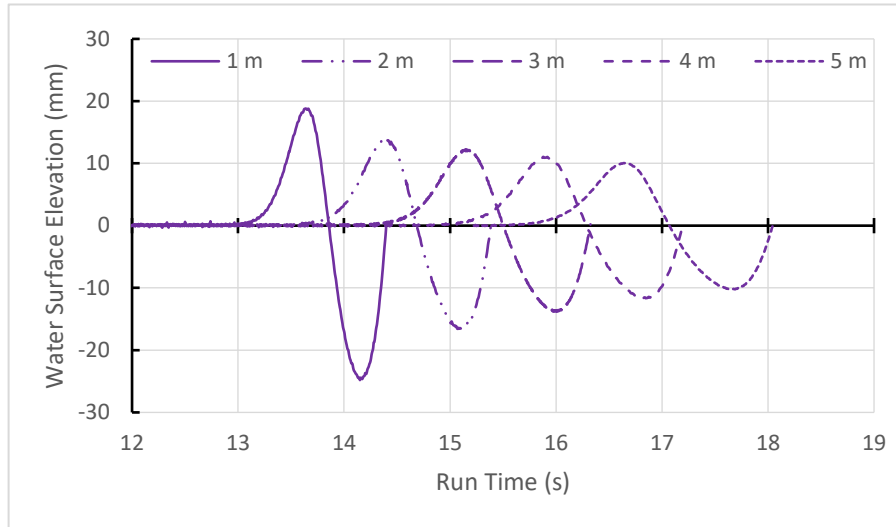
**Figure C4** - *The first shallow water wave for model AMC 00-01 ( $V = 2.75\,m/s$ ; $Fr_h = 2.27$) at five different lateral separations in 0.15 m water depth. The height decays with propagation but the apparent period increases (refer to the "start and "end" lines in Figure C3). Also of note are the disproportionate crest height in the near field ($y = 1L$) and the gradually reducing asymmetry between crest height and trough depth. This asymmetry is partially responsible for decay rate discrepancy in the very near field.*

## C.3     Decay Rate

Use of the developed decay equation requires knowledge of the fundamental wavenumber and hence the group celerity of the packet. In deep water, where none of the waves are affected by depth, the relationships between waves are absolute. Where waves are fully depth affected, the celerity limit of $\sqrt{gh}$ would give the same effect. In intermediate water depths, where waves are depth affected to differing degrees depending on their wavelengths, the relationship is more complex and relative. In reality, though, waves propagating as a group are never fully depth affected to the point of being absolutely non-dispersive; only the crest of the first wave could be considered as fitting the definition of non-dispersive (with celerity of $\sqrt{gh}$). **Figure C3** shows this clearly, with none of the salient features of the first wave being parallel to each other and therefore travelling at different speeds.

Using the relationship developed in Appendix B, the decay equation for the first (apparent) wave in shallow water would be:

$$u(x,t) \propto \left[1 + 4\left(\frac{y}{\sqrt{gh}}\right)^2\right]^{-\frac{1}{4}}$$

[C1]

Where $u$ is the wave height at lateral position $y$ relative to the wave height at the sailing line (taken as unity), and so ranges between *unity* at the sailing line to *zero* towards infinity. Again, the relationship is approximate, since the group celerity is only approximately equal to $\sqrt{gh}$ across the first (apparent) wave.

As this method predicts the wave height at a position relative to the height at a known location, values of $u$ for each experimental data point are relative to one selected position. In all cases the known location is taken as the most distant probe, being the one generally most consistent in its results. The method applied to an experimental data set is:

251

- Set the "$u$" value for the furthest probe measurement according to [C1].
- Calculate the "$u$" value for intermediate probe positions according to $u_2 = u_1 H_2/H_1$
- Calculate the theoretical value of $u$ according to [C1].
- Plot the calculated $u$ values against the theoretical values for different values of $y/c_g$ ($y/\sqrt{gh}$ in the shallow water condition).

In all versions of the graphed data, the theoretical and experimental values of $u$ will coincide at one point (the furthest probe position).

In the case of the shallow water experiments, the relative heights can be plotted against $y$ rather than $y/\sqrt{gh}$ for a fixed water depth. When comparing across multiple depths, $y/\sqrt{gh}$ must be used.


## C.4    Variation with Depth

As depth decreases relative to the vessel length, the strength of the first apparent wave increases. It becomes dominant when $h/L < \sim 0.15$. At this point the first apparent wave becomes the most dominant in height and certainly the most dominant in apparent period. Fourier analysis as well as estimates based on wave parameters show that the energy of the first wave as a percentage of the total wake energy increases as depth decreases. This is discussed in *Appendix ZA* (Fig. ZA12).

The packet behaviour of this first wave becomes very defined at shallow depths. Increased depth leads to an increased rate of dispersion, which moves more energy out of the first packet and into the main packet as they propagate away from the sailing line. The stronger dispersion rate in the first packet at intermediate depths means its decay becomes less predictable, since the decay method is premised on a fixed group celerity. If wave components fall out of the first packet faster due to dispersion, the group celerity of the first packet would vary more with propagation.

Localised interference effects in the very near field make the near-field wave heights unreliable. Also, during analysis it was obvious that many near-field traces were contaminated with spikes and high frequency waves evident at the wave crests, though they were not evident in the medium to far field. In most of the presented model-scale decay data, results at the first probe ($y = 1\ m$) have been discarded. ***Figure C5*** is an example of near-field, shallow water instability of the first apparent wave, in that case caused partly by the forefoot spray sheet.

Some of the near-field instability in shallow water can be overcome by comparing the decay of only the first apparent wave crest; the first crests having more stable decay than the first troughs. In practical terms though, there is little interest in wave wake heights in the near field.
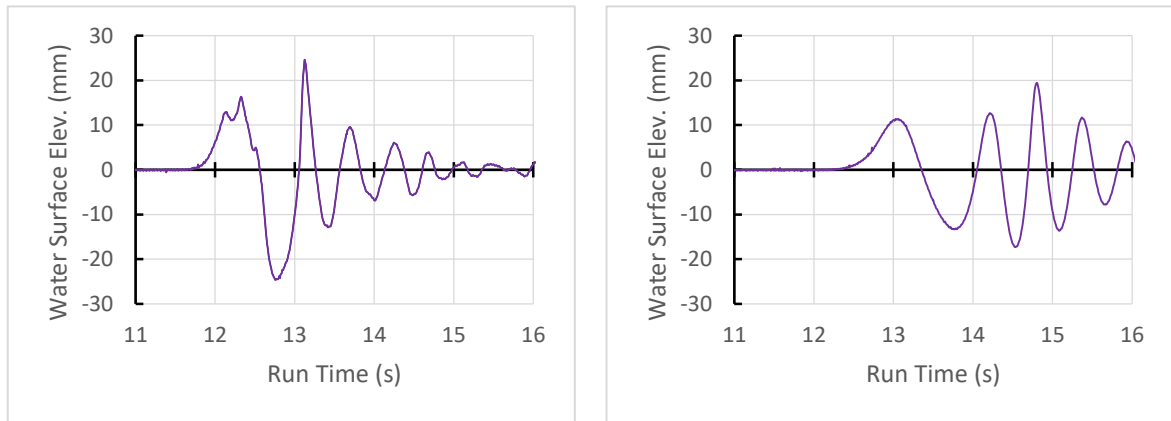
**Figure C5** – *Example of instability of the first wave crest and exaggeration of the depth of the first trough in shallow water at ~1L from the sailing line (left) and subsequent stability at ~2L from the sailing line (right). (AMC 00-01: $V = 3.5\ m/s; h = 0.15\ m; y = 1\ m$ left, $y = 2\ m$ right).*

## C.5    Variation with Depth Froude Number

Analysis of experimental data demonstrates that the derived wave decay relationship is invalid around the depth critical speed. Below this, wakes are of a deep water form, with packets comforming to the decay relationship. At depth super-critical speeds, wakes are as previously described, with a single leading wave (or apparent wave) followed by a packet of shorter waves slowly decaying in period.

## C.6    Examples

*Figures C6* and *C7* show examples of actual and predicted wave height decay for the first shallow water wave over a range of super-critical speeds at two depth conditions. Three points are most notable:

a.  the first near-field probe heights are unreliable;
b.  decay at the depth-critical speed is of a different form;
c.  the prediction improves as water depth decreases as the components of the first wave become less dispersive.

*Figures C6* and *C7* include data for their respective depth-critical speeds and the height decay has a more linear or weakly non-linear form, but quite obviously different to other speeds.

*Figure C8* shows examples of a power decay, which is the commonly accepted wave decay functions. A power decay with a constant exponent can be fitted to [C1] but over a limited lateral separation, since the approximated power decay rate changes laterally. The value of the negative decay exponent becomes larger away from the sailing line, approaching its limit of *-0.5* in the far field. The accuracy of [C1] improves as the water depth decreases.

The two examples presented show that the experimental decay rate is slightly faster than the theoretical decay rate. The explanation for this is simple. The theoretical rate is based on an assumed group celerity of $\sqrt{gh}$. The actual group celerity is something slightly less than this; dependent on the degree of weak dispersion within the first wave. A higher group celerity means less time to decay, leading to lower actual decay at a given lateral separation. Height decay has a time dependency.

253

*Figure C9* demonstrates how near-field inaccuracies in interpreting height can substantially change a power decay interpretation.
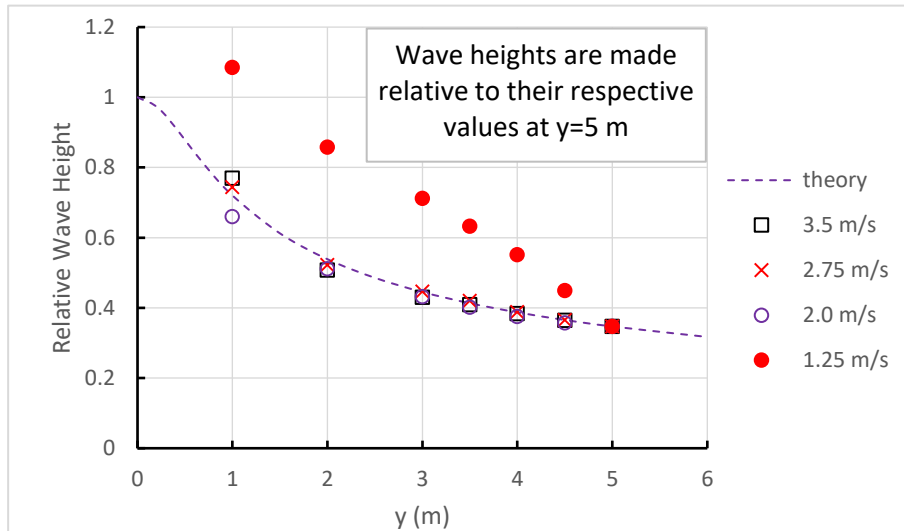


**Figure C6** – *Shallow water wave height decay comparison for model AMC 00-01 ($h = 0.15\ m$). The depth-critical speed is $V_{crit} = 1.213\ m/s$. In general, all results follow the equation described by [C1], except around the depth-critical speed where the wave form and propagation are different. The close fit, even for the near-field location, is due to the shallow water depth and the increasing relative strength of the first (apparent) wave as water depth decreases. The shallower the water, the closer the fit.*
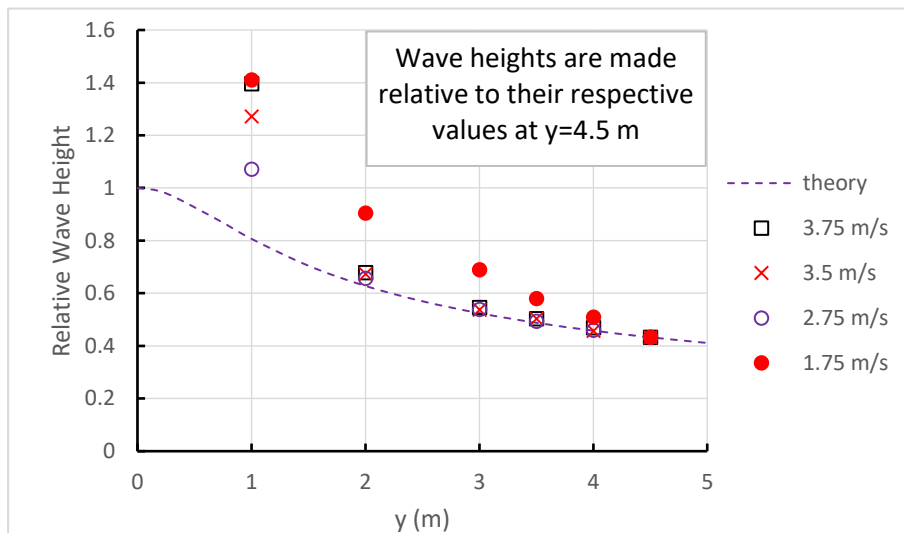


**Figure C7** – *Shallow water wave height decay comparison for model AMC 00-01 ($h = 0.3\ m$). The depth-critical speed is $V_{crit} = 1.716\ m/s$. The depth-critical speed condition and the near-field probes diverge from the theoretical decay.*
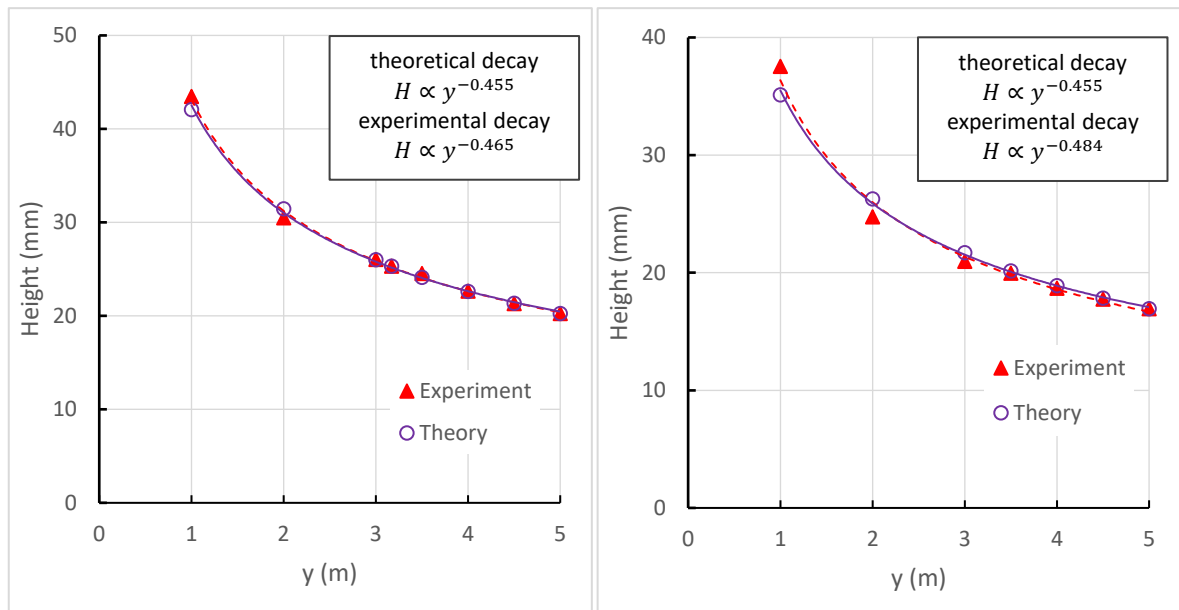
**Figure C8** – Model *AMC 00-01 at* $h = 0.15\ m$; $V = 2.75\ m/s$ *(left) and* $V = 3.5\ m/s$ *(right), with power decay curves fitted to the theoretical and experimental data of Figure C6. In very shallow water and high depth super-critical speeds, the experimental data closely fits the theory. Power decay curves (solid purple line for theory, dashed red line for experiment) are fitted to correlate with present wave wake practice, noting that the exponent values are slightly less than -0.5. The theoretical decay is identical in both cases; the group celerity being determined by the depth alone.*
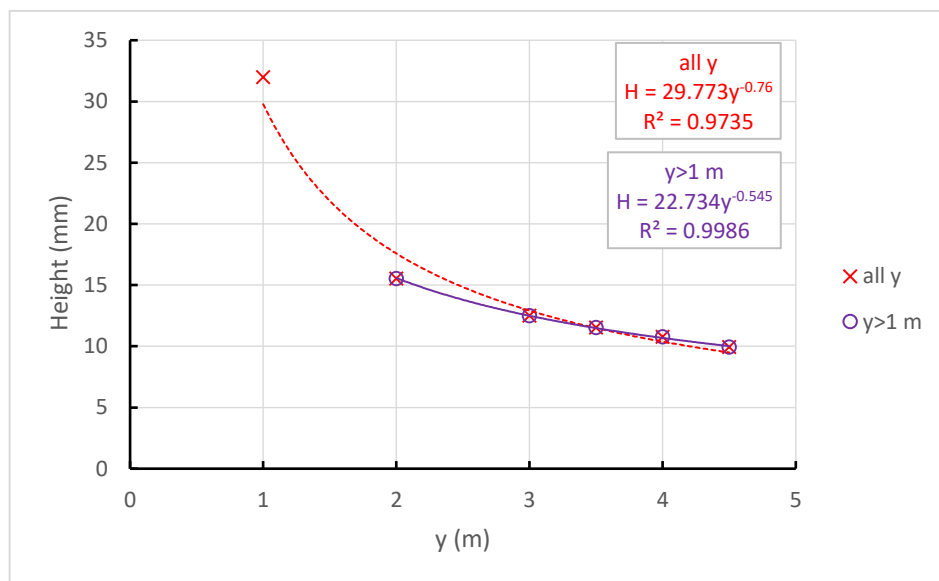


**Figure C9** – *Example of the industry-standard interpretation of height decay using a power relationship for model AMC 00-01 ($V = 3.75\ m/s$; $h = 0.3\ m$; $Fr_h = 2.19$). If all data from near to far fields are considered, the apparent power decay exponent becomes large; distorted by the extreme wave height in the near field. Taking only values at $y > 1\ m$ ($y/L \sim 2$ and beyond), the exponent comes down to -0.545. Reducing the wave height value at $y = 2\ m$ from 15.54 to 15.0 mm (reduced by 3.5%), the power decay exponent becomes -0.5. The theoretical lower limit of the decay equation exponent is -0.5. In practical terms, the value in the very near field is inconsequential. Apart from near-field effects, vessels would not operate at such a depth Froude number so close to shorelines.*

# Appendix D – Shallow Water Wavefront Propagation

## D.1    Measurement of Salient Shallow Water Wave Features

When assessing shallow water wave wakes, it became apparent that the period of the leading wave changed (increased) with increasing lateral separation. This contrasts with the deep-water condition where the period of the maximum wave is stable; being a function of the packet group celerity. Moreover, the salient features of the leading wave travelled at different speeds, including speeds in excess of the linear shallow water limit of $\sqrt{gh}$. This assessment led to the conclusions that there was an underlying solitary wave component within the leading wave and that the leading wave was comprised of multiple waves trapped within a very weakly dispersive condition.

Most wave features, such as zero crossing points, crests and troughs, are easy to discern from model results. The zero crossing points in particular are discernible in the tabulated water surface elevation data to the nearest time-sampling unit. When viewed at a large scale, crests and troughs are often contaminated by very small ripples. The technique used here to determine the probable time position of the crest or trough was to fit a curve to the data points around the inflexion and determine the exact time position of the maximum/minimum elevation. The exact position of the maximum/minimum could vary according to the order of polynomial fitted, but not by more than a few time-sampling units.

The definition of the start of the first wave is more complex. In deep water, where the packet shape is more symmetrical about the maximum wave height and the wave height tends to zero at the ends of the packet, the beginning of the first wave is effectively indeterminable. Taking the first determinable point, usually a zero crossing point (up or down), is the only option, the problem then being to identify the same point at successive lateral positions. If this is possible, the question then is if this is actually the same wave at successive lateral positions, or just the same packet feature. Packet dynamics says that it's only ever the same feature; not necessarily the same wave.

For shallow water waves, the packet shape makes analysis easier. **Figure D1** shows a typical shallow water wave packet, comprised of a large leading wave followed by several waves of shorter period and reducing height. Unlike the deep-water condition, where the maximum wave is almost always the most energetic wave and occurs in the middle of the packet (by definition, where the packet envelope has its maximum bounds), the most energetic wave in shallow water is almost always the leading wave. However, the most energetic wave in a shallow water packet may not always be the highest wave, and only becomes so if $\lambda/h$ is sufficiently large. This is further discussed in the Section 5.

In the study of solitary waves, Lighthill (1978) makes the comment that a notional wavelength for a solitary wave can be measured between nominal points of surface elevation, which were suggested as *3%* of its crest height. Although the waves measured here are not solitary waves and may not even be cnoidal in form, taking the starting point of the first wave as *3%* of the corresponding amplitude of the first crest proved reasonable, repeatable and consistent. **Figure D2** shows this graphically.

Another method previously proposed by Cox (2000) in relation to shallow water, restricted channel effects, was to find the still-water intercept of the slope of the leading wave face. This is shown in *Figure D2*. It can be seen in *Figure D2* that all wake waves exhibit very straight slopes about their zero crossing points, except for the first down-crossing of the first wave in a shallow water condition, which is distorted by the speed-trapped component waves that go to make up the first wave. It does provide a very consistent and simple means of determining a starting time for the first wave, but whether or not it actually has any relevance to the wave propagation itself is another matter.
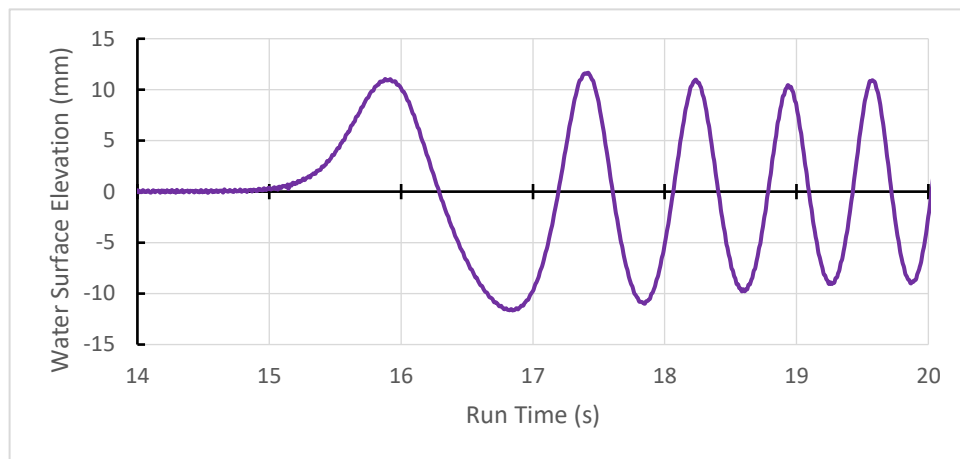


**Figure D1** – *Wave trace for model AMC 00-01 at $V = 2.75 \ m/s$, $y = 4.0 \ m$, $h = 0.15 \ m$, $Fr_h = 2.27$.*
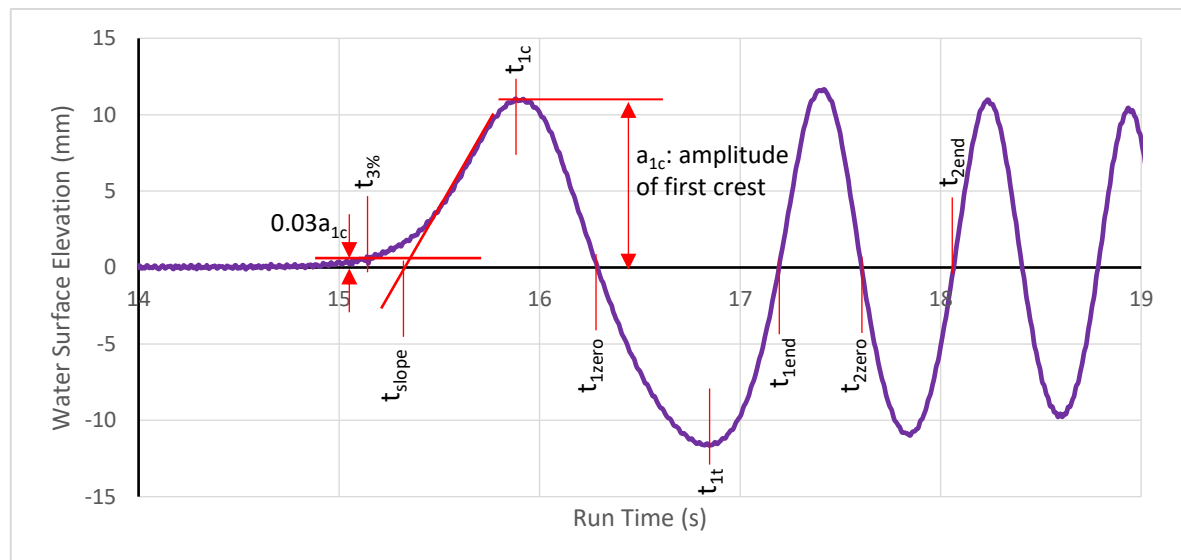


**Figure D2** – *Interpretation of the salient features of the first shallow water waves, showing the definition of the nominal start point based on 3% of the first crest amplitude (Lighthill, 1978) and intercept of the initial wave slope.*

257

## D.2    Propagation of the First Wave

Several experiments in shallow water were studied to determine how the first wave propagated. The common literature, including Havelock's 1908 paper on the subject of depth-affected wake waves, make sweeping generalisations about wave wake patterns. The depth super-critical pattern shown by Havelock (1908, Fig. 9) would probably be regarded as incorrect, exhibiting convex crests behind the leading wavefront.

*Figure D3* shows the standard shallow water wave propagation geometry developed by Havelock, as well as an extension of that geometry to the experimental arrangement of having several wave probes positioned laterally from the sailing line. To aid the analysis, the lateral celerity, $c_L$, is defined as the propagation rate of a particular wave feature along the lateral probe line. The limiting Havelock wavefront would be that delineated by the depth celerity limit of a water wave ($\sqrt{gh}$), which makes an angle to the sailing line according to:

$$\alpha = \sin^{-1}\left(\frac{\sqrt{gh}}{V}\right) \qquad \text{[D1]}$$

and so

$$c_L = \frac{\sqrt{gh}}{\cos\alpha} \qquad \text{[D2]}$$

Similarly, the inverse lateral celerity of the wavefront (in seconds per metre) conforming to [D1] and [D2], as used in the experimental analysis, is:

$$\frac{1}{c_L} = \sqrt{\frac{1}{(gh)} - \frac{1}{V^2}} \qquad \text{[D3]}$$
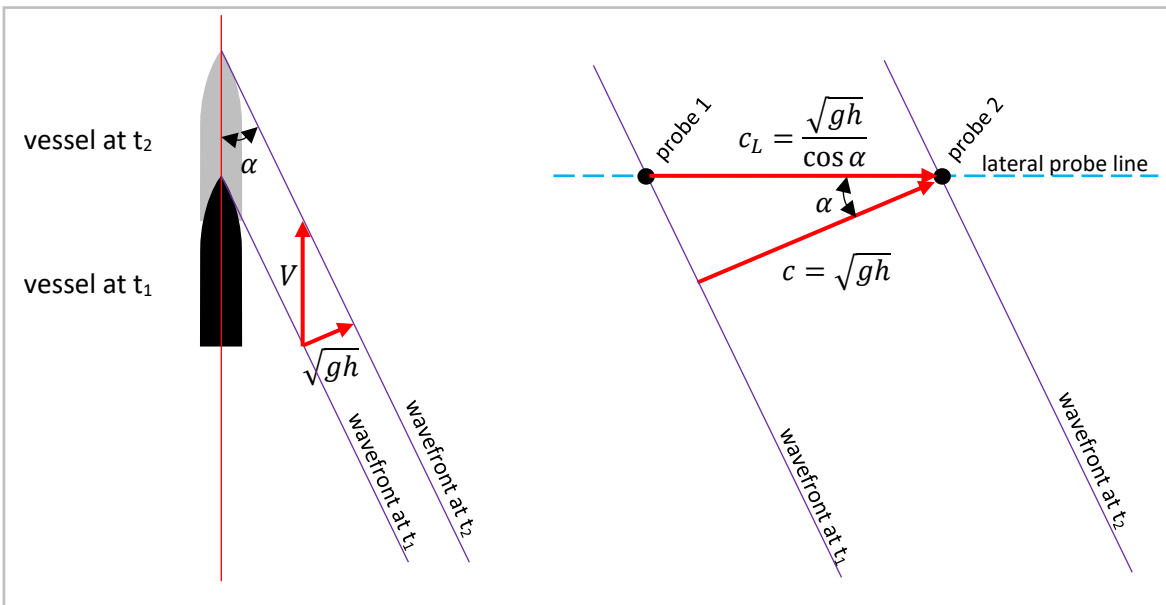


**Figure D3** – *Geometry of the wavefront, based on the assumption by Havelock (1908) that the wavefront cannot propagate faster than the depth-limited value of $\sqrt{gh}$. As shown by experiments, there are parts of the first wave that do propagate ahead of the wavefront at an apparent speed greater than $\sqrt{gh}$.*

258

Several experimental results were studied in detail. One example is shown in **Figure D4**, for $h = 0.15\ m$ and $V = 2.75\ m/s$. This figure plots the lateral position of various features of the first and second waves against the run time of the wave wake recording (water surface elevation). Eight wave probes were positioned along a single lateral line up to *5 m* (about five waterline lengths) abreast of the sailing line. A laser was used to record the time when the forward towing post passed the lateral probe line, denoted in **Figure D4** as "*t-bow*," corrected for the distance between the forward towing post and the forward end of the static waterline. The model had a planing hull and there would be variance between the forward end of the static and dynamic waterlines, with the *dynamic bow* lagging behind the *static bow*. The salient features of the first two waves noted in **Figure D2** are listed in **Table D1**, along with the corresponding line of best fit and goodness of fit value ($R^2$). For both the first and second wave, the times marked "*1 zero*" and "*2 zero*" denote the mid zero crossing points, which were always zero down-crossings.
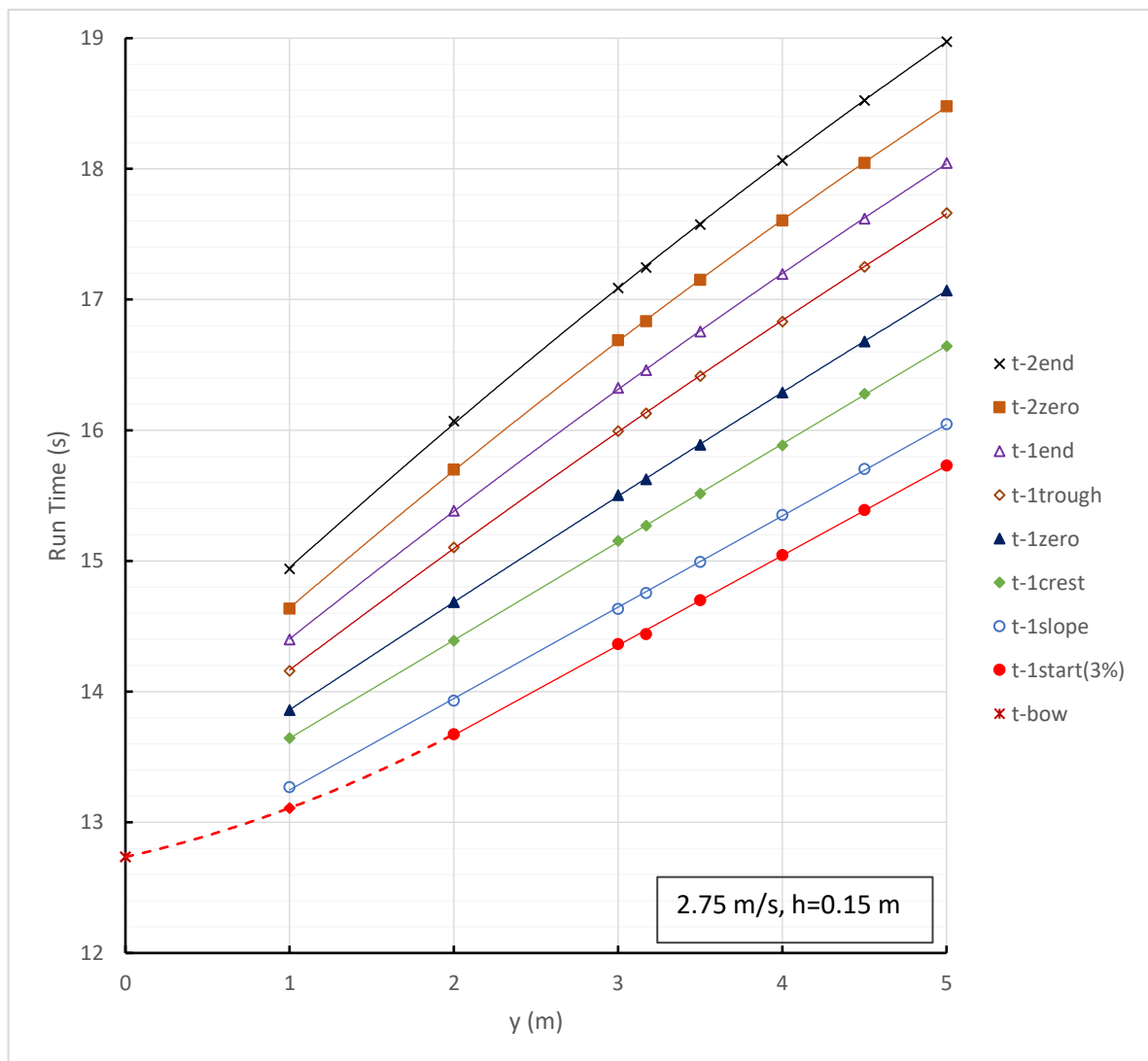


**Figure D4** – *Salient temporal/spatial features of the first and second waves for model AMC 00-01, a planing monohull form with nominal static waterline length of 1.04 m travelling at 2.75 m/s in a water depth of 0.15 m.*

**Table D1** – *Salient features of Figure D4.*

| Feature | Line of Best Fit | Goodness of Fit (R²) |
|---|---|---|
| 1 start(3%) | t = 0.6875y+12.292 | 0.9996 |
| 1 slope | t = 0.6987y+12.550 | 0.9998 |
| 1 crest | t = 0.7506y+12.893 | 0.9999 |
| 1 zero | t = -0.0076y²+0.8475y+13.0206 | 1.0000 |
| 1 trough | t = -0.0192y²+0.9874y+13.1971 | 1.0000 |
| 1 end (2 start) | t = -0.0228y²+1.0455y+13.3806 | 1.0000 |
| 2 zero | t = -0.0311y²+1.1451y+13.5256 | 1.0000 |
| 2 end | t = -0.0319y²+1.1972y+13.7830 | 0.9999 |

*Figure D4* and *Table D1* have several salient features:

a.  The propagation of the very initial upswelling ($t_{1start3\%}$) associated with the first nominal wave is not (and cannot be) linear in the near field ($0\ m < y < 2\ m$). The waves radiate from a travelling source and at the point of initiation at the sailing line ($y = 0$) must be packed into an infinitely short packet. As the first wave radiates, the head of the packet cannot travel faster than the water depth dictates (non-linear effects excepted) and the tail of the packet exists at the sailing line.

At some point, the first nominal wave, which is likely to be comprised of several depth-affected (and hence *speed-trapped*) component waves, has fully left the sailing line and propagates freely. That point depends on the period of the component waves of the first wave, but it is just past $y = 2\ m$ for the example in *Figure D1* and marks the point where the far-field lateral propagation of the wavefront becomes linear with time. It's expected that the slope of the dashed line between *0-2 m* would tend to zero at the sailing line.

b.  The two nominal start points of the first wave, being *3%* of the first crest amplitude ($t_{1start3\%}$) and the intercept of the wave slope ($t_{1slope}$), as well as the crest of *wave 1* ($t_{1c}$), have very definite linear relationships with lateral separation. That would suggest that these three features propagate along some form of the Havelock shallow water wavefront, dependent on the vessel speed and water depth (and possibly wave amplitude, as will be discussed).

c.  The transient measurement points after the first wave crest, consisting of zero crossing points, end points and troughs of the first and second waves, and crest of the second wave, gradually increase in non-linearity (of the feature line) with lateral distance and time separation from the propagating wavefront. The lines of best fit in *Table D1* are all quadratic equations, though there may be more representative natural relationships (power or exponential), given more data. The curve fitting process was purposely limited to a quadratic, since it is possible to fit an equation to any number of points given a polynomial of high enough order. That, however, would be best regarded as coercion rather than accuracy. The goodness of fit values show that the relationships are perfectly defined, even for the simplest quadratic curve fit.

d.  Calculation of the celerity of the second wave shows it to be propagating at slightly less than $\sqrt{gh}$. This wave, and all the waves that follow, would be slowly dispersing, but at a rate so slow that a distant shoreline would still most likely see a similar pattern of waves, but with some height attenuation.

e.  The period of the first wave, taken nominally as $(t_{1end} - t_{1start3\%})$, is gradually increasing with lateral separation. However, since the beginning of *wave 1* has a linear lateral propagation rate but the end of *wave 1* has non-linear lateral propagation rate, it is possible to determine a probable point where the apparent period of the first wave ceases to increase by equating $dt/dy$ for each curve. In this example, it would equate to about eight boatlengths of lateral separation, though this highly dependent on the curve fitted to the data points and the extent of extrapolation into the far field (fitting a higher order polynomial can lead lines that diverge). It should be regarded as indicative but not accurate.

The slope of those curves in **Figure D4** with a linear relationship between run time and lateral separation (highlighted in Table D1) can be compared with the equation for the inverse lateral celerity of the wavefront [D3]. The wavefront is a feature that shallow water wave theory regards as somewhat absolute, since a wave should not be able to propagate ahead of this without exceeding the depth-limited wave celerity. Based on this example of *2.75 m/s* vessel speed and *0.15 m* water depth, the calculated inverse lateral celerity is *0.74 s/m*. However, **Table D1** shows that both wave start points, based on *3%* of the wave amplitude and the intercept of the slope, do actually travel ahead of the Havelock wavefront. The first crest, with an inverse celerity of *0.75 s/m*, is the feature that is closest in form to the actual Havelock wavefront (inverse celerity *0.74 s/m*). The time difference between the theoretical inverse celerity of the Havelock wavefront and that of the first crest is only about two time-sampling units (*0.011 s*) per metre of lateral separation, which is well within the error of interpreting the position of the salient wave features.

The angle of the propagation of the wavefront can be calculated for the start point of *wave 1* ($t_{1start3\%}$) using [D2] and knowing that the slope of the line shown in **Table D1** must equal the inverse lateral celerity. It is calculated as *33.5°*, against *26.2°* for the Havelock wavefront, based on a celerity limit of $\sqrt{gh}$. Unlike the discrepancy of two sampling units in correlating the first wave crest with the Havelock wavefront, this discrepancy of angle equates to eleven sampling units (*0.055 s*) per metre of lateral separation, which is no longer considered to be within the expected uncertainty in interpreting the time series.

If non-linear effects are accounted for and that part of the wave ahead of the first crest is allowed to propagate at a speed greater than $\sqrt{gh}$, the actual propagation angle of the very initial upswelling of wave 1 ($t_{1start3\%}$) is *27.9°* and its speed of propagation is *1.286 m/s* against the shallow water limit of *1.213 m/s* for $h = 0.15\ m$. This correlates with **Figure D6** (right), discussed later.

### D.3 Correlating First Wave Features with the Havelock Wavefront

Review of other test conditions showed a consistent relationship between the Havelock wavefront and the first crest, provided the vessel speed was sufficiently super-critical. At speeds closer to the critical speed, correlation with the Havelock wavefront shifted from the first crest to the beginning of the first wave. This is shown in **Figure D5**, though for only limited conditions due to the time required to determine the relevant wave angles.

The deviation between the Havelock wavefront and the beginning of the first wave cannot be explained by experimental uncertainty. In **Figure D5** for instance, the ($t_{1start3\%}$) data point shown at $Fr_h = 2.21$ would only correspond with the wavefront if the water depth was increased from *150 mm* to *176 mm*. The consistency at higher depth Froude numbers suggests another mechanism occurring, which is almost certainly due to non-linear effects in shallow water. In the example cited above, $\lambda/h \approx 19$ in the far field. Lighthill (1978) would consider this as a long wave, where the celerity limit of $\sqrt{gh}$ applies ($\lambda/h > 14$, according to Lighthill). The Shore Protection Manual (Coastal Engineering Research Center (CERC) (U.S.), 1984) uses $\lambda/h > 25$ as the shallow water definition, though probably to extend linear wave theory for the engineering purposes the Shore Protection Manual was primarily intended.
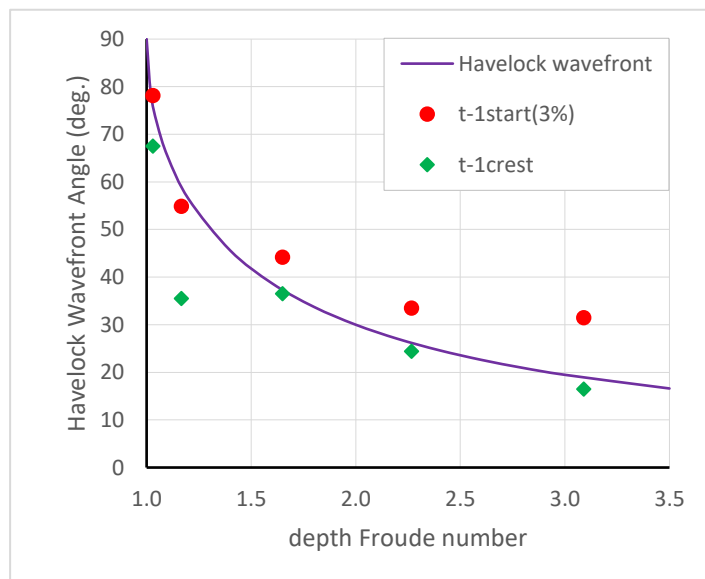


**Figure D5** – *Comparison of the theoretical Havelock wavefront angle with the apparent values measured at different depth Froude numbers, assuming the limiting wave propagation speed is $\sqrt{gh}$. When non-linear effects are accounted for, the discrepancy between the theoretical value and the first upswelling ($t_{1start3\%}$) reduces. Near the depth-critical speed, the very start of the first wave correlates with the theoretical value. At higher depth super-critical speeds, the first crest corresponds with the theoretical value and part of the first wave travels ahead of the wavefront due to non-linear, shallow water effects. All data points, apart from those at $Fr_h = 1.16$, are for $h = 0.15\ m$ and from very stable tests. The data at $Fr_h = 1.16$ are from a test that was somewhat contaminated by residual noise.*

## D.4   Example Shallow Water Wake Patterns

Two examples of shallow water wake patterns are presented, based on the time series records in two shallow water conditions. These are shown in **Figure D6**. The left figure is at a depth Froude number just above the critical speed and the right figure is at a depth super-critical speed.

**Figure D7** shows the first wave lead, defined as the apparent distance that the far-field projected first wavefront intersects the sailing line ahead of the model. Newman (1977) makes the comment that:

*"Figure 6.17 shows a commonly observed feature, namely that the apex of the sectors containing the Kelvin waves is displaced upstream from the ship's bow by an amount typically as large as on ship length."*

Similarly, **Figures D6** and **D7** would show the same in shallow water. The upstream displacement is known to occur around the depth-critical speed, but there are no apparent comments in the literature regarding upstream displacement of the Havelock wavefront at super-critical speeds. Havelock (1908) does not discuss this, or show it figuratively.
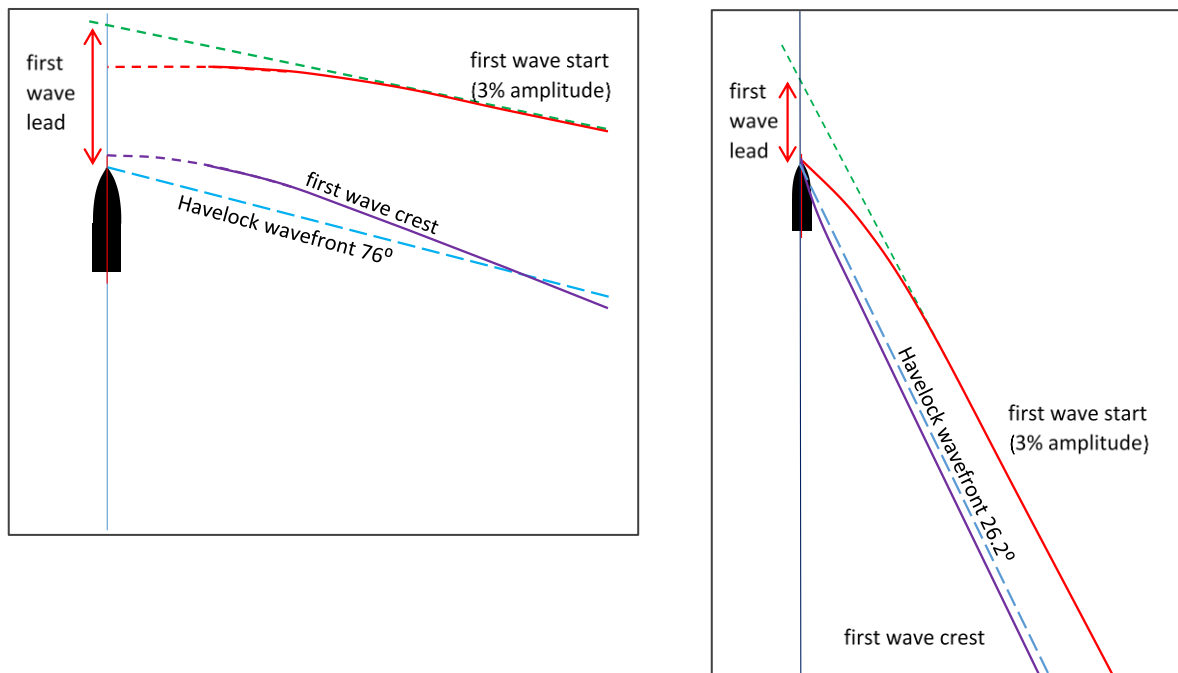


**Figure D6** – *Wake patterns of the initial upswelling and first wave crest at super-critical speeds for $h/L_{WL} = 0.144$. The **left** figure is at $V = 1.25\ m/s$ and $Fr_h = 1.03$. The **right** figure is at $V = 2.75\ m/s$ and $Fr_h = 2.27$. Figures are drawn to scale, with the vessel length representing the model's static waterline length of 1.04 m. The wave features are assembled from eight laterally spaced probes (left figure) and five probes (right figure), plus the zero point at the sailing line (taken as the point where the forward end of the static waterline passed the lateral probe line). Nominal speeds were used to calculate the Havelock wavefront; average speeds are always fractionally higher, reducing the wavefront angle and reinforcing the argument.*
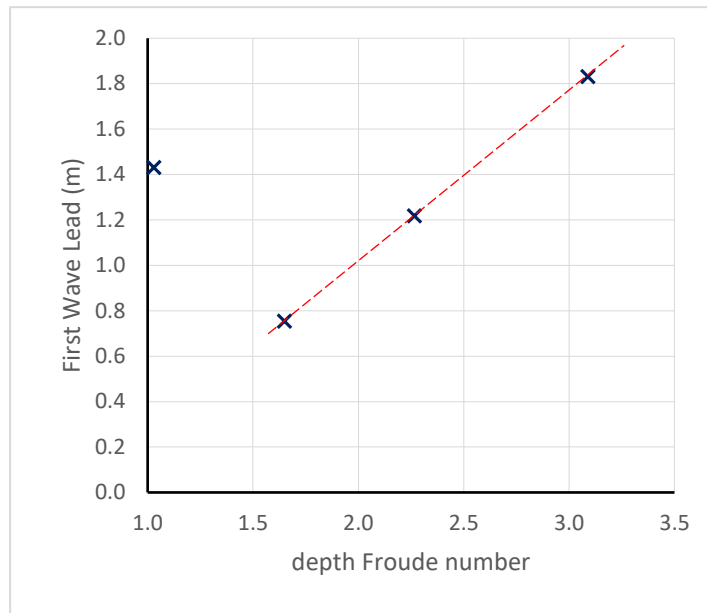
**Figure D7** – *First wave lead as a function of depth Froude number for $h = 0.15\ m$. The higher depth Froude numbers demonstrate a linear relationship. At or around the depth-critical speed, the position of the first wave is known to migrate along the sailing line relative to the vessel and eventually detach – it doesn't always occur at the same relative position.*

## D.5    Discussion of Figure D6

### Left ($Fr_h = 1.03$):

- The green dashed line at the start of the first wave is the projection of the steady state, far-field wavefront. In the far field ($y > 3\ m$), the wavefront has a linear form.
- At a speed just above the depth-critical speed, there is definitely a component of the first wave travelling ahead of the vessel. The first wave lead, in terms of a time separation between the first upswelling and the vessel's bow, is *1.14 s* (about *1.43 m*), which cannot be attributed to an experimental anomaly. Even the first wave probe, positioned laterally at $y = 1\ m$, records the first upswelling at *0.86 s* (about *1.08 m*) ahead of the bow. That correlates with the well-known phenomenon of solitary waves forming around the bow, detaching and propagating independently.
- The first probe, positioned at $y = 1\ m$, is marked by the juncture between the dashed and solid upswelling and crest lines. It is assumed that in the near field, from $0\ m \le y \le 1\ m$, these wave features do not contract back to the forward end of the vessel's waterline.
- The calculated Havelock wavefront at $\alpha = 76°$ is shown. It certainly does not conform to the first wave crest, as it does at higher super-critical depth Froude numbers, but is closer to the upswelling of the first wave, which is propagating in the far field at an angle of $80^o$ to the sailing line.
- ***Figure D8*** represents the far-field wave trace in this condition (very right-hand extremities in Figure D6-left) and the first wave of solitary form is evident.

### Right ($Fr_h = 2.27$):

- The nominal speed of *2.75 m/s* was used in the calculations. The recorded average was *2.778 m/s*, which is *1.0%* faster. Using the recorded average reduces the Havelock

wavefront angle from *26.17°* to *25.89°*, which only reinforces the argument. The purpose of this experiment was to demonstrate the existence of difference in wave angles and not to quantify the magnitude.

- Once the depth super-critical speed of the model exceeds the depth super-critical celerity of the solitary wave it generates, the wake pattern forms into the more expected shallow water pattern. The wave crest approximately conforms to the Havelock wavefront angle (as shown also in Figure D5) but the start of the first wave very definitely travels ahead of this, at a propagation angle of *27.9°* and a celerity approximately *6%* faster than $\sqrt{gh}$.

- The initial upswelling becomes stable and linear with lateral separation at about $y = 2\ m$ and beyond. Before that ($y < 2\ m$), the first wave (or rather its component sub-waves) has not had sufficient time or propagation distance to "unpack", or spread out fully.
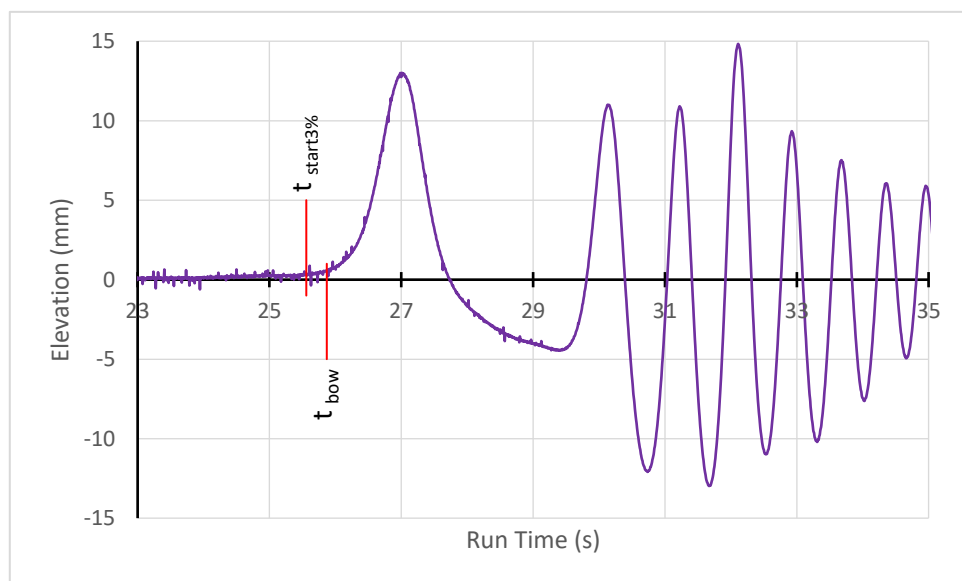


**Figure D8** - *Wave trace for model AMC 00-01 at $V = 1.25\ m/s$, $y = 5.0\ m$, $h = 0.15\ m$, $Fr_h = 1.03$. Of note is how the first wave initially resembles a solitary wave form (symmetrical about $t = 27\ s$), followed by the remnants of a drawdown ($t \approx 29\ s$) that leads into a weakly dispersive wave packet.*

### D.6    Linear Growth in First Wave Lead at Super-Critical Speeds

The premise for this is that there is essentially no difference between the wake waves in the deep water condition and the shallow water condition. What is different is how these waves propagate; the deep water condition allowing for full dispersion and the shallow water condition tempering dispersion. In deep water, the packet disperses and spreads. In shallow water, the first several waves that would otherwise have formed as they do in deep water become "*speed trapped*" by the shallow water and travel together. There is weak dispersion across these component waves that make up the first wave, which is why the period of the first shallow water wave apparently increases with lateral separation. **Figure D9** explains this further.

Although the vessel speed is close to the depth-critical speed at $h = 0.9\ m$, the ratio of $h/L$ is sufficiently small that the vessel is essentially operating in deep water. The individual packet waves have been numbered, commencing with *wave 1* and delineating into half waves according

265

to whether it is above the mean water level ("crest") or below the mean water level ("trough"). Dividing each wave into halves improves the accuracy of the trends.
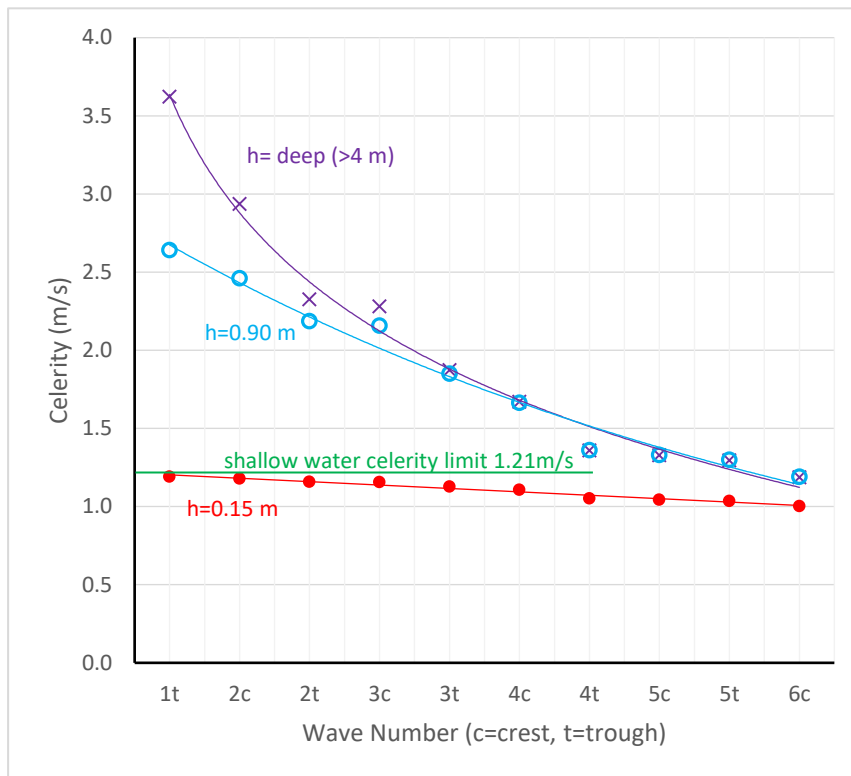


**Figure D9** – *Model AMC 00-01 wave celerity analysis for $V = 2.75 \ m/s$, $y = 4.5 \ m$, $h = 0.9 \ m$, $Fr_h = 0.93$. The parameters for each individual half wave (crest and trough) have been taken from the $h = 0.9 \ m$ condition (practically deep water, with $h/L = 0.86$) and transposed into deep ($h = 4.0 \ m$) and shallow ($h = 0.15 \ m$) water. The parameters of the very first half wave, wave "1 crest", are practically indeterminable and so not shown. The data are discrete but are joined for clarity.*

The celerity of each wave half is calculated for three conditions: the actual test condition of $h = 0.9 \ m$, deep water ($h > 4 \ m$, by way of transposition), and shallow water ($h = 0.15 \ m$, by way of transposition). There are three particular points to note.

Firstly, the tested condition at $h = 0.9 \ m$ is not quite deep water and the first few half waves (up to and including the third crest) are slightly depth affected, shown by a decrease in wave celerity. Beyond that, the waves are too short to be depth affected.

Secondly, the maximum wave, which is *wave 6* in deep water, is not depth affected at all at $h = 0.9 \ m$. That is important, since it implies that maximum waves can be measured in water much shallower than the vessel's static waterline length without undue effects (with a caveat, presented later). The rule-of-thumb is that measurements in water deeper than $0.56 L_{WL}$ will yield the equivalent maximum wave to that in deep water, even though the leading waves may be depth affected.

Thirdly, if each half wave were transposed into shallow water ($h = 0.15 \ m$), the first half wave (*1t*) becomes fully speed limited by depth and the successive half waves travel at speeds slowly

decreasing across the packet. This is important, as it reinforces the premise that waves generated in shallow water and those generated in deep water are related. The first wave of a packet generated in shallow water is potentially a composite of several "*speed-trapped*" waves travelling at slightly different depth-affected speeds, giving rise to an apparent dispersion or "period stretching" of the first wave with increasing lateral separation. As mentioned, it is expected that this would stabilise and possibly start to reduce in the very far field, as the slower components of the first shallow water wave fall behind or get consumed by the weakly dispersive waves following the first.

If this is the case, then the start of the first shallow water wave would have to propagate a particular distance from the sailing line before it was fully unpacked.[130] That distance would be approximately the transposed wavelength of the first wave (half wave crest plus half wave trough), being the longest and fastest wave in deep water. In this example, that is about *2.49 m*. Correcting this wavelength (approximately) to a lateral distance by multiplying by $\cos(\alpha)$ gives *2.23 m* as the lateral distance it takes for the first shallow water wave to unpack. That can be seen in *Figure D4*, where the very start of the first wave becomes stable (dashed line becomes solid).

Also, we know that at high speeds the period of the first wave in deep water is approximately constant, so that the wavelength of the longest component wave of the first shallow water wave would be approximately constant. That leads to *Figure D10*, which shows that the wavefront of the first wave upswelling pivots around the approximate point where the first wave is fully unpacked. In reality, it is likely that the apparent linearity of the first wave lead shown in *Figure D7* is not a straight line, but a function of $\sin(\alpha)$, which defines the Havelock wavefront.
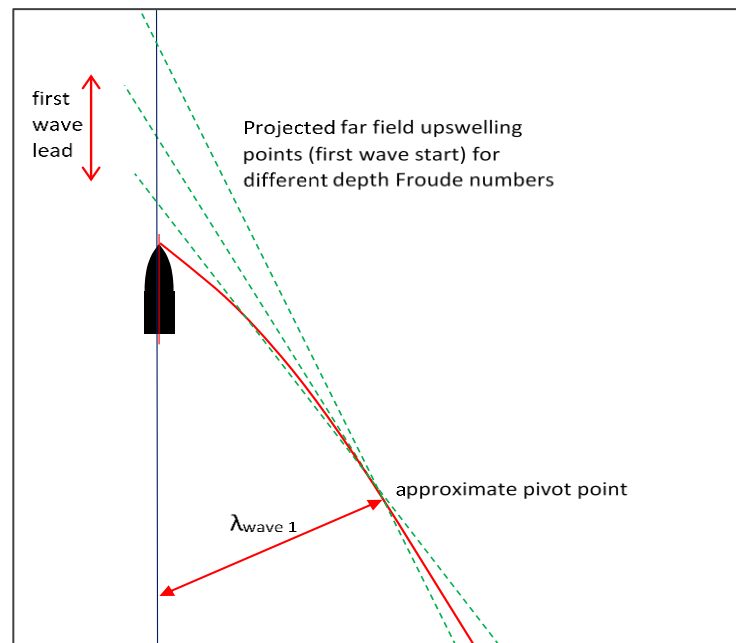


*Figure D10* – *Possible explanation for the apparent linearity and growth of the first wave lead at higher depth super-critical speeds. At high speeds, the wave periods become more constant and so the shallow water wavelength becomes constant. Once it propagates away from the sailing line and into the far field, the wavefront becomes stable. The pivot point becomes the point where the first wave has propagated one wavelength and the projected far field wavefronts pass through this point.*

---

[130] More can be found in *Appendix C* and the discussion of Figure C2.

**D.7    The Depth Transition Paradox**

A series of experiments were conducted where wake waves from model AMC 00-01 were generated in (practically) deep water ($h = 0.9\ m$) and propagated onto a shallow shelf ($h = 0.15\ m$) over a very steep ($\sim 42°$) transition (Drobyshevski, 2017). These were compared with tests conducted at a constant deep-water depth of *0.9m*. A peculiarity arose before the depth transition. In the experiments, the depth transition from *0.9 m* to *0.15 m* depth started at $y = 3.17\ m$ from the sailing line and finished at $y = 4.0\ m$ from the sailing line. For an example speed, the wake trace at $y = 3.0\ m$ in the deep-water section of the transition case was compared to the wake trace at the $y = 3.0\ m$ constant *0.9 m* depth case, with the assumption that they would be identical. They were not.

Although both wake traces were recorded at the same lateral separation and both were at the same water depth, the later waves in the transition case had attenuated in height. The first few waves were identical, but heights attenuated after that. The explanation is simple but not the mechanism.

As the first wave passes the wave probe, the whole packet is still in deep water. However, as the mid-section of the packet passes through the probe, the leading waves have already passed over the depth transition and into the far field shallow water. The probe represents a spatial not a temporal record. It would appear that changes in packet energy flow at the head of the propagating packet, as well as reflection of energy off the sloped transition, was reducing the energy of those waves yet to enter the shallow water, reducing their height. The energy within a packet is transient and dynamic, but the literature does not make specific mention of transient packet energy changes due to external influences. Reflection and refraction are well understood (Mei, 1989; refer also Appendix G), but the mechanisms by which the rearward leakage of energy is disrupted are secondary to the argument.

The further implication of this is that if waves are measured in water that is not reasonably consistent in depth, the maximum wave itself may not be depth affected but may be affected by its relationship to other waves in the packet, especially those leading waves that may have passed into shallow water. *Figure D11* shows this schematically. *Figure D12* shows an experimental example.

In its practical application, measurement of the maximum wave in deep water alone is not enough to ensure that correct values are obtained; the whole packet and especially the leading waves must not be excessively affected by depth.
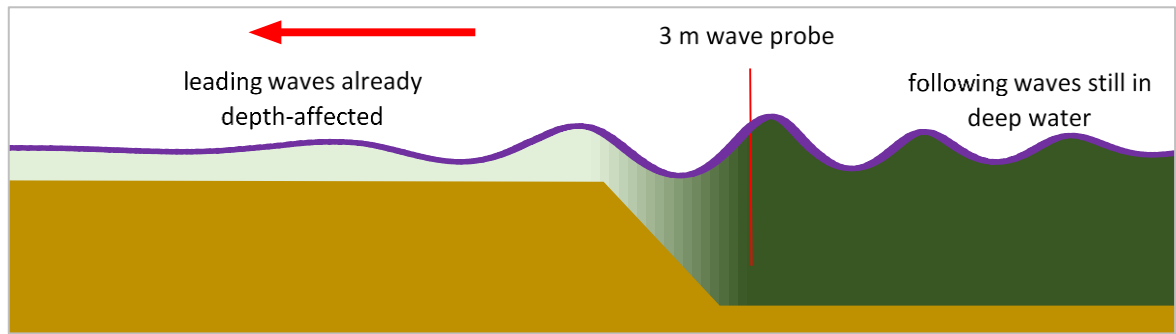
**Figure D11** – *Deep water generated wave wake packet propagating from deep to shallow water (right to left). By the time the maximum (highest) wave passes the wave probe, the leading waves are already in the far-field shallow water, partially reflecting off the transition and then becoming weakly dispersive. The diagram is schematic, and the wave elevations have been exaggerated.*
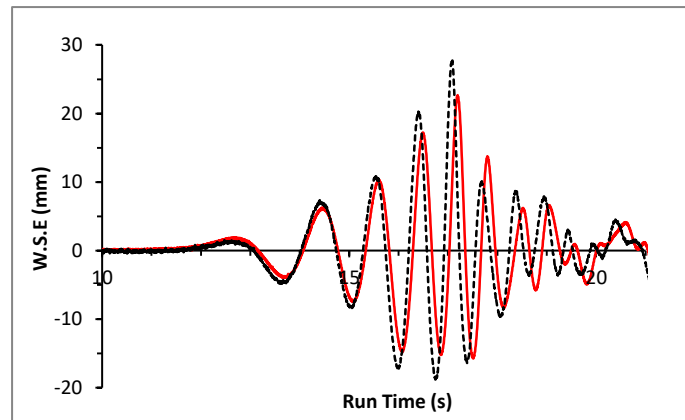


**Figure D12** – *Adaptation of Fig. 15a from Drobyshevski (2017). The results are from model AMC 00-01, at $V = 3.5\ m/s; Fr_h = 1.18; Fr_L = 1.09$. The constant deep-water condition ($h = 0.9\ m$) is shown as the dashed line, and the transition condition ($h = 0.9\ m\ to\ 0.15\ m$) is shown as the solid line. The traces were recorded at the last deep-water probe ($y = 3\ m$) before the start of the depth transition ($y = 3.17\ m$). The traces have similar forms, except that the transition case shows the deep-water waves increasingly attenuated in height due to a disruption in the rearward energy leakage caused by the weakening dispersion of the leading waves in shallow water and reflections off the transition.*

269

# Appendix E – First Wave in Very Shallow Water

## E.1    Introduction

Historically, solitary wave theories have been used to describe very shallow water waves, especially those close to breaking (McGowan, 1894; Munk, 1949; and Li and Raichlen, 2001, as three of many examples). As shallow water wave theories were further developed, the consensus was that solitary waves represented the terminal condition of a wave moving from the deepest to the shallowest water, transforming from an Airy form to a cnoidal form and finally to a solitary form. Solitary waves have the benefit of simpler computations compared to cnoidal waves, which themselves have been described by approximated theories to reduce computational complexity (Fenton,1990 and Iwagaki,1968, as examples).

The previous analysis of tests of model AMC 00-01 in *150 mm* water depth ($h \sim 0.15L$) alluded to the existence of a solitary wave component *buried beneath* (or *integrated into*) the first shallow water wave at depth super-critical speeds. Although the first wave had an obvious periodic form, the wavefront was travelling at speeds greater than the crest speed of $\sqrt{gh}$ and Fourier analysis showed a long-period component of consistent spectral energy. At the *150 mm* water depth and analysing the first wave as a single wave, the ratio of $\lambda/h$ was around *10* in the near field but was increasing with lateral separation due to the packet nature of the first wave and shorter wave components slowly dispersing out of the wave, increasing its apparent period. The ratio $\lambda/h \sim 10$ would not qualify a periodic wave as *shallow*.

In this investigation of model AMC 00-01 in *100 mm* water depth, the solitary form is evident and dominant. The calculated ratio of $\lambda/h$ increased to $\sim 16$, based on the leading crest as a solitary wave. Unlike the *150 mm* depth condition, the height of the leading wave was quite stable at $Fr_h > \sim 2$, once away from the vessel. It is therefore likely that the formation of a dominant leading solitary wave depends on the depth being sufficiently shallow and the leading crest being sufficiently high. The relevant relationships are further expanded in discussion following.

*Figure E1* shows one example of a wave wake in very shallow water. In this figure, only the leading wave is shown and at different lateral positions of up to $\sim 5L$. Three features are notable:

    a.   the nearest wave probe ($y = 1\,m;\ \sim 1L$) shows a superimposed wave in the trough, thought to be part of the slowly dispersing waves following the first crest and falling away as the first crest slowly moves ahead of the other waves. It is not evident at subsequent wave probes and is not thought to be a second solitary wave shed from the first;

    b.   once the leading crest has moved ahead, its height remains approximately constant with lateral separation. This is a strong indication of the first crest having a dominant solitary form;

    c.   the crest remains consistent in form with propagation, but the trough stretches in the far field. Their form is different to that seen in slightly deeper depths, where the trough becomes only slightly asymmetrical. In this very shallow water case, the troughs become increasingly asymmetrical, as if the leading crest were moving up and out of the trough in the far field.

*Figure E2* is a modification of *Figure E1*, with all leading crests aligned. The stable upswelling and height are clear.

270

## E.2    Very Shallow Water, Far-Field Form

In this condition, the far field wave wake begins to resemble an undular bore, with a hydraulic jump occurring just behind the leading crest. Such a feature is usually created with a constant flow at a depth super-critical speed passing into water of increasing depth, causing the formation of the hydraulic jump and the sub-critical undular bore made up of cnoidal waves (Lighthill, 1978). If the wave function itself rather than increased channel cross-section became the mechanism for reducing flow speed, and by changing the frame of reference (waves moving across stationary water), the undular bore would form.
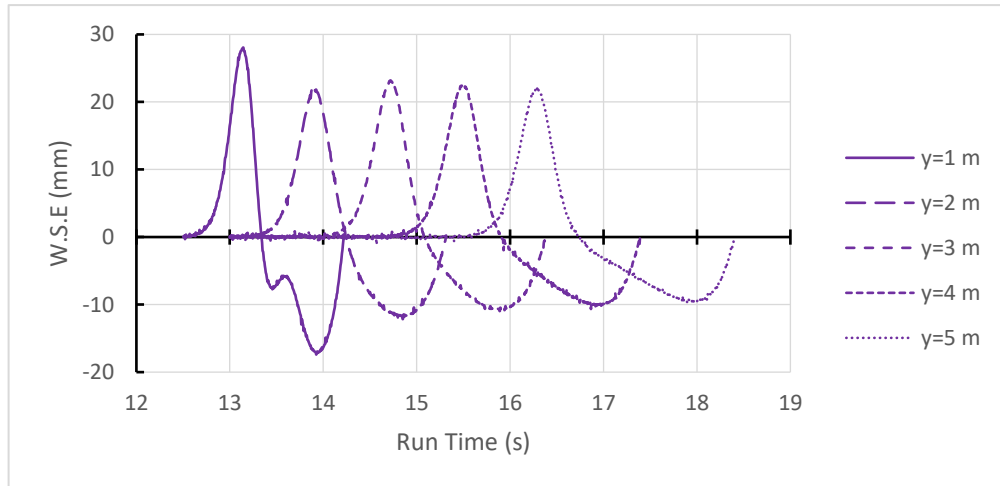


**Figure E1** – *Model AMC 00-01 first wave in very shallow water ($h = 0.1\ m$; $h/L = 0.096$; $V = 2.0\ m/s$; $Fr_h = 2.02$). Of note are the stable crest heights at $y \geq 2\ m$, very limited spreading of the first crest, spreading of the trough following and the decay of the trough depth with lateral separation.*
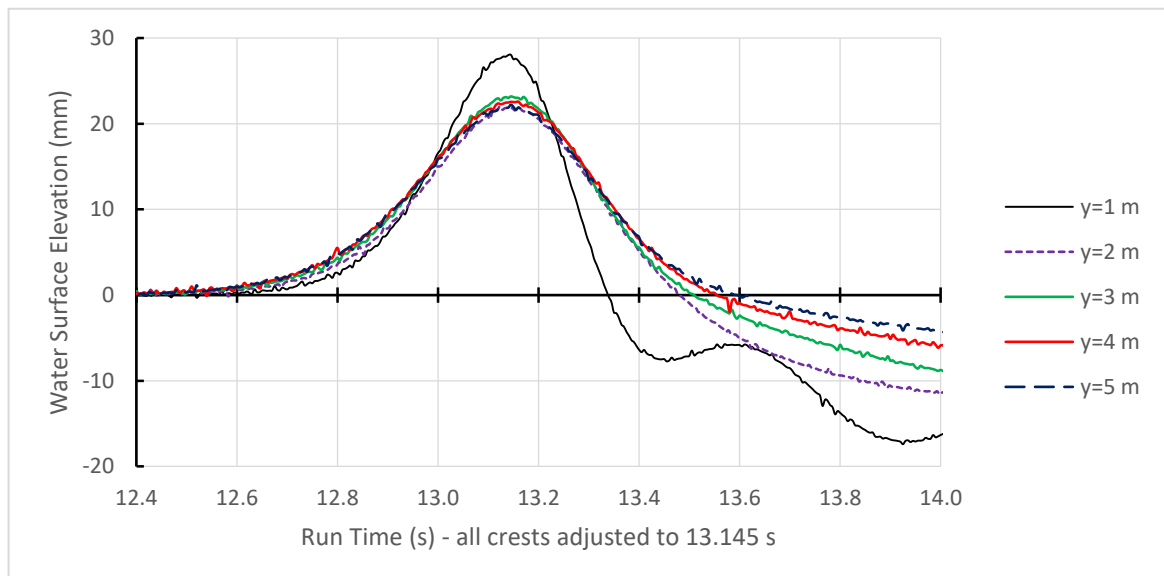


**Figure E2** – *Modification of Figure E1, with all crests aligned. There was insufficient lateral separation at $y = 1\ m$ for the leading solitary crest to move clear of the weakly dispersive packet following. The rate of dispersion and subsequent wake transformation depend on the water depth and number of wave cycles respectively, both of which are inhibiting dispersion in the near field, shallow water condition. Once sufficiently clear, the stability of the solitary crest is evident.*

271

The leading solitary component must move at a slightly depth super-critical speed by any of the present solitary wave theories, providing the requisite conditions for the leading, super-critical flow. After that, the transition to sub-critical flow would happen in the trough trailing the solitary crest, leading to the *jump* to a sub-critical flow (the small waves following). In this particular frame of reference, the jump itself would stretch as the super-critical leading crest moved away from the sub-critical waves following, stretching the trough. This is what is shown in ***Figure E1***. The difference between this example and a static example of flow in a channel is that the channel waves appear stationary, since the mechanism to bring about the super-to-sub critical flow change is a change of depth, not a progression of the wave function. The wake waves cannot be made stationary only by a change of frame of reference.

Given sufficient lateral separation and crest amplitude, the question of whether the leading solitary wave is able to separate itself from the rest of the wake arises, as it may appear to do around the depth-critical speed in restricted channels with the shedding of a train of solitary waves. The question becomes whether the divergent wake was generated by the model as a coherent wave function and must propagate as such, or if the solitary wave is or can transform into a separate, distinct entity. The super and sub-critical parts in ***Figure E1*** are clearly stretching apart at the first trough.[131] Further experimental results and discussion can be found in *Appendix ZD*.

***Figure E3*** explains this schematically for the experimental example of ***Figures E1*** and ***E2***. The strength of a bore $\beta$ is referred to as the ratio of the change in flow cross-section to the super-critical flow cross-section, which for a rectangular channel of constant width simplifies to $\beta = (h_1 - h_0)/h_0$ (Lighthill, 1978). Specific physical conditions for the formation of an undular bore are maintained, such as the strength $\beta < \sim 0.3$ and the speed in the super-critical region being not much above $\sqrt{gh}$. Increased ratios lead to a breaking bore, which may be seen when a super-critical wake shoals; the leading solitary wave may not break but the shorter waves following become unstable if $(h_1 - h_0)/h_0 > \sim 0.3$ (though can vary).

Another feature of an undular bore is that the amplitude of the wave following the jump is around $0.6(h_1 - h_o)$, which can be derived from linear theory and the requirement that energy is lost at the jump. By linear theory, *20%* of energy is lost at the jump, but by non-linear theory as little as *5%* may be lost at the jump if the strength is weak (Lighthill, 1978). ***Figure E3*** (*right*) shows the parameters of the hydraulic jump and undular bore, assumed for the shallow water wave wake condition. This wave trace is later reproduced as ***Figure E13*** and the value of $a/(h_1 - h_0)$ is exactly *0.6* as predicted. This is quite consistent at other depth super-critical speeds for the same model and depth condition.

---

[131] A wave wake is formed as a coherent function and not as individual waves; whether the head is able to propagate super-critically and detach is the question. However, there are examples where this is possible. Craig *et al.* (2006) reported on numerical and physical non-linear interactions of solitary waves in water. Their experiments show that solitary water waves are not pure solitons by definition, as the interactions (collisions) produced small oscillatory residuals. However, they also demonstrated that the post-interaction solitary waves were able to shed their oscillating tails and propagate independently (Craig *et al.*, 2006, Fig. 10). Those waves, having been formed as pure solitary waves, are not the same as vessel divergent waves, which are formed as a single group (and with possible multiple sub-groups) with their form varying from solitary at the very head to near-sinusoidal at the very tail of the packet in shallow water.

272
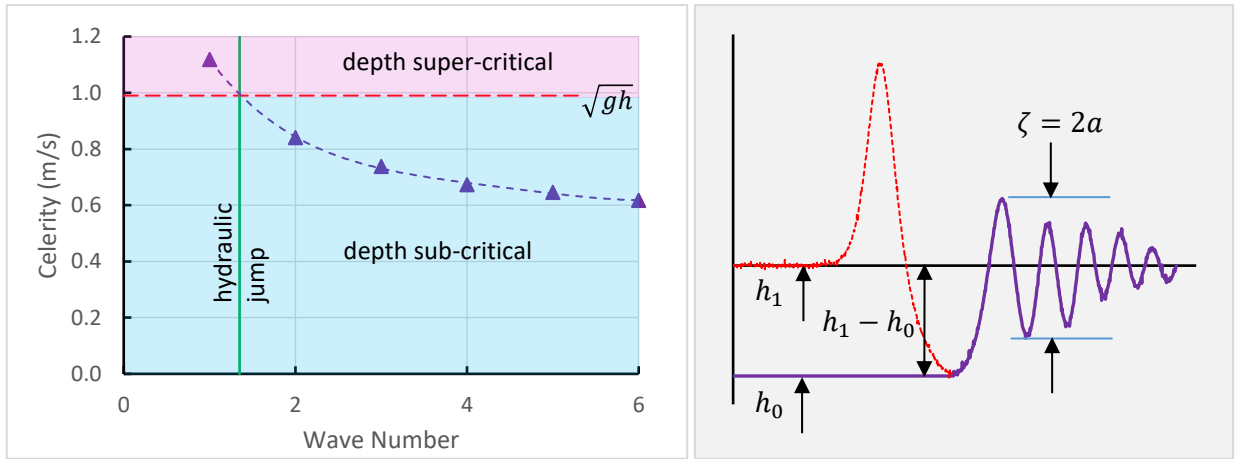
**Figure E3** – *Left*: *Schematic of the discretised wave celerities from Figure E13 (following) and how they explain the super-critical/sub-critical nature of very shallow water wave wakes, the apparent formation of a hydraulic jump resembling an undular bore, and the stretching of the first trough (the point of flow change from super to sub-critical) with increasing lateral separation. The first (super-critical) crest is possibly able to disassociate itself (decouple) from the trailing (sub-critical) waves and so leads to the increasing trough width and asymmetry of Figure E1.* ***Right:*** *Parameters relevant to the hydraulic jump. The leading solitary wave (red dashed line) forms the super-critical condition necessary for the formation of the bore. The undular bore itself is the solid line.*

### E.3 Comparison of the First Wave Crest with Solitary Wave Forms

Dingemans (1997) presents a summary of solitary wave solutions for five theories.[132] The three most common solutions are those of Korteweg de Vries (KdV), the improved Boussinesq equations (iBq), and Benjamin-Bona-Mahoney (BBM).[133] The water surface elevation $\zeta$ is given by:

$$\zeta(x,t) = H \operatorname{sech}^2\left(\frac{x - ct}{\Delta}\right) \qquad \text{[E1]}$$

where the wave celerity $c$ and the width $\Delta$ are shown in **Table E1**. The width $\Delta$ is the inverse of the wavenumber $k$ and therefore the nominal wavelength of a solitary wave is $2\pi\Delta$.

---

[132] These equations are for first-order approximations. As such, they can be used with sufficient accuracy up to $H/h = {\sim}0.5$, which adequately covers wave wakes. The increasing wave non-linearity above this point results in a decaying crest Froude number growth that can only be managed with higher order wave solutions. Fenton (1972, Fig. 1) gives an excellent account of higher order wave celerity solutions against a first order Boussinesq celerity, and Yamashita and Kakinuma (2014, Fig. 3) do the same for KdV solutions.

[133] According to Dingemans, Bousinnesq's original solitary wave derivation had errors that were only discovered in the 1970s. The improved equations correct the error in the width $\Delta$ with the added $c/\sqrt{gh}$ term.

– *Parameters for solitary wave equations (from Dingemans, 1997) (see footnotes 132 and 133).*

| Solution | celerity, c | width, Δ |
|----------|-------------|----------|
| KdV | $\left(1 + \dfrac{1}{2}\dfrac{H}{h}\right)\sqrt{gh}$ | $\sqrt{\dfrac{4h^3}{3H}}$ |
| BBM | $\left(1 + \dfrac{1}{2}\dfrac{H}{h}\right)\sqrt{gh}$ | $\sqrt{\dfrac{4h^3}{3H}\dfrac{c}{\sqrt{gh}}}$ |
| iBq | $\sqrt{g(h + H)}$ | $\sqrt{\dfrac{4h^3}{3H}\left(\dfrac{c}{\sqrt{gh}}\right)}$ |

The leading shallow water wave at several model test conditions were assessed for their correlation with KdV and iBq solitary wave profiles. ***Figure E4*** shows examples where correlation was achieved.

***Figure E4 (a)*** is a very shallow water, near-field ($y\sim1L$) result. In this case the wave front conforms to the KdV solution, having travelled insufficient wave cycles to assume its more consistent, far-field form. The back of the wave is being distorted by the divergent waves following, which are of a different form (Stokes III and therefore not considered overly shallow) and hence distorting the leading part of the wave function from a pure solitary form into a solitary/periodic form.

***Figure E4 (b)*** is a very shallow water, far-field ($y\sim5L$) result, showing increasing consistency on both the front and back of the wave. The wave form has developed from a KdV form to an iBq form as it propagates – a feature which is further discussed in Appendix ZF.

***Figure E4 (c)*** is from the deep-to-shallow test series, where waves were generated in *0.1 m* water depth and allowed to propagate over a step into *0.85 m* water depth. At the depth step, the first wave maintained the same form as (b), with only a slight moderation of height.

***Figure E4 (d)*** is in slightly deeper water ($h = 0.15\,m$) at a mid-field position ($y\sim3L$), but close to the depth critical speed ($Fr_h = 1.04$) where solitary waves are known to form. In this case the form is evident in the upswelling but falls away after the crest under the influence of the following shorter divergent waves. At other depth super-critical speeds in this water depth the correlation was less convincing – further suggesting that at intermediate depths the first shallow water divergent wave has a solitary component, but buried beneath a stronger, shallow water periodic form (probably of a cnoidal form).

Qualitatively, any leading shallow-water crest at the head of a wake packet would be best initially described by the KdV solution. Such a crest would be considered as the limiting condition of periodic waves in water so shallow as to be fully depth affected, hence of the KdV form. The justification of this end condition of periodic waves is commonly quoted (Munk (1949) and Palais (2008) as examples). In contrast, a stand-alone solitary wave (or waves) generated under specific conditions might conform to a Boussinesq solution (or improved form when describing its profile). The fact that near-field leading crests appear to conform better to a KdV form and far-field leading crests appear to conform better to an iBQ form would support that assertion – the further the first crest is from the vessel, the more likely that an increasing portion of that crest assumes a solitary wave form as the rest of the trailing, weakly dispersive cnoidal components of the wave

function fall behind. Visually, *Figure E1* would support this. Apart from crest celerity differences (discussed following), the differences are quite minor; the Boussinesq profile being slightly fuller than a KdV.
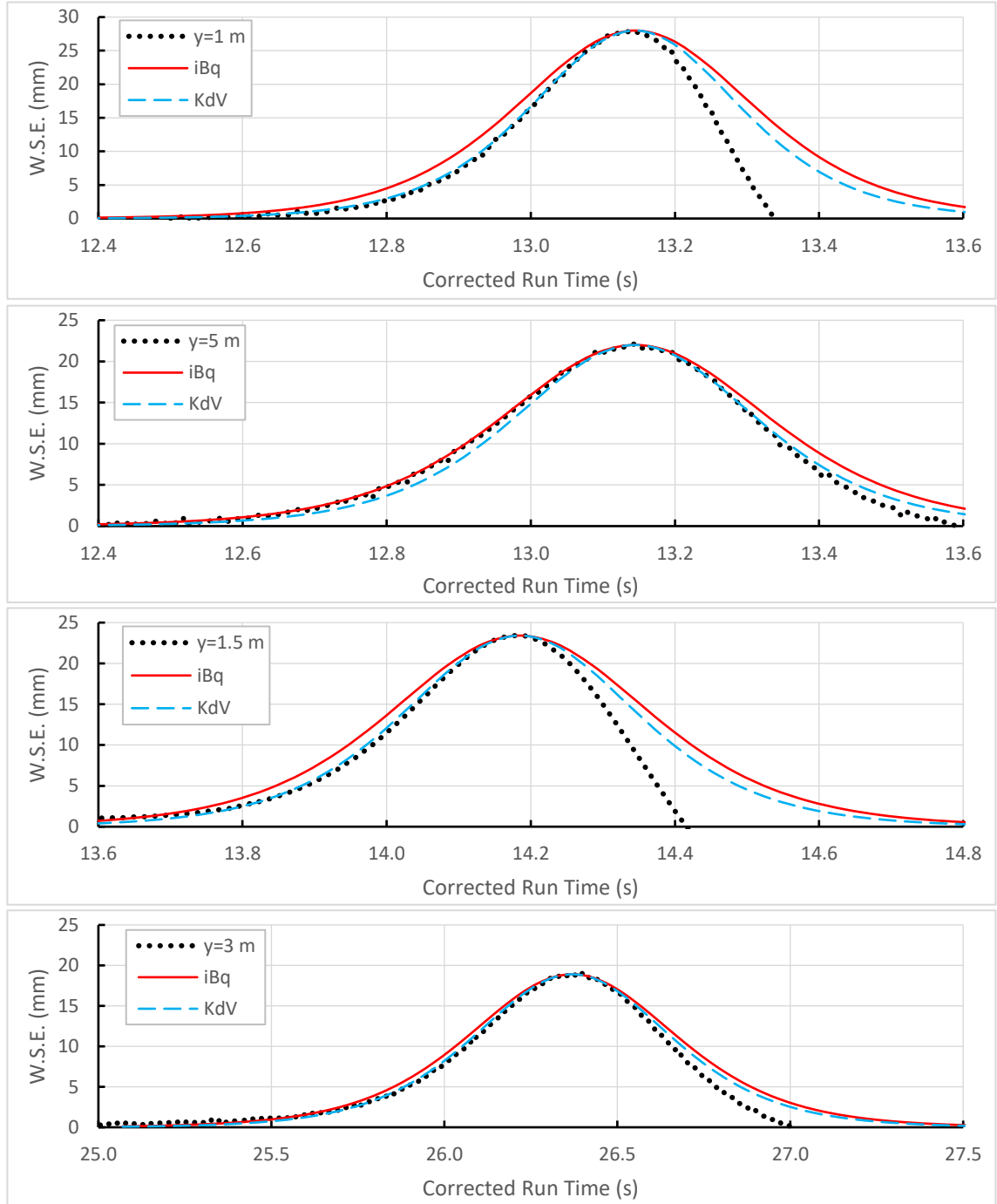


**Figure E4**. *Comparison of shallow water first waves with three solitary wave solutions for model AMC 00-01. **Top to bottom**: (a) $h = 0.1\ m$, $V = 2\ m/s$, $y = 1\ m$; (b) $h = 0.1\ m$, $V = 2\ m/s$, $y = 5\ m$; (c) $h = 0.1/0.9\ m$, $V = 2\ m/s$, $y = 1.5\ m$ (edge of shallow section); (d) $h = 0.15\ m$, $V = 1.25\ m/s$, $y = 3\ m$ (critical speed). In the far field the initial upswelling more closely resembles the iBq profile, but in the near field or at the critical speed it more closely resembles the KdV profile.*

## E.4 Relationship Between Depth, Leading Crest Height and Leading Solitary Waves.

Although there is not absolute agreement, several authors have concluded that waves approach their shallow water condition when $\lambda/h \geq \sim 16$ (Fenton,1999, and Dean and Dalrymple,1991, as examples). Lighthill (1978) suggests an even lower value of $\sim 14$. The examples given here would appear to confirm that $\lambda/h = 16$ is representative. Setting $\lambda/h = 16$ as the lower limit of the definition of fully shallow and using the relationships in **Table E1**, the minimum conditions for $H/h$ can be calculated, where $H$ is the crest height only, as required for a solitary wave (often referred to as amplitude $a$). For the KdV solution, $\lambda/h \geq 16$ when the crest height, $H$, of the leading wave is such that $H/h \geq 0.206$ (the exact form being $\pi^2/48$).

Similarly, for the improved Boussinesq solution, the relationship is $H/h \geq 0.259$ [the exact form being $1/(48/\pi^2 - 1)$]. So, depending on the solitary wave theory chosen, the height of the leading crest height needs to be at least *20-25%* of the water depth to assume a dominant solitary wave form, though it's most likely to be closer to the KdV solution initially, at around *20%*.

*Figure E5*, taken from Fenton (1999), delineates between Stokes and Cnoidal theories at an Ursell number of *40* as proposed by Hedges (1995). For values of $\lambda/h = 16$ and $H/h \geq 0.206$, the Ursell number would be about *53*, placing it marginally higher than Hedges' demarcation. As a further example, *Figure E6* is a graphical representation of the relationship between wave celerity and Ursell number for cnoidal waves presented by Wiegel (1960, Fig. 8) and reproduced by Mei (1989, Ch. 11 Fig. 5.3). The conjunction of curves occurs at an Ursell number of about *47*, which is midway between Hedges' value of *40* and the value of *53* used here as the limiting condition for a dominant, leading solitary wave to form. That may be coincidence, but it may also be related.
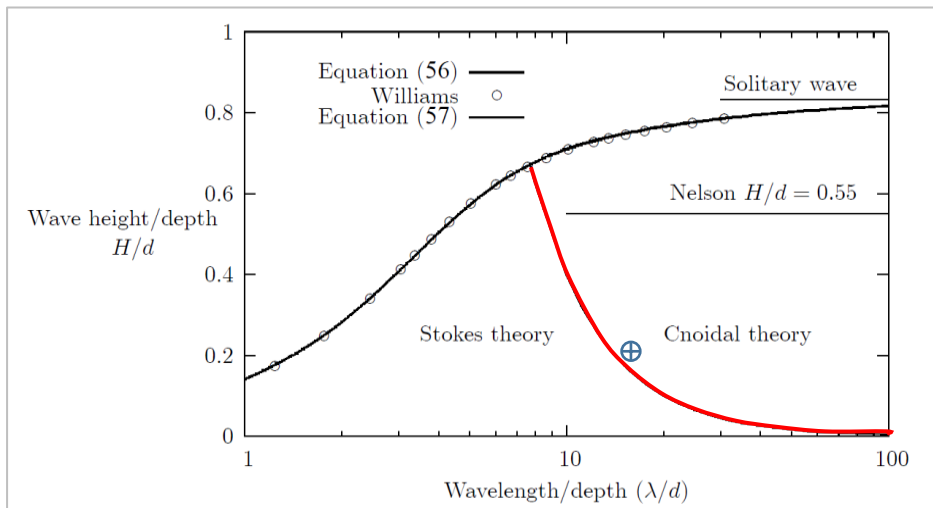


**Figure E5** – *Reproduced from Fenton (1999), Fig. 2, with reference to Hedges (1995). Note that $d \equiv h$. The line of demarcation between cnoidal and Stokes theories is shown at an Ursell number of 40 (red line). The value of $H/h = 0.206$ and $\lambda/h = 16$ proposed here gives an Ursell number of about 53, shown as a crossed marker, which moves the Fenton/Hedges line fractionally higher.*
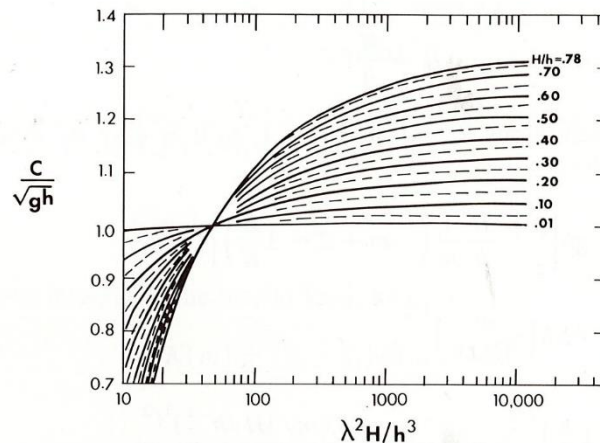
**Figure E6** – *Graph of cnoidal wave celerity (non-dimensionalised against depth) against Ursell number (or Stokes number) for different ratios of H/h (first shown in Wiegel, 1960, Fig. 7 and reproduced here from Mei, 1989, Ch. 11 Fig. 5.3). Those curves to the left of the conjunction can be described by Stokes' wave theories and those to the right of the conjunction are best described as cnoidal waves. The conjunction at $U_R \sim 47$ is midway between Hedges' value of 40 and the value assumed here of 53.*

### E.5    Very Shallow Water First Crest Celerity

For model AMC 00-01, a selection of very shallow water wave wake results at depth super-critical speeds were assessed for the relative position of the first wave crest. If the crest propagates as a solitary wave, it would propagate ahead of the Havelock wavefront. All the celerity equations in **Table E1** are functions of water depth and crest height, and so must be greater than the $\sqrt{gh}$ limit imposed by Havelock (1908) for any positive wave.

**Figure E7** shows clearly that the first crests in very shallow water travel ahead of their respective Havelock wavefronts (solid red lines). Modified wavefronts, based on a KdV solitary wave crest celerity of $[1 + H/(2h)]\sqrt{gh}$, are shown as dashed lines, with $H$ taken as the median crest height value (at $y = 3\ m$). This is unlike the experimental results at $h = 150\ mm$ (*Appendix ZE*), where the first crest aligned with the traditional Havelock wavefront but the first upswelling propagated ahead of the wavefront, and with the linear distance between the first wave upswelling and wave crest increasing linearly with increasing lateral separation. That suggested there was a solitary component to the first wave, but with the water not sufficiently shallow for it to dominate the first wave.

**Table E1** shows that the crest celerity depends on the solitary wave solution chosen, with the celerities of the KdV and BBM solutions being slightly faster than that of the improved Boussinesq solution for any positive value of crest height.[134,135] As discussed, it's more likely that the KdV solution would be most applicable, at least in the near field, as it describes the end of a

---

[134] Dark solitons, or travelling depressions described by the non-linear Schrödinger equation, have been observed experimentally in shallow water (Chabchoub *et al.*, 2013). These conform to the wider, more formal definition of solitons and are not immediately analogous to the near-solitons (more rightly just solitary waves) observed in ship studies.

[135] Remembering that the solitary wave celerities in Table E1 are first-order approximations that increasingly over-predict celerity as the ratio of $H/h$ increases due to non-linear effects. Refer to footnote 132.

277

transformation from a periodic to a solitary form rather than the pure solitary form of the Boussinesq solution.
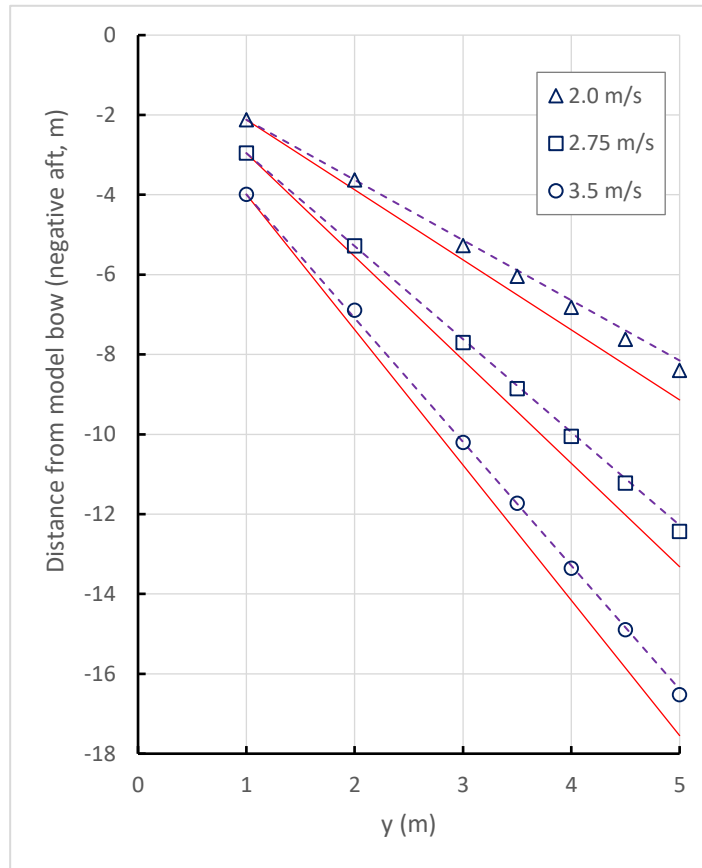


**Figure E7** – *Positions of the first crests of Model AMC 00-01 at three super-critical speeds in 0.1 m water depth. This is considered as an extremely shallow depth, with $h/L = 0.096$. The depth-critical speed is 0.99 m/s. The solid (red) lines show the classical Havelock wavefronts based on $\sqrt{gh}$ and the dashed (purple) lines show the Havelock wavefronts based on the KdV solitary wave celerity given in Table E1. The Boussinesq form of the solitary wave celerity would give marginally slower wavefronts, lagging slightly behind the KdV form. The consistency of crest positions with the solitary wave form of the Havelock wavefront is demonstrated. Note that the axes are scaled differently for clarity. Calculated wavefronts are notionally aligned to their respective crest positions at $y = 1\ m$.*

For comparison, the catamaran model AMC 17-05 was tested in extremely shallow water, with $h/L = 0.045$ and at depth sub-critical, trans-critical and super-critical speeds. Similar results to the monohull model were expected, based on the very shallow water depth relative to model length. However, other mitigating factors and testing limitations prevented any direct correlation.

Catamaran model AMC 17-05 is much longer than the monohull model AMC 00-01, limiting lateral wave probe distances to just over one boatlength maximum and constraining results to the very near field. **Table E2** is an example of the measured first crest parameters at various speeds, with wavenumbers, wavelengths and periods calculated assuming the first crest has a solitary form.

Moreover, the catamaran's very high slenderness ratio limited the generated wave heights such that any solitary wave component at depth super-critical speeds was not dominant, even with the extremely shallow depth relative to length. The catamaran model had a slenderness ratio of *9.0,* compared to the monohull model slenderness ratio of *4.75*. Scaled to the same static waterline

length, the monohull model would have a displacement almost seven times that of the catamaran model. The exaggeration of the monohull wave forms, in particular the leading solitary wave, would be almost wholly due to the excessive displacement and should not be erroneously (mischievously or nefariously) attributed to differences in hull form for the purpose of promoting one hull form over another. The fact remains that the two principle vessel design parameters determining wave wake parameters are length and displacement.

**Figure E8** shows the leading crest positions for model AMC 17-05 for different speeds at $h = 0.16\ m$. Some speeds have been removed for clarity. The depth-critical speed ($\sqrt{gh} = 1$) is *1.25 m/s* and so all speeds are depth super-critical. The Havelock wavefronts (based on $\sqrt{gh}$) are shown as dashed lines. Only the speeds of *1.46 m/s* and *1.63 m/s* exhibit any tendency for the leading crests to move ahead of their Havelock wavefronts away from the model; the others exhibiting the typical pattern of moderately shallow water. The *1.30 m/s* speed does exhibit a mild initial tendency for the leading crest to move ahead in the very near field, but it falls behind with increasing lateral separation.

The limited lateral separation of barely more than one boatlength does not afford the leading crest sufficient wave cycles for any leading solitary component to move ahead of the trailing periodic waves. It is noted in **Table E2** that the two speeds with the lowest wavenumbers are those that exhibit the faster moving crests in **Figure E8**, as they have undergone more wave cycles before each wave probe. In comparison, the monohull under similar super-critical conditions had wavenumbers in excess of *4*, or more than double the highest value for the catamaran. Greater lateral separation and increased wave cycles are conducive to stable results.

The leading crest heights are also the highest anywhere in each time series, improving the strength of any solitary component. Regardless, the requisite ratio of $H/h$ to form strong, leading solitary waves was not satisfied, and it was only satisfied with the monohull model due to its excessive displacement.

**Table E2** – *Low Wash Catamaran model AMC 17-05 first crest data at $h/L = 0.045$, assuming the leading crest is of a solitary wave form. Depth critical speed is 1.25 m/s. Wave data is at model scale.*

| $V_{ship}$ (kn) | $V_{model}$ (m/s) | $H_{crest}$ (mm) | k (rad.m$^{-1}$) | $\lambda$ (m) | T (= $\lambda/c$), (s) |
|---|---|---|---|---|---|
| 8 | 1.30 | 15.85 | 1.704 | 3.688 | 2.81 |
| 9 | 1.46 | 21.93 | 2.004 | 3.136 | 2.35 |
| 10 | 1.63 | 20.28 | 1.927 | 3.261 | 2.45 |
| 11 | 1.79 | 16.33 | 1.729 | 3.634 | 2.76 |
| 12 | 1.95 | 14.50 | 1.629 | 3.856 | 2.95 |
| 15 | 2.44 | 12.64 | 1.521 | 4.130 | 3.17 |
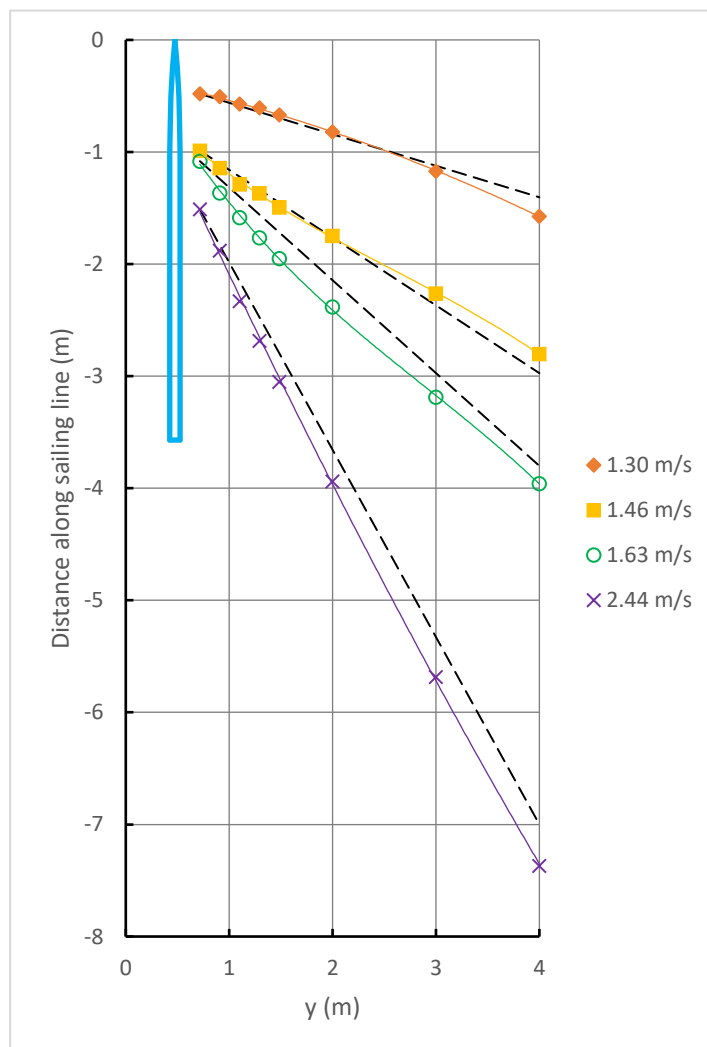


**Figure E8** – *Leading wave crest positions for depth super-critical speeds in very shallow water for catamaran model AMC 17-05. Although the water depth was extremely shallow ($h/L = 0.045$), the combination of low leading wavenumber, limited lateral separation ($y/L < 1.12$), and low displacement did not generate a dominant solitary wave that could consistently move ahead of the classical Havelock wavefront. Only the slightly super-critical speeds of 1.46 m/s and 1.63 m/s, where solitary component of the leading crest is strongest, is their presence apparent.*

## E.6 Very Shallow Water Wave Form Comparison – Catamaran and Monohull

As discussed, the catamaran model AMC 17-05 was tested in very shallow water relative to its length but did not generate the dominant leading solitary wave seen in the relatively heavier monohull model AMC 00-01. *Figure E9* shows the time series for the catamaran at the fastest depth-supercritical speed ($Fr_h = 1.95$) and second-furthest wave probe ($y/L = 0.84$), and for the monohull at a similar depth Froude number ($Fr_h = 2.02$) but the nearest wave probe ($y/L = 0.96$).

The waves following the drawdown are barely depth affected. The maximum wave would be classed as Stokes II with $\lambda/h = 3.94$, putting it just outside *practically deep* and at a point where it has the practical attributes of a deep water wave.

A conclusion drawn from *Figure E9* and the figure discussion is that the dominance of the leading solitary wave is a function of the slenderness ratio. The direct relationship between wave height and slenderness ratio, such that $H = f(\nabla^{\frac{1}{3}}/L)$, is a well-known relationship in the field of wave wake analysis.
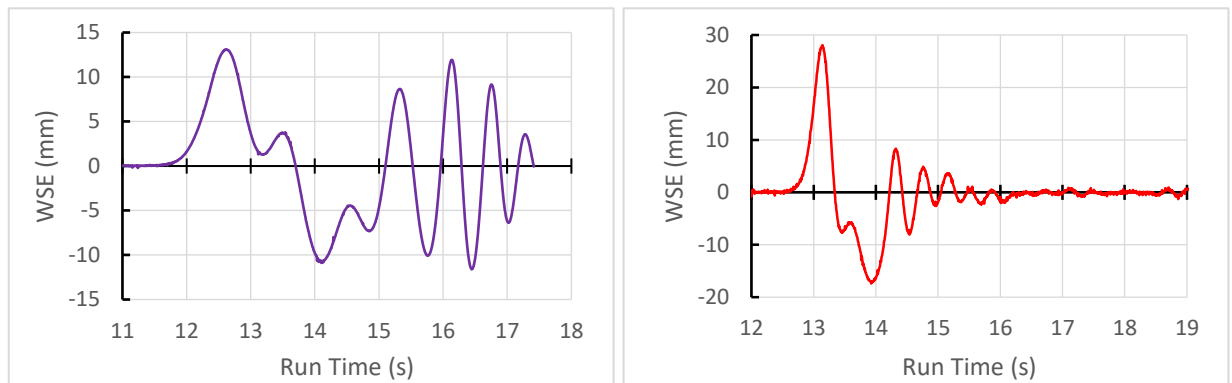


**Figure E9** – *Left: near-field wake trace for a low wash catamaran model AMC 17-05 at super-critical speed in very shallow water ($h = 0.16\,m; V = 2.44\,m/s; y/L = 0.84; h/L = 0.045; Fr_h = 1.95$). **Right**: near-field wake trace for monohull model AMC 00-01 at super-critical speed in very shallow water ($h = 0.1\,m; V = 2.0\,m/s; y/L = 0.96; h/L = 0.096; Fr_h = 2.02$). Both exhibit the same leading solitary wave and trailing periodic waves, the difference being the relative strengths of these for each model, with the catamaran wake still dominated by the trailing divergent packet. The catamaran leading crest does not meet the requirement of $H/h > \sim 0.2$ for the leading crest to be a dominant solitary wave. However, $(h_1 - h_0)/h_0 < \sim 0.3$ in both cases; there is a strong semblance of an undular bore for the monohull but weakly so for the catamaran.*

As a comparison to the first wave analysis of the monohull model shown in *Figure E2*, a similar analysis is shown for the catamaran model in *Figure E10* with all leading crests adjusted to coincide at the same run time. The forms are similar, but the increased influence of the waves following is seen in the catamaran results. Note that the most distant wave probe for the catamaran ($y = 4\,m, y/L = 1.12$) is in an equivalent position to the nearest probe for the monohull ($y = 1\,m, y/L = 0.96$).
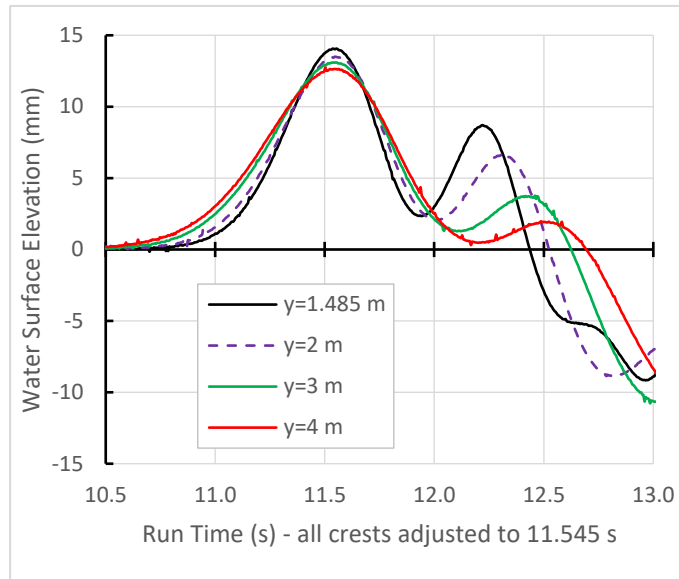
**Figure E10** – *Catamaran model AMC 17-05 in very shallow water ($h = 0.16\ m$; $V = 2.44\ m/s$; $h/L = 0.045$; $Fr_h = 1.95$), with leading crests adjusted to coincide. The weak dispersion and decay of the second crest is similar to that of the monohull, but more pronounced.*

### E.7 Relationship between Trans-Critical Wake and Residuary Resistance Peak

It is widely known and reported that critical speed effects reach their peak at slightly depth sub-critical speeds, typically around $Fr_h \approx 0.9$. The criterion against which to judge this peak can only be attributed to one of three variables: wave height (which is fraught with inconsistencies), leading crest angle, or residuary resistance.

Wave height, particularly that of the leading crest, is often quite inconsistent. Blockage and or restricted channel width can affect how the leading crest develops. Leading crest angle was reported by Robbins (2013, Figures 28 and 69) as approaching *90 deg.* at $Fr_h \approx 0.9$ and was apparently unaffected by the degree of shallowness. The extreme rate of change of leading crest angle with $Fr_h$ around the depth-critical speed complicates experimental stability and repeatability.

Residuary resistance is possibly the most stable method of assessment, but with caution. Resistance tests are usually undertaken in a towing tank, but blockage could distort the results in the very shallow water conditions. It is known that residuary resistance decreases markedly around the critical speed as the transverse waves are no longer able to travel with the vessel due to the depth restrictions on their celerity. At that critical condition the transverse waves would be fully depth affected, and at a certain sub-critical speed the waves would not be depth affected to any practical extent and linear theory would describe adequately the relationship between transverse wave celerity and vessel speed.

The standard definition of deep water has as its upper limit $\lambda/h = 2$, and the adopted definition of *practically deep* is based on the nominal upper limit of $h/\lambda = 0.28$ ($\lambda/h = 3.5$) proposed by Lighthill (1978). Using the linear wave theory relationship between transverse wave celerity and vessel speed of $V = \sqrt{(g\lambda)/(2\pi)}$, the upper limit for *deep* would be $Fr_h = 0.56$ and for *practically deep* would be $Fr_h = 0.75$. Above the *practically deep* depth Froude number limit, the

transverse waves become rapidly depth affected until reaching a terminal condition where they are fully shallow at $\sqrt{gh}$. These limits concur with Havelock (1908, Table III).

Few comparable examples are available, though there are three notable references that complement the results of model AMC 17-05. The first is Doctors *et al.* (1991, Fig. 5), with one reported shallow water condition ("$d/L = 0.2857$", where $d \equiv h$) recording the critical speed. The critical speed of the only other shallow water condition reported fell outside of the graph range ("$d/L = 0.1$", $F = 0.316$ at the depth-critical speed, where $F \equiv Fr_L$). For the single condition of interest reported, the last experimental data point before the decrease in wave resistance coefficient occurred at $Fr_h \approx 0.91$. Interestingly, the corresponding theoretical decrease occurred at $Fr_h = 1$, suggesting that this may have been a codified constraint (i.e., transverse waves taken as valid until $Fr_h = 1$ when the linear response becomes indeterminate) and therefore one reliant on the linear shallow water celerity limit of $\sqrt{gh}$. Lyakhovitsky (2007, Sec. 3.4) presents similar findings from theoretical resistance estimates in shallow water, showing a wave resistance peak at $Fr_h = 1$.

The second example is a series of numerical and experimental comparisons of catamaran models comprised of Wigley hull forms at different water depths and restricted channel widths (Doctors, 1994, Figures 3a and 3b). The lateral width restrictions may have influenced the results, but in the two shallow water tests ($h/L = 0.25$) the peak in wave resistance coefficient occurred at $Fr_h \approx 0.90$ experimentally and $Fr_h = 1$ numerically. Greater credence is placed on the experimental results: one reflects reality; the other reflects an interpretation of reality dependent on the model used.

The third example is found in the experimental results of Dand *et al.* (1999), notably Fig. 1. Mean sinkage was also a strong indicator of the pre-critical peak in shallow water effects (Dand *et al.*, 1999, Fig. 5 and 6).

Interestingly, in these experimental examples, restricted channel width and or water depth did not seem to change the depth Froude number at which the peak wave drag coefficient occurred; they only influenced its magnitude. This concurs with the findings of Robbins (2013) and the apparent disjuncture between wave angle and shallowness at the peak condition.

A possible explanation for the wave resistance coefficient peak at $Fr_h \sim 0.9$ can be found in the formation of solitary components in the leading wave, with reference to ***Figure E3*** and ***Table E1***. The depth sub-critical, shallow water wave train may be best described by the KdV equations, as previously discussed. If the water were sufficiently shallow relative to vessel length, the solitary component of the wave function at the front of the leading crest would become fully depth affected at a slightly depth sub-critical vessel speed (the solitary component's celerity being a function of height and depth, not just depth). Assuming the fully shallow limit is reached according to the assumed condition of $\lambda/h \geq \sim 16$, this would occur when $Fr_h = (1 + \pi^2/96)^{-1}$, or *0.907*. If an iBQ form is assumed, the peak would occur slightly earlier at $Fr_h = [1 + 1/(48/\pi^2 - 1)]^{-1/2}$, or *0.891*.[136] The difference is minor, though the argument here for the applicability of the KdV form is stronger – the solitary component having formed at the head of a depth-restricted periodic wave packet and not alone. At this slightly depth sub-critical vessel speed, the celerity of the front of the leading wave becomes super-critical, leading to the condition where the wave resistance may begin to reduce. At some point, when the leading

---

[136] Derived using the relationships for solitary wave celerity and width in Table E1, knowing that $\lambda = 2\pi\Delta$ and assuming a limiting shallow water condition of $\lambda/h \geq 16$.

solitary wave has energised itself sufficiently, the argument for use of the iBq form would apply. That would concur with Fig. 10(b) of Lee *et al.* (1989) (though no explanation was offered by the authors), as discussed in Section 5.

Adopting the shallow water limit of $\lambda/h \geq 14$ proposed by Lighthill (1978) (and referred to here as *practically shallow*), and assuming the KdV form, the peak would occur at $Fr_h = (1 + 2\pi^2/147)^{-1}$, or *0.882*. Lighthill's definition of *shallow* is the lowest value found in the literature and can be considered as a lower bound.

There is an analogy between the criticality of a generated solitary wave at slightly sub-critical vessel speeds and the development of shock waves. In aerodynamics, the term *critical Mach number* ($M_{crit}$) refers to an aircraft's Mach number when the flow over its wings reaches a Mach number of unity and a shock wave forms. Variables such as compressibility, planform and sectional shape can vary $M_{crit}$ considerably (and complicate the analogy for compressible and incompressible flows), but the value for the (non-lifting) fuselage is around *0.9*, which concurs with the value calculated here.

An interesting set of experiments would be to confirm the position of the peak in wave drag coefficient approaching depth-critical speed and conditions that might influence it.


## E.8    Very Shallow Water and Depth-Critical Speed

Solitary waves form at trans-critical speeds but become more dominant if restriction occurs due to depth and or width constraints. Studies of this condition are made somewhat academic by full-scale limitations such as lack of stable depth, difficulty in controlling vessel speed in this dynamically unstable condition and achieving the low $h/L$ ratio necessary for the solitary wave to be dominant. It is well reported that solitary waves, formed under the specific trans-critical conditions in restricted channels, can evolve into a train of solitary waves ahead of the vessel at model scale. It is a phenomenon rarely observed at full scale due to the inability to replicate consistent conditions.

Depth trans-critical test results for model AMC 00-01 were analysed for qualitative features in the leading waves. *Figure E11* presents two conditions: $Fr_h = 0.91$ (*left*) and $Fr_h = 1.01$ (*right*) and in very shallow water ($h/L = 0.096$). The first (*left*) condition represents the speed at which a leading KdV solitary wave would begin to propagate super-critically and the second (*right*) condition represents the speed traditionally considered as the depth-critical speed. Both produce similar wave patterns. The depth super-critical condition appears to produce the highest waves (both solitary and periodic), which would seem contrary to what is the general trend with peak resistance.

In both cases it is quite obvious that the third solitary crest begins to fall behind in the far field, due partially to its diminishing height (and the influence of height on solitary wave celerity), but also due to the lack of a supporting boundary in a restricted channel that might otherwise stop the crest-wise leakage of energy. Given sufficient lateral separation, all three leading solitary waves may deteriorate into a KdV periodic form, starting with the *least solitary* wave (third crest) and eventually all three waves. That is certainly evident in the pattern of the solitary wave crests.
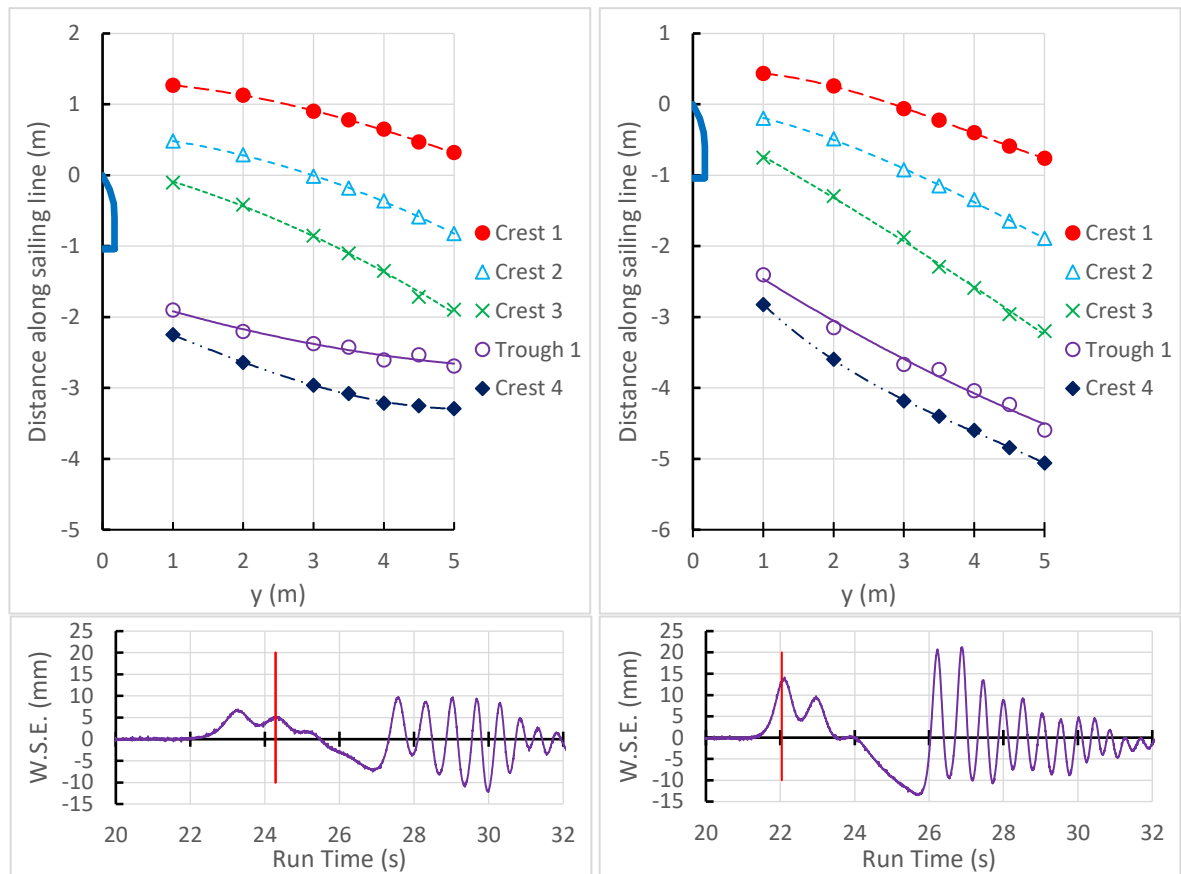
**Figure E11** – *Leading crest and trough positions at depth trans-critical speeds for model AMC 00-01 ($h = 0.1\,m, h/L = 0.096$). **Left**: $Fr_h = 0.91$; **Right** $Fr_h = 1.01$. The corresponding wave traces at $y = 3\,m$ are also shown for comparison. The leading crests have the form of solitary waves with a convex crest, but the third crest is beginning to fall behind in the far field as the strength of its solitary component diminishes and the wave decays into a periodic KdV form. The fourth crest, being the leading crest of the sub-critical packet, has a more typical high-speed, concave crest shape.*

### E.9    Wave Energy

Of interest for environmental assessment is the distribution of energy within the shoaling wake. Wakes generated in deep water and propagating to shallow water have a tendency for a more even distribution of energy throughout the wake. The maximum wave within a deep-water wake accounts for around *50%* of the total divergent wave energy in the very near field ($y/L{\sim}1$), decaying in the far field as the packet disperses, the number of waves increases, and the relative strength of the maximum wave diminishes.

In contrast, shallow water wakes concentrate the bulk of the energy into fewer waves, which are slower to change with propagation due to their weakly dispersive nature. The distribution of energy is dependent on depth, speed and vessel form, but the general guide is that the first wave contains at least half the total wake energy when $h/L < {\sim}0.15$. An example of the rapid shift in energy towards the head of a depth super-critical wake is shown in *Figure E12*. In deep water, dispersion and increasing lateral separation increases the number of waves and reduces the energy of the maximum wave, but overall packet energy is maintained. In the shallow water cases, weakening dispersion increasingly maintains energy at the head of the packet.

285
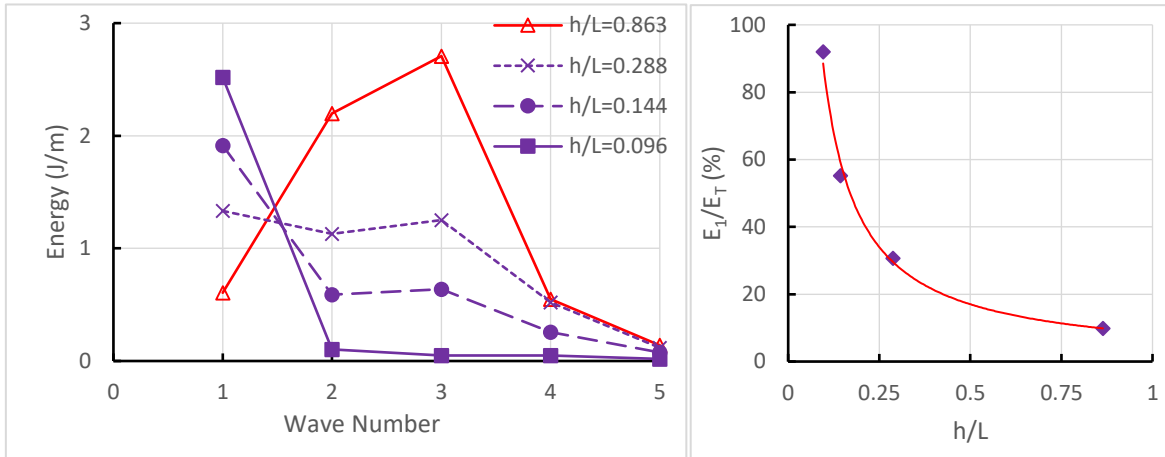
**Figure E12** – *Experimental results for model AMC 00-01 at different values of $h/L$ from practically deep to very shallow. The term "wave number" refers to individual waves as they appear in the trace and not "wavenumber". **Left**: energy of individual waves ($E = \rho g H^2 \lambda/8$), using the appropriate linear or non-linear theory to estimate $\lambda$. In the deep condition ($h/L = 0.863$), the wave with the highest energy is characteristically towards the centre of the packet. As the water shoals, energy is trapped in the head of the wake at increasing levels due to the weakening dispersion (data markers are joined for clarity; the abscissae are otherwise discrete). **Right**: ratio of energy of the first wave ($E_1$) to the total packet energy ($E_T$) against $h/L$, showing the accelerated growth of energy of the first wave as the depth decreases. This is of particular consequence for the depth super-critical operation large, high-speed ferries in semi-open waterways.*

*Figure E13* shows the very shallow water wake of model AMC 00-01 at a lateral separation of ~$2L$. It has the familiar form of a hydraulic jump, as discussed in Appendix E (Figure E3). Only the first six waves have been analysed, with subsequent waves judged as adding immeasurably to the total energy (wave six accounts for just *0.12%* of the total wake energy). Energy was calculated using the linear form $E = \frac{1}{8}\rho g H^2 \lambda$, with wavelength calculated according the appropriate shallow water or non-linear theory. The first wave, considered as *long*, conforms to the hyperbolic approximation to cnoidal theory (Iwagaki, 1968). The subsequent waves are much shorter and can be regarded as Stokes III waves.

The results are shown in *Table E3*. They clearly demonstrate that the first wave, assumed in this instance to be a periodic wave (but most likely isn't completely), accounts for most of the total wake energy - in this case almost *93%*. If the first wave is treated as a solitary wave and the energy per unit crest width calculated according to [E2] (from Munk, 1949):

$$E = \frac{8}{3\sqrt{3}} \rho g (Hh)^{3/2} \tag{E2}$$

the energy of the first crest is *2.99 J/m*, which is just *5%* less than the linearised energy with non-linear theory wavelength for *wave 1*. Even with the difference between [E2] for a solitary wave and $E = \frac{1}{8}\rho g H^2 \lambda$ for a periodic wave being the lack of a trough in the solitary wave analysis, the results are very similar.

286
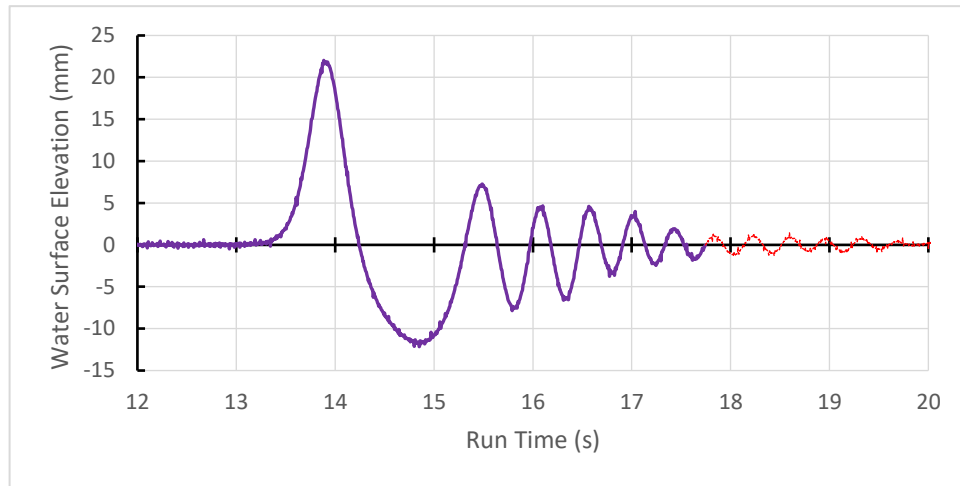
**Figure E13** – *Model AMC 00-01 at $y = 2\ m$ (~2L) in very shallow water ($h/L = 0.096$, $V = 2.0\ m/s$, $Fr_h = 2.02$). The first six waves (commencing with up-crossings) are highlighted.*

**Table E3** – *Discretised Energy Analysis of Figure E13. The depth-critical speed ($\sqrt{gh}$) is 0.99 m/s.*

| Wave | 1 | 2 | 3 | 4 | 5 | 6 |
|---|---|---|---|---|---|---|
| H (mm) | 34.0 | 15.1 | 11.0 | 8.0 | 5.7 | 3.6 |
| T (s) | 2.02 | 0.65 | 0.50 | 0.44 | 0.43 | 0.41 |
| λ (m) | 2.224 | 0.547 | 0.369 | 0.296 | 0.277 | 0.259 |
| c (m/s) | 1.10 | 0.84 | 0.74 | 0.67 | 0.65 | 0.63 |
| E (J/m) | 3.153 | 0.152 | 0.055 | 0.023 | 0.011 | 0.004 |

Similar calculations were performed for model AMC 00-01 at the same water depth and lateral separation over a range of depth super-critical speeds, with the following generalised results:

- regardless of whether it was considered as a periodic or solitary wave, the first wave contained at least *90%* of the total wake energy;
- the energy of the first wave followed a similar trend to that of the maximum wave in deep water – slowly decreasing towards a constant value as speed increased;
- the wave periods of the waves following the first wave were consistent and independent of speed;
- with the energy of the first wave calculated using the solitary wave energy formula in [E2], the energy of the first wave as a percentage of the total wake energy was very consistent at around *92%*, and independent of speed (provided it was depth super-critical).

## E.10    Wave Decay

Waves will only follow predictable decay rates where they propagate as a packet. Interference between different packets within the propagating wake will render wave decay calculations pointless.

Appendix C discussed how certain parts of a shallow water wave wake have predictable decay characteristics, notably the leading shallow water wave. That is because this wave is itself a packet of waves that are unable to fully and quickly disperse due to the depth limitation present since their generation at the sailing line. In that case the group celerity necessary to calculate the decay is easily determined, being $\sqrt{gh}$.

In the case of very shallow water where the leading wave is dominated by a solitary form, the Schrödinger-based decay equation does not apply as the leading wave form approaches a single wave rather than a packet. However, the trough depth did appear to conform better, suggesting that the trough parameters are related more to the trailing periodic waves than the leading crest. *Figure E14* shows analysis of the leading crests and trailing troughs of model AMC 00-01 in very shallow water. The left figure demonstrates that the crest height does not comply when the solitary wave dominates. The right figure shows that the trough depth does comply, but more so at higher depth super-critical speeds. Further discussion can be found in the figure caption.
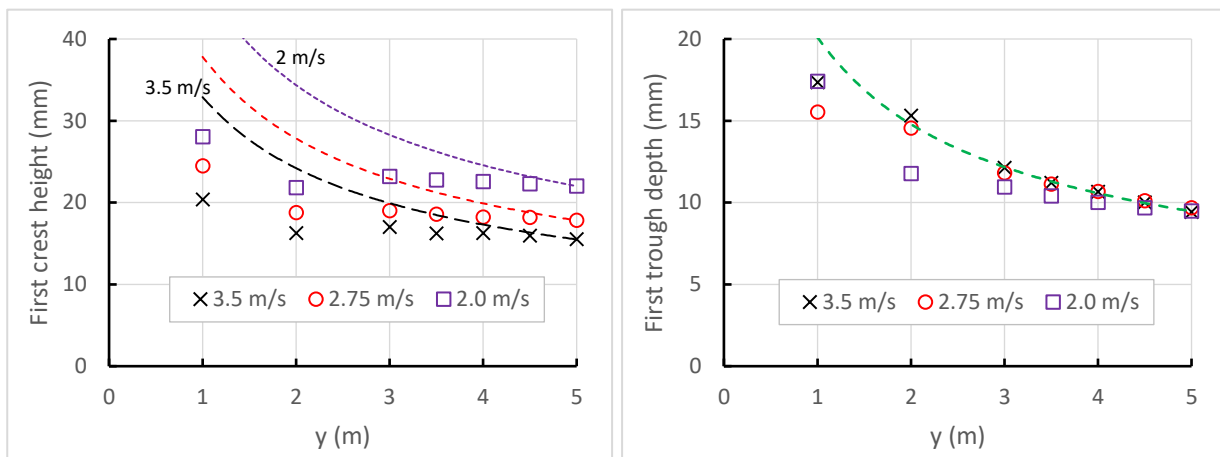


**Figure E14** *– Model AMC 00-01, decay of the first wave components in very shallow water ($h/L = 0.096$). Crest height is shown on the left and trough depth is shown on the right. These are compared to their respective decay equation (Appendix C, [C1], shown as dashed lines made relative to the value at $y = 5\ m$), based on a group celerity of $\sqrt{gh}$. The crests exhibit no correlation whatsoever, though do have a very consistent height stability with minimal decay in the far field. This is consistent with a predominately solitary wave form. The troughs show far better correlation with the calculated decay rate (only one decay curve shown – the others are almost identical). This suggests that the depth-restricted periodic wave packet is defined principally by the trough if the water depth is shallow enough; the strength of the solitary component increasing with increasing $\lambda/h$. In the complementary shallow-to-deep tests, where wave wakes were generated in shallow water and allowed to propagate to deep water, the rapid collapse of the first shallow water crest upon reaching deep water would suggest that its energy has bled back into the packet as it changes from its shallow water solitary to its deeper water periodic form.*

## Appendix F – Wave Wake in Extremely Shallow Water

### F.1    Introduction

A series of experiments were conducted on model AMC 00-01 in extremely shallow water – so shallow as to be considered un-navigable in practice. The experiment was designed for two purposes: to further demonstrate the detachment and free propagation of the leading solitary wave, and to study the relevance to wave wakes of the depth Froude number limit of a uniform stream flow on the generation of solitary waves (McCowan, 1894; Benjamin and Lighthill, 1954).

From Table E1 of Appendix E, the first order depth Froude number of a solitary wave crest can be easily recognised as $Fr_{h,KdV} = [1 + H/(2h)]$ for a KdV solitary wave form and $Fr_{h,iBq} = \sqrt{(H+h)/h}$ for a Boussinesq form (original and improved). Applying the flow depth Froude number limits of McCowan ($Fr_h \sim 1.25$), and Benjamin and Lighthill ($Fr_h \sim 1.21$), and comparing first order and higher order models, these would be realised according to **Table F1**:[137]

**Table F1**: *Solitary wave crest height/depth relationships required to achieve the stated flow depth Froude number limits of McCowan (1894) and Benjamin and Lighthill (1954).*

|  | **McCowan** | **Benjamin and Lighthill** |
|---|---|---|
| First order KdV | $H/h = 0.50$ | $H/h = 0.42$ |
| First order iBq | $H/h = 0.56$ | $H/h = 0.46$ |
| Yamashita and Kakinuma (2014) | $H/h = 0.60$ | $H/h = 0.49$ |

**Note**: *At $H/h = 0.5$, the crest Froude number discrepancy between the first and higher order relationships is 3%. At $H/h = 0.3$ the discrepancy is 1%. At breaking ($H/h \sim 0.83$), it increases to 10%.*

The intention was to attempt to generate $H/h$ ratios in this range to understand how a uniform flow depth Froude number limit might apply to wave wakes. The scenarios are not quite identical physically: in the open flow condition the water is moving and the bottom (and the wave itself) is stationary; in the wave wake case the bottom and water are stationary, but the wave moves. Figure G4 of Appendix G shows how the shallow water effect on wave height is greatest at a vessel condition of $Fr_h \sim 1.25$. Below this, a wake has the traditional form of a critical speed wake, dominated by leading solitary waves. Above this speed, where the wake has the accepted super-critical form, the industry-standard dialogue refers only to long-crested waves of an apparent periodic form, without mention of solitary wave components. It is evident that solitary waves are not limited only to the depth trans-critical speed range.

Clearly, the only two means available for increasing $H/h$ experimentally are to increase the solitary wave height or decrease the water depth. Once the model is well into the depth super-critical speed range, height can only be increased by increasing displacement. Reducing

---

[137] Limits above which solitary waves, in the form of precursor solitary waves, cannot be generated by a uniform flow.

slenderness ratio by maintaining displacement and decreasing length, which then increases the $h/L$ ratio, would not give the same result, since reducing length alone would increase the height relative to length but not necessarily the absolute height.[138] The other way would be to reduce the water depth, with the obvious limitation that the model should not ground at any time.

To overcome these limitations, the water depth was reduced to *52 mm*, and the model was fixed in heave and trim to replicate its dynamic planing attitude. This reduced its static displacement to around *40%* of its usual test value of *10.55 kg*, but with extra virtual displacement caused by the induced lift from planing bottom pressure. This added two further limitations: it would only apply at one speed, since the dynamic trim and sinkage of a planing hull are speed dependent; it would be almost impossible to calculate the dynamic lift and hence displacement augment with accuracy. The fastest speed would be the closest to reality, with the effect at slower speeds less than desired, as the dynamic lift component reduces with reducing speed. This is because the fully planing speed for this vessel, where the dynamic lift equals the vessel weight, would not occur until a speed of about *4.9 m/s* ($Fr_\nabla \approx 3.35$), which is well beyond the test range. At the fastest test speed of *3.5 m/s*, the positive dynamic stern sinkage would result in a stern draft greater than the at-rest draft, and this could not be replicated in the very shallow water without the model grounding.

## F.2     <u>Leading Crest Height and Crest Angle</u>

The lack of displaced volume (and reduced dynamic virtual displacement at slower speeds) resulted in leading waves of insufficient height to approach the required $H/h$ values of **Table F1**. **Figure F1** shows the measured values at the nearest lateral probe ($h/L = 0.05$, solid circles). As anticipated, the discrepancy is diminished at higher speeds when the dynamic lift increases and offsets the deficit in displaced volume. Even so, the peak in crest height at a model condition of $Fr_h = {\sim}1.25$ concords with Figure G4 of Appendix G. The steady crest height in the vessel speed range $1.25 < Fr_h < 4.25$ is almost certainly due to the variability in dynamic bottom lift plus static buoyancy.

---

[138] Increasing the $h/L$ ratio would reduce the dominance of the leading crest. At the same time, the shorter model length would generate waves with shorter periods, which are less affected by depth. Wave height relative to vessel length would increase, but wave height relative to depth would increase less, or not at all.
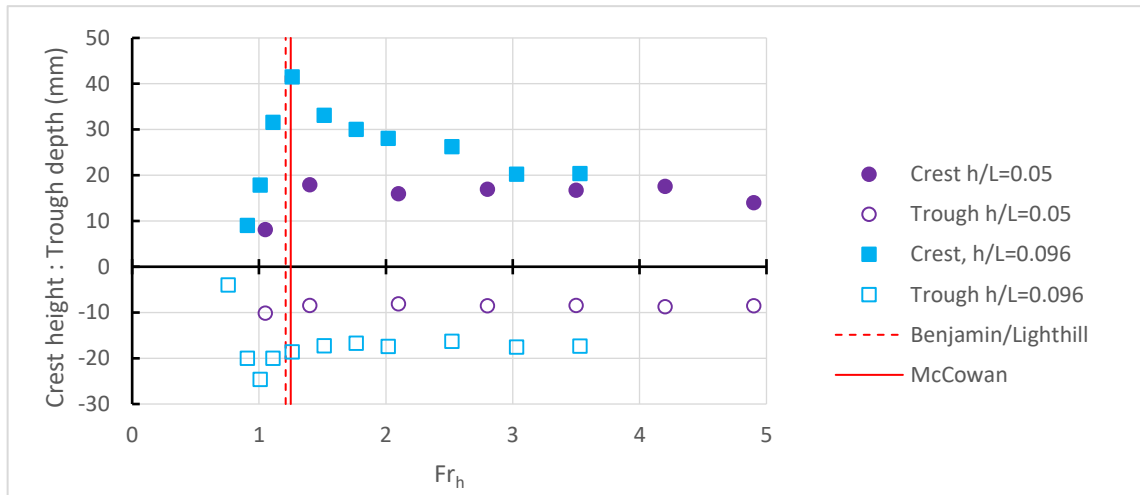
**Figure F1** – *Crest height/trough depth for AMC 00-01 in extremely shallow water ($h/L = 0.05$), with results from previous experiments ($h/L = 0.096$) where the model was free to heave and trim. The $h/L$ ratio is notionally 0.05 (based on the standard static waterline length for model AMC 00-01). The slenderness ratio in this artificial setup could not be determined; no normalisation of wave parameters has been undertaken. As with the slightly deeper condition of $h/L = 0.096$, the crest height peaks at $Fr_h \approx 1.25$, as inferred from McCowan (1894), and Benjamin and Lighthill (1954), and the trough depth is deepest around a depth critical speed of unity. The near-constant crest height at higher speeds is a function of the fixed model setup peculiar to these experiments.*

As a note, the maximum crest height shown in **Figure F1** ($h/L = 0.096$, solid squares) has a crest celerity depth Froude number of *1.208* based on its KdV celerity. This may be coincidence, but it might also be that the limiting depth Froude number of a vessel-generated solitary wave crest is ~1.21 and occurs at a vessel depth Froude number of around the same value.

Regardless of the tempered crest heights, the leading crest angles were well predicted by the shallow water solitary wave celerity equations, as shown in **Figure F2**. The exception to this was in the model trans-critical and low super-critical ranges, where crests tended to lag the calculated solitary wave celerities slightly but lead the linear shallow water celerity of $\sqrt{gh}$. Only at model depth Froude numbers greater than ~1.5 did the wavefront of the leading crest approach a consistent linearity.
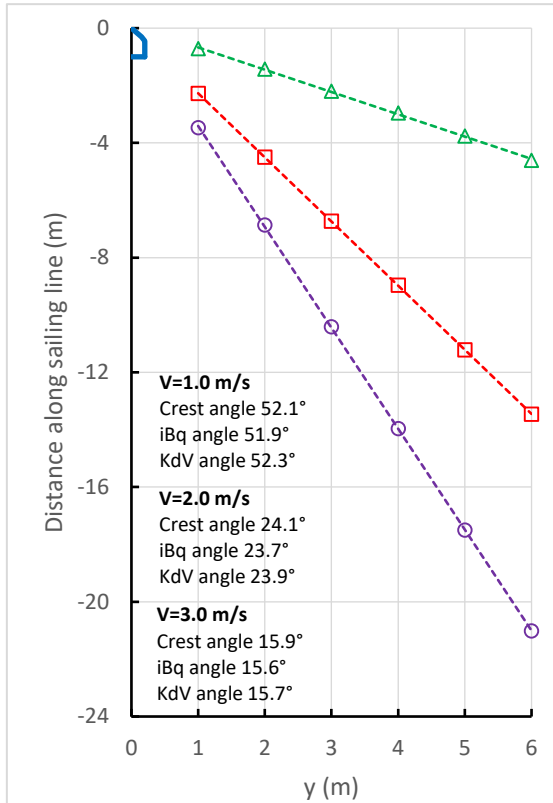
**Figure F2** – *Leading crest positions at three vessel speeds (model AMC 00-01). The $V = 1.0\ m/s$ ($Fr_h = 1.4$) dashed crest line assumes a linear form, though there is a slight convexity. The small discrepancies in angles are most likely due to the increasing influence of the model basin depth irregularities as the $H/h$ ratio increases, as well as non-linear effects.*

*At slower vessel speeds the measured crest angles lag the predictions; at higher speeds they lead. This confirms the observation at other depths that the vessel depth Froude number must reach about 1.5 before the leading crest shape becomes perfectly linear and the angle stabilises close to its predicted value.*

*Vessel speeds shown are nominal; the actual speeds used in calculations were time-averaged from the recorded data. From the uncertainty analysis (Appendix M), the maximum uncertainty in the crest angle is in the order of ±0.2° at this water depth and is the same for both iBq and KdV forms.*

That is a peculiar result, as it occurred even if the crest height (and by inference the solitary wave celerity, which is a function of crest height) decayed with lateral separation. In all cases presented here the predicted crest angles use crest height values at the most distant probe unless noted otherwise. The fact that the crest angle maintained its linearity regardless of its local height implies that the crest celerity was pre-determined, and the crest adjusted to suit – possibly shedding small crests as was noted in other shallow water experiments. A crest angle varying according to the local crest height decreasing with lateral separation would produce a curved (convex) wavefront; the lower, far-field crests travelling slower and falling behind the linear wavefront. Convex crest shapes in depth super-critical wake waves were noted by Havelock (1908, Fig. 9), but that was due to (weak) dispersion of the super-critical wake packet. Shallow water, depth super-critical wakes are more commonly observed and recorded with concave wavefronts, though that may depend on the degree of shallowness. The mechanism for the linear solitary wavefront irrespective of local crest height is not obvious but would be worth exploring.

### F.3    Solitary Wave Energy

The energy per unit crest width (*J/m*) of a solitary wave is taken as $E = 8\rho g\sqrt{(Hh)^3}/\left(3\sqrt{3}\right)$ (Munk, 1949), which can be rewritten as:

$$E = \tfrac{2}{3}\rho gH\nabla \qquad\qquad\qquad [F1]$$

where $\nabla$ is the volume per unit crest width of the wave in *m³/m*. The volume per unit crest width is effectively the area under the wave profile (evaluated between $\pm\infty$), which can be a spatial area (*in m²*) or a temporal area (*in ms*), depending on how the wave is recorded. As noted in Appendix E, the profile of a solitary wave is in the form $\zeta(x,t) = H sech^2[(x - ct)/\Delta]$, and the

first order spatial and temporal volumes (profile areas), and commensurate values for the KdV and iBq solitary wave solutions, are shown in **Table F2**.

**Table F2** – *Solitary wave volumes.*

| | spatial | temporal |
|---|---|---|
| Volume per unit width: m³/m; m²s/m (area under crest profile: m²; ms) | $\nabla = \int_{-\infty}^{\infty} \zeta \, dx = 2H\Delta$ | $\nabla_t = \int_{-\infty}^{\infty} \zeta \, dt = \dfrac{2H\Delta}{c}$ |
| Volume, KdV form | $\nabla = \sqrt{\dfrac{16Hh^3}{3}}$ | $\nabla_t = \dfrac{\sqrt{\dfrac{16Hh^2}{3g}}}{\left(1 + \dfrac{H}{2h}\right)}$ |
| Volume, iBq form | $\nabla = \sqrt{\dfrac{16Hh^2(H+h)}{3}}$ | $\nabla_t = \sqrt{\dfrac{16Hh^2}{3g}}$ |
| $\dfrac{\text{Volume iBq}}{\text{Volume KdV}}$ | $= \sqrt{\dfrac{H+h}{h}}$ $= Fr_{h,iBq}$ | $= \left(1 + \dfrac{H}{2h}\right)$ $= Fr_{h,KdV}$ |

Notes:

a. '$c$' is the appropriate solitary wave celerity (KdV or iBq form) and '$\Delta$' is the solitary wave width;

b. On its own, the temporal volume '$\nabla_t$' has no particular absolute meaning. However, multiplying the temporal volume by the solitary wave celerity $c$ will give the spatial volume. This is useful, as most wave wake records are temporal (from fixed wave probes) and not spatial (numerical, or from photographs);

c. These relationships are applicable for $H/h < 0.3$, where non-linearity is weaker and accounts for less than 1% discrepancy in the crest's depth Froude number.

From **Table F2**, a solitary wave of the iBq form is fuller and therefore has greater energy than a solitary wave of the KdV form with the same height.[139] Close analysis of leading shallow water waves has shown that those measured close to the vessel and at lower ratios of $H/h$, where the solitary wave is still forming or is not dominant, more closely approximate a KdV form. Conversely, those in the far field and at higher ratios of $H/h$ more closely approximate an iBq form. Stated again, the KdV form represents the end of the transition from sinusoidal to solitary and the iBq form is more of a pure solitary wave. Daily and Stephan (1952), who conducted experiments generating single solitary waves and measuring their parameters, found from five possible profile options (which did not include a KdV form) that the waves most closely conformed to a Boussinesq profile.

It is proposed that the solitary wave at the head of a very shallow water wake must be energised to enable it to disassociate itself from the wake and propagate freely. Its energy is increased through packet dispersion, however weak, where some of the energy normally cycling through

---

[139] $Fr_{h,iBq}$ and $Fr_{h,KdV}$ are always $> 1$ for any positive wave.

the packet is trapped at the non-dispersive head, increasing the volume of the solitary wave. Once a pure solitary wave form is achieved, it is free to propagate alone as if generated as a pure solitary wave in the first instance. In this way it is analogous to the change of phase when water boils – the KdV form representing the gradual change of temperature as a liquid, and the difference in energy between the KdV and iBq solitary wave forms representing the latent heat of vaporisation.

If this were the case, the energy increase of the iBq form over the KdV form is in accordance with the increased volume, as shown in **Table F2** and [F1]. The energy ratio is therefore directly related to $Fr_{h,iBq}$ (spatially) or $Fr_{h,KdV}$ (temporally).

It is well known that the permanence of a solitary wave (equating to a permanent solution analytically) is due to a balance between non-linear effects, which would lead to steepening and asymmetry, and dispersion. It may be the case that, in the initial stages of formation of a solitary wave in a wave wake, this balance does not exist, and energy is transferred to the head of the wake to complete the balance. Benjamin and Lighthill (1954) also state "*For it is known that, for every Froude number between 1 and some limiting value, a uniform supercritical stream may form without frictional effects into a solitary wave.*"

In a numerical study of the evolution of solitary waves, Wei and Kirby (1998) showed that evolving solitary waves reach height stability at a distance of $\sim 150h$, which decreases as $H/h$ increases. That demonstrates that the more dominant solitary waves reach a permanent state earlier in their propagation. This has direct relevance to wave wakes and to the quote above from Benjamin and Lighthill. Given sufficient lateral separation, every super-critical wake could develop a leading solitary wave that detaches and propagates independently. Depth instability, and bottom and internal friction, would most likely mitigate this to the point where it was practically impossible, except in the case of large, high-speed ferries operating in near-coastal, shallow-water routes.

**Figure F3** is an example of the changing wave profile with propagation in very shallow water. Near and far field profiles at $V = 2.0 \ m/s$ ($h/L = 0.05; Fr_h = 2.8$) are compared with the calculated iBq and KdV forms, further validating the evolution of the first crest profile from a KdV form to an iBq form as it propagates. This change comes with increasing volume and therefore energy relative to crest height. The far field profile at the higher speed of $V = 3.0 \ m/s$ shows almost complete agreement with the iBq profile (refer to Figure F4 following and the decoupling of the solitary crest in the far field).

**Figure F4** demonstrates the evolution of the leading solitary wave in a propagating shallow water wake regarding its changing energy content. Two depth super-critical speeds are shown, comparing the calculated KdV and iBq energies of the leading crest with the measured energy based on the actual volume under the crest. There is experimental variability, but the general trend is consistent. In the near field, the calculated energy (based on measured crest volume) is equivalent to that of a KdV form (based on calculated crest volume, Table F2). With increasing lateral separation, the energy level increases to the level of the more energetic iBq form. The $V = 3.0 \ m/s, y = 6 \ m$ condition of **Figure F4** is a particularly good example of the free propagation of the leading solitary wave in the far field. Both the *2.0 m/s* and *3.0 m/s* far-field profiles correlate with **Figure F3**; the *2.0 m/s* profile has not quite achieved its full energy level and therefore has not fully completed its disassociation, in contrast to the *3.0 m/s* profile.
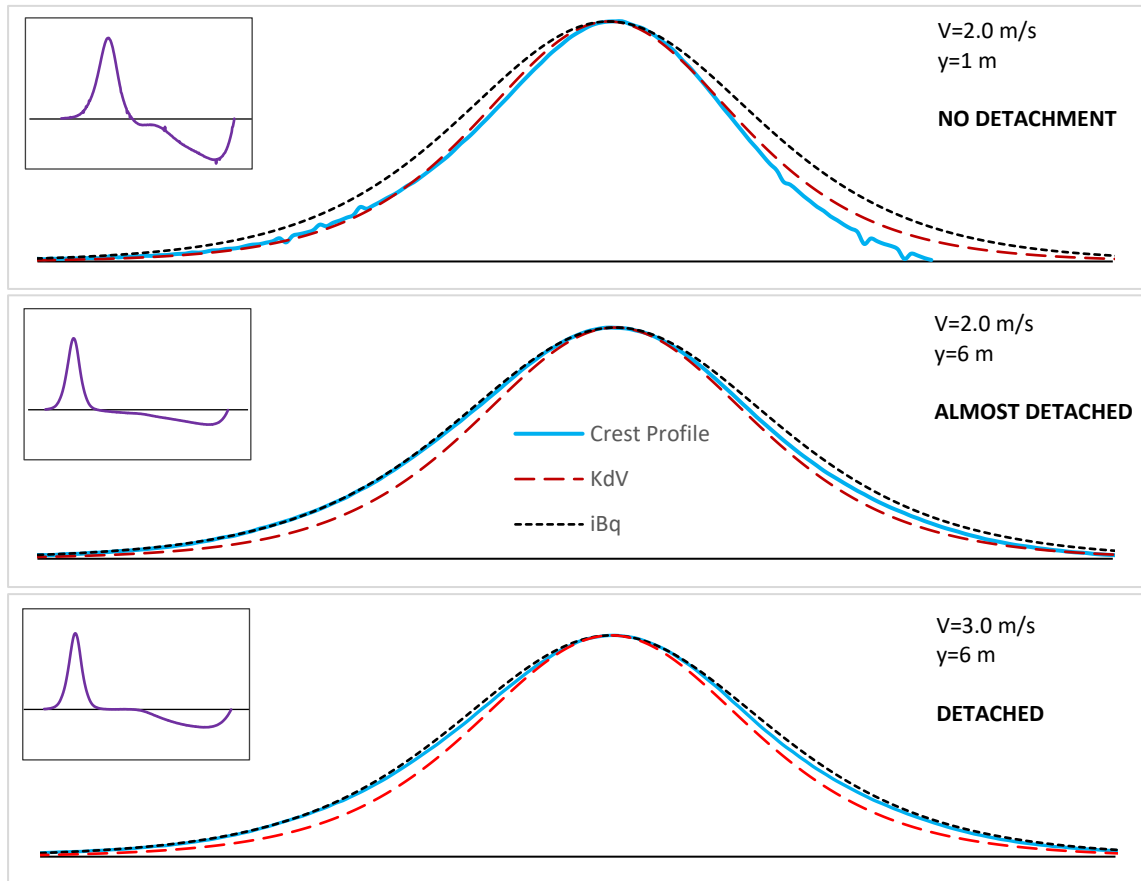
**Figure F3** – *Evolution of the leading solitary crest at different lateral positions and model speeds (wave propagation right to left). The top two figures at $V = 2.0 \; m/s$ show the change in profile from a KdV to iBq form with propagation from near field ($y = 1 \; m$; ~1L) to far field ($y = 6 \; m$; ~6L), demonstrating an increasing volume and therefore increasing energy content relative to height. The lower figure at a higher speed in the far field shows an almost complete agreement with the iBq form. Refer to Figure F4 and the partial/full detachment of the solitary crests in the far field in this case.*
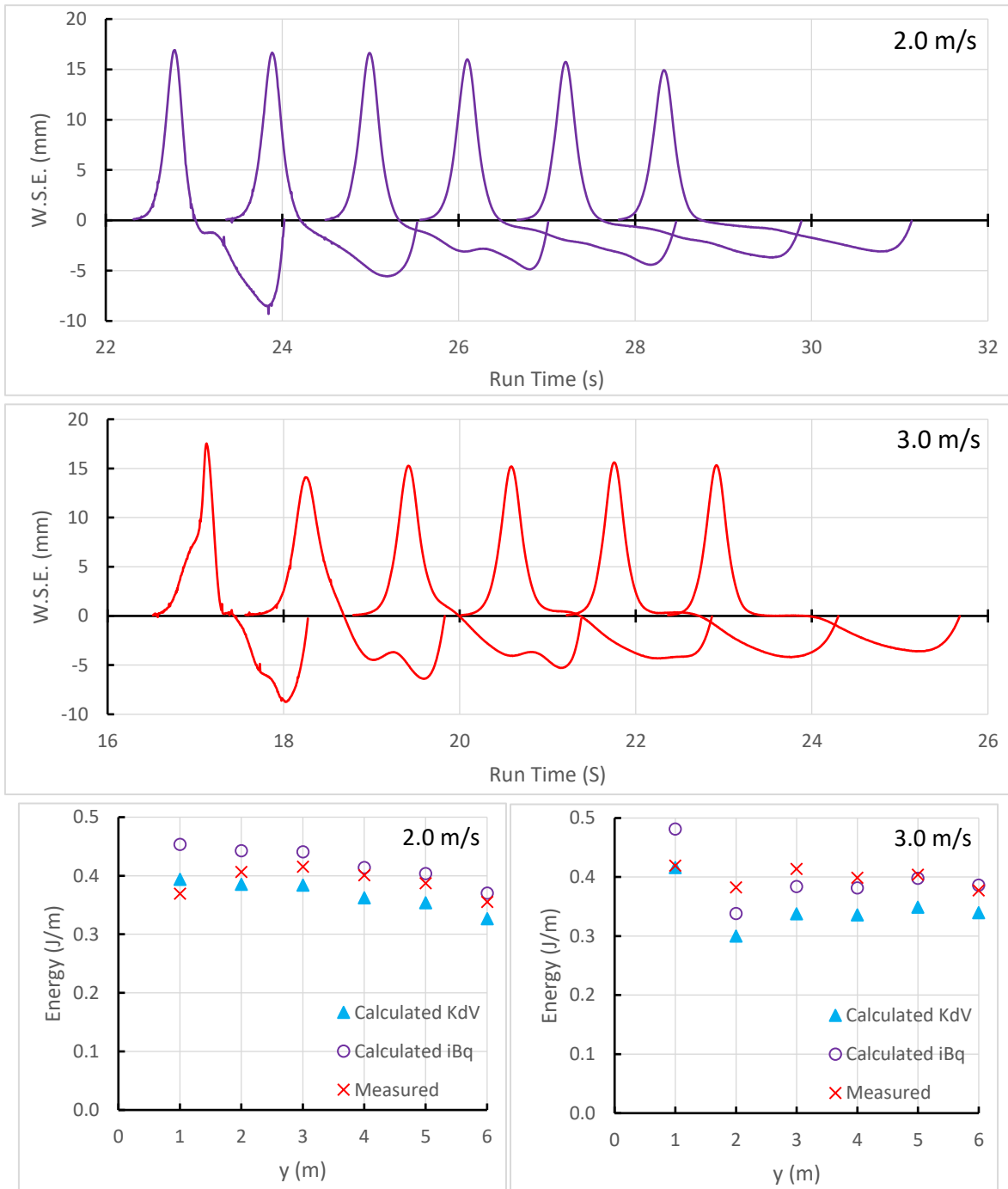
**Figure F4** – *Solitary wave energy comparison for two extremely shallow test conditions ($h = 52\ mm$) for model AMC 00-01 with six wave probes at $y = 1\ m \rightarrow 6\ m$ ($\sim 1L \rightarrow \sim 6L$). Only the first crests and troughs are shown. The calculated energy is from [F1] and Table F2. The measured energy is from [F1], with $\nabla$ from the numerical integration of each wave crest profile. Most notable is how the leading solitary wave energy evolves from a KdV value in the near field to an iBq value in the far field. The 2.0 m/s results are most descriptive in that regard; the 3.0 m/s crests having experimental irregularities that change the volume (most likely increased model spray at high speeds at the 1 m probe).*

### F.4    Note on the Celerity Discrepancy as Non-Linearity Increases.

It is noted that the discrepancy between the first-order KdV approximations and the higher order relationships increases as $H/h$ increases. At $H/h = 0.3$ the difference in crest Froude number is *1%* (over-predicted by the first-order approximations). In this experiment, values of $H/h$ in the order of *0.3* were obtained; in the experiments discussed in Appendix G, values closer to *0.5* were achieved in the shallow water area.

The effects of increasing non-linearity were too small to be isolated. For instance, applying a *1%* non-linearity discrepancy in crest celerities in *Figure F2* is shown in *Table F3*. It shows that the measured crest angles are greater (and hence crest celerity is slightly faster) than the non-linear correction would show, in which case non-linearity can be ignored if the $H/h$ ratio is not too large. It is also to be noted that the measured and calculated angles are very much encroaching on the limits of accuracy of the experiments of ~±0.2° (refer Appendix M).

**Table F3** – *Measured crest angle and calculated non-linear crest celerity angle (refer Figure F2)*

| Model Speed (m/s) | Measured crest angle (deg) | Calculated crest angle (corrected) (deg) |
|---|---|---|
| 1.0 | 52.1 | 51.6 |
| 2.0 | 24.1 | 23.6 |
| 3.0 | 15.9 | 15.5 |

*Note*: Model speeds are nominal. The actual speeds used to calculate the crest angles were time-averaged from the experimental results.

# Appendix G – Very Shallow Water Wake: Transition Shallow to Shallower

## G.1 Introduction

Experiments were conducted to propagate the very shallow water wave wake of model AMC 00-01 into even shallower water. The test section was *100 mm* deep ($h/L = 0.096$) and the wake transitioned into water *48 mm* deep ($h/L = 0.046$) beyond a lateral separation of $y = 2\ m$, with at *1:5* transition slope between. This is shown in **Figure G1**. The transition depth of *48 mm* was determined largely by the availability of materials (hence the odd number), as well as the requirement that the depth be shallow enough to force changes to the wake but not so shallow as to cause breaking due to shoaling.
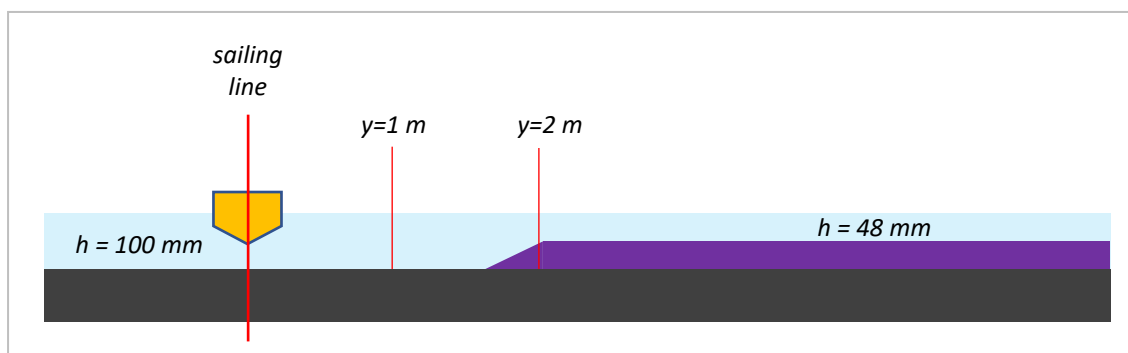


<u>**Figure G1**</u> *– Sectioned schematic of shallow water transition experimental setup (not to scale).*

The purpose of the experiment was four-fold:

a. to force the undular bore formed at the $h = 0.1\ m$ condition to become unstable (turbulent or breaking), demonstrating that the very shallow water wake does conform to general bore relationships;
b. to determine qualitatively how the bore changes when the parameters causing it change;
c. to observe changes to the leading solitary wave on transition;
d. to determine if the leading solitary wave component of the wake is able to fully disassociate itself from the trailing periodic wake and propagate independently.

The practical need for such an experiment is to resolve the components of the shallow water wake and how they might affect shorelines and shoreline users. Doyle *et al.* (2001) studied the shallow water wakes of large, high-speed ferries. They noted that wakes generated in very shallow water were dominated by a large leading wave that carried most of the wake energy. It was postulated that this wave was non-dispersive and therefore maintained its energy but was also subjected to shoaling and a commensurate growth in height. These are probably somewhat true (though lacking proper qualification), but they don't explain the nature of the wave itself and are based on an inherent assumption that the leading wave of a shallow water wave wake is periodic in nature.

The relatively abrupt depth transition of *1:5* was unavoidable. In other published numerical and experimental studies, a depth transition of *1:20* is considered more appropriate to minimise

reflections. Taylor (2016) reports on a numerical study by Orszaghova (2012) where a *1:20* transition caused a very slight reflection. In that case the incident wave was a single solitary wave and so the reflection was visible. In the case of the experiments here, where the solitary wave precedes a trailing periodic wake, determination of the reflection would be impossible.

Mei (1989) calculates transmission and reflection coefficients for an incident wave normal to a step, with Mei's subscripts *1* and *2* signifying before and after the step. There are two possible combinations: wave moving deep-to-shallow or shallow-to-deep. In this case we consider only the deep-to-shallow case, in which case the equations of Mei (1989) are given as:

*Transmission coefficient:*

$$T_1 = \frac{H_2}{H_1} = \frac{2}{1 + \sqrt{h_2/h_1}} \tag{G1}$$

*Reflection coefficient:*

$$R_1 = \frac{H_{1,after}}{H_{1,before}} = \frac{1 - \sqrt{h_2/h_1}}{1 + \sqrt{h_2/h_1}} \tag{G2}$$

For the experimental arrangement used ($h_1 = 100\ mm$ and $h_2 = 48\ mm$), the transmission and reflection coefficients are $T_1 = 1.18$ and $R_1 = 0.18$. Reflection would be impossible to detect in the wake at any scale. There are several limitations in using these equations. Firstly, the incident waves were not normal to the step. That introduces a second set of equations that account for refraction (Mei, 1989, Section 4.3) and depends on wavenumber, which is ill-defined for solitary waves in the classical sense. Secondly, the waves are assumed to be plane waves with a particular frequency. Vessel periodic wake waves are not perfectly plane or of constant frequency. A leading solitary wave may be. The purpose of these experiments was not to quantify wave parameters but to qualify them. It will be shown that the height of the leading solitary crest on the shelf was generally less than in deeper water and so the transmission coefficient was less than one.

Appendix E (Figure E12) showed the calculated energy of the first wave in one shallow water model test example ($h/L = 0.096$) accounted for over *90%* of the total wake energy. It also showed the form of the leading wave in the shallow water wake to be dominated increasingly by a solitary wave as the ratio of $h/L$ reduced. Given sufficient propagation distance and shoaling water, the leading solitary wave could begin to move ahead of the rest of the wake. Not only would it travel faster, the observations of Doyle *et al*. (2001) would make it a potentially dangerous wave if it arrived without warning.

Another factor that favours such waves from larger high-speed vessels is the relative $L/T$ ratio, which tends to increase with increasing length. The $h/L$ ratio necessary for safe navigation at speed reduces as a consequence, so it is more likely that larger vessels can be operated at high speeds in relatively shallower water than small craft. As a simple example, a small recreational vessel of length *5 m* (dynamic draft about *0.7 m*, including propeller) could not operate safely at high speed in water shallower than about *1 m*, yet this $h/L$ ratio scaled to the length of the *126 m Stena HSS 1500* ferry would equate to a depth of about *25 m*, which would be considered more than adequate for safe navigation for a such a vessel with a draft of *4.8 m*. The importance of understanding these extremely shallow water phenomena lies not with recreational craft but with the potential danger of larger high-speed vessels operating in shallow channels.

299

### G.2    Transformation of the Undular Bore

The undular bore form from previous model tests is shown in *Appendix E* (Figures E3 and E13). The undular form was not perfect, though Grimshaw (2011) notes that the term "*undular bore*" is somewhat generic. Many of the characteristics of an undular bore, such as the ratio of wave amplitude to water level change and the length of the bore *w.r.t.* time were met, but the periodic wave train retained a slowly decreasing wave period and not a constant period that defines an undular bore. It was also discussed that certain criteria must be satisfied for an undular bore to form, namely that the bore strength, $\beta = (h_1 - h_0)/h_0$, should be less than ~0.3, and the speed in the super-critical region should be not much above $\sqrt{gh}$. These are generally satisfied in very shallow water: the bore strength can only be sufficiently increased in water so shallow as to make it impractical for general navigation at depth super-critical speeds; the speed of the bore is governed by the speed of the solitary wave that precedes it and promotes its generation.

The celerity of a solitary wave at the point of breaking is a little less than $1.3\sqrt{gh}$ (Fenton, 1972, Fig. 1; Yamashita and Kakinuma, 2014, Fig. 3). Only when the solitary wave dominates the wave wake can the celerity of the leading shallow water wake wave be considered as well above $\sqrt{gh}$. If it is not dominant, as it the case when $H/h$ is less than about *0.2* ($H$ being the leading crest height above still water), the solitary component propagates as part of a leading wave with celerity $\sqrt{gh}$ that itself is a component of a wider wave wake described by a KdV function decaying from weakly solitary at the head to periodic at the tail. At even lower ratios of $H/h$, the KdV solution breaks down and the wake is described best by a periodic Stokes solution and an increasingly inconsequential solitary component that is barely discernible (*Appendix D*).

Similarly, the strength of the bore in this experimental example can only be increased by two means – increasing the ratio between the super and sub-critical flow celerities or with very shallow water to accentuate the bore. As pointed out, in the vessel wake analogue of a bore the flow celerity differential only increases with increased $H/h$ (meaning increasingly shallow water or reduced slenderness ratio), but it becomes impractical to generate wave wakes in extremely shallow water. To overcome this, the experiment was designed to create a shallow water wake in the form of an undular bore preceded by a leading solitary wave, then propagate that wake into even shallower water to force a transformation.

Apart from breaking due to shoaling, another limitation of this proposal was the loss of solitary wave celerity as it moved from shallow into very shallow water. This was partly offset by the even greater loss of celerity of the trailing waves. When the wake propagated from *100 mm* to *48 mm* depth, the leading solitary wave ($H\sim22\ mm$ average) lost *23%* of its celerity, but the trailing periodic waves lost at least *31%* celerity, assuming their celerity to be depth sub-critical (limited to $\sqrt{gh}$ ). The experimental results showed what was anticipated – that the bore would lose strength once it reached the shallow water. If any transformation from undular to turbulent was to occur, it would most likely occur only within the early propagation phase in the very shallow water where the bore retained sufficient strength.

Pelinovsky *et al*. (2015) provide a condition for transition between undular and breaking bores based on observed field data. They showed that the ratio $h_1/h_0 < 1.5$ would form an undular bore and $h_1/h_0 > 1.5$ would form a breaking (turbulent) bore.[140] Given the ratios expected, a value of *1.5* would be difficult, if not impossible, to achieve. However, the bores studied by Pelinovsky *et al*. (2015) were all river bores, where (mostly) the bore is stationary relative to the depth change but the water is moving. The bores generated in a wave wake are moving and the condition of super-criticality is generated by the preceding solitary wave. It is likely therefore that an undular bore created at one depth could never be transformed into a breaking bore under any conditions: once established as an undular bore, it cannot be *un-made*. At best, the individual periodic waves may become unstable, forming either individual breaking bores or breaking partially; losing some energy and re-forming as (smaller) periodic waves. This is not dissimilar to the shoaling of small wavelets in shallow water with minimal bottom slope, where wave crests periodically break to shed energy and height rather than break and form a bore. To do this, the waves need to be of a spilling form, implying short and steep.

Benjamin and Lighthill (1954) make the comment that the periodic waves of a bore arising from a stream flow with depth Froude number greater than ~1.21 (or ~1.25: a value from McCowan, 1894) may begin to break to provide the requisite loss of energy at the bore. They note that "*if this is so the reduction of $r$* (non-dimensionalised energy per unit mass) *by breaking of this first wave would lead to waves 'a little lower' than the wave of greatest height being formed behind any bore of moderate strength.*" That would appear to have happened in this experimental example.

Observations of the model tests showed quite conclusively that the first sub-critical wave following the leading wave (second crest overall) did shed a turbulent wake on the region about *0.25 m* to *0.75 m* past the transition. It is also possible that those following also did the same, though it was less clear once in the turbulent wake of the first bore wave. This can be seen in **Figure G2**.

Le Roux (2007), quotes Grilli *et al*. (1997), who found that waves do not break on slopes greater than *12°*. The slope of the transition between the shallow and very shallow sections (Figure G1) was *1:5*, or *11.3°*. It is unlikely therefore that any of the waves would have been subjected to breaking at the transition itself. Similarly, there were glassy (non-turbulent) areas before and after waves, suggesting that bottom roughness did not initiate the turbulence.

---

[140] Pelinovsky *et al*. (2015) state the ratio in terms of parameter $H/h$, where $H$ is the height of the bore above the bottom and $h$ is the unperturbed (super-critical) depth. As their symbols have generic wave wake meanings, the symbols of $h_1$ and $h_0$ (Lighthill, 1978) are substituted here. Note also that Benjamin and Lighthill (1954), and Mei (1989) use $h_2$ and $h_1$, just to confuse the matter.
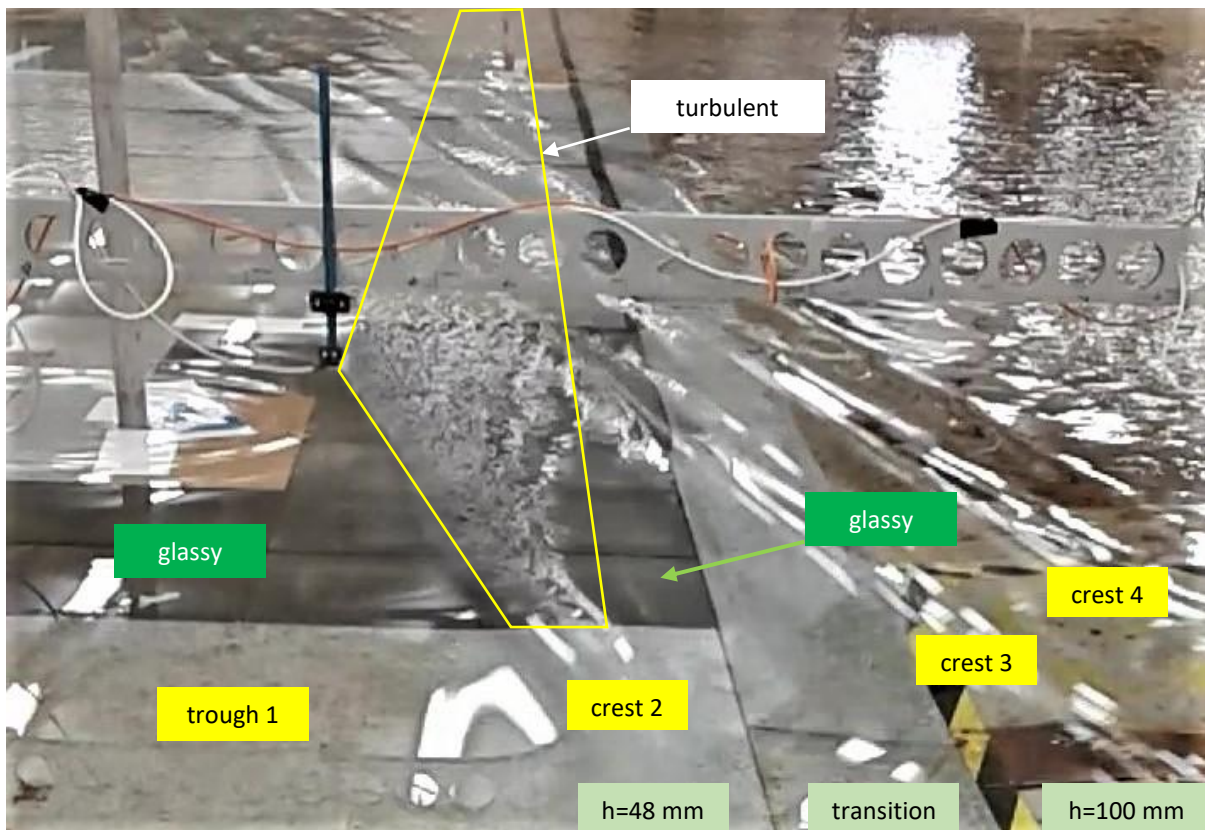
**Figure G2** – *Photograph at 3 m/s model speed, taken from a video recording. The sailing line is to the right and the waves are propagating to the left. The leading (solitary) crest has already passed to the left of the image. The turbulent region is evident along the narrow band shown, irrespective of the bottom roughness (galvanised steel sheeting or brick pavers). Note the glassy surface before and after the turbulent zone, suggesting that bottom roughness is not the cause. From the wave probe records, the first periodic wave progressively lost height and energy in the very shallow water to the point where it was almost consumed by those following.*

Further into the very shallow water, the second crest (first wave of the undular bore) began to decay in height rapidly and slowed relative to the crests following. Lee *et.al* (1989, p. 580 and Fig. 3) also note the subsidence of waves trailing a leading solitary wave, though offer no explanation. *Figure G3* shows the amplitude/depth of the leading solitary crest, leading trough and first periodic crest in two depth conditions. In the transition condition, the rapid decay of the trough depth and particularly the periodic wave amplitude can be seen, to the point where the following crests became difficult to track at the more distant probes. As noted in *Figure G2*, the periodic waves following became unstable at a distance into the shallow water and broke, leaving a zone of turbulence at the surface. The transformation of the leading wave had a deleterious effect on the periodic waves following. In these extreme conditions, where almost all the total wake energy is contained in the leading wave, changes in the trailing waves become somewhat academic.
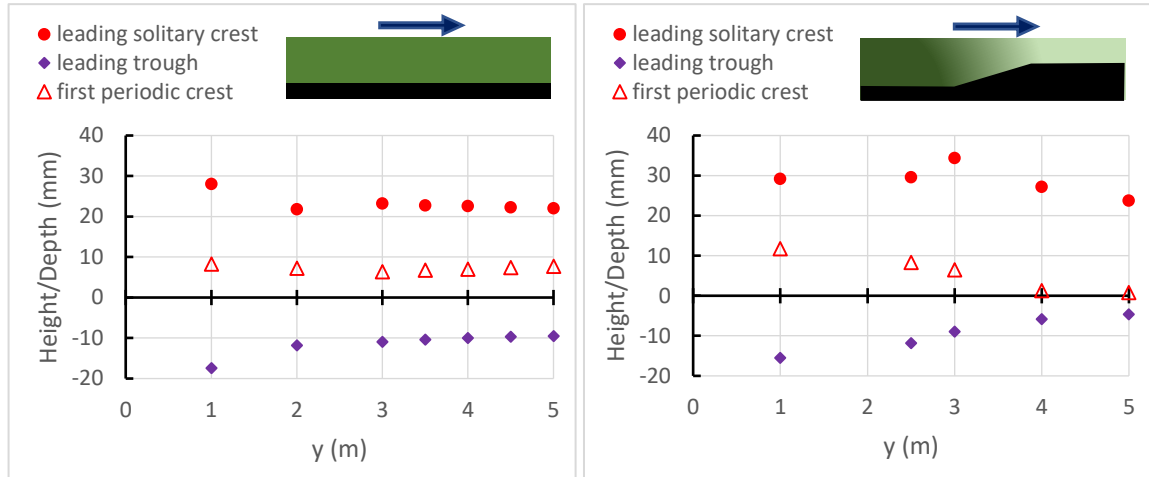
**Figure G3** – *Constant and variable depth comparison of the first few wave features at a model speed of 2.0 m/s.* **Left**: *Constant 100mm depth.* **Right**: *100mm to 48mm transition (refer Figure G1). Note the steadiness of waves in the constant depth condition where dispersion is weak. In the transition condition, the first crest (amplitude as a solitary wave above still water) tended to maintain a more constant value at other speeds. Of note is the collapse of the leading trough (as the leading solitary crest begins to detach) and first periodic crest (due to bore instability) once into the very shallow water beyond $y = 2\,m$.*

### G.3     Solitary Waves Under Transition

As expected, the speed of the leading wave slowed on reaching the very shallow water, leading to a more acute Havelock wavefront angle (based on the vector components of the vessel speed and the solitary wave celerity). Although the crest celerity reduced in shallow water, the depth Froude number of crest propagation increased.[141] The crest amplitude in the very shallow water tended to reduce to a value where the solitary wave's depth Froude number was around *1.25*; the upper limit for generation of solitary waves in super-critical flows (McCowan, 1984), as well as the solitary wave of maximum height (Benjamin and Lighthill, 1954). This may be coincidental, since this limit applies at the time of generation and not necessarily to propagation/transformation, but it may also explain several other observed phenomena.

The limiting height condition at $Fr_h = {\sim}1.25$ concurs with the test results of a small number of models in shallow water, as shown in **Figure G4**. Models were tested in water of varying relative lateral widths: model AMC 97-30 was tested at $\sim 1L$ from the wall (blockage *1.8%*); AMC model 17-05 was tested at $\sim 2L$ from the wall (blockage *1.2%*); AMC model 00-01 was tested at $\sim 7L$ from the wall (blockage ≤*1.2%*). Near-field results are presented in this instance; far-field results are similar but from fewer model tests (AMC model 00-01 only). The peak in leading crest height, which also tends to be the highest wave in shallow water, coincides with McCowan's proposed limiting depth Froude number. Above this, the first crest breaks close to the vessel due to excessive steepness - a phenomenon observed in both shallow and deep-water wave wakes.

---

[141] Adopting the KdV celerity equation, the depth Froude number simply becomes $Fr_{h,KdV} = [1 + H/(2h)]$, though only where the first-order approximation was valid ($H/h < {\sim}0.5$, error in crest $Fr_h$ <3%). This would be analogous to $(1 + \Delta)$ of Grimshaw *et al.* (2007) and Grimshaw *et al.* (2009), where $\Delta$ is the flow criticality parameter ($= Fr_h - 1$ for the flow, not to be confused with the solitary wave width used here).

Conversely, the maximum depth of the following trough occurs at $Fr_h = \sim 1$; the exception being the single catamaran model, which experienced a deeper trough at higher depth Froude numbers. This may not be an experimental aberration as there are several concurrent data points.

The occurrence of the maximum shallow water, leading wave height at $Fr_h = \sim 1.25$ has particular relevance to vessel operations. Delineation of vessel wave wake regimes according to depth Froude number is standard practice, though there are variations in the values. Trans-critical speeds were traditionally taken as those between $0.8 < Fr_h < 1.2$, but more recent variations shorten this to $0.75 < Fr_h < 1.0$, with anything above $Fr_h = 1.0$ taken as super-critical. If the most energetic and damaging wave in shallow water is the leading crest, and it reaches its peak value around $Fr_h \sim 1.25$, there may be reasonable cause to extend the trans-critical region. Alternatively, the adoption of four speed regimes – sub-critical, trans-sub-critical, trans-super-critical and super-critical, may be the preferred outcome.
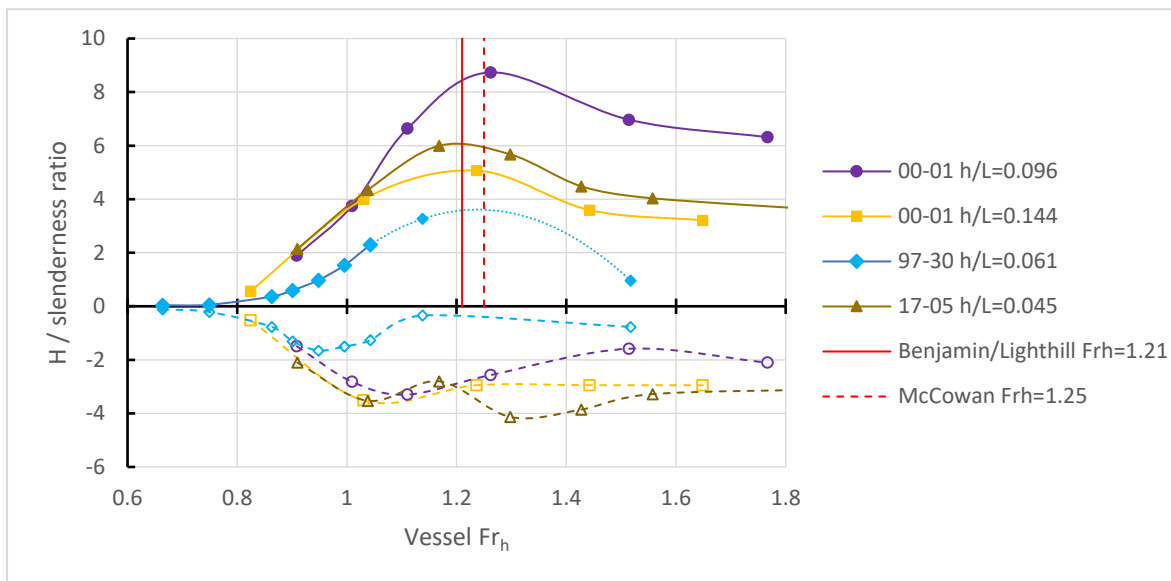


**Figure G4** – *Amplitude of leading crest (solid lines) and depth of the following trough (dashed lines) against depth Froude number for three models at different $h/L$ ratios and at $y \sim 1L$. Models 00-01 and 97-30 are monohulls, and 17-05 is a low-wash catamaran. Amplitudes/depths have been normalised by the slenderness ratio – the traditional non-dimensional parameter relevant to wave height. In all cases the leading crest peaks at $Fr_h \sim 1.25$, as predicted by McCowan (1894). The trough minimum occurs earlier, except for the catamaran which exhibits an extended range. Similar trends were evident at wider lateral positions. Although $Fr_h \sim 1$ has long been considered the worst case for vessels in restricted waterways, a higher value would be warranted for vessels in open, shallow water.*

Upon reaching the very shallow water, the leading crest began to shed a turbulent wake, visible after approximately *1.0 m* of very shallow water propagation ($y \sim 3\ m$). It will be noted from **Figure G9** (following) that this marks the point where the calculated very-shallow-water Havelock wavefront becomes asymptotic to the crest line, indicating the end of transition between the two test depths. Similarly, projecting the (dashed) Havelock wavefronts of the shed crest (based on their KdV solitary wave celerities) shows that they almost perfectly intersect with the lines of *crest 1* at the beginning of the very shallow water region ($y = 2\ m$). **Figure G10** (following) shows this. It is well understood that a solitary wave needs to shed energy in the form of additional solitary waves to maintain steady-state propagation in the shallower water, though this is the first example known in a super-critical wave wake model test. A numerical example can be found in

Schaper and Zielke (1984, Fig. 7), reproduced here in *Figure G8* (following), though only for a single solitary wave under depth transition.

Similarly, it is noted in both photographs and the wake traces that the leading crest begins to shed a separate crest at around $y = 3\ m$ and beyond. This is visible in *Figure G5*. Further analysis of this crest shed from the leading wave is illustrated in *Figures G6* and *G7*. *Figure G9* plots the positions of this shed crest against its calculated Havelock wavefront based on a KdV solitary wave celerity, demonstrating that this shed wave is also of a solitary form. *Figure G8* shows one example of a shed crest profile and compares it to the calculated KdV and iBQ solitary wave profiles. The back of the wave conforms perfectly to a KdV profile and the overall profile conformity in general is very good, considering the experimental nature of the wave.

Benjamin and Lighthill (1954) make the comment that weak undular bores evolve into a train of sinusoidal waves and strong undular bores evolve into a train of solitary waves. Grimshaw (2011) confirms this, adding that the effects become pronounced as $t \to \infty$. The transformed solitary wave, and hence trailing bore, may be considered to have transformed from a weaker to a stronger bore in the very shallow water, which ultimately was the aim of the experiment. That may be a reason for the formation of the turbulent wake of the leading crest, though this could only be confirmed with more extreme transformation examples.
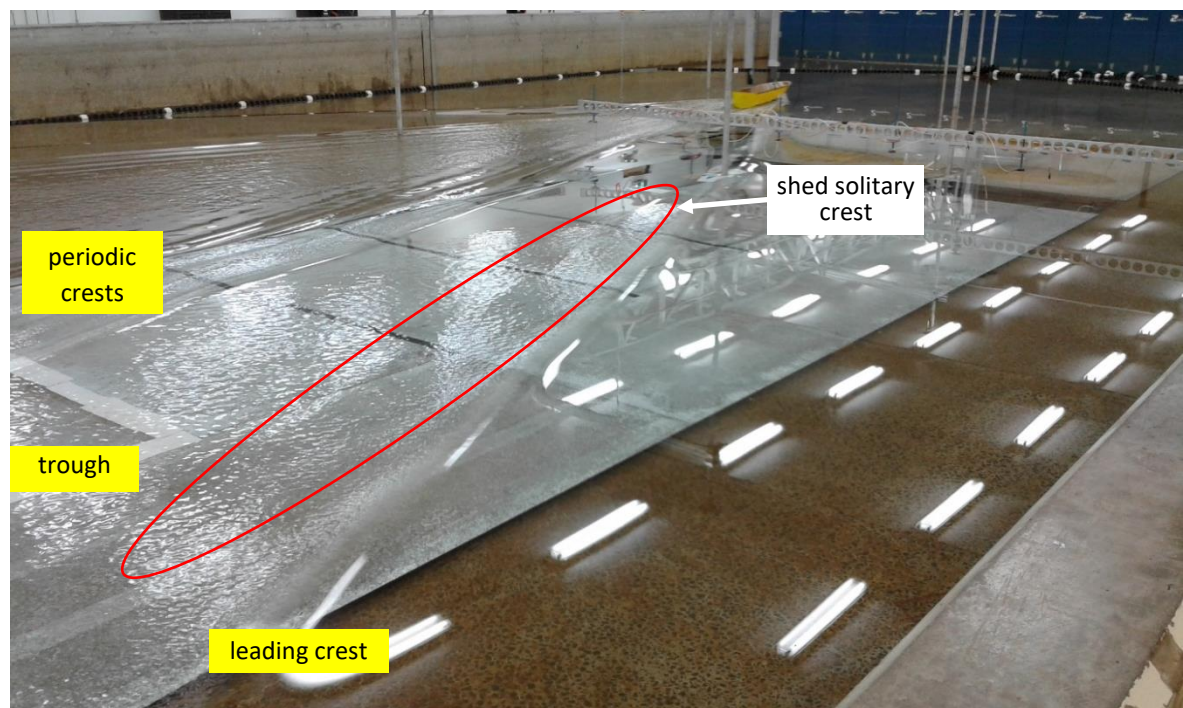


**Figure G5** – *Test at 3.25 m/s. The very shallow section (silver colour) extended just beyond the measurement area but was later widened to study the leading crest propagation. It is possible to see the small solitary crest shed by the leading solitary crest (more readily visible at larger scale). There is also turbulence evident in the trough after the leading crest but commencing only about 1.0 m after the depth transition. Before this trough turbulence, the trough is glassy. Note also the leading crest/following crests in the background at a constant depth on the opposite side of the sailing line (top of photo).*
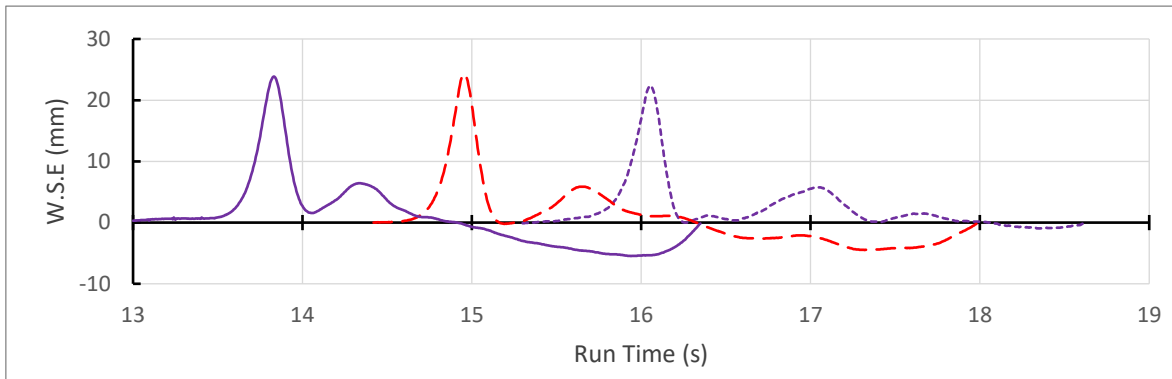
**Figure G6** – *Leading crest and trailing trough at a model speed of 3.0 m/s,  $h = 48$  mm, for the 4, 5 and 6 m probes. The 6 m trace has been truncated slightly due to basin wall reflections. Note the formation of a smaller crest after the leading crest (visible in photographs) and the stable amplitude of the first shed crest at around 7 mm. The first trough after the leading crest does not dip below the still water level, suggesting that the leading crest is a solitary wave in the process of disassociating itself from the rest of the wake.*
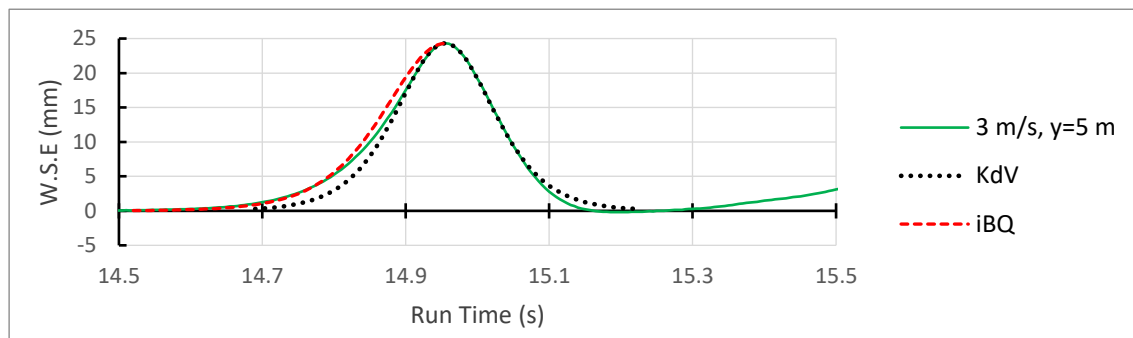


**Figure G7** – *Solitary wave profiles, comparing calculated values to experimentally measured values. The leading face of the first crest is best approximated by the fuller form of the iBQ profile. The back of the first crest is best approximated by a KdV profile, which has a slightly slimmer form. The back of the crest is associated with trailing periodic waves and so the wave function is expected to have a KdV form, with the wave function decaying as it trails from the leading solitary wave at its head.*
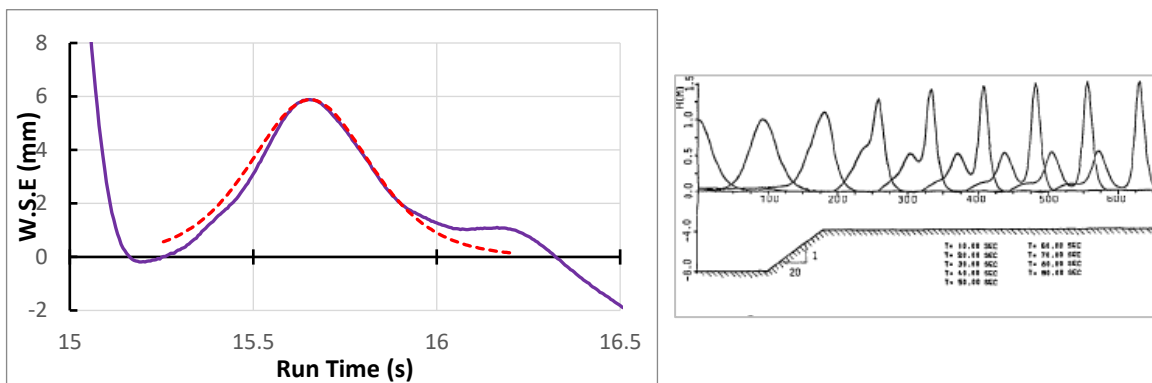


**Figure G8** – ***Left:*** *Shed solitary wave shown at the  $y = 5$  m probe of Figure G6 (propagation right to left). The fitted form (dashed red line) is a KdV profile (an iBQ profile would be fuller). The fit is quite reasonable, considering the experimental derivation of the wave form, with a particularly good fit on the back of the wave.* ***Right:*** *Schaper and Zielke (1984), Fig. 7 (propagation left to right), showing a numerical simulation of a solitary crest shedding over a step, but from a single solitary wave without trailing waves.*

## G.4    Number of Solitary Waves After Transformation

Taylor (2016) presents a review of simplified methods to calculate the number of solitary crests after transformation as a function of the ratio of depth change. The ratio in these experiments was *48:100* (*0.48*). The predicted outcome is "*two large solitary waves are produced with a much smaller third one and some very small trailing oscillations*" (Taylor, 2016).

The experiments here are an almost perfect *1:10* scale of Fig. 5 of Taylor (from Orszaghova *et al.*, 2012, Fig. 8), except for the slope of the transition. The *6 m* result of **Figure G6** may confirm three waves, though the height of the second crest is *30%* lower than predicted. Also, the three waves are clearly evident, even though the transformation distance is only about $80h_1$ into the shallow water. Orszaghova *et al.* (Fig. 8) and Schaper and Zielke (1984) (Fig. 7, Figure G8 right) at a similar position show the second and third crests to not have fully detached from each other; only separating at about twice the experimental distance here. That seems peculiar; the *perfect* conditions of a numerical analysis would be expected to yield the fastest and cleanest transformation. In comparison, experimental results, and those where the leading solitary crest was not crested in isolation, would be expected to take longer to reach a steady-state outcome.
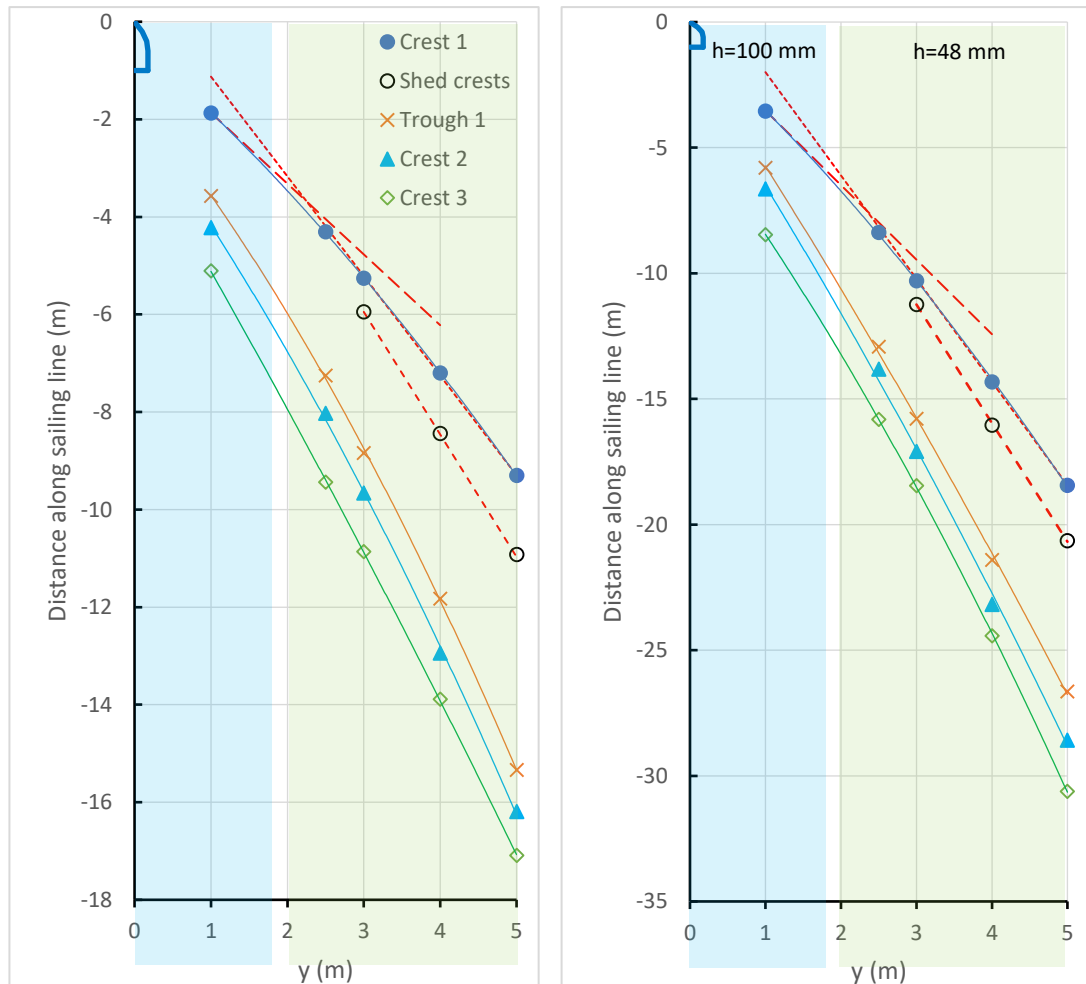


**Figure G9** – *Wave features for two depth super-critical wakes propagating into very shallow water: **Left** – 2.0 m/s; **Right** – 3.5 m/s. The depth varies according to Figure G1. The Havelock wavefronts at the 100 mm depth (value at $y = 1\ m$) and 48 mm depth (value at $y = 4\ m$), based on the respective KdV solitary wave celerities, as well as those of the shed solitary crest, are shown as dashed lines. The leading crests and shed crests conform perfectly to the calculated celerities for solitary waves. The figures are not to scale.*
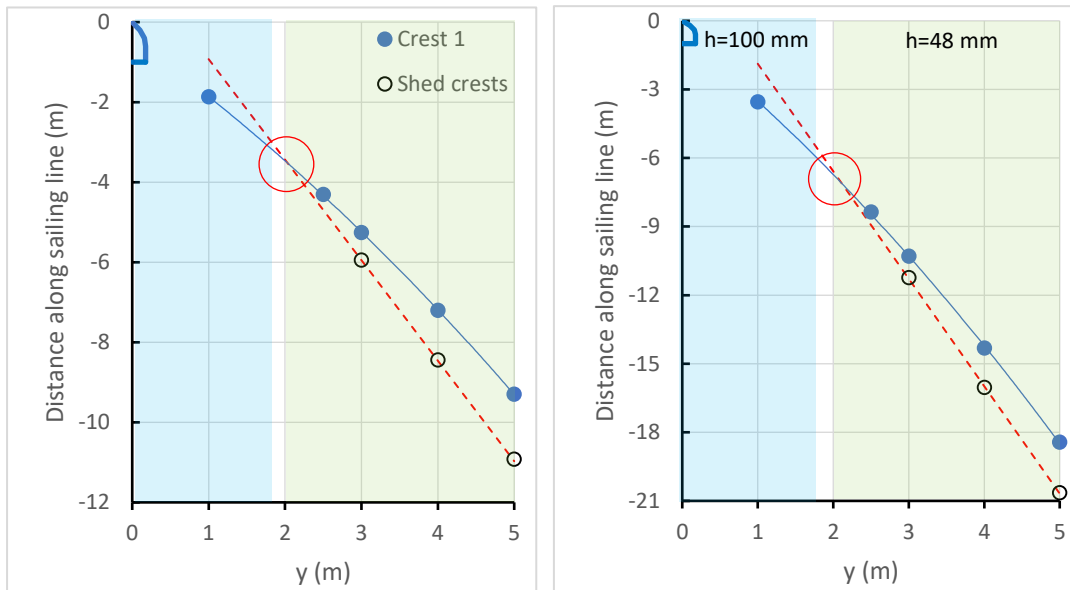
**Figure G10** – *Detail from Figure G9, showing the intersection of the line of the leading crest with the projected Havelock wavefront of the small shed crest (based on a KdV solitary wave celerity) at the beginning of the very shallow water ($h = 48\ mm\ at\ y = 2\ m$): **Left** – 2.0 m/s; **Right** – 3.5 m/s. The depth varies according to Figure G1. This demonstrates that the leading solitary crest must shed additional solitary crests as part of its stabilising transformation into shallower water. The figures are not to scale.*

## G.5 Detachment (Decoupling) of the Leading Crest

Possibly the most controversial aspect of the experiments was to understand if it was possible for the leading crest to transform fully into a solitary wave, disassociate itself from the rest of the wake, and propagate independently – controversial in that it appears never to have been reported before in the context of wave wake. At first glance it would not be thought possible, since all wake waves were formed by the same source and could be considered as components of a broader, propagating wave function.

Solitary waves are known to have properties that differentiate them from periodic waves, but they are consistently referred to as one of the end conditions of the KdV equations as $m \rightarrow 1$, the other being sinusoidal waves as $m \rightarrow 0$.[142] It may be more appropriate to consider solitary waves as being more than simply an end state; a better analogy being the boiling of water, with latent heat leading to a change of phase without a change of temperature. In this case, '$m$' is the somewhat analogous to the change in temperature, but it doesn't explain the change of state that would allow the solitary wave to disassociate and escape from the wave function that describes its generation.

Under certain conditions, numerical examples have demonstrated the ability for the flow over an obstruction to generate detached solitary waves upstream and detached undular flows downstream. Grimshaw *et al.* (2009) gives examples of this in two cases over a hole at critical and super-critical conditions (criticality parameter $\Delta = 0$; $\Delta > 0$) (Grimshaw *et al.*, 2009, Fig. 2 and

---

[142] With 'm' being the modulus of the Jacobi elliptic function, which reflects the degree of shallowness relative to the wave parameters and how that shapes the wave profile.

Fig. 4, with Fig. 4 reproduced here as Figure G11).[143] Super-critical flow over a step also exhibits a similar feature (Grimshaw *et al.*, 2007, Fig. 3(b)), as well as non-constant periods in the undular bore.
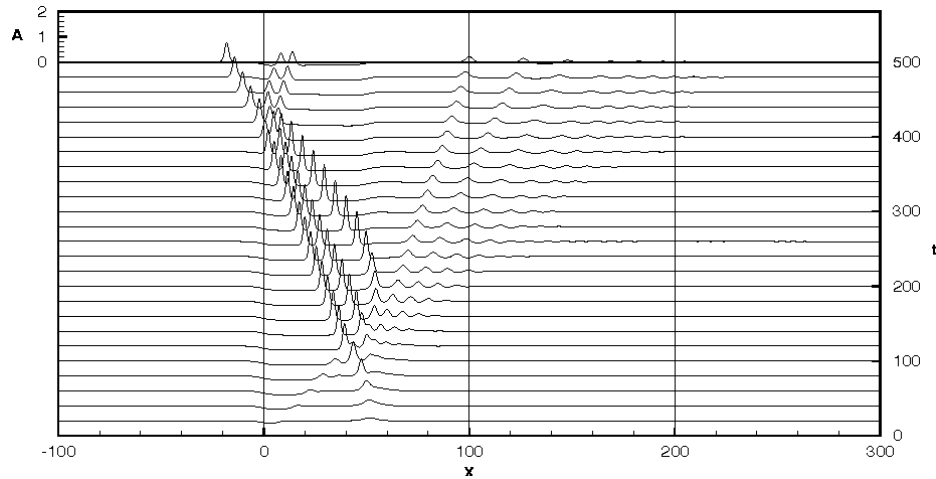


**Figure G11** – *Reproduced from Grimshaw et al. (2009), Fig. 4. The x-axis represents spatial location and the y=axis represents time. Simulations are at 20 s intervals. The hole is 50 units long, positioned at $0 \leq x \leq 50$. The criticality parameter, $\Delta$ (= $Fr_h - 1$), is positive, indicating a flow speed $> \sqrt{gh}$.*

To test for this, an additional wave probe was positioned at $y = 6\,m$ (~$6L$). If the leading wave were to move away, it must do so as a singular crest and without forming any appreciable following trough. Limitations on the basin width meant that only the first few seconds could be captured after the leading crest passed the last probe before basin wall reflections contaminated the trace.

*Figure G6* shows that the first trough following the leading crest never dips below the still water level as it propagates out (within the limits of experimental error), providing some evidence that the leading crest can disassociate itself from the rest of the wake and propagate freely. This is not wholly dissimilar to the shedding of the residual periodic tail after the collision of two solitary waves in water, with the tail shed completely (Craig *et al.*, 2006). Further examples of detached solitary waves can be found in Appendix F.

Although this would only happen under extreme conditions, it may have relevance to the shoaling of large ferry wakes in shallow coastal waters. Not only would a leading solitary wave contain most of the wake energy, it would travel increasingly faster than the rest of the wake in shoal water and arrive without warning, thereby satisfying the observations of Doyle *et al.* (2001).

---

[143] Note that most of the figures in Grimshaw *et al*. (2009) are incorrectly captioned with hole length $L = 100$, which relates only to their Fig. 3. The rest are clearly at $L = 50$ according to the wave patterns and text.

# Appendix H – Wave Propagation from Shallow to Deep Water

## H.1     Introduction

The shallow-to-deep experiments were designed to test the composition of the first shallow water wave. If the wave was not a single wave but a packet of waves speed constrained by the depth, removing the speed constraint would allow the wave to decompose into component waves that would disperse normally. That was achieved by generating the waves in shallow water and allowing them to propagate into deep water where they would be fully dispersive.

Model test basin constraints limited the lateral separation that could be achieved. It was not possible to have a gently sloping transition from the shallow to deep sections, so an abrupt transition was arranged. It was recognised that there may be losses due to reflection at the step, but previous experiments propagating waves from deep to shallow over abrupt and sloped transitions suggested that losses at the step were not substantial. The experiments were intended to be qualitative more than quantitative – the fact that there may be losses should not change materially how the waves transform.

*Figure H1* shows a schematic of the experimental arrangement. Two shallow depths were tested ($h = 0.1\ m$; $h = 0.15\ m$); achieved by adjusting the basin water depth rather than adjusting the structure forming the shallow water area. The transition was positioned at *1.5 m* abreast of the sailing line to allow adequate time for the shallow water wave wake to form and for comparison with previous experiments in a shallow condition without the step (closest probe at $y = 1\ m$). The model used (AMC 00-01) afforded the greatest lateral separation relative to model length, least depth effect in the deep section, and had a form and slenderness ratio typical of small recreational craft.
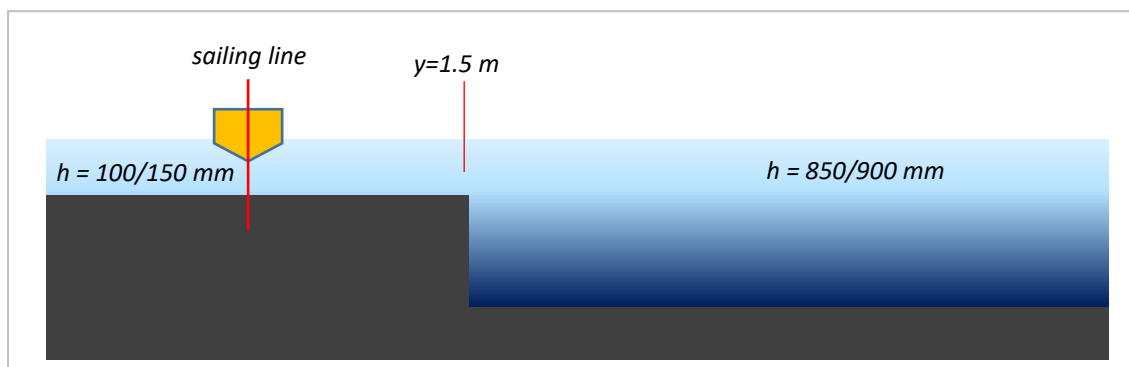


**Figure H1** – *Schematic of the experimental setup. Two shallow depths were tested (100 mm and 150 mm). The depth change was achieved by changing the basin water level, hence the depth variation in the deep section. The abrupt transition was fitted with a vertical seal.*

The shallow water wake was compared with previous full-width, shallow water tests and the results are equivalent. Once the wake moved into deep water, the first wave quickly decomposed into a packet with a deep-water form as the wave components of the first shallow water wave became substantially more dispersive. *Figure H2* demonstrates this. Also, the first large, trailing wave was identified (Figure H2 – circled red). Tracking its time as it propagated (taken as the

median zero crossing at each wave probe) displayed an almost perfect linear relationship, as shown in **Figure H3**. The wave had an average period of *0.59 s*, which would give $\lambda \sim 0.52\ m$ at $h = 0.15\ m$. That would make this wave as close enough to *practically deep* in the *0.15 m* shallow water section ($\lambda/h = 3.47$), so it would not be materially depth affected or undergo refraction across the depth transition. Its propagation would hold consistent over moderate distances. The same model in a fully deep condition at the same speed has a maximum wave with period slightly longer at *0.65 s*.
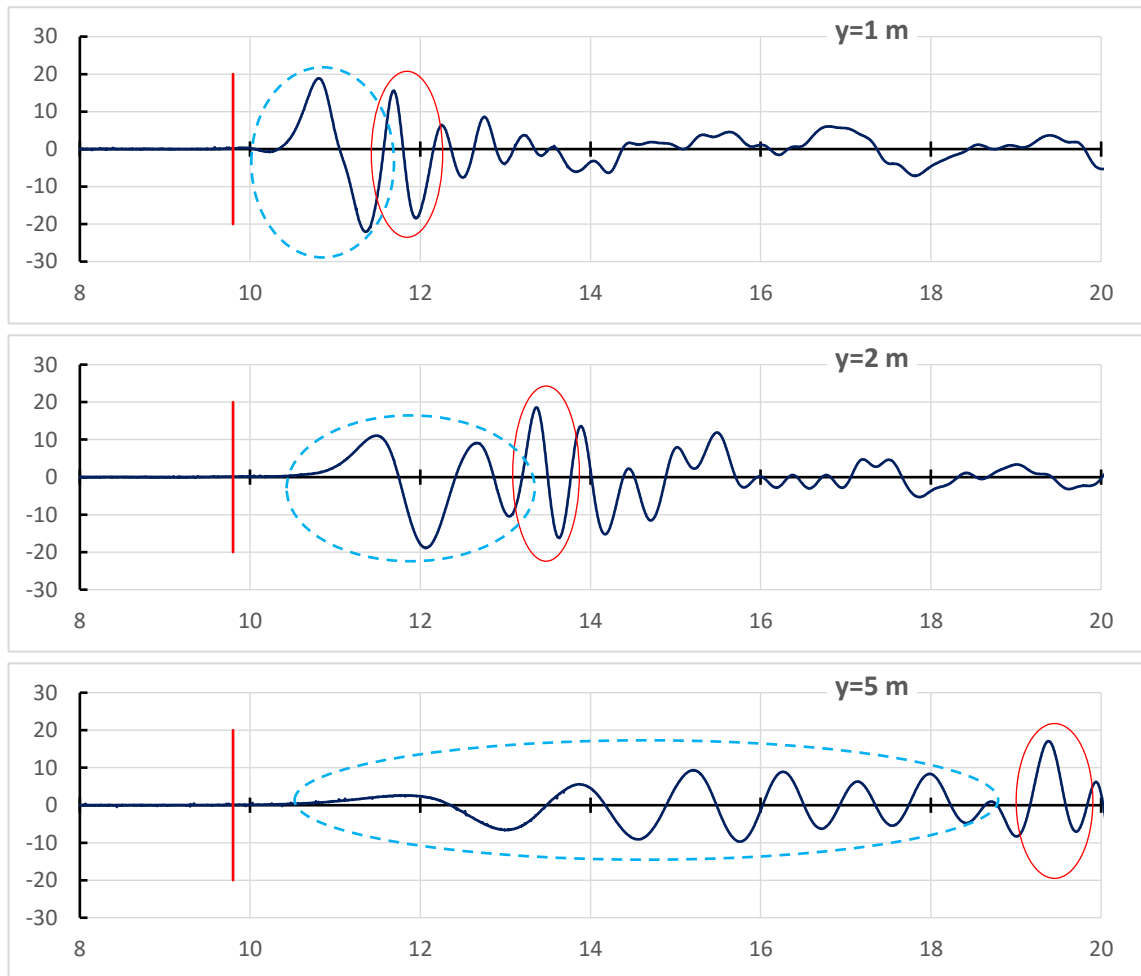


**Figure H2** – *Traces for $V = 2.75\ m/s$; $Fr_h = 2.27$ – shallow (150 mm) to deep (900 mm). The elevation is in mm and the run time is in seconds. The 1 m probe (top) is in shallow water and shows the expected undular bore form. The 2 m probe (centre) is the first deep water probe (transition at 1.5 m) and shows the first wave beginning to decompose. The 5 m probe (bottom) is the furthest deep-water probe and shows that the first wave has decomposed into a deep-water packet form, with envelope evident around 10 s to 19 s. The bow crossing is marked at 9.8 s. The decomposing first shallow water wave is circled by the dashed blue line and the first of the more dispersive trailing waves is circled in red.*

**Figure H3** – *Time of the first trailing wave (circled red, Figure H2) in shallow water relative to the sailing line ($t = 0$), taken as the median zero crossing point. The wave has an average period of approximately 0.59 s, which would make it practically unaffected by depth in both the shallow and deep areas (celerity and wavelength varies by just 5% in the different depths as a Stokes $3^{rd}$ order wave). Refraction would be minimal. It is quite likely that this wave represents the deep-water maximum wave. The maximum wave is the only fully dispersive wave that can be tracked as it propagates due to its innate relationship with the packet envelope.*
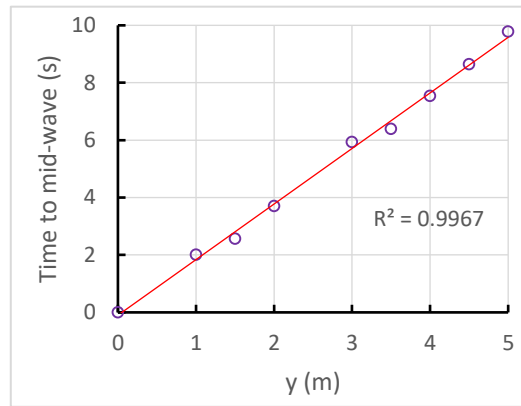


**Figure H4** shows the Fourier analysis for the decomposing first wave of **Figure H2** (within the dashed blue line), and **Table H1** shows the relative energy levels (as a function of area under the curves) and median frequencies. With allowances for energy losses due to reflections as the waves pass over the depth transition and the simple numerical analysis used to determine the area under the curve (Reimann midpoint method), the relative power and median frequency are maintained with lateral separation.



**Figure H4** – *Fourier analysis of the decomposing first packet of Figure H2 (dashed blue line).*

**Table H1** – *Analysis of Figure H4.*

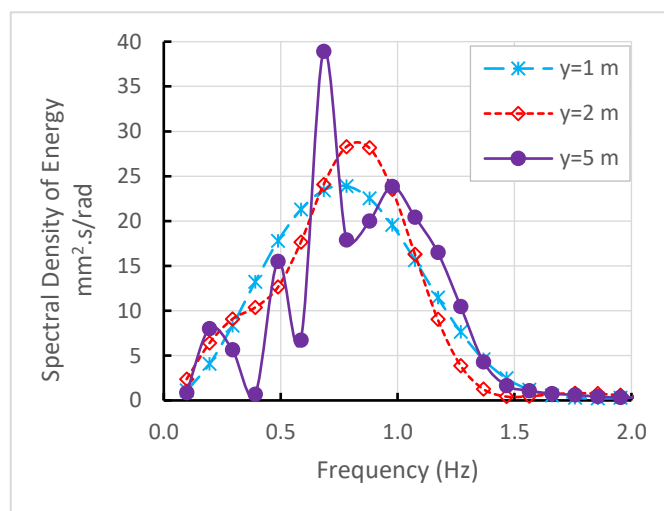|  | y=1 m | y=2 m | y=5 m |
|---|---|---|---|
| Area under curve (mm²/rad) | 19.87 | 19.25 | 19.07 |
| Median frequency (Hz) | 0.81 | 0.79 | 0.85 |

## G.2    Relative position of the first crest

From past work on the same model in shallow water of constant depth, the existence of a leading solitary wave component of the first shallow water wave was postulated. Analysis of the shallow-to-deep tests would tend to confirm this.

The celerity of a solitary wave is dependent on the depth of water beneath its crest and is equal to $\sqrt{g(h+H)}$ in a pure (Boussinesq) form or $[1+H/(2h)]\sqrt{gh}$ in a terminally shallow (KdV) form.[144] In very shallow water, the celerity of any solitary wave component would be slightly faster than the periodic wave components with their celerity limited to $\sqrt{gh}$. However, testing at model scale does not allow sufficient lateral separation for the celerity difference to manifest as separate waves, except in extremely shallow water when solitary wave components of a vessel's wake dominate.

In the shallow-to-deep case, any solitary wave component would have the tendency to propagate faster. Ignoring the contribution of crest height to celerity (assuming $H/h$ is small) gives a lower celerity bound of $\sqrt{gh}$; at $h = 0.15\ m$ its celerity would be at least *1.21 m/s* and at $h = 0.90\ m$ its celerity would be *2.97 m/s*, though in the deep case it is most likely that a solitary wave with valid parameters in shallow water could not exist in solitary wave form at the increased depth and would devolve into a periodic wavetrain.

*Figure H5* shows the position of the first crest relative to the sailing line and to the model for two shallow-to-deep conditions. These are analogous to aerial photographs of the first crests. The speeds are all super-critical in the shallow water section, ranging from $1.65 \leq Fr_h \leq 3.09$. As the crests flatten in the far field, the determination of the actual crest maxima increases in uncertainty. To minimise errors, the crest time series in each instance was fitted with a polynomial that (visually) matched the plotted time series data points. From these polynomials the crest maxima were derived, accurate to the nearest sampling unit (*0.005 s*). The relative smoothness of curves in *Figure H5* suggests this approach is at least consistent, if not accurate.

The shallow water crests align very closely with their respective calculated Havelock wavefronts, which is to be expected. However, in deep water the crests form angles with a shallow water form, but having critical speeds of just under *3 m/s*. That would suggest that the leading waves are of a solitary form, or at least propagate as if they were. It is known that the critical speed wake pattern peaks early at about $Fr_h = 0.9$, which in this case would be a model speed about $V = 2.6\ m/s$ in the deep section. This is well reflected in *Figure H5*. At model speeds less depth-critical in the deep section, the first crest begins to catch up to the model; at higher speeds it falls behind.

Keller (1949), as described by Munk (1949) demonstrated that "*the solitary wave represents the extreme case for certain types of periodic waves.*"[145] This implies that they do not need to be of the classical crest-only form for periodic waves to have the same characteristics as solitary waves.

At speeds less than *2.0 m/s* the leading waves displayed a tendency to collapse very quickly once they reached the deeper water. This is the reason why the crests of *Figure H5* commence at *2.0 m/s*, representing the minimum speed at which waves remained stable when propagating from shallow to deep water.

---

[144] As first order approximations, which are valid for $H/h < {\sim}0.5$ where non-linear effects are limited.

[145] These papers were published together and there is a degree of synergy.

313

*Figure H6* shows the time series of several probes at $V = 1.75 \, m/s$, which was the highest speed where the first crest could not be tracked. The bow is marked in red. The *1.5 m* probe represents the last of the shallow water probes. The first crest becomes essentially indeterminate in the deeper water.

Of note is the existence of a small, propagating wave that exists around the bow in shallow water and eventually begins to move ahead of it in deep water.[146] This would be consistent with the trend in *Figure H5* but was not analysed due to the very small wave height and increased risk of error. However, it is clearly evident in *Figure H7*, with the water surface elevation magnified for clarity. Not only does the wave appear to be moving faster than the model in the far field (and deep water), it appears to be maintaining its height with lateral separation.

It has been suggested that this small wave may be a transient feature caused by the model acceleration, but that does not correlate with what is shown in *Figure H5*, where the height of the first crest is substantial at higher speeds and exhibits a similar trend. It is suggested that this wave would exist at full scale under the same conditions.
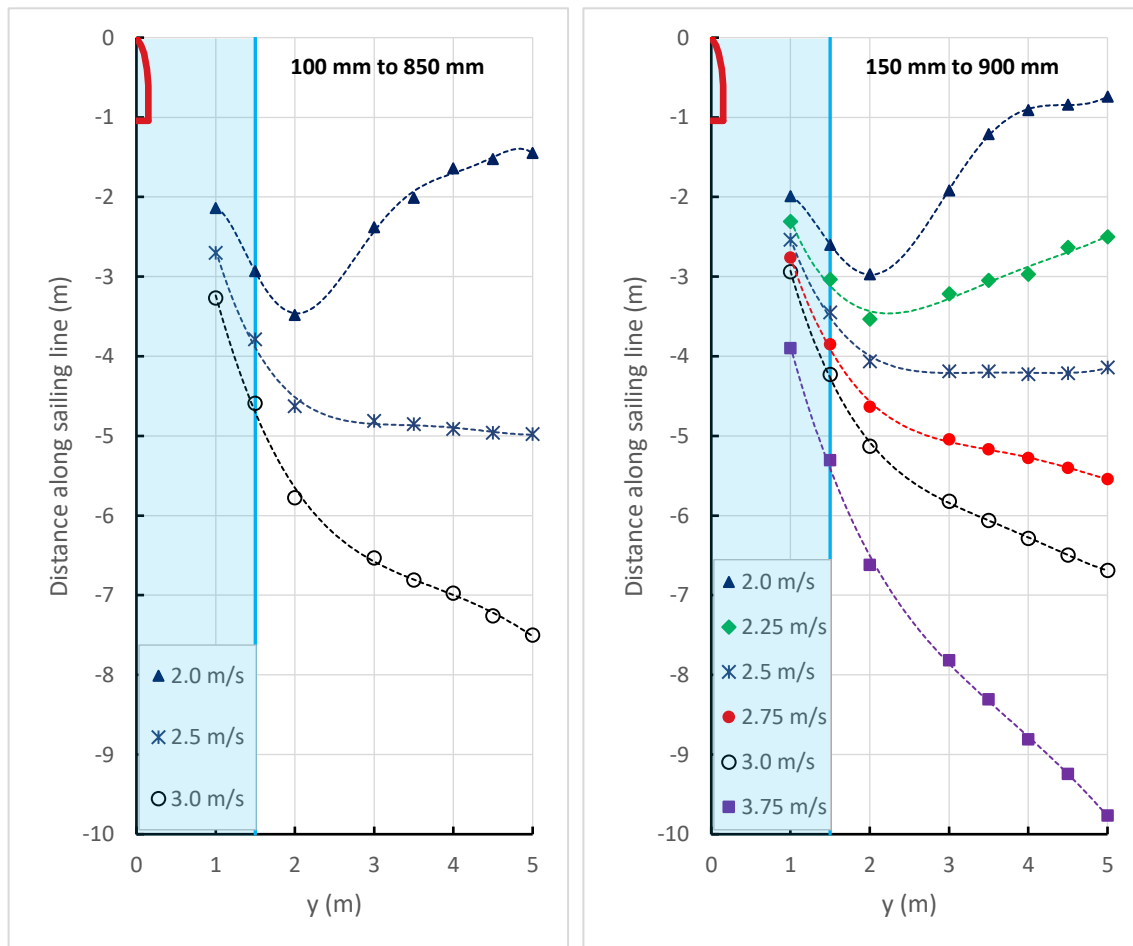


**Figure H5** – *Relative positions of the first wave crest in shallow-to-deep tests. The model is at depth super-critical vessel speeds in the shallow water region, marked in blue. The left figure is at $h = 100mm$ to $850 \, mm$ and the right figure is at $h = 150mm$ to $900 \, mm$. The model is shown, and the figure is to scale.*

---

[146] i.e., not a localised surge/drawdown around the model only.

An alternative explanation for this small crest is the disintegration of a leading solitary component of the shallow water wake. In shallow water, the wake front is headed by a component of the wave function that is fully depth affected and therefore limited by the water depth. This represents the fully non-dispersive component of the shallow water wake, which is followed by waves with increasing dispersiveness. Once into the deep water, the solitary components move ahead at its increased celerity but at the same time loses strength and dissipates (in essence a hysteresis effect). That would also explain the convex pattern of the first crest in the far field, as the leading solitary component both slows and disintegrates in the deeper water (*Figure H5*, *2 m/s* as an example).

One further feature of the shallow-to-deep tests was the reverse of that observed in deep-to shallow tests. Once the leading waves enter the deep water and become fully dispersive, they appear able to cycle energy back through the wave wake at an increasing rate (Davis, 2018). In the depth constrained shallow water, where dispersion is weak, the cycling of energy through the packet is much slower. The trailing waves still in the shallow water tended to increase in height by as much as *20%* compared to the equivalent constant depth test condition, once the leading waves were in the deep water. That also suggests that reflections on the abrupt depth change are minimal. This height variation has implications for wave wake measurement and the positioning of wave probes.
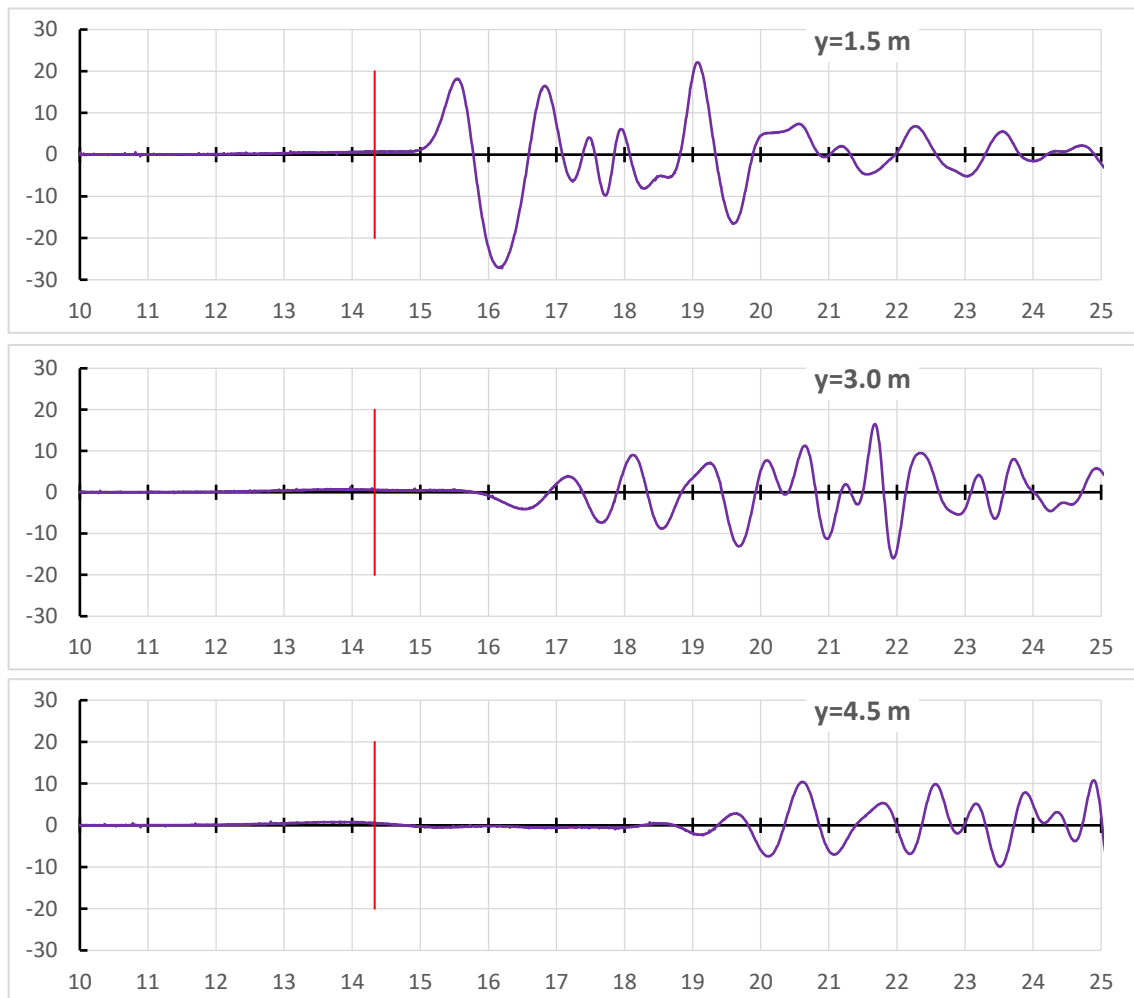
**Figure H6** – *Wave traces at $V = 1.75 \ m/s$ at three lateral separations: 1.5 m (shallow); 3.0 m (deep); 4.5 m (deep). Water surface elevation is in mm and the run time is in seconds. The bow is marked at 14.33 s. Note how quickly the first large crest collapses once into deeper water – only at speeds of 2.0 m/s and above were the crests determinable in the deep water. Note also the existence of a small crest at the bow position that slowly moves ahead of the model. Wave reflections have not been cropped.*
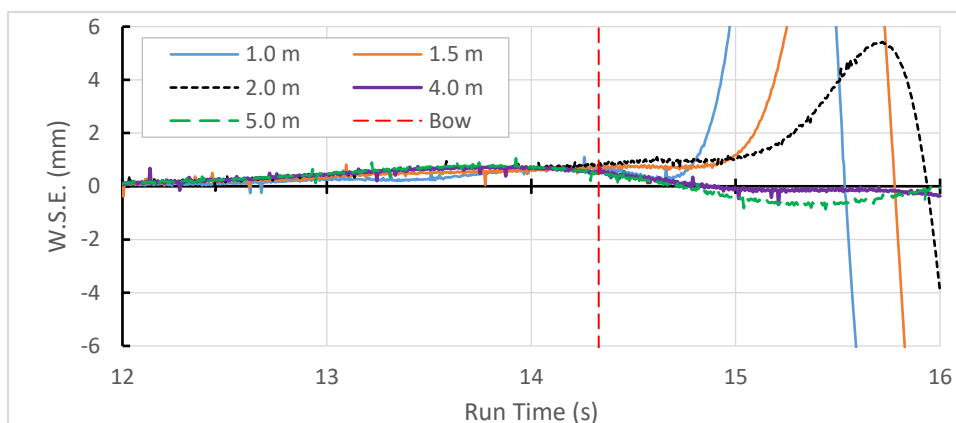


**Figure H7** – *Magnification of traces at $V = 1.75 \ m/s$, with bow position (forward end of static waterline) shown. The dynamic waterline at the bow would move aft about 0.1 s, which is inconsequential to the argument. The small crest appears to be moving out ahead of the model in the far field and does not appear to be reducing in height. At the $y = 5 \ m$ probe the wave is of a periodic form, though there isn't another definite periodic wave until around 18 s run time.*

316

### G.3    Propagation of the first several wave features.

*Figure H8* shows the relative positions of several wave features for $V = 2.75 \ m/s$:

> *Initial Upswelling* – taken as the point where the water surface elevation is *3%* of the height of the first crest, following the proposition by Lighthill (1978). As with the method used to determine the crest maxima in *Figure H5*, a curve of best fit was used to improve accuracy. As a word of caution, *Figure H8* would appear to show the initial upswelling beginning to move ahead of the model, though this may not be exactly representative of reality. The initial upswelling appears to be perpendicular to the sailing line but the first crest decays with lateral separation. Every subsequent *3%* of the decaying local first crest height would move the measured start point further forward (height decays, therefore *3%H* reduces). Regardless, it is clear from close examination that the initial upswelling is at least *perpendicular* to the sailing line.

> *First Wave Crest* – As per the method used in *Figure H5* (fitted parabola to smooth WSE).

> *End of First Wave, Beginning of Second Wave* – waves are considered between either zero up-crossings or down-crossings. The end of the first wave is therefore the zero-crossing point after the first wave cycle. As a zero-crossing point, its position is quite determinate.

> *Second Crest* – as with the first crest but tending to be even more determinate as wave height increases.

> *End of Second Wave* – as per the end of the first wave.

The Havelock wavefront (based on $\sqrt{gh}$) is shown and corresponds closely to the first crest. Also of interest is how the end of first wave asymptotically approaches a tangent line $55^o$ to the sailing line in the far field, which is what would be expected of a far field, deep-water wave wake. *Figure H9* shows a similar plot to *Figure H8*, but at the higher speed of $V = 3.75 \ m/s$. At this speed the position of the first upswelling becomes markedly indeterminate.

317
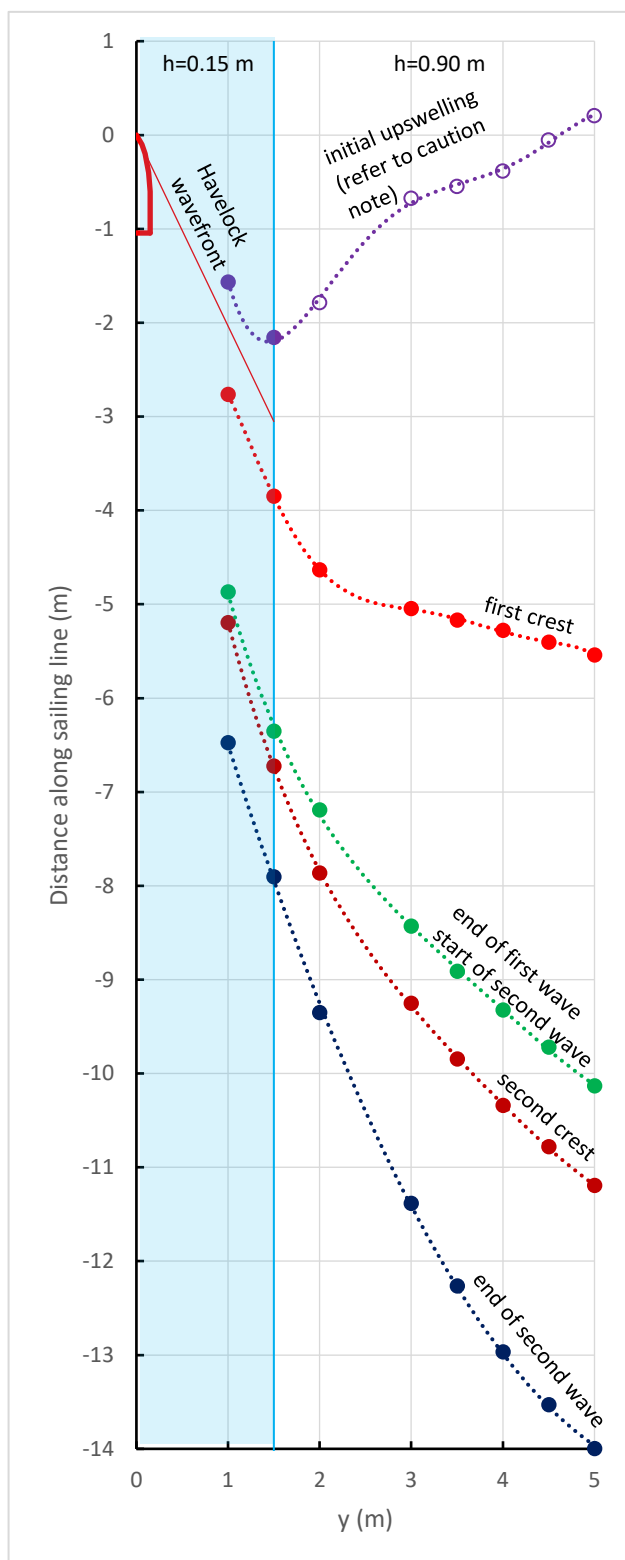
**Figure H8** – *relative positions of several wave features at $V = 2.75\ m/s$. Rapid dispersion becomes evident in the far field. "End of wave" refers to a zero up-crossing.*
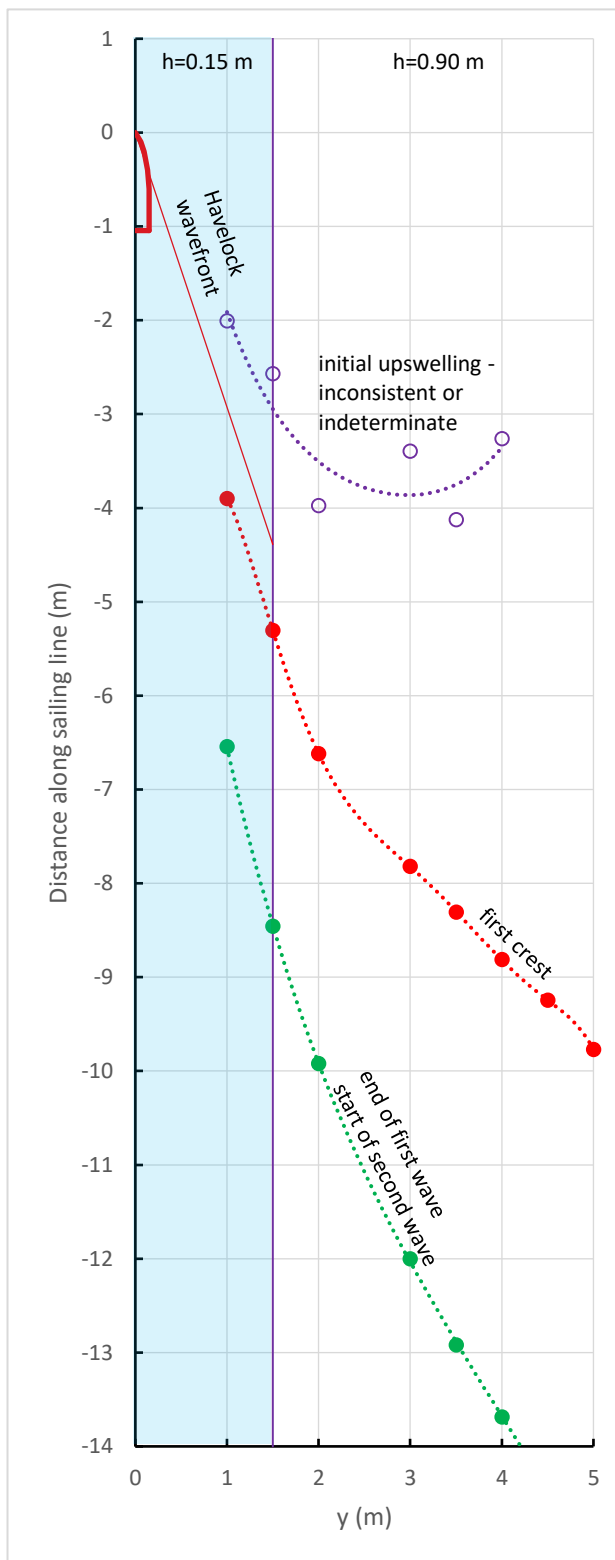
**Figure H9** – *relative positions of several wave features at $V = 3.75\ m/s$. **Caution**: the initial upswelling is very inconsistent in its precise location.*

### G.4    Kelvin Mach Angle in Shallow and Deep Water

The so-called Kelvin Mach Angle, which describes the apparent narrowing of the Kelvin wave angle at high speeds ($Fr_L > \sim 0.573$) in deep water, was plotted and found to be reasonably consistent with the most current theories.[147] The predicted angle of the maximum wave determined using the method of Ma *et al*. (2016) is consistent in the deep-water section, even after propagation from shallow water. The Ma *et al*. (2016) equations for a monohull are delineated into three speed ranges:

$$\psi^M \approx \text{Kelvin Angle} \quad \text{for } Fr_L < \sim 0.573 \tag{H1a}$$

$$\psi^M \approx \arctan\left[0.116/(Fr_L)^2\right] \quad \text{for } 0.573 < Fr_L < 0.85 \tag{H1b}$$

$$\psi^M \approx \arctan\left[0.08(1 + 0.6/Fr_L)/Fr_L\right] \text{ for } Fr_L \geq 0.85 \tag{H1c}$$

However, it is not consistent in constant shallow depths, even though the authors claim it would be. It falls apart in very shallow water when the first wave becomes dominant in height, at around $h/L < \sim 0.15$. ***Figure H10*** shows the position of the highest waves at three speeds; *2.0 m/s* using [H1b], and *2.75 m/s* and *3.75 m/s* using [H1c]. At the slower speeds two distinct packets could be tracked. At *3.75 m/s* only one packet was evident.

There is slight misrepresentation of this contraction, as noted by Darmon *et al*. (2014). The Kelvin wedge does retain a constant angle at all speeds, but the wedge of waves of maximum height contracts away from the Kelvin wedge with increasing $Fr_L$.

---

[147] The deep-water limit proposed by Ma *et al*. (2016) of $Fr_L = \sim 0.573$, below which the Kelvin angle is constant, corresponds to the nominal condition at which the transverse wavelength equals twice the water depth ($Fr_h = \sqrt{\pi^{-1}} = 0.564$).

**Figure H10** – *Predicted incidence of the highest divergent wave peaks at high length Froude numbers for three shallow-to-deep tests (150 mm to 900 mm, shallow in blue). There is reasonable correlation in this deep water condition (ignoring lateral offset), but not at constant shallow depths where the first wave dominates.*
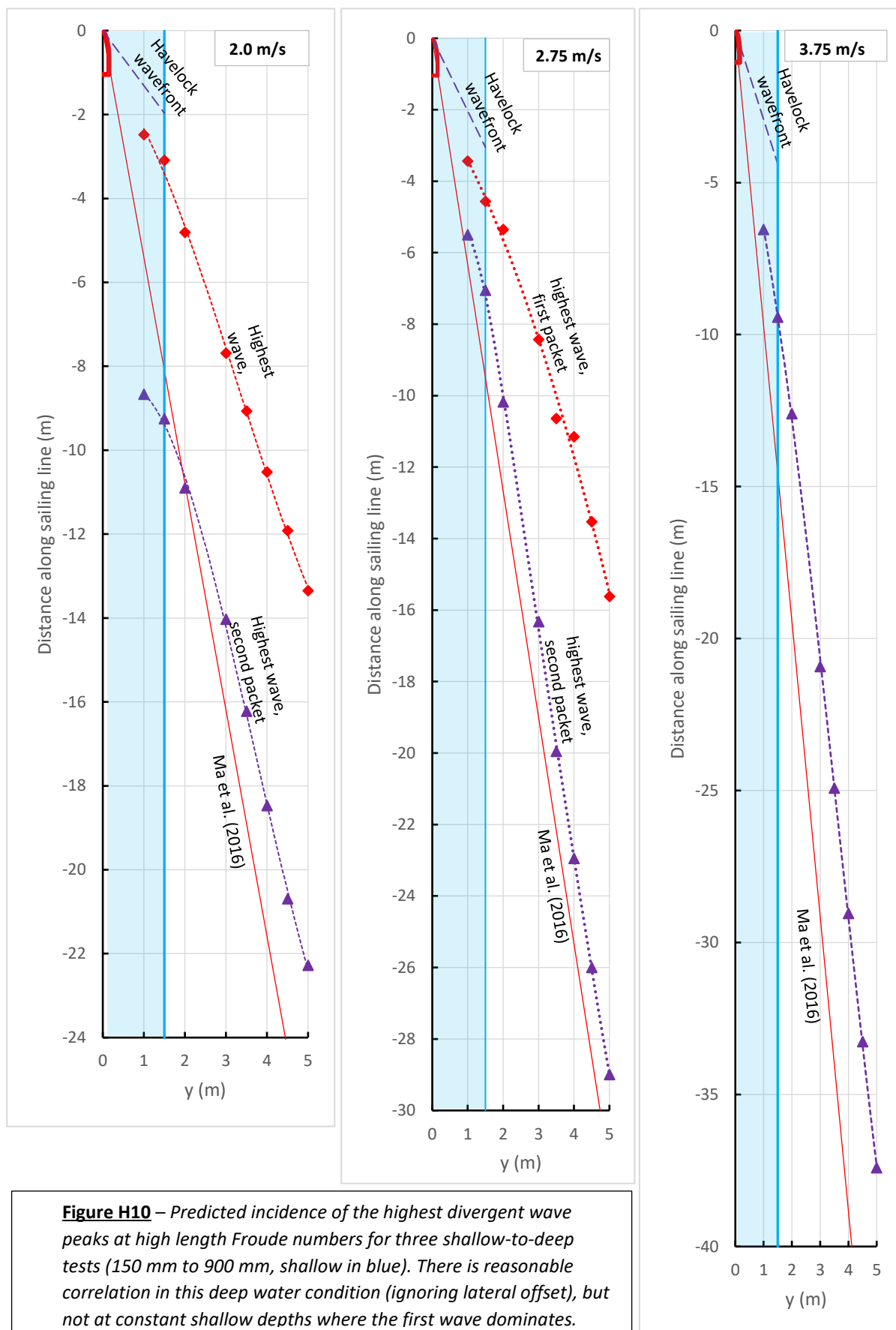
# Appendix J – Gordon River Analysis: Correlation Between Bed Shear Stress and Turbidity

## J.1    Introduction

In order to develop a method of determining the erosion potential of a wave wake, any new measure must be validated against existing measures. There would be little point continuing further with bed shear stress analysis that produced a robust response within itself but was unverified or less responsive in the real world.

The problem becomes one of relating erosion to vessel wake waves and not just waves in general. *Figure J1* shows schematically how a vessel's wake is linked to erosion.
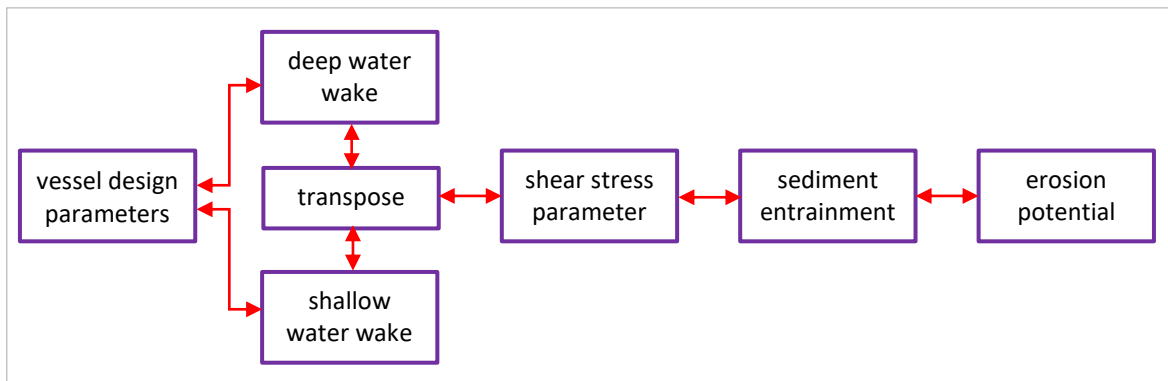


**Figure J1** – *Schematic of the development and inter-relation between elements linking vessels to the wake created and the measure of their erosive potential. The process must be reversible if operational restrictions are to be assessed for new routes.*

The data available is in terms of two sets of parameters – the vessel wave wake, characterised by the height and period of the highest wave in deep water, and the recorded turbidity at mid depth in *0.5 m* of water. Section 8 introduced the parameter *S'*, which is the quotient of actual bed shear stress and threshold bed shear stress, indicating the amount of excess shear stress at the bed in terms of multiples of the threshold value. It also introduced the parameter $A_{nett}$, which is the integration of the excess shear stress values beneath a shoaling wave from threshold ($S' = 1$) through to breaking.

The Gordon River turbidity data, having been recorded at one depth only, cannot directly validate the $A_{nett}$ parameter. That would require turbidity records at several depths from initiation of turbidity through to breaking. All that could be verified with the data available is the relationship between the excess shear stress, *S'*, and turbidity. It is postulated that any relationship at the measurement depth of *0.5 m* would be consistent at any depth. A similar (though poorly controlled and documented) series of experiments reported by Ozeren *et al.*, (2016) concluded that:

> *The measurements showed that the measured turbidity near the shore increased with increasing boat speed. At planning [sic] speeds, even though the maximum wave height is lower than the critical value, the measured turbidity increased. Previous laboratory*

321

*experiments with the same instruments in mixtures of water and silty sediments at various concentrations showed that there is a linear relation between the turbidity level and suspended sediment concentration.*

There are three statements that are pertinent here. The first two are completely erroneous - that turbidity near the shore increased with increasing vessel speed and turbidity increased with increasing wave height (Ozeren *et al.*, 2016, Fig. 8). Unfortunately, their statements are not supported by their published *Fig. 8*, which is divided into two parts – *wave height against turbidity* and *wave height against vessel speed*. Merging the two, there is a clear increase in turbidity and wave height with increasing vessel speed, then a gradual decrease. ***Figure J2*** is a re-construction of the data presented by Ozeren *et al*. (2016).
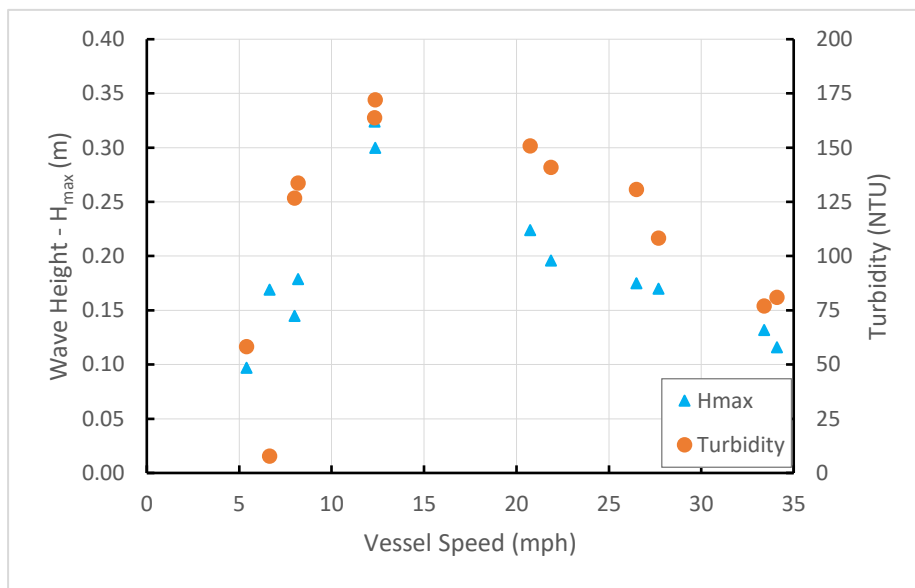


**Figure J2** – *Re-construction of data published by Ozeren et al. (2016), Fig.8, which does not support their claim that turbidity increased with increasing vessel speed. Turbidity peaks at the approximate speeds predicted for depth effects ($Fr_h = 1.0$ at $V = 12.1$ mph) and increased dynamic planing effects ($Fr_{\overline{v}} = 1.75$ at $V = 13.4$ mph). Above this, turbidity clearly decreased with increasing speed, as did wave height.*

It must be noted that wave period, in the context of its importance to turbidity and erosion, was mentioned once by Ozeren *et al*. (2016), who claimed it was measured but then neglected to report or discuss it further.

***Figure J2*** implies immediately that turbidity is almost directly related to wave height, though that is only part of the story. Turbidity was measured at only one location. What is not evident is how wave period would have increased the depth to which turbidity was generated. Also, the turbidity was recorded after the passing of all waves in the wake, but the turbidity was characterised in the standard manner by only a single wave – the highest wave.

The third point made by Ozeren *et al*. (2016) was that there may be a linear relationship between turbidity levels and concentrations of suspended sediment. This is an important assumption in the attempt to link sediment entrainment to turbidity and turbidity to vessel waves, and hence to vessel parameters. It is unfortunate that the two erroneous conclusions weigh heavily on the potential validity of this statement.

## J.2    Severity of entrainment and its relationship to wave parameters

The parameter *severity of entrainment, S',* or *excess shear stress,* is the selected parameter to characterise the degree of sediment entrainment. It assumes that excess shear stress will entrain sediment and to increasing levels with increasing shear stress excess. Following from **Figure J1**, where *shear stress parameter* and *sediment entrainment* are two separate elements of the process, the link between the two must be developed.

The Gordon River turbidity data was analysed for relationships between principal and composite wave parameters, erosion parameters and measured turbidity (Appendix K). Threshold wave parameters were identified, and only those runs with recorded elevated turbidity of at least *3 NTU* were used for analysis. When *S'* was calculated for each run in the 2004 Gordon River trials, the depth-corrected wave height was applied, and a correction was applied to account for the turbidity sensor being at half depth in *0.5 m* of water and not at the bed.

**Figure J3** demonstrates that there is an intrinsic relationship between wave power and $S'_{0.5}$ (severity of entrainment at $h = 0.5\ m$) that is inherent within the developed method for calculating $S'_{0.5}$. The strength of the goodness of fit for field experiments cannot be explained otherwise. Previous work has demonstrated a close correlation between wave packet characteristics and wave power, but only within a particular packet of waves and not between different packets. Wave power is not discounted as a prime determinant of erosion potential, however its close correlation *within* wave packets but mediocre correlation *between* the packets of different vessels is not the relationship sought for development into an over-arching regulatory approach.
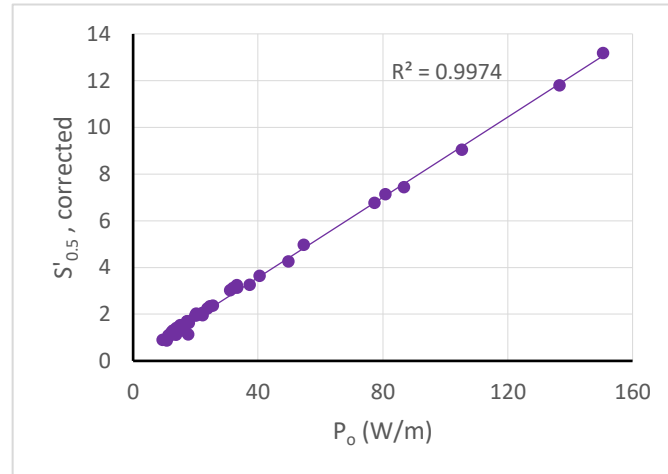


**Figure J3** – *Excess shear stress (S') at $h = 0.5\ m$ against deep water wave power, calculated using the waves recorded in the Gordon River tests. The goodness of fit ($R^2$) value, being nearly unity, implies an intrinsic mathematical relationship between wave power and the severity of entrainment rather than an environmental relationship. The absence of a perfect goodness of fit is most likely due to the wave height corrections from deep to shallow water. It must be remembered that this only links the vessel parameters to the shear stress parameter and not to sediment entrainment itself, so this intrinsic relationship should hold for any wave and not just those measured.*

The principal parameters of wave height and wave period do not exhibit the same intrinsic relationship as the composite parameter of wave power. **Figure J4** shows the relationship between *S'* at *0.5 m* depth and three parameters: $H_o$ (deep water wave height, assumed with

good reason to be at the *4 m* wave probe location); $H_{0.5}$ (deep water wave height transposed to the *0.5 m* turbidity measurement depth according to the relevant wave theory); *T* (period of the maximum wave):

> $H_o$ – a general trend is exhibited, but one that would otherwise have been expected. The scatter can only partly be explained by the nature of the field tests, since the calculation of $S'_{0.5}$ requires just wave height, wave period (or wavelength) and water depth. The only variable from field measurements is the relationship between wave height and period (hence wave steepness), and therefore the interpretation of the maximum wave. Actual correlation between $S'_{0.5}$ and elevated turbidity is not introduced at this point.

> $H_{0.5}$ – of note is the almost straight-line variance of $S'_{0.5}$ with wave height for the highest recorded waves. Smaller waves do not exhibit any better correlation using the deep water or transposed height values, which is expected as the smaller waves generally have shorter periods and are less affected by the water depth.

> *T* – this is most interesting, exhibiting scatter that defies the robust relationship in **Figure J3**. How can the composite parameter of wave power exhibit an intrinsic relationship with $S'_{0.5}$ when one of its principal parameters exhibits almost no relationship? In fact, there is a relationship, but within waves and not necessarily between them. When wave data points of $H_o$ and *T* are paired, it becomes obvious that one tempers the other, such that the composite value of power forms its intrinsic relationship with $S'_{0.5}$. For any particular value of $S'_{0.5}$, waves with a greater height also have a corresponding shorter period and vice versa, such that wave power is maintained as a constant. That also suggests that there is unlikely to be a useful relationship between $S'_{0.5}$ and wave steepness (for a constant $S'$, maintaining a constant power relationship between wave parameters requires an inverse proportionality between $H^2$ and $T$; wave steepness requires inverse proportionality between $H$ and $T^2$).



**Figure J4** – *Severity of entrainment against measured deep-water maximum wave height ($H_o$), transposed maximum wave height at the turbidity measurement depth ($H_{0.5}$) and period of the maximum wave (T) for the Gordon River data. Deep water maximum wave height (left) exhibits a general trend, with the scatter considerably tightened when maximum wave height is corrected to the 0.5 m turbidity recording depth (centre). Period of the maximum wave exhibits considerable scatter.*

## J.3    Elevated Turbidity and its relationship to wave parameters.

Correlation between elevated turbidity and wave parameters from the Gordon River tests has already been discussed in Appendix K, but further specific comments are made. ***Figure J5*** compares elevated turbidity with principal wave parameters. Only runs which recorded an elevated turbidity of at least *3 NTU* are included, being the sensitivity threshold of the equipment used.

Firstly, both wave height parameters $H_o$ and $H_{0.5}$ exhibit very tepid relationships to elevated turbidity, except to say that there are increasing trends, but with wide-ranging bounds. The relatively short wave periods ($\leq 3\ s$) and with waves categorised at *fairly long* at worst ($7 \leq \lambda/h \leq 14$) would not substantially alter wave heights. Secondly, wave period exhibits a tighter trend and with a narrower, more defined threshold base. Overall, these are opposite to those of ***Figure J4***, which relates excess shear stress to principal wave parameters.



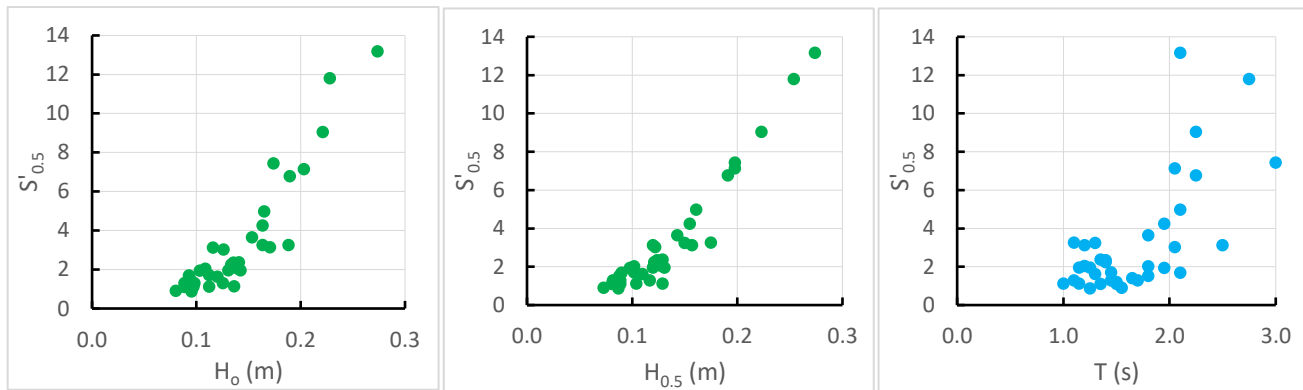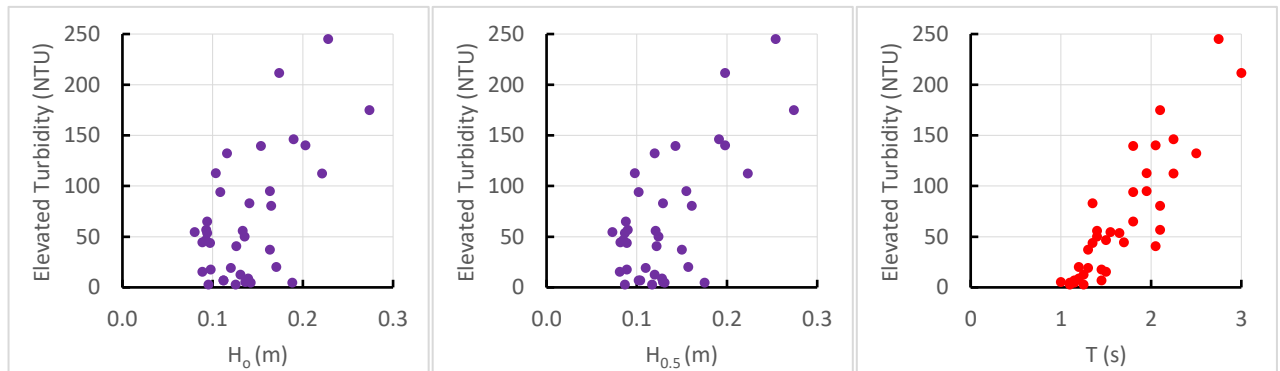**Figure J5** – *Elevated turbidity against measured deep-water maximum wave height (Hₒ), transposed maximum wave height at the turbidity measurement depth (H₀.₅) and period of the maximum wave (T) for the Gordon River data. Both wave height variations exhibit essentially the same widely-bounded trend. Wave period has a more developed trend.*

When comparing principal wave parameters to composite wave parameters, an interesting pattern occurs that may explain casual field observations.[148] ***Figure J6*** shows elevated turbidity against *energy per unit wave height* ($E_o/H_o$) and *energy* ($E_o$), both for the deep-water condition (the un-transposed wave probe readings). Turbidity values are the original mid-depth records. The previously determined threshold values of $E_o/H_o = 260 J/m^2$ and $E_0 = 30 J/m$ are shown. Once sediment entrainment was initiated, at least to the extent where the plume was high enough to initiate a record at half depth, turbidity increased substantially for little additional energy.

The rapid entrainment may be due to turbidity measurements being taken at half depth. It may also be due to the action of the leading waves – those waves that precede the passing of the maximum wave. A threshold amount of energy is necessary to firstly initiate sediment movement at the bed, even though this initial movement may not lead to transient, vertical entrainment. The leading waves energise the sediment and the maximum wave (or group of waves around the

---

[148] Refer also to von Krusenstierna (1990), Fig. 6.2(a), which shows a similar initial, rapid increase in erosion rate with increasing wave power, followed by a slower, steady increase. At higher wave power levels, the erosion rate accelerated again. Wave power is the preferred parameter of some geographers and coastal engineers.

maximum) create the vertical plume. A physical analogy would be the melting and heating of ice – the initial energy input provides the latent heat component without temperature change and subsequent energy input increases temperature.
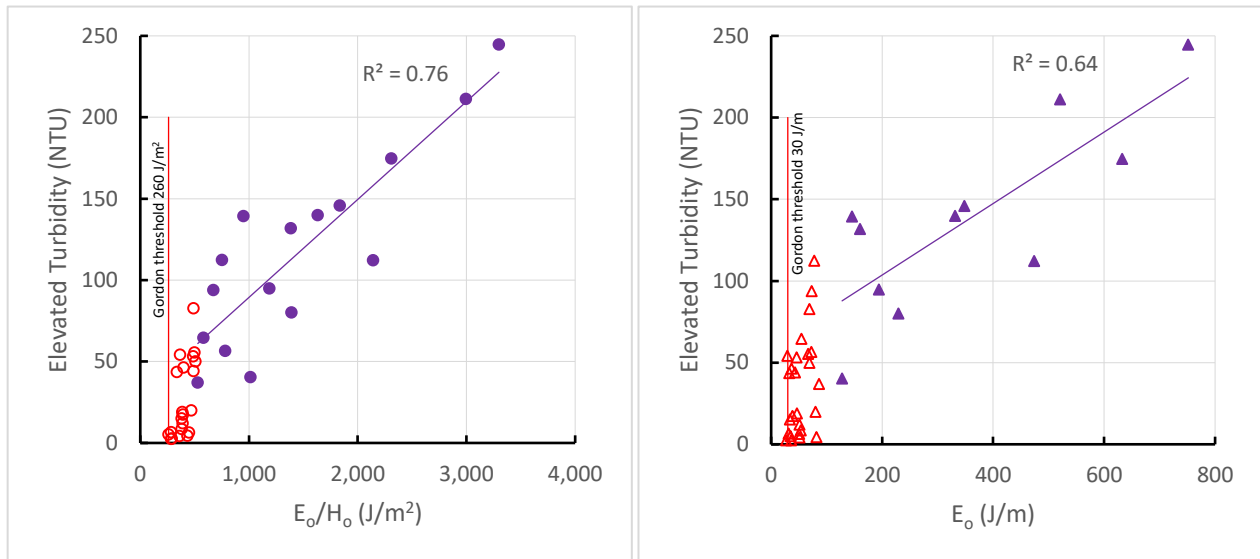


**Figure J6** – *Gordon River results for those tests recording at least 3 NTU elevated turbidity. **Left**: elevated turbidity against energy per unit wave height (deep water), the low energy measurements (hollow, red) covering the range from the turbidity threshold of 260 J/m² up to twice the threshold (520 J/m²). **Right**: elevated turbidity against wave energy (deep water), the initial measurements (hollow red) covering the range from the turbidity threshold of 30 J/m up to thrice the threshold (90 J/m). Note the rapid increase in turbidity for little additional energy, followed by a steady increase once turbid. This correlates with Fig. 6.2(a) of von Krusenstierna (1990).*

**Figure J7** gives a better understanding of the development of *S'* for the waves in a propagating packet. The waves are for the *QG Cowan* and the *Large Ski Boat* (Macfarlane and Cox, 2003), with only full wave numbers (wake trace waves numbered sequentially and commencing with a zero up-crossing) shown. The packet-wise trend is consistent, with a shift in the relative position of the maximum wave according to vessel speed (wave *4 ½* for the slower *Large Ski Boat* at $Fr_L = 0.56$ and wave *6* for the faster *QG Cowan* at $Fr_L = 2.0$). The sailing line lateral offset for the *QG Cowan* and *Large Ski Boat* was *23 m*, more than the *50 m* used on the Gordon River. If a simple (-⅓) wave height decay exponent was applied to the increased lateral offset, the wave heights would reduce by *23%* from *23 m* to *50 m* lateral separation, with a further reduction at *0.5 m* depth due to shoaling of such short period waves. That would reduce the maximum wave $S'_{0.5}$ values from *4.5* at *23 m* lateral separation to *3.07* at *50 m* lateral separation, both vessels having almost identical values. Coincidentally, all the hollow red data markers in **Figure J6**, representing the rapid initiation phase of turbidity, had $S'_{0.5}$ values ranging from *1* to *3.3*, so the depth and distance corrected $S'_{0.5}$ values of all waves in the packets for the *QG Cowan* and *Large Ski Boat* would be within the turbidity initiation region.

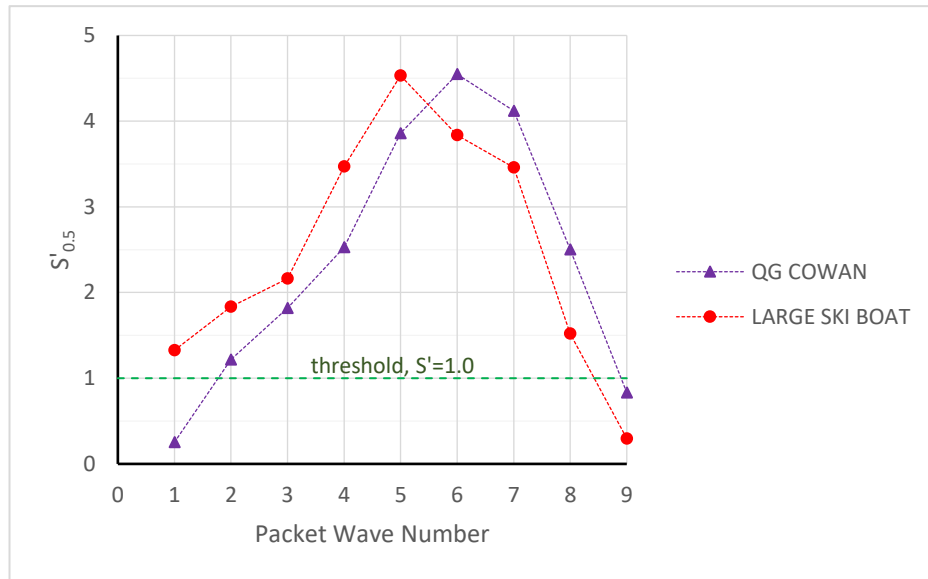**Figure J7** – *Excess shear stress, S'$_{0.5}$, calculated at a water depth of 0.5 m for the packet waves of two vessels – QG Cowan ($L = 6.75\ m, V = 31.88\ kn$) and the Large Ski Boat ($L = 5.3\ m, V = 7.78\ kn$). The sediment is assumed to be unconsolidated sand, with $D = 0.075\ mm$. It is expected that the offset in parameter values for the QG Cowan towards the latter packet waves is due to the higher vessel speed. Data points represent discrete events (individual waves) but are joined for clarity.*

## J.4     The Link between Bed Shear Stress and Sediment Entrainment

To complete the schematic of **Figure J1**, the link between bed shear stress and sediment entrainment must be established. Excess bed shear stress is defined by *S'* and sediment entrainment is defined by elevated turbidity.

**Figure J8** presents the Gordon River data that exhibited active turbidity ($\geq 3\ NTU$) and compares the two deep water composite energy parameters of *energy per unit wave height* and *energy* against two variables – S'$_{0.5}$ (degree of excess bed shear stress at *0.5 m* water depth) and S'$_{0.5}$/NTU (quotient of excess bed shear stress and elevated turbidity).

### S'$_{0.5}$ *and Energy Parameters*

These variables link waves to sediment entrainment potential only. Deep water wave energy has better correlation than energy per unit wave height, though it was shown in Section 8 that the ultimate link between the severity of erosion measure, $A_{nett}$ and vessel wake parameters is the same for *energy* and *energy per unit wave height*. $E_o/H_o$ is preferred because of its demonstrated relationship to wave runup, which is a potential erosion mechanism for low, long-period waves.

Although **Figure J3** shows that wave power has an obvious intrinsic relationship with S'$_{0.5}$, its relationship to S'$_{0.5}$/NTU is poor at low levels of wave power (not shown here).

### Energy Parameters and S'$_{0.5}$/NTU

This is most interesting. By dividing the excess shear stress parameter by the recorded elevated turbidity, the form of any correlation can be determined. From **Figure J8**, and for both energy parameters (*E* and *E/H*), waves right at the derived thresholds (vertical red lines) would have a degree of developed bed shear, but no turbidity at half depth (the

depth of the nephelometer), hence the parameter $S'_{0.5}/NTU$ would be infinite. A modest increase in the energy parameter brings little additional excess shear stress, but enough elevated turbidity to reduce the parameter $S'_{0.5}/NTU$ substantially. After a certain multiple of the energy parameter is reached, in this case about double the *energy per unit wave height* and treble the *energy*, the parameter $S'_{0.5}/NTU$ settles to an approximate constant value. That reflects the results of **Figure J6**, where there was a rapid entrainment of sediment followed by a steady state growth in turbidity. Caution not to overstate the strength of the constancy of the relationship must be applied, given the vertical scale of the parameter $S'_{0.5}/NTU$.
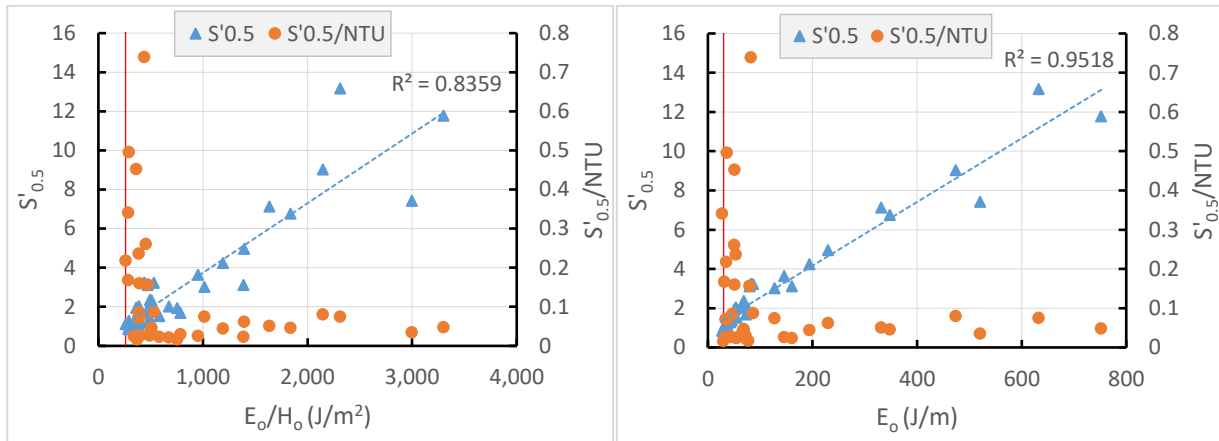


**Figure J8** – *Comparative graphs of S'$_{0.5}$ (excess shear stress) and S'$_{0.5}$/NTU (quotient of excess shear stress and elevated turbidity) for two deep water energy measures – energy per unit wave height (left) and energy (right). The deep-water condition is used as it is simpler to apply. Although energy has a better correlation with excess shear stress, the relationships between both energy measures and the excess shear stress/turbidity parameter are almost identical. The initial rapid growth of turbidity at the inception of excess energy above the relevant threshold, followed by a (relatively) steady state growth, is also evident.*

In summary, **Figure J8** confirms the (relatively) constant relationship between excess bed shear stress and elevated turbidity once the initial, rapid, elevated turbidity growth phase has stabilised. The statement of Ozeren *et al*. (2016), claiming a linear relationship between turbidity level and suspended sediment concentration, would appear to be consistent with the relationship between elevated turbidity and the bed shear stress mechanism initiating it.

# Appendix K – Correlation of the Severity of Erosion Method with the 2004 Gordon River Data

### K.1      Introduction

The Gordon River data from 2004 is the only known local data available where there has been an attempt to record turbidity and vessel wakes in controlled experiments. In the case of those experiments, the application of the proposed method for assessing erosion severity would not necessarily be valid, since turbidity was measured at one shallow water condition (mid-depth in *0.5 m* of water) and this may not reflect the preceding accumulation of bottom stress as a wave shoals.

It also ignores the fact that the wake measured consisted of several waves of varying height and period, yet the erosion severity calculations are for a single wave only. This may not necessarily invalidate the approach, as was found by Bauer *et al*. (2002):

> "*Maximum onshore values of cumulative (sediment) flux were attained within only 4-6 normalised time increments, which indicates that net onshore transport ceased relatively early in the boat-wake event (within about 30 s). Such bank-directed fluxes ordinarily yield sediment accretion in the near-bank region, but this was not the case at the study site. Suspended sediments were flushed out of the system by downstream currents before they had time to settle, and net transport was persistently downstream despite weak onshore tendencies.*"

For the purpose of illustration, eight vessel runs with varying wave parameters were selected for analysis. Their principal parameter values are shown in ***Table K1***. The sediment size is assumed as *0.075 mm*. A ninth wave was also analysed, and the results plotted independently. It was selected due to its lack of conformity in previous assessments; probably the result of experimental error (the recorded turbidity was far above that expected from the wave parameters). Its lack of conformity was confirmed in this analysis.

**Table K1 -** *Selected Gordon River wave parameters assessed.*

| Run | Height (mm) | Period (s) | Turbidity at *h=0.5 m* (NTU) |
|:---:|:---:|:---:|:---:|
| 1 | 174 | 3.0 | 211 |
| 2 | 163 | 1.95 | 95 |
| 3 | 164 | 1.3 | 37 |
| 4 | 221 | 2.25 | 112 |
| 5 | 274 | 2.1 | 175 |
| 6 | 228 | 2.75 | 249 |
| 7 | 126 | 2.05 | 40 |
| 8 | 165 | 2.1 | 80 |
| 9 | 153 | 1.8 | 139 |

The measurement point was in *4 m* water depth and the longest wave period recorded was *3.0 s*. Defining *practically deep* as equivalent to the $h/\lambda > 0.28$ limit proposed by Lighthill (1978) and calculating the deep-water wavelength of a *3 s* period wave to be *14 m*, the longest wave

recorded in the 2004 Gordon River trials just meets the *practically deep* criterion. Height attenuation with distance is also ignored, since the waves were recorded well into the far-field (*50 m* from the sailing line) and the distance between the wave measurement point and turbidity measurement point, though apparently not recorded, was not far according to the photographs taken at the time. This is quite normal for riverine environments, where cross-sections are more "U-like" and depths hold fairly close to the banks.

Although there were *32* individual vessel passes with elevated turbidity readings greater than *5 NTU*, limitations of reasonable time allowed only one-quarter of those to be assessed. Further assessment would only have been undertaken in case of exceptionally good or exceptionally poor correlation. In fact, that was the case with the first three wave conditions, which resulted in a perfect correlation between erosion severity and recorded turbidity and led to the assessment of a further five waves. The perfect correlation was short-lived.


## K.2    Discussion of Results

*Figure K1* is the log-log plot of the area under the $S'$ curve from threshold to $h = 0.5\ m$ against measured elevated turbidity at $h = 0.5\ m$ (measured at half-depth). Both the total area (from $S' = 0$ to $S'_{0.5}$) and nett area (from $S' = 1$ to $S'_{0.5}$) are shown. Of interest is that the total and nett areas exhibit the same goodness of fit. That is to be expected, since the threshold stress with depth is almost constant (refer Section 8, Figure 8.3). The corresponding values for wave 9 are shown as hollow markers.

It is not unreasonable to expect that the severity of erosion measure, $\int S'$, would not be a particularly good indicator of the measured elevated turbidity at one measurement point, as it is intended to be a measure of the accumulation of stress beneath a shoaling wave and not an instantaneous measure. The only proper way to assess this would be to take elevated turbidity measurements at various depths beneath the shoaling wave, as was done in the field trials reported by Bauer *et al*. (2002).

*Figure K2* is a linear graph of elevated turbidity against the deep-water *energy per unit wave height* ($E_o/H_o$). The correlation between the simple measure of $E_o/H_o$ and turbidity is obvious and of importance in developing a simplified but robust methodology for assessing the environmental viability of vessel operations. Also of note is the equation of the line of best fit, which implies a threshold value of $E_o/H_o = 242\ J/m^2$ below which the elevated turbidity will be zero. This compares to a value of $260\ J/m^2$ derived from the full analysis of the Gordon River trials.

*Figure K3* is the same as *Figure K2*, but with elevated turbidity measured against $S'_{0.5}$: the severity of erosion at $h = 0.5\ m$. The relationship is satisfactory but not to the quality of $E_o/H_o$ as an indicator of a wave's potential to instigate sediment movement.
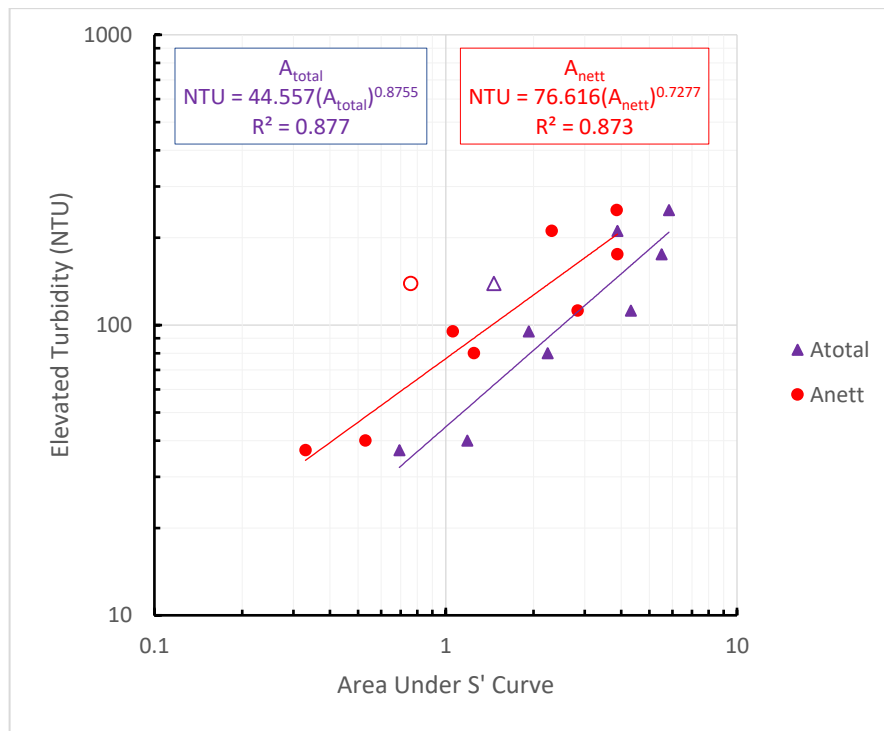
**Figure K1** – *Elevated turbidity as a function of the area under the $S'$ curve for nine waves. Wave 9 is shown with hollow markers but is otherwise excluded from the assessment. The almost identical response using $A_{total}$ and $A_{nett}$ would suggest that any relationship is incidental (as opposed to coincidental). This is further demonstrated in the curves following.*
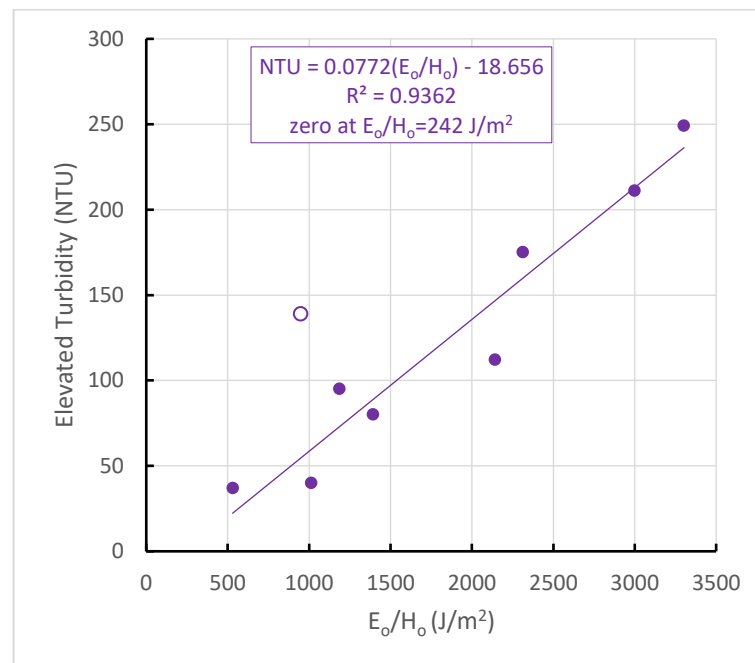


**Figure K2** – *Linear plot of elevated turbidity against $E_o/H_o$ (energy per unit wave height in deep water). The relationship is remarkably good, as expected. The result for wave 9 is shown as a hollow marker but has been excluded from assessment.*

331

Plot showing "NTU = 8.6985(S'_{0.5})^{1.329}, R² = 0.8047" on log-log axes of Elevated Turbidity (NTU) against S'_{0.5}.

**Figure K3** – *Log-log graph of elevated turbidity against severity of erosion at $h = 0.5\,m$. Although there is a trend, the relationship with $E_o/H_o$ in Figure K2 is stronger. The result for wave 9 is shown as a hollow marker but is excluded from the relationship.*

### K.3    Use of Linear Wave Theory

As discussed, linear wave theory remains the most commonly used wave theory due to its comparative simplicity compared to non-linear theories. In the initial development of this severity of sediment entrainment (erosion) methodology, linear wave theory was used to calculate shoaling wave parameters. Although this was then superseded by the use of non-linear theories (but with the shear stress equation of Komar and Miller (1973) based on linear theory), it was felt that if the methodology proved representative and repeatable then the relativity of the defining erosion severity parameter, $S'$, might not be diminished by the use of linear theory: absoluteness - probably; relativity - less likely.
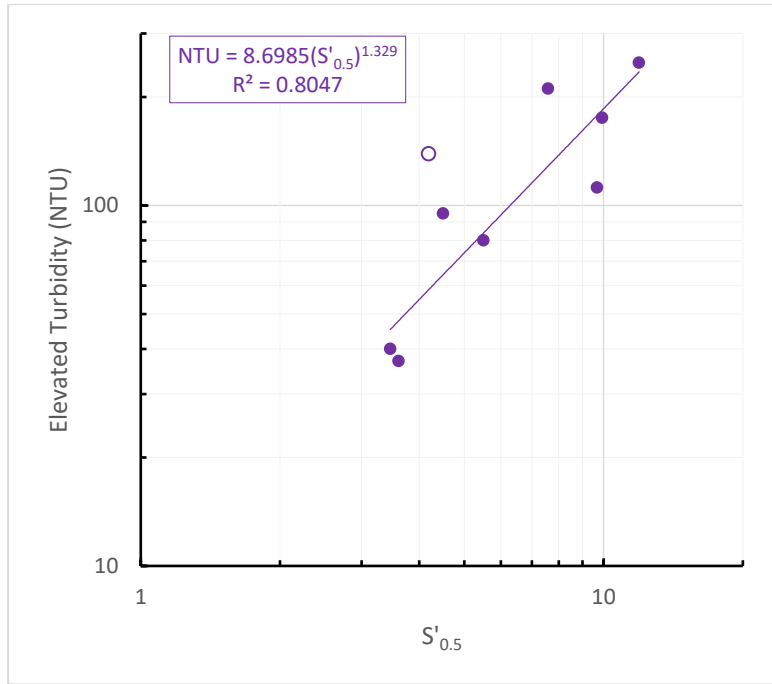
***Figure K4*** shows a small selection of results and demonstrates the predictability afforded by linear theory. The wave parameters $\{H_o = 0.1\,m;\ 1\,s\ \leq T \leq 8\,s\}$ were not calculated through to breaking. Points of breaking were calculated but by varying wave period for particular values of $H_o$ and $h$.

Except for the $T = 1\,s$ curve, the curves show a consistent relationship between $h$ and $S'$. Moreover, at the point of breaking it was found that $S'_b\sqrt{k_s/H_o} = const.$, which can be re-arranged to $S'_b\sqrt{H_b}/H_o = const.$, where $k_s$ is the shoaling factor and $S'_b$ is the severity of sediment suspension at breaking. Given the convoluted, iterative way in which the transformed wave parameters are derived, as well as the definition of $S'$, such a definite response would be particularly useful if this method were to be expanded as a means of grading vessel wave wakes for erosion potential. The strength of correlation of the even more simplified parameter $E_o/H_o$ renders this inconsequential.
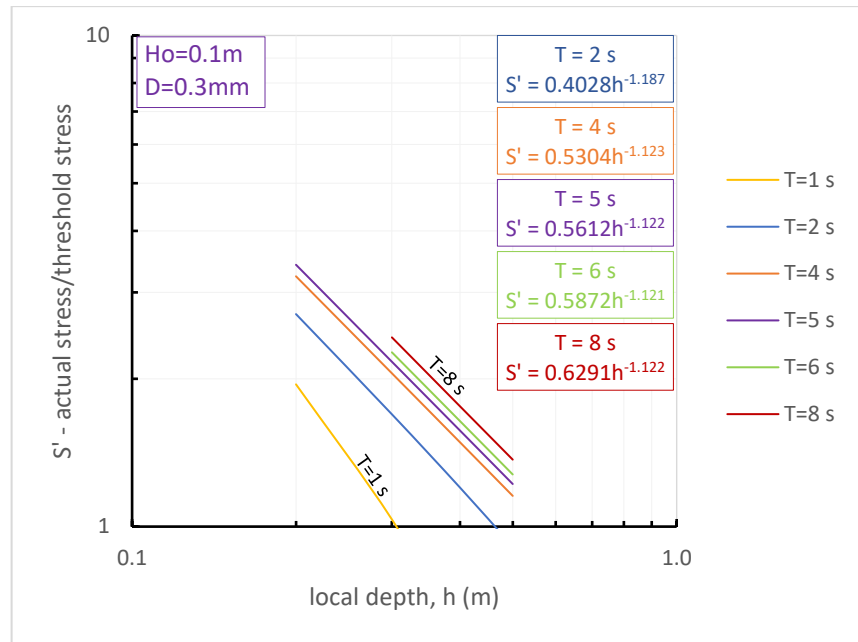
**Figure K4** – *Severity of sediment suspension (S') against h for $H_o = 0.1 \, m$ using linear wave theory at log-log scale. The consistency in the equation exponent for values of $T > 1 \, s$ is clear.*

## K.5 Comparison of Linear and Non-linear Wave Theories Applied to Erosion Thresholds

Different wave models are investigated to determine their effect on the erosion prediction method proposed. Two assumptions have so far been made when reviewing the wave theories. Firstly, it is assumed that bottom friction would negligible and can be ignored. This is not an unreasonable assumption, since bottom friction requires depth-affected wave propagation in the order of hundreds of wavelengths to become a substantive quantity. Secondly, wave diffraction has been ignored. This may be a less reasonable proposition but would be dependent on the lateral distance between the wave measurement point and the turbidity measurement point. In the case of the Gordon River tests the lateral distance between the points wave and turbidity measurement was much smaller than the lateral distance between the sailing line and the wave measurement point (in the order of *10:1*), so that the height attenuation due to dispersion would have been less than *4%*.

In terms of wave shoaling, waves with periods shorter than *3 s* in a practical sense, or *2 s* in an (engineering) absolute sense, do not shoal to any degree and there is little justification for the added complexity of correction based on water depth. The error in this would be no greater than the substantial scatter caused by variations in experimental procedures. *Figure K5* shows the extent of shoaling for four wave periods – three covering the wave period range of the Gordon River results from $1 \, s \leq T \leq 3 \, s$ and one longer wave period as a contrast. The slight reduction in height as waves begin to feel the bottom is due to a brief, relative increase in group celerity before the waves become fully depth-affected. This reduction in height is necessary to maintain constant energy flux, which is a function of group celerity.

Ignoring wave shoaling is of particular importance for the analysis of small craft wave wakes, since period of the maximum wave would be expected to remain below *3 s* at all speeds.
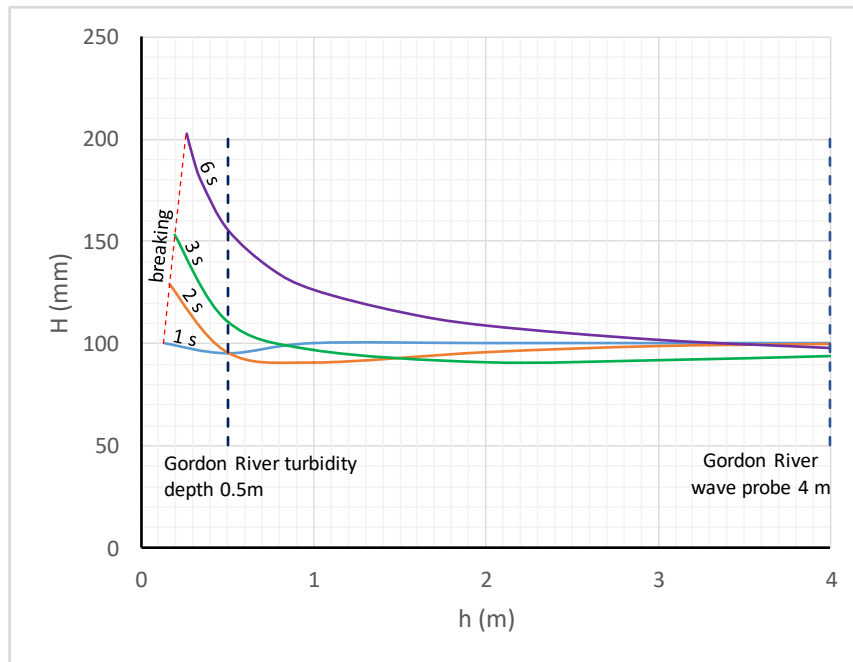
**Figure K5** – *Wave shoaling for four waves from $h_b \leq h \leq 4\ m$, with $H_o = 100\ mm$. The wave probe depth (4 m) and turbidity measurement depth (0.5 m) for the 2004 Gordon River tests are shown, justifying the assumption that wave shoaling for those test results can be reasonably ignored.*

## K.6    Erosion Thresholds

Previously, sediment entrainment thresholds were calculated for a range of conditions, with focus on those of the 2004 Gordon River turbidity experiments. The resulting graph is shown in **Figure 2** for $h = 0.5\ m$ and $D = 0.075\ mm$ sand (unconsolidated). Wave height was varied to account for deep water values and transposed values (termed *local height*) at the turbidity measurement depth of *0.5 m*.

The case for applicability to the Gordon River turbidity experiments is as discussed previously; the recorded wave periods are low and almost all the waves would not shoal. The wave parameters recorded at the *4 m* wave probe depth would be similar to those at the *0.5 m* turbidity measurement depth.

**Figure K6** shows the deviation to the local wave height assumption if non-linearity is accounted for. Two conditions are presented.

a.  ***Non-linear, local height.***
    This makes the same assumptions as the original linear model, in that the wave height is assumed to be the actual height at the threshold depth, but with the local wavelength derived from the appropriate non-linear theory as opposed to the empirical, depth-dependent simplification proposed by Fenton and McKee (1989), and commonly used in practical applications. The shear loads at the bed are a function of wavelength. In essence, this would mark the difference in using approximated wavelengths and non-linear theory wavelengths, and the difference is clearly small.

    The non-linear, local height curve of **Figure K6** spans three non-linear theories:

    - Stokes 3$^{rd}$ Order from $H = H_b$ to $H = 100\ mm$ $(T_b \leq T \leq 1\ s)$;

- Stokes $2^{nd}$ Order from $H = 80\ mm$ to $H = 60\ mm$ $(1\ s < T \le 3\ s)$;
- Hyperbolic (*Iwagaki $5^{th}$ Order*) from $H = 57\ mm$ to $H = 80\ mm$ $(3\ s < T \le 10\ s)$.

Inherent within this spanning of non-linear theories is a degree of discontinuity at the boundaries of applicability, especially near breaking where all non-linear theories become unreliable. Moreover, the capacity of these theories to realistically describe such small waves and those with obviously unusual, if not unrealistic, parameters (such as $h = 76\ mm$ and $T = 10\ s$) is to be questioned.

### b. *Non-linear, deep water height*

In this case the wave height referred from the curve is assumed to be the deep-water wave height and not the local wave height at $h = 0.5\ m$, such that $H = H_o$. For each datum used to generate the curve, the deep-water wave height was transposed to *0.5 m* water depth using the appropriate non-linear theory for calculating the threshold. In effect, this curve would collapse to the non-linear, local height curve of *condition (a)* on transposition.

This approach may have limited practical application in sheltered waterways. **Figure K7** relates wave period to water depth in terms of *absolutely deep* and *practically deep*. It may be impossible to achieve sufficient depth in sheltered waterways for anything but the shortest period waves to propagate initially as deep-water waves, implying that the wake waves of vessels other than small craft would have been generated in shallow water to begin with. Similarly, if a sufficiently deep depth was experienced to enable the generation and initial propagation of wake waves as deep-water waves, the bathymetry may not provide sufficient lateral separation for waves to disperse before becoming depth-affected. In that instance the interpretation of wake traces may become problematic.

Some salient points referring to the *non-linear local height* and *non-linear deep-water height* curves:

- The curves converge at short periods, where shoaling becomes negligible.
- There is a band of divergence around $1\ s \approx T \approx 2\ s$ where the waves measured in deep water are slightly higher than they are at $h = 0.5\ m$. This is the result of the relative increase in group celerity experienced by waves as they begin to feel the bottom, causing a slight reduction in height of generally less than *10%*.
- At periods longer than about *2 s* the curves again diverge, this time in the opposite sense. The height recorded in deep water would be less than that of the same wave at the $h = 0.5\ m$ depth, the result of shoaling. This is a period/wavelength/depth-dependent phenomenon; the disparity increases with increasing period and decreasing depth as the wavelength attenuates.
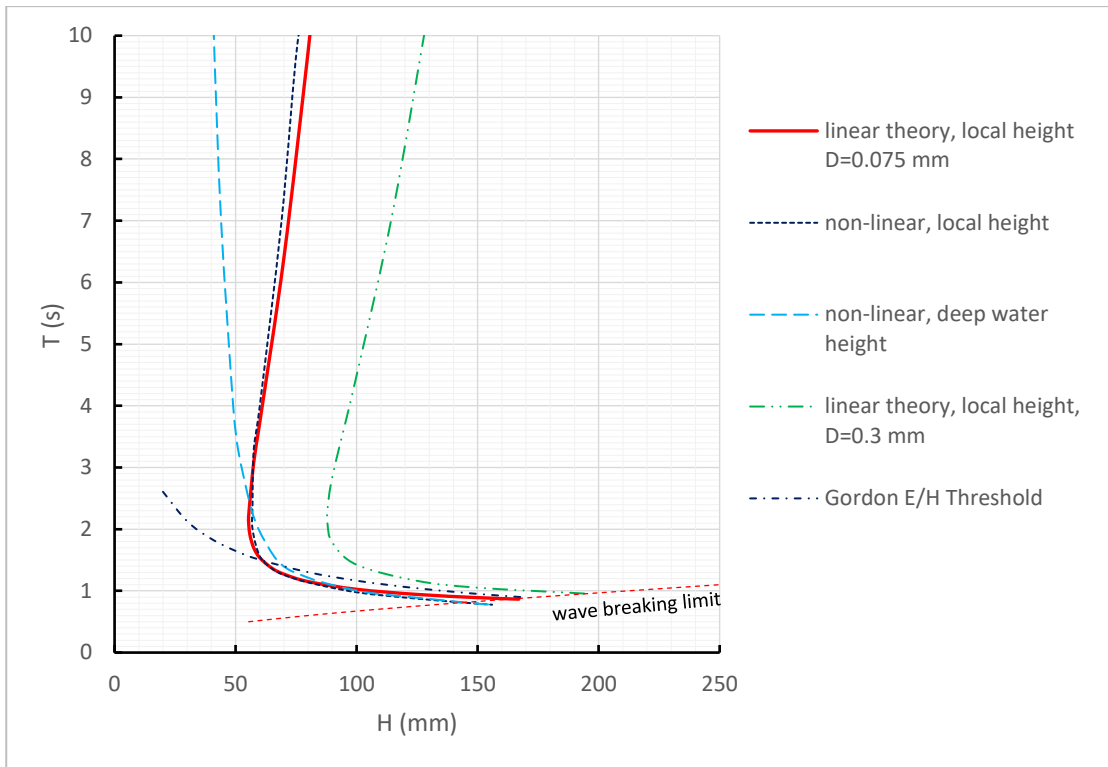
**Figure K6** – *Sediment entrainment thresholds for $h = 0.5\ m, D = 0.075\ mm$ (unconsolidated sediment) using linear and non-linear theories. A fourth threshold with increased sediment diameter is shown for comparison. The linear and non-linear theories assuming wave height is measured at the 0.5 m depth are essentially equivalent. The non-linear theory assuming the wave height is measured in deep water would collapse to the non-linear, local height curve on transposition. The energy per unit wave height curve is based on linear theory (Gordon $E/H$ threshold of 260J/m².*

## K.7    Energy Per Unit Wave Height Thresholds

Energy per unit wave height is the simplified measure of erosion potential, based on the premise that sediment entrainment and subsequent displacement is a satisfactory indicator of erosion. As discussed previously, the $E/H$ limit derived for the Gordon River studies and plotted at different wave heights such that $HT^2 = constant$, closely follows the erosion threshold of the Gordon River study for short-period waves.

In the instance where period remains low ($T < 2\ s$), the value of $E/H$ is little affected by differences between wave theories, as is the case with shoaling. Wave height briefly decreases due to a small increase in group celerity as short-period waves begin to feel the bottom, but the reduction in height is around *10%* at best. Adjustment to $E/H$ thresholds to account for non-linear wave theories may only be justified for longer period thresholds, suggesting larger sediment size.

336

**Figure K7** – *Relationship between wave period and depth for absolutely deep and practically deep, showing how unusual it would be in practice for sheltered waterways to experience longer-period vessel wake waves generated in deep water. The delineated waterway types (sheltered river, sheltered bay, open bay) are for illustration only.*
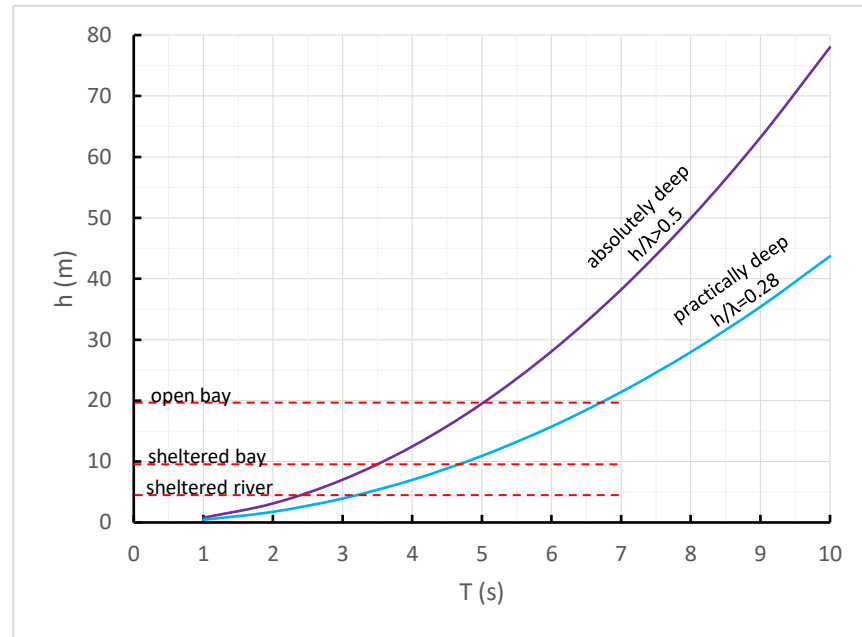
## K.8    Application to Severity of Erosion

The analysis of the severity of erosion, defined as the area under the normalised sediment stress curve from $h_t$ to $h_b$, was based on non-linear wave theory. A comparison of the resulting curves for non-linear and linear theories was presented, but only in a qualitative sense. Linear theory may work adequately in coastal engineering studies where the ratio of wave length to water depth (measure of shallowness) is not small and therefore the Ursell number is small, but it falls apart as the Ursell number becomes large in the nearshore zone.

As a quantitative example, **Table K2** presents a comparison between linear and non-linear theory for two waves with deep water wave parameters within the range of interest for vessel wake waves. When comparing values of $S'$ and $A_{nett}$, percentage differences mean nothing – real variance comes in orders of magnitude. Reference is made to Section 8, Table 8.4.

Of note are the under-prediction by linear theory of wavelength and breaker height, hence an under-prediction of sediment entrainment. This is also the case when applying lower order, non-linear methods, such as Stokes second-order, in shoaling water.

**Table K2** – *Example parameters for two waves using linear and non-linear theories.*

|  | $h_t$ | | $h_b$ | | $H_b$ | | $\lambda_t$ | | $\lambda_b$ | | $S'_b$ (=$S_b/S_{t,b}$) | | $A_{total}$ | | $A_{nett}$ | |
|---|---|---|---|---|---|---|---|---|---|---|---|---|---|---|---|---|
|  | linear | non-lin | linear | non-lin | linear | non-lin | linear | non-lin | linear | non-lin | linear | non-lin | linear | non-lin | linear | non-lin |
| $H_o = 0.1\ m, T = 4\ s$ | 0.687 | 0.715 | 0.195 | 0.221 | 0.152 | 0.221 | 10.220 | 10.666 | 5.525 | 8.079 | 4.116 | 7.303 | 0.895 | 1.205 | 0.404 | 0.711 |
| $H_o = 0.2\ m, T = 2\ s$ | 1.133 | 1.267 | 0.270 | 0.291 | 0.172 | 0.226 | 5.389 | 6.019 | 3.157 | 4.130 | 6.719 | 10.202 | 2.159 | 2.592 | 1.296 | 1.616 |

# Appendix L – Wind Waves

## L.1 Introduction

The intention of this section is three-fold:

a. to understand fully one of the most energetic and persistent sources of change to sheltered water environments;
b. to understand how individual wind wave parameters change with varying conditions and how the parameters relate to each other, rather than relying on composite values such as energy;
c. to investigate possible relationships between parameters and how those relationships compare to vessel wake waves.

Understanding how the environment reacts to changing wind wave parameters helps with the understanding of how it would react to the varying wave wake parameters. The most important relationships are that wind wave height is mainly a function of wind speed and wind wave period is mainly a function of fetch. A novel approach to analysing wind waves is presented.

## L.2 Methodology and Limitations

The most comprehensive and practical sources of wind wave data are the Shore Protection Manual (*SPM*) (Coastal Engineering Research Center (CERC) (U.S.), 1984), last updated and published in 1984, which has been replaced by the Coastal Engineering Manual (*CEM*) (United States, 2006) and a newer wind wave methodology that is, in fact, somewhat simplified in parts compared to the *SPM*.

The methods and equations derived are not absolute. Wind wave fields are not uniform, hence the use of spectral analysis to determine principal values of height and period under particular conditions. Similarly, wind gradients are not uniform and are functions of atmospheric and environmental factors such as temperature and terrain.

Moreover, the methods and equations tend to be skewed more towards coastal engineering problems, where wind, fetch and wave parameters may reach extreme values.[149] The applicability and computational stability of the hindcasting equations may become questionable in certain circumstances, notably fetch extremes (short and long), short durations (which are cautioned against in the *CEM*) and very low wind speeds.[150] Unfortunately, the *CEM* (and *SPM* before it) does not follow what should be standard practice for the derivation of empirical equations from experiments and observations by stating limits of applicability.

## L.3 SPM and CEM

The *SPM* has separate equations for shallow and deep water. When $h \gg \lambda$, the shallow-water equations devolve to the deep-water equations. The *CEM* is similar in format but does away with the shallow water equations, based on studies that purport to show that the deep-water

---

[149] Demirbilek *et al*. (1993), whose work forms the basis of the *CEM* hindcasting method as well as the USACE wind wave modelling software, refer to an upper wind speed limit ($U_{10}$) of 250 m/s!

[150] Though Demirbilek *et al*. (1993) refer to a $U_{10}$ value of 1 m/s as a lower bound of applicability.

equations return wind wave parameter values that are sufficiently accurate for use in shallow water (*CEM* p.II-2-49, para (d) Shallow water). For sheltered waterways where fetches and wind speeds are limited, it is likely that this would be the case, since the expected wind wave heights and periods are unlikely to be depth-affected to any appreciable degree during their formation and are likely only depth affected just prior to reaching the lee shore.

The deep-water equations in the *SPM*, as preferred by the *CEM*, do not appear to properly reflect wind wave growth to maturity. The deep-water approximations are of a form where, given unbounded environmental parameters such as fetch and wind speed, would generate unbounded wave parameters and wave growth. This clearly cannot be the case in real life. To compensate, upper limits for wind wave height and period are adopted in the *SPM/CEM* to truncate the growth. Those limits are also questionable.

*CEM 2015 deep-water wind wave relationships:*

$$\frac{gH_{m_0}}{u_*^2} = 4.13 \times 10^{-2} \left(\frac{gX}{u_*^2}\right)^{\frac{1}{2}}$$

[L1]

*and*

$$\frac{gT_p}{u_*} = 0.651 \left(\frac{gX}{u_*^2}\right)^{\frac{1}{3}}$$

[L2]

*where*:
$X$      = fetch in metres
$H_{m_0}$      = significant wave height in metres
$T_p$      = period spectral peak in seconds
$u_*$      = friction velocity: a function of the wind speed at *10* metres elevation, in m/s,
       and $u_*^2 = 0.0011 U_{10}^2 + 3.5 \times 10^{-5} U_{10}^3$ (but refer to discussion following)

*CEM fully-developed wave conditions*:

$$\frac{gH_{m_0}}{u_*^2} = 211.5$$

[L3]

*and*

$$\frac{gT_p}{u_*} = 239.8$$

[L4]

*SPM 1984 deep-water wind wave relationships:*

$$\frac{gH}{U_A^2} = 1.6 \times 10^{-3} \left(\frac{gF}{U_A^2}\right)^{\frac{1}{2}}$$

[L5]

*and*

$$\frac{gT}{U_A} = 0.2857 \left(\frac{gF}{U_A^2}\right)^{\frac{1}{3}}$$

[L6]

339

*where*:

| | |
|---|---|
| $F$ | = fetch in metres |
| $U$ | = wind speed in m/s |
| | = $R_T U_{10}$ |
| $R_T$ | = air/sea temperature correction; default is 1.1 based on $(T_a - T_s) = -3^o C$ |
| $U_A$ | = "adjusted" wind speed in m/s |
| | = $0.71 U^{1.23}$ |

*SPM fully-developed wave conditions*:

$$\frac{g H_{m_0}}{U_A^2} = 0.2433 \qquad\qquad\qquad \text{[L7]}$$

*and*

$$\frac{g T_m}{U_A} = 8.134 \qquad\qquad\qquad \text{[L8]}$$

## L.4    Relationship between *SPM* and *CEM*

It is possible to develop a relationship between $U_{10}$ (wind speed at *10 m* reference height), $U_A$ (*SPM* adjusted wind speed) and $u_*$ (*CEM* friction velocity). Whenever the generic term "wind speed" is used it is always assumed to be the $U_{10}$ value. Knowing that $C_D = u_*^2 / U_{10}^2$ and that $u_*^2 = 0.0011 U_{10}^2 + 3.5 \times 10^{-5} U_{10}^3$, for any value of $U_{10}$ a corresponding value of $U_A$ and $u_*$ can be calculated. It is possible to develop an explicit relationship, since the equation for $u_*^2$ is a cubic and there are three roots to this equation (in the case of this equation all roots are real since the discriminant is greater than zero), but it is simpler just to tabulate. **Table L1** shows this.

**Table L1** – *Relationships between SPM and CEM wind parameters (in m/s) given $U_{10}$.*

| $U_{10}$ | *CEM*: $u_*$ | *SPM*: $U_A$ |
|---|---|---|
| 1.25 | 0.042 | 1.05 |
| 2.5 | 0.086 | 2.46 |
| 5.0 | 0.179 | 5.78 |
| 7.5 | 0.277 | 9.51 |
| 10.0 | 0.381 | 13.55 |
| 12.5 | 0.490 | 17.83 |
| 15.0 | 0.605 | 22.32 |
| 17.5 | 0.724 | 26.97 |
| 20.0 | 0.849 | 31.79 |

### *CEM* Friction Velocity $u_*$

The *CEM*, referring to Demirbilek *et al.* (1993, Eqn. 1) introduces the concept of friction velocity $u_*$, which is defined by:

$$T = \rho C_D u_*^2 \qquad\qquad\qquad \text{[L9]}$$

where $T$ is the sea surface stress, $C_D$ is the drag coefficient and $\rho$ is the air density. The drag coefficient listed in the *CEM* (eqn. II-2-36) and in the WISWAVE 2.0 software developed by Demirbilek *et al*. (1993) is:

$$C_D = 0.001(1.1 + 0.035U_{10}) \hspace{4cm} [L10]$$

However, Demirbilek *et al*. (1993, Eqn. 7) state the equation for the drag coefficient as:

$$C_D = 0.001(1.1 + 0.035U_{10})U_{10} \hspace{3.5cm} [L11]$$

This equation for the drag coefficient has an additional $U_{10}$ term after the parentheses, which does not appear in the *CEM* or in the *WISWAVE 2.0* code. However, it cannot be a typographical error according to the following explanation of Demirbilek *et al*. (1993) accompanying their equation 7:

> *"This form, although parabolic, nearly represents a straight line approximation of the drag coefficient versus wind speed for low values of wind speed."*

That is true. At low wind speeds, [L11] approximates a straight line, but it is clearly a quadratic as noted by their reference to its *parabolic form*, compared to [L10] which, without the additional $U_{10}$ term, has a linear form. It can only be concluded that [L11] is not a typographical error, but it's origin and relationship to the hindcasting method is unclear and confusing. Moreover, in explaining the logic of the *WISWAVE 2.0* software in Appendix D of Demirbilek *et al*. (1993, Eqn. 1), the authors revert to the linear form of [L10].

### L.5    Limit Wave Speed

Application of the *SPM* shallow water equations with water depth set to "deep" (h>>λ) demonstrates the relationships derived from the deep-water equations, but only in the condition where waves are fetch limited. Given sufficient fetch and assuming the wind to be continuous (not duration-limited), the wind waves will eventually reach mature limits and the seas are considered to be fully developed. The *SPM* states that the limit of momentum transfer is when the wave speed equals the adjusted wind speed $U_A$, which is always greater than $U_{10}$ for all values of $U_{10} > {\sim}2.7\ m/s$. The mechanism that allows fully-developed wind waves to travel faster than the wind is a non-linear process where energy from shorter waves is transferred to longer waves (described colourfully as *the long waves consuming the short ones*).[151]

Using the *SPM* equations for deep water wave period limit (fully-developed seas) and applying the premise that the developed wave speed cannot be faster than the adjusted wind speed, linear wave theory would give $gT_m/U_A = 2\pi$. However, the fully-developed limit equation from *SPM* is

---

[151] For the purpose of discussion, an additional mechanism is proposed. Much of the study of wind waves has been based on the statistical analysis of data from field measurements. The wind speed used is an averaged parameter (mean, significant, or otherwise), accounting for the fact that the wind speed is never constant. In a fully-developed wind wave climate, the waves would have been exposed to gusts where wind speeds exceeded the statistical average and transferred additional momentum to the waves accordingly. Waves in deep water approach what can be considered an almost frictionless state, so once they receive the additional momentum they would propagate as such. The mature wave parameters, including wave speed, would therefore approach something reflecting the maximum wind speed, whereas the recorded wind speed is taken as an averaged value. This does not appear to be discussed in the literature.

$gT_m/U_A = 8.134$, implying that the period of a fully developed wave results in a wave that travels *29.5%* faster than the adjusted wind speed ($8.134 = 1.295 \times 2\pi$).

Similarly, using the *CEM* method for fully-developed wind wave period of $gT_p/u_* = 239.8$ [L4] gives a limiting wave speed of $38.165u_*$, which can be related to $U_{10}$ using the relationship that $C_D = u_*^2/U_{10}^2$ combined with [L10] to give $u_*^2 = 0.0011U_{10}^2 + 3.5 \times 10^{-5}U_{10}^3$. The relationship between $u_*$ and $U_{10}$ allows the *CEM* limit wave speed to be compared to the *SPM* adjusted wind speed $U_A$, since both $u_*$ from the *CEM* and $U_A$ from the *SPM* can be written as functions of $U_{10}$. This is shown graphically in **Figure L1**. Although the limit wave speed appears to become asymptotic to $U_A$ at around *25 m/s*, the two actually diverge above this. There is reasonable correlation $[(V_{wave} - U_A)/U_A < 3\%]$ at $U_{10}$ wind speeds above around *12 m/s*, with deteriorating correlation at slower speeds. At $U_{10}$ wind speeds below around *5 m/s* the limit wave speed of the *CEM* is almost *18%* faster than the adjusted wind speed.

Given that hindcasting equations are empirical, or semi-empirical by nature, and there can be considerable variance in calculated values due to the wide variation in conditions (wind gradient and wind speed averaging being a prime examples), it is most likely that the *CEM* limit for fully-developed wind wave period was an attempt to overcome the inherent discrepancies of the earlier *SPM* limit, given the (practical) correlation between the *CEM*'s wave speed limit (*V_wave CEM*) and $U_A$ shown in **Figure L1**.
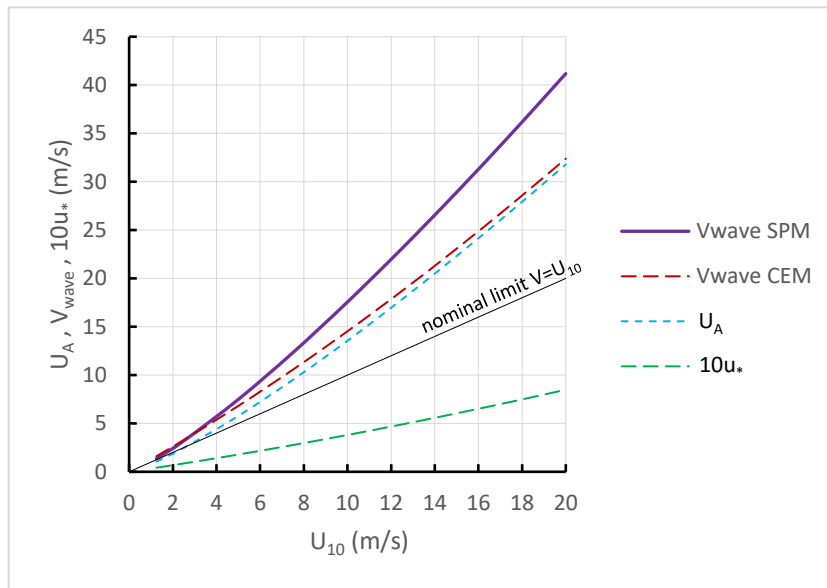


**FIGURE L1** – *Relationships between wind speed at 10 m height ($U_{10}$) and calculated wind speed values (adjusted wind speed $U_A$ from the SPM and friction velocity $u_*$ from the CEM) and the corresponding limit wave speed values "V_wave SPM" and "V_wave CEM." Note that the SPM limit wave speed is much faster than U_A by a constant value of around 30%. The nominal limit line of $V = U_{10}$ is a reference line only (since the graph axes are not of equal scale).*

### L.6    Limit Wind Wave Steepness

Of all the wave parameters that could define the establishment and growth to maturity of a wind wave field, wave steepness is possibly the most descriptive. The caveat to this is that the limit wave steepness must arise from maturity in wave height and period and not just reaching a point of an intrinsic relationship between height and period that yields constant wave steepness. Without that caveat it may be possible that waves could continue to grow yet maintain a constant wave steepness, disqualifying the premise that wave growth to the point of constant wave steepness signifies a mature, fully-developed sea. Both the *SPM* and the *CEM* rely only on height and period to define a fully-developed wind wave climate, yet it can be shown that their hindcasting equations produce intrinsic relationships between wave height and period that would avoid the problem of constant wave steepness with unbounded height and period parameters.

For that reason, it is best to define wave steepness as a function of fetch Froude number $Fr_F$ , where $Fr_F = v/\sqrt{gF}$ (using $v$ as a generic wind speed, since the *SPM* uses $U_A$ and the *CEM* uses $u_*$), and not wind speed or fetch alone. Waves grow in height and period with increasing fetch and wind speed, and fetch Froude number is the quotient of these two parameters, acting to balance the two growth factors.

It can easily be shown that the relationship between wave steepness and fetch Froude number at a constant wind speed and where wind waves are immature is:

$$\frac{H}{\lambda} \propto F_F^{1/3}$$

[L12]

***Figure L8*** (following), based on the *SPM* shallow water wind wave hindcasting equations with h>>λ, demonstrates that relationship absolutely, but within reason. If the *SPM* deep water hindcasting equations are applied the curve exponent becomes exactly ⅓ everywhere, but without the equations having any inherent limits to wave growth. This is shown in ***Figure L9***. This apparent unfettered growth, where wind waves under a constant wind speed grow in height and period with fetch and growth is truncated by nominal height/period limits does not reflect physical processes. An example of this anomaly is shown in ***Figure L2*** (following), reproduced from *CEM* Fig. II-2-23, where wind wave height growth continues uninterrupted up to the nominal limit value. The power exponent in the growth phase is one-half ($H \propto \sqrt{F}$), as is predicted by the *CEM* deep water wind wave height equation, then suddenly assumes a zero value (signifying a constant value of wave height). Growth rate decay is not possible with the height and period equations of the form used in the deep-water simplification, hence the nominally truncated growth.
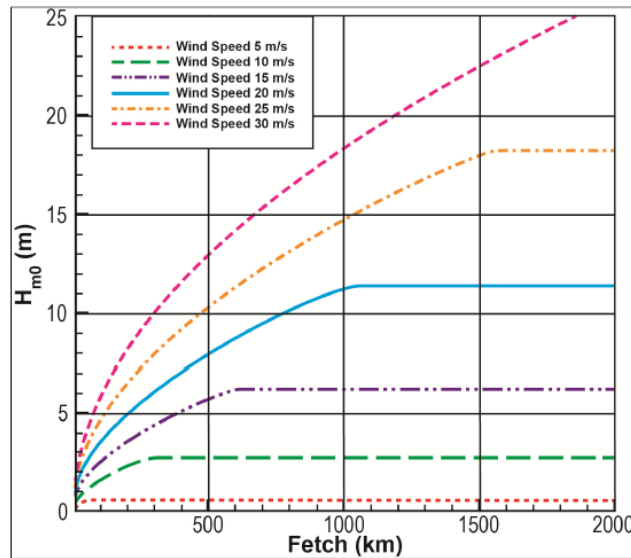
343

Figure II-2-23. Fetch-limited wave heights.

**Figure L2** – *CEM wind wave heights, reproduced from CEM Fig. II-2-23. The growth in height for various wind speeds, truncated abruptly by a nominal wave height limit, is clear. The power exponent of the growth portion is ½, as expected from the equation used. The corresponding wave period graph is similar in form.*

**Figure L2** presents another inconsistency in the *CEM* hindcasting method. The horizontal portion of each wind speed curve represents the fully matured wind wave height, yet the values do not correspond with [L3]. **Table L2** demonstrates this and shows the increasing disparity between the graphical and analytical expressions.

**Table L2** – *Height growth limits: difference between the CEM graph and the CEM equation.*

| $U_{10}$ (m/s) | 10 | 15 | 20 | 25 |
|---|---|---|---|---|
| $u_*$ | 0.381 | 0.605 | 0.849 | 1.111 |
| H limit – Fig. L2 (m) | 2.72 | 6.26 | 11.33 | 18.38 |
| H limit – Eqn. [L3] (m) | 3.13 | 7.88 | 15.52 | 26.61 |

By using the graphed limits for wave height and back-calculating the constant in the height limit equation (stated to be *211.5*), the constant is not constant but varies with wind speed. This is best demonstrated by the complementary *CEM* period graph (*CEM* Fig. II-2-24). The stated limiting period is given by [L4], which implies a linear relationship between the fully-developed period limit and $u_*$. *CEM* Fig. II-2-24 shows a linear relationship, but with wind speed and not $u_*$. Doubling the wind speed doubles the period limit, but the relationship between wind speed and $u_*$ is non-linear, as shown in the nomenclature for [L1] and [L2]. That is why the stated *constants* for the height and period limits are not constants but are actually variable constants. It makes little difference in the understanding of wind waves; their growth in sheltered waterways would never reach maturity.

## L.7 Derivation of Wind Wave Steepness Limits

The deep-water wind wave hindcasting equations of both the *SPM* and *CEM* have stated limits to height and period, said to represent fully-developed seas (SPM: [L7] and [L8]; CEM: [L3] and [L4]). The limits are non-dimensionalised in such a manner that wind speed variables such as $U_A$ and $u_*$ (*SPM* and *CEM* respectively) cancel out in the calculation of wave steepness using linear wave theory, leaving only a constant. That constant wave steepness is identical for both methods and is equal to *0.0231*, or approximately *1/43.3*.

The fact that both share the same limiting steepness suggests that the intrinsic relationship between height and period and the relative rate of their growth has been retained, but the wind speed driving the momentum transfer has been modified between the two methods. It may also suggest that the *CEM*'s wave height and period limits were simply derived from the *SPM* values using the relationship between $U_A$ and $u_*$.

Another contradiction arises. As stated, the limiting wind wave steepness is independent of wind speed using linear wave theory in deep water and the relevant height and period limit condition equations. However, using the graphed values of limiting height and period in the CEM (Fig. II-2-23 and Fig. II-2-24), the limit wave steepness is slowly reducing with increasing wind speed, with a mean value of about *1/25*.

*Figure L1* shows how the *CEM* value of limit wave speed, $V_{wave}$ CEM (wind wave speed limit in a fully-developed sea), is reasonably close to the *SPM* adjusted wind speed $U_A$, particularly in the range of interest to coastal engineers, who are mostly interested in elevated wind speeds. Assuming the *CEM* wind wave period equation and fully-developed limit to be correct, using the *CEM* general deep-water hindcasting equations [L1] and [L2], and knowing the limit condition in [L4], the height limit condition can be checked. Rearranging [L2] in terms of $gX/u_*^2$ (which is the inverse square of the *CEM* fetch Froude number) and substituting into [L1] gives the corresponding height limit as $gH_{m_0}/u_*^2 = 292$. The *CEM* published equation [L3] has a constant of *211.5*, which appears incorrect.

Using these revised limit conditions, the limit wave steepness can be calculated, such that $H/\lambda = 1/31.3$. This new value of *1/31.3* compares to the value of *1/43.3* from the published *SPM*/*CEM* limits and *1/29* from the shallow water equations when wave speed is limited to the adjusted wind speed, $U_A$ and with $h \gg \lambda$. Plotting out a range of wave parameters using the *SPM* shallow-water equations shows how they become asymptotic to a wave steepness of *1/29* without the need to apply any wave speed limit. This is discussed in *Figure L8* following.

## L.8 General Wind Wave Relationships

Coastal engineers are more interested in high wind speeds and long fetches found in coastal regions rather than sheltered waterways. These hindcasting equations are to be considered as an empirical representation of reality, not a mirror image of it. It is quite likely that the validity of these equations becomes questionable at the extremes, including the lighter winds and short fetches of sheltered waterways. Certainly, the application of equations such as that for calculating the adjusted wind speed $U_A$, where the equation constant must be dimensional for the equation to be valid, does not give comfort to those seeking a mathematically rigorous approach.

345

### L.8.1 Derived Deep-Water Wind Wave Relationships (SPM 1984)

Given that $Fr_F$ denotes the fetch Froude number and is equal to $U_A/\sqrt{(gF)}$,

$$H \propto \frac{U_A^2}{g} \cdot \frac{1}{Fr_F} \qquad \text{[L13]}$$

*and*

$$T \propto \frac{U_A}{g} \cdot \frac{1}{Fr_F^{2/3}} \qquad \text{[L14]}$$

For constant $U_A$ (constant U) and without duration limit, the following relationships can be derived:

i.  $H \propto Fr_F^{-1}$

Which implies that $H \propto \sqrt{F}$, where $U$ is constant.

ii.  $T \propto Fr_F^{-2/3}$

Which implies that $T \propto \sqrt[3]{F}$, where $U$ is constant.

iii.  $T \propto H^{2/3}$ and $H \propto \left(\sqrt{T}\right)^3$

These are important intrinsic relationships between height and period, which clearly show that wave parameters do not grow in isolation.

iv.  $P \propto Fr_F^{-8/3}$ and $E \propto Fr_F^{-10/3}$

A particular relationship to note is that, for a constant wind speed, $E \propto F^{5/3}$, which demonstrates that energy remains modest provided the fetch is limited. This is shown in **Figure L11**.

v.  $h/\lambda \propto Fr_F^{1/3}$

This is shown in **Figure L8** (shallow water equations with $h \gg \lambda$) and **Figure L9** (deep water equations).

vi.  $h/\lambda \propto P^{-1/8}$

Refer to discussion relating to vessel waves.


### L.8.2 Graphed Relationships and Discussion *(L3 to L11 grouped)*

**Figure L3** shows the variation of wave power with height for different wind speeds and varying fetch lengths from *100 m* to *10,000 m*. The curves have the same basic form, with slight variation in exponent. At high wind speeds in a fetch-limited environment (where $U_A$>>*wave speed*) the exponent approaches the calculated value of *2⅔*. At slower wind speeds the exponent also marginally decreases. This is important for sheltered waterways where wind speed is low because a relationship of $P \propto H^{2.5}$ implies that wave steepness is constant and an exponent approaching *2.5* would confirm this.

*Figure L4* is the combined form of *Figure L3*, without grouping according to wind speed. The line of best fit shows an overall average exponent of *2.5*, suggesting that the constant wave steepness proposal is reasonable when applied to grouped data. The reason why the exponent of the group is slightly different to the exponent of the individual curves of constant wind speed of *Figure L3* is demonstrated by the schematic in *Figure L4* – the individual curves of constant wind speed combine to form an envelope. The lower bound of the envelope represents fetch-limited wind wave growth and the upper bound of the envelope represents the fully-developed wave field (mature growth).

It is possible that the vessel wave wake records exhibiting the same $P \propto H^{2.5}$ relationship may in fact be a composite of many curves of $P \propto H^n$, with a combined data exponent of *2.5*. That implies that there are intrinsic relationships between height and period, as well as vessel parameters. The relationships between vessel parameters and wave parameters, at least at high speeds, are known (such as $T \propto \sqrt{L}$ and $H \propto L/\sqrt[3]{\nabla}$), but there does not appear to have been any attempt previously to identify innate relationships between wave wake height and period. The 2004 Gordon River data showing $P \propto H^{2.5}$ is shown as *Figure L5*.

*Figures L6 and L7* show the relative growth in wind wave height and period in fetch-limited and wind speed-limited conditions, as would be expected in sheltered waterways. They exhibit the convexity/concavity that demonstrate the progressive ease of increasing height and the progressive difficulty of increasing period as wind speed increases. Also reconfirmed are the increasing wave energy and power dependence on wave height as fetch and wind speeds grow.

Referring to the 2004 Gordon River erosion studies and the derived height/period thresholds of *114 mm* and *1.1 s* respectively, it is unlikely that wind waves on the Gordon River in excess of these values would be generated, except in very extreme conditions. A worst-case fetch of *500 m* (assumed to be along a straight stretch of the river where waves would impinge on a down-fetch bend), the wind speed exceeding the threshold wave values is around *8.5 m/s*, or *16.5 kn*. After correcting the wind speed for terrain and vegetation, this must be considered an extreme event. For that reason, the shoreline stability of the Gordon River is more likely to be influenced by other riverine and climatic events and less likely due to wind wave climate.

In *Figure L8* (wave steepness against fetch Froude number – *SPM* shallow water equations), fetch Froude number provides the effective non-dimensional link between adjusted wind speed and fetch to balance out the relative effects of these two parameters. Three (arbitrary) zones are shown: fully-developed, where the wave climate is mature; transition, where the decreasing wind/wave speed relativity is slowing growth; fetch-limited, where there is insufficient distance for wind waves to mature. In generating this graph, the wind speeds ($U_{10}$) ranged from *0.5 m/s* to *20 m/s* and the fetch from *50 m* to *50 km*, which are well beyond the limits of the preceding graphs where wave parameter maturity was not full achieved.

Two limits are shown also. The nominal breaker limit of approximately *1/7* (or *0.142*) is well-established. The wave steepness limit, which comes about when the waves are fully matured, was derived empirically by adjusting all possible variables in the shallow water hindcasting equations (fetch, adjusted wind speed and depth) to find the minimum value, which is approximately *1/29*. This conflicts with the height and period limits stated in the *SPM/CEM* for deep water waves, which would give a wave steepness limit of approximately *1/43*.

The deep-water hindcasting equations imply that wave steepness is a function of $Fr_F^{1/3}$ and that relationship is demonstrated absolutely in the section of data where wave parameters are

immature. That corresponds to strong winds and short fetches, generating large wave steepness. Large steepness implies a far greater ratio of height to period, which corresponds to the general relationship between erosion rates and wind waves in fetch-limited waterways. Small steepness implies light winds and long fetches, allowing period growth to catch up to height growth as the wave parameters mature.

*Figure L9* exhibits the unconstrained growth of height and period when the deep-water wind wave equations are used. The unconstrained growth in height and period, followed by truncation at nominal limits, results in a similar pattern as demonstrated by *Figure L2*. The notionality of the height and period (hence wave steepness) limits is shown by the fact that data exists beyond the limit. Although it is of little consequence for sheltered waterways given their short fetches, the rigour of the deep-water equations is questionable.

The log-log graph of *Figure L10* shows the relative growth and maturity of height, period and wave steepness with fetch. Of note is the relatively short fetch-limited initial state where the relationships derived from the deep-water equations are valid. For most of the fetch the waves are in transition, moving from their fetch-limited state to the limit of momentum transfer and then into the non-linear state where interactions between waves continue the growth process. The wave steepness, however, reaches its limiting value earlier.

*Figure L11* shows graphically how the relative growth of each can be predicted from the deep-water equations. Of interest is the relative rate of growth, especially early in the fetch where height and not period dominates. The near-linearity of $E/H$ is interesting considering this parameter's influence on erosion.
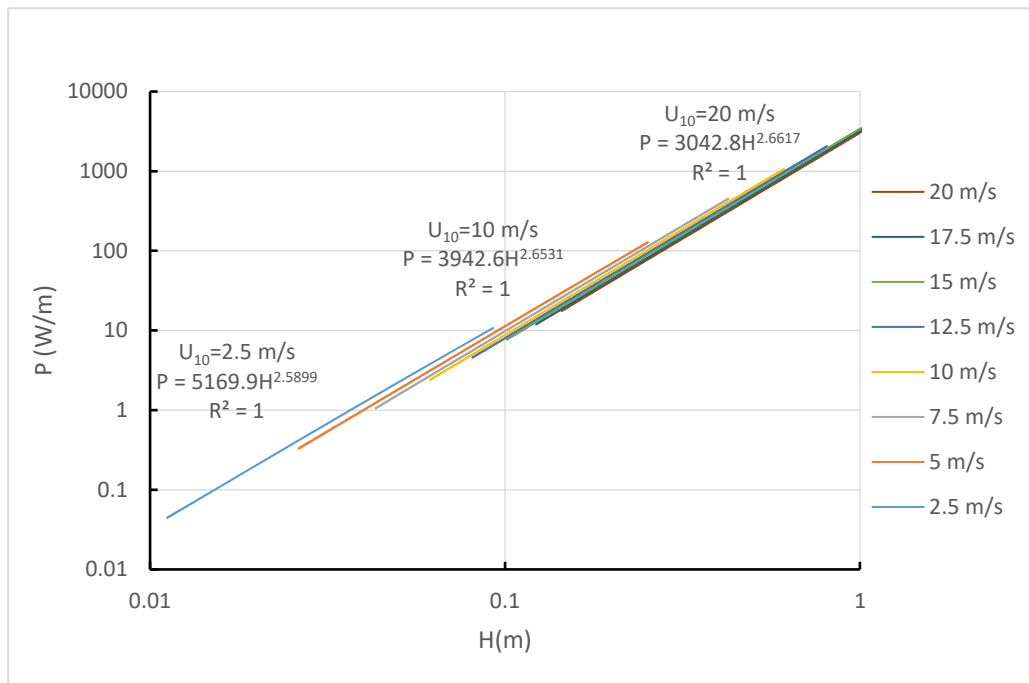


**Figure L3** – *Power against height (log-log) for constant wind speeds and varying fetch lengths.*
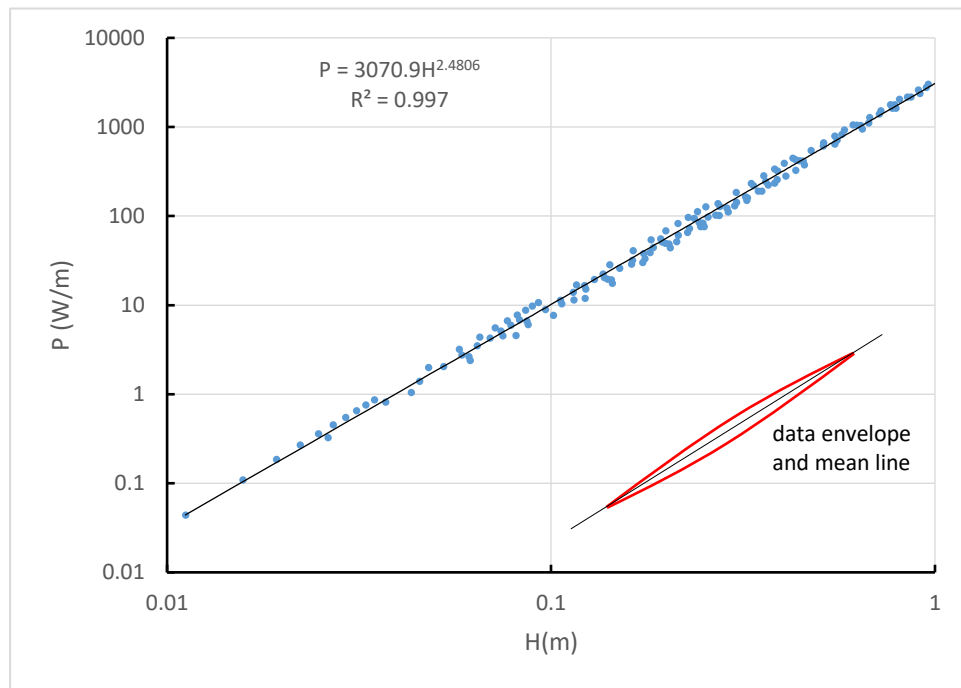
**Figure L4** – *Wave power against height (log-log), combined data of Figure L3. As with wake waves, there is an intrinsic relationship between wave power and wave height, which implies that the growth in wave height and period for a given wind speed (and by extension of the argument to wave wake terms – for a given vessel) are inter-related.*
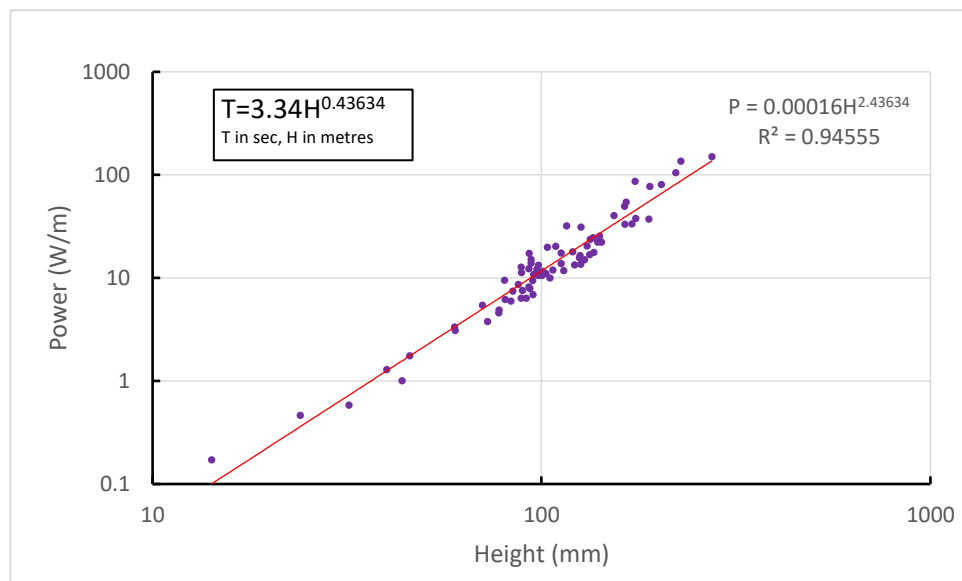


**Figure L5** – *Wave power against height from the 2004 Gordon River tests (for the maximum wave). An exponent of 2.5 would result in a constant value of wave steepness. The general relationship between the recorded wave height and period is shown. The near-intrinsic relationship for vessel wake waves concurs with the wind waves in Figure L4.*
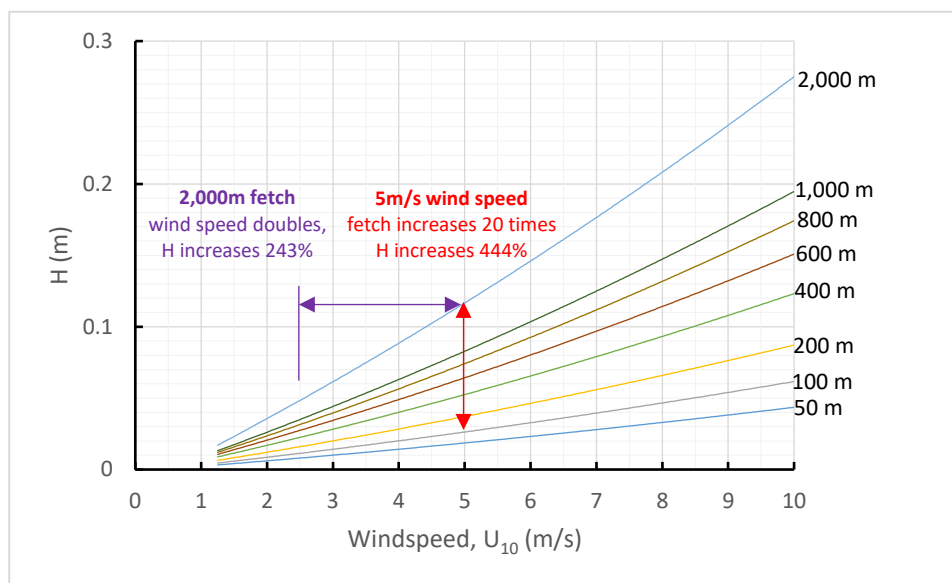
**Figure L6** – *Wind wave height against wind speed for different values of fetch, with wind speeds and fetches in the range expected in sheltered waterways.*
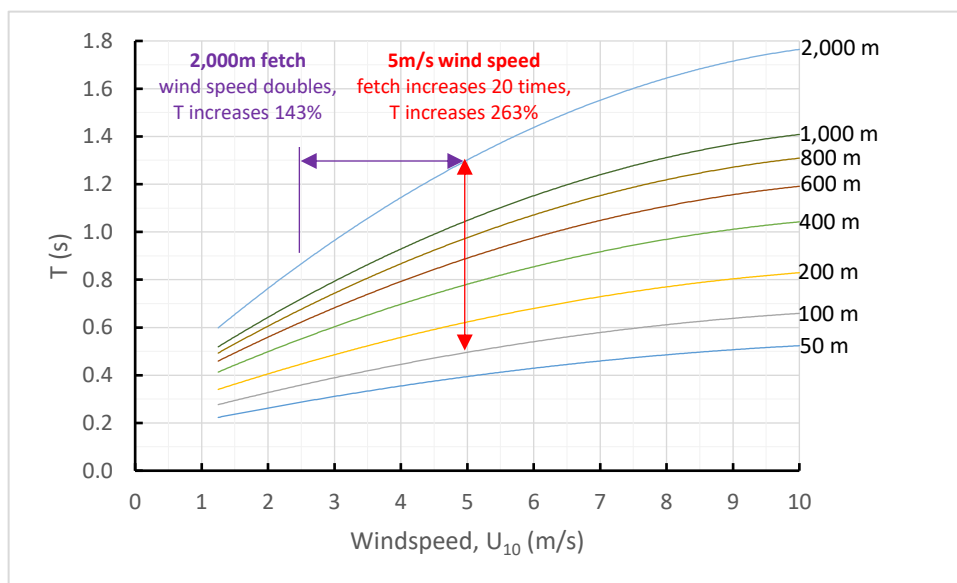


**Figure L7** – *Wind wave period against wind speed for different values of fetch, with wind speeds and fetches in the range expected in sheltered waterways.*
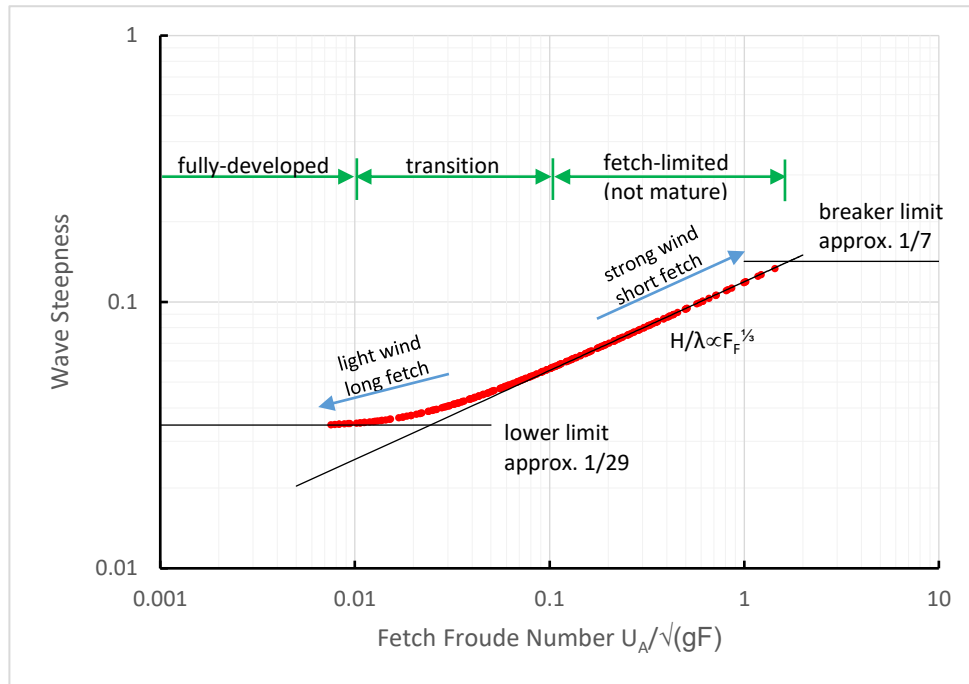
**Figure L8** – *Log-log graph of* wind *wave steepness against fetch Froude number, based on the SPM 1984 shallow water hindcasting equations with h>>λ. These equations give the expected form of the change in wave steepness through to maturity.*
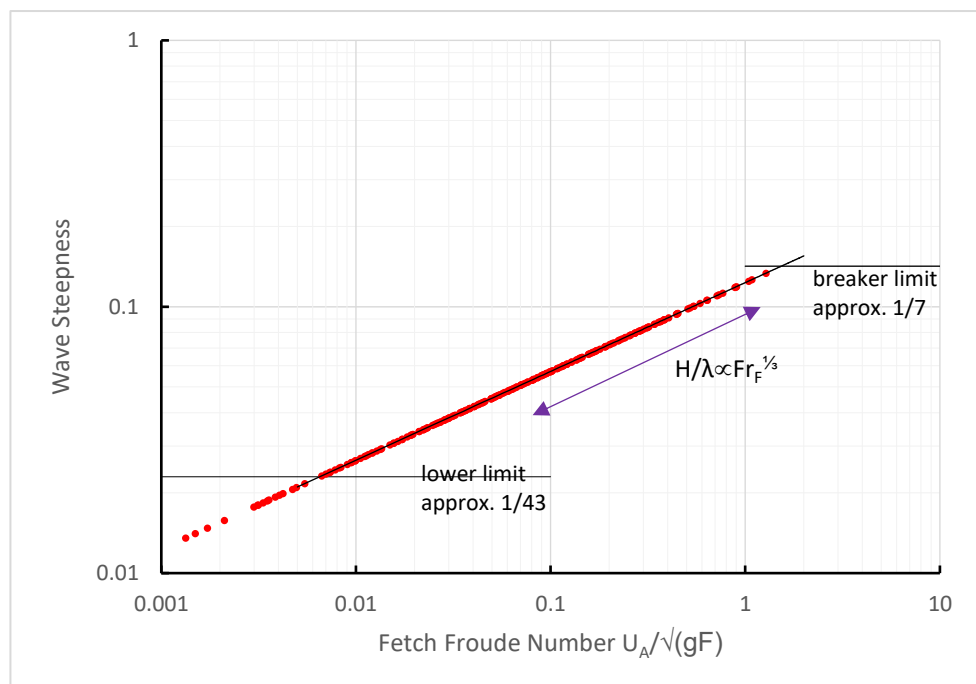


**Figure L9** – *Log-log graph of* wind *wave steepness against fetch Froude number, based on the SPM 1984 deep water hindcasting equations. The CEM 2015 deep-water equations yield essentially the same results. The wave steepness limit of 1/43 is based on the nominal limiting (mature) height and period, and the limiting wave steepness is the same for both the SPM 1984 and CEM 2015 equations. It has been shown to be questionable. The implication from the deep-water hindcasting equations is that the growth of height and period is unfettered until the nominal mature height and period limits are reached, which does not reflect reality.*

351

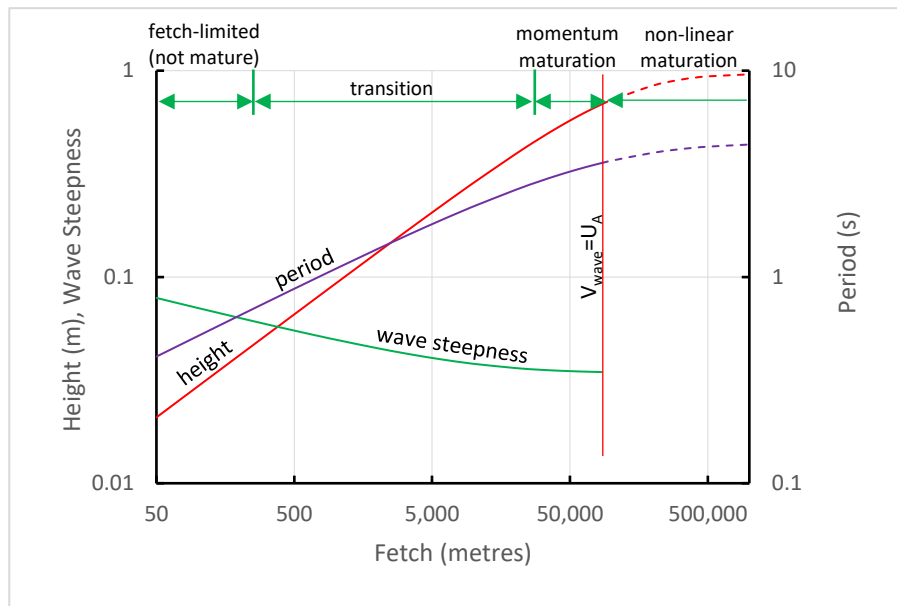**Figure L10** – *Example of the growth of the individual wind wave measures – height, period and steepness – with increasing fetch at 5 m/s nominal wind speed ($U_{10}$) in log-log form. The limiting condition of the maximum wave speed equal to the adjusted wind speed is shown. Although the equations for height and period (shallow water equations with h>>λ) will continue to allow growth in height and period beyond this limit condition, the wave steepness becomes constant at or before the limit. The (nominal) growth phases of Figure L8 are also shown; the transition ranging from fetch Froude numbers of about 0.1 to 0.01. Note how the fetch-limited range, where the wave relationships derived from the deep-water equations remain valid, is relatively short. The relative growth rates of height and period with fetch are evident.*
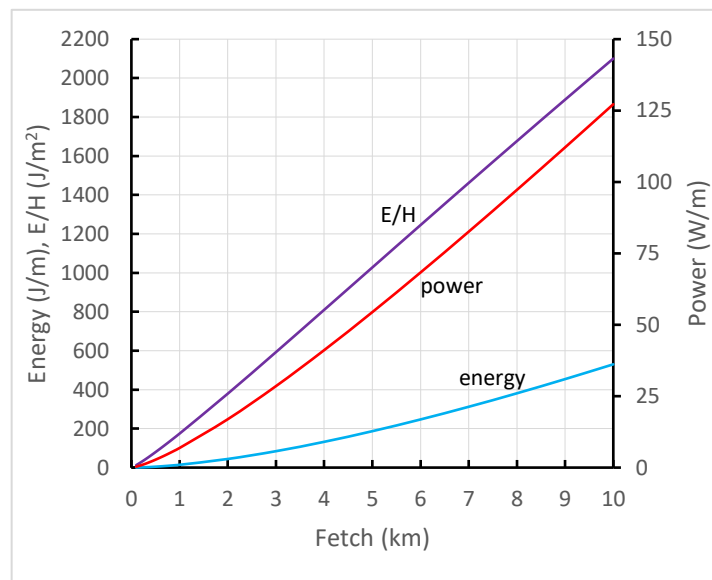


**Figure L11** – *Growth of wind wave energy, power and energy per unit wave height with fetch for a wind speed of 5 m/s. Energy, being equally a function of height and period, grows slowly at first and then accelerates as wave period grows with fetch. Power, which is skewed more towards height and not period, grows more evenly. Energy per unit wave height is almost linear with fetch. The relevant relationships with fetch for a constant wind speed and immature sea are: $E \propto F^{5/3}$, $P \propto F^{4/3}$ and $E/H \propto F^{7/6}$.*

## L.9    Wind Waves and Erosion Thresholds

*Figure L12* shows erosion thresholds of wave height and period for different sediment sizes in *0.5 m* water depth. Overlaid are contours of hindcast wind waves using the *SPM* shallow water equations with $h \gg \lambda$, with wind speeds ranging from *2.5 m/s* to *20 m/s* in *2.5 m/*s increments and fetches ranging from *100 m* to *1,000 m* in *100 m* increments. There is no obvious relationship between any of the erosion thresholds and the wind wave contours, excepting that relationships such as $Fr_F \propto (E/H)^{-3/7}$ can be demonstrated.

The non-linear threshold limit for *0.075 mm* sediment can be exceeded by wind waves generated at any reasonable fetch and wind strength. The fact that sheltered riverine environments in particular may be in dynamic equilibrium suggests that rivers are not exposed to sufficiently strong winds or long fetches to cause on-going erosion. There are many mitigating reasons as to why this may be, not the least being the lack of reasonable fetch (except during specific, limited intervals when wind direction is streamwise and erosion is most likely at downwind bends) and local topography and vegetation that attenuate wind speed. For these reasons it is likely that the equilibrium of very sheltered riverbanks is not impacted by wind waves much, if at all, and other riverine processes (such as tidal flows, floods and seasonal flows), land use, vegetation and waterway usage (principally vessel traffic) are the dominant causes of change.

*Figure L13* is an annotated version of *Figure L2* with data points from the newer Gordon River erosion tests, grouped according to recorded turbidity. The zero turbidity results (green markers) not only lie below the proposed *energy per unit wave height* limit of *260 J/m²* (refer Appendix ZG), they also follow the general trend of wind waves. The erosion test results exhibiting turbidity (red markers) lie well above the wind wave envelope and in a region of wind wave heights/periods more consistent with open waterways.
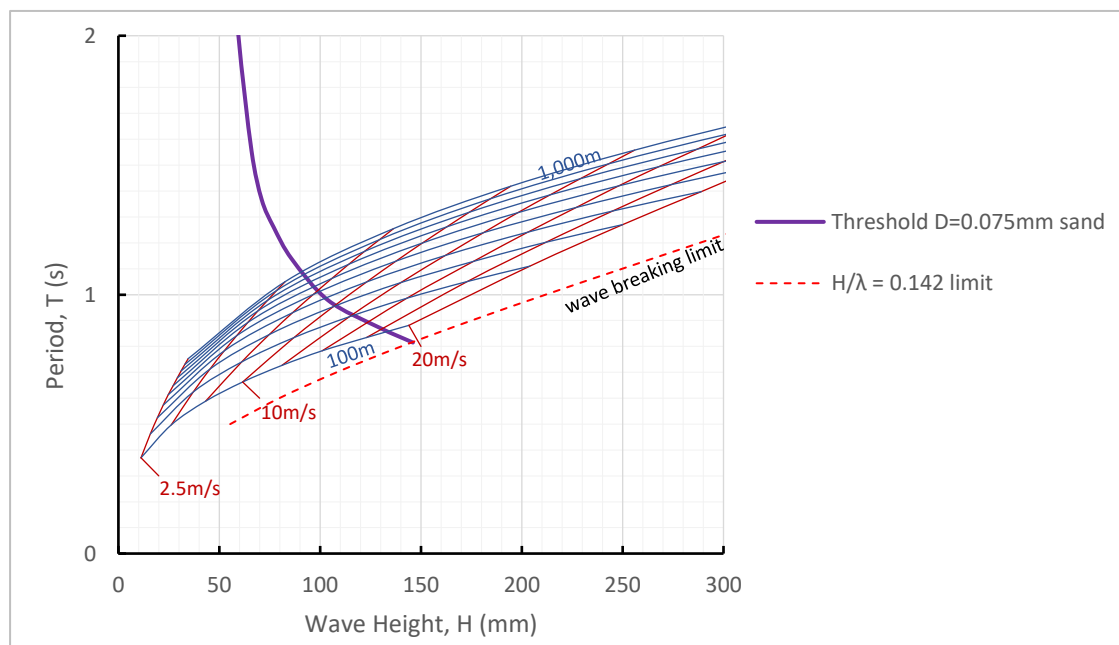


**Figure L12** – *Contours of hindcast wind waves from 2.5 m/s to 20 m/s wind speed in 2.5 m/s increments, and 100 m to 1,000 m fetch in 100 m increments, representing a riverine wind wave climate, overlaid on the non-linear sediment movement threshold at 0.5 m water depth. There is no defined relationship between the wind wave contours and the erosion threshold. The skew of wind wave parameters shows how fetch-limited wind waves grow faster in height than in period.*

353
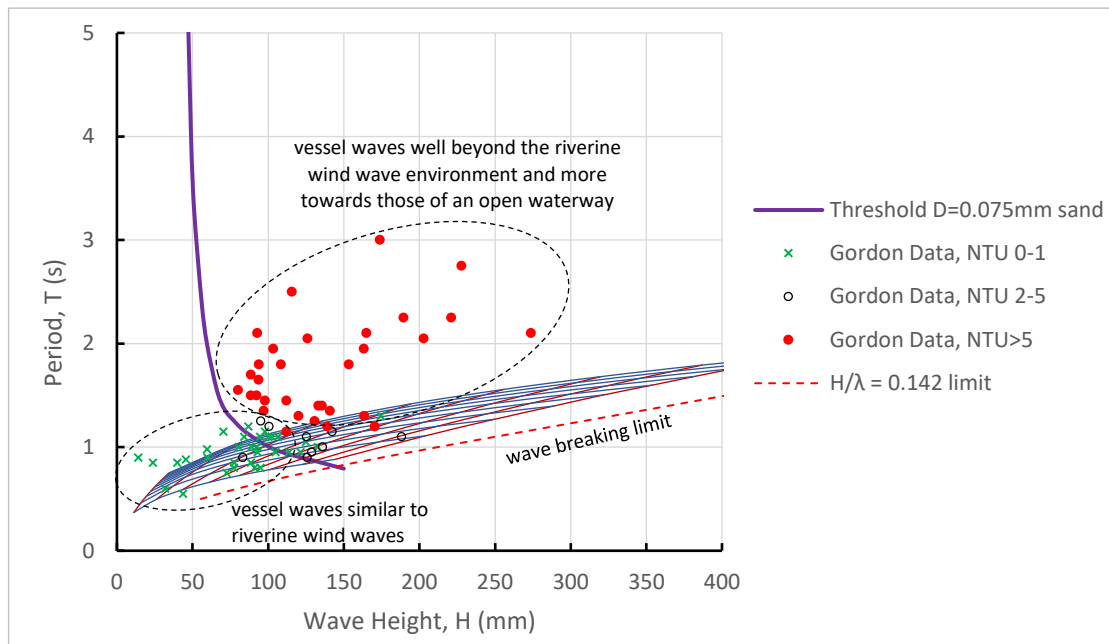
**Figure L13** – *Figure L12 with the 2004 Gordon River erosion tests added, grouped according to no turbidity (NTU 0-1), initiated turbidity (NTU 2-5) and turbid (NTU>5). The spread of "no turbidity" results closely follow the wind wave envelope relevant to this riverine environment (100 m to 1,000 m fetch). The "turbid" results lay distinctly outside the wind wave envelope. Vessel wake waves tend to grow more evenly in height and period whereas wind waves in a sheltered waterway cannot grow in period without increased fetch. The data have not been corrected for sensor vertical position (which moves the erosion data to the left). The threshold curve is based on non-linear theory.*

# Appendix M – Error Analysis and Uncertainty

## M.1     Introduction

In keeping with the themes of the study, the emphasis in the error and uncertainty analysis is on qualification and less so on quantification. It is a simple process to conduct experiments, measure parameters and make a statement on the extent of experimental uncertainty, but that cannot be taken as an expression of the accuracy of a wave wake assessment and the applicability of the results. The understanding of the inherent variability must be made well beyond the experiments themselves, as this is where the greatest uncertainty lies.

The description of errors and their uncertainty are given for three cases – model testing, full-scale testing and results analysis.

## M.2     Model testing and the quantification of uncertainty

### M.2.1   Sources of uncertainty

Error can be accumulated through the following sources of uncertainty:

*Vessel Dimensions*: This is not a parametric analysis of the effect of different vessel dimensions on the generated wake waves. In a regulatory application, the most likely vessel parameters recorded would be the basic hull form (number of hulls), static waterline length and displacement. The effects of other hull dimensions and ratios such as B/T and L/B ratio are ignored.

The static waterline length could be measured to an accuracy of about *0.1%*, but it is known to vary dynamically. In extreme cases at very high speeds, the dynamic waterline length could approach half to two-thirds that of the static condition. Moreover, the forward end of the waterline is a nominal datum and does not necessarily correlate with the waves generated. The fact that ship waves can be crudely approximated by a point source somewhat trivialises the analysis of model dimensional accuracy.

At model scale, displacement has been measured to the nearest gram with a calibration accuracy less than that. For the lightest model tested (AMC 99-17), an error of *1 g* represents *0.026%* of the displacement. At full scale, determination of displacement is less accurate. It requires drafts to be read from draft marks that may or may not have been positioned accurately. For every *1 mm* inaccuracy measuring drafts, caused either by reading error or incorrect positioning of draft marks, the error in calculated displacement would be about *0.4%.* When the hydrostatic parameters are unknown, such as with the estimation of the weight of recreational craft using published data, the level of uncertainty could be in the order of *±10%* with limited (but undefined) confidence. That is the most significant challenge in a regulatory application.

*Lateral separation*: limited to the error of reading the measurement as well as variation in probe position once mounted. The uncertainty is in the order of *±1 mm*; this is an absolute uncertainty and so the relative uncertainly decreases as lateral separation increases. For the nearest probe ($y = 1\,m$) and with a height decay exponent of *-0.5*, the uncertainty in wave height due to lateral separation uncertainty would be *0.1%*. At the most distant probe ($y = 6\,m$), it would be *0.02%*.

Water surface elevation and time are measured at each probe, therefore the two measurements that might be affected are wave decay (which is barely quantifiable at best) and crest mapping.

*Wave height*: Instrumentation calibration was completed for every test and at least daily. The uncertainty in the wave height is a function of the signal voltage and calibration factor uncertainty, which Macfarlane (2012) states as *4.5 mV* and *0.5%* respectively. One source of structural uncertainty is that the model for assessing wave wakes assumes a quasi-static visualisation of waves as they pass through each probe, whereas they are dynamic and changing as the waves transmute. In the time the packet takes to pass through a probe, it and the waves within change in form. The model bias from the quasi-static interpretation cannot be readily accounted for, but it is assumed to be a secondary source of error.

*Wave period*: A standard sampling rate of *200 Hz* is adopted. There is uncertainty within the data acquisition and processing software, but it is understood to be orders of magnitude smaller than other sources. Using the analysis for model AMC 00-01 in the deep-water condition (worst case), the uncertainty in measuring wave height is calculated at *±0.5 mm* (see M.2.3 following). Wave period is measured between zero crossings. A typical value of $\partial H/\partial t$ at a maximum wave zero crossing is in the order of *235 mm/s*, and a water surface elevation uncertainty of *0.5 mm* would therefore be a time uncertainty of *≈0.002 s*, which is less than one-half of one time step of *0.005 s*. A typical period of the maximum wave at high speed for model AMC 00-01 is around *130* time steps.

*Water depth*: The AMC model test basin concrete floor has depth variability in the order of *±2 mm*, though not everywhere. Depth is measured by a metre rule, with an assumed uncertainty of *±1 mm* when the meniscus is accounted for. During shallow water testing, the depth was measured at several points leading up to the wave probes and the variation was never more than *2 mm* (*±1 mm*). The water depth uncertainty in way of the test area is therefore taken as *±2 mm*.

*Vessel speed*: The present model test basin towing apparatus uses an electric motor to drive a continuous chain that pulls the model and its mounting frame along a suspended track. A nominal speed in entered into the motor controller and the actual instantaneous speed is recorded during the testing at each time step. The nominal speed has a systematic relative error of *2.2%* compared to the mean run speed ($V/V_{nom} = 1.022$). In most cases, the nominal speed and related quantities such as Froude number are reported for simplicity, but the averaged speed has been used in calculations where a numerical rather than a schematic interpretation is required.

The speed uncertainty within the recorded values comes from two sources: the variation of speed across the steady-state run time and the calibration of the speed sensor. The variation in steady-state speed is cyclical, with a period of about *1 s* that decreases slightly (but inconsistently) as speed increases. It is unlikely to be a function of elasticity in the chain drive; using the simple spring frequency equation $T = 2\pi\sqrt{m/k}$ where $m$ is the mass and $k$ is the spring constant, the period would be proportional to $\sqrt{m}$. In this case the mass could be substituted with an equivalent mass representing vessel drag and system friction, and these generally increase with increasing speed.[152] Complicating this is the fact that the drive chain length (carriage to motor) reduces as each run progresses, which may change its effective spring constant as the number of

---

[152] This is slightly simplistic. At a steady-state speed the mass of the carriage and model would not have any effect, but in reality the system is undergoing cyclical velocity change and there would be an inertial component of the system mass.

links under tension reduce (and system *play* changes). That is opposite to what was occurring, suggesting the cyclical speed variation is in the motor controller.

There is one mitigating factor with vessel speed variation and that is that wave generation has an associated hysteresis effect. Wave parameters do not change instantaneously, and this dampens out their variation. If the uncertainty analysis were carried through using the speed and depth uncertainty in shallow water tests, the uncertainty could be greater than the measured values at slow speeds. That would cause random variation in results and a lack of repeatability. The fact that experimental results are quite repeatable with satisfactory precision would also imply satisfactory accuracy. Macfarlane (2012) states the speed uncertainty to be *0.01 m/s*. Based on analysis of a sample of the results in this study, the standard deviation in speed was *±0.02 m/s*, and applying a *95%* confidence interval of *2σ*, the uncertainty in speed is taken as *±0.04 m/s.*

*Ancillary Variables*: These include acceleration due to gravity, water density, water temperature, errors caused by incorrect modelling of vessel running trim caused by being towed, errors of scaling (inability to account for viscous and other effects, and absence of propulsion equipment effects as examples) and wake wave breaking not modelled correctly. Scaling errors could be regarded as model bias induced by structural uncertainty. They are all considered to be secondary sources of uncertainty that are an order of magnitude less than the main sources.

## M.2.2   Analysis of results

Ignoring the secondary sources of uncertainty, wave height is taken to be a function of four parameters – model speed $V$, water depth $h$, wave probe calibration factor $C_{wp}$ and wave probe voltage $V_{wp}$. Applying a propagation of uncertainty, the uncertainty in wave height $\delta_H$ is:

$$\delta_H = \sqrt{\left(\frac{\partial H}{\partial V}\delta_V\right)^2 + \left(\frac{\partial H}{\partial h}\delta_h\right)^2 + \left(\frac{\partial H}{\partial C_{wp}}\delta_{C_{wp}}\right)^2 + \left(\frac{\partial H}{\partial V_{wp}}\delta_{V_{wp}}\right)^2}$$

[M1]

There are no known analytical relationships between wave height, vessel speed and water depth, and they must be described numerically to determine their partial derivatives.

Three analyses are presented to establish benchmark values of uncertainty and the relative influence of each source. They include a deep-water condition, a range of shallow water conditions, and a shallow water condition to establish the uncertainty in crest angle.

### M.2.3 Deep water condition: model AMC 00-01 at $h = 0.9\ m$ and $y = 3\ m$

**Figure M1** is used to determine the relationship between wave height and model speed. It has the expected form of a low and high-speed section. The greatest wave height occurs slightly later than expected ($Fr_L \approx 0.64$), which is possibly due to the dynamics of the heavy planing hull and local wave interference. The decreased wave height at *1.5 m/s* is consistent for this model and is most likely due to wave cancellation caused by an active transverse system.

Wave height at high speed would usually decrease gradually. For the sake of an analytical relationship, the trend line shown was used.

**Figure M2** demonstrates that the results in the model test basin depth of $h = 0.9\ m$ are equivalent to previous experiments in a deeper facility ($h = 2.2\ m$). The very deep-water experiments show the anticipated gradual reduction in wave height at high speeds.

**Figure M3** determines the relationship between wave height and water depth for four speeds. Once deeper than about *0.9 m*, depth has no influence on this model. At the slowest speed the generated wavelengths are short, and even shallow depths have almost no influence.

The component uncertainties used in this example are:

$\delta V_{wp} = \pm 4.5 \times 10^{-3}\ V$
$\delta C_{wp} = \pm 3.3 \times 10^{-3}$
$\delta V = \pm 0.04\ m/s$

Results are shown graphically in **Figure M4**.

**Table M1** shows the relative and absolute uncertainties in wave height and the relative contributions of the three component parameters.
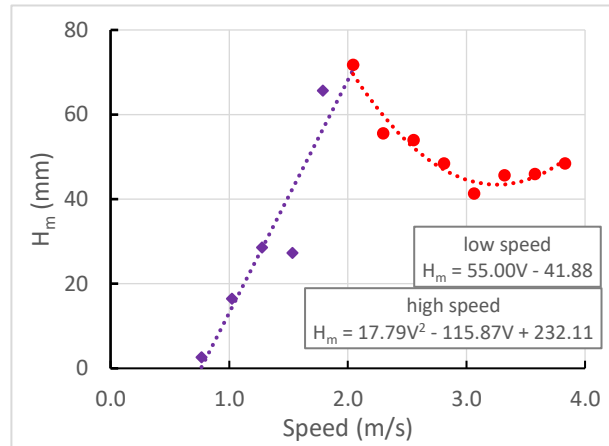


**Figure M1** – *Model AMC 00-01: $h = 0.9\ m$; $y = 3\ m$. Maximum wave height against speed delineated into low and high-speed regions.*



**Figure M2** – *Model AMC 00-01: $y = 3\ m$. Maximum wave height against speed for two deep-water conditions, showing that depth effects at $h = 0.9\ m$ are minimal.*



**Figure M3** – *Model AMC 00-01: $y = 3\ m$. Maximum wave height against water depth for four speed conditions. There is no effect deeper than 0.9 m.*

**Table M1** – *Deep water wave height uncertainty*
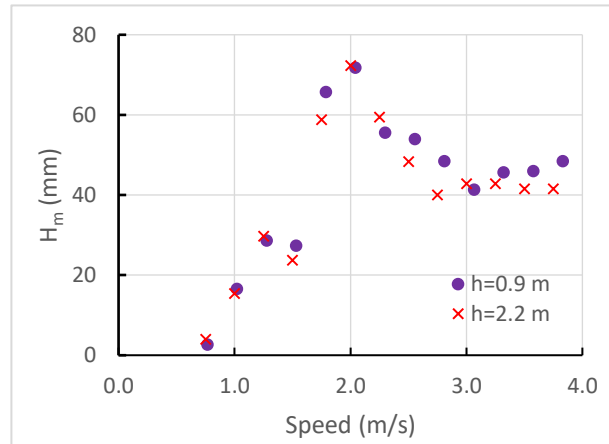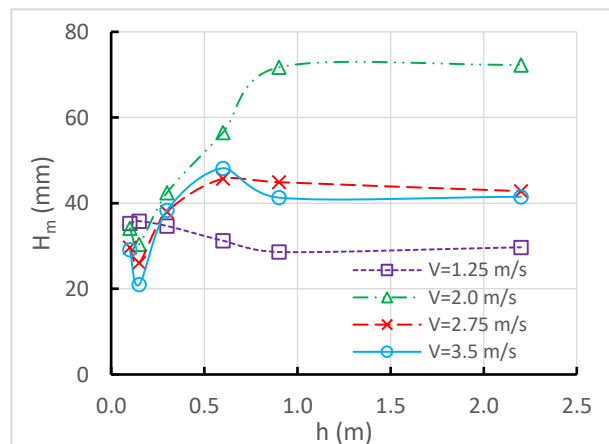
| V$_{nom}$ (m/s) | H (mm) | δH (mm) | δH/H % | relative contribution % | | |
| --- | --- | --- | --- | --- | --- | --- |
| | | | | wave probe voltage | wave probe calibration | model speed |
| 0.75 | 2.6 | 2.2 | 84.6 | 0.0 | 0.0 | 100.0 |
| 1.00 | 16.5 | 2.2 | 13.3 | 0.0 | 0.0 | 100.0 |
| 1.25 | 28.6 | 2.2 | 7.7 | 0.0 | 0.0 | 100.0 |
| 1.50 | 27.3 | 2.2 | 8.1 | 0.0 | 0.0 | 100.0 |
| 1.75 | 65.7 | 2.2 | 3.3 | 0.0 | 0.0 | 100.0 |
| 2.00 | 71.7 | 2.2 | 3.1 | 0.0 | 0.0 | 100.0 |
| 2.25 | 55.5 | 1.4 | 2.5 | 0.0 | 0.0 | 99.9 |
| 2.50 | 53.9 | 1.0 | 1.9 | 0.1 | 0.1 | 99.8 |
| 2.75 | 48.4 | 0.6 | 1.3 | 0.2 | 0.1 | 99.6 |
| 3.00 | 41.3 | 0.3 | 0.7 | 1.2 | 0.6 | 98.2 |
| 3.25 | 45.6 | 0.1 | 0.2 | 9.0 | 5.2 | 85.8 |
| 3.50 | 45.9 | 0.5 | 1.0 | 0.4 | 0.3 | 99.3 |
| 3.75 | 48.4 | 0.8 | 1.7 | 0.1 | 0.1 | 99.8 |
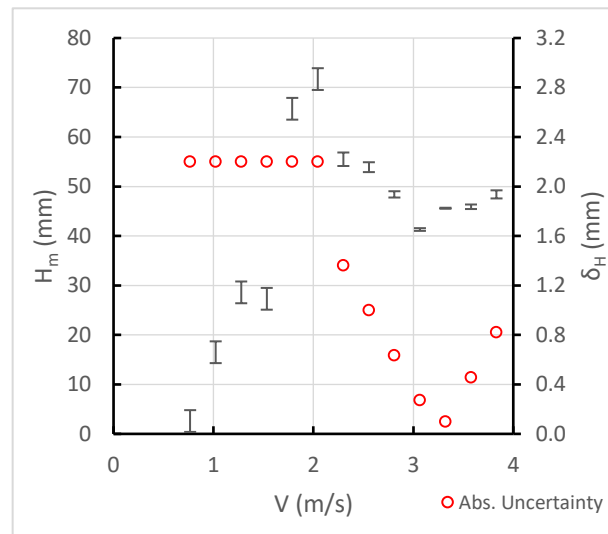


**Figure M4 -** *Wave height uncertainty in the deep-water condition. At slow speeds the uncertainty is substantial and only the high-speed results have relative uncertainties of a few percent. In the deep-water condition, almost all of the uncertainty comes from the uncertainty in model speed. The relative uncertainty in the instrumentation is only significant whenever $\partial H / \partial V$ is small, such as around 3.25 m/s according to the relationship in Figure M1, but the absolute uncertainty remains small.*

**M.2.4   Shallow water condition**: model AMC 00-01 at $h = 0.15\ m$ and $y = 3\ m$

Four speed conditions were investigated, as shown in **Table M2**. The propagation of uncertainties is similar to the deep-water condition, except that water depth becomes important. **Figure M3** was used to determine $\partial H/\partial h$ at $h = 0.15\ m$, which was taken as the average of the slopes either side of $h = 0.15\ m$. At very shallow depths, the leading wave contained an increasing amount of the total wake energy and so its wave height increased. At deeper depths, a wave further back in the packet becomes the maximum wave. **Figure M5** was used to determine $\partial H/\partial V$ at $h = 0.15\ m$ and $y = 3\ m$.

The component uncertainties used in this condition were:

$$\delta V_{wp} = \pm 4.5 \times 10^{-3}\ V$$
$$\delta C_{wp} = \pm 2.9 \times 10^{-3}$$
$$\delta V = \pm 0.04\ m/s$$
$$\delta h = \pm 2\ mm$$

**Figure M6** shows the uncertainty in shallow water. In general, the sources of uncertainty are model speed and water depth, with the relative influence of depth increasing with increasing speed.
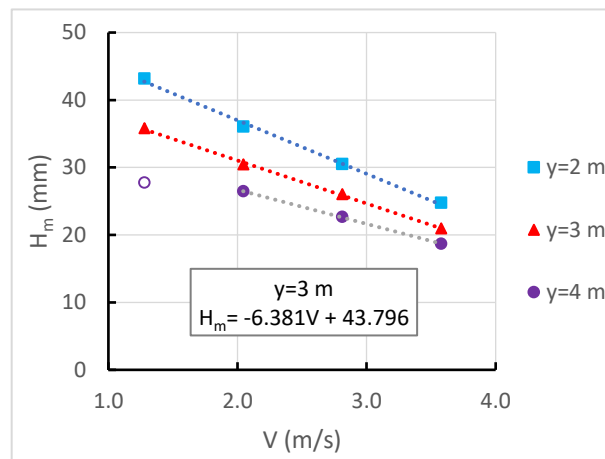


**Figure M5** – *Model AMC 00-01: $h = 0.15\ m$. Maximum wave height against speed for three lateral separations.*

**Table M2 –** *Shallow water wave height uncertainty*

| | | | | relative contribution % | | | |
|---|---|---|---|---|---|---|---|
| $V_{nom}$ (m/s) | H (mm) | δH (mm) | δH/H % | wave probe voltage | wave probe calibration | model speed | water depth |
| 1.25 | 35.8 | **0.3** | 0.7 | 1.1 | 0.5 | 98.0 | 0.5 |
| 2.00 | 30.4 | **0.3** | 1.0 | 0.8 | 0.3 | 72.6 | 26.4 |
| 2.75 | 26.0 | **0.3** | 1.1 | 0.8 | 0.2 | 73.3 | 25.7 |
| 3.50 | 21.0 | **0.4** | 1.8 | 0.5 | 0.1 | 45.5 | 54.0 |

360

**Figure M6 -** *Wave height uncertainty in the shallow water condition ($h = 0.15\ m$). Relative uncertainty increases with increasing speed, due largely 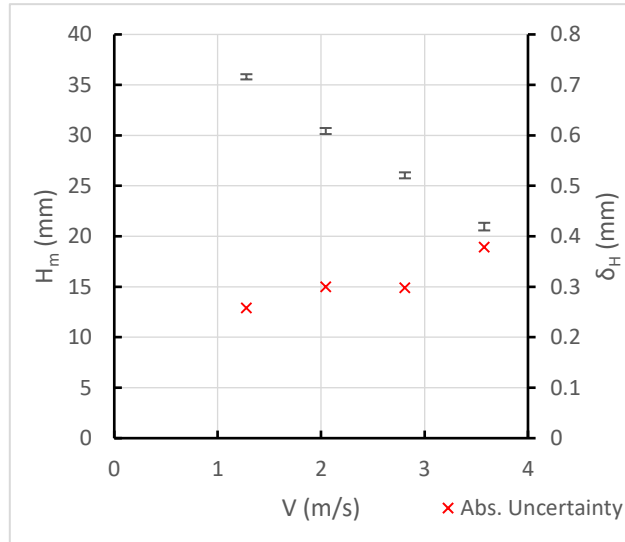to reducing wave heights as speed increases. The relative contributions of model speed and water depth change as speed increases. As with the deep-water condition, instrumentation uncertainty is almost inconsequential.*

**M.2.5 Shallow water leading wave angle**: model AMC 00-01 at $h = 0.15\ m$ and $y = 3\ m$

There are analytical relationships between the leading crest angle and the parameters of water depth and model speed. There is also a relationship between the leading crest angle and wave height, though it depends on the $h/L$ ratio and whether the first wave is dominated by a solitary wave form. If the leading crest is not dominated by a solitary wave form (whose celerity depends on water depth and wave height), the crest's celerity would be limited to $\sqrt{gh}$ and therefore without influence of wave height. As it transpires, wave height has a very minor influence on the crest angle (refer Tables M3 and M4 following), which diminishes further as depth increases. For that reason, a separate analysis using $\sqrt{gh}$ and excluding wave height is not warranted.

The relationships between leading crest angle $\alpha$ and experimental parameters are given by [M2] (Boussinesq) and [M5] (Korteweg de Vries). The partial derivatives with respect to wave height, water depth and model speed are given by [M3] and [M4] for the Boussinesq form and [M6], [M7] and [M8] for the KdV form (note that the equations give uncertainty in $\alpha$ in radians):

*Boussinesq*:

$$\alpha = \sin^{-1}\left(\frac{\sqrt{g(h+H)}}{V}\right) \tag{M2}$$

$$\frac{\partial \alpha}{\partial H} = \frac{\partial \alpha}{\partial h} = \frac{g}{2V\sqrt{g(h+H)}\sqrt{1 - \frac{g(h+H)}{V^2}}} \tag{M3}$$

$$\frac{\partial \alpha}{\partial V} = -\frac{\sqrt{g(h+H)}}{V^2\sqrt{1 - \frac{g(h+H)}{V^2}}} \tag{M4}$$

361

**Korteweg de Vries**:

$$\alpha = \sin^{-1}\left[\frac{\left(1 + \frac{H}{2h}\right)\sqrt{gh}}{V}\right]$$ [M5]

$$\frac{\partial \alpha}{\partial H} = \frac{\sqrt{gh}}{2hV\sqrt{1 - \frac{gh\left(1 + \frac{H}{2h}\right)^2}{V^2}}}$$ [M6]

$$\frac{\partial \alpha}{\partial h} = \frac{\frac{g\left(1 + \frac{H}{2h}\right)}{2V\sqrt{gh}} - \frac{H\sqrt{gh}}{2Vh^2}}{\sqrt{1 - \frac{gh\left(1 + \frac{H}{2h}\right)^2}{V^2}}}$$ [M7]

$$\frac{\partial \alpha}{\partial V} = -\frac{\left(1 + \frac{H}{2h}\right)\sqrt{gh}}{V^2\sqrt{1 - \frac{gh\left(1 + \frac{H}{2h}\right)^2}{V^2}}}$$ [M8]

The uncertainty in wave height measurement is taken from **Table M2** as $\partial H = \pm 0.4\ mm$, which is the worst case derived. Applying a propagation of uncertainty, the uncertainties in the leading wave angles are shown in **Tables M3** and **M4,** and they are in the order of *±0.2° to ±0.3°*. As water depth increases, the relative contribution of depth decreases. Model speed remains by far the greatest source of uncertainty.

**Table M3** – *Uncertainty in leading wave angle for two conditions – Boussinesq form*

| | | | | | relative contribution % | | |
|---|---|---|---|---|---|---|---|
| $V_{nom}$ (m/s) | h (mm) | α (deg) | δα (deg) | δα/α % | water depth | model speed | wave height |
| 2.75 | 100 | 22.7 | **0.3** | 1.5 | 3.4 | 96.5 | 0.1 |
| 3.00 | 52 | 15.6 | **0.2** | 1.4 | 11.1 | 88.4 | 0.4 |

**Table M4** – *Uncertainty in leading wave angle for two conditions – Korteweg de Vries form*

| | | | | | relative contribution % | | |
|---|---|---|---|---|---|---|---|
| $V_{nom}$ (m/s) | h (mm) | α (deg) | δα (deg) | δα/α % | water depth | model speed | wave height |
| 2.75 | 100 | 22.7 | **0.3** | 1.5 | 0.4 | 98.0 | 1.6 |
| 3.00 | 52 | 15.6 | **0.2** | 1.4 | 3.9 | 90.3 | 5.8 |

## M.3    Full-scale Trials and the Sources of Uncertainty

*Vessel condition:* The two principal vessel dimensions recorded during full-scale trials are static waterline length and displacement. Owners of commercial vessels (usually) have at their disposal information such as a stability book that assists with condition recording. As noted, there is an inherent degree of uncertainty due to the limitations of draft mark surveys. It is usually impossible to ascertain the condition of recreational vessels unless they are weighed. Published weights may be incorrect or incomplete (such as the difference between *dry weight* and *lightship*). Similarly, static waterline length is rarely recorded due to the variable loading conditions, and the high operating Froude numbers of small craft give rise to substantial dynamic variation.

In a regulatory application, under-reporting of vessel weight could become an area of abuse. The assessment of a vessel's wave wake potential can only be made statistically, which relies on the two principal inputs of length and displacement. Individual wave wake certification of recreational craft is untenable unless done in a type approval regime.

*Instrumentation*: Macfarlane (2012) notes the wave probe uncertainties using field trials instrumentation are *±5.5 mV* for voltage (typical) and *1.0%* for calibration factor. Provided calibration is undertaken regularly, both these factors are considered to be insignificant, as they were for model experiments. The uncertainty due to the instrumentation is not the primary source of error.

*Speed*: The measurement of speed itself has a small uncertainty, depending on how it is achieved. However, the maintenance of a steady-state speed is a primary source of error. Wave wake generation comes with inherent transient effects and a rate-dependent hysteresis that is inherently non-linear. The failure to achieve a steady state speed well before the measurement probes would cause every probe to record varying states of wake generation (varying within each probe's record and between probes)

The stability of the transverse system period is dependent on the length of the steady-state condition, especially at higher speeds when the wavelength of the transverse system becomes long compared to the vessel. As shown in Figure 4.8 of Section 4, the shorter period transverse system waves generated during acceleration are evident. They tend not to affect the maximum wave, which occurs relatively earlier in the temporal record.

Lastly, the stability of the divergent system relies on the continuous energy input of the vessel. If the speed is reduced abruptly after passing the wave probes, the divergent system will diffract (it effectively becomes "open-ended" if input energy is cut at the source). That would cause a slight decrease in far-field wave heights, with an unwarranted reliance on hysteresis to offset it. In field trials, conducting experiments in two directions encourages the helmsman to continue past the wave probes at speed to gain an adequate acceleration distance for the next test. Model scale experiments, conducted in one direction, can experience this structural uncertainty but steady-state numerical analyses do not. The extent of the uncertainty has never been quantified.

*Water Depth*: Model tests are mostly predicated on maintaining a constant water depth. That is a rare occurrence at full scale. As with speed, the effects of fluctuations in water depth are smoothed by hysteresis. Waves do not alter their parameters instantly.

Uncertainty arising from variable depth has two conditions. The first is variability at the sailing line, so that the waves generated may have forms that change over time. Provided the trans-critical speed range is avoided, the extreme non-linearities of that range can also be avoided. The

363

second is variability in depth as waves propagate. Apart from wave parameter change due to shoaling, changes in the maximum wave can occur when part of the packet is in water much deeper/shallower than the depth at the maximum wave. The attempt by Ozeren *et al.* (2016) to measure wave heights almost at the point of breaking would introduce additional non-linearities that are almost impossible to account for with certainty.

Water depth and vessel speed are inter-related. At model scale with a towed model, the model speed control has a minor uncertainty but a great effect. At full scale, or at model scale with a self-propelled model, changes in vessel resistance with changing water depth can cause instability in vessel resistance and therefore speed, so much so that it becomes almost impossible to replicate conditions around the depth-critical speed where the speed/resistance relationship is dynamically unstable. A further complication to this is found with planing vessels (almost all recreational craft forms), which experience speed instability as they transition from displacement to planing mode. It has long been a (colloquial) observation that small craft can be made to "*get over the hump*" with simple adjustments to the seating positions of passengers.[153]

*Course*: The need to maintain a straight, defined course cannot be overstated. Curved approaches to the wave measurement area affect the waves - focussing waves on the inside of curves and diffracting them on the outside.

The lateral separation must be maintained at a known location. It may not seem important to maintain a fixed lateral separation for all test speeds – the results could be corrected (with inherent error) provided the actual lateral separation is known for each test. That would require application of a decay rate when only one or two probes are used, but Section 7 demonstrates that actual decay rates are not well defined.

Ozeren *et al.* (2016), as discussed in Appendix A8, conducted a large number of field trials with lateral separation varying by around *100%*. The courses were mapped using GPS instrumentation, but there was no recorded attempt to mark a course. The uncertainty incurred between the vessel parameters and wave parameters would have been considerable. They are not alone in their experimental methodology; the over-utilisation of 21st century instrumentation offering precision uncertainty.

*Ambient Conditions*: An unfortunate consequence of open water testing is unfavourable ambient conditions. Wind waves are of concern to small craft experiments where the wind wave heights and periods may not be dissimilar to those of the vessel. The effect decreases with increasing vessel size, but that can be offset by the navigational requirement to conduct trials of larger vessels in more open waters.

There are also problems with contamination from passing vessel traffic and variability of results due to currents. Seiching has also been encountered during field trials. It is possible to filter out

---

[153] The Bristol Bay gill netting boats operating in Alaska use a combination of shallow water and planing hull dynamics to achieve adequate laden performance. The very short fishing season and regulatory design limits result in vessel designs with extremely low L/B ratios capable of catching large quantities of salmon and returning to port quickly to unload. A heavily laden vessel, unable to reach planing speeds in deeper water due to its increased resistance *hump*, will transit to very shallow water (*~1-2 m*) where the reduced resistance allows it to plane. Once *on the plane* and past the hull's natural resistance *hump*, it can return to deeper water and maintain planing speeds. The dynamic planing resistance *hump* and shallow water resistance *hump* are examples of speed instabilities that are a source of error in self-propelled model tests and full-scale testing.

some of the effects of wind waves, but the filtering techniques have inherent uncertainty that deteriorates the closer the ambient wave parameters approach the vessel wave parameters.


**M.4     Sources of Uncertainty During Analysis.**

Over the whole process of generation, propagation, measurement and analysis, the greatest source of uncertainty is in the interpretation of wave wake records. The precision afforded by using controlled model testing conditions and calibrated instrumentation has no relationship to the accuracy of the results in terms of how the parameters recorded are a measure of the wave wake of a vessel. Lack of accuracy innate to the interpretation of results cannot be offset by precision of measurement.

Additionally, there is an inherent problem of definition in the analysis, in that it's uncertain if what we are measuring is what it proports to be, or what we define it to be. It's easy to measure a wave, but we have no way of knowing what that wave is comprised of and what it represents. That is certainly the case for shallow water waves, but also for deep water waves where there may be multiple wave packets with similar characteristic wavenumbers causing local constructive/destructive interference. A Fourier analysis may only indicate the combined effect and not the individual components. That gives rise to parameter uncertainty. Repeating experiments only reduces experimental uncertainty and not parameter uncertainty.

There is also a known, but difficult to quantify, uncertainty when applying analytical wave equations to calculate parameters such as shallow water wavelength. In some ways there is little point trying to quantify the uncertainty, as there is likely to be a natural variation due to the packet-like nature of waves and the fact that a discretised wave is only the nett result of multiple components at a particular point in space and time.

Summarising Sections 3-7, the analysis uncertainty can arise from:

a.  interference between wave systems, which is dependent on the number of wave packets, their packet wavenumbers (which determines how they propagate relative to each other), the strength of the transverse system (which is a function of vessel parameters, vessel speed and water depth). Multihulls experience exaggerated effects at slow speeds;
b.  the position of the wave cut relative to the waves within the total system;
c.  the water depth; with its effect dependent on the vessel speed and the fact that the effect is different for each wave and any point in time and space. Similarly, the composition of the first wave in very shallow water is unclear, even if the wave itself is clear;
d.  wave height decay, which at best is an approximation.


*Figure M7* shows the results of field trials against the AMC's wave wake database prediction. The WWDB scales numerous vessel results based on basic form (monohull or multihull). The bounds of the prediction reflect the variation in the scaled results, but not the total uncertainty.
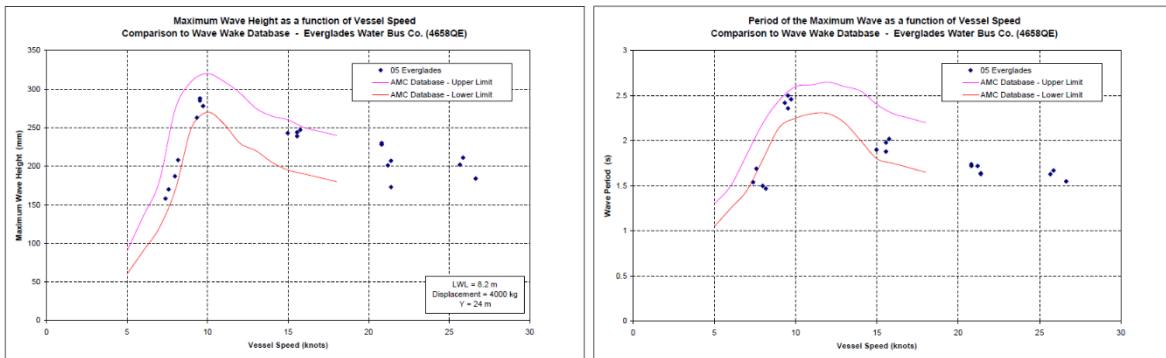
365

**Figure M7** – *Reproduced from Macfarlane and Cox (2003), Fig. D63 and D64: Comparison of full-scale results of an 8.2 m monohull vessel (discrete points) against the upper and lower limit predictions of the AMC's wave wake database.* **Left** – *maximum wave height against speed.* **Right** *–period of the maximum wave against speed. The limits of the prediction are <u>not</u> a measure of total uncertainty; they are the variation in the scaled results of the large number of vessels that make up the database. Inherent within those limits is the uncertainty of the analysis that made up the entries of the database, which would further increase overall uncertainty.*

## M.5    The Mitigating Factor

Wave wake analysis is rarely a study of percentages but of orders of magnitude. As an example, the Gordon River threshold energy from Appendix K is calculated at *~30 J/m* in *0.5 m* water depth. In an unpublished set of (commercial-in-confidence) experiments conducted on the Sydney Harbour JetCats in 1994, the energy of the maximum wave reached a peak value in excess of *30,000 J/m* at the vessel's *hump* speed (*15.0 kn*, or $Fr_L = 0.48$) in *13 m* water depth, with high-speed values around *10,000 J/m* or less.[154]

Without this naturally-occurring variation in wave energy, wave wake analysis and its attendant uncertainties would possibly be a pointless exercise.

***Bibliography***:

Taylor, J.R. (1997). *An introduction to error analysis: the study of uncertainties in physical measurements*. Sausalito CA: University Science Books

Taylor, B.N. and Kuyatt, C.E. (1994). *NIST Technical Note 1297: Guidelines for Evaluating and Expressing the Uncertainty of NIST Measurement Results*. National Institute of Standards and Technology, United States Department of Commerce – Technology Administration. Washington: U.S. Government Printing Office.

---

[154] The JetCats had a waterline length of *~30 m* and a stated displacement at trials of *100 t*. Measurements were made in *~13 m* water depth at a lateral separation of *~50 m*. The vessels were used on the outer harbour where wave wake was not a primary operational consideration. The vessels were sold off in 2008/9.